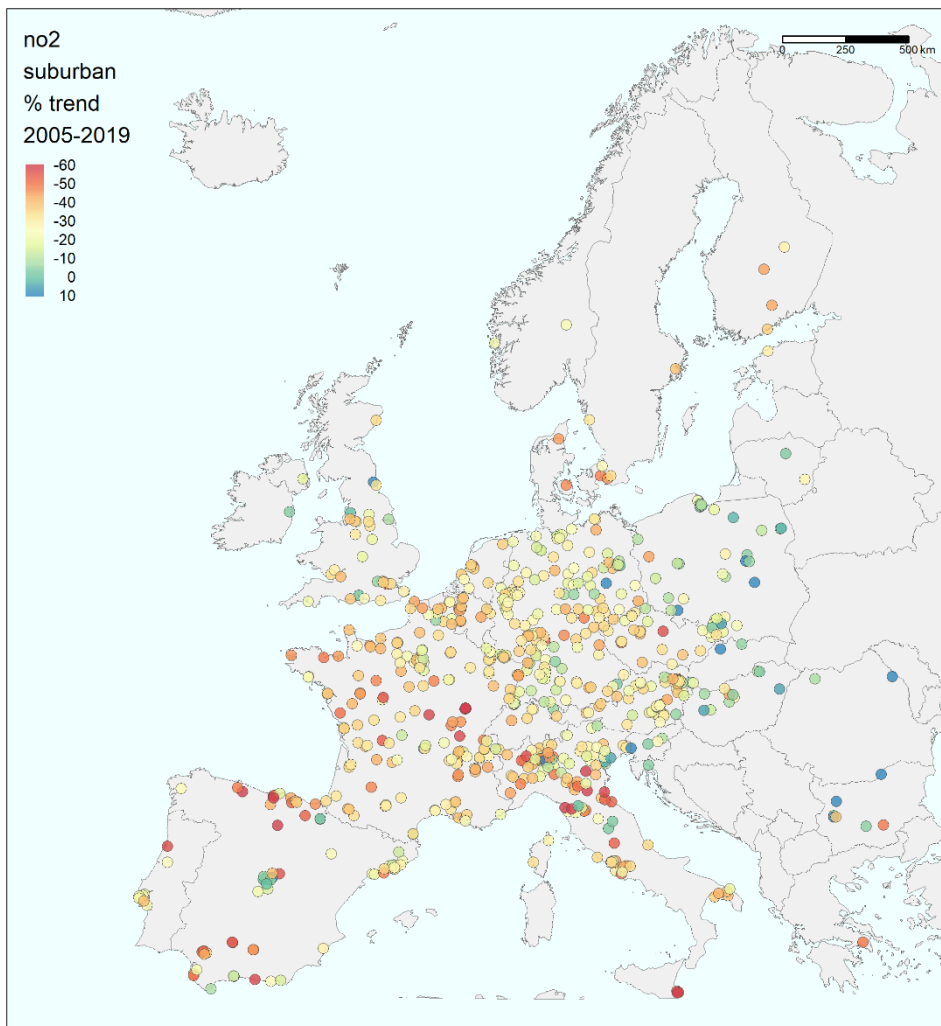


Long-term trends of air pollutants at national level 2005-2019

November 2021



Authors:

Sverre Solberg (NILU), Augustin Colette (INERIS), Blandine Raux (INERIS),
Sam-Erik Walker (NILU), Cristina Guerreiro (NILU)

ETC/ATNI consortium partners:

NILU – Norwegian Institute for Air Research, Aether Limited, Czech Hydrometeorological Institute (CHMI), EMISIA SA, Institut National de l'Environnement Industriel et des risques (INERIS), Universitat Autònoma de Barcelona (UAB), Umweltbundesamt GmbH (UBA-V), 4sfera Innova, Transport & Mobility Leuven NV (TML)

European Environment Agency
European Topic Centre on Air pollution,
transport, noise and industrial pollution



Cover design: EEA
Layout: ETC/ATNI

Legal notice

The contents of this publication do not necessarily reflect the official opinions of the European Commission or other institutions of the European Union. Neither the European Environment Agency, the European Topic Centre on Air pollution, transport, noise and industrial pollution nor any person or company acting on behalf of the Agency or the Topic Centre is responsible for the use that may be made of the information contained in this report.

Copyright notice

© European Topic Centre on Air pollution, transport, noise and industrial pollution, 2021

Reproduction is authorized, provided the source is acknowledged.

Information about the European Union is available on the Internet. It can be accessed through the Europa server (www.europa.eu).

The withdrawal of the United Kingdom from the European Union did not affect the production of the report.

Data reported by the United Kingdom are included in all analyses and assessments contained herein, unless otherwise indicated.

Author(s)

Sverre Solberg (NILU), Augustin Colette (INERIS), Blandine Raux (INERIS), Sam-Erik Walker (NILU), Cristina Guerreiro (NILU)

ETC/ATNI c/o NILU
ISBN 978-82-93752-33-2

European Topic Centre on Air pollution, transport, noise and industrial pollution
c/o NILU – Norwegian Institute for Air Research
P.O. Box 100, NO-2027 Kjeller, Norway
Tel.: +47 63 89 80 00
Email: etc.atni@nilu.no
Web : <https://www.eionet.europa.eu/etcs/etc-atni>

Contents

Summary	5
Acknowledgements	6
1 Introduction	7
2 Models and methods	8
2.1 Analyses of the air quality observations	8
2.1.1 Data completeness	8
2.1.2 Air pollutant indicators, metrics and indices	3
2.1.3 Statistical tests	4
2.1.4 Air pollutant emissions	5
2.2 AirGAM	5
2.2.1 Input data to AirGAM	6
3 Results. Trends of air pollutants and air quality	7
3.1 Results from analyses of measurement data	7
3.1.1 Sulfur dioxide	7
3.1.2 Nitrogen dioxide	11
3.1.3 Ozone	17
3.1.4 Particulate Matter	27
3.1.5 Air Quality Index	33
3.2 Results from AirGAM calculations for NO ₂ , PM ₁₀ , PM _{2.5} and O ₃	35
3.2.1 Preliminary AirGAM results for VOC	41
4 Summary and conclusions	43
5 References	44
Annex 1 National trends in air concentrations as calculated from in-situ measurements	46
Annex 2 National trends in air concentrations as calculated by AirGAM and reported emissions	278
5.1 Country AT	278
5.2 Country BE	279
5.3 Country BG	281
5.4 Country CH	281
5.5 Country CZ	282
5.6 Country DE	284
5.7 Country DK	285
5.8 Country EE	286
5.9 Country ES	287
5.10 Country FI	288
5.11 Country FR	289
5.12 Country GB	290
5.13 Country GR	291
5.14 Country HR	292
5.15 Country HU	293
5.16 Country IE	294
5.17 Country IT	295
5.18 Country LT	296
5.19 Country LU	297
5.20 Country ME	298

5.21 Country MK	299
5.22 Country NL	300
5.23 Country NO	301
5.24 Country PL.....	302
5.25 Country PT.....	303
5.26 Country RO.....	304
5.27 Country SE.....	305
5.28 Country SI.....	306
5.29 Country SK.....	307

Summary

The aim of this study is to investigate the development of European air pollutant concentrations during a 15-years period (2005-2019) and how the changes in pollutants relate to the emission data over the same period. Surface concentrations of SO₂, NO₂, PM₁₀, PM_{2.5} and O₃ in different types of areas (rural, suburban, urban, traffic) are analysed.

All emitted pollutants (SO₂, NO₂, PM₁₀, PM_{2.5}) show significant downward trends. The largest decrease is seen for sulphur dioxide for which the levels at industrial sites in 2019 are comparable to that of rural sites at the beginning of the period (2005). A reduction of the order of 60-70 % is found, and the agreement between reported emissions and measured concentrations are quite good.

For NO₂, a mismatch between the trend in air concentrations and NO_x emissions is found. Whereas the overall NO_x emissions are reported to be reduced by around 45 % over the period, the surface concentrations of NO₂ have dropped by around 30 % on average. When looking into individual countries, substantial variations are found, and for some countries the agreement between national NO_x emissions and measured NO₂ concentrations are good. This mismatch could not be explained by interannual variations in weather conditions as this is accounted for by the applied statistical methods. There are, however, several possible reasons why the trends in NO₂ concentrations and NO_x emissions differ. Changes in the fleet of vehicles could lead to a change in the NO₂/NO_x concentration ratio at roadside stations, and this ratio could also be influenced by changes in the ambient ozone level.

For PM data (PM₁₀ and PM_{2.5}) the surface PM concentrations show stronger downward trends than the reported emissions. This is likely an effect of the importance of secondary aerosols which are mitigated by other activities than the direct PM emissions, thus leading to additional reductions compared to the abatement of primary emissions alone. For PM₁₀ an overall reduction in surface concentrations of the order of 30-38 % is found during 2005-2019. The reduction of the direct emissions of PM₁₀ is 5-10 percentage units smaller than this. Similar results are found for PM_{2.5}, but due to the substantially less amount of measurement data, these findings are more uncertain.

O₃ is not emitted but is a result of a hemispheric baseline level with the addition of photochemical episodes creating O₃ in the atmosphere from precursors as NO_x, VOC, CO and methane. During the period 2005-2019 the annual mean ozone concentration has increased slightly while the high peaks have been reduced. The increase in mean level is explained by hemispheric transport and reduced titration by NO as a result of reduced NO_x levels in the atmosphere. The reduction in high ozone peaks is expected when the general NO_x level in Europe is reduced.

Acknowledgements

Christoffer Stoll at NILU is acknowledged for assistance with the observation databases. Sabine Eckhardt also at NILU is acknowledged for extracting ERA5 data from ECMWF. Luca Liberti at EEA is acknowledged for being the task manager.

1 Introduction

It is well documented that air pollution poses a serious threat for human health and ecosystems. It has been mitigated since the 1970s, in particular through international policy instruments such as the Geneva Convention on the Long Range Transboundary Air Pollution (CLRTAP, 1979) and, as far as Europe is concerned, the National Emission Ceiling Directives (EC, 2001, 2016), which set objectives to be achieved by the implementation of national and local regulations. In order to assess the magnitude of the threat, and the efficiency of mitigation strategies and policies, scientific assessments based on tools to monitor and predict atmospheric composition changes were developed. The CLRTAP launched the European Monitoring and Evaluation Programme (EMEP, www.emep.int), with a dedicated in situ monitoring network, and the European Commission released a number of air quality directives (EC, 1996, 2004, 2008) defining common monitoring principles for countries of the European Union as well as maximum air pollution levels not to be exceeded to ensure a clean air for European citizen.

Decades after having initiated emission reduction strategies and dedicated monitoring networks, several studies taking stock of long-term air quality monitoring have been performed by the EC and the CLRTAP to assess the efficiency of air pollution mitigation strategies (Colette et al., 2016; EEA, 2009, 2020; Maas and Grennfelt 2016). The topic has also been of interest for the scientific community with a number of articles devoted to the assessment of air quality trends and relating them to the efforts achieved in terms of emission reductions. The majority of such studies were focused on ozone (Cooper et al., 2020; Lefohn et al., 2016; Vautard et al., 2006; Sicard et al., 2013; Derwent et al., 2003; Derwent et al., 2010; Jonson et al., 2006; Wilson et al., 2012; Fleming et al., 2018; Simpson et al., 2014) to name just a few, and excluding all the scientific body devoted to tropospheric ozone at a larger scale. But there has also been studies investigating nitrogen and particulate matter trends: (Colette et al., 2011; Guerreiro et al., 2014; Barmpadimos et al., 2012; Turnock et al., 2015; Banzhaf et al., 2015; Turnock et al., 2016; Tørseth et al., 2012).

Several of those investigations relied on both observations and models to discuss policy effectiveness, in general by feeding one or several chemistry-transport models with reported air pollutant emissions before comparing the results with observations to conclude on the effectiveness of policy implementation (Colette et al., 2017; Wilson et al., 2012; Colette et al., 2011).

In this report the trends are studied by two different methods: One method analysing the observations by linear statistics to update the knowledge of the current status of trends in the European air quality, and one method using a nonlinear regression tool (GAM) developed recent years for EEA trend studies in which the daily concentrations are linked to local meteorological data (Solberg et al., 2021). The results from both methods are presented based on aggregated European data in the main report, and for each individual country in the annexes. Both methods also relate the trends in air pollutant concentrations to the reported emission changes over the 2005-2019 period to the extent possible.

In this study, a 15 year period is studied: 2005-2019, the latest year being constrained by the availability of validated observation released for the year 2019 in 2021 by the European Environment Agency. Compared to earlier studies looking at shorter periods a 15 years period makes it easier to conclude on statistical significance of the trends. In addition, larger geographical areas become available for the analysis.

The methods and their respective input data are described in Chapter 2, and the results in Chapter 3 where the trend of the various air pollutants of interest are discussed (Sulphur dioxide – SO₂, nitrogen dioxide – NO₂, ozone – O₃, Particulate matter finer than 10µm and 2.5µm – PM₁₀ and PM_{2.5}) as well as the trends of the Air Quality index in order to provide a synthetic overview of air quality evolution that captures the change for all individual compounds. A summary is given in Chapter 4.

2 Models and methods

2.1 Analyses of the air quality observations

For this study, we rely on the air quality monitoring databases hosted by the European Environment Agency (EEA). Up to 2012, these datasets were gathered in the AIRBASE database, for which we used the v8 release. After 2013, the EEA database moved to the Air Quality e-reporting system. Only validated data are used. A technical difficulty lied in matching these two databases because many stations changed names and codes over time. Instead of station names, the matching is performed using the Sampling Point Identification, which is the most reliable meta-data about the consistency of a given record.

The EEA databases differentiate sampling point area (urban, suburban and rural) and typology (background, traffic, industrial). For synthesis, we differentiate background types at urban, suburban and rural areas and also considered separately traffic stations and industrial stations (yet without distinction of whether traffic or industrial stations are located in urban, suburban or rural areas).

2.1.1 Data completeness

All the surface data available included in the database is used in the present study. We did not apply any outlier detection or filtering considering that the impact of spurious data will be minimised in the aggregation of statistic over a large dataset. We did however perform a completeness check so that too short records were not included in the trend analysis. First the completeness in any given year is assessed so that all datasets (days or hours) within a year where less than 75% of the record are available are discarded. In a second step, we also removed a given station if less than 75% of the years in the 18 year time period (i.e. 5 years or more) were not available.

Regarding temporal resolution, most observations for NO₂, SO₂ and O₃ are available as hourly data so that we used only those records, which allow to investigate daily maximum behaviour and diurnal variations. For PM₁₀ and PM_{2.5} there is however a mix of hourly and daily values according to the measurement method used, but most relevant indicators are defined on the basis of daily means. As a consequence, we averaged all raw hourly records and checked for redundancy before aggregating them in the raw data available as daily means. This aggregation did not include a verification of missing data over a given day.

A specific work was performed to identify collocated measurements of O₃ and NO₂ in order to discuss Ox (as O₃ + NO₂) trends, but also to compare the relative trends of O₃ and NO₂ at a consistent set of stations. Ideally NO should also be added to O₃ and NO₂ to derive total Ox, but that would have led to a selection of too few stations because of the scarce collocation of O₃, NO₂ and NO measurements. Likewise, we identified collocated measurements of PM₁₀ and PM_{2.5} to compare the trends of fine and coarse PM.

Because until 2007, French authorities reported PM hourly concentrations from automatic devices (TEOM, Beta gages) without applying any correction factor to account for the volatilisation of some PM compound during the measurement phase, daily values could not be directly used before that date in that country. Nevertheless, as it was done by the other countries at that time, a correction of annual mean values was applied (factor 1.3, (Malherbe et al., 2017)) so that only annual mean statistics of PM₁₀ can be used for the purpose of this study for France up to 2006.

The total number of air quality stations by station type and pollutant available during the period 2005-2019 in the European Union (27 countries) and the UK is given in Figure 1. In 2005, about 5000 records (combinations of stations and pollutants) were available, but in 2019 this number exceeds 10000 records. A steady increase of the number of stations is found for all station types and pollutants. Over the early 2000's, the PM monitoring network has developed drastically, so that the proportion of gaseous monitoring devices is reduced. Before 2007, PM_{2.5} stations locations were scarce.

After having applied the completeness checks for trend assessment described above, we kept about 5000 records. If only stations covering the whole period had been selected, the number of station would have been constant in time, but we see here an increase in the number of sites over the first few years because of the relaxed completeness criteria that selects records with only 75% of valid years (i.e. over 2005-2019 for all pollutants except for PM_{2.5} where the time period is 2008-2019). A clear issue occurred in 2013, the year when the EEA system changed from Airbase to AQ e-reporting. As can be seen in the total number of available records, there is no anomaly in the data reported overall. This lower number of available sites in 2013 can be due either to a lower number of reported data, or a change in sampling point identifiers (which would impair the matching of several records with the reminder of the period, making them irrelevant for trend assessment). The vast majority of selected stations passing completeness criteria are located in the 27 countries of the European Union and the UK. But we also captured a few additional stations located mainly in Norway and Switzerland, as well as Iceland, North Macedonia, and Gibraltar.

Apart from this anomaly of 2013, there is no systematic trend in the distribution of station type after 2005. The number of PM monitoring sites increased gradually, so that ozone and NO₂ monitoring became relatively less important.

Figure 1: Number of air quality monitoring station by pollutant (top) and station type (bottom), in the 27 countries of the European Union and UK (EU28) available over the 2005-2019 time period (left) and passing the completeness criteria for trend assessment in absolute (middle) and relative (right) numbers

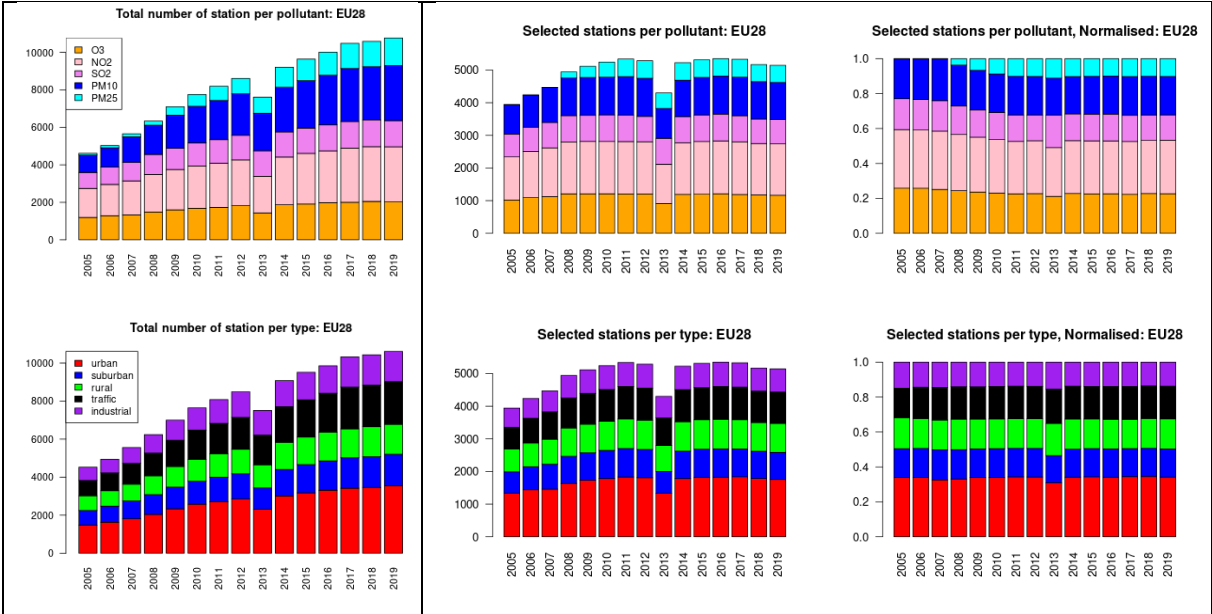


Table 1: Number of stations per country and typology passing completeness criteria and therefore included in the present trend assessment for each pollutants

Pollutant	SO2					NO2					O3					PM10					PM25				
	Annual Mean																								
Station Type	urban	suburban	rural	traffic	industrial	urban	suburban	rural	traffic	industrial	urban	suburban	rural	traffic	industrial	urban	suburban	rural	traffic	industrial	urban	suburban	rural	traffic	industrial
AT	9	17	21	0	18	18	42	26	33	6	11	33	41	4	1	20	40	18	13	7	6	4	2	2	0
BE	4	8	9	2	17	5	11	15	2	20	4	8	17	1	5	5	12	10	1	15	7	9	8	0	6
BG	6	1	1	2	3	6	0	1	2	1	6	1	1	2	2	11	6	1	3	3	4	1	1	0	0
CY	0	0	0	0	0	0	0	0	0	0	0	0	1	0	0	0	0	0	0	0	1	2	1	0	0
CZ	11	8	6	2	1	14	10	6	15	1	14	9	16	3	0	28	19	5	13	1	12	7	2	3	1
DE	35	14	31	12	12	88	57	52	95	19	80	58	58	6	12	80	48	45	83	18	47	15	16	33	7
DK	0	0	0	0	0	3	0	2	3	0	3	0	2	1	0	0	0	0	0	0	0	0	0	1	0
EE	1	0	2	1	2	1	0	2	1	2	1	0	3	1	2	1	0	1	1	2	3	0	3	0	1
ES	43	20	25	58	96	53	33	32	82	105	46	42	48	47	71	26	9	18	40	54	14	10	13	15	26
FI	0	0	4	0	4	3	1	4	10	2	2	0	8	0	0	2	2	0	14	0	5	2	1	5	0
FR	34	16	4	1	47	139	39	9	37	16	110	66	29	0	0	106	24	2	14	23	40	2	3	1	0
GR	0	0	0	1	0	0	1	0	1	1	0	1	0	1	1	0	1	0	0	0	0	0	0	0	0
HR	0	0	0	0	0	2	0	0	2	0	1	0	0	0	0	0	0	0	2	0	0	0	0	0	0
HU	5	7	1	6	1	6	7	1	7	1	6	7	2	1	1	6	6	2	6	1	0	0	0	1	0
IE	2	0	1	1	1	1	0	1	1	0	1	1	3	0	0	1	3	1	1	0	0	1	0	0	0
IT	23	8	5	21	19	80	33	30	90	22	61	27	29	4	3	52	21	12	50	14	37	7	15	14	5
LT	2	0	0	2	2	2	0	0	4	3	1	0	4	4	2	4	0	0	5	4	0	0	0	3	0
LU	2	0	1	0	0	1	0	2	0	0	2	0	3	0	0	0	1	0	0	0	2	0	0	0	0
LV	0	0	0	0	0	0	0	0	0	0	0	0	0	0	0	0	0	0	0	0	0	0	0	0	0
MT	0	0	0	0	0	0	0	1	0	0	1	0	1	0	0	0	0	0	0	0	0	0	0	0	0
NL	0	1	4	0	0	9	3	17	15	0	3	3	17	4	0	2	3	16	11	0	3	1	1	0	0
PL	42	3	9	1	3	38	3	10	5	3	23	2	15	0	0	49	3	4	3	2	41	1	4	5	1
PT	2	2	2	2	3	9	1	4	5	5	11	4	7	0	3	6	3	4	6	3	3	0	4	1	0
RO	2	0	0	3	0	2	0	0	0	1	0	0	0	0	1	0	1	0	0	1	3	0	0	0	0
SE	2	0	0	0	0	5	0	1	6	0	5	0	8	0	0	3	0	2	9	0	2	0	3	5	0
SI	3	1	0	1	0	3	1	1	1	0	5	1	3	1	0	4	2	2	1	0	1	1	1	1	0
SK	4	1	0	2	0	2	0	0	4	0	4	2	4	0	0	10	2	0	4	1	1	0	0	1	0
CH	2	2	2	1	0	0	0	0	0	0	0	0	0	0	0	0	0	0	0	0	0	0	0	0	0
GB	12	0	4	2	5	28	2	12	15	8	30	2	18	1	4	4	0	0	3	2	21	2	2	12	6
GI	0	0	0	1	0	0	1	0	1	0	0	1	0	0	0	0	0	0	1	0	0	0	0	1	0
IS	0	0	0	1	0	0	0	0	1	0	0	0	0	0	0	0	0	0	1	0	0	0	0	0	1
MK	0	0	0	2	1	0	0	0	0	0	0	0	0	2	2	0	0	0	0	0	0	0	0	0	0
NO	0	0	0	0	1	1	2	0	7	0	0	0	6	0	0	4	1	0	8	1	3	2	0	10	0

2.1.2 Air pollutant indicators, metrics and indices

We intended to be as comprehensive as possible in terms of statistical indicators, computing for each year: annual, seasonal, monthly, weekly (per day of the week), daily information and corresponding quantiles on the basis of daily means for all compounds. For NO₂ and O₃ we also computed indicators aggregated on the basis of hourly observations to derive daily maxima and include diurnal profiles.

We also included a few additional metrics because of their relevance with regards to the European Directive on Air quality (EC, 2008), or health and ecosystem impacts. For ozone, the hourly daily maximum was used to compute the number of days above 120 µg/m³ (long-term objective), 180 µg/m³ (information threshold) and 240 µg/m³ (alert threshold). The daily maximum 8-hr average was also used to derive 4DMA8: the annual fourth highest peak, which is considered to be the most representative of ozone peaks. The summertime mean of daily maximum ozone is sometimes used as an indicator of ozone peaks, but it should be noted that in many locations in Europe most summer days are not characterized by high ozone levels. In turn, the summertime average is also largely influenced by moderate ozone levels. That is why we use the 4th highest value observed in the summer to provide an indication of the highest peaks (Colette et al., 2016). We also computed health-related metrics: SOMO35 and SOMO10 (sum of ozone daily maxima in excess of 35 ppbv and 10 ppbv, (Malley et al., 2015)) and ecosystem-related metrics: AOT40c and AOT40f (accumulated ozone over 40 ppbv between May and July for crops and between April and September for forests). For NO₂ we considered but eventually excluded the number of hours above 200 µg/m³ because of the low number of occurrences at most stations. Similarly, the number of days above 125 µg/m³ and hours above 350 µg/m³ were excluded for SO₂. For PM₁₀ we computed the number of days above 50 µg/m³ daily limit value.

We also computed air quality indices by country for all air pollutants, using the definition of EEA recalled in Table 2 that consists in defining intervals for each air pollutants, the index being subsequently defined as the worst level across available air pollutant observations at a given station. Computing the index therefore requires availability of all pollutants at a given station, which is far from being the case so that modelling is used by EEA as gap filling. In order to avoid such gap filling, we rather compute the index level for all pollutants and take the median by pollutant for all stations in a given country. The country air quality index is then defined here as the worst category for all pollutants.

Table 2: Definition of the EEA Air Quality Index (Source: airindex.eea.europa.eu)

	Good	Fair	Moderate	Poor	Very poor	Extremely poor
Particles less than 2.5 µm (PM _{2.5})	0-10	10-20	20-25	25-50	50-75	75-800
Particles less than 10 µm (PM ₁₀)	0-20	20-40	40-50	50-100	100-150	150-1200
Nitrogen dioxide (NO ₂)	0-40	40-90	90-120	120-230	230-340	340-1000
Ozone (O ₃)	0-50	50-100	100-130	130-240	240-380	380-800
Sulphur dioxide (SO ₂)	0-100	100-200	200-350	350-500	500-750	750-1250

2.1.3 Statistical tests

The statistical method applied for the trend detection is Mann-Kendall (with a p-value of 0.05) and we compute the actual slope using the Sen-Theil approach. Both techniques differ from the more classical least square regression in the fact that they focus on the distribution of pairs of changes, aggregating their sign for Mann-Kendall, or using the median of differences for Sen-Theil. They are thus less sensitive to outliers, but also to autocorrelation and non-normality in the distribution.

The trends presented here are given in unit change per year ($\mu\text{g}/\text{m}^3/\text{yr}$ in most cases). But we also provide the relative change which is useful to infer order of magnitudes over various pollutants/indicators. The relative change is computed from the Sen-Theil slope, multiplied by the overall duration, and normalised by the estimated level at the beginning of the period. The estimated level at the beginning of the period is the linear fit over the whole time series taken for the year 2005, which minimises the effect of interannual variability compared to using directly the value for the year 2005. Those estimated 2005 levels are used for normalisation of both observed concentrations and emissions in the timeseries. A similar approach is used when comparing distribution or monthly/weekly/daily cycle for the beginning and end of the period, where we use the linear fit for 2005 and 2019 instead of the actual cycle for those years.

In several figures, the distribution of relative changes are presented as boxplot that provide the inner 25th- to 75th percentiles (filled boxes), median (horizontal line) as well as the 5th and 95th percentiles (whiskers) and individual values outside of that later interval (dots).

2.1.4 Air pollutant emissions

We used the National air pollutant emission (Primary PM₁₀ and PM_{2.5}, nitrogen oxides - NO_x, ammonia - NH₃, volatile organic compounds - VOC and sulfur oxides - SO_x), reported to the Convention on Long Range Transboundary Air Pollutant and European National Emission Ceiling Directive. Those were obtained for the EU28 (as EU27 and the UK) from the EMEP Centre for Emission Inventories and Projections¹ (Emission as used in EMEP models), in the version of July 2021.

2.2 AirGAM

The AirGAM model has been presented and documented in previous reports and thus only the main features is given in this report. The AirGAM model is an air quality trend and prediction model developed in EEA projects over the years 2017-2021 (ETC/ATNI, 2019; ETC/ACM, 2018; ETC/ACM, 2017). It is based on GAM (Generalized Additive Modelling) regression for estimating trends in daily observed pollutant concentrations at air quality monitoring stations, adjusting for eventual trends in corresponding meteorological data. The model has been developed primarily for the compounds NO₂, O₃, PM₁₀ and PM_{2.5} but can also be used for other compounds, such as VOCs.

Input meteorological data consist of temperature, wind speed and direction, planetary boundary layer height, relative and absolute humidity, cloud cover and precipitation over the period considered. In addition to the meteorological variables the model also incorporates time variables such as day of the week, day of the year, and overall time, representing the model's trend term. The trend analysis is performed at each station separately. Thus, the model only considers the temporal features of concentrations and meteorology at a station without any spatial correlations or dependencies between stations.

The AirGAM model proved useful for analysing the effect of the lockdown during the pandemic in 2020 on European NO₂ levels (Solberg et al., 2021), and a detailed model documentation is in preparation (Walker et al., 2021, *to be submitted*).

There are a number of settings defining choices in the AirGAM model. In the present study, non-linear smooth trends were assumed for all species. Furthermore, the control parameter *use_season* was set to 1, meaning that the relationships between explanatory variables (temperature, humidity, mixing height, etc) and air concentrations are sought for each half year independently (Walker et al., 2021). Tests revealed, however, that the differences compared to running for the whole year without any seasonal split, was very small for NO₂ and PM. This setting is mainly designed for O₃, but for the present study, O₃ was only run for the summer half year (April-September) and thus the *use_season* setting didn't have any effect for that compound.

A screening of the AirGAM results was also applied. Previous applications (ETC/ATNI, 2019; ETC/ACM, 2018; ETC/ACM, 2017) have revealed that the AirGAM model fails for a certain number of stations, and further inspections have indicated that dubious monitoring data showing unphysical artefacts could explain a number of these cases. This includes sudden shifts in the concentration levels, substantial differences in the mean value from one year to the next, fixed concentration levels during extended time periods etc. In addition, it is reasonable that the AirGAM model fails also for stations where the pollutant levels are determined by processes which are not related to local meteorological conditions. This would typically regard remote stations for which the long-range air mass transport is dominant.

¹ <https://www.ceip.at/webdab-emission-database/emissions-as-used-in-emep-models>, accessed 11/8/2021

As in previous applications, the AirGAM results was screened according to Pearson's linear correlation coefficient, r , in the following way:

- For NO_2 and O_3 : $r > 0.65$
- For PM_{10} and $\text{PM}_{2.5}$: $r > 0.55$

The reason for differing between the species was that the model performance is generally better for NO_2 and O_3 than for PM.

The stations were grouped into three categories depending on the metadata station area and station type given in the EEA database in this way:

- Traffic: All sites with 'type' = traffic
- Suburban: Sites with 'area' starting with urban or suburban and not 'type' = traffic
- Rural: Sites with 'area' starting with rural and not 'type' = traffic

Industry sites were not used in the AirGAM analyses since they were considered being too little homogeneous with respect to nearby emissions and local surroundings. In the country subchapters, the meteorologically adjusted trends are compared with the national total emissions for the Suburban and Rural category (see above), while compared to the national emissions for road traffic for the Traffic category. The time series in the country subchapters show the median (blue full line) as well as the 25 percentile and 75 percentile for all stations given as blue shaded area.

2.2.1 Input data to AirGAM

All available monitoring data for NO_2 , O_3 , PM_{10} and $\text{PM}_{2.5}$ for the period 2005-2019 were downloaded from EEA by mid-June from the available web services at that time. Since then, a new Air Quality Portal has been released and the Airbase (2005-2012) and AQER (2013-2019) monitoring data are now accessible from the web page:

<https://aqportal.discomap.eea.europa.eu/index.php/users-corner/>

All NO_2 and O_3 data are given as hourly averages whereas PM_{10} and $\text{PM}_{2.5}$ could be given as hourly or daily values depending on the instrumentation and measurement method.

For use in the AirGAM model, the raw data were aggregated into daily values, i.e. daily means for NO_2 and PM and MDA8 (max daily 8-h running mean) for O_3 as defined in the EU directive. When calculating these daily quantities a data capture criterion of 75 % was applied or else a missing value was assigned to that day.

Furthermore, a data capture criterion of 75 % was also applied to the number of years with data and the amount of data within each year, i.e.: 75 % of the years 2005-2019 should have at least 75 % valid daily data for the station to be used in the AirGAM model. For this study, covering 15 years, the criterion was relaxed to 11 years with valid data (75 % of 15 = 11.25).

As for the analyses of the measurement data (Chapter 2.1), national reported emission data were extracted from Centre on Emission Inventories and Projections (CEIP).

For the input meteorological data to the AirGAM model, we used ERA5 data for the meteorological input to the model provided by the European Center for Medium-Range Weather Forecast (ECMWF). These data has a spatial resolution of 30 km:

<https://www.ecmwf.int/en/forecasts/datasets/reanalysis-datasets/era5>).

3 Results. Trends of air pollutants and air quality

This chapter presents the results of the trend calculations by the two applied methods; Chapter 3.1 for the non-parametric, linear Mann-Kendall/Theil Sen's slope method and Chapter 3.2 for the AirGAM model.

3.1 Results from analyses of measurement data

3.1.1 Sulfur dioxide

The time series presented in Figure 2 display, for each typology of stations, the median of annual mean values at all available European stations as well as the distribution for all sites of the relative changes between the beginning and the end of the period (as boxplots). The corresponding quantitative SO₂ trends are provided in Table 3.

The trends of sulfur dioxide present the largest decrease of all pollutants, and they are always significant as indicated by the very small p-values. The decrease is such that at industrial sites, the levels in 2019 are comparable to that of rural sites at the beginning of the period. The relative changes in the Europe-wide composite computed as the median of all annual mean values between 2005 and 2019 depends on station types: -58% (traffic), -67% (industrial), and -61% (urban background).

In order to provide an indication whether the trend is steady, slowing down, or increasing in time, we also computed the same trends over the first and second halves of the period. Comparing the linear fits over the first and second halves of the period (2005-2012 and 2012-2019), one can notice a slight flattening of absolute decrease in more recent years. Focusing on EMEP rural sites, it should be noted that most of the decrease for SO₂ had been actually observed in the 1990s, with up to 90% decreases (Colette et al., 2016; Tørseth et al., 2012; Aas et al., 2019). The slower decrease in recent years is more visible closer to the sources at urban and industrial sites with decrease about 50% and 10% over the first and second decade, respectively.

Figure 2: Time series of the European-wide composite (median) of annual mean SO₂ (µg/m³) per station type and area (red: urban background, blue suburban background, green: rural background, black: traffic, violet: industrial) between 2005 and 2019. The dashed lines show the linear fit between 2005 & 2012 and between 2012 & 2019. The boxplots on the right-hand side show the distribution of relative changes (%) between 2005 and 2019 for all stations of each typology

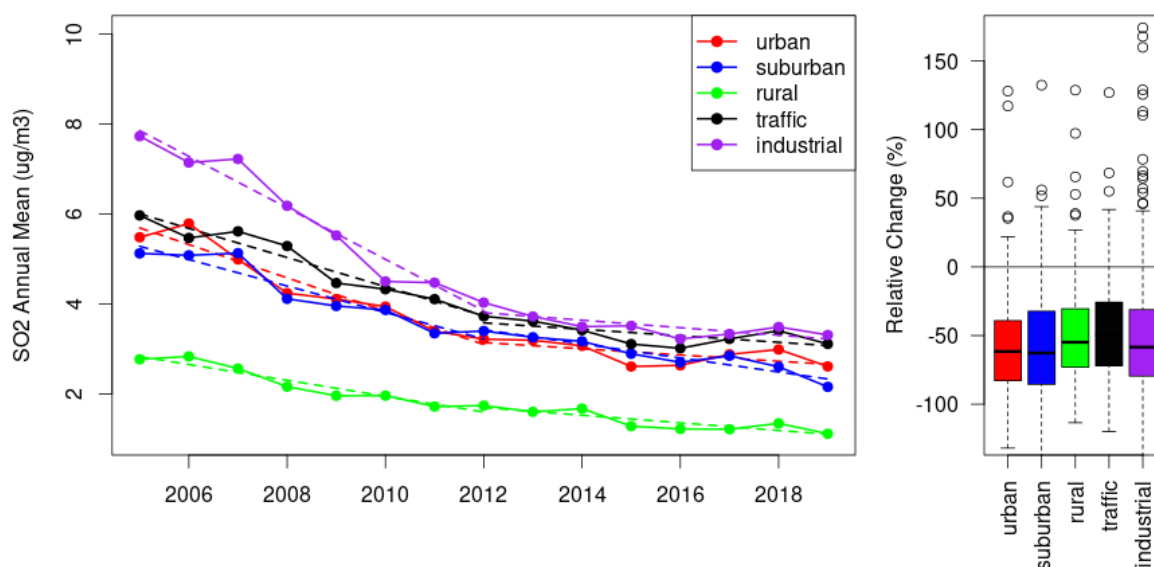


Table 3: Summary of observed SO₂ annual mean trends for various station typology: total number of station, 5th and 95th quantiles of Sen Theil slopes at all European stations, trend of the median of the European-wide composite (Sen-Theil slope, µg/m³/yr), significance of the European-wide composite (Mann-Kendall p-value, MK p-val) and percentage change between : 2005 and 2019, 2005 and 2012, 2012 and 2019 for the European-wide composite (% change)

Metric	Station Type	Number of Stations	5th and 95th quantile of trends	Trend of Median	MK p-val of Median	Relative Change (2019 vs 2005, %)	Relative Change (2012 vs 2005, %)	Relative Change (2019 vs 2012, %)
Annual Mean	urban	246	[-0.82;0.02]	-0.21	0.00	-60.6	-46.0	-9.0
Annual Mean	suburban	109	[-0.79;0.04]	-0.19	0.00	-55.6	-39.0	-21.0
Annual Mean	rural	132	[-0.37;0.06]	-0.12	0.00	-66.4	-44.0	-24.0
Annual Mean	traffic	125	[-0.80;0.07]	-0.22	0.00	-58.4	-38.0	-9.0
Annual Mean	industrial	236	[-1.14;0.14]	-0.32	0.00	-67.4	-51.0	-9.0

The trends of the European-wide composites (median over all stations of the annual means) displayed in Figure 2 are all significant as indicated with the Mann-Kendall statistics of Table 3 that are well below 0.05. There are however a few sites where the relative trend is smaller (or even positive) in the boxplots of Figure 2. The map of trends at all urban, suburban and rural sites are plotted in Figure 3. Those smaller decrease, or even increases are really scattered, and would need to be investigated at site level. Such a level of investigation is beyond the scope of our European-wide assessment and would not change our overall conclusions. Besides these localized increases, it is difficult to point out significant spatial patterns in the maps of Figure 3.

Figure 4 presents a comparison between reported SO_x emission between 2005 and 2019 and observed annual mean SO₂ concentrations, both normalized at their 2005 levels (the intercept of the linear fit is used to estimate 2005 levels and minimize the effect of interannual variability). For each country with at least 5 stations of typology “traffic”, “industrial”, or any “background” type, the median observation of the corresponding type is computed, and subsequently the European median over the selected countries is shown. The total number of stations and corresponding relative changes in emissions and concentrations are also provided in Table 4, some relative decrease exceed 100% (i.e. reaching negative concentrations in 2019) because a linear approximation is used to fit the trends.

The relation between emission and concentration is not straightforward, and Chemistry-Transport Models (CTM) should be involved for a more detailed analysis, but it remains insightful to compare their qualitative evolution. The consistency between the rate of change in emissions of SO_x and observed concentrations SO₂ is quite good over the whole period (75% reduction reported in emission against 60% in concentration observed at background sites overall in Europe). Note that because we compare to country total reported emissions, in Table 3 we take the median observed trend over all stations of background typology in any given country where more than 5 stations are available for the whole period. As can be seen in Figure 4, the agreement is very good until 2007, but after that year a substantial gap is seen until the end of the period. This mismatch was even more clear in the corresponding figure covering the 2000-2017 period in (Colette and Rouil, 2020).

Figure 3: Map of SO₂ trends (in µg/m³/yr) at all urban, suburban and rural background sites in Europe between 2005 and 2019. Significant trends are displayed as dots, and un-significant trends as diamonds

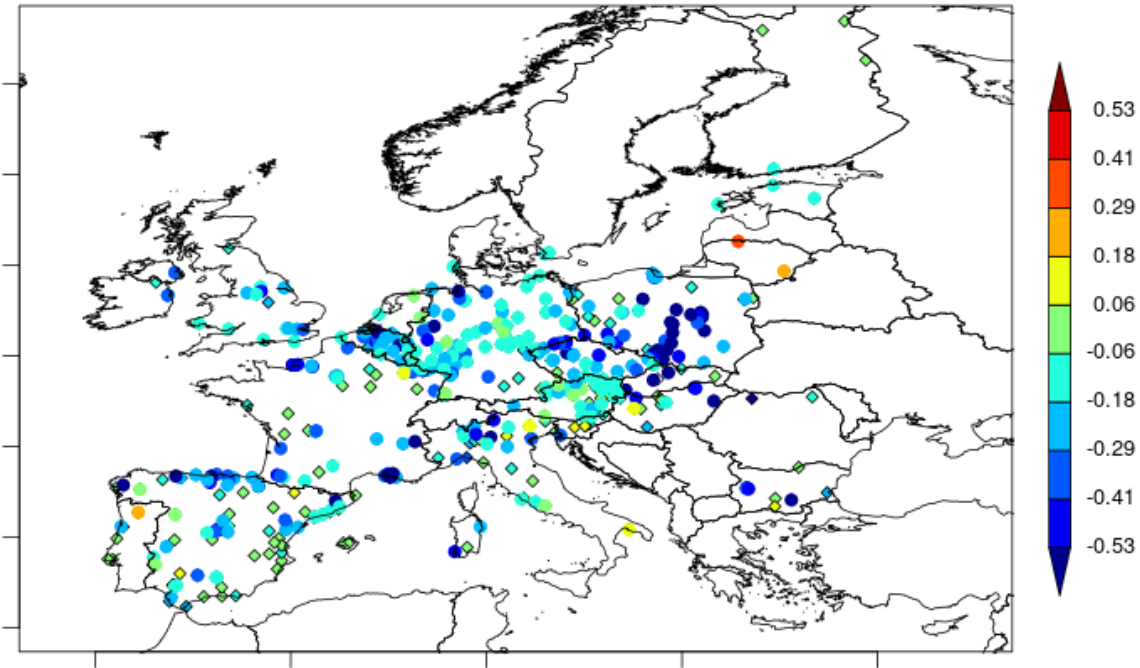


Figure 4: Time series of country median SO₂ observed at traffic (black), industrial (violet) and background (cyan) sites (solid lines), and corresponding national SO_x emissions (dashed line) normalised to estimated 2005 levels (%). The median is taken over countries where more than 5 stations of each typology is available. The total number of stations is provided in brackets. Straight lines are the linear fits of emissions and concentration at background stations over the whole period

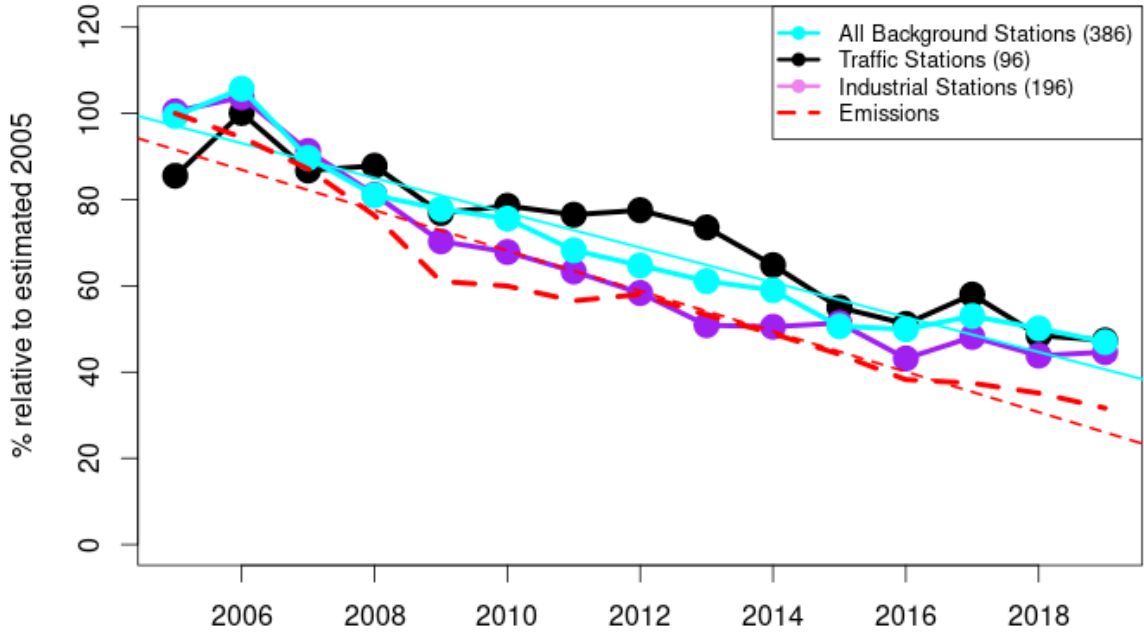


Table 4: Change, relative to 2005 (in %), for emissions and concentrations, as median over countries with at least 5 stations of any typology (Nsta, otherwise indicated as "NA")

	SOx/SO ₂			NOx/NO ₂			PPM10/PM10			PPM25/PM25		
	Nsta	Emis	Conc	Nsta	Emis	Conc	Nsta	Emis	Conc	Nsta	Emis	Conc
AT	47	-74,1	-44,1	86	-45,4	-30,5	78	-34,3	-41,3	12	-46,3	-36,9
BE	21	-97,7	-94,7	31	-60,3	-38,0	27	-55,0	-37,4	24	-57,9	-46,5
BG	8	-101,4	-32,7	7	-50,6	-21,5	18	-8,0	-41,6	-	-	-
CY	-	-	-	-	-	-	-	-	-	-	-	-
CZ	25	-63,7	-51,5	30	-47,9	-32,3	52	-24,5	-34,1	21	-21,5	-24,9
DE	80	-56,3	-65,5	197	-38,0	-27,0	173	-31,5	-34,3	78	-47,5	-35,5
DK	-	-	-	-	-	-	-	-	-	-	-	-
EE	-	-	-	-	-	-	-	-	-	-	-	-
ES	88	-103,7	-37,2	118	-57,8	-29,7	53	-31,4	-41,8	37	-24,9	-20,9
FI	-	-	-	8	-57,0	-35,2	-	-	-	-	-	-
FR	54	-95,4	-87,5	187	-59,3	-34,8	132	-58,7	-41,1	45	-70,1	-52,0
GB	16	-102,7	-63,5	42	-66,5	-31,4	-	-	-	25	-26,1	-31,9
GR	-	-	-	-	-	-	-	-	-	-	-	-
HR	-	-	-	-	-	-	-	-	-	-	-	-
HU	13	-25,5	-36,5	14	-46,3	-19,1	14	-8,3	-25,1	-	-	-
IE	-	-	-	-	-	-	-	-	-	-	-	-
IT	36	-104,0	-41,1	143	-67,9	-38,5	85	-28,1	-35,9	59	-23,2	-28,1
LT	-	-	-	-	-	-	-	-	-	-	-	-
LU	-	-	-	-	-	-	-	-	-	-	-	-
LV	-	-	-	-	-	-	-	-	-	-	-	-
MT	-	-	-	-	-	-	-	-	-	-	-	-
NL	-	-	-	29	-53,4	-30,4	21	-46,7	-42,1	-	-	-
PL	54	-71,6	-57,1	51	-22,5	-11,6	56	-25,0	-15,5	46	-25,5	-33,7
PT	-	-	-	14	-59,4	-38,7	13	-49,3	-36,7	-	-	-

	SOx/SO ₂			NOx/NO ₂			PPM10/PM10			PPM25/PM25		
	Nsta	Emis	Conc	Nsta	Emis	Conc	Nsta	Emis	Conc	Nsta	Emis	Conc
RO	-	-	-	-	-	-	-	-	-	-	-	-
SE	-	-	-	6	-40,2	-34,3	5	-33,2	-38,1	-	-	-
SI	-	-	-	-	-	-	-	-	-	-	-	-
SK	-	-	-	-	-	-	12	-53,7	-36,2	-	-	-
EU28	442	-75,0	-60,0	963	-45,1	-30,5	743	-28,5	-37,7	347	-30,1	-33,4

The sharp decrease in emissions after 2007 is mainly due to reductions in emissions from the industrial sector and the energy production and distribution sector in the lee of the economic downturn of 2008 (EEA, 2018). No such decrease is observed at traffic sites. At stations of background type (urban, suburban and rural), a decrease is noted in 2008 but quickly followed by a recovery with concentrations increasing again in 2009. The decrease in 2008 was observed at industrial sites but it was then followed by less strong reduction than reported in emissions inventories.

There are also some noteworthy differences depending on the countries (Table 3). Whereas the observed rate of decline in SO₂ observations is slower than the decline of emissions in Austria, Bulgaria, France, Spain, United Kingdom, Italy, Poland, the opposite is found for Germany and Hungary

It is not possible to investigate further this issue with the material available here because we ignore the effect of the transport and transformation of SO₂ in the atmosphere and comparing nation-wide emission and point observations raise spatial representativeness issues. Nevertheless, this discrepancy should trigger follow-up works to understand why the 2008 economic downturn seemed to have had a smaller impact on observed SO₂ concentration trends compared to reported emissions.

3.1.2 Nitrogen dioxide

The median trend of annual mean of nitrogen dioxide over Europe is displayed in Figure 5 as the time series of the median across all European sites. It shows a clear downward trend for all station types. The interannual variability is low. The relative changes are within -20% to -50% for the central interquartile part of the distribution across all stations. They are similar for all station types, except for rural and industrial stations where the median relative change is larger. For all site typologies except traffic stations, the linear fits over the beginning (2005-2012) and end (2012-2019) of the period indicated as dashed straight lines suggests that there is no strong change in the rate of decline. But a closer look at Table 5 shows that for industrial sites, the relative changes were about twice as large over the 2005-2012 period compared to 2012-2019.

Figure 5: Time series of the European-wide composite (median) of annual mean NO₂ (µg/m³) per station type and area (red: urban background, blue suburban background, green: rural background, black: traffic, violet: industrial) between 2005 and 2019. The dashed lines show the linear fit between 2005 & 2012 and between 2012 & 2019. The boxplots on the right-hand side show the distribution of relative changes (%) between 2005 and 2019 for all stations of each typology

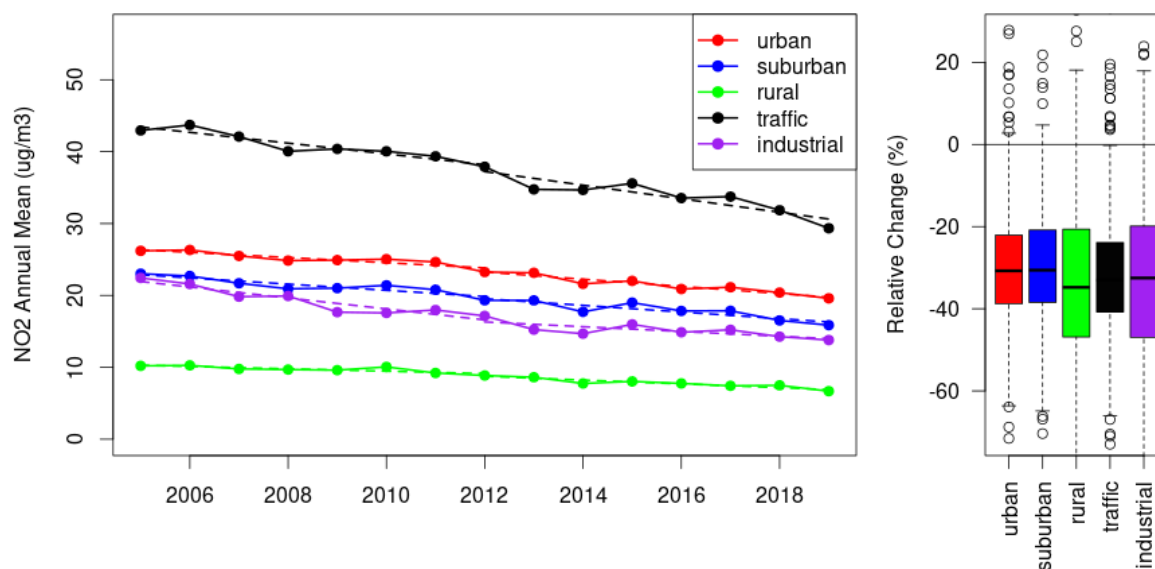


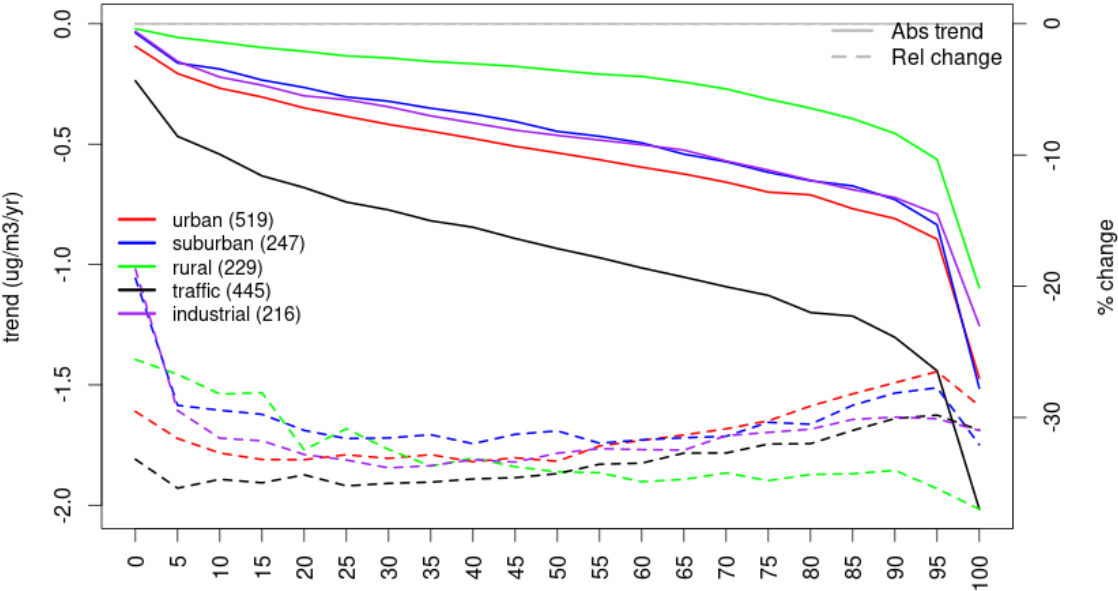
Table 5: Summary of observed NO₂ annual mean trends for various station typology: total number of station, 5th and 95th quantiles of Sen Theil slopes at all European stations, trend of the median of the European-wide composite (Sen-Theil slope, µg/m³/yr), significance of the European-wide composite (Mann-Kendall p-value, MK p-val) and percentage change between : 2005 and 2019, 2005 and 2012, 2012 and 2019 for the European-wide composite (% change)

Metric	Station Type	Number of Stations	5th and 95th quantile of trends	Trend of Median	MK p-val of Median	Relative Change (2019 vs 2005, %)	Relative Change (2012 vs 2005, %)	Relative Change (2019 vs 2012, %)
Annual Mean	urban	519	[-1.25;-0.08]	-0.48	0.00	-26.8	-10.0	-9.0
Annual Mean	suburban	247	[-1.00;-0.02]	-0.49	0.00	-31.7	-13.0	-10.0
Annual Mean	rural	229	[-0.71;0.04]	-0.25	0.00	-35.3	-11.0	-13.0
Annual Mean	traffic	445	[-2.11;-0.05]	-0.92	0.00	-31.5	-12.0	-11.0
Annual Mean	industrial	216	[-1.16;0.09]	-0.57	0.00	-40.2	-24.0	-9.0

In order to discuss the relative evolution of low and high NO₂ values, the absolute and relative trends of percentiles 0 to 100 are given in Figure 6. At each monitoring sites, the percentiles distribution of daily mean NO₂ is computed every year to derive the absolute trend and relative change of each corresponding percentiles. The Figure provides the median trend and change for each percentile by typology of station. It appears that the absolute largest declines are found for highest percentiles. On the contrary, the relative changes are larger for the lower/medium percentiles (up to 40%), whereas

the peaks have only declined by 30% at urban and suburban sites. The fact that high values are less efficiently reduced than medium levels (in relative terms) was more prominent in earlier assessment focused on the 2000-2017 period.

Figure 6: For NO₂ and each typology of station, absolute trend (solid lines) and relative change (dashed lines) of the percentiles of daily means



This larger decline of high NO₂ levels in absolute terms is also seen in diurnal cycles Figure 7. The diurnal cycle displays a usual two-peak (morning/evening) profile. What is noticeable is the relative change per hour of the day, where it appears clearly that those peaks were not reduced as efficiently as lower values (see dashed lines in the lower panel of Figure 7). Likewise, Figure 8 shows the trends by day of the week. This weekly cycle illustrates that NO₂ levels observed in 2019 in working days are similar to those of weekends in 2005, even at traffic sites. But here, in relative terms, it is the weekday trends that are larger than during weekends.

There is some geographical variability in NO₂ annual mean trends (Figure 9). In particular, a lower relative decline is found over Germany, Austria and Poland compared to other countries. The comparison between the trends in emissions and observation is presented in Figure 10 and the corresponding numbers are in Table 4. As mentioned in Section 0, this comparison must be handled with care, and Chemistry-Transport Model results should be included to be more conclusive.

Again, the agreement between emission and concentration trends was quite good up to 2008, but after 2009 the mismatch becomes clear for all station types. A strong consistency between NO₂ concentration trends monitored at background, traffic and industrial sites can be noted. The mismatch between NO_x emissions and NO₂ concentrations is quite systematic over European countries with enough measurement sites, so that the comparison over EU27+UK points out a disagreement: 45% reduction in emissions, whereas NO₂ concentrations only decreased by 30% (see Table 3). This finding raises some concerns regarding the level of ambition that policy measures should achieve to deal with high NO₂ levels still observed in major cities.

Figure 7: Top: diurnal cycle of NO₂ at various station type estimated from the whole time series in 2005 (solid lines) and 2019 (dashed lines). Bottom: corresponding absolute (solid lines) and relative (dashed lines) trends

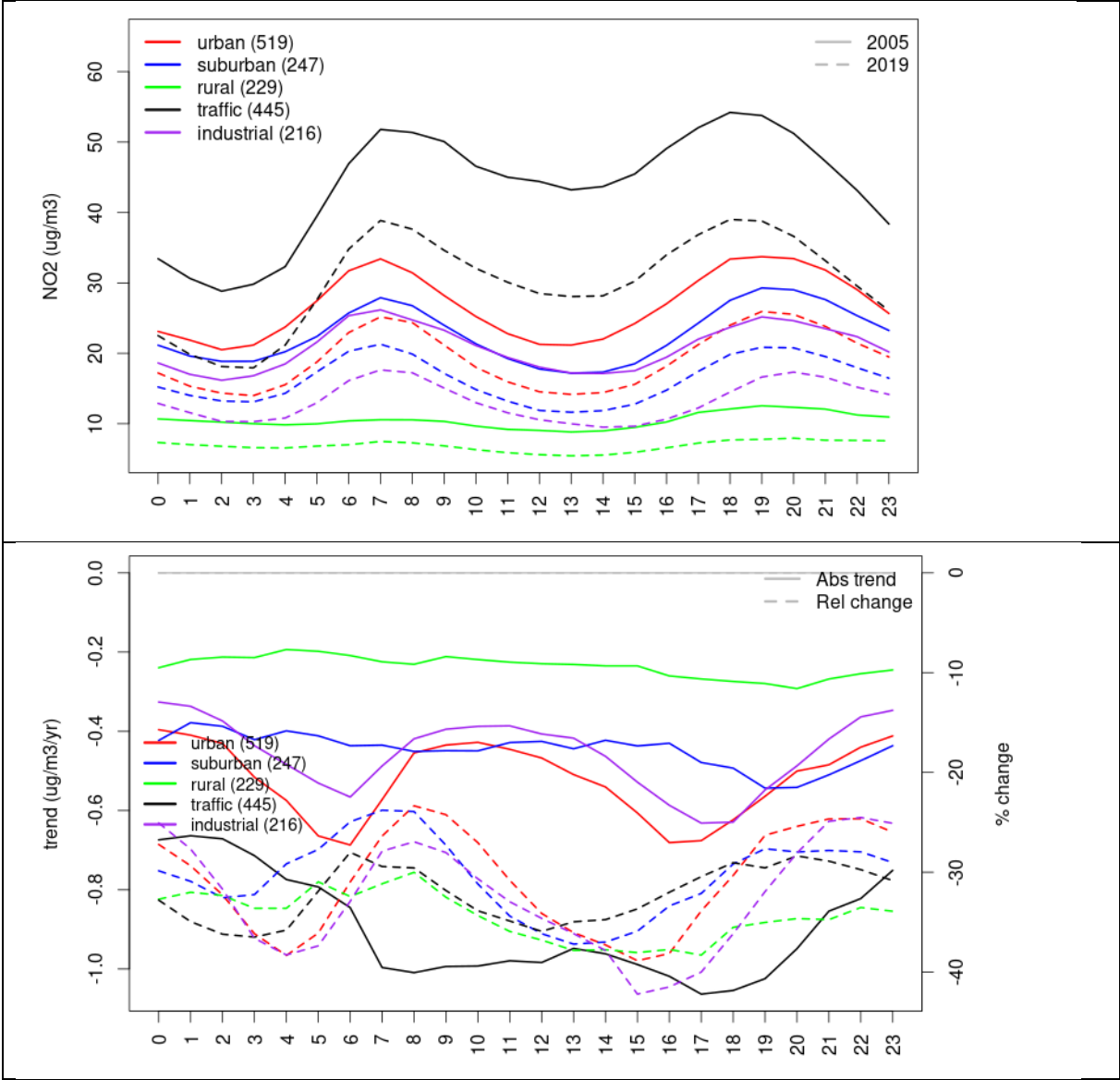


Figure 8: Top: weekly cycle of NO₂ at various station type estimated from the whole time series in 2005 (solid lines) and 2019 (dashed lines). Bottom: corresponding absolute (solid lines) and relative (dashed lines) trends

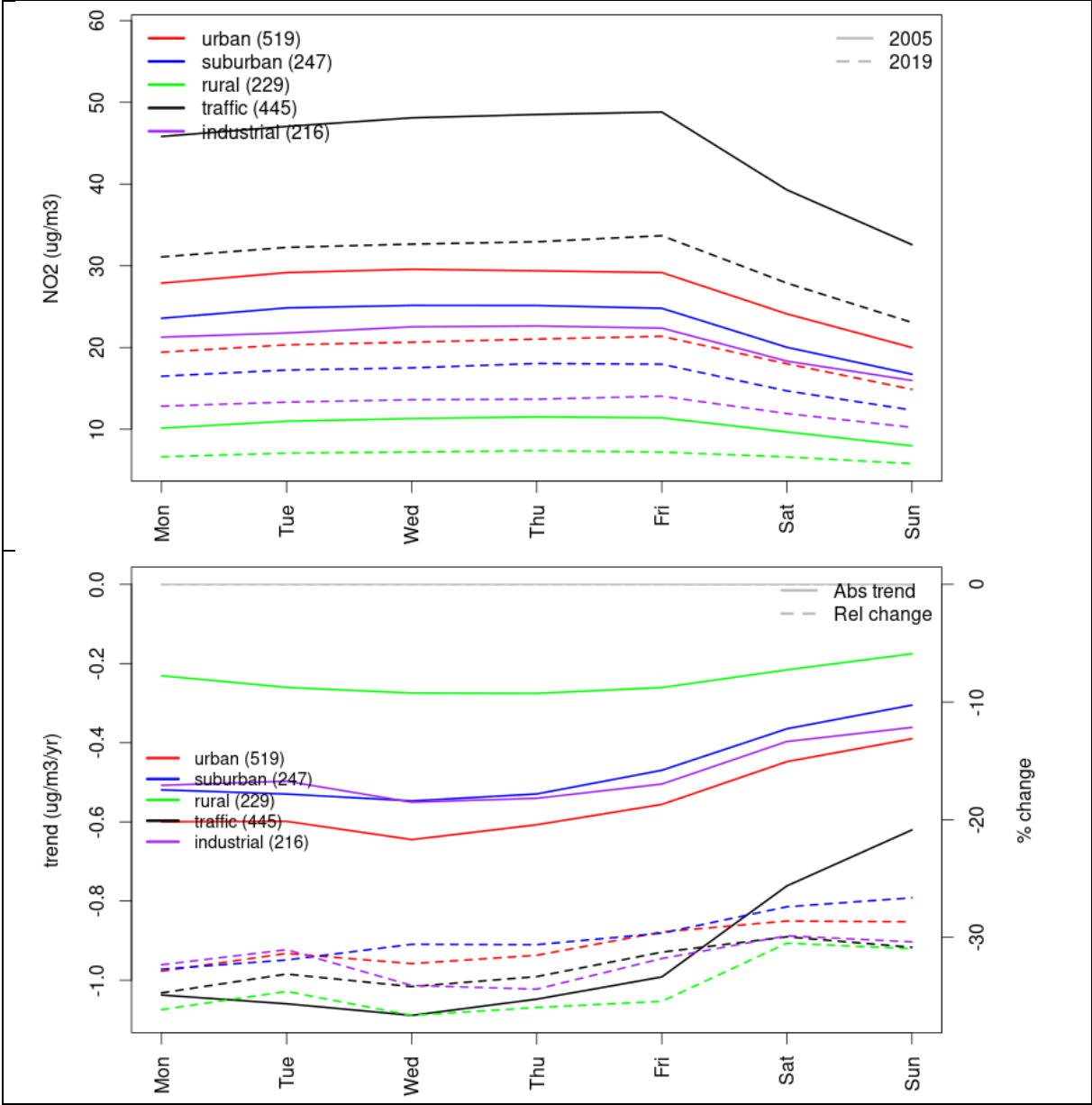


Figure 9: Map of NO₂ trends (in µg/m³/yr) at all urban, suburban and rural background sites in Europe between 2005 and 2019

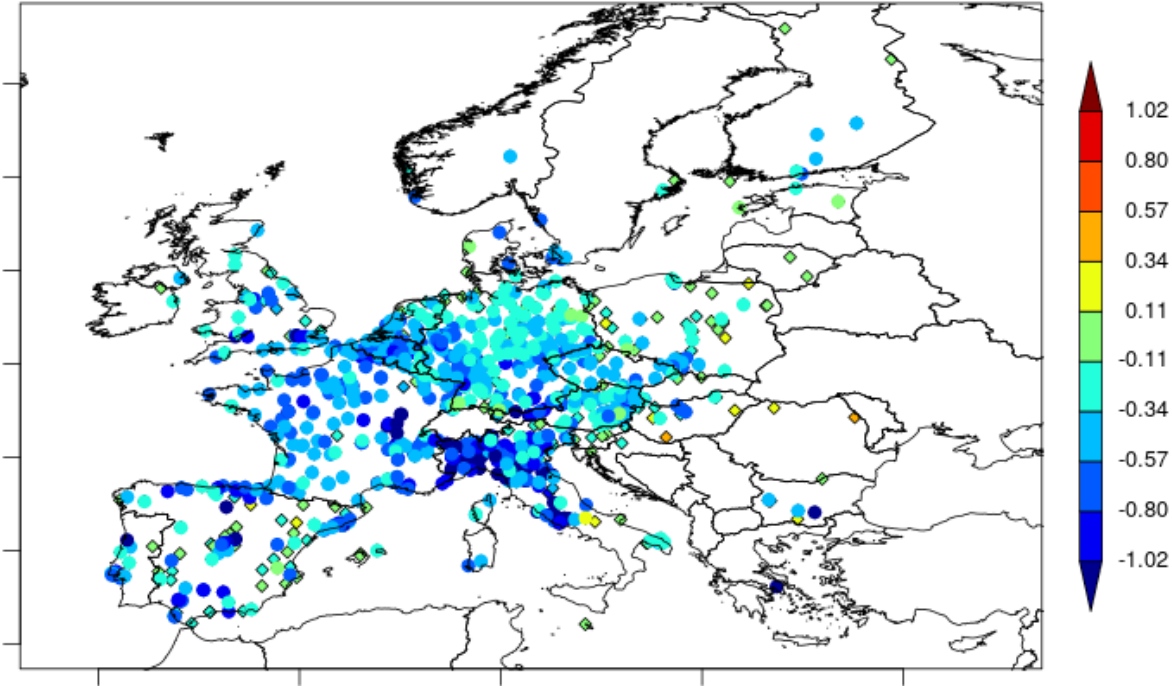
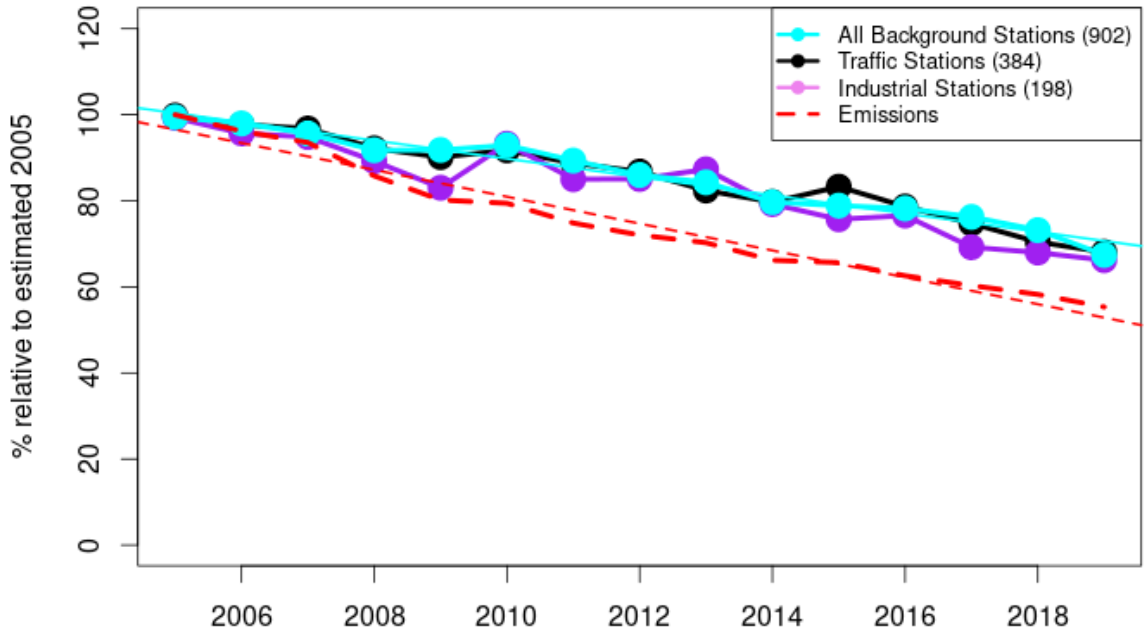


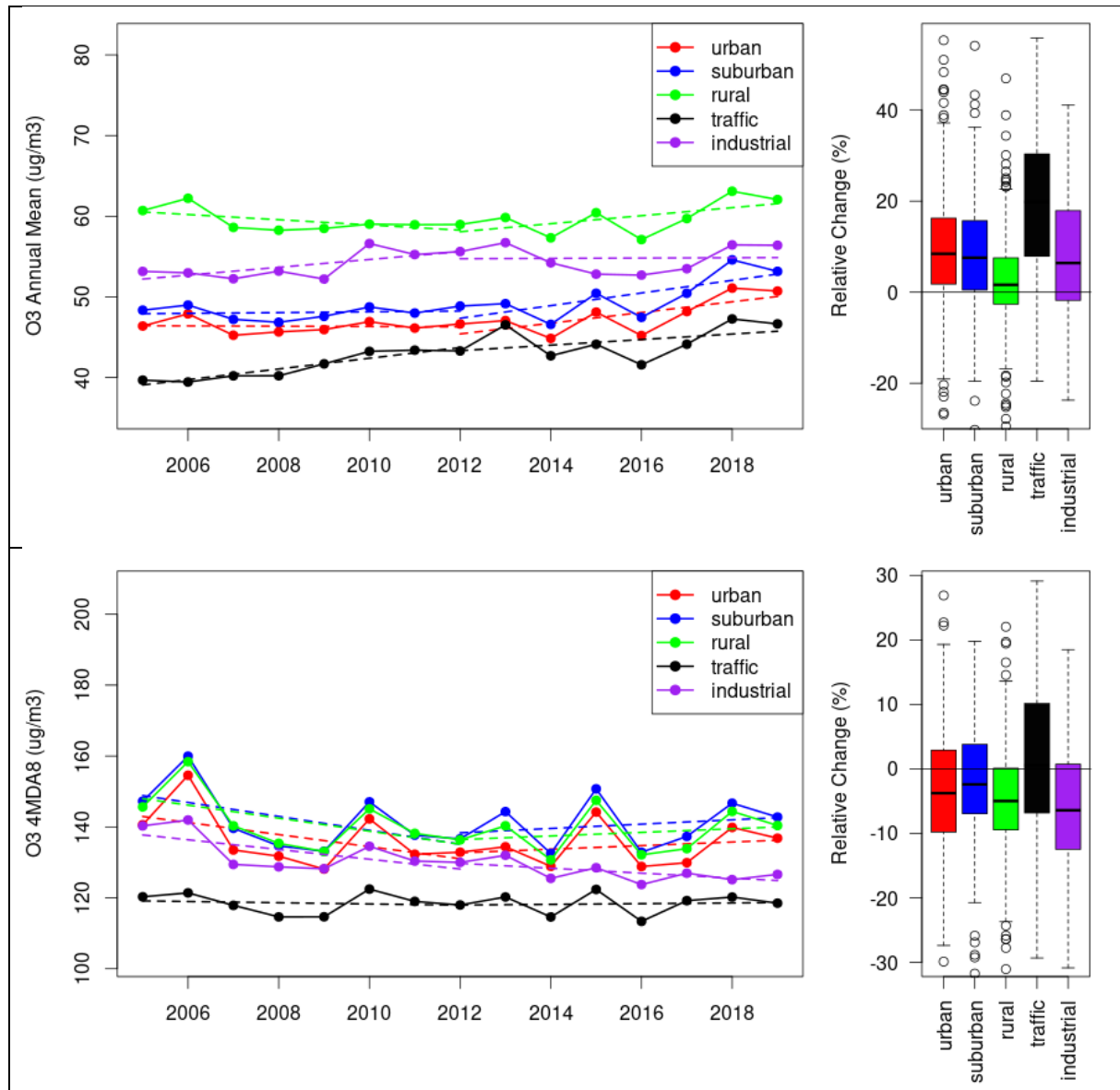
Figure 10: Time series of country median NO₂ observed at traffic (black), industrial (violet) and background (cyan) sites (solid lines), and corresponding national NO_x emissions (dashed line) normalised to estimated 2005 levels (%). The median is taken over countries where more than 5 stations of each typology is available. The total number of stations is provided in brackets. Straight lines are the linear fits over the whole period



3.1.3 Ozone

For ozone, opposite trends have been identified in the past depending on the metrics with decreases of high ozone peaks, whereas annual mean ozone increased or displayed no significant trends (Fleming et al., 2018; Simpson et al., 2014). This finding is confirmed here: annual mean ozone increases while peaks decrease (Figure 11). The increase of annual mean can be substantial, especially at traffic sites where it reaches almost 20% over Europe (Table 6).

Figure 11: For ozone annual mean (top), fourth highest daily peak (4MDA8, second row), number of days of exceedance of hourly maxima over the target value $120\mu\text{g}/\text{m}^3$ (third row), and OX (as O_3+NO_2) annual mean (bottom): Time series of the European-wide composite (median) per station type and area (red: urban background, blue suburban background, green: rural background, black: traffic, violet: industrial) between 2005 and 2019. The dashed lines show the linear fit between 2005 & 2012 and between 2012 & 2019. The boxplots on the right-hand side show the distribution of relative changes (%) between 2005 and 2019 for all stations of each typology



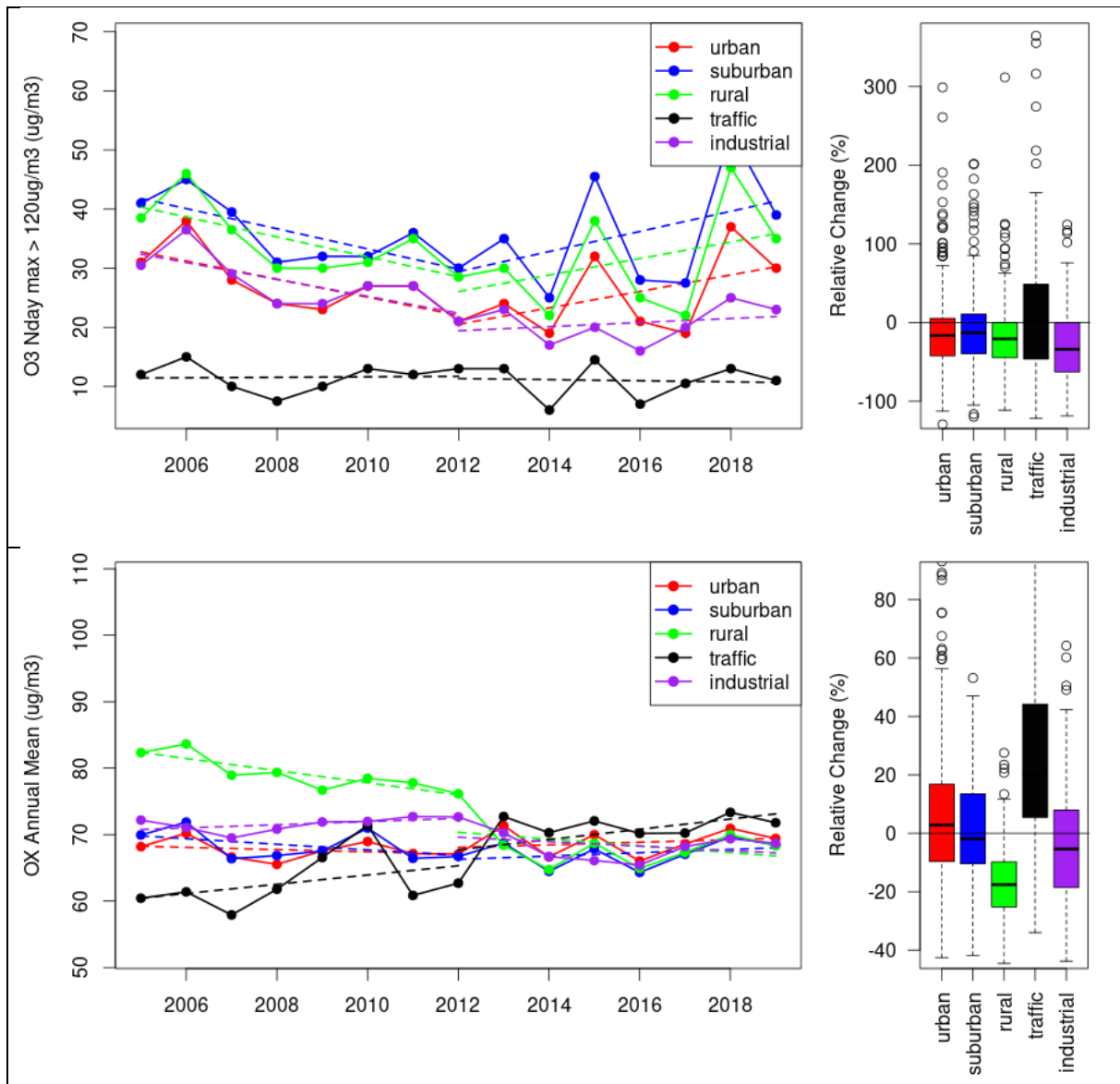


Table 6: Summary of observed ozone indicator trends for various station typology: total number of station, 5th and 95th quantiles of Sen Theil slopes at all European stations, trend of the median of the European-wide composite (Sen-Theil slope, $\mu\text{g}/\text{m}^3/\text{yr}$), significance of the European-wide composite (Mann-Kendall p-value, MK p-val) and percentage change between : 2005 and 2019, 2005 and 2012, 2012 and 2019 for the European-wide composite (% change)

Metric	Station Type	Number of Stations	5th and 95th quantile of trends	Trend of Median	MK p-val of Median	Relative Change (2019 vs 2005, %)	Relative Change (2012 vs 2005, %)	Relative Change (2019 vs 2012, %)
Annual Mean	urban	431	[-0.45;0.78]	0.28	0.06	9.2	0.0	6.0
Annual Mean	suburban	268	[-0.42;0.83]	0.32	0.04	10.4	1.0	6.0
Annual Mean	rural	344	[-0.55;0.68]	0.11	0.55	2.8	-4.0	3.0
Annual Mean	traffic	83	[-0.32;1.43]	0.50	0.00	18.7	12.0	3.0
Annual Mean	industrial	110	[-0.54;1.00]	0.13	0.23	3.5	6.0	0.0
4MDA8	urban	431	[-1.75;1.06]	-0.30	0.62	-3.2	-8.0	2.0
4MDA8	suburban	268	[-1.85;1.12]	-0.23	0.49	-2.4	-9.0	2.0
4MDA8	rural	344	[-1.74;0.84]	-0.50	0.43	-5.2	-9.0	1.0
4MDA8	traffic	83	[-1.99;1.65]	-0.01	0.69	-0.1	-1.0	0.0
4MDA8	industrial	110	[-2.45;1.29]	-0.69	0.00	-7.6	-7.0	-2.0
Nday max > 120 $\mu\text{g}/\text{m}^3$	urban	431	[-1.80;0.89]	-0.25	0.58	-25.1	-42.0	25.0
Nday max > 120 $\mu\text{g}/\text{m}^3$	suburban	268	[-2.23;1.09]	-0.14	0.73	-10.2	-40.0	27.0
Nday max > 120 $\mu\text{g}/\text{m}^3$	rural	344	[-2.49;0.91]	-0.56	0.32	-36.1	-44.0	23.0
Nday max > 120 $\mu\text{g}/\text{m}^3$	traffic	83	[-1.39;0.83]	0.00	0.54	0.0	-24.0	0.0
Nday max > 120 $\mu\text{g}/\text{m}^3$	industrial	110	[-2.50;0.94]	-0.50	0.01	-52.3	-38.0	-22.0
SOMO35	urban	430	[-173.90;126.90]	-5.16	0.84	-2.0	-12.0	15.0
SOMO35	suburban	267	[-184.89;162.00]	11.60	0.77	3.7	-12.0	12.0
SOMO35	rural	344	[-229.88;123.81]	-12.20	0.92	-3.5	-13.0	9.0
SOMO35	traffic	81	[-180.50;199.47]	59.10	0.01	39.5	13.0	11.0
SOMO35	industrial	109	[-240.15;193.16]	-2.43	0.84	-0.8	-1.0	5.0
SOMO10	urban	431	[-201.11;274.29]	65.29	0.32	5.7	-1.0	6.0
SOMO10	suburban	268	[-230.12;313.24]	87.21	0.32	7.1	-2.0	6.0
SOMO10	rural	344	[-258.27;249.75]	15.40	0.77	1.1	-4.0	4.0
SOMO10	traffic	83	[-202.82;531.15]	199.66	0.00	21.0	18.0	3.0
SOMO10	industrial	110	[-288.39;382.86]	79.25	0.37	6.1	5.0	2.0
AOTcrops	urban	430	[-769.51;485.11]	11.02	1.00	1.2	-37.0	20.0
AOTcrops	suburban	267	[-886.55;620.02]	90.55	0.77	7.8	-35.0	17.0
AOTcrops	rural	343	[-924.54;570.87]	-116.70	0.62	-9.8	-39.0	17.0
AOTcrops	traffic	79	[-559.17;640.19]	51.69	0.32	11.9	-13.0	14.0
AOTcrops	industrial	108	[-1024.79;582.61]	-177.12	0.23	-19.3	-31.0	3.0
AOTforest	urban	430	[-1157.80;789.71]	-154.34	0.62	-11.3	-20.0	20.0
AOTforest	suburban	267	[-1383.67;989.43]	24.09	1.00	1.4	-20.0	17.0
AOTforest	rural	344	[-1704.03;1016.61]	-391.36	0.32	-21.1	-23.0	13.0

Metric	Station Type	Number of Stations	5th and 95th quantile of trends	Trend of Median	MK p-val of Median	Relative Change (2019 vs 2005, %)	Relative Change (2012 vs 2005, %)	Relative Change (2019 vs 2012, %)
AOTforest	traffic	82	[-1219.24;1197.45]	258.16	0.11	38.7	5.0	13.0
AOTforest	industrial	109	[-1551.32;895.91]	-281.34	0.37	-18.4	-19.0	8.0
OX	urban	378	[-1.29;1.65]	0.13	0.49	2.8	-2.0	1.0
OX	suburban	186	[-1.29;1.24]	-0.11	0.62	-2.4	-4.0	1.0
OX	rural	220	[-2.37;0.18]	-1.17	0.00	-21.3	-8.0	-3.0
OX	traffic	73	[-0.85;3.40]	0.92	0.00	22.9	8.0	4.0
OX	industrial	85	[-1.83;1.44]	-0.29	0.05	-6.1	2.0	-2.0

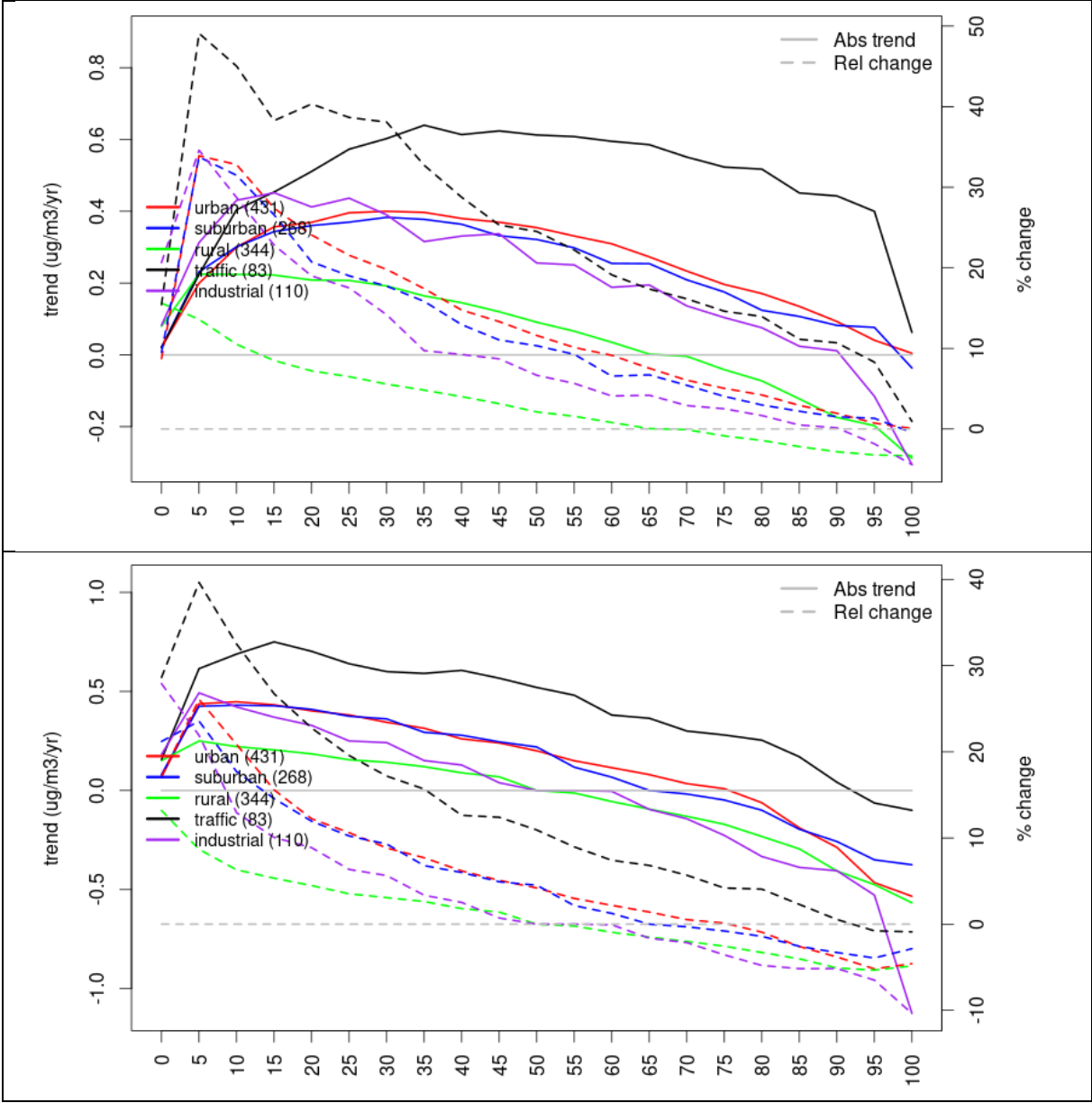
Amongst all the factors that bear upon surface ozone, the recent increase of annual mean ozone is generally attributed to hemispheric transport (Cooper et al., 2014) or reduced titration as a result of NO_x emission decreases (Monks et al., 2015). The clear difference between rural sites and other typologies indicates that the decreased titration has more impact on the recent trends in Europe than hemispheric transport.

The ozone peaks are assessed from the fourth highest annual daily maximum of 8hr running mean called “4MDA8” trend. This metric is taken instead of the summertime average because when only a handful of significant ozone air pollution episode occur in a year for a given station, the summertime average of daily maxima is not really representative of high ozone episodes. Ozone peaks decrease over the period, of about 2 to 5% at background sites, but the trend of the European composite is not significant. There is a flattening of the downward trend over recent years, with several increases reported over the period 2012-2019 even for ozone peaks.

The number of days of exceedance of the target value 120µg/m³ for the daily maximum hourly ozone is also given in Figure 11. The interannual variability is even stronger than for 4MDA8, with outstanding years in 2015, 2018, and 2019. More exceedances are found at suburban sites, they declined by 10% between 2005 and 2019, but increased by 27% between 2012 and 2019.

The trends of daily maxima and daily mean ozone percentiles illustrate well the difference between ozone trends for high and low concentrations (Figure 12). High quantiles of the daily maxima decrease by about 5% at all sites, while at urban background sites low quantiles increase by more than 10% below the 20th percentile. It is only at rural and industrial sites that some decreases of the highest quantiles in daily means are seen.

Figure 12: For ozone and each typology of station, absolute trend (solid lines, left y-axis) and relative change (dashed lines, right y-axis) of the percentiles of daily mean (top) and daily maxima (bottom) over the period 2005-2019

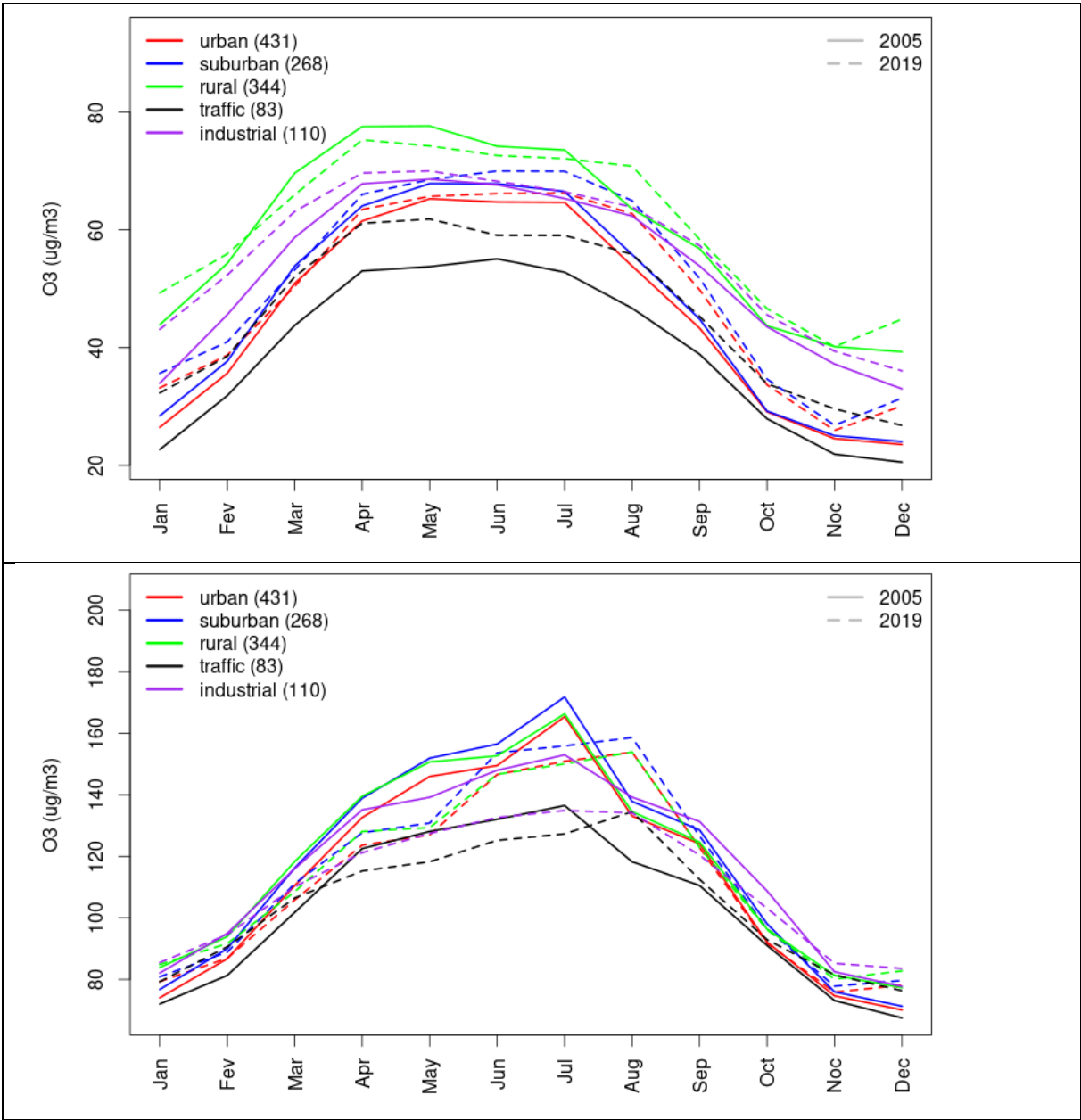


The trends in ozone health and ecosystem exposure are influenced by both high and low percentiles of ozone distributions. As an indicator of human health impact, SOMO35 (sum of ozone daily maxima in excess of 35 ppbv) is mainly relevant at urban and suburban sites where its trend is not significant and the relative change is -2% to +3.7% over the whole period, respectively to each station typology (Table 6). By also taking into lower values of ozone daily maxima (from 10ppbv upwards), SOMO10 is more influenced by the titration effect than SOMO35, so that the increase at urban sites is still un-significant but reaches 5.7% (Table 5). Regarding ecosystem exposure, AOT40 for crops is reduced by 9.8% at rural sites but the interannual variability is so large that the trend is not significant. Likewise, for forests, a non-significant 21.1% reduction is observed.

Ozone displays a strong seasonal cycle illustrated in Figure 13 for both ozone daily means and daily maxima. Here the monthly cycles at the beginning (2005) and end (2019) of the period are compared

by using estimated values for the years 2005 and 2019 based on a linear fit rather than the actual monthly cycle for those years to minimize the impact of interannual variability. To compute these estimated values for 2005 and 2019, we take the monthly cycle for either daily max or daily mean, and for each year over the period. Then a linear regression is done for each month taking the 15 values between 2005 and 2019. And the fitted value for the years 2005 and 2019 are used rather than the actual monthly cycle of 2005 or 2019, which would be very sensitive to the actual choice of the starting/ending years because of interannual variability. If we discard the winter months and traffic sites, when ozone levels are lower, consistent decreases are still found for both ozone max and means, with a notable exception for the month of August, where the recent trend contributed to increase ozone levels. This feature was not visible in earlier assessment (Colette and Rouil, 2020) focusing on 2000-2017, highlighting the strong impact of the years 2018 & 2019 on the trend.

Figure 13: Monthly cycle of daily mean (top) and daily maxima (bottom) ozone at various station type estimated from the whole time series in 2005 (solid lines) and 2019 (dashed lines)



The ozone diurnal cycles are shown in Figure 14. The cycles are estimated for 2005 and 2019, and absolute and relative trends are also available on the Figure. For all sites, the increase occurs all day long and it is smaller only during the morning hours. Note that those cycles are averaged over a full year and would be shifted if considered only over summer.

Figure 14: Top: diurnal cycle of ozone at various station types estimated from the whole time series in 2005 (solid lines) and 2019 (dashed lines). Bottom: corresponding absolute trend (solid lines) and relative changes (dashed lines)

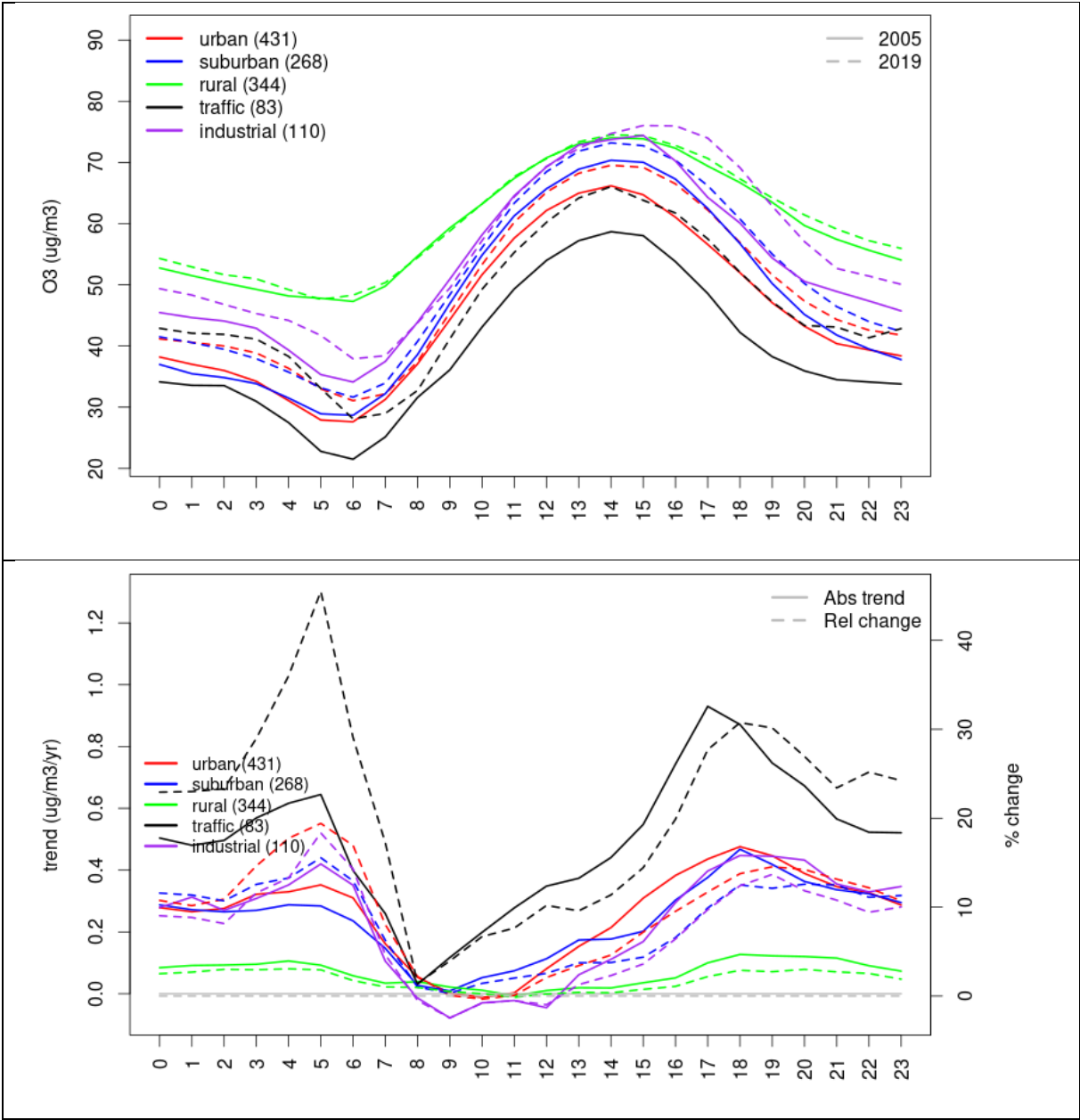


Figure 15: Top: diurnal cycle of OX (as NO₂+O₃) at various station types estimated from the whole time series in 2005 (solid lines) and 2019 (dashed lines). Bottom: corresponding absolute trend (solid lines) and relative changes (dashed lines)

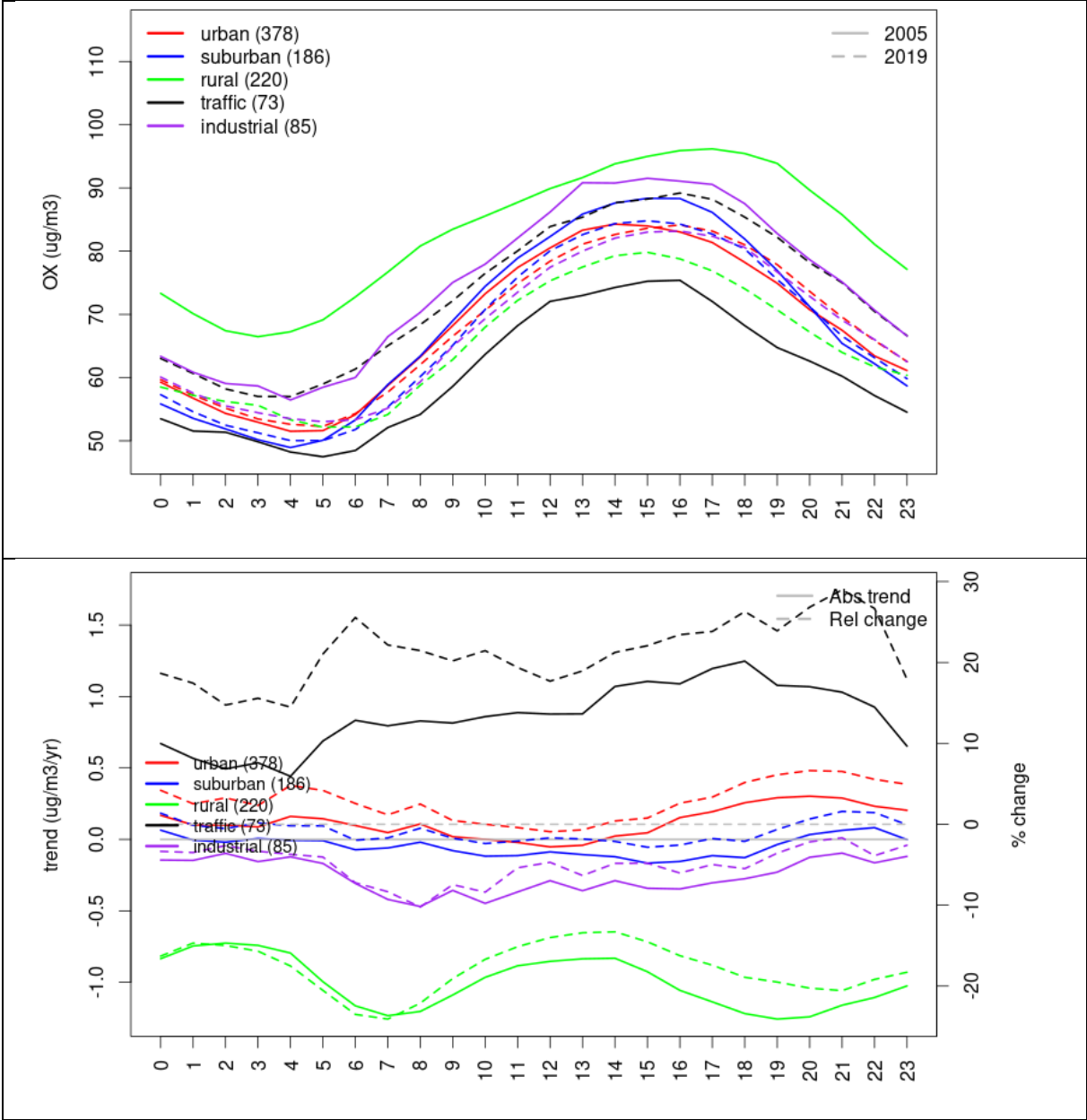
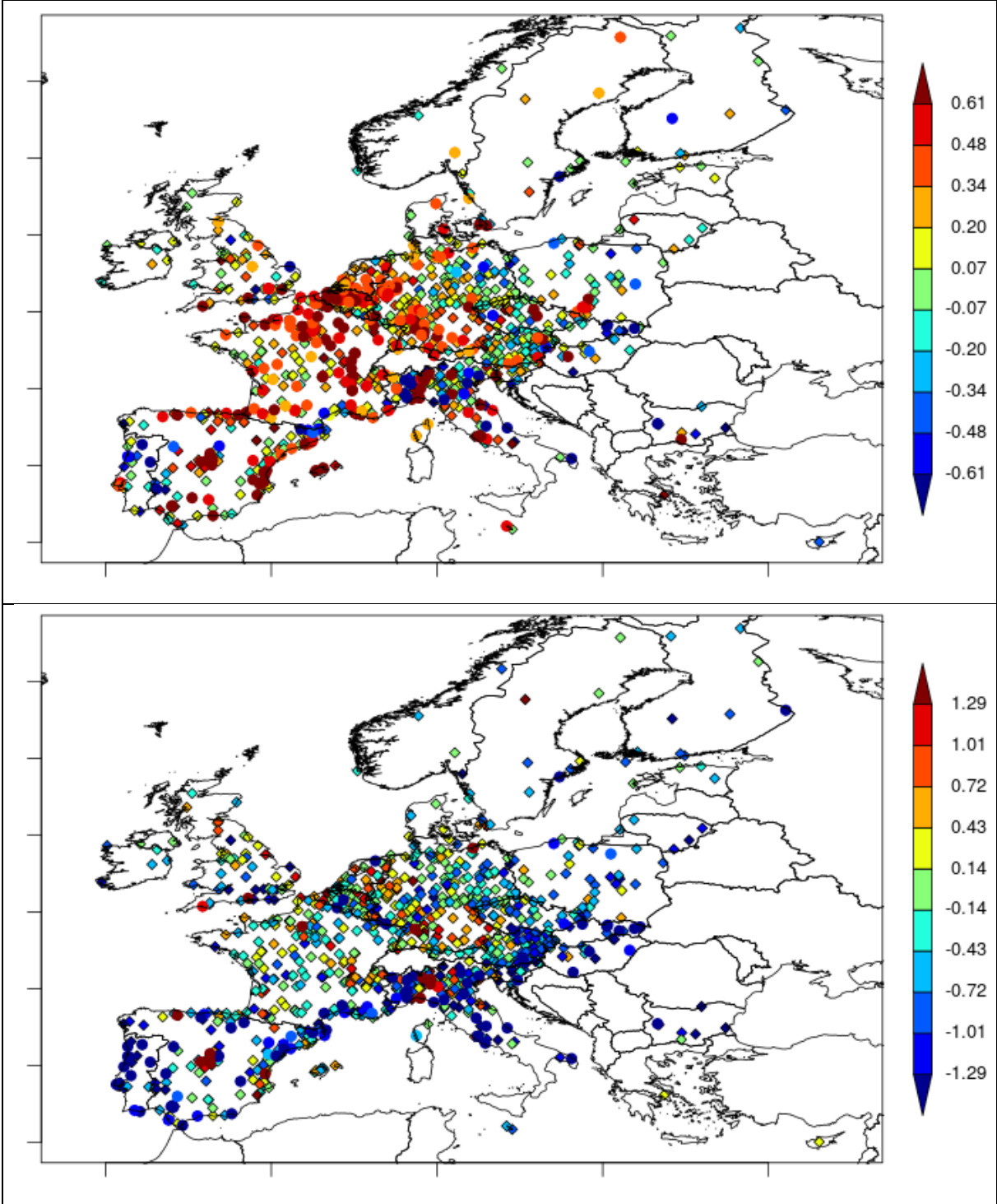


Figure 15 shows the diurnal cycle of O_x defined as the sum of O₃ and NO₂ concentrations. Because of the fast O₃/NO₂ reaction, it is chemically relevant to consider the trend of their sum. They also both have adverse health effects. And, as mentioned above, their trends are opposite (at least in terms of daily means), so that it is difficult to conclude whether, for instance, ozone increases at urban sites should really be a concern for human exposure if it is associated with nitrogen dioxide decreases. O_x trends are significantly decreasing at rural sites (-21.3%), and significantly increasing at traffic sites (+22.9%) (Figure 11). At urban, suburban, and industrial sites un-significant changes within about 5% are found, Table 6.

The maps of the trends observed over Europe at background sites are given in Figure 16 for ozone annual mean and 4MDA8. Decreases in ozone annual mean are recorded over Central/Eastern Europe (Austria, Czech Republic and Poland) while there are more increases in Western Europe, in particular

in Spain and South Eastern France. There is however no strong latitudinal gradient that would be expected from different chemical regimes and photolysis rates. The amplitude of ozone peaks (as 4MDA8) is slightly less reduced in Germany (to be related to the lower NO₂ decreases discussed in Section 3.1.2) and a couple of individual stations in Spain.

Figure 16: Map of O₃ annual mean (top) and 4MDA8 (bottom), in µg/m³/yr at all urban, suburban and rural background sites in Europe over 2005-2019



The relative evolution of ozone concentration in Europe is put in perspective with emissions of its precursor in Table 7. A more in-depth analysis of the effectiveness of emission mitigation policies in reducing ozone levels in Europe would require the implementation of regional and global chemistry-transport models in order to take into account the effect of meteorology, intercontinental transport, but also long-lived precursors such as methane. Nevertheless, this table allows pointing out the important gap between the rate of change of the emission of ozone precursors, and the observed ozone evolution. Considering only the countries with at least 5 ozone stations of any typology, the emissions of NMVOC and NO_x decreased over 2005-2019 by 46% and 34%, respectively. At the same time, annual ozone increased by 6% and the peaks (4MDA8) decreased, but only by 4% (these changes are given for all station types for synthesis purposes in Table 6, but the details per typology is given in Table 6). This gap is systematic for the European countries included in Table 6 and raises legitimate questions in relation to the effectiveness of air quality policies to deal with ozone issues in the European countries. This is essentially because European anthropogenic emission will only contribute to ozone formation in excess to a baseline constituted of natural ozone (from soil and biogenic emissions) and hemispheric background. This baseline is substantial and can be about 80µg/m³ in summer. Assessing policy effectiveness in mitigating ozone would require focusing on the ozone concentration in excess of that baseline, which would therefore need to be computed more precisely.

Table 7: Change, relative to 2005 (in %), for emissions of NO_x and VOC and concentrations of ozone annual mean and peaks, as median over countries with at least 5 stations of any typology (Nsta, otherwise indicated as "NA")

	Nsta	Emis NO_x	Emis VOC	Conc AVG	Conc MDA8
AT	85	-46,3	-45,4	3,1	-6,4
BE	29	-61,3	-60,3	17,9	0,4
BG	8	-31,6	-50,6	-4,7	-15,2
CY	-	-	-	-	-
CZ	39	-31,0	-47,9	2,8	-4,3
DE	196	-39,2	-38,0	6,9	0,3
DK	-	-	-	-	-
EE	-	-	-	-	-
ES	136	-49,7	-57,8	7,7	-5,0
FI	10	-62,6	-57,0	-0,8	-10,5
FR	205	-59,6	-59,3	11,1	-2,4
GB	50	-59,9	-66,5	4,6	-1,5
GR	-	-	-	-	-
HR	-	-	-	-	-

	Nsta	Emis NOx	Emis VOC	Conc AVG	Conc MDA8
HU	15	-42,2	-46,3	1,8	-11,0
IE	-	-	-	-	-
IT	117	-54,1	-67,9	2,8	-6,6
LT	-	-	-	-	-
LU	-	-	-	-	-
LV	-	-	-	-	-
MT	-	-	-	-	-
NL	23	-19,2	-53,4	13,3	-0,1
PL	40	-16,2	-22,5	-1,1	-7,2
PT	22	-46,7	-59,4	-0,2	-14,7
RO	-	-	-	-	-
SE	13	-42,5	-40,2	1,6	-5,4
SI	-	-	-	-	-
SK	-	-	-	-	-
EU28	988	-33,8	-46,0	5,8	-3,7

3.1.4 Particulate Matter

Strong significant downward trends of annual mean PM₁₀ concentrations were observed in Europe since 2005 for all station types (Figure 17). The decrease over all European stations of annual mean PM₁₀ is 37% at urban sites Table 8. The comparison of trends in the earlier and later part of the period indicate no flattening out at urban and suburban sites, but a slower rate of change in recent years at traffic, industrial and rural sites. For annual mean PM_{2.5} concentrations, only the decrease after 2008 can be considered because of the scarcity of the network before that date. All trends are significant and the decrease of annual mean PM_{2.5} is similar to that of PM₁₀: 38.4% at urban sites.

Figure 17: For PM10 (top) and PM2.5 (bottom) annual means: Time series of the European-wide composite (median) per station type and area (red: urban background, blue suburban background, green: rural background, black: traffic, violet: industrial) between 2005 and 2019. The dashed lines show the linear fit between 2005 & 2012 and between 2012 & 2019. The boxplots on the right-hand side show the distribution of relative changes (%) between 2005 and 2019 for all stations of each typology

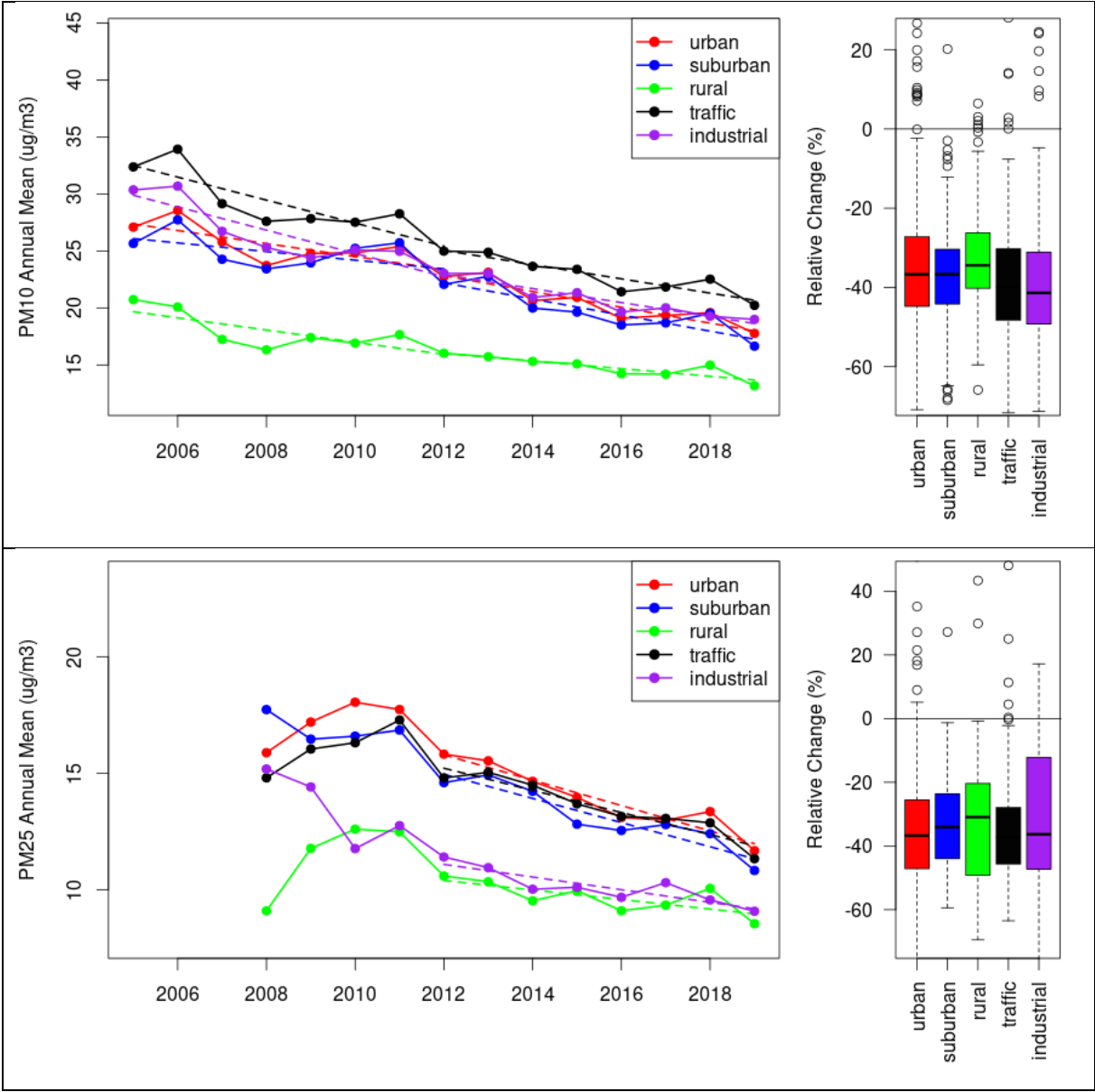


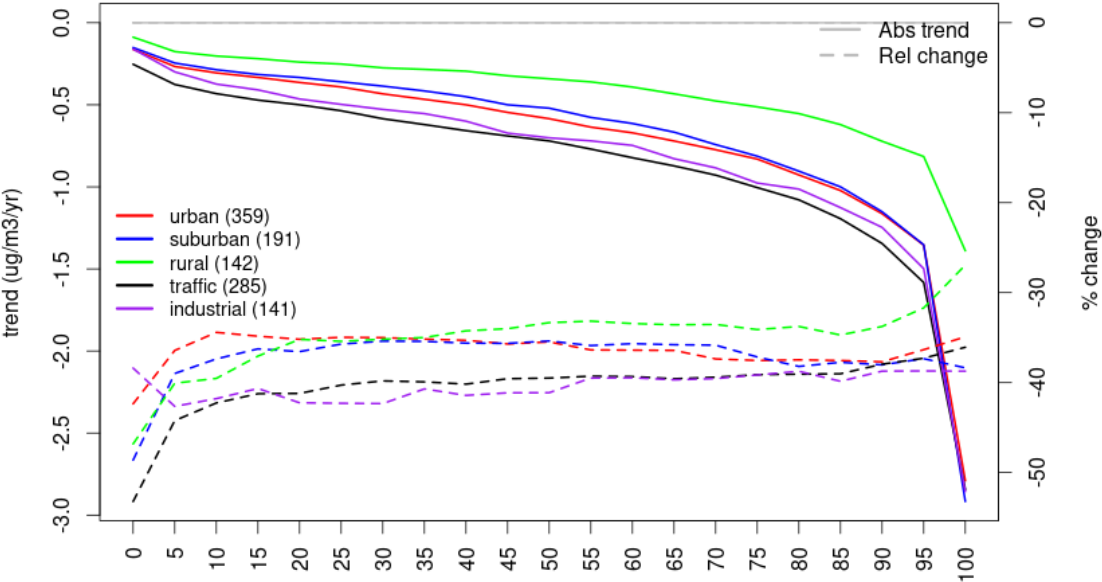
Table 8: Summary of observed PM indicator trends for various station typology: total number of station, 5th and 95th quantiles of Sen Theil slopes at all European stations, trend of the median of the European-wide composite (Sen-Theil slope, $\mu\text{g}/\text{m}^3/\text{yr}$), significance of the European-wide composite (Mann-Kendall p-value, MK p-val) and percentage change between : 2005 and 2019, 2005 and 2012, 2012 and 2019 for the European-wide composite (% change)

Pollutant	Metric	Station Type	Number of Stations	5th and 95th quantile of trends	Trend of Median	MK p-val of Median	Relative Change (PM10: 2019 vs 2005, %) (PM25: 2019 vs 2008, %)	Relative Change (2012 vs 2005, %)	Relative Change (2019 vs 2012, %)
PM ₁₀	Annual Mean	urban	424	[-1.42;-0.09]	-0.68	0.00	-36.9	-15.0	-13.0
PM ₁₀	Annual Mean	suburban	207	[-1.54;-0.28]	-0.65	0.00	-36.2	-10.0	-14.0
PM ₁₀	Annual Mean	rural	143	[-0.93;-0.01]	-0.42	0.00	-32.4	-19.0	-9.0
PM ₁₀	Annual Mean	traffic	293	[-1.70;-0.22]	-0.79	0.00	-37.1	-22.0	-11.0
PM ₁₀	Annual Mean	industrial	152	[-1.72;0.04]	-0.74	0.00	-38.0	-24.0	-12.0
PM ₁₀	Nday > 50 $\mu\text{g}/\text{m}^3$	urban	359	[-5.42;0.01]	-1.79	0.00	-87.2	-43.0	-58.0
PM ₁₀	Nday > 50 $\mu\text{g}/\text{m}^3$	suburban	191	[-5.68;-0.14]	-1.44	0.00	-81.4	-15.0	-57.0
PM ₁₀	Nday > 50 $\mu\text{g}/\text{m}^3$	rural	142	[-2.00;0.00]	-0.46	0.00	-88.1	-26.0	-47.0
PM ₁₀	Nday > 50 $\mu\text{g}/\text{m}^3$	traffic	285	[-6.77;-0.05]	-2.30	0.00	-84.2	-55.0	-47.0
PM ₁₀	Nday > 50 $\mu\text{g}/\text{m}^3$	industrial	141	[-5.67;0.00]	-1.80	0.00	-92.9	-58.0	-45.0
PM _{2.5}	Annual Mean	urban	256	[-1.40;-0.06]	-0.57	0.00	-38.4	N/A	-24.0
PM _{2.5}	Annual Mean	suburban	67	[-0.91;-0.04]	-0.57	0.00	-38.7	N/A	-24.0
PM _{2.5}	Annual Mean	rural	80	[-0.80;-0.04]	-0.30	0.05	-30.9	N/A	-14.0
PM _{2.5}	Annual Mean	traffic	114	[-1.11;0.02]	-0.42	0.00	-30.3	N/A	-22.0
PM _{2.5}	Annual Mean	industrial	54	[-1.03;0.09]	-0.46	0.00	-39.2	N/A	-17.0

The trends of PM₁₀ and PM_{2.5} in Table 8 cannot be directly compared as they rely on different monitoring networks (about half as many PM_{2.5} stations compared to PM₁₀). We must therefore limit the comparison to those sites which measure PM₁₀ and PM_{2.5} at the same time. Then we only include 74 and 36 urban and rural sites, respectively. For urban sites, PM₁₀ and PM_{2.5} relative changes between 2008 and 2019 are broadly consistent: 22 and 27% reduction, respectively. But for rural sites, PM₁₀ decrease faster (-16%) than PM_{2.5} (-7%).

Following the reduction in annual mean PM₁₀, the number of days when the regulatory limit value (50 $\mu\text{g}/\text{m}^3$) is exceeded, is strongly reduced: 81 to 93% (Table 8). Yet, in relative terms, the highest PM₁₀ peaks decrease less than the rest of the distribution at rural sites (Figure 18). A lower rate of decline of high peaks at rural locations could be a sign of sustained (or even increasing) frequency of natural outbreaks (of desert dusts or wildfires) which would be masked by other factors at urban sites. The fact that this lower rate of decline of high peaks at urban sites would tend to exclude an increasing frequency of meteorological factors such as strong stagnation events.

Figure 18: For PM10 and each typology of station: absolute trend (solid lines, left y-axis) and relative change (dashed lines, right y-axis) of the percentiles of daily mean over the period 2005-2019



The monthly PM_{10} cycle show a winter maximum at urban, suburban and traffic sites both for the 2005 and 2019 estimates (Figure 19). The amplitude of the monthly cycle has been reduced in time at all station types. It is in summer (when PM_{10} levels are lower) that the relative reduction has been more limited, in particular because of the contribution of natural sources (including secondary organic aerosols formed from biogenic VOCs). Decreasing trend in PM_{10} and $\text{PM}_{2.5}$ concentrations are recorded in all European countries. Lower rate of declines are seen in Germany for both PM_{10} and $\text{PM}_{2.5}$, and in Spain (only for $\text{PM}_{2.5}$).

Figure 19: Top: monthly cycle of daily mean of PM10 at various station type estimated from the whole time series in 2005 (solid lines) and 2019 (dashed lines). Bottom: absolute trend (solid lines, left y-axis) and relative change (dashed lines, right y-axis) of the percentiles of daily mean over the period 2005-2019

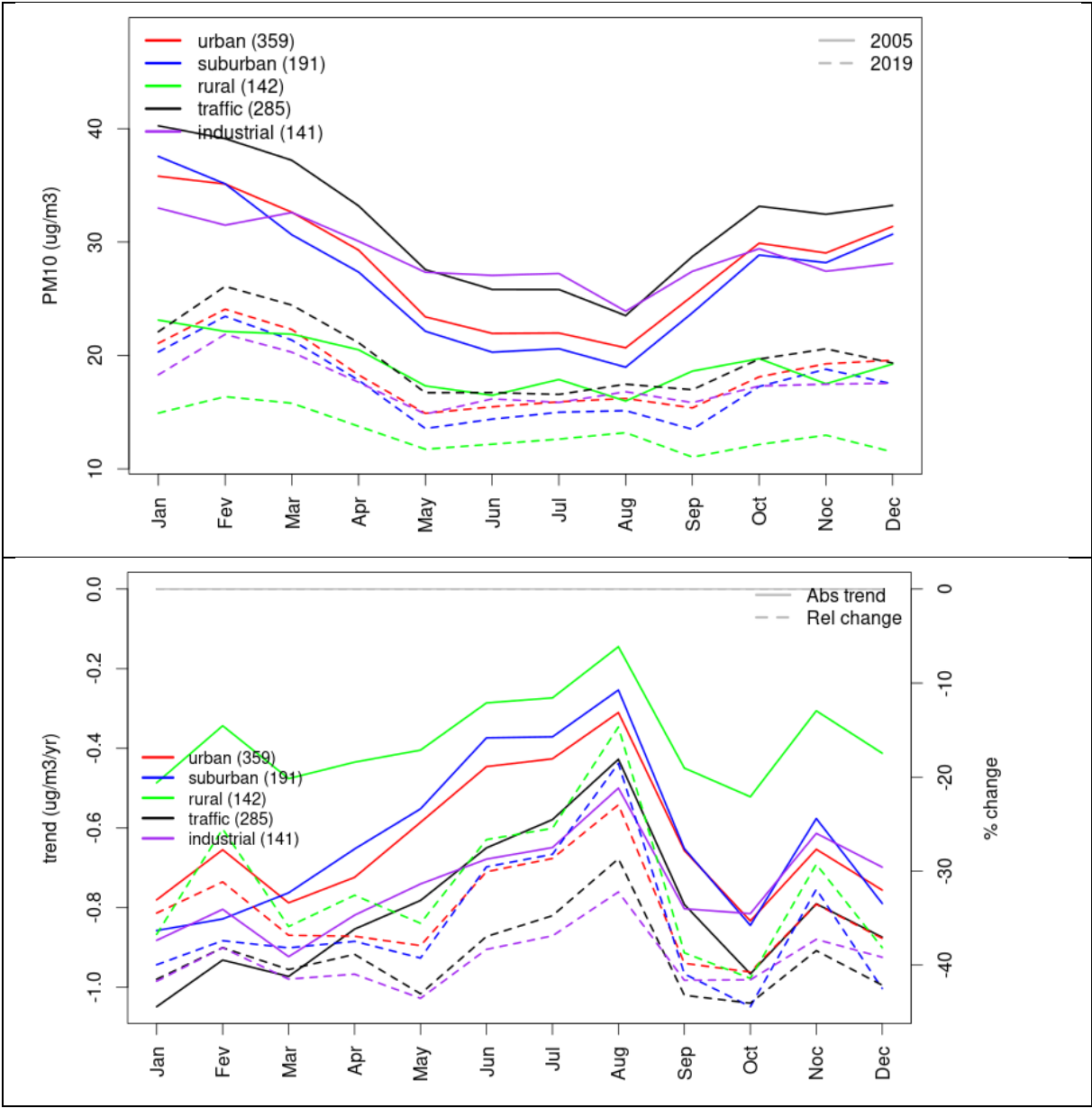
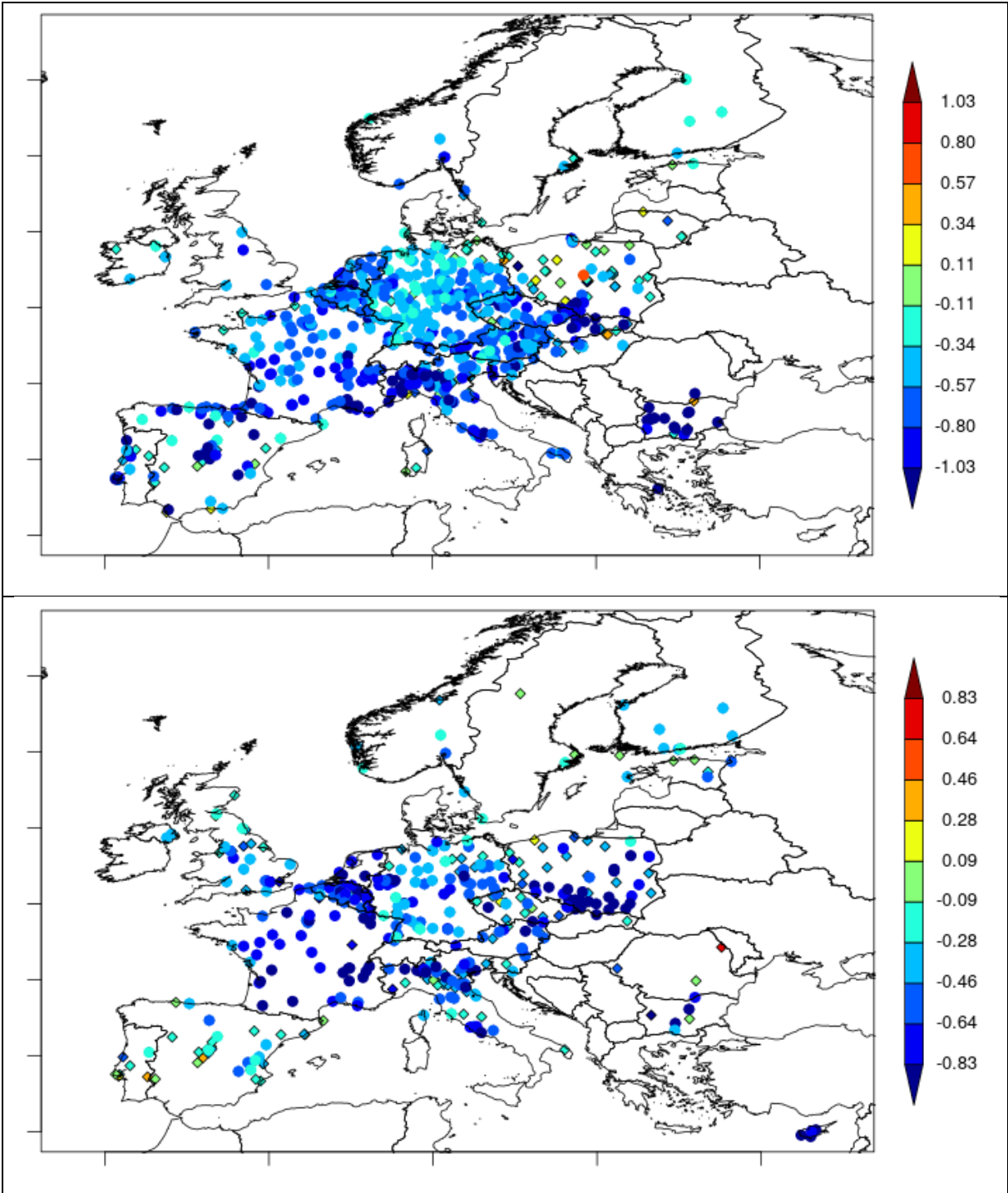
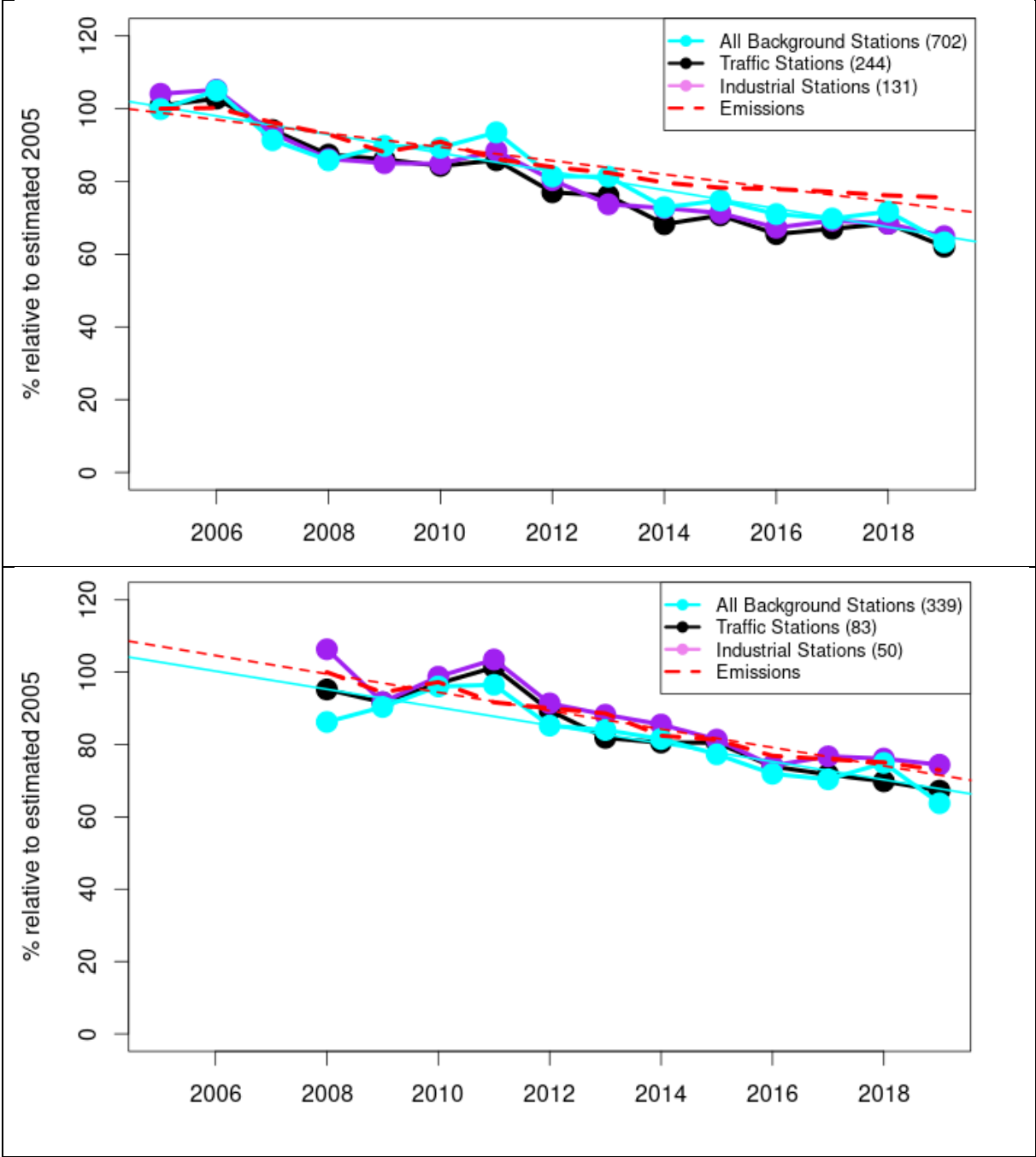


Figure 20: Map of PM10 annual mean (top) and PM2.5 annual mean (bottom), in $\mu\text{g}/\text{m}^3/\text{yr}$ at all urban, suburban and rural background sites in Europe over 2005-2019



The comparison between emissions and observation by country displays a good correlation (Figure 21). As for SO_2 and NO_2 , this comparison remains very qualitative until chemistry-transport models are involved for a more detailed assessment. Over countries where the network is dense enough, PM_{10} and $\text{PM}_{2.5}$ concentrations decreased respectively by 38% and 33% (Table S.3), whereas the corresponding changes in primary emissions were 28% and 30%. The decreases are larger in observed concentrations, which was expected considering the importance of secondary aerosols, which are mitigated by decreasing other precursors than primary PM. The difference between PM_{10} and $\text{PM}_{2.5}$ trends shall not be further interpreted as this comparison is not for collocated measurements.

Figure 21: Time series of country median PM10 (top) and PM2.5 (bottom) observed at traffic (black), industrial (violet) and background (cyan) sites (solid lines), and corresponding country PPM10 and PPM2.5 emissions (dashed line) normalised to estimated 2005 levels. The total number of stations is provided in brackets. Straight lines are the linear fit over the whole period



3.1.5 Air Quality Index

The evolution of air quality in Europe is synthesized in Figure 22 using the EEA air quality index that categorizes air pollutant (PM_{2.5}, PM₁₀, NO₂, O₃ and SO₂) concentrations in 6 ranges: good, fair, moderate, poor, very poor and extremely poor. For a given day and location, the category is computed for each pollutant (taking daily max instead of daily means where relevant), and the index accounts for the worst category of all 5 pollutants. Because of the non-colocalization of various pollutants in the

monitoring network, and its substantial development since 2005, it is difficult to compute the index over a long time period for each station. To cope with this limitation, a median index either by country or over the whole EU27+UK is computed.

Figure 22: For the whole Europe Union: overall air quality index (percentage of days in a given year) and distribution of daily categories per pollutant (light blue: good, light green: fair, yellow: moderate, orange: poor, red: very poor, violet: extremely poor, see Table S.1)



A slight improvement is found for the overall index. In 2005, less than half of the days were “fair”. This proportion reaches about 60% by 2019 with slightly less days classified as “moderate” or “poor”. The use of a median value over the whole Europe (as EU27+UK) evens out the variability so that no “good”, “very poor”, or “extremely poor” days appear.

Figure 22 also show the long-term evolution of the good/fair/moderate/poor/very poor/extremely poor categories by pollutant over Europe. The number of “good” days for NO₂, PM₁₀ and PM_{2.5} has increased clearly. But for ozone, the distribution has not changed substantially, and the daily categories for SO₂ were already good at the beginning of the period.

The long-term evolution of the network presented in Figure 1 does not suggest that there could be significant sampling biases related to a change in station typology. The number of stations has increased dramatically but the relative proportion of urban/rural sites remained quite constant. An important effect could be due to the development of PM monitoring that would rather be unfavourable to the air quality trend.

3.2 Results from AirGAM calculations for NO₂, PM₁₀, PM_{2.5} and O₃

The total change in percent over the period 2005-2019 for NO₂, PM₁₀, PM_{2.5} and O₃ (summer half year only) for the annual mean concentrations are given in Figure 23 for each of the three categories of stations as explained above. Table 9 - Table 11 list these values for NO₂, PM₁₀ and PM_{2.5} together with the reported changes in emission. These values were calculated as:

$$X_{rel} = [100 \times (X_{2019} - X_{2005}) / X_{2005}]$$

where X₂₀₁₉ and X₂₀₀₅ refers to the met.adjusted long term trend concentration in 2019 and 2005, respectively, for each of the individual countries. Note that these values for the changes in the emissions differ from those under Chapter 3.1 since the ones tabulated under Ch. 3.1 are based on a linear fit to the emission data (the Theil Sen’s slope) during the entire period, whereas in the present chapter the actual values in 2005 and 2019 were used.

For the AirGAM study, the national total emissions were used when comparing to the rural, suburban and urban background sites whereas the national emissions from road traffic were used when comparing with traffic sites. In the following, all the estimated trends in air pollutant concentrations refer to the meteorologically adjusted trends, meaning that the “noise” in long-term data caused by interannual variations due to anomalous weather situations are filtered out.

Annex 2 presents the comparison between met.adjusted trends as calculated by the AirGAM model and the national emissions as given by CEIP for each country, separately. For each country and station category these plots show the median (blue line) and spread (25 and 75 percentile as blue shaded area) of the met.adjusted long-term trend calculated by the AirGAM model for all stations in the respective country/category. The red line gives the national emissions as given by CEIP from road traffic when compared to sites in the traffic category and from all sources when compared to the other two categories.

Figure 23 indicates geographical difference in the changes in air concentrations over the 2005-2019 period with less reductions in parts of eastern Europe, as also indicated by the national emission data. Note that we could not compute the AirGAM trends for PM₁₀ and PM_{2.5} over France due to the lack of long-term monitoring data. The reason for this was that the only daily based PM data were available for France before 2010 and only hourly data after that, and we did not want to merge daily based and hourly based time series data. Note also that no screening of the number of stations were used when calculating the trends for each station category and country in Table 9 - Table 11. This will introduce

uncertainties for countries with few stations (even down to one single station) but was kept as this to avoid losing information.

Fairly similar downward trends were calculated for the various stations categories of NO_2 , ranging from 27 to 32 % as a median (Table 9). As opposed to this, the reported emission data for NO_x ranges from 43-48% (depending on whether all sources or just road traffic were included). Thus, a clear deviation between the official NO_x emission data and the measured NO_2 concentrations (even when taking into account the effect of inter-annual meteorological variations) are found, similar to what is discussed under Ch 3.1.

The mismatch between the reduction in observed NO_2 concentrations and the reported emissions of NO_x could not be explained by changes in meteorology. Thus, it raises a question on a possible discrepancy between emission data and actual efficiency of mitigation measures for NO_x , but also on the role of other factors such as the NO_2/NO_x ratio of the emissions, changes in baseline hemispheric ozone concentration and natural emissions. NO_2 constitutes only of the order of 5-15% of the total NO_x emissions, and changes in the fleet of vehicles (e.g. diesel versus petrol cars) could lead to a trend in the NO_2/NO_x air concentration ratio, particularly at roadside stations. Furthermore, the ambient ozone concentration is controlling the equilibrium NO_2/NO_x , meaning that close to the emissions, the NO_2 concentration is a sum of the direct emission and the NO_2 formed from ozone reacting with NO , thus counteracting the effect of the emission reductions. Finally, substantial differences are revealed when looking at the trends for individual countries and for different types of monitoring stations. Smaller reductions in NO_2 than the NO_x emission reductions are seen at traffic sites in most countries, but for rural/suburban/urban background sites a good agreement is seen between the trends in NO_x emissions and NO_2 concentrations in some countries as Germany, Czech Republic and Switzerland. The overall mismatch between trends in NO_2 concentrations and NO_x emissions is thus most likely explained by a combination of deficiencies in the emission data, atmospheric processes, and geographical differences.

For PM_{10} and $\text{PM}_{2.5}$, the situation is the opposite as for NO_2/NO_x discussed above, meaning that the concentrations of PM have dropped more than direct emissions of these species. For PM_{10} we estimate a median reduction in concentration at suburban and urban background sites of 34-35 % during 2005-2019 and 30 % at background rural sites, while the reported emissions give reductions of 27 % and 25 %, respectively (Table 10). A similar discrepancy was found in Chapter 3.1 and could be explained by the importance of secondary aerosols, which are mitigated by decreasing other precursors than primary PM. For traffic sites, we find a good agreement between the reported emissions from road traffic and the observed reduction in concentrations (37 % vs 35 %).

The estimated reductions in $\text{PM}_{2.5}$ at suburban/urban background sites and rural background sites is 34 % and 24 %, respectively, while the reported emissions give reductions of 34 % and 23 %, respectively (Table 11). For traffic sites, the reported emissions of $\text{PM}_{2.5}$ from road traffic is significantly higher than observed at traffic sites (49% vs 32 %). Due to the limited amount of data and often shorter time periods of measurements, these numbers should be interpreted with care.

Table 9 - Table 11 and the annual time series as shown in the Annex2, reveal substantial differences among the countries. Furthermore, the reported emission data are far from linear in several countries. Particularly strong deviations from linearity are seen in some East European countries as Estonia, Poland, and North Macedonia.

The agreement between the met-adjusted AirGAM trends and the emission data as shown in Annex2 varies from very good agreement for some countries/species/site categories to no agreement for other combinations, and it is difficult to summarize these findings in a few sentences. The deviation from linear slopes is, however, fairly strong in many countries.

Figure 23: Total change in the mean concentration (%) of NO₂, PM₁₀, PM_{2.5}, and O₃ during the period 2005-2019 relative to 2005 as estimated by AirGAM for three categories of stations: i) all traffic sites; ii) urban and suburban background; iii) rural background. For O₃ the data are based on the mean of the daily max 8-h running mean during the summer half year

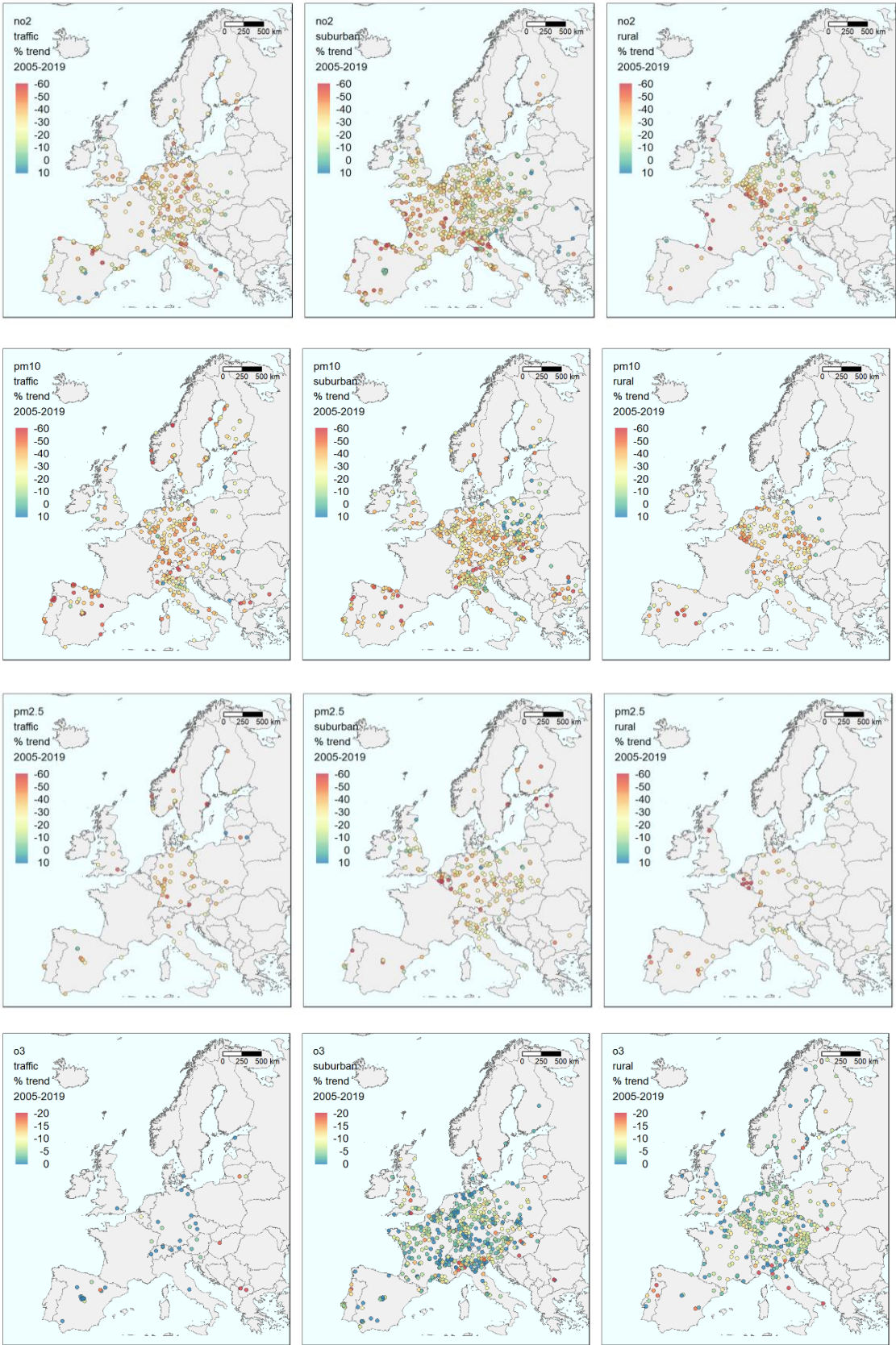


Table 9: The relative emission reduction (%) according to CEIP, and the median relative reduction in measured concentration of NO₂ during 2005-2019 as given by the met-adjusted trend for three categories of stations in each country

	Emis (rural)	Conc (rural)	Emis (sub/urban)	Conc (sub/urban)	Emis (traffic)	Conc (traffic)
AT	42	12	42	28	52	27
BE	51	40	51	38	54	39
BG	-	-	44	4	-	-
CH	34	26	34	35	35	30
CZ	40	36	40	31	39	23
DE	31	32	31	25	45	33
DK	52	26	52	47	62	48
EE	40	25	40	28	48	56
ES	52	47	52	31	57	32
FI	42	30	42	40	64	34
FR	48	49	48	33	47	32
GB	53	34	53	31	54	31
GR	-	-	48	50	50	34
HR	-	-	40	3	26	15
HU	36	5	36	10	45	30
IE	-	-	43	3	-	-
IT	51	41	51	34	60	29
LT	-	-	16	15	12	2
LU	66	22	66	18	-	-
NL	43	26	43	36	50	41
NO	-	-	31	22	33	35
PL	23	8	23	11	-15	10
PT	47	23	47	21	42	21
RO	-	-	34	-3	-	-
SE	-	-	33	34	51	32
SI	-	-	46	6	36	35
SK	-	-	42	-20	49	-4
Median	45	28	43	27	48	32

Table 10: The relative emission reduction (%) according to CEIP, and the median relative reduction in concentration of PM₁₀ during 2005-2019 as given by the met-adjusted trend for three categories of stations in each country

	Emis (rural)	Conc (rural)	Emis (sub/urban)	Conc (sub/urban)	Emis (traffic)	Conc (traffic)
AT	26	30	26	32	57	40
BE	40	44	40	34	53	38
BG	-	-	18	34	26	35
CH	22	42	22	38	23	45
CZ	19	34	19	37	27	35
DE	18	28	18	31	42	36
DK	-	-	-	-	44	46
EE	-	-	56	50	32	56
ES	18	31	18	43	53	43
FI	-	-	29	27	18	31
GB	-	-	19	22	37	34
GR	-	-	52	42	48	32
HR	-	-	-	-	44	13
HU	17	26	17	35	39	27
IE	33	23	33	27	45	27
IT	23	23	23	30	54	29
LT	-	-	18	1	-3	14
LU	-	-	43	44	-	-
ME	-	-	-	-	-5	-15
MK	-	-	-	-	9	53
NL	34	35	34	34	59	33
NO	-	-	31	33	38	48
PL	22	6	22	18	-39	22
PT	35	19	35	40	41	53
RO	-	-	4	46	-	-
SE	27	42	27	45	1	43
SI	36	32	36	29	21	29
SK	47	-1	47	37	37	41
Median	25	30	27	34	37	35

Table 11: The relative emission reduction (%) according to CEIP, and the median relative reduction in observed concentration of PM_{2.5} during 2005-2019 as given by the met-adjusted trend for three categories of stations in each country

	Emis (rural)	Conc (rural)	Emis (sub/urban)	Conc (sub/urban)	Emis (traffic)	Conc (traffic)
AT	38	43	38	33	66	48
BE	47	66	47	40	-	-
BG	3	24	3	40	-	-
CZ	18	20	18	34	37	29
DE	33	31	33	31	54	38
DK	-	-	-	-	56	37
EE	55	24	55	60	-	-
ES	8	33	8	40	62	29
FI	36	7	36	43	48	23
GB	17	41	17	24	49	32
HU	-	-	5	14	49	41
IE	-	-	38	5	-	-
IT	20	25	20	25	64	28
LT	-	-	-	-	8	-39
LU	-	-	53	68	-	-
NO	-	-	37	36	54	45
PL	21	16	21	23	-26	32
PT	25	64	25	34	46	39
SE	-	-	44	44	29	61
SI	35	21	35	21	32	21
SK	-	-	51	35	49	9
Median	23	24	34	34	49	32

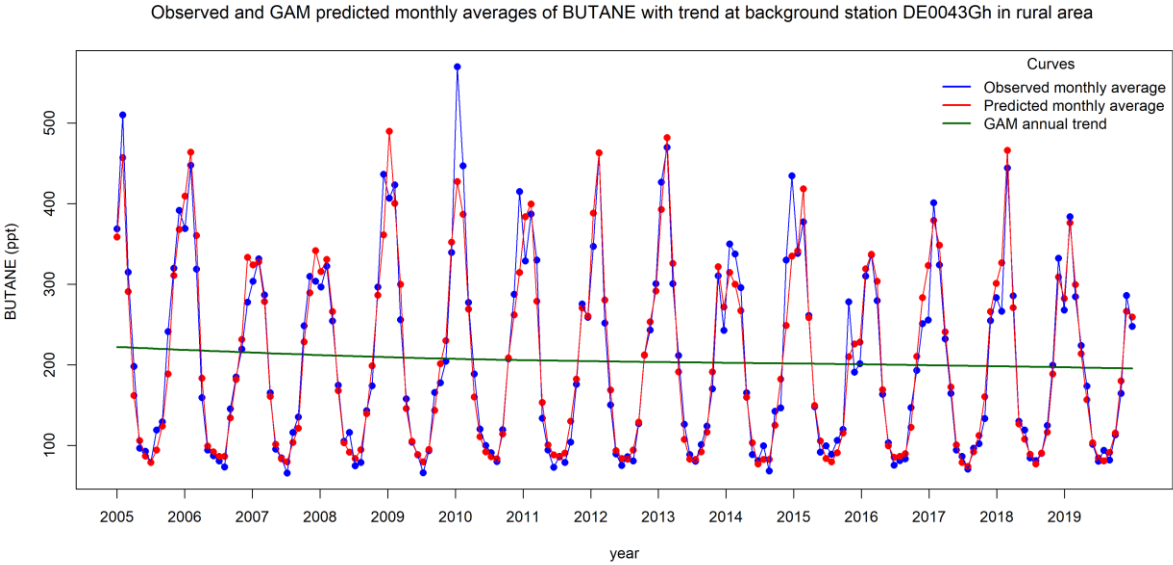
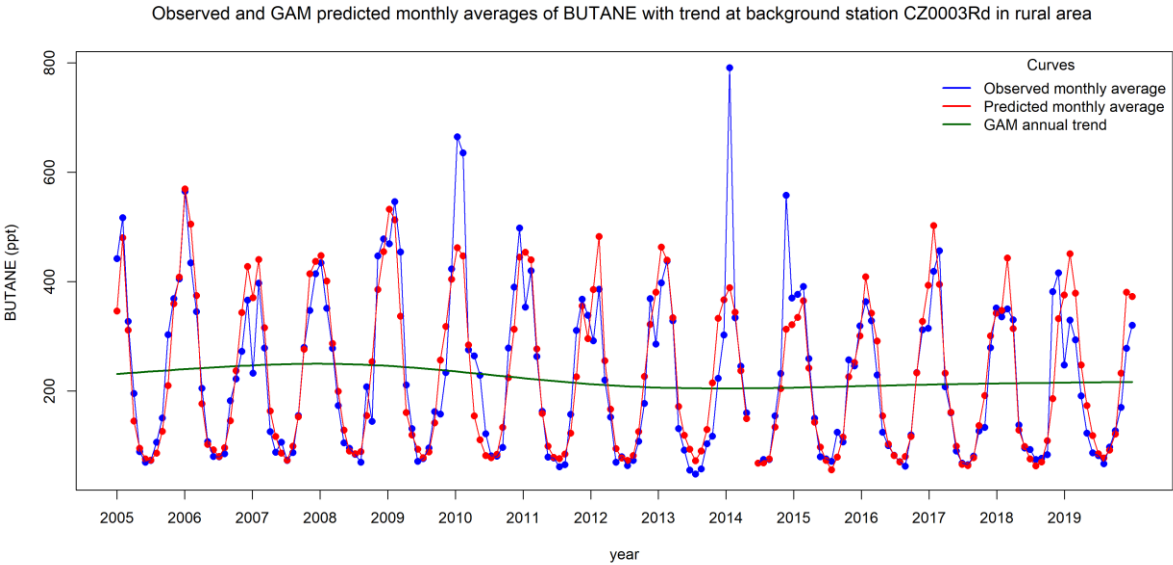
3.2.1 Preliminary AirGAM results for VOC

The VOC data in Airbase/AQER is presently sparse and little documented in the literature. The AirGAM model could in principle be applied also to these data in a similar way as for NO₂ or PM provided that time series of sufficient length and data quality exist. At the moment, the model was tested out for time series of n-butane reported to WDCRG/EBAS (World data centre for reactive gases/EMEP data base) at two rural background stations, Kosetice in the Czech Republic and Hohenpeissenberg in Germany.

A further challenge with VOC data is that the reported emission data only exist for emission sectors and not for individual species. Thus, the modelled and observed trends in single species could not easily be compared to the emission data. N-butane as shown below is emitted from a variety of emission sources (natural gas leakage, fuel evaporation, road traffic etc). Figure 24 shows the monthly mean concentrations observed and modelled by the AirGAM model as well as the estimated met-adjusted trend over the period 2005-2019. These results show a good agreement between observed and modelled data which is a very encouraging result considering that these sites are located in background rural areas that presumably are significantly influenced by long-range transport of pollutants.

In the future, it is recommended to investigate the data availability of the various VOCs in Airbase/AQER and proceed with AirGAM modelling if it turns out feasible for the available species.

Figure 24: Observed (blue) and modelled (red) monthly mean concentrations of n-butane at two rural background stations (Kosetice and Hohenpeissenberg) during 2005-2019. The green curve shows the long-term met-adjusted trend function



4 Summary and conclusions

Detailed trend calculations of air pollutants for the periods 2005-2019 based on two separate methods have been applied. We find that the trends of sulphur dioxide present the largest decrease of all pollutants. The decrease is such that at industrial sites, the levels in 2019 are comparable to that of rural sites at the beginning of the period (2005). A reduction of the order of 60-70 % is found, and the agreement between reported emission data and measured concentrations are quite good.

For NO₂, a mismatch between the trend in air concentrations and NO_x emissions is found. While the overall NO_x emissions are reported to be reduced by around 45 % over the period, the measured NO₂ data indicate a decline of the order of only 30 %. This is a clear finding from both methods. Strong differences between countries are found, though, with better agreement between emissions and measurements in some areas. The relative changes in NO₂ are found to be largest for the lower/medium percentiles whereas smaller reductions are found for the highest peaks.

This mismatch could not be explained by changes in meteorology as this is accounted for. Possible reasons for this mismatch could be the NO₂/NO_x ratio of the emissions, changes in baseline hemispheric ozone concentration and natural emissions. Changes in the fleet of vehicles could lead to a trend in the NO₂/NO_x air concentration ratio at roadside stations, and this ratio could also be influenced by the ambient ozone concentration and thus by long-term trends in ozone. The mismatch between NO_x emissions and NO₂ concentrations is most clearly seen at traffic sites, whereas for rural/suburban/urban background sites a good agreement is found in some countries as Germany, Czech Republic and Switzerland. The overall mismatch between trends in NO₂ concentrations and NO_x emissions is thus most likely explained by a combination of deficiencies in the emission data, atmospheric processes, and geographical differences.

For PM data (PM₁₀ and PM_{2.5}) we find an opposite mismatch, meaning that the PM concentrations show stronger downward trends than the reported emissions. This is likely an effect of the importance of secondary aerosols which are mitigated by other activities than the direct PM emissions, and thus leading to larger reductions than the primary emissions alone. Depending on statistical approach, station type etc, we estimate an overall reduction in PM₁₀ of the order of 30-38 % during 2005-2019 while the direct emissions give a reduction that is 5-10 percentage units smaller. Similar results are found for PM_{2.5}, but due to the substantially less amount of measurement data, these findings are more uncertain.

For O₃, our findings are in line with earlier studies, implying that the annual mean ozone concentration has increased while the high peaks have been reduced. The increase in mean levels is explained by hemispheric transport and reduced titration by NO as a result of reduced NO_x levels. The reduction in high ozone peaks is expected when the general NO_x level in Europe is reduced. It must be noted however that the decrease in the peaks is much more limited over the 2005-2019 period than earlier documented for 2000-2017. Whereas previous ETC report highlighted statistically significant downward trends about 10% in peak ozone, when considering the 2005-2019 period, the decrease is only a few percent and not significant. This is particularly induced by outstanding high ozone years in 2018 and 2019.

5 References

- Aas, W., et al., 2019, *Global and regional trends of atmospheric sulfur*, Scientific Reports, 9, 953, 10.1038/s41598-018-37304-0.
- Banzhaf, S., et al., 2015, *Dynamic model evaluation for secondary inorganic aerosol and its precursors over Europe between 1990 and 2009*, Geosci. Model Dev., 8, 1047-1070, 10.5194/gmd-8-1047-2015.
- Barmpadimos, I., et al., 2012, *One decade of parallel fine (PM_{2.5}) and coarse (PM₁₀–PM_{2.5}) particulate matter measurements in Europe: trends and variability*, Atmos. Chem. Phys., 12, 3189-3203, 10.5194/acp-12-3189-2012, 2012.
- CLRTAP, 1979, Convention on Long Range Transboundary Air Pollution, UNECE, Geneva.
- Colette, A., et al., 2011, *Air quality trends in Europe over the past decade: a first multi-model assessment*, Atmos. Chem. Phys., 11, 11657-11678.
- Colette, A., et al., 2016, *Air pollution trends in the EMEP region between 1990 and 2012*, NILU, Oslo, 2016.
- Colette, A., et al., *EURODELTA-Trends, a multi-model experiment of air quality hindcast in Europe over 1990–2010*, Geosci. Model Dev., 10, 3255-3276, 10.5194/gmd-10-3255-2017, 2017.
- Colette, A., and Rouil, L., 2020, *Air Quality Trends in Europe: 2000-2017*, Assessment for surface SO₂, NO₂, Ozone, PM₁₀ and PM_{2.5}, 2020.
- Cooper, O. R., et al., 2014, *Global distribution and trends of tropospheric ozone: An observation-based review* Elementa, 10.12952/journal.elementa.000029.
- Cooper, O. R., et al., 2020, *Multi-decadal surface ozone trends at globally distributed remote locations*, Elementa: Science of the Anthropocene, 8, 10.1525/elementa.420.
- Derwent, R. G., et al., 2003, *Photochemical ozone formation in north west Europe and its control*, Atmospheric Environment, 37, 1983-1991, [https://doi.org/10.1016/S1352-2310\(03\)00031-1](https://doi.org/10.1016/S1352-2310(03)00031-1).
- Derwent, R. G., et al., 2010, *Ozone in Central England: the impact of 20 years of precursor emission controls in Europe*, environmental science & policy, 13, 195-204.
- EC, 1996, Council Directive 96/62/EC of 27 September 1996 on ambient air quality assessment and management, Brussels.
- EC, 2001, Directive 2001/42/EC of the European Parliament and of the Council of 27 June 2001 on the assessment of the effects of certain plans and programmes on the environment.
- EC, 2004, Directive of the European Parliament and of the Council of 15 December 2004 relating to arsenic, cadmium, mercury, nickel and polycyclic aromatic hydrocarbons in ambient air.
- EC, 2008, Directive 2008/50/EC of the European Parliament and of the Council of 21 May 2008 on ambient air quality and cleaner air for Europe, European Commission, Brussels.
- EC, 2016, Directive (EU) 2016/2284 of the European Parliament and of the Council of 14 December 2016 on the reduction of national emissions of certain atmospheric pollutants, amending Directive 2003/35/EC and repealing Directive 2001/81/EC, European Commission, Brussels.
- EEA, 2018, *Air Quality in Europe - 2018 Report*, Copenhagen, 2018.
- ETC/ACM, 2018, *Discounting the effect of meteorology on trends in surface ozone: Development of statistical tools*, ETC/ACM Technical paper 2017/15.
- ETC/ACM, 2018, *Trends in measured NO₂ and PM. Discounting the effect of meteorology*, Eionet-Report - ETC/ACM 2018-9.

- ETC/ATNI, 2019, *Statistical modelling for long-term trends of pollutants. Use of a GAM model for the assessment of measurements of O3, NO2 and PM*, Eionet Report - ETC/ATNI 2019/14.
- Fleming, Z. L., et al., 2018, *Tropospheric Ozone Assessment Report: Present-day ozone distribution and trends relevant to human health*.
- Guerreiro, C. B. B., et al., 2014, *Air quality status and trends in Europe*, *Atmospheric Environment*, 98, 376-384, <https://doi.org/10.1016/j.atmosenv.2014.09.017>.
- Jonson, J. E., et al., 2006, *Can we explain the trends in European ozone levels?*, *Atmos. Chem. Phys.*, 6, 51-66, 10.5194/acp-6-51-2006.
- Lefohn, A. S., et al., 2016, *Responses of human health and vegetation exposure metrics to changes in ozone concentration distributions associated with changing emissions patterns in the European Union, United States, and China*, *Atmospheric Environment*, submitted, 2016.
- Malherbe, L., et al., 2017, *Analyse de Tendances Nationales en Matière de Qualité de l'Air*, LCSQA, Verneuil en Halatte.
- Malley, C. S., et al., 2015, *Trends and drivers of ozone human health and vegetation impact metrics from UK EMEP supersite measurements (1990–2013)*, *Atmos. Chem. Phys.*, 15, 4025-4042, 10.5194/acp-15-4025-2015.
- Monks, P. S., et al., 2015, *Tropospheric ozone and its precursors from the urban to the global scale from air quality to short-lived climate forcer*, *Atmos. Chem. Phys.*, 15, 8889-8973.
- Sicard, P., et al., 2013, *Decrease in surface ozone concentrations at Mediterranean remote sites and increase in the cities*, *Atmospheric Environment*, 79, 705-715, <https://doi.org/10.1016/j.atmosenv.2013.07.042>.
- Simpson, D., et al., 2014, *Ozone - the persistent menace: interactions with the N cycle and climate change*, *Current Opinion in Environmental Sustainability*, 9-10, 9-19.
- Solberg, S., et al., 2021, *Quantifying the Impact of the Covid-19 Lockdown Measures on Nitrogen Dioxide Levels throughout Europe*, 12, 131, <https://doi.org/10.3390/atmos12020131>, 2021.
- Tørseth, K., et al., 2012, *Introduction to the European Monitoring and Evaluation Programme (EMEP) and observed atmospheric composition change during 1972-2009*, *Atmos. Chem. Phys.*, 12, 5447-5481, 10.5194/acp-12-5447-2012.
- Turnock, S., et al., 2015, *Modelled and observed changes in aerosols and surface solar radiation over Europe between 1960 and 2009*, *Atmospheric Chemistry and Physics*, 15, 9477-9500.
- Turnock, S., et al., 2016, *The impact of European legislative and technology measures to reduce air pollutants on air quality, human health and climate*, *Environmental Research Letters*, 11, 024010.
- Vautard, R., et al., 2006, *Are decadal anthropogenic emission reductions in Europe consistent with surface ozone observations?*, *Geophys. Res. Lett.*, 33, L13810, 10.1029/2006GL026080.
- Walker, S.-E., et al., 2021, *The AirGAM air quality trend and prediction model*, *Geosci. Model Dev.*, (to be submitted).
- Wilson, R. C., et al., 2012, *Have primary emission reduction measures reduced ozone across Europe? An analysis of European rural background ozone trends 1996-2005*, *Atmos. Chem. Phys.*, 12, 437-454.

Annex 1

National trends in air concentrations as calculated from in-situ measurements

Air Quality Trends in Europe : 2005-2019

-

INERIS

January 27, 2022

Contents

1	Austria	49
2	Belgium	58
3	Bulgaria	67
4	Switzerland	75
5	Czechia	81
6	Germany	90
7	Denmark	99
8	Estonia	107
9	Spain	115
10	Finland	124
11	France	132
12	Great Britain	141
13	Greece	150
14	Croatia	158
15	Hungary	165
16	Ireland	173
17	Italy	181
18	Lithuania	190
19	Luxembourg	198
20	Republic of North Macedonia	206

21 Netherlands	212
22 Norway	221
23 Poland	228
24 Portugal	237
25 Romania	246
26 Sweden	254
27 Slovenia	262
28 Slovakia	270

1 Austria

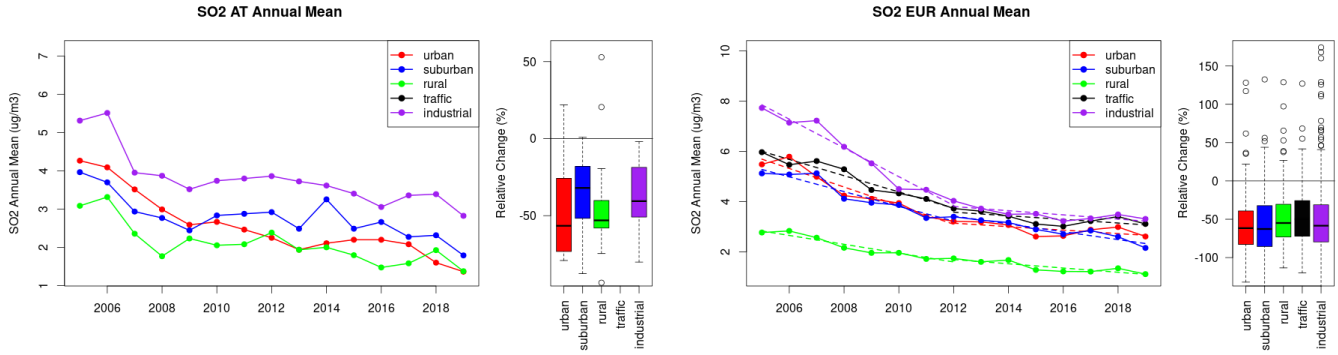


Figure S.1: Time series of the Austria (left) and European-wide composite (median) of annual mean SO₂ (ug/m³) per station type and area (red: urban background, blue suburban background, green: rural background, black: traffic, violet: industrial) between 2005 and 2019. In the European composite, the dashed lines show the linear fit between 2005 & 2012 and between 2012 & 2019. The boxplots on the right-hand side show the distribution of relative changes (%) between 2005 and 2019 for all stations of each typology in Austria and in Europe.

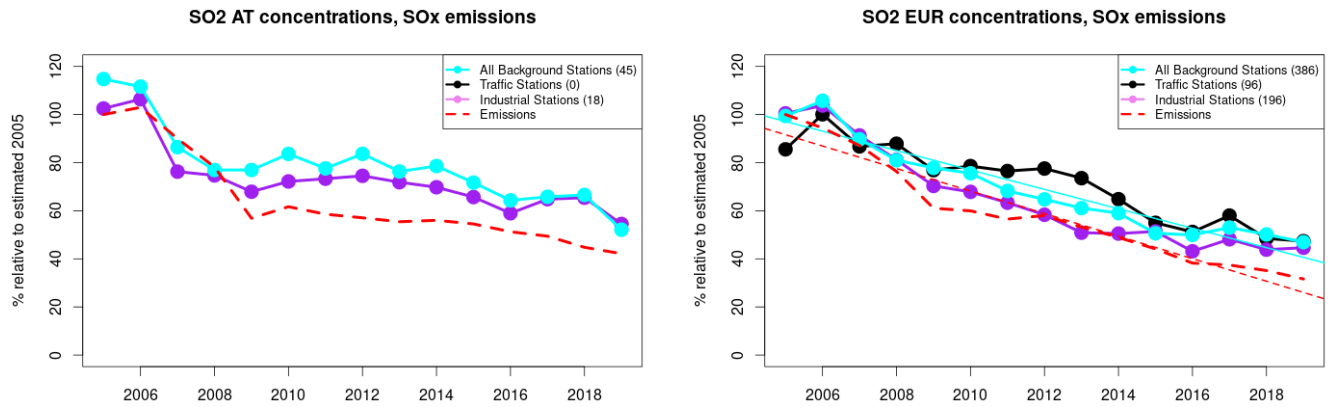


Figure S.2: Time series of 2005-2019 (left) and European (right) median SO₂ observed at traffic (black), industrial (violet) and background (cyan) sites (solid lines), and corresponding SO_x emissions (dashed line) normalised to estimated 2000 levels (%). The median is taken over where more than 5 stations of each typology is available. The total number of stations included is provided in brackets. In the European composite, straight lines are the linear fits over the whole period.

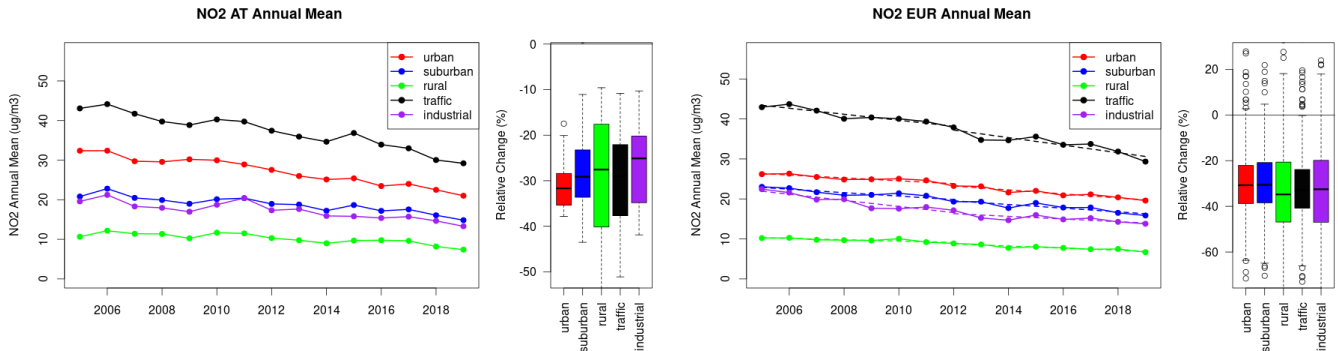


Figure S.3: Time series of the Austria (left) and European-wide composite (median) of annual mean NO₂ (ug/m³) per station type and area (red: urban background, blue suburban background, green: rural background, black: traffic, violet: industrial) between 2005 and 2019. In the European composite, the dashed lines show the linear fit between 2005 & 2012 and between 2012 & 2019. The boxplots on the right-hand side show the distribution of relative changes (%) between 2005 and 2019 for all stations of each typology in Austria and in Europe.

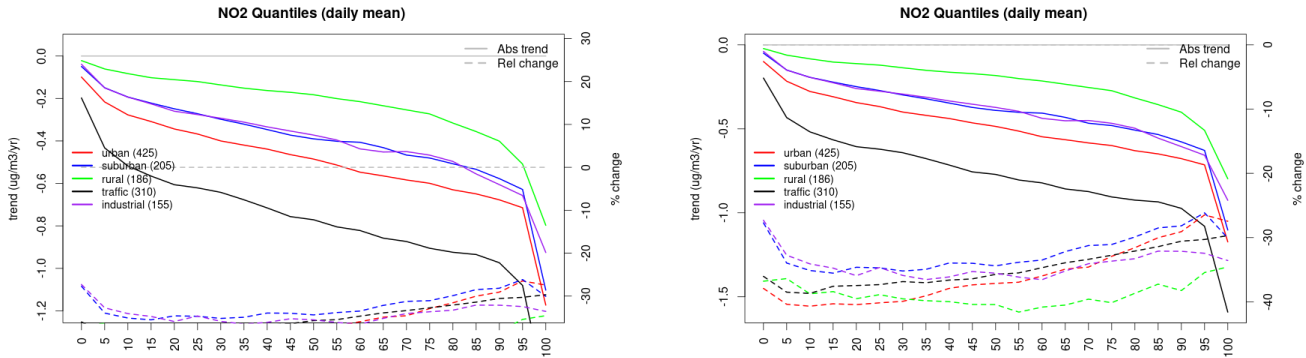


Figure S.4: For NO₂ in Austria (left) and Europe, and for each typology of station: absolute trend (solid lines, left y-axis) and relative change (dashed lines, right y-axis) of the percentiles of daily means.

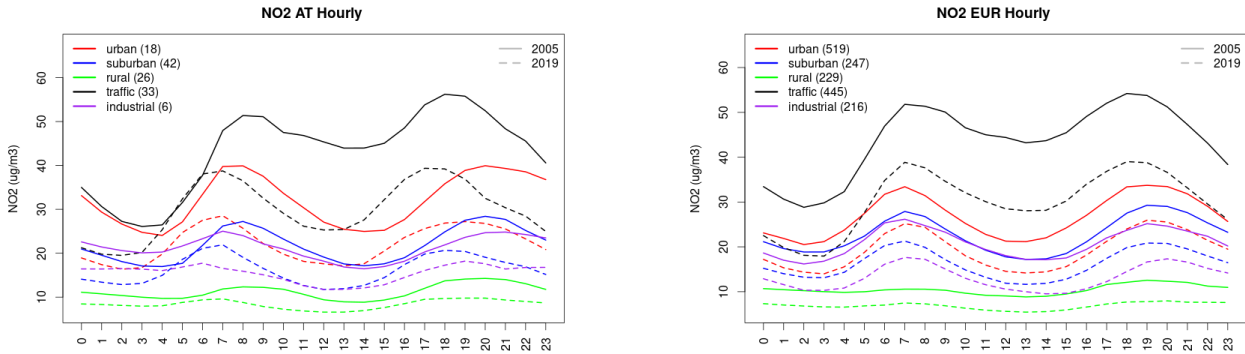


Figure S.5: Diurnal cycle of daily mean NO₂ for Austria (left) and Europe (right) at various station types estimated from the whole time series in 2005 (solid lines) and 2019

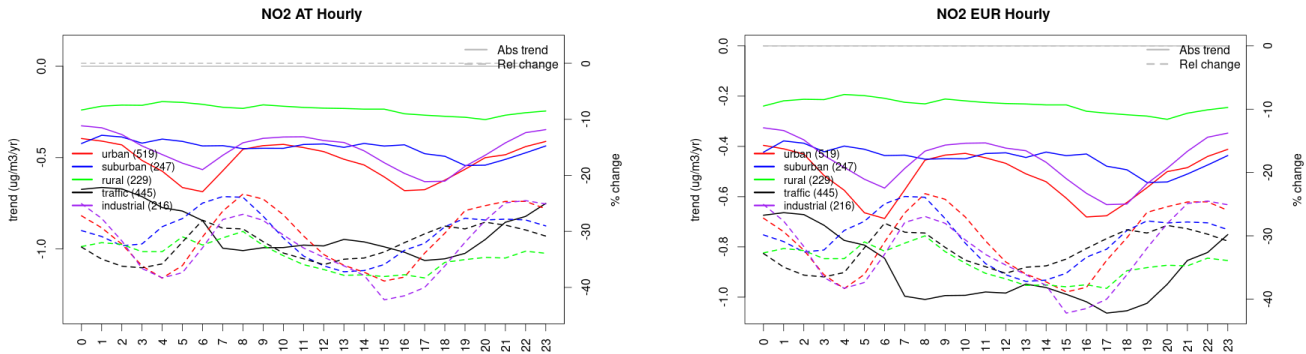


Figure S.6: Absolute (solid lines, left axis) and relative (dashed lines, right axis) trends in the diurnal cycle for Austria (left) and Europe (right) of NO₂ at various station type.

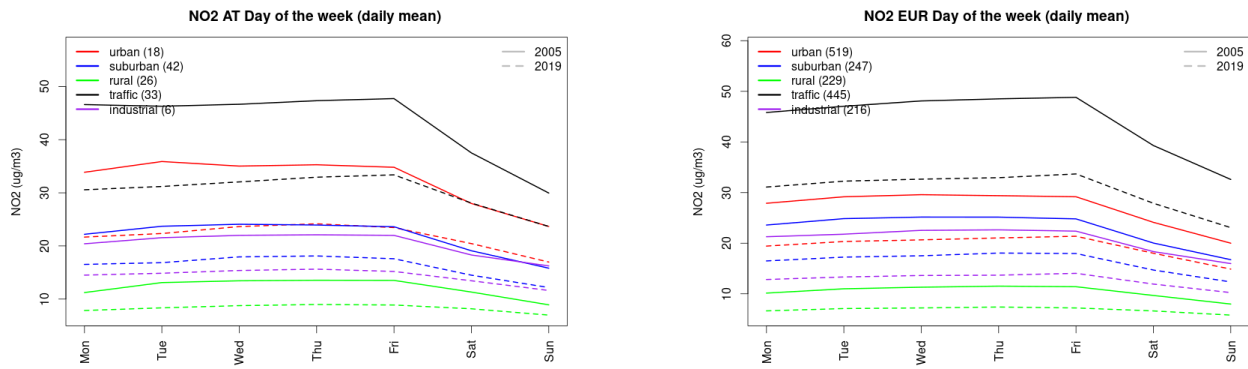


Figure S.7: Weekly cycle of daily mean NO2 for Austria (left) and Europe (right) at various station types estimated from the whole time series in 2005 (solid lines) and 2019

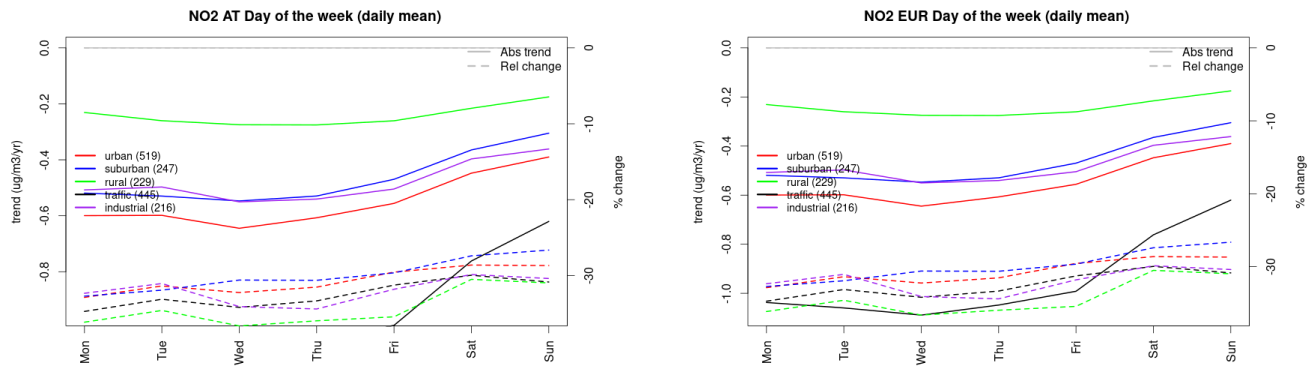


Figure S.8: Absolute (solid lines, left axis) and relative (dashed lines, right axis) trends in the weekly cycle for Austria (left) and Europe (right) of NO2 at various station type.

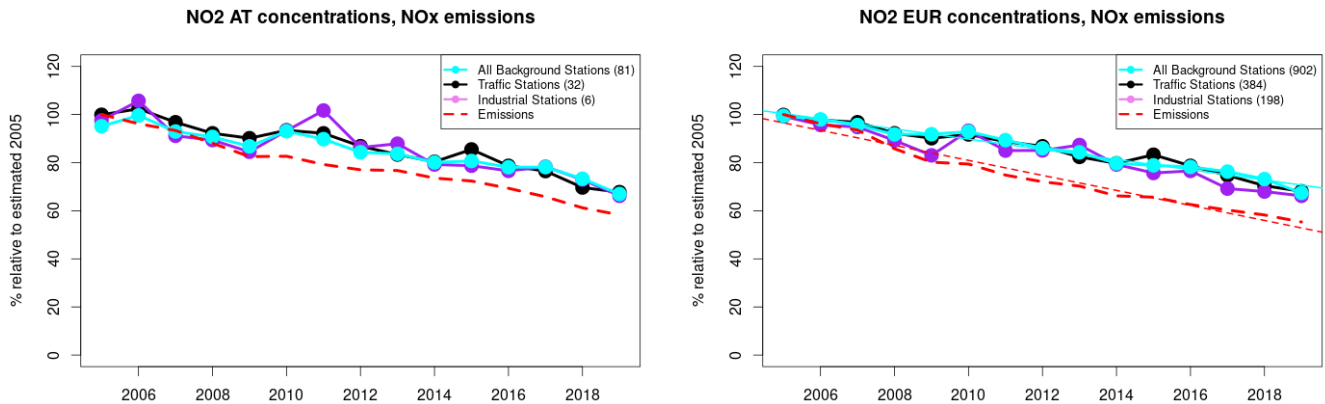


Figure S.9: Time series of 2005-2019 (left) and European (right) median NO2 observed at traffic (black), industrial (violet) and background (cyan) sites (solid lines), and corresponding NOx emissions (dashed line) normalised to estimated 2000 levels (%). The median is taken over where more than 5 stations of each typology is available. The total number of stations included is provided in brackets. In the European composite, straight lines are the linear fits over the whole period.

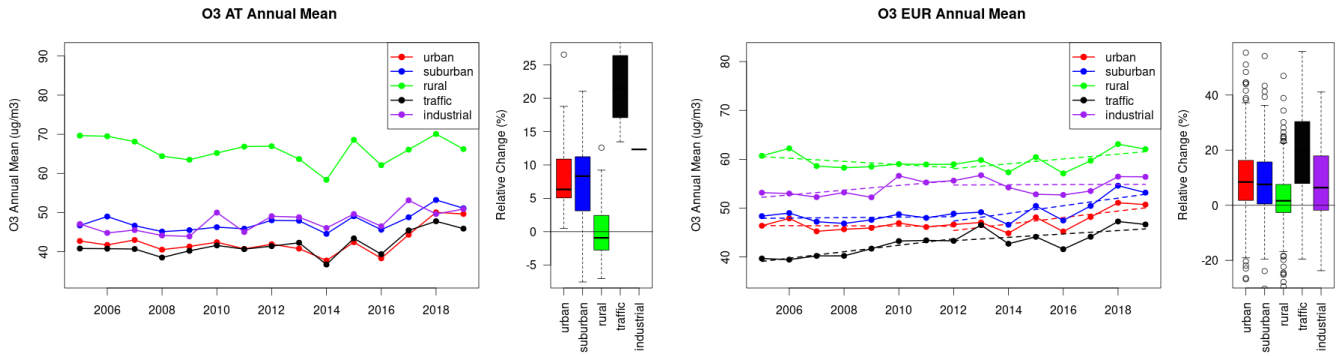


Figure S.10: Time series of the Austria (left) and European-wide composite (median) of annual mean ozone ($\mu\text{g}/\text{m}^3$) per station type and area (red: urban background, blue suburban background, green: rural background, black: traffic, violet: industrial) between 2005 and 2019. In the European composite, the dashed lines show the linear fit between 2005 & 2012 and between 2012 & 2019. The boxplots on the right-hand side show the distribution of relative changes (%) between 2005 and 2019 for all stations of each typology in Austria and in Europe.

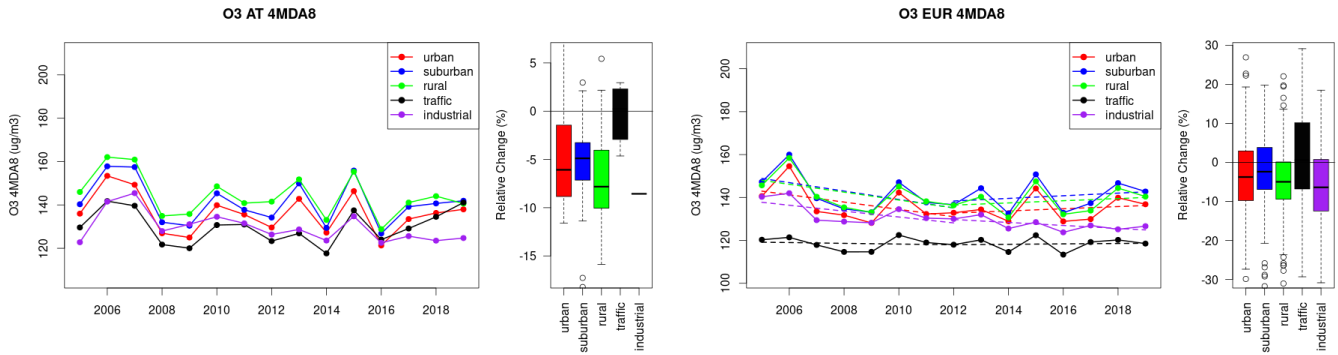


Figure S.11: Time series of the Austria (left) and European-wide composite (median) of O3 fourth highest daily peak (4MDA8, $\mu\text{g}/\text{m}^3$) per station type and area (red: urban background, blue suburban background, green: rural background, black: traffic, violet: industrial) between 2005 and 2019. In the European composite, the dashed lines show the linear fit between 2005 & 2012 and between 2012 & 2019. The boxplots on the right-hand side show the distribution of relative changes (%) between 2005 and 2019 for all stations of each typology in Austria and in Europe.

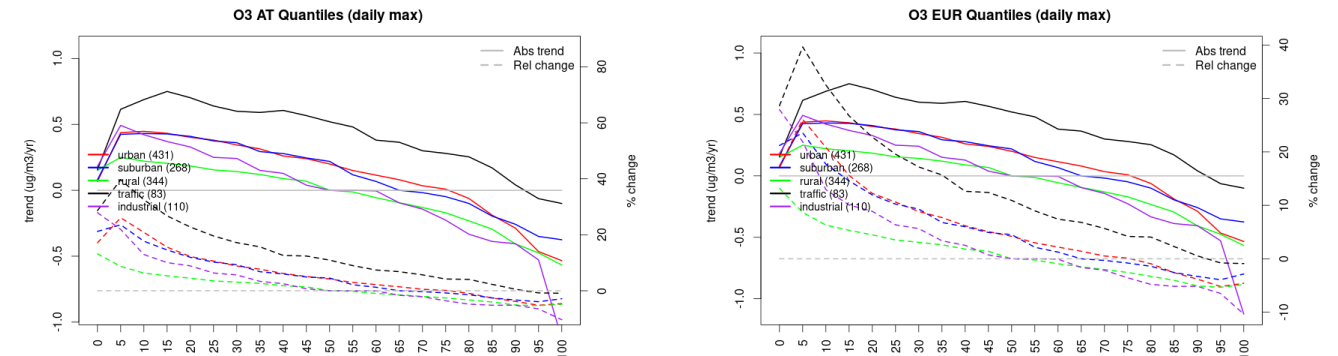


Figure S.12: For ozone in Austria (left) and Europe, and for each typology of station: absolute trend (solid lines, left y-axis) and relative change (dashed lines, right y-axis) of the percentiles of daily maxima.

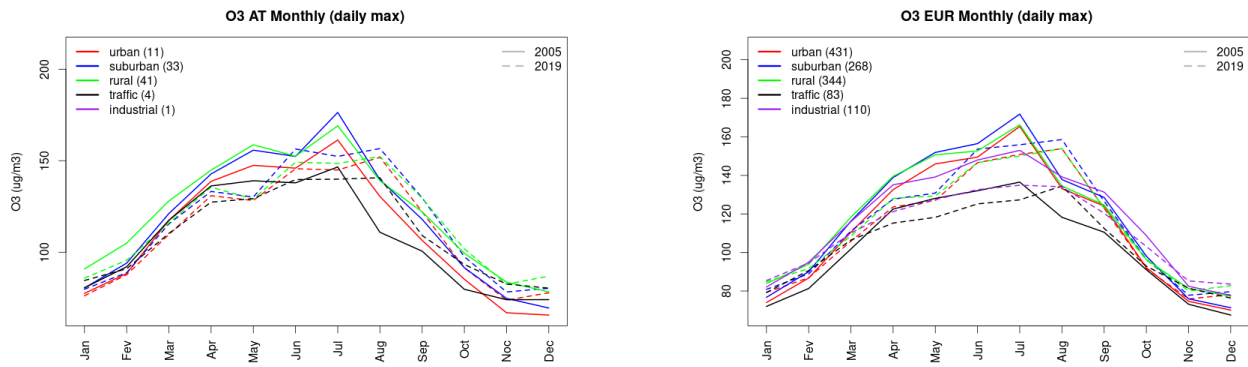


Figure S.13: Monthly cycle of daily max ozone for Austria (left) and Europe (right) at various station types estimated from the whole time series in 2005 (solid lines) and 2019

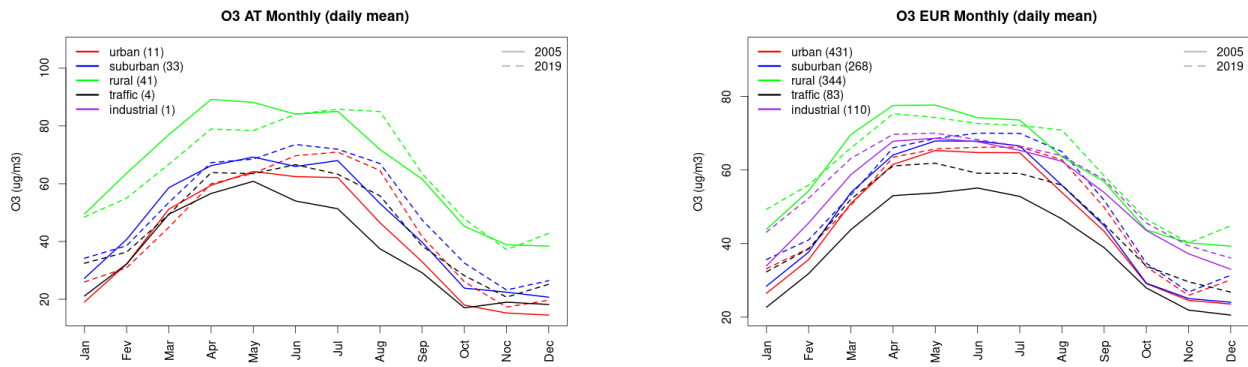


Figure S.14: Monthly cycle of daily mean ozone for Austria (left) and Europe (right) at various station types estimated from the whole time series in 2005 (solid lines) and 2019

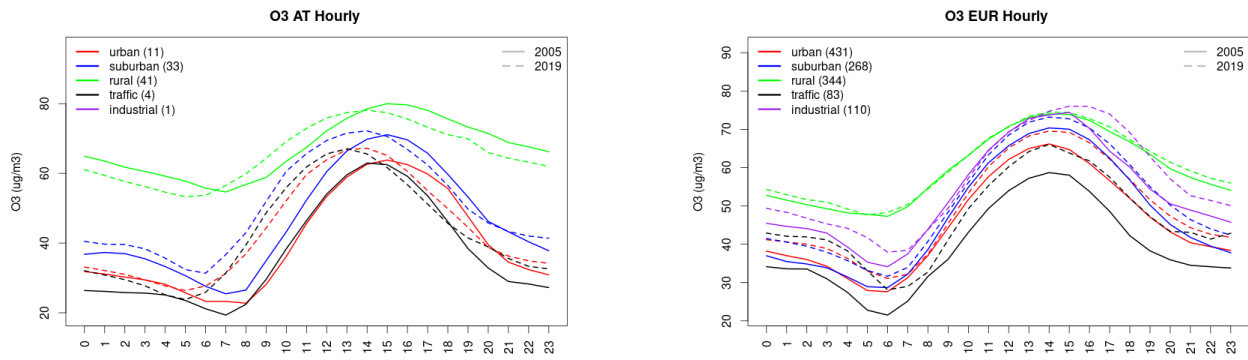


Figure S.15: Diurnal cycle of daily mean ozone for Austria (left) and Europe (right) at various station types estimated from the whole time series in 2005 (solid lines) and 2019

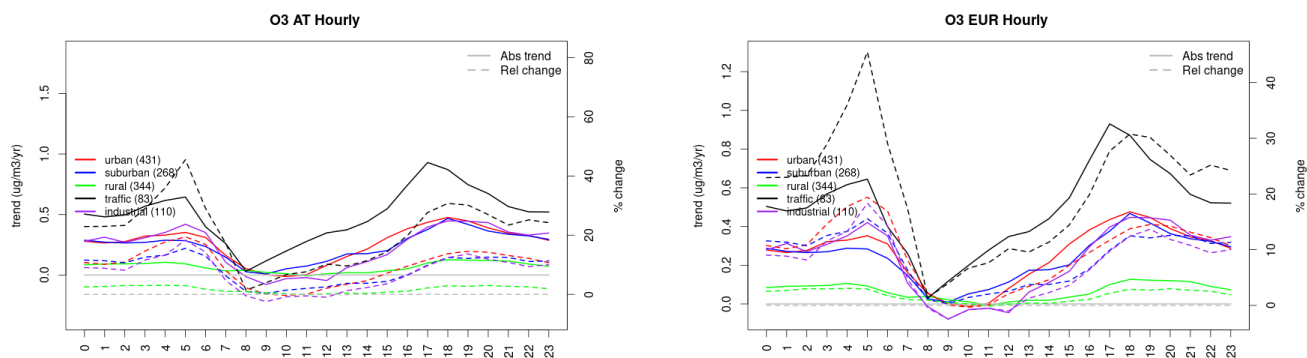


Figure S.16: Absolute (solid lines, left axis) and relative (dashed lines, right axis) trends in the diurnal cycle for Austria (left) and Europe (right) of ozone at various station type.

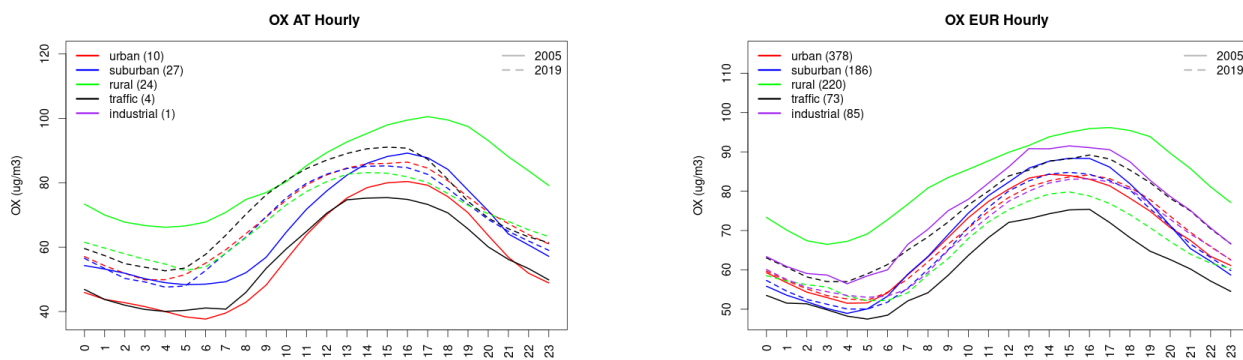


Figure S.17: Diurnal cycle of daily mean OX (as NO₂+O₃) for Austria (left) and Europe (right) at various station types estimated from the whole time series in 2005 (solid lines) and 2019

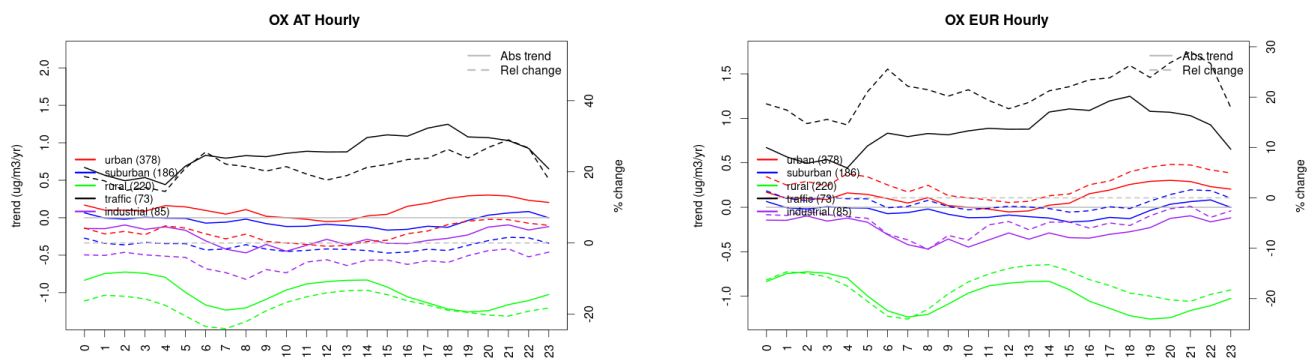


Figure S.18: Absolute (solid lines, left axis) and relative (dashed lines, right axis) trends in the diurnal cycle for Austria (left) and Europe (right) of OX (as NO₂+O₃) at various station type.

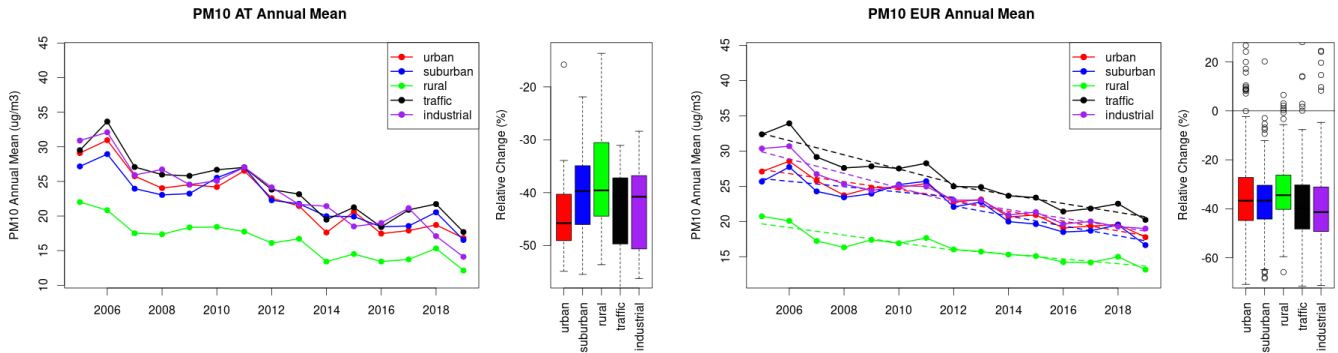


Figure S.19: Time series of the Austria (left) and European-wide composite (median) of annual mean PM10 ($\mu\text{g}/\text{m}^3$) per station type and area (red: urban background, blue suburban background, green: rural background, black: traffic, violet: industrial) between 2005 and 2019. In the European composite, the dashed lines show the linear fit between 2005 & 2012 and between 2012 & 2019. The boxplots on the right-hand side show the distribution of relative changes (%) between 2005 and 2019 for all stations of each typology in Austria and in Europe.

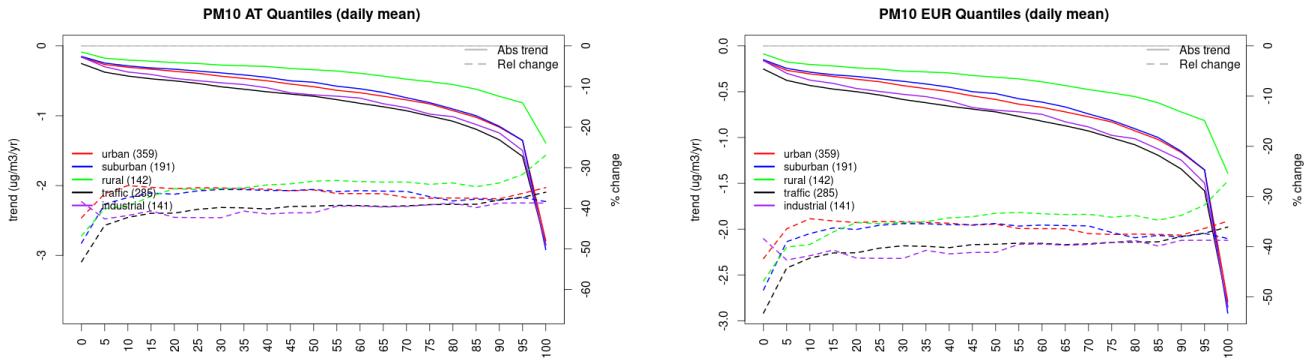


Figure S.20: For PM10 in Austria (left) and Europe, and for each typology of station: absolute trend (solid lines, left y-axis) and relative change (dashed lines, right y-axis) of the percentiles of daily means.

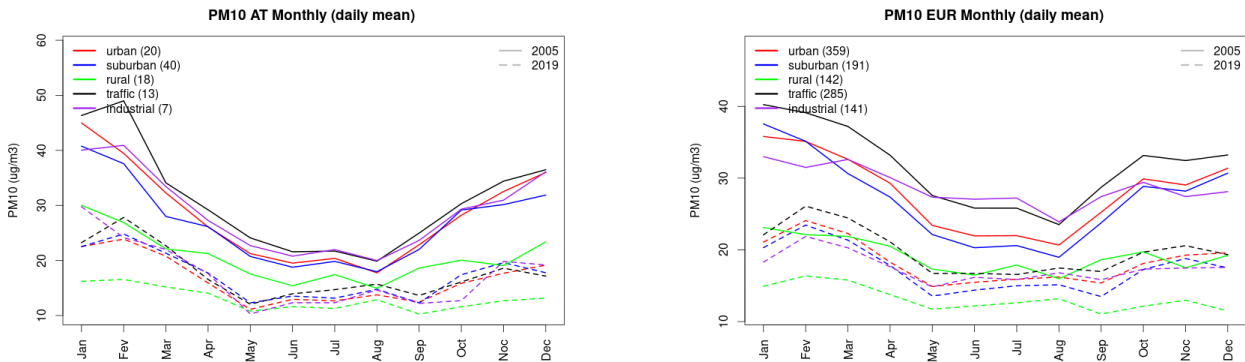


Figure S.21: Monthly cycle of daily mean PM10 for Austria (left) and Europe (right) at various station types estimated from the whole time series in 2005 (solid lines) and 2019

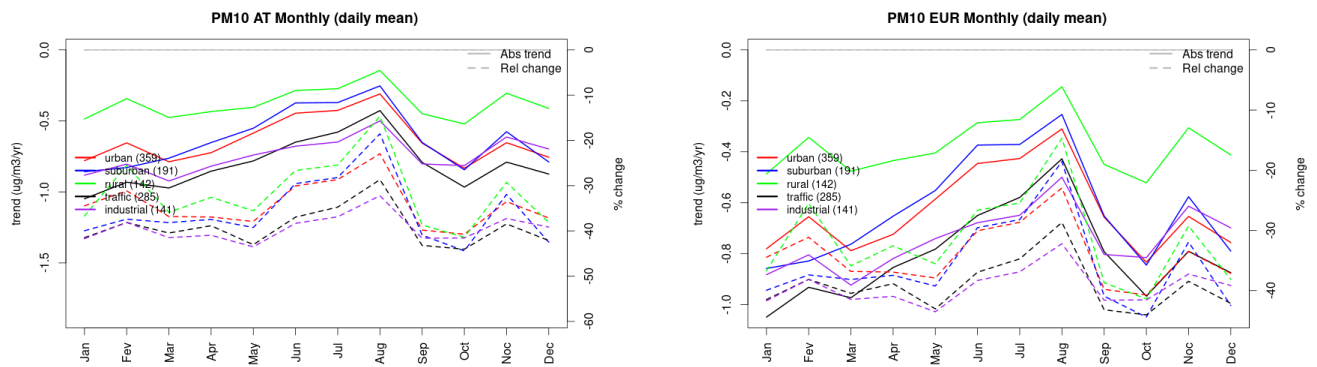


Figure S.22: Absolute (solid lines, left axis) and relative (dashed lines, right axis) trends in the monthly cycle for Austria (left) and Europe (right) of PM10 at various station type.

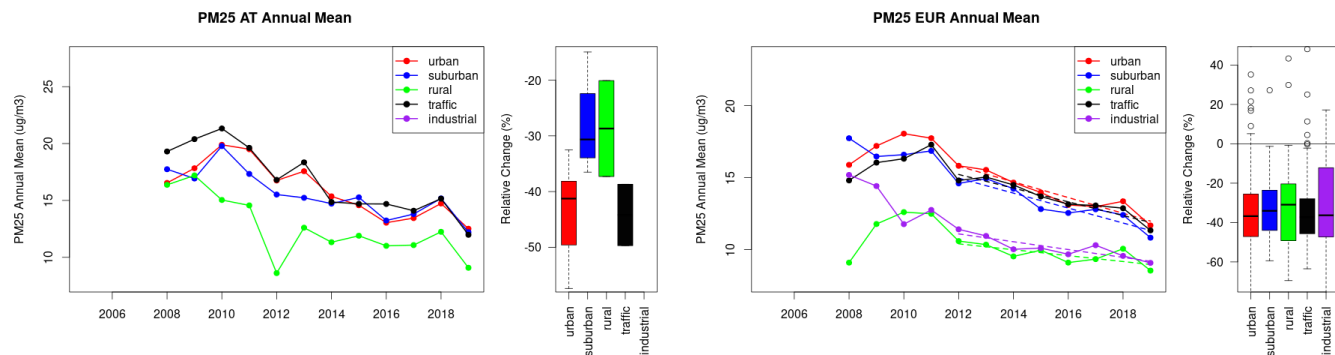


Figure S.23: Time series of the Austria (left) and European-wide composite (median) of annual mean PM25 ($\mu\text{g}/\text{m}^3$) per station type and area (red: urban background, blue suburban background, green: rural background, black: traffic, violet: industrial) between 2005 and 2019. In the European composite, the dashed lines show the linear fit between 2005 & 2012 and between 2012 & 2019. The boxplots on the right-hand side show the distribution of relative changes (%) between 2005 and 2019 for all stations of each typology in Austria and in Europe.

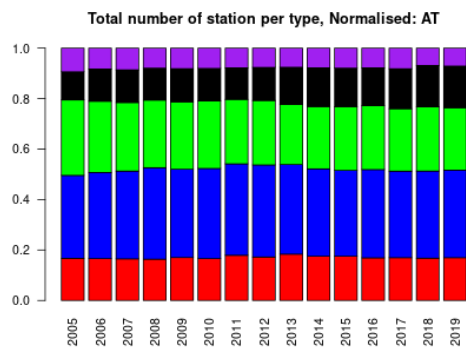
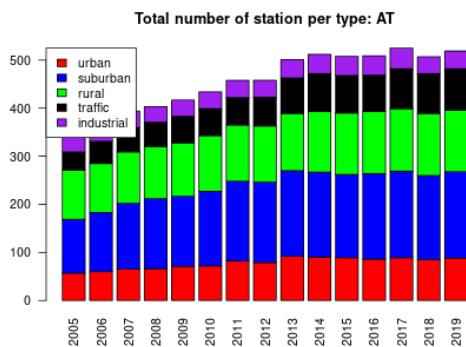
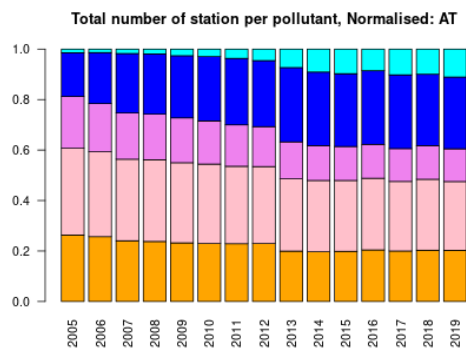
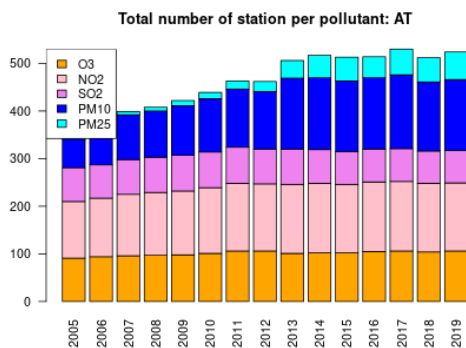
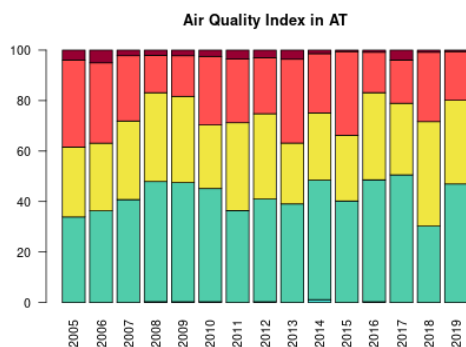


Figure S.24: For Austria: overall air quality index (percentage of days in a given year) and distribution of daily categories per pollutant (light blue: good, light green: fair, yellow: moderate, orange: poor, red: very poor, violet: extremely poor).

2 Belgium

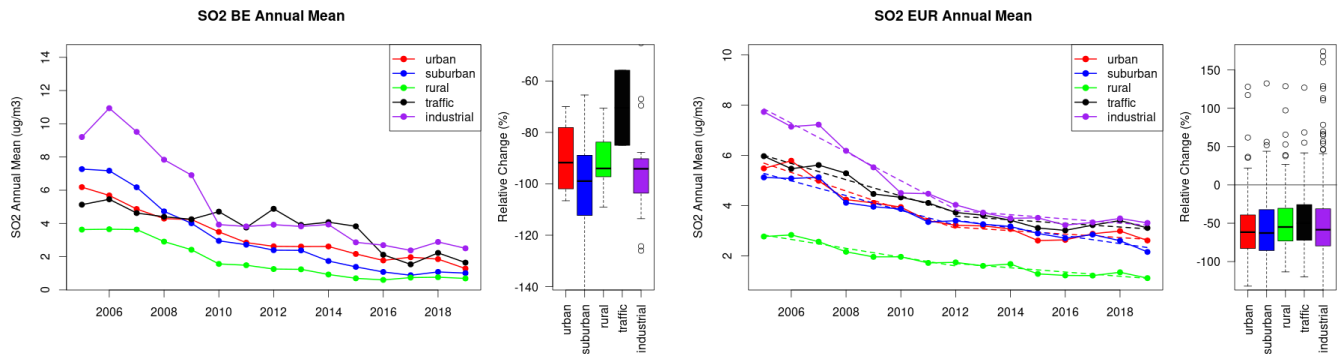


Figure S.25: Time series of the Belgium (left) and European-wide composite (median) of annual mean SO₂ (ug/m³) per station type and area (red: urban background, blue suburban background, green: rural background, black: traffic, violet: industrial) between 2005 and 2019. In the European composite, the dashed lines show the linear fit between 2005 & 2012 and between 2012 & 2019. The boxplots on the right-hand side show the distribution of relative changes (%) between 2005 and 2019 for all stations of each typology in Belgium and in Europe.

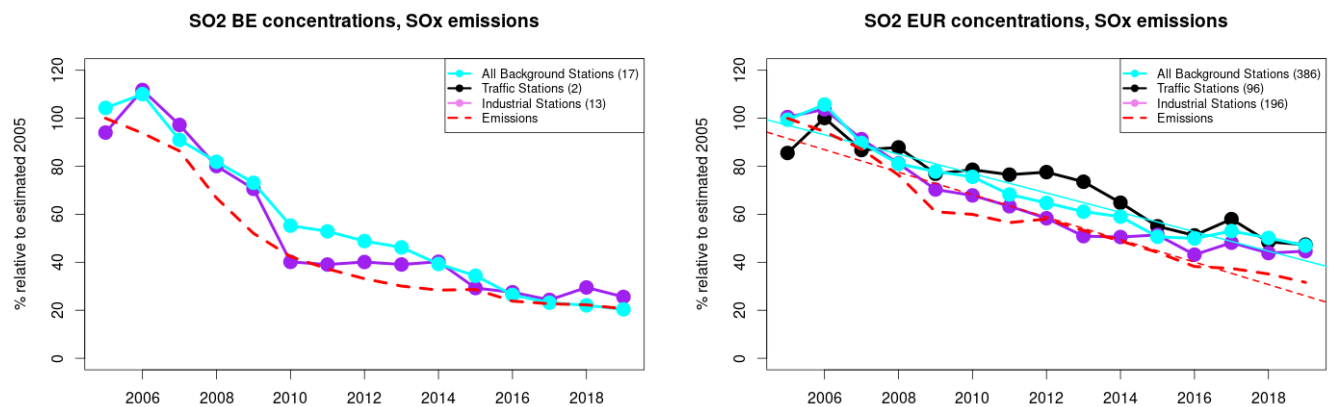


Figure S.26: Time series of 2005-2019 (left) and European (right) median SO₂ observed at traffic (black), industrial (violet) and background (cyan) sites (solid lines), and corresponding SO_x emissions (dashed line) normalised to estimated 2000 levels (%). The median is taken over where more than 5 stations of each typology is available. The total number of stations included is provided in brackets. In the European composite, straight lines are the linear fits over the whole period.

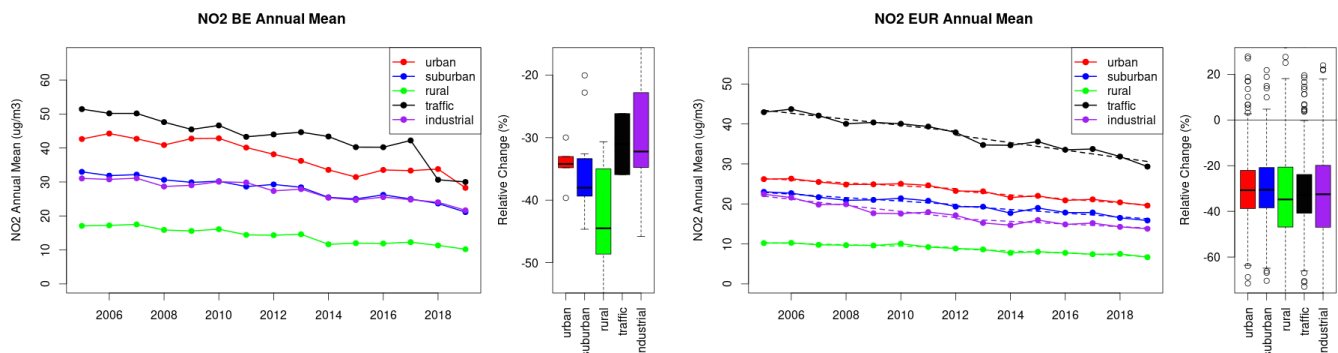


Figure S.27: Time series of the Belgium (left) and European-wide composite (median) of annual mean NO₂ (ug/m³) per station type and area (red: urban background, blue suburban background, green: rural background, black: traffic, violet: industrial) between 2005 and 2019. In the European composite, the dashed lines show the linear fit between 2005 & 2012 and between 2012 & 2019. The boxplots on the right-hand side show the distribution of relative changes (%) between 2005 and 2019 for all stations of each typology in Belgium and in Europe.

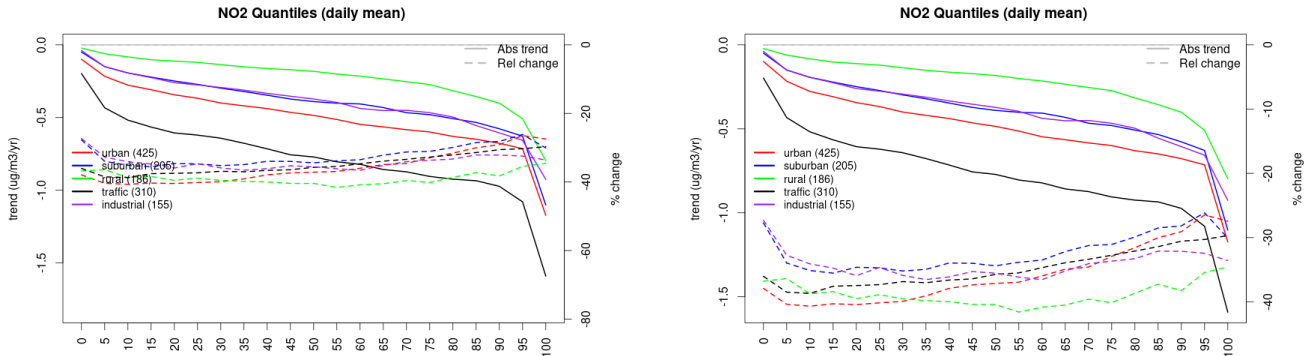


Figure S.28: For NO₂ in Belgium (left) and Europe, and for each typology of station: absolute trend (solid lines, left y-axis) and relative change (dashed lines, right y-axis) of the percentiles of daily means.

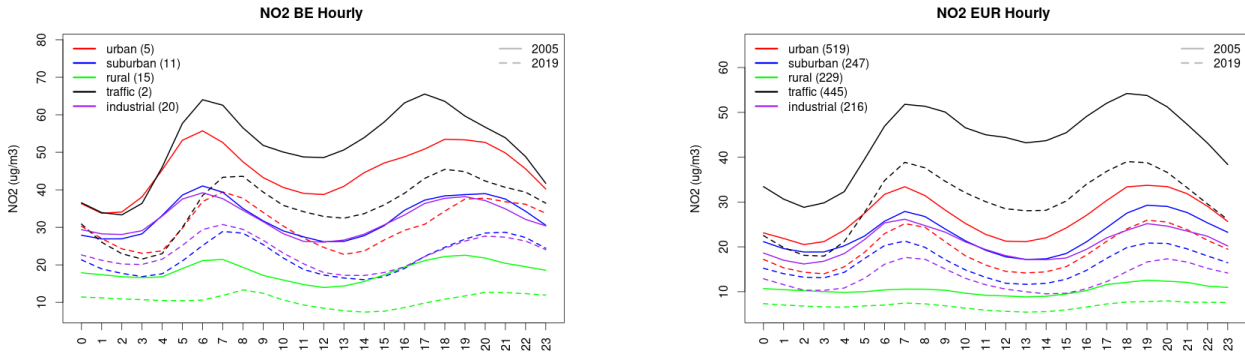


Figure S.29: Diurnal cycle of daily mean NO₂ for Belgium (left) and Europe (right) at various station types estimated from the whole time series in 2005 (solid lines) and 2019

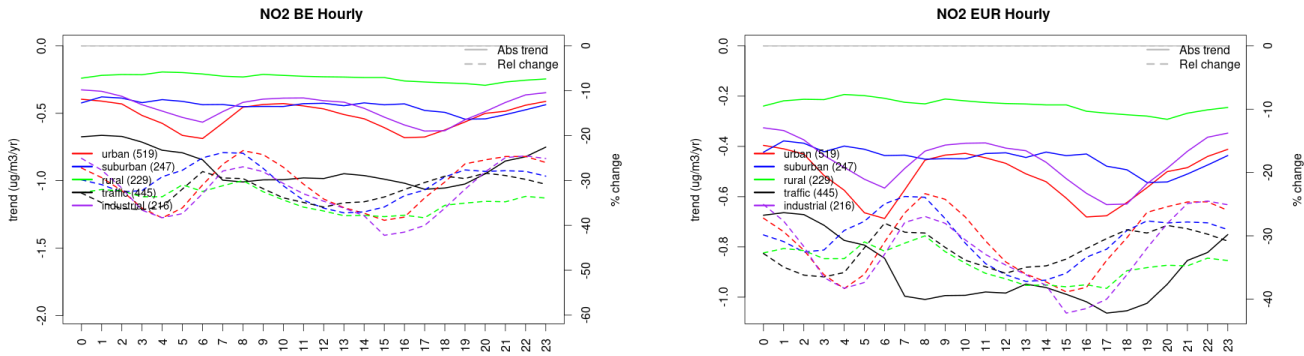


Figure S.30: Absolute (solid lines, left axis) and relative (dashed lines, right axis) trends in the diurnal cycle for Belgium (left) and Europe (right) of NO₂ at various station type.

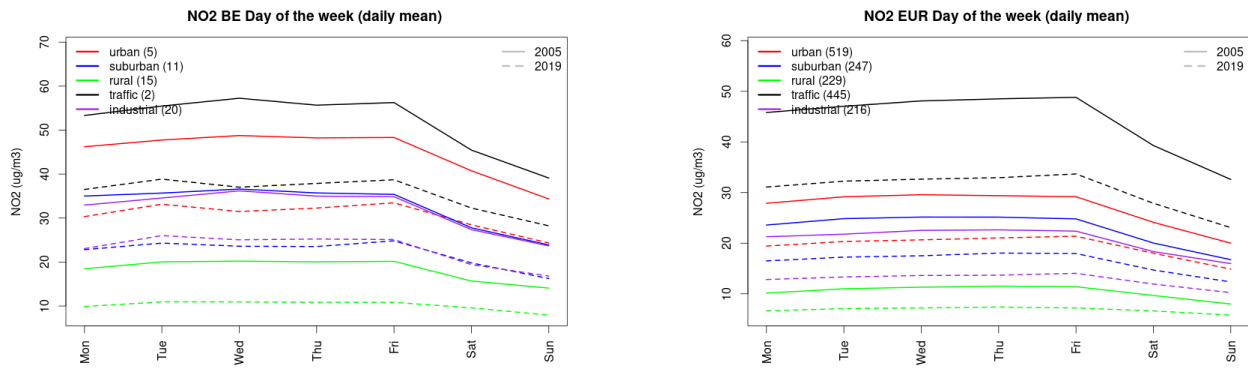


Figure S.31: Weekly cycle of daily mean NO₂ for Belgium (left) and Europe (right) at various station types estimated from the whole time series in 2005 (solid lines) and 2019

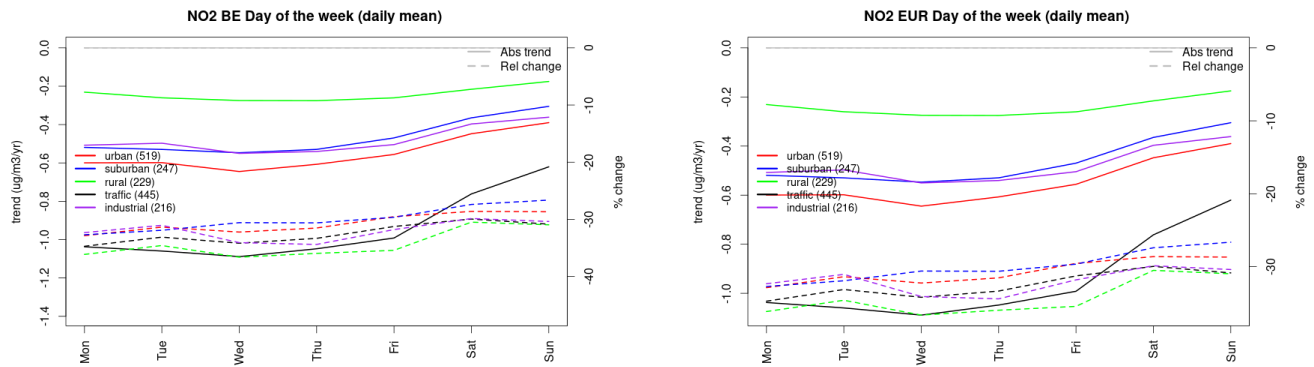


Figure S.32: Absolute (solid lines, left axis) and relative (dashed lines, right axis) trends in the weekly cycle for Belgium (left) and Europe (right) of NO₂ at various station type.

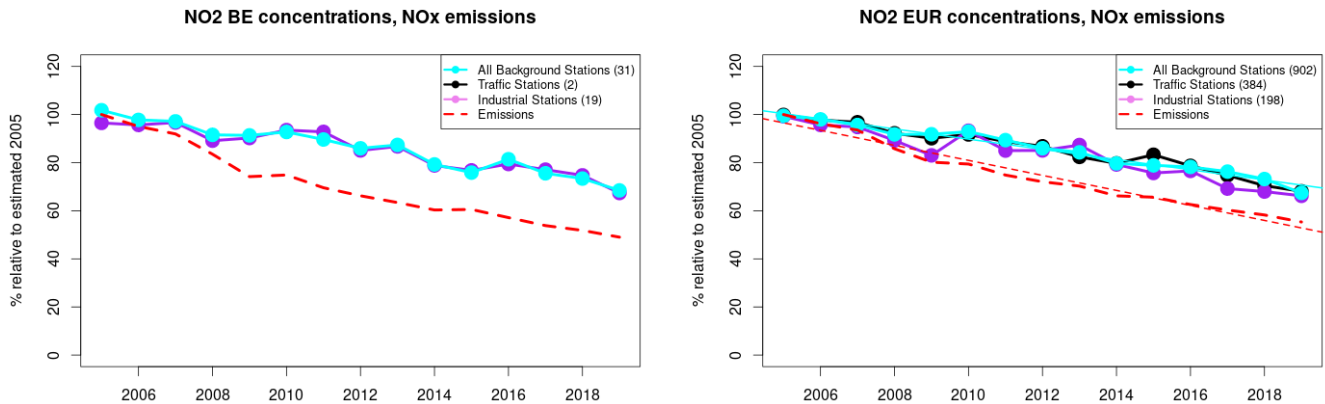


Figure S.33: Time series of 2005-2019 (left) and European (right) median NO₂ observed at traffic (black), industrial (violet) and background (cyan) sites (solid lines), and corresponding NO_x emissions (dashed line) normalised to estimated 2000 levels (%). The median is taken over where more than 5 stations of each typology is available. The total number of stations included is provided in brackets. In the European composite, straight lines are the linear fits over the whole period.

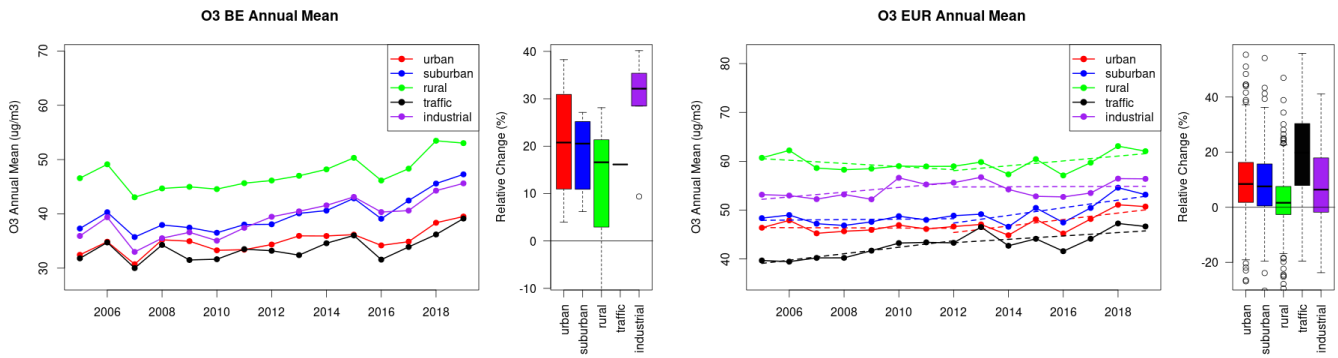


Figure S.34: Time series of the Belgium (left) and European-wide composite (median) of annual mean ozone ($\mu\text{g}/\text{m}^3$) per station type and area (red: urban background, blue suburban background, green: rural background, black: traffic, violet: industrial) between 2005 and 2019. In the European composite, the dashed lines show the linear fit between 2005 & 2012 and between 2012 & 2019. The boxplots on the right-hand side show the distribution of relative changes (%) between 2005 and 2019 for all stations of each typology in Belgium and in Europe.

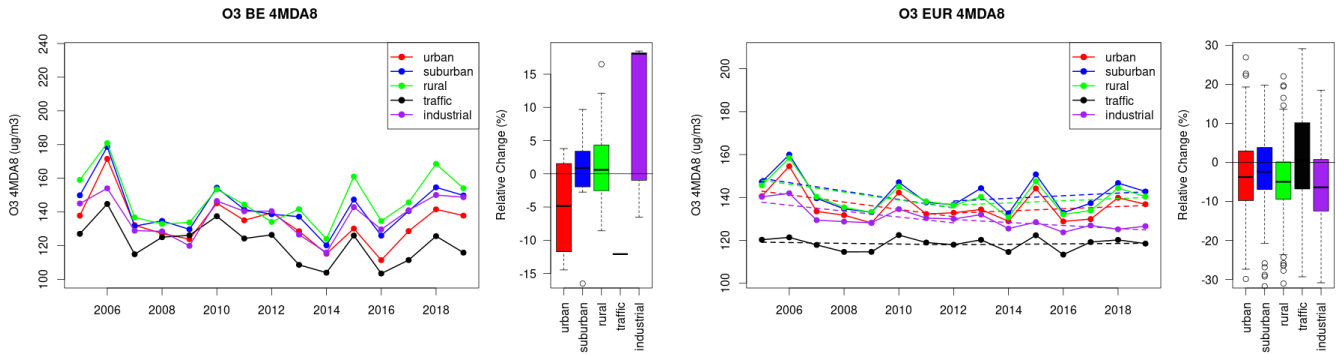


Figure S.35: Time series of the Belgium (left) and European-wide composite (median) of O3 fourth highest daily peak (4MDA8, $\mu\text{g}/\text{m}^3$) per station type and area (red: urban background, blue suburban background, green: rural background, black: traffic, violet: industrial) between 2005 and 2019. In the European composite, the dashed lines show the linear fit between 2005 & 2012 and between 2012 & 2019. The boxplots on the right-hand side show the distribution of relative changes (%) between 2005 and 2019 for all stations of each typology in Belgium and in Europe.

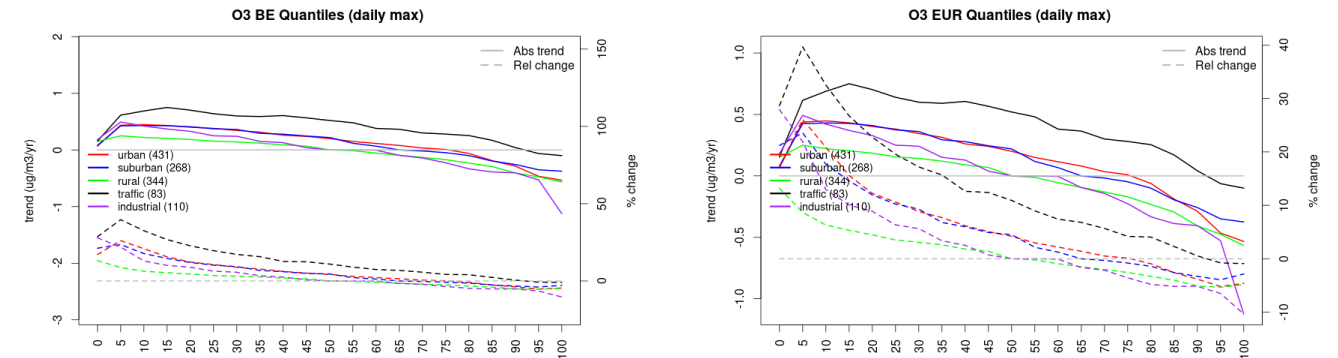


Figure S.36: For ozone in Belgium (left) and Europe, and for each typology of station: absolute trend (solid lines, left y-axis) and relative change (dashed lines, right y-axis) of the percentiles of daily maxima.

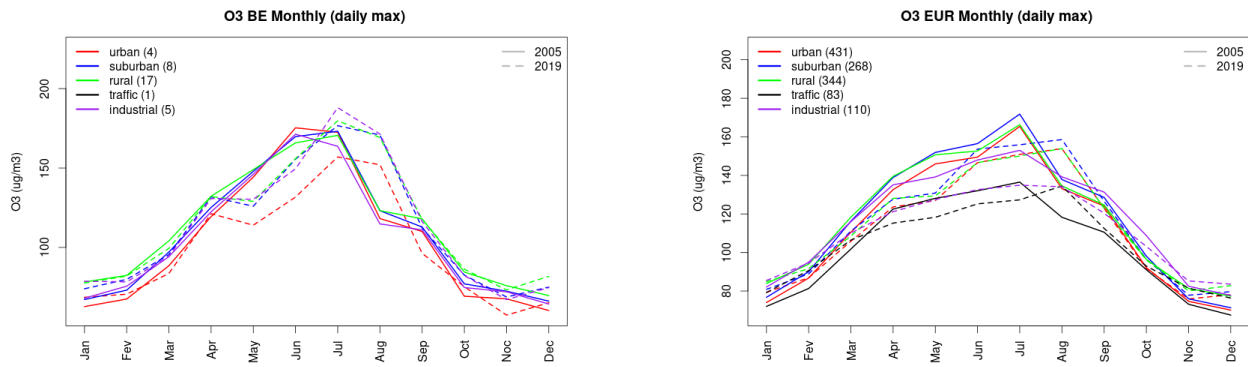


Figure S.37: Monthly cycle of daily max ozone for Belgium (left) and Europe (right) at various station types estimated from the whole time series in 2005 (solid lines) and 2019

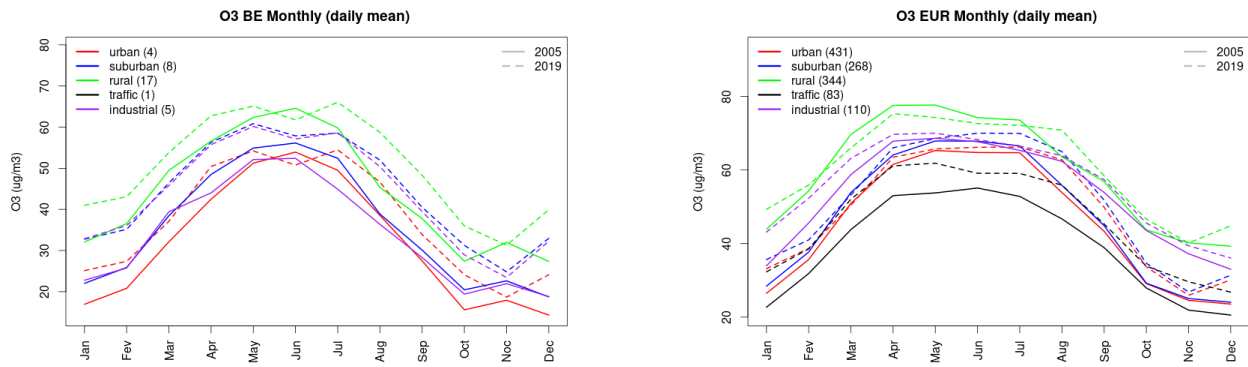


Figure S.38: Monthly cycle of daily mean ozone for Belgium (left) and Europe (right) at various station types estimated from the whole time series in 2005 (solid lines) and 2019

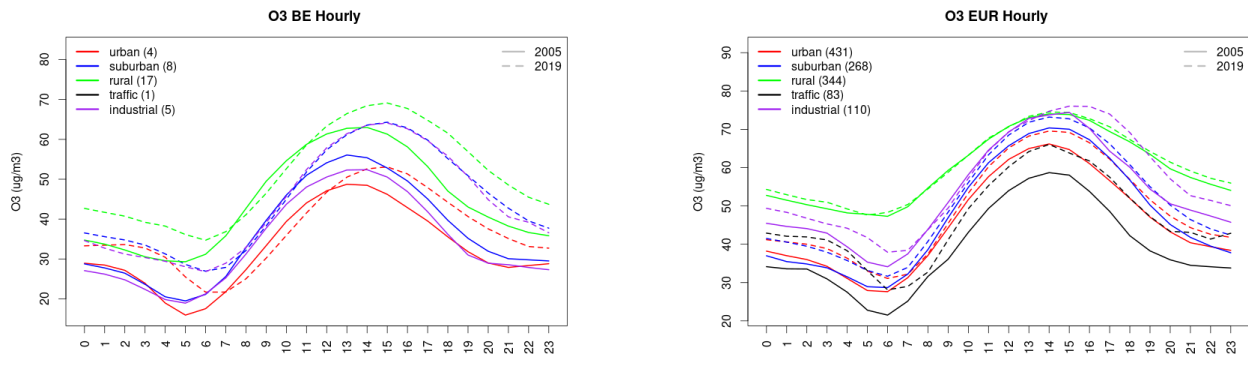


Figure S.39: Diurnal cycle of daily mean ozone for Belgium (left) and Europe (right) at various station types estimated from the whole time series in 2005 (solid lines) and 2019

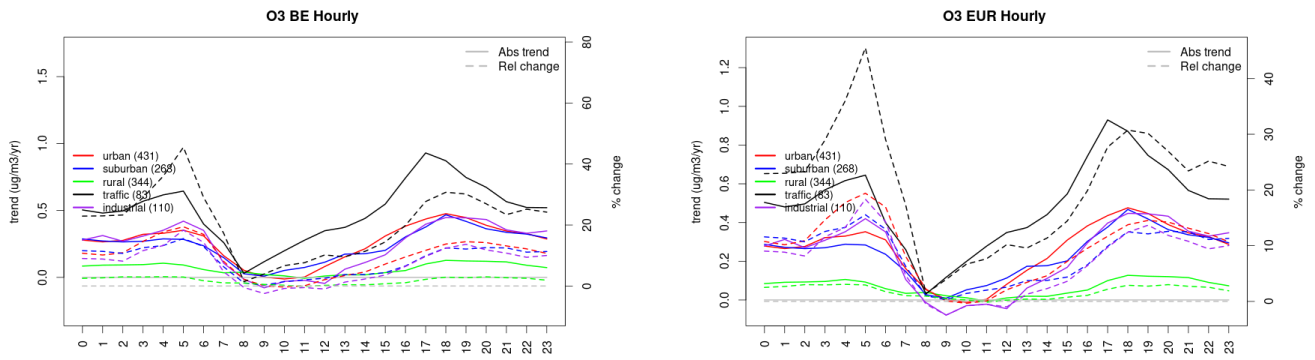


Figure S.40: Absolute (solid lines, left axis) and relative (dashed lines, right axis) trends in the diurnal cycle for Belgium (left) and Europe (right) of ozone at various station type.

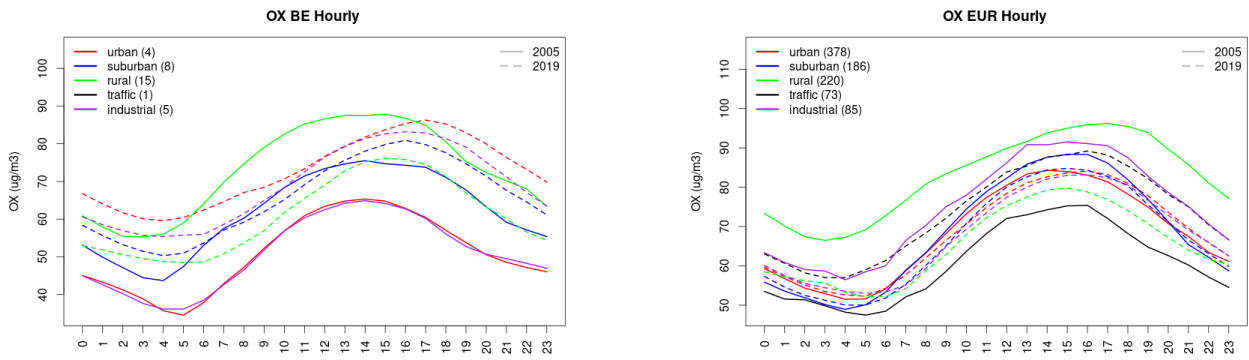


Figure S.41: Diurnal cycle of daily mean OX (as NO₂+O₃) for Belgium (left) and Europe (right) at various station types estimated from the whole time series in 2005 (solid lines) and 2019

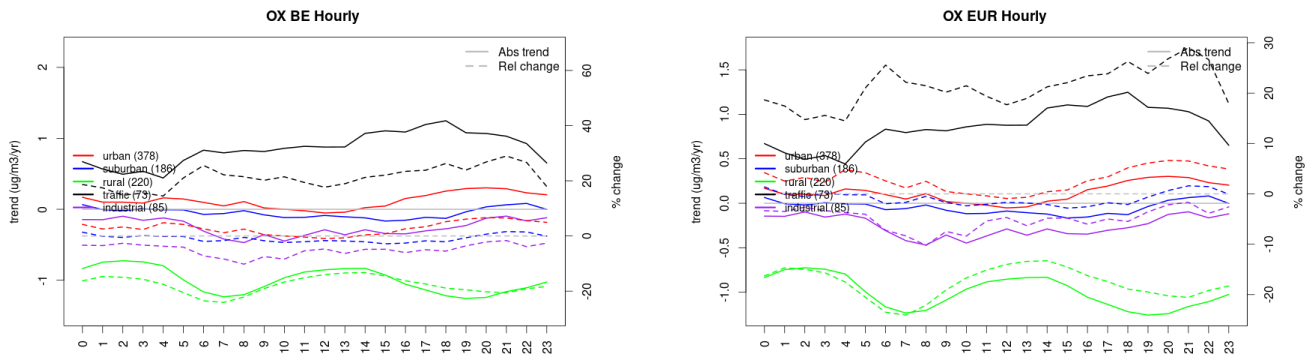


Figure S.42: Absolute (solid lines, left axis) and relative (dashed lines, right axis) trends in the diurnal cycle for Belgium (left) and Europe (right) of OX (as NO₂+O₃) at various station type.

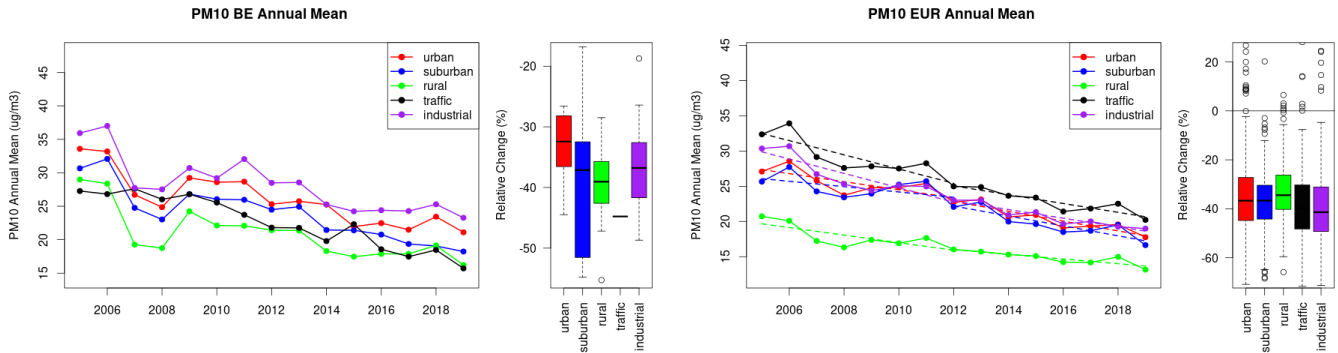


Figure S.43: Time series of the Belgium (left) and European-wide composite (median) of annual mean PM10 ($\mu\text{g}/\text{m}^3$) per station type and area (red: urban background, blue suburban background, green: rural background, black: traffic, violet: industrial) between 2005 and 2019. In the European composite, the dashed lines show the linear fit between 2005 & 2012 and between 2012 & 2019. The boxplots on the right-hand side show the distribution of relative changes (%) between 2005 and 2019 for all stations of each typology in Belgium and in Europe.

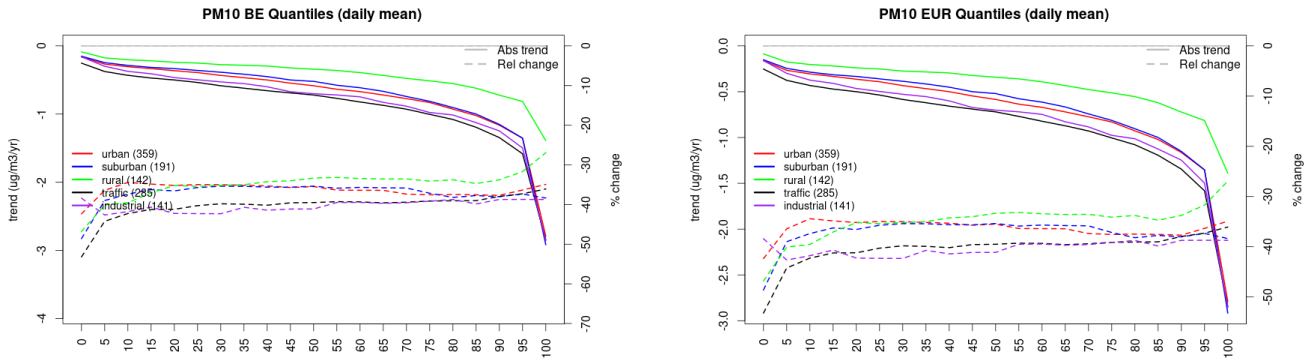


Figure S.44: For PM10 in Belgium (left) and Europe, and for each typology of station: absolute trend (solid lines, left y-axis) and relative change (dashed lines, right y-axis) of the percentiles of daily means.

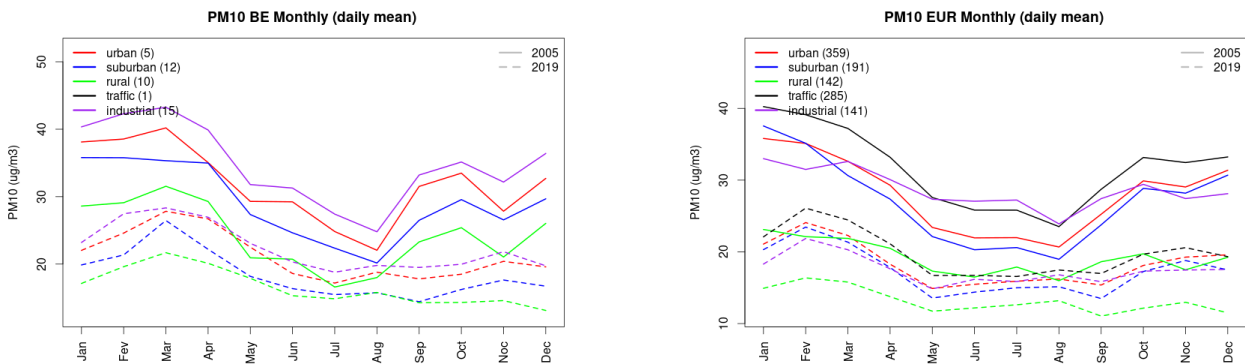


Figure S.45: Monthly cycle of daily mean PM10 for Belgium (left) and Europe (right) at various station types estimated from the whole time series in 2005 (solid lines) and 2019 (dashed lines).

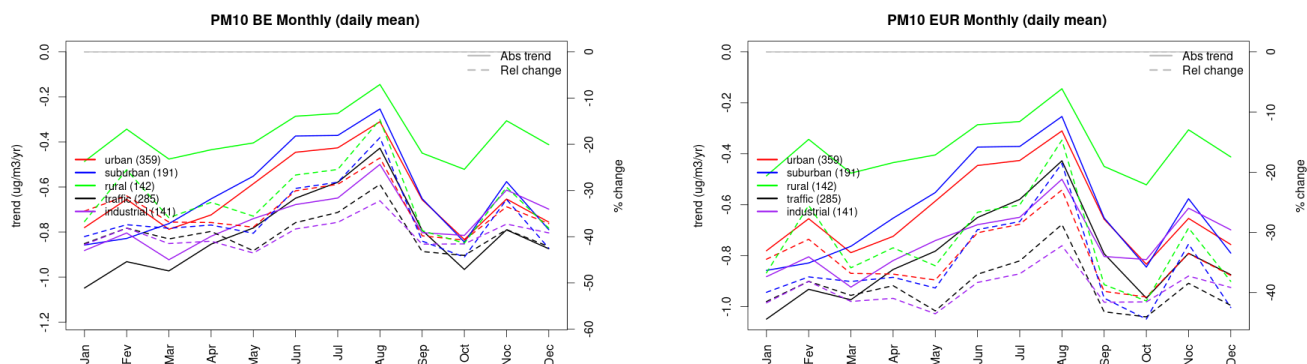


Figure S.46: Absolute (solid lines, left axis) and relative (dashed lines, right axis) trends in the monthly cycle for Belgium (left) and Europe (right) of PM10 at various station type.

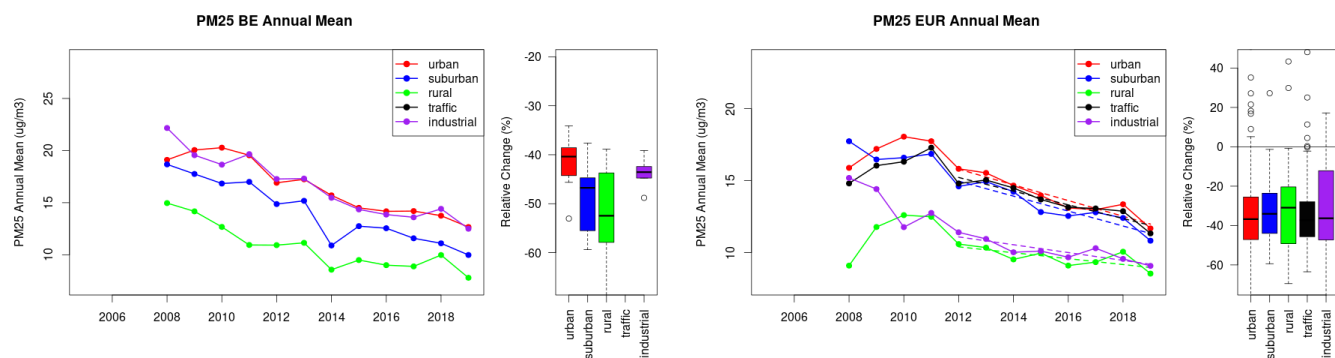


Figure S.47: Time series of the Belgium (left) and European-wide composite (median) of annual mean PM25 ($\mu\text{g}/\text{m}^3$) per station type and area (red: urban background, blue suburban background, green: rural background, black: traffic, violet: industrial) between 2005 and 2019. In the European composite, the dashed lines show the linear fit between 2005 & 2012 and between 2012 & 2019. The boxplots on the right-hand side show the distribution of relative changes (%) between 2005 and 2019 for all stations of each typology in Belgium and in Europe.

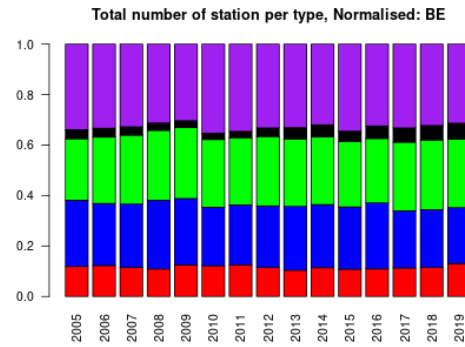
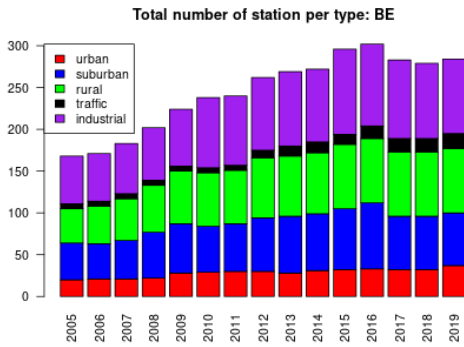
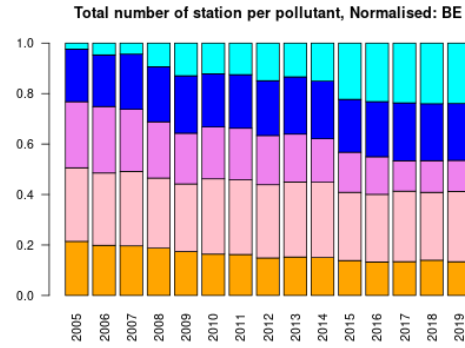
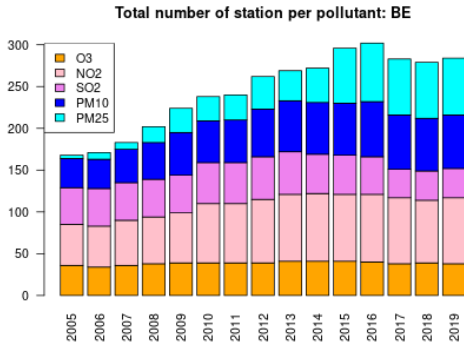
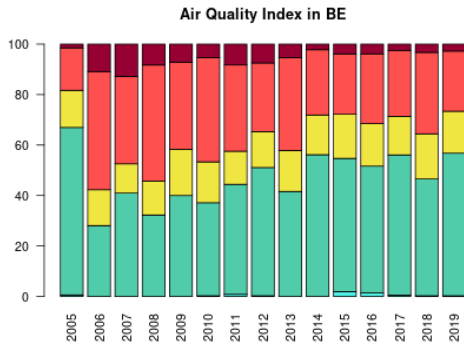


Figure S.48: For Belgium: overall air quality index (percentage of days in a given year) and distribution of daily categories per pollutant (light blue: good, light green: fair, yellow: moderate, orange: poor, red: very poor, violet: extremely poor).

3 Bulgaria

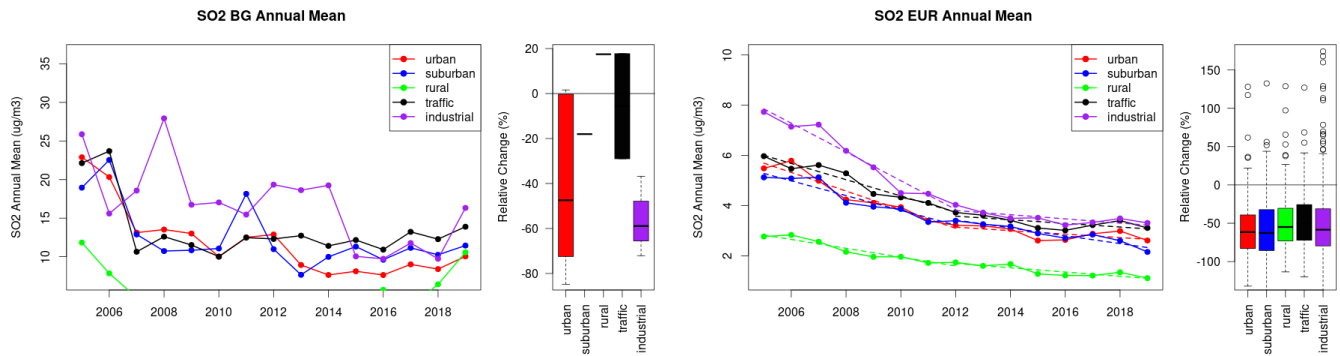


Figure S.49: Time series of the Bulgaria (left) and European-wide composite (median) of annual mean SO₂ (ug/m³) per station type and area (red: urban background, blue suburban background, green: rural background, black: traffic, violet: industrial) between 2005 and 2019. In the European composite, the dashed lines show the linear fit between 2005 & 2012 and between 2012 & 2019. The boxplots on the right-hand side show the distribution of relative changes (%) between 2005 and 2019 for all stations of each typology in Bulgaria and in Europe.

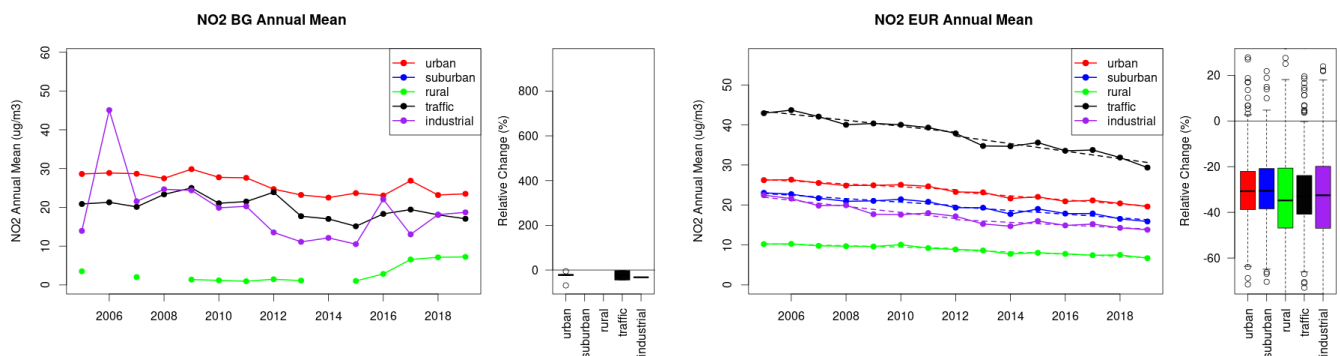


Figure S.50: Time series of the Bulgaria (left) and European-wide composite (median) of annual mean NO₂ (ug/m³) per station type and area (red: urban background, blue suburban background, green: rural background, black: traffic, violet: industrial) between 2005 and 2019. In the European composite, the dashed lines show the linear fit between 2005 & 2012 and between 2012 & 2019. The boxplots on the right-hand side show the distribution of relative changes (%) between 2005 and 2019 for all stations of each typology in Bulgaria and in Europe.

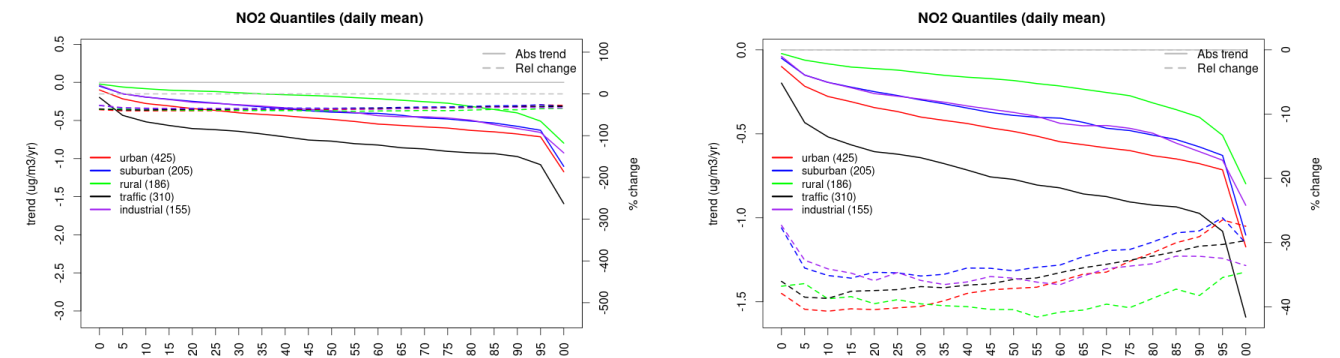


Figure S.51: For NO₂ in Bulgaria (left) and Europe, and for each typology of station: absolute trend (solid lines, left y-axis) and relative change (dashed lines, right y-axis) of the percentiles of daily means.

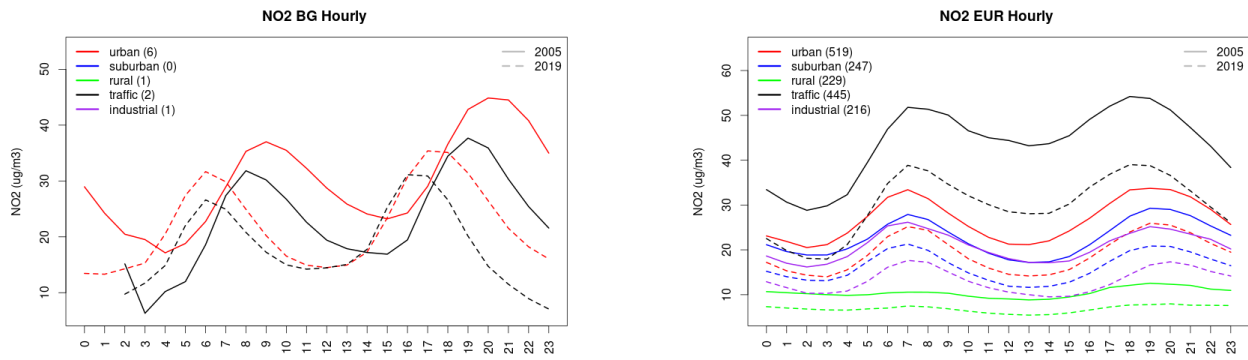


Figure S.52: Diurnal cycle of daily mean NO₂ for Bulgaria (left) and Europe (right) at various station types estimated from the whole time series in 2005 (solid lines) and 2019

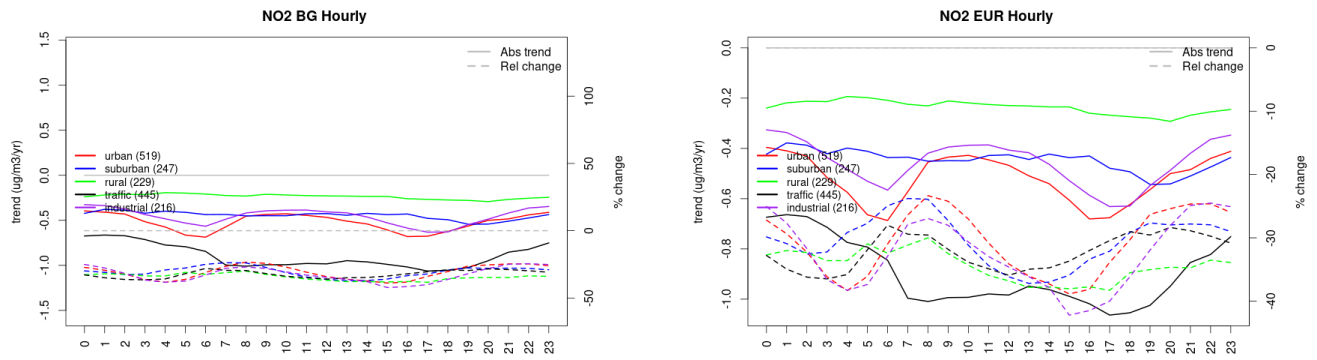


Figure S.53: Absolute (solid lines, left axis) and relative (dashed lines, right axis) trends in the diurnal cycle for Bulgaria (left) and Europe (right) of NO₂ at various station type.

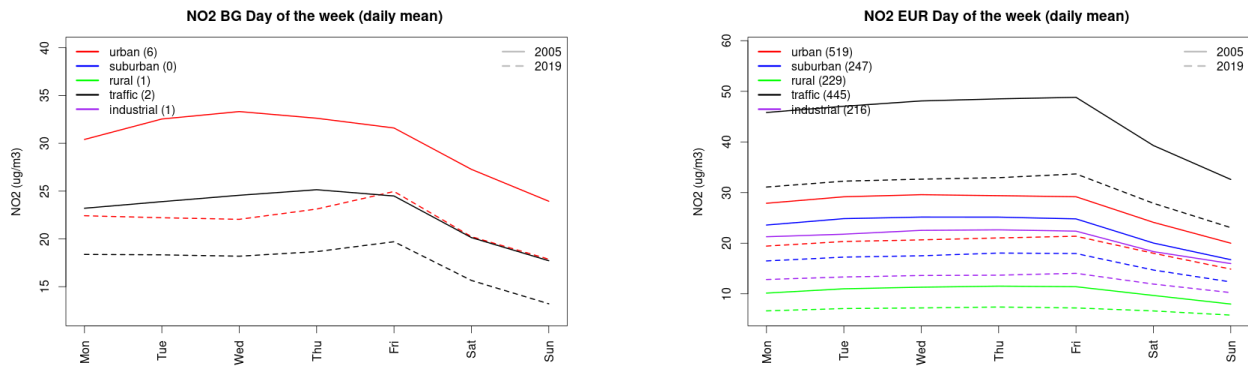


Figure S.54: Weekly cycle of daily mean NO₂ for Bulgaria (left) and Europe (right) at various station types estimated from the whole time series in 2005 (solid lines) and 2019

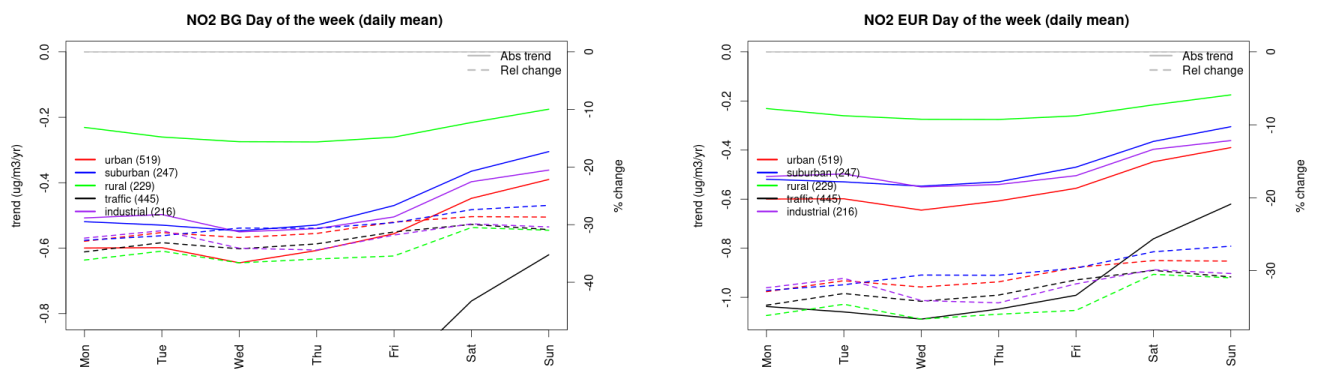


Figure S.55: Absolute (solid lines, left axis) and relative (dashed lines, right axis) trends in the weekly cycle for Bulgaria (left) and Europe (right) of NO₂ at various station type.

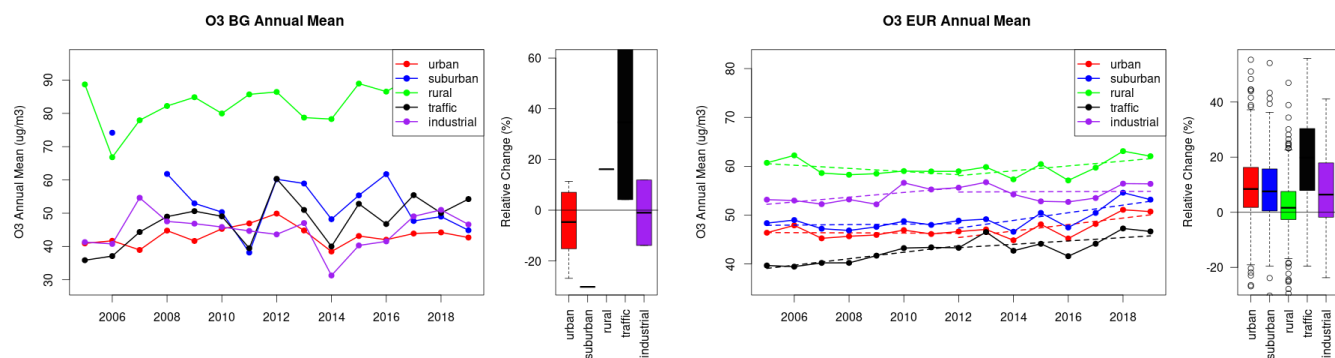


Figure S.56: Time series of the Bulgaria (left) and European-wide composite (median) of annual mean ozone (ug/m³) per station type and area (red: urban background, blue suburban background, green: rural background, black: traffic, violet: industrial) between 2005 and 2019. In the European composite, the dashed lines show the linear fit between 2005 & 2012 and between 2012 & 2019. The boxplots on the right-hand side show the distribution of relative changes (%) between 2005 and 2019 for all stations of each typology in Bulgaria and in Europe.

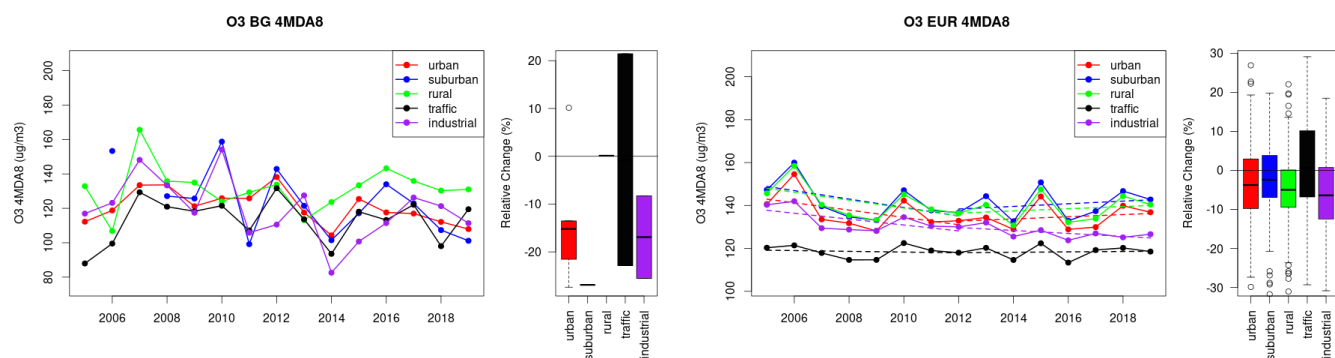


Figure S.57: Time series of the Bulgaria (left) and European-wide composite (median) of O₃ fourth highest daily peak (4MDA8, ug/m³) per station type and area (red: urban background, blue suburban background, green: rural background, black: traffic, violet: industrial) between 2005 and 2019. In the European composite, the dashed lines show the linear fit between 2005 & 2012 and between 2012 & 2019. The boxplots on the right-hand side show the distribution of relative changes (%) between 2005 and 2019 for all stations of each typology in Bulgaria and in Europe.

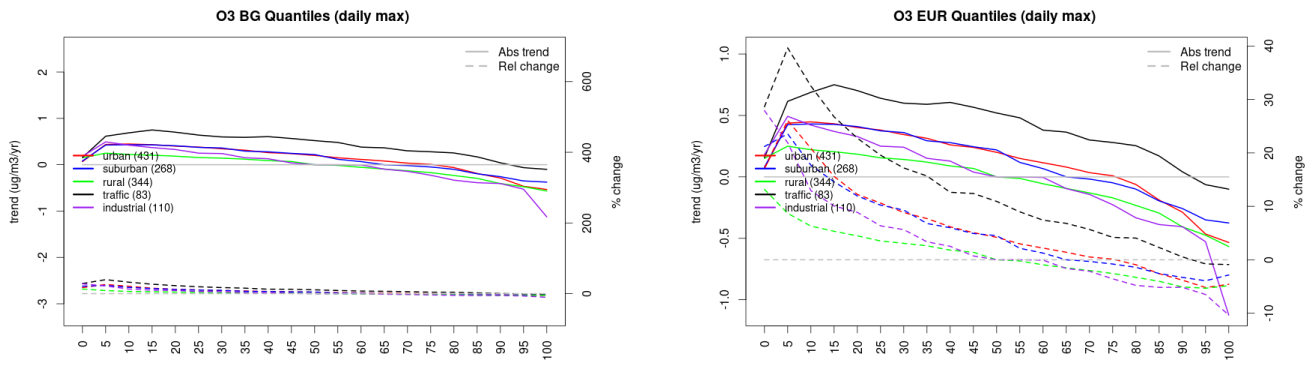


Figure S.58: For ozone in Bulgaria (left) and Europe, and for each typology of station: absolute trend (solid lines, left y-axis) and relative change (dashed lines, right y-axis) of the percentiles of daily maxima.

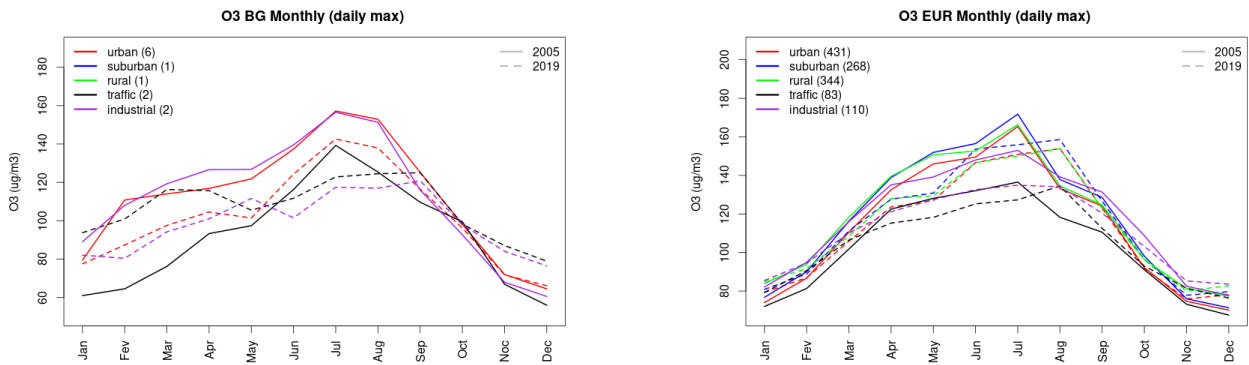


Figure S.59: Monthly cycle of daily max ozone for Bulgaria (left) and Europe (right) at various station types estimated from the whole time series in 2005 (solid lines) and 2019

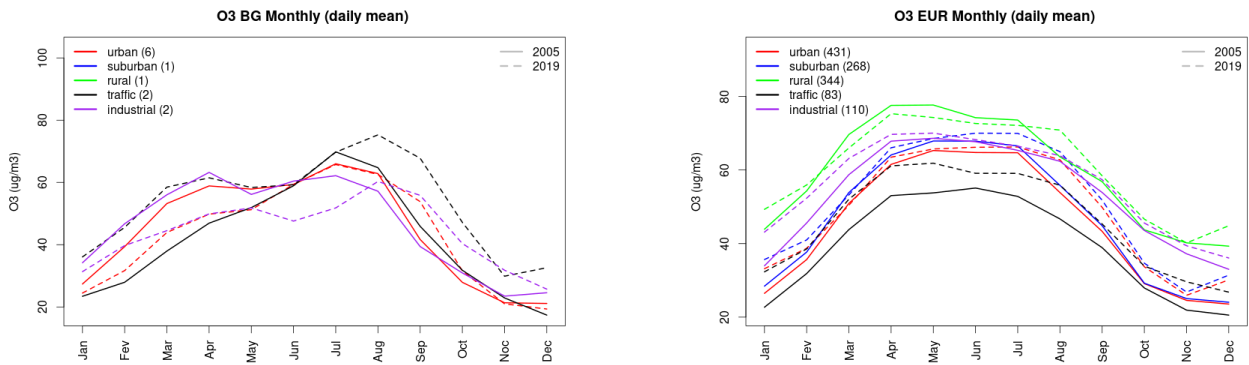


Figure S.60: Monthly cycle of daily mean ozone for Bulgaria (left) and Europe (right) at various station types estimated from the whole time series in 2005 (solid lines) and 2019

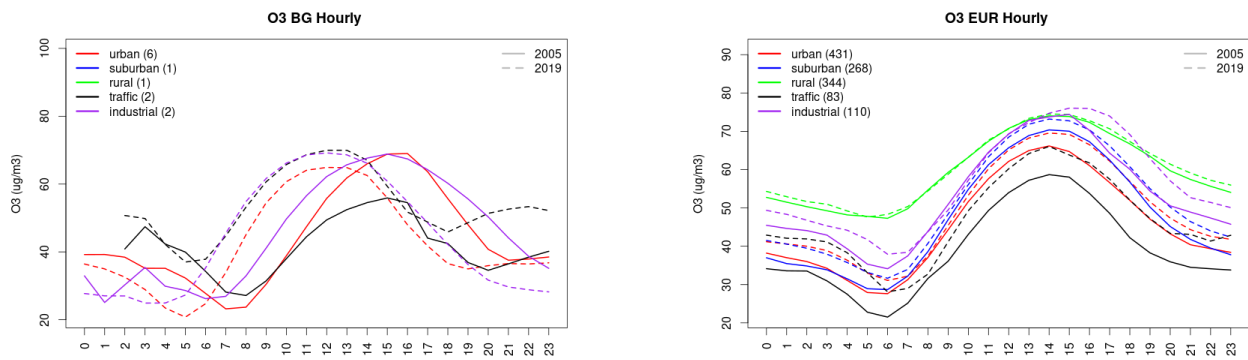


Figure S.61: Diurnal cycle of daily mean ozone for Bulgaria (left) and Europe (right) at various station types estimated from the whole time series in 2005 (solid lines) and 2019

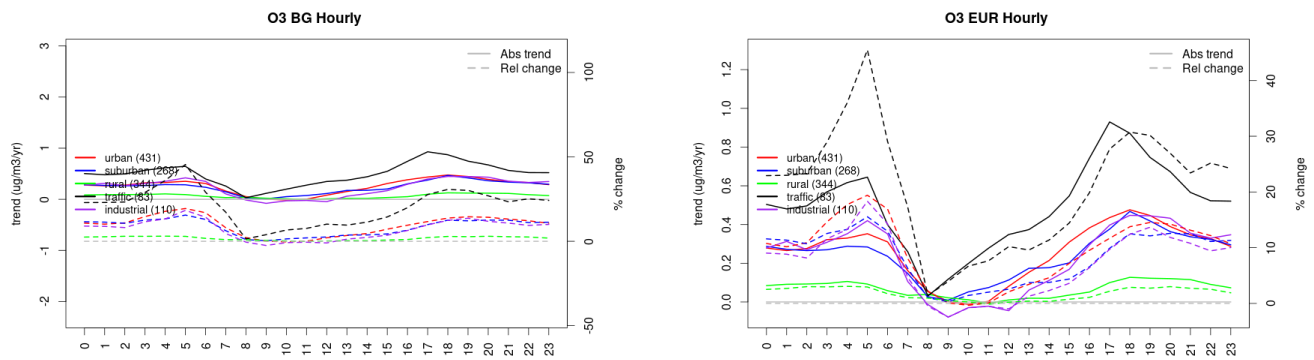


Figure S.62: Absolute (solid lines, left axis) and relative (dashed lines, right axis) trends in the diurnal cycle for Bulgaria (left) and Europe (right) of ozone at various station type.

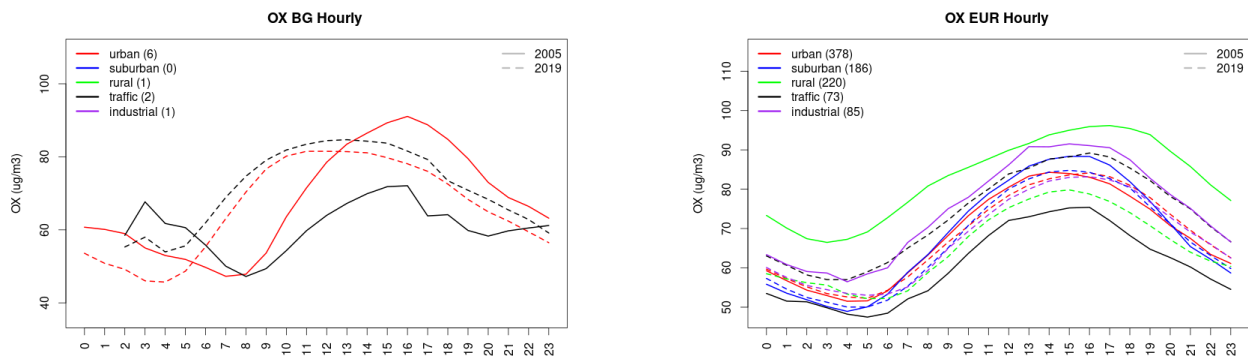


Figure S.63: Diurnal cycle of daily mean OX (as NO2+O3) for Bulgaria (left) and Europe (right) at various station types estimated from the whole time series in 2005 (solid lines) and 2019

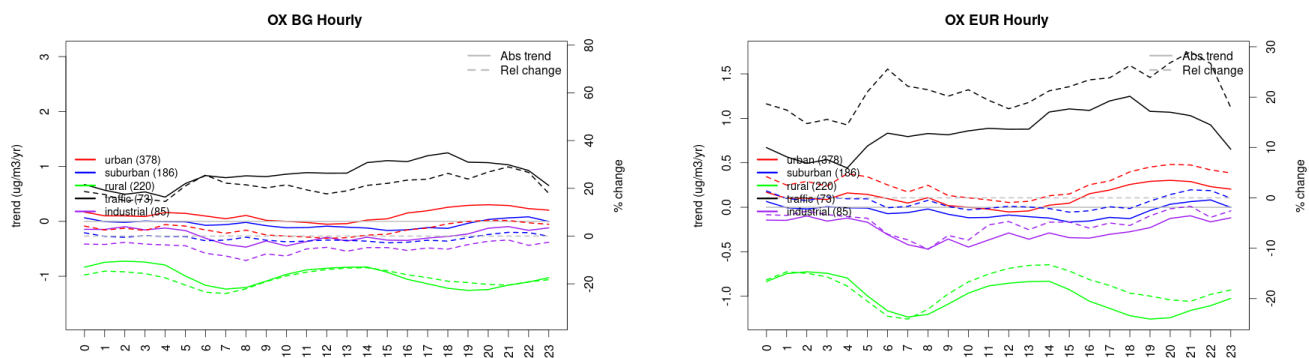


Figure S.64: Absolute (solid lines, left axis) and relative (dashed lines, right axis) trends in the diurnal cycle for Bulgaria (left) and Europe (right) of OX (as NO₂+O₃) at various station type.

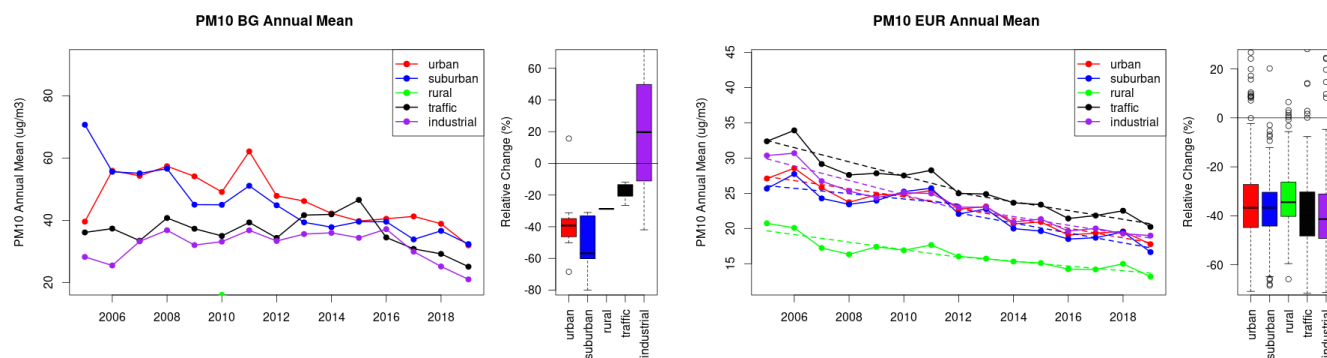


Figure S.65: Time series of the Bulgaria (left) and European-wide composite (median) of annual mean PM₁₀ (ug/m³) per station type and area (red: urban background, blue suburban background, green: rural background, black: traffic, violet: industrial) between 2005 and 2019. In the European composite, the dashed lines show the linear fit between 2005 & 2012 and between 2012 & 2019. The boxplots on the right-hand side show the distribution of relative changes (%) between 2005 and 2019 for all stations of each typology in Bulgaria and in Europe.

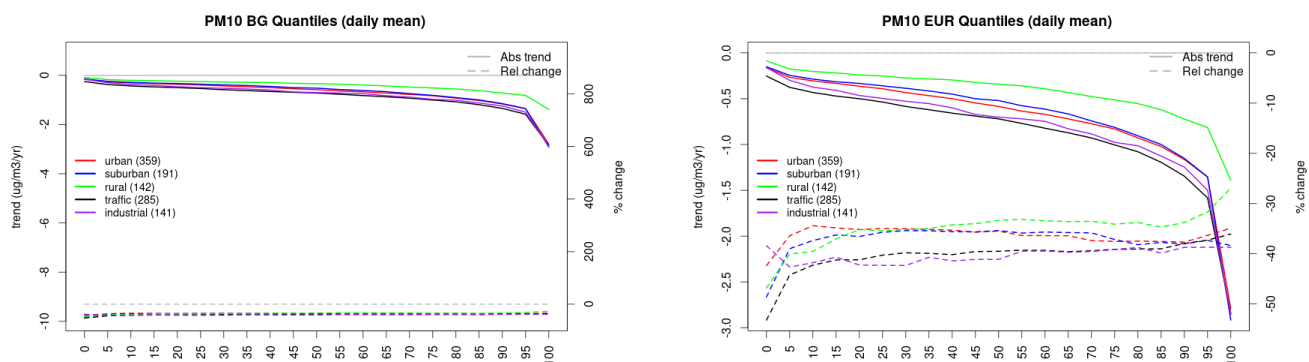


Figure S.66: For PM₁₀ in Bulgaria (left) and Europe, and for each typology of station: absolute trend (solid lines, left y-axis) and relative change (dashed lines, right y-axis) of the percentiles of daily means.

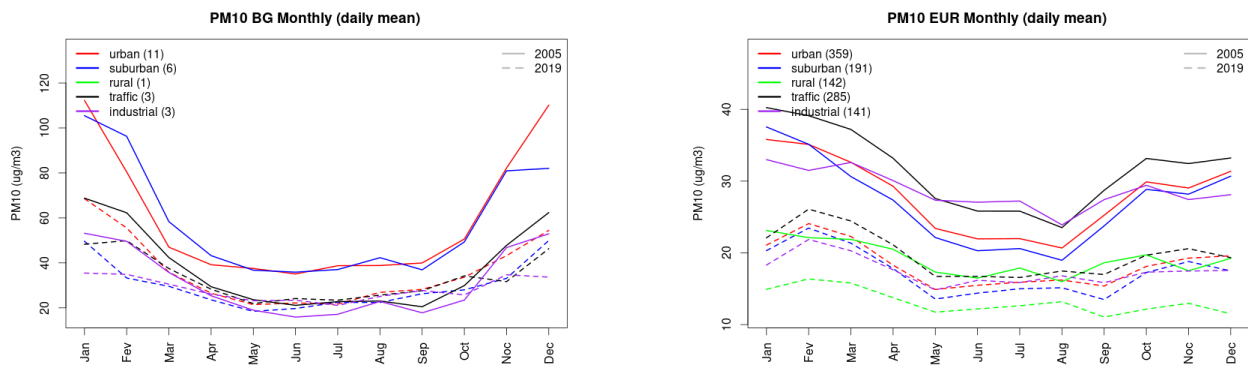


Figure S.67: Monthly cycle of daily mean PM10 for Bulgaria (left) and Europe (right) at various station types estimated from the whole time series in 2005 (solid lines) and 2019

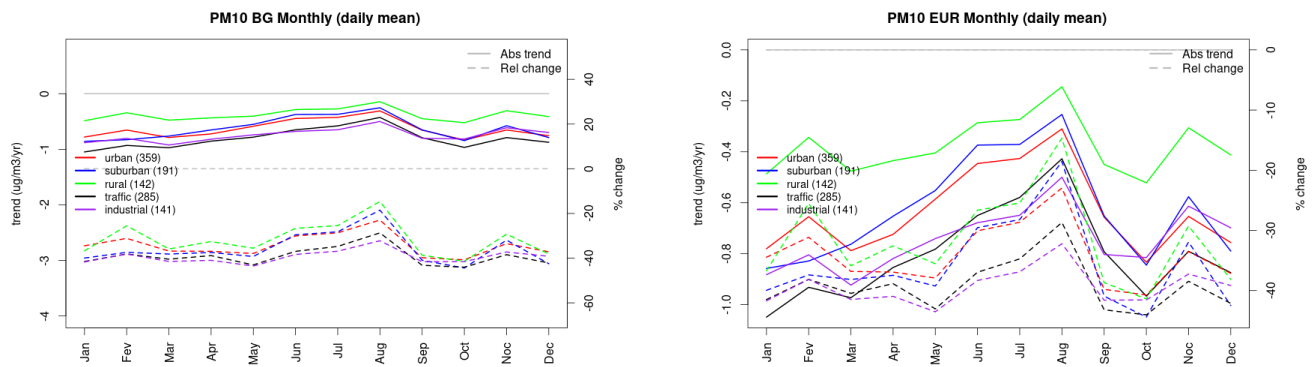


Figure S.68: Absolute (solid lines, left axis) and relative (dashed lines, right axis) trends in the monthly cycle for Bulgaria (left) and Europe (right) of PM10 at various station type.

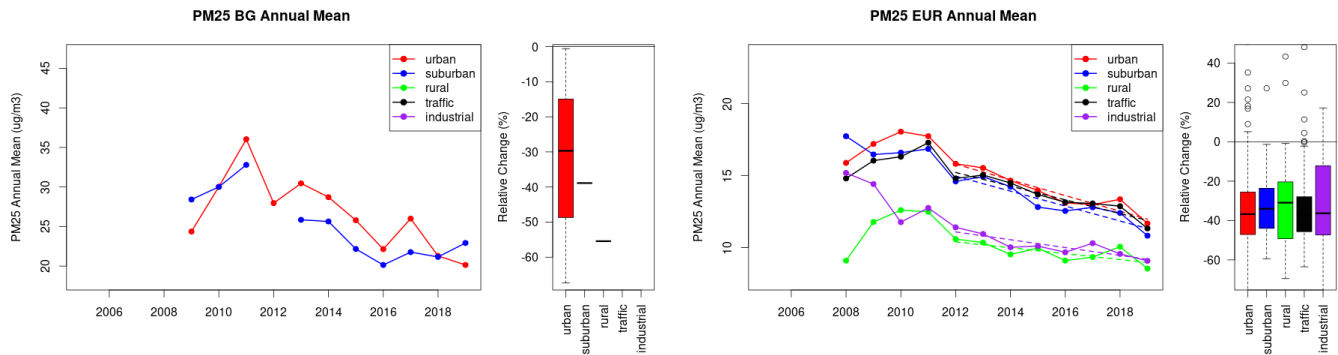


Figure S.69: Time series of the Bulgaria (left) and European-wide composite (median) of annual mean PM25 ($\mu\text{g}/\text{m}^3$) per station type and area (red: urban background, blue suburban background, green: rural background, black: traffic, violet: industrial) between 2005 and 2019. In the European composite, the dashed lines show the linear fit between 2005 & 2012 and between 2012 & 2019. The boxplots on the right-hand side show the distribution of relative changes (%) between 2005 and 2019 for all stations of each typology in Bulgaria and in Europe.

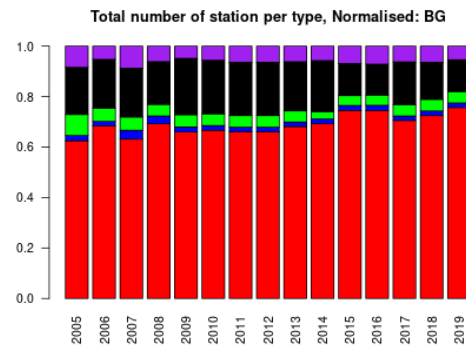
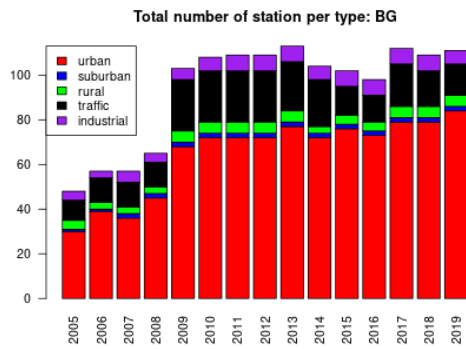
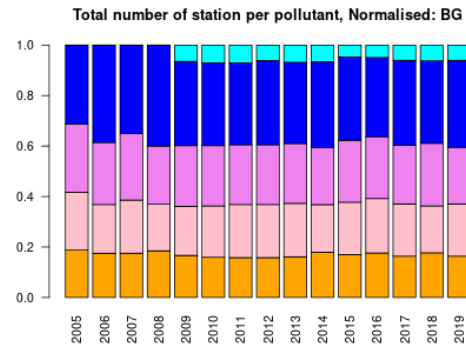
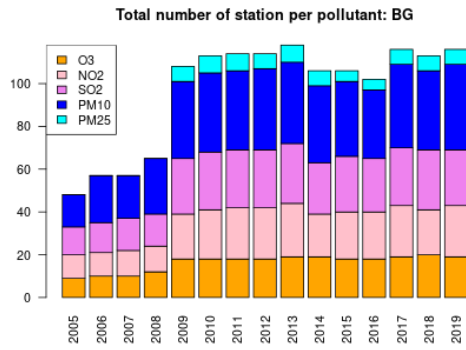
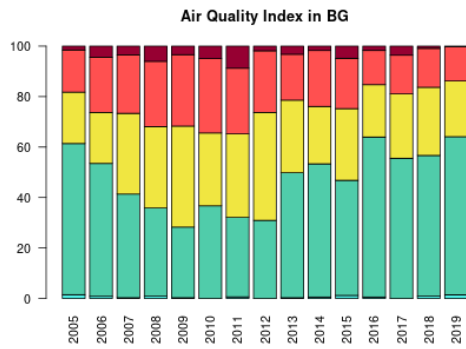


Figure S.70: For Bulgaria: overall air quality index (percentage of days in a given year) and distribution of daily categories per pollutant (light blue: good, light green: fair, yellow: moderate, orange: poor, red: very poor, violet: extremely poor).

4 Switzerland

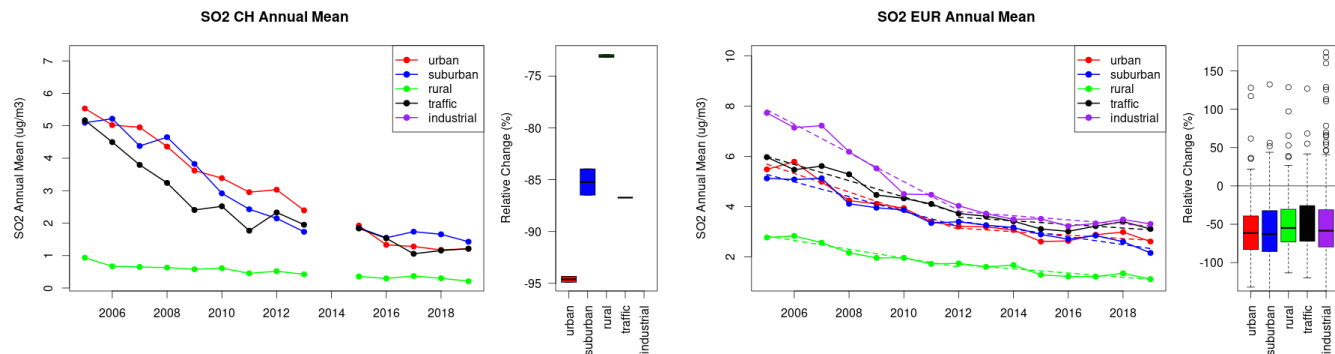


Figure S.71: Time series of the Switzerland (left) and European-wide composite (median) of annual mean SO₂ (ug/m³) per station type and area (red: urban background, blue suburban background, green: rural background, black: traffic, violet: industrial) between 2005 and 2019. In the European composite, the dashed lines show the linear fit between 2005 & 2012 and between 2012 & 2019. The boxplots on the right-hand side show the distribution of relative changes (%) between 2005 and 2019 for all stations of each typology in Switzerland and in Europe.

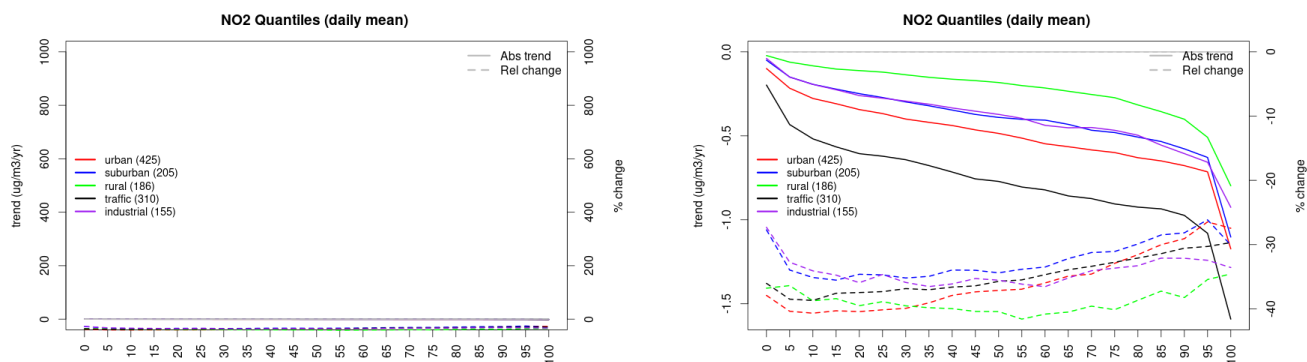


Figure S.72: For NO₂ in Switzerland (left) and Europe, and for each typology of station: absolute trend (solid lines, left y-axis) and relative change (dashed lines, right y-axis) of the percentiles of daily means.

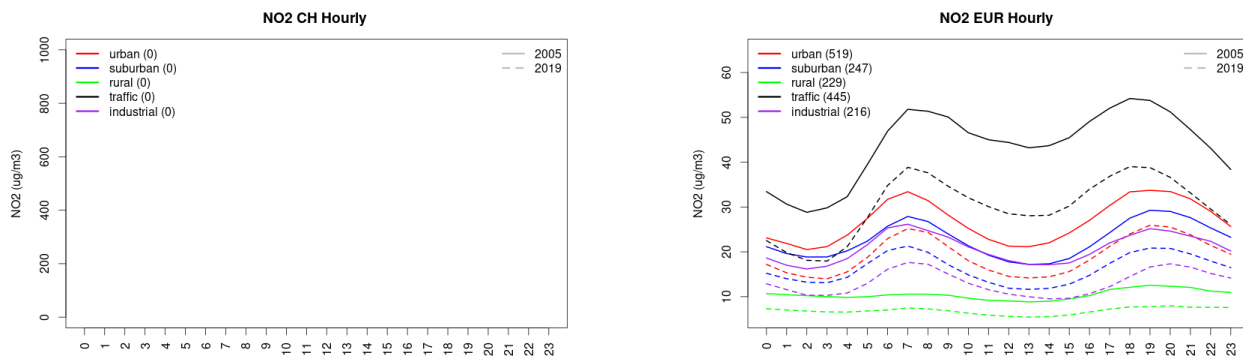


Figure S.73: Diurnal cycle of daily mean NO₂ for Switzerland (left) and Europe (right) at various station types estimated from the whole time series in 2005 (solid lines) and 2019

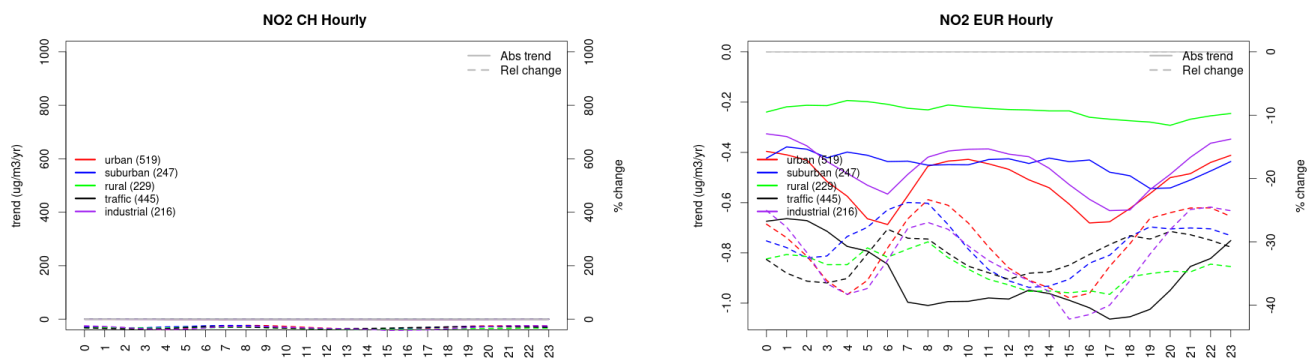


Figure S.74: Absolute (solid lines, left axis) and relative (dashed lines, right axis) trends in the diurnal cycle for Switzerland (left) and Europe (right) of NO₂ at various station type.

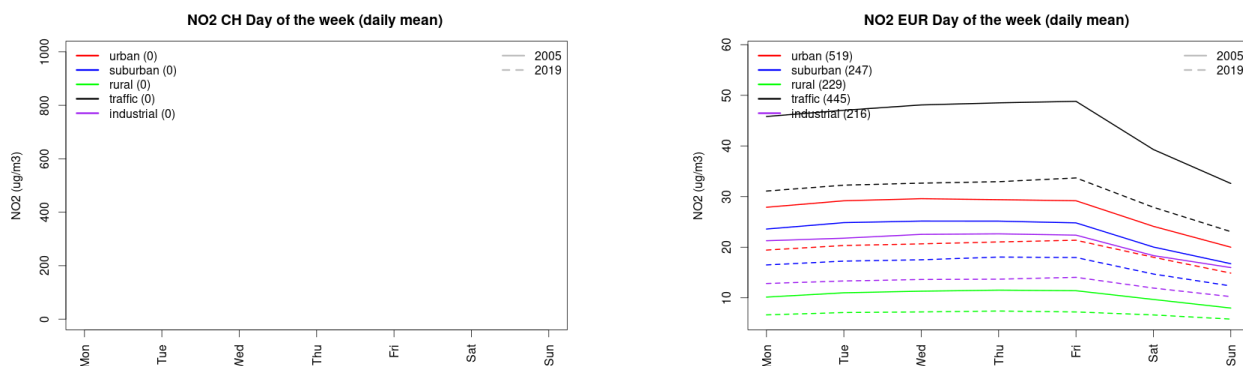


Figure S.75: Weekly cycle of daily mean NO₂ for Switzerland (left) and Europe (right) at various station types estimated from the whole time series in 2005 (solid lines) and 2019

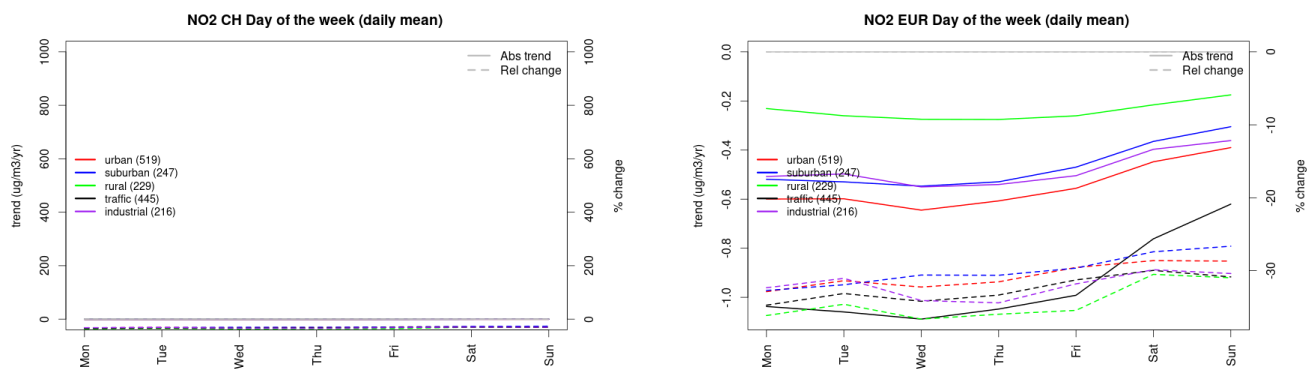


Figure S.76: Absolute (solid lines, left axis) and relative (dashed lines, right axis) trends in the weekly cycle for Switzerland (left) and Europe (right) of NO₂ at various station type.

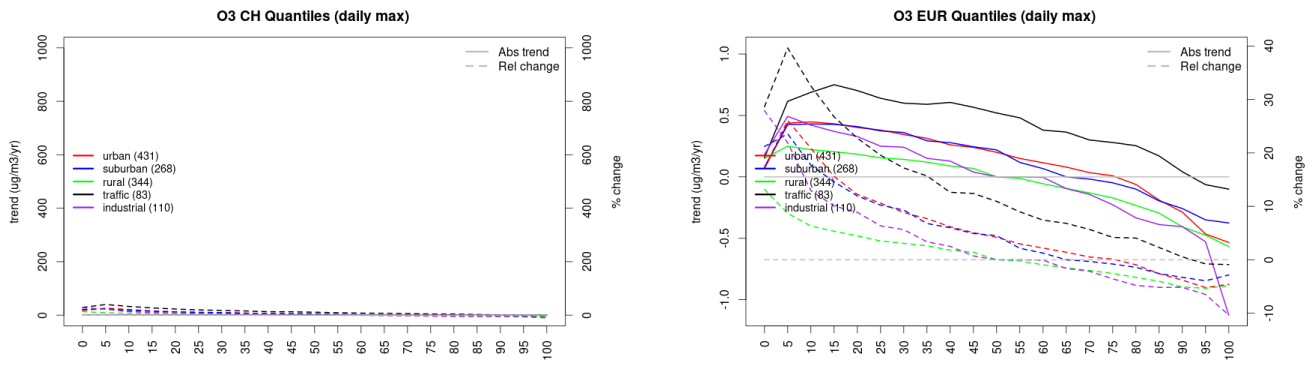


Figure S.77: For ozone in Switzerland (left) and Europe, and for each typology of station: absolute trend (solid lines, left y-axis) and relative change (dashed lines, right y-axis) of the percentiles of daily maxima.

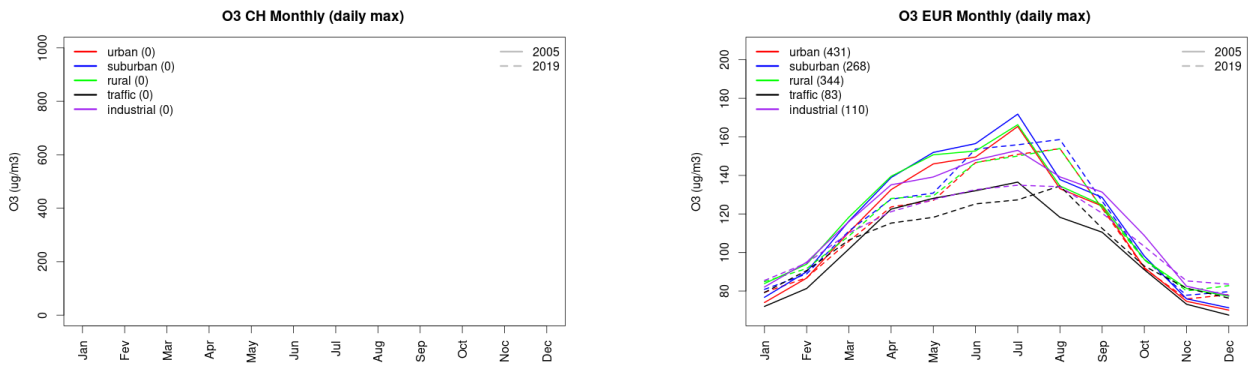


Figure S.78: Monthly cycle of daily max ozone for Switzerland (left) and Europe (right) at various station types estimated from the whole time series in 2005 (solid lines) and 2019

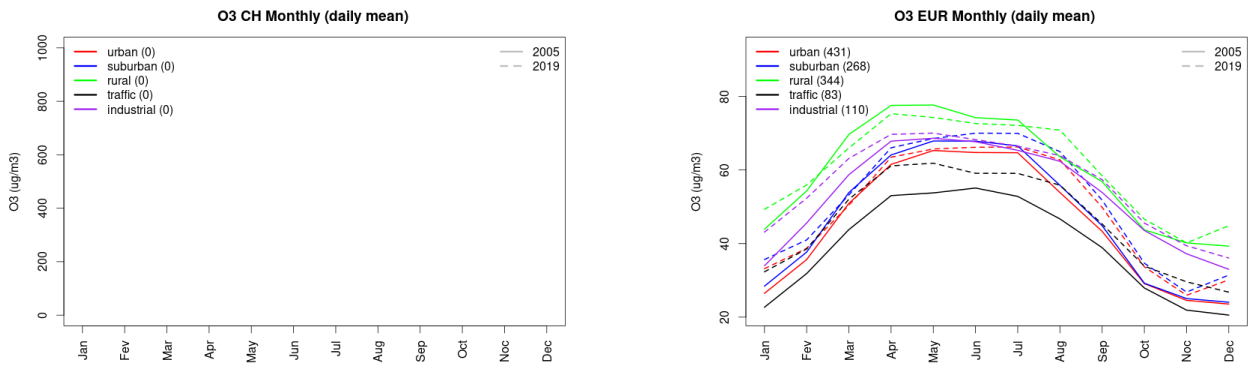


Figure S.79: Monthly cycle of daily mean ozone for Switzerland (left) and Europe (right) at various station types estimated from the whole time series in 2005 (solid lines) and 2019

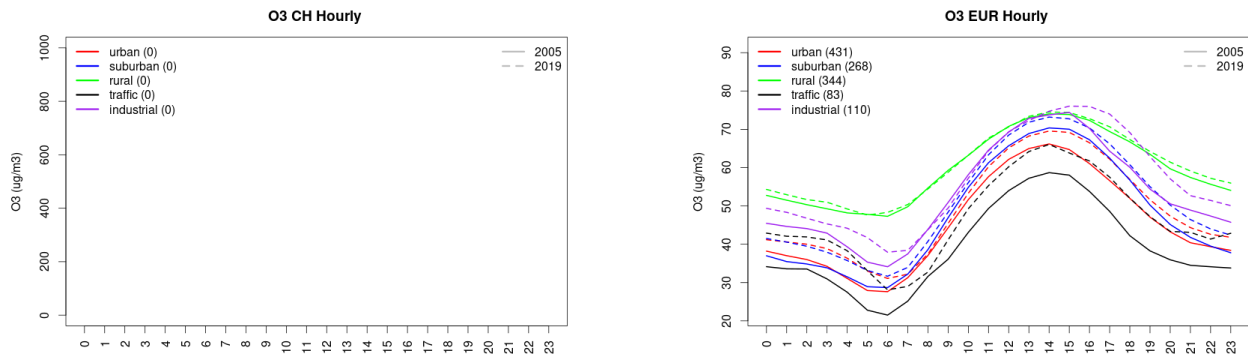


Figure S.80: Diurnal cycle of daily mean ozone for Switzerland (left) and Europe (right) at various station types estimated from the whole time series in 2005 (solid lines) and 2019

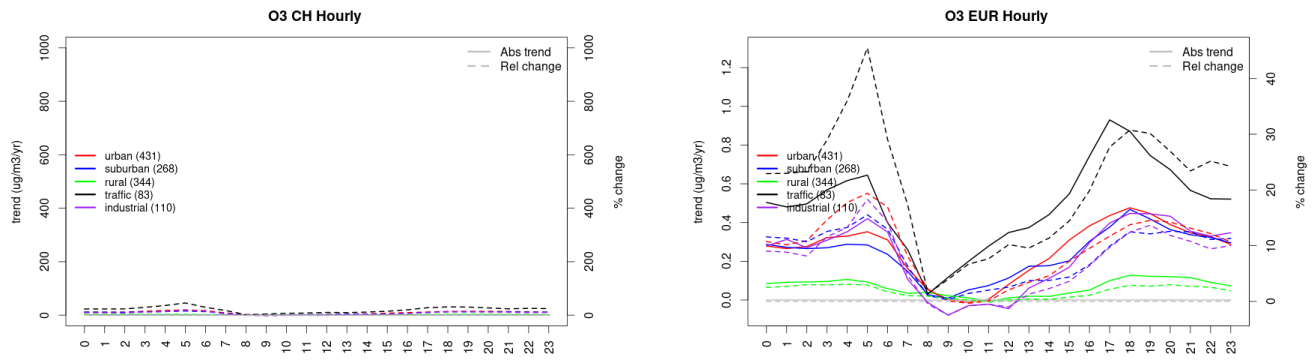


Figure S.81: Absolute (solid lines, left axis) and relative (dashed lines, right axis) trends in the diurnal cycle for Switzerland (left) and Europe (right) of ozone at various station type.

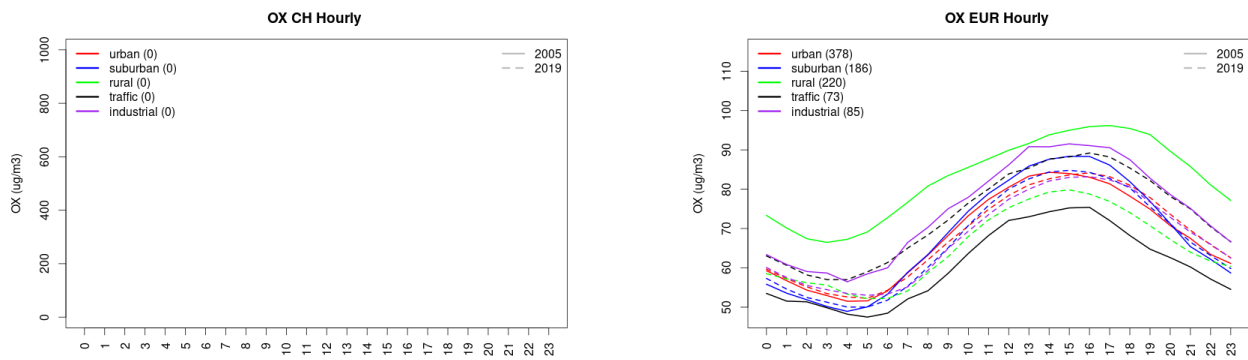


Figure S.82: Diurnal cycle of daily mean OX (as $\text{NO}_2 + \text{O}_3$) for Switzerland (left) and Europe (right) at various station types estimated from the whole time series in 2005 (solid lines) and 2019

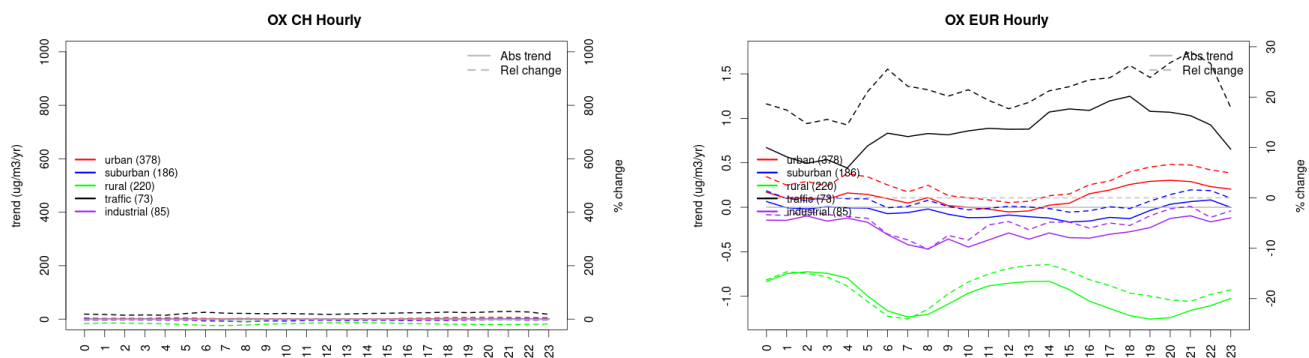


Figure S.83: Absolute (solid lines, left axis) and relative (dashed lines, right axis) trends in the diurnal cycle for Switzerland (left) and Europe (right) of OX (as NO₂+O₃) at various station type.

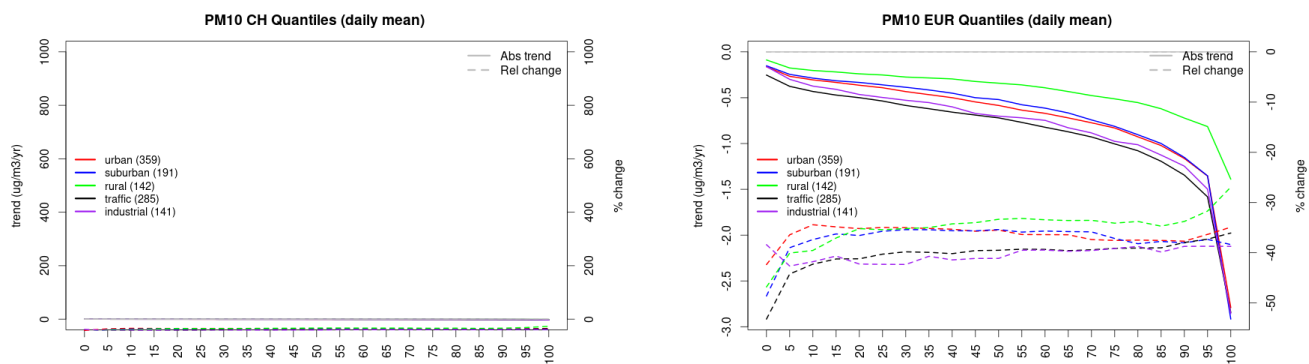


Figure S.84: For PM₁₀ in Switzerland (left) and Europe, and for each typology of station: absolute trend (solid lines, left y-axis) and relative change (dashed lines, right y-axis) of the percentiles of daily means.

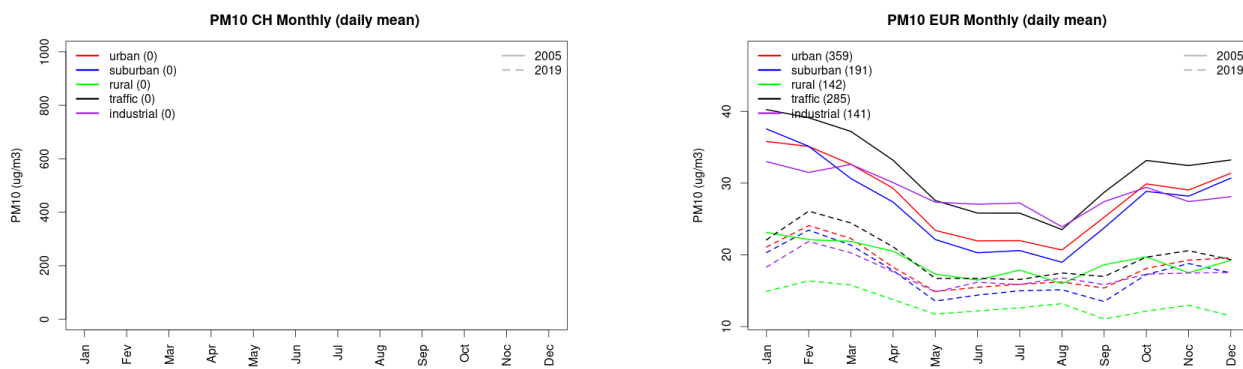


Figure S.85: Monthly cycle of daily mean PM₁₀ for Switzerland (left) and Europe (right) at various station types estimated from the whole time series in 2005 (solid lines) and 2019

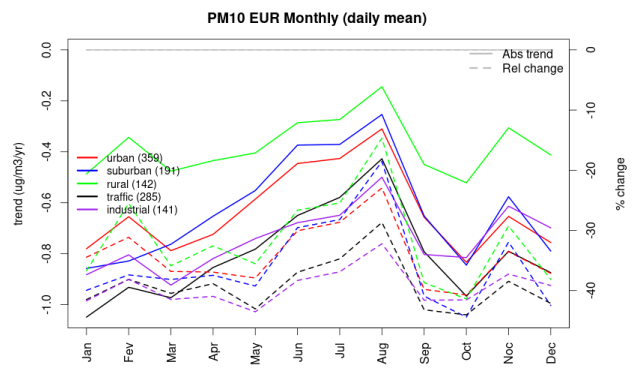
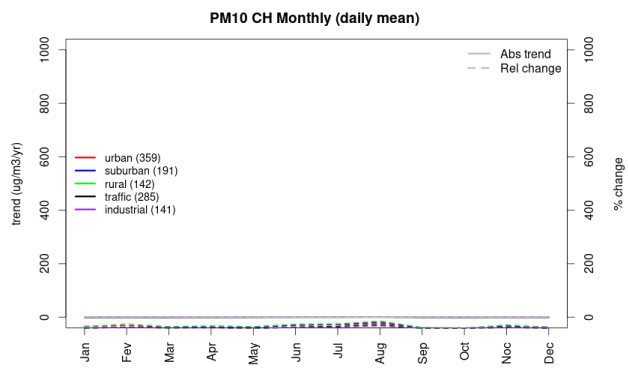


Figure S.86: Absolute (solid lines, left axis) and relative (dashed lines, right axis) trends in the monthly cycle for Switzerland (left) and Europe (right) of PM10 at various station type.

5 Czechia

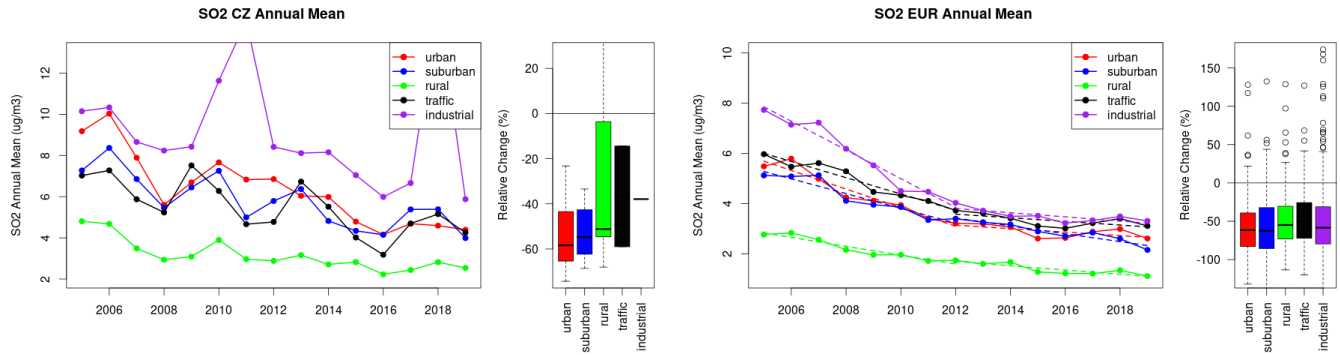


Figure S.87: Time series of the Czechia (left) and European-wide composite (median) of annual mean SO₂ (ug/m³) per station type and area (red: urban background, blue suburban background, green: rural background, black: traffic, violet: industrial) between 2005 and 2019. In the European composite, the dashed lines show the linear fit between 2005 & 2012 and between 2012 & 2019. The boxplots on the right-hand side show the distribution of relative changes (%) between 2005 and 2019 for all stations of each typology in Czechia and in Europe.

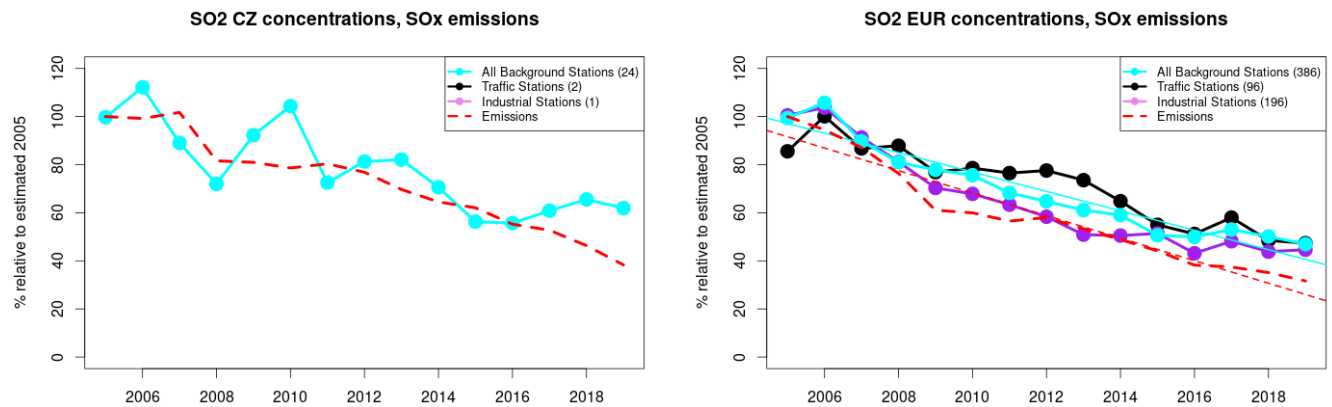


Figure S.88: Time series of 2005-2019 (left) and European (right) median SO₂ observed at traffic (black), industrial (violet) and background (cyan) sites (solid lines), and corresponding SO_x emissions (dashed line) normalised to estimated 2000 levels (%). The median is taken over where more than 5 stations of each typology is available. The total number of stations included is provided in brackets. In the European composite, straight lines are the linear fits over the whole period.

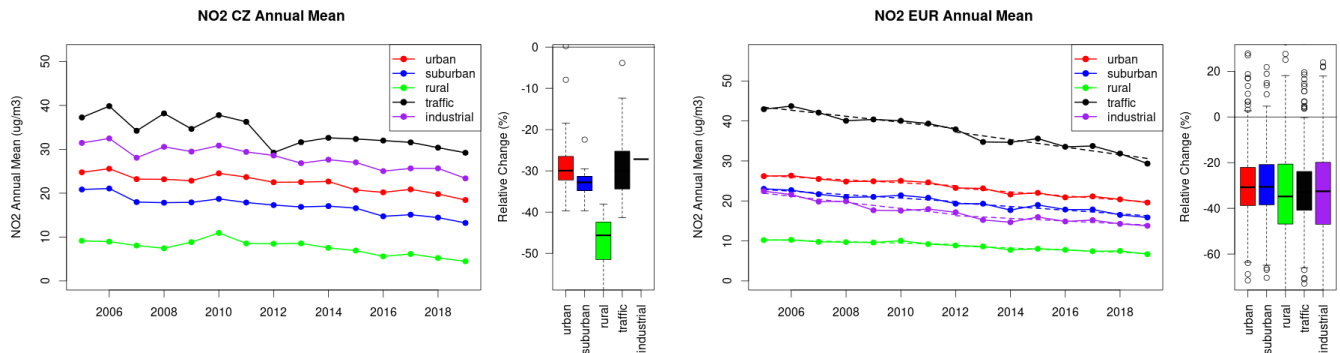


Figure S.89: Time series of the Czechia (left) and European-wide composite (median) of annual mean NO₂ (ug/m³) per station type and area (red: urban background, blue suburban background, green: rural background, black: traffic, violet: industrial) between 2005 and 2019. In the European composite, the dashed lines show the linear fit between 2005 & 2012 and between 2012 & 2019. The boxplots on the right-hand side show the distribution of relative changes (%) between 2005 and 2019 for all stations of each typology in Czechia and in Europe.

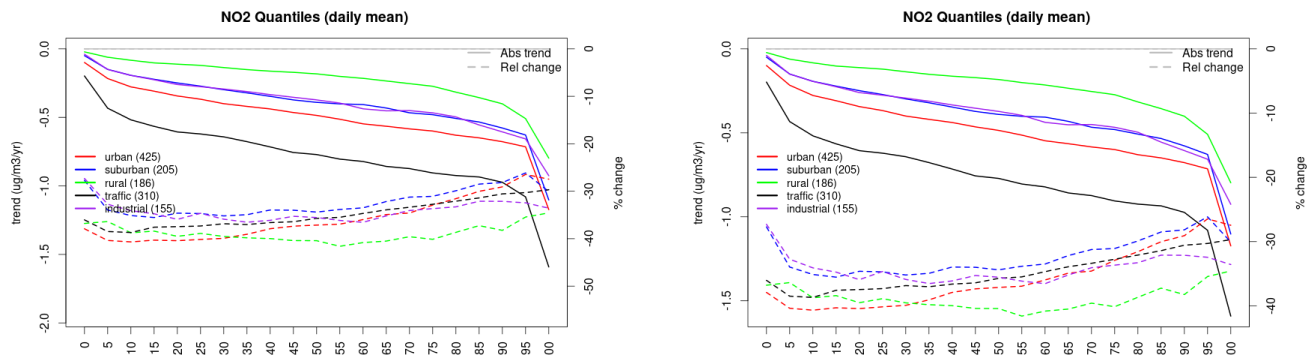


Figure S.90: For NO₂ in Czechia (left) and Europe, and for each typology of station: absolute trend (solid lines, left y-axis) and relative change (dashed lines, right y-axis) of the percentiles of daily means.

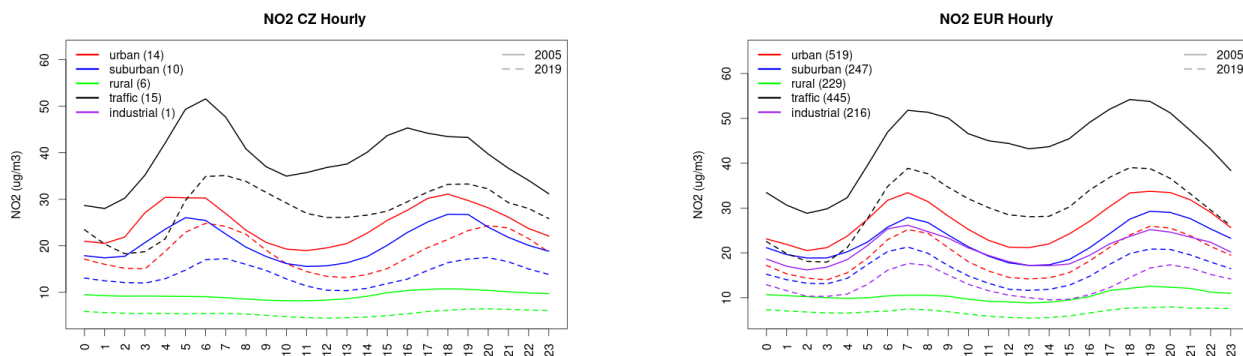


Figure S.91: Diurnal cycle of daily mean NO₂ for Czechia (left) and Europe (right) at various station types estimated from the whole time series in 2005 (solid lines) and 2019

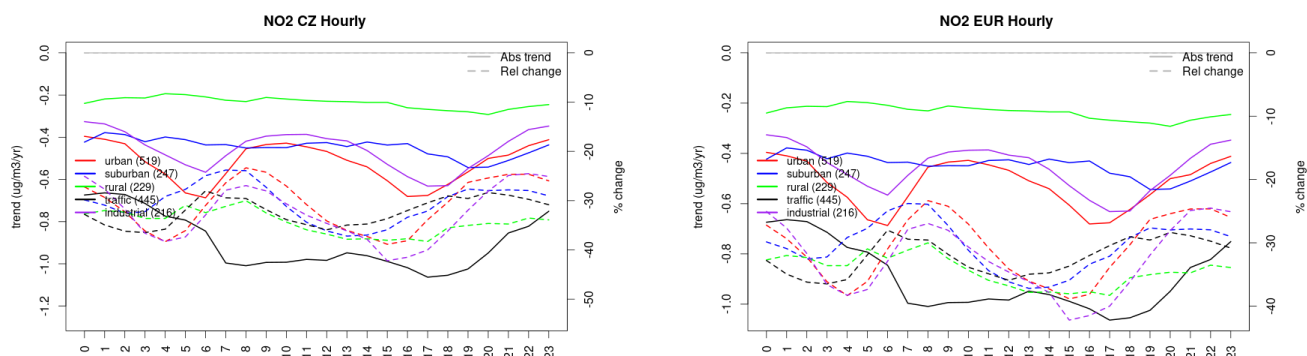


Figure S.92: Absolute (solid lines, left axis) and relative (dashed lines, right axis) trends in the diurnal cycle for Czechia (left) and Europe (right) of NO₂ at various station type.

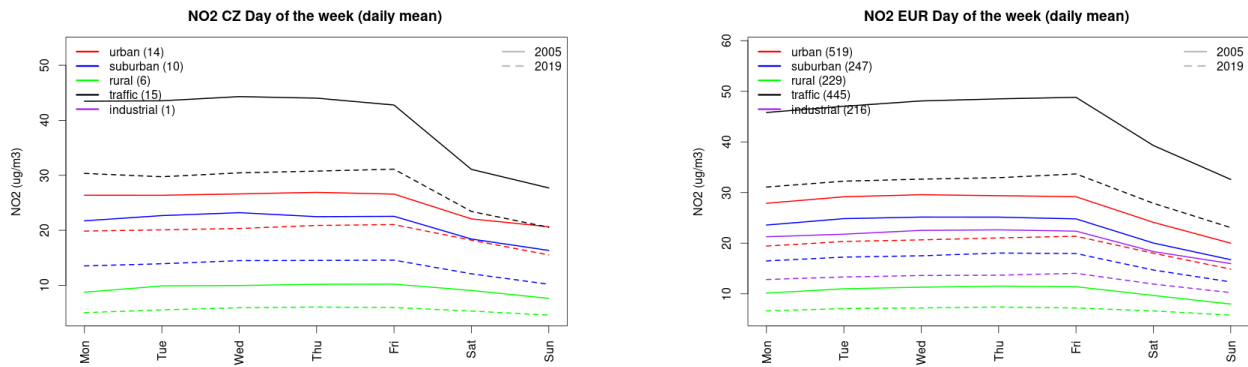


Figure S.93: Weekly cycle of daily mean NO2 for Czechia (left) and Europe (right) at various station types estimated from the whole time series in 2005 (solid lines) and 2019

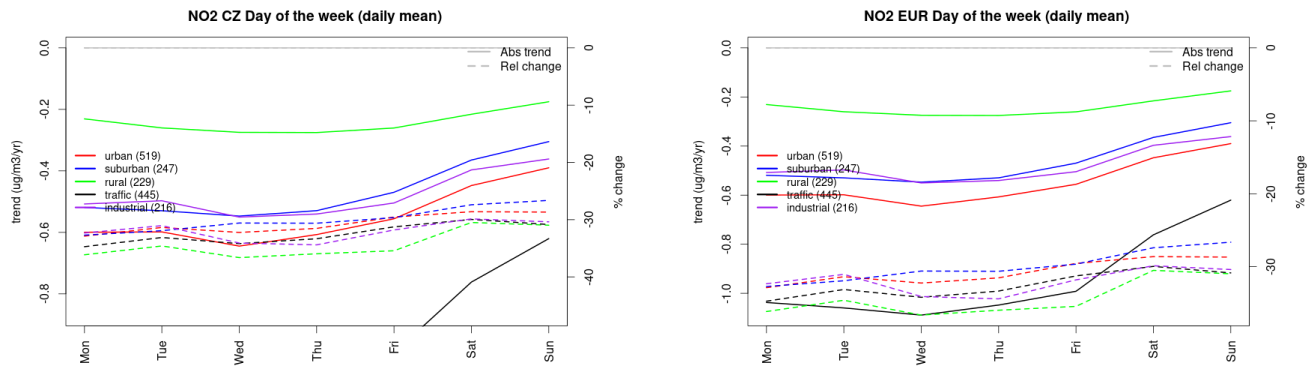


Figure S.94: Absolute (solid lines, left axis) and relative (dashed lines, right axis) trends in the weekly cycle for Czechia (left) and Europe (right) of NO2 at various station type.

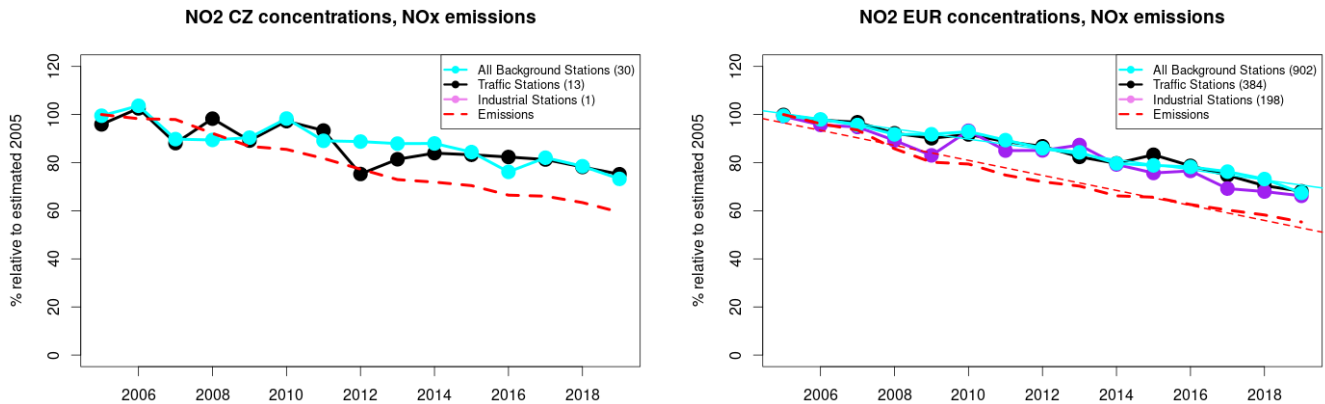


Figure S.95: Time series of 2005-2019 (left) and European (right) median NO2 observed at traffic (black), industrial (violet) and background (cyan) sites (solid lines), and corresponding NOx emissions (dashed line) normalised to estimated 2000 levels (%). The median is taken over where more than 5 stations of each typology is available. The total number of stations included is provided in brackets. In the European composite, straight lines are the linear fits over the whole period.

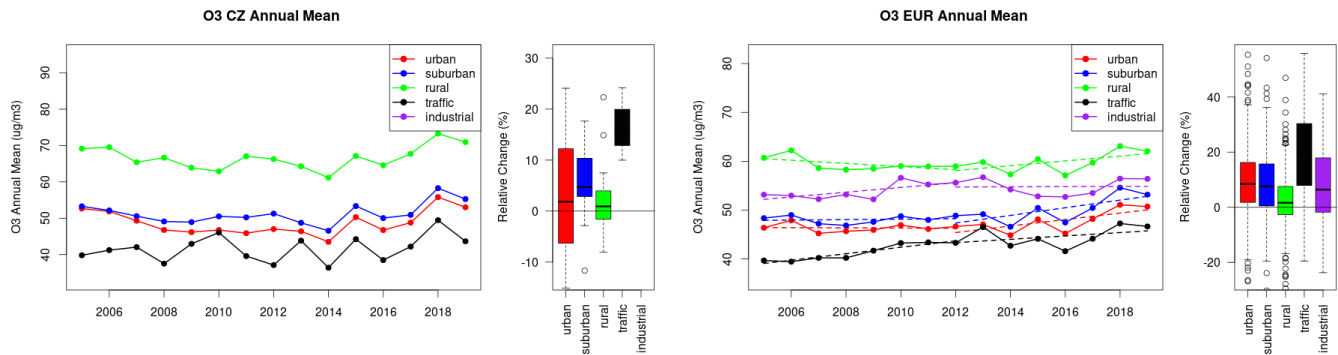


Figure S.96: Time series of the Czechia (left) and European-wide composite (median) of annual mean ozone ($\mu\text{g}/\text{m}^3$) per station type and area (red: urban background, blue suburban background, green: rural background, black: traffic, violet: industrial) between 2005 and 2019. In the European composite, the dashed lines show the linear fit between 2005 & 2012 and between 2012 & 2019. The boxplots on the right-hand side show the distribution of relative changes (%) between 2005 and 2019 for all stations of each typology in Czechia and in Europe.

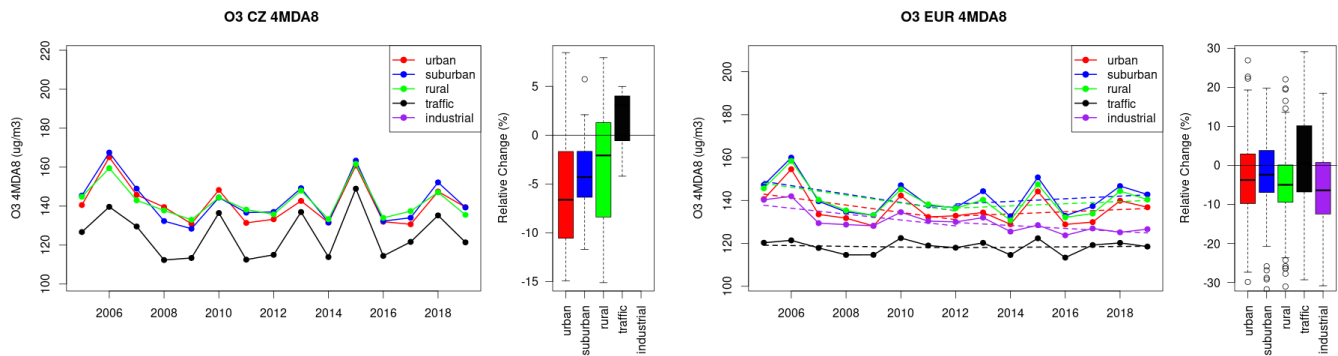


Figure S.97: Time series of the Czechia (left) and European-wide composite (median) of O3 fourth highest daily peak (4MDA8, $\mu\text{g}/\text{m}^3$) per station type and area (red: urban background, blue suburban background, green: rural background, black: traffic, violet: industrial) between 2005 and 2019. In the European composite, the dashed lines show the linear fit between 2005 & 2012 and between 2012 & 2019. The boxplots on the right-hand side show the distribution of relative changes (%) between 2005 and 2019 for all stations of each typology in Czechia and in Europe.

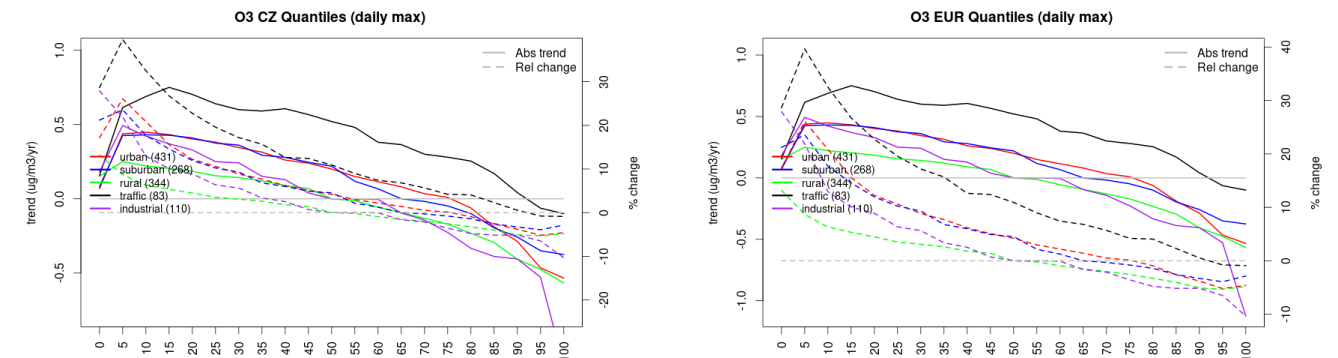


Figure S.98: For ozone in Czechia (left) and Europe, and for each typology of station: absolute trend (solid lines, left y-axis) and relative change (dashed lines, right y-axis) of the percentiles of daily maxima.

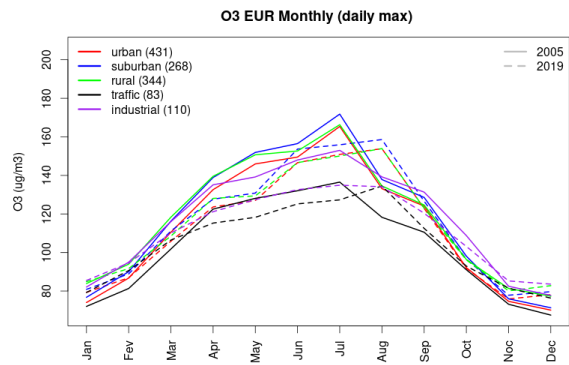
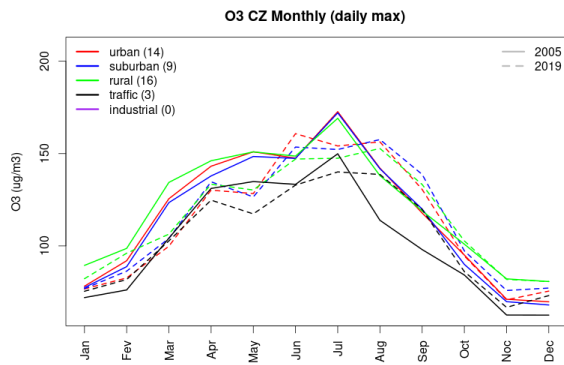


Figure S.99: Monthly cycle of daily max ozone for Czechia (left) and Europe (right) at various station types estimated from the whole time series in 2005 (solid lines) and 2019

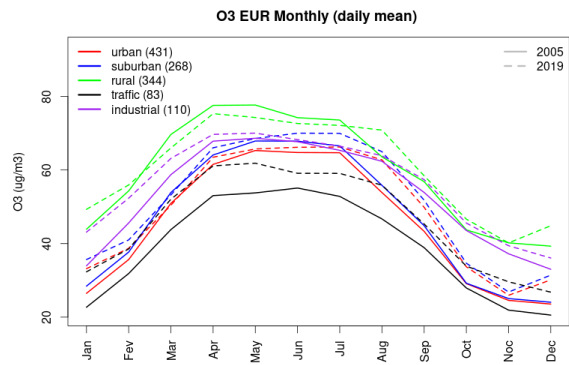
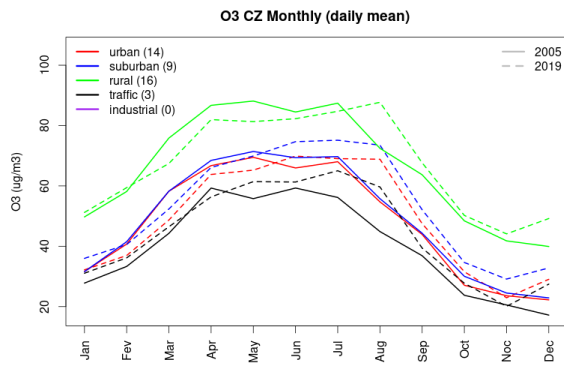


Figure S.100: Monthly cycle of daily mean ozone for Czechia (left) and Europe (right) at various station types estimated from the whole time series in 2005 (solid lines) and 2019

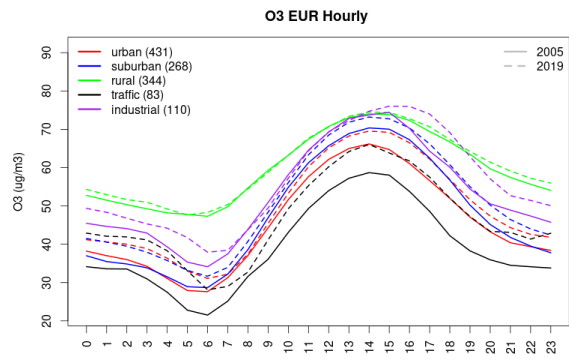
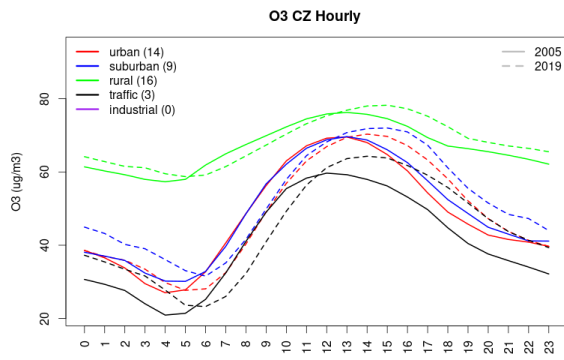


Figure S.101: Diurnal cycle of daily mean ozone for Czechia (left) and Europe (right) at various station types estimated from the whole time series in 2005 (solid lines) and 2019

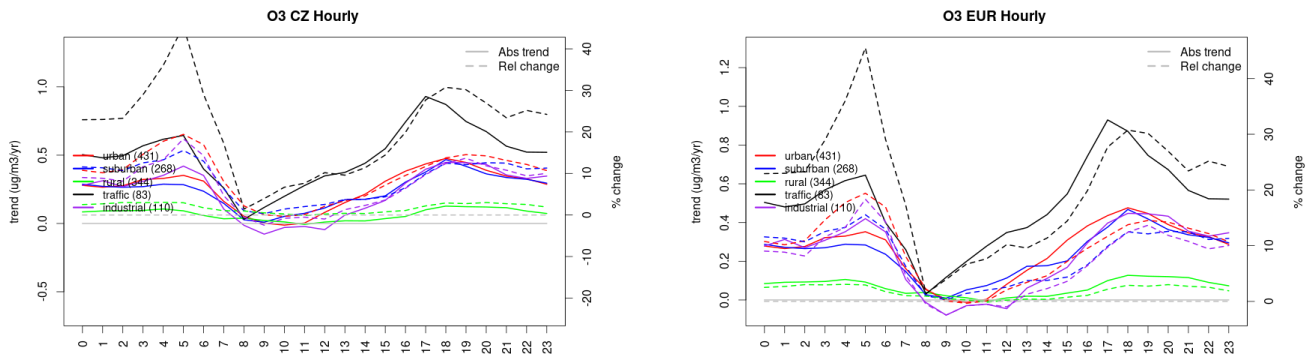


Figure S.102: Absolute (solid lines, left axis) and relative (dashed lines, right axis) trends in the diurnal cycle for Czechia (left) and Europe (right) of ozone at various station type.

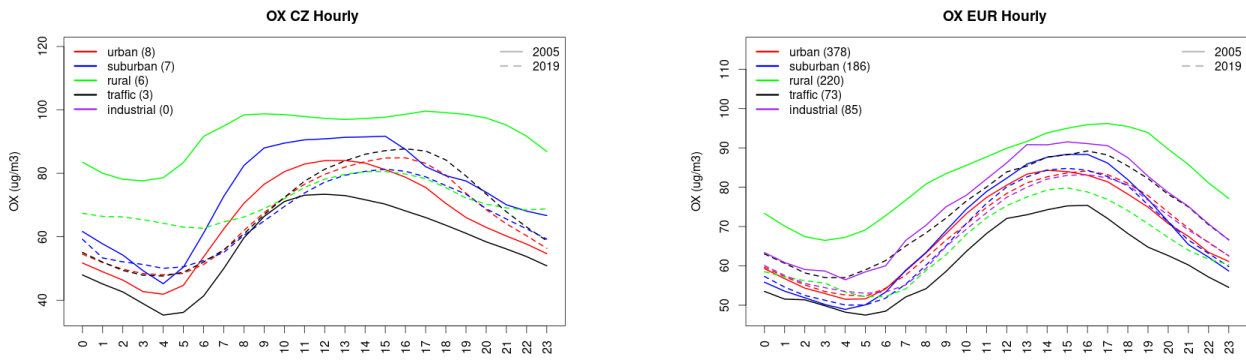


Figure S.103: Diurnal cycle of daily mean OX (as NO₂+O₃) for Czechia (left) and Europe (right) at various station types estimated from the whole time series in 2005 (solid lines) and 2019

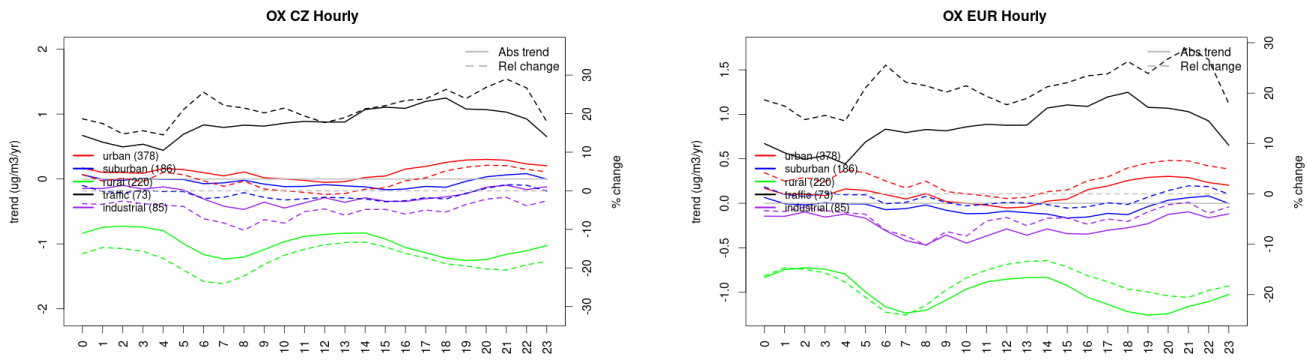


Figure S.104: Absolute (solid lines, left axis) and relative (dashed lines, right axis) trends in the diurnal cycle for Czechia (left) and Europe (right) of OX (as NO₂+O₃) at various station type.

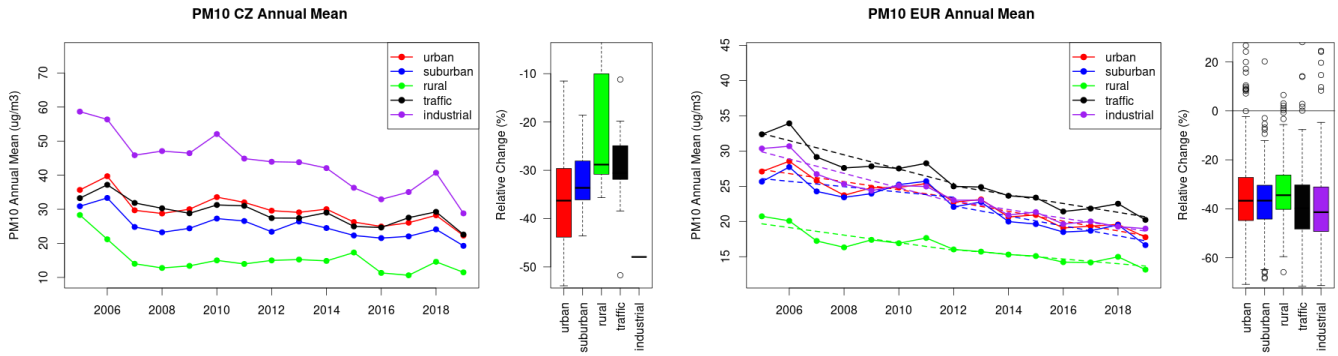


Figure S.105: Time series of the Czechia (left) and European-wide composite (median) of annual mean PM10 ($\mu\text{g}/\text{m}^3$) per station type and area (red: urban background, blue suburban background, green: rural background, black: traffic, violet: industrial) between 2005 and 2019. In the European composite, the dashed lines show the linear fit between 2005 & 2012 and between 2012 & 2019. The boxplots on the right-hand side show the distribution of relative changes (%) between 2005 and 2019 for all stations of each typology in Czechia and in Europe.

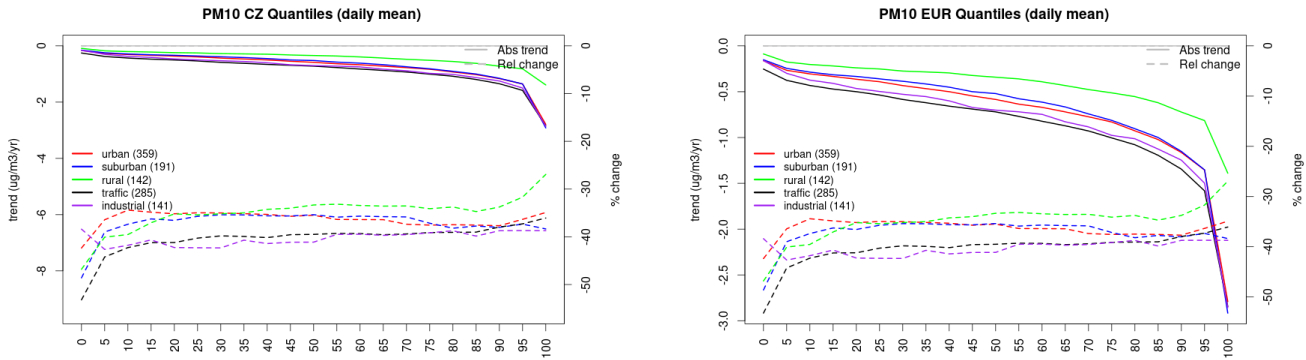


Figure S.106: For PM10 in Czechia (left) and Europe, and for each typology of station: absolute trend (solid lines, left y-axis) and relative change (dashed lines, right y-axis) of the percentiles of daily means.

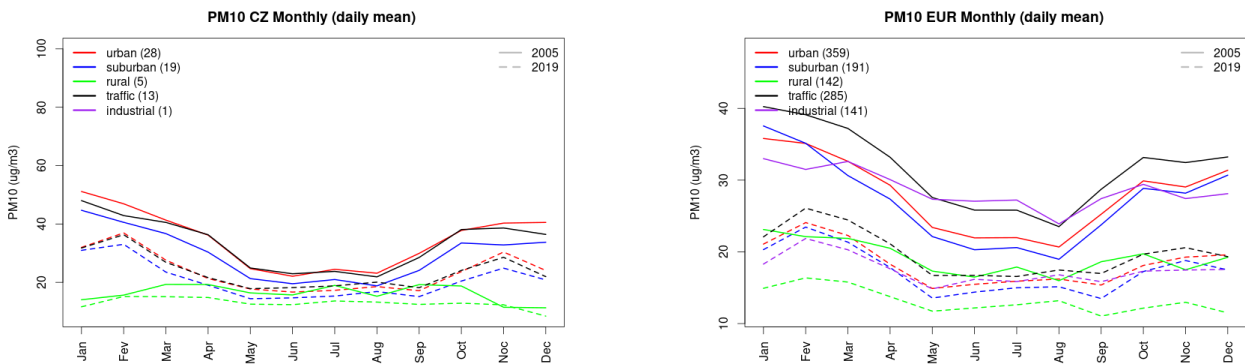


Figure S.107: Monthly cycle of daily mean PM10 for Czechia (left) and Europe (right) at various station types estimated from the whole time series in 2005 (solid lines) and 2019

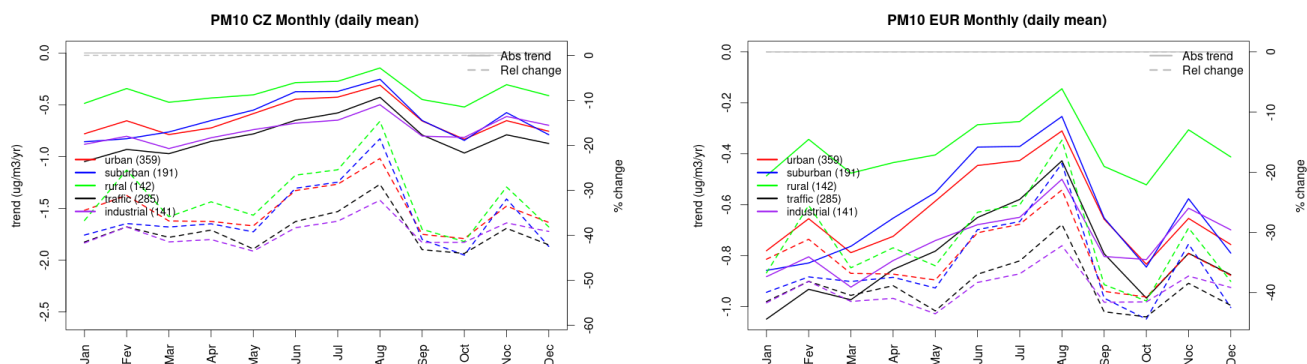


Figure S.108: Absolute (solid lines, left axis) and relative (dashed lines, right axis) trends in the monthly cycle for Czechia (left) and Europe (right) of PM10 at various station type.

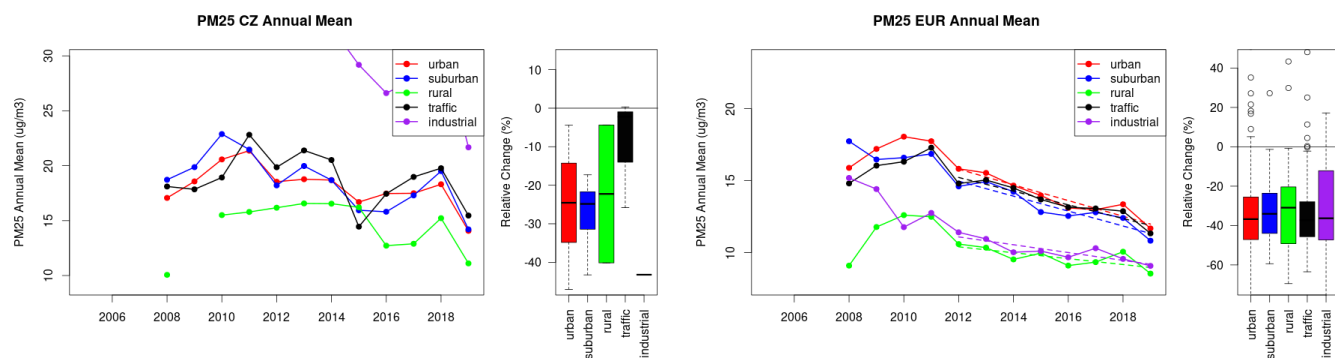


Figure S.109: Time series of the Czechia (left) and European-wide composite (median) of annual mean PM25 ($\mu\text{g}/\text{m}^3$) per station type and area (red: urban background, blue suburban background, green: rural background, black: traffic, violet: industrial) between 2005 and 2019. In the European composite, the dashed lines show the linear fit between 2005 & 2012 and between 2012 & 2019. The boxplots on the right-hand side show the distribution of relative changes (%) between 2005 and 2019 for all stations of each typology in Czechia and in Europe.

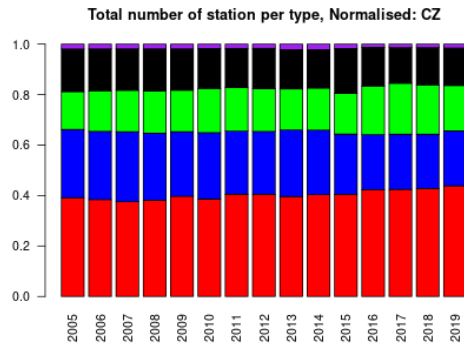
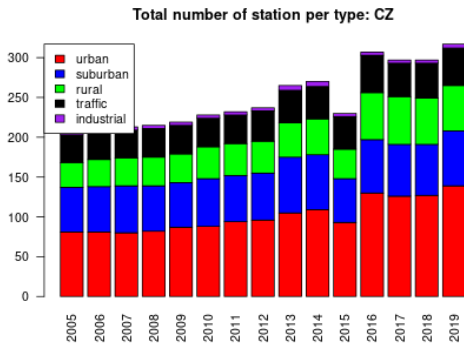
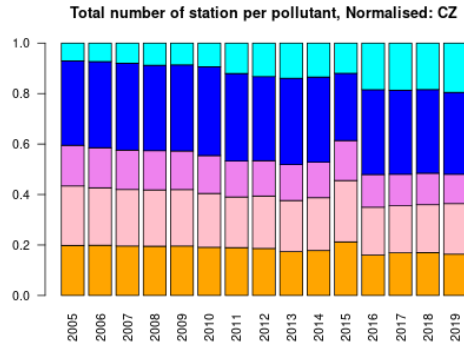
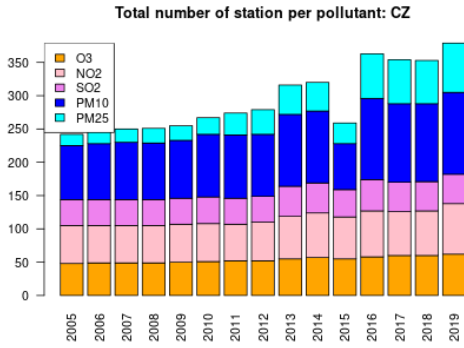
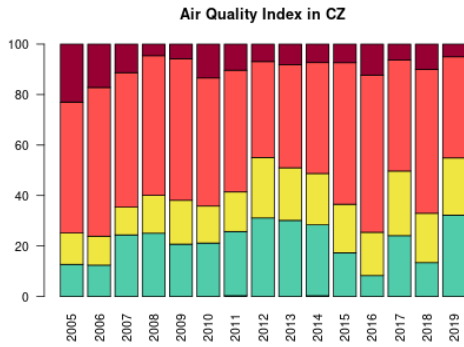


Figure S.110: For Czechia: overall air quality index (percentage of days in a given year) and distribution of daily categories per pollutant (light blue: good, light green: fair, yellow: moderate, orange: poor, red: very poor, violet: extremely poor).

6 Germany

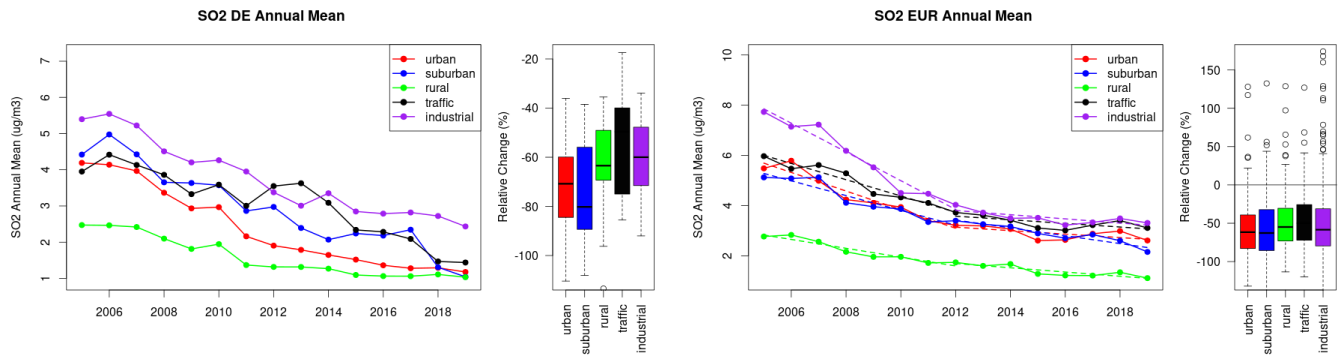


Figure S.111: Time series of the Germany (left) and European-wide composite (median) of annual mean SO₂ (ug/m³) per station type and area (red: urban background, blue suburban background, green: rural background, black: traffic, violet: industrial) between 2005 and 2019. In the European composite, the dashed lines show the linear fit between 2005 & 2012 and between 2012 & 2019. The boxplots on the right-hand side show the distribution of relative changes (%) between 2005 and 2019 for all stations of each typology in Germany and in Europe.

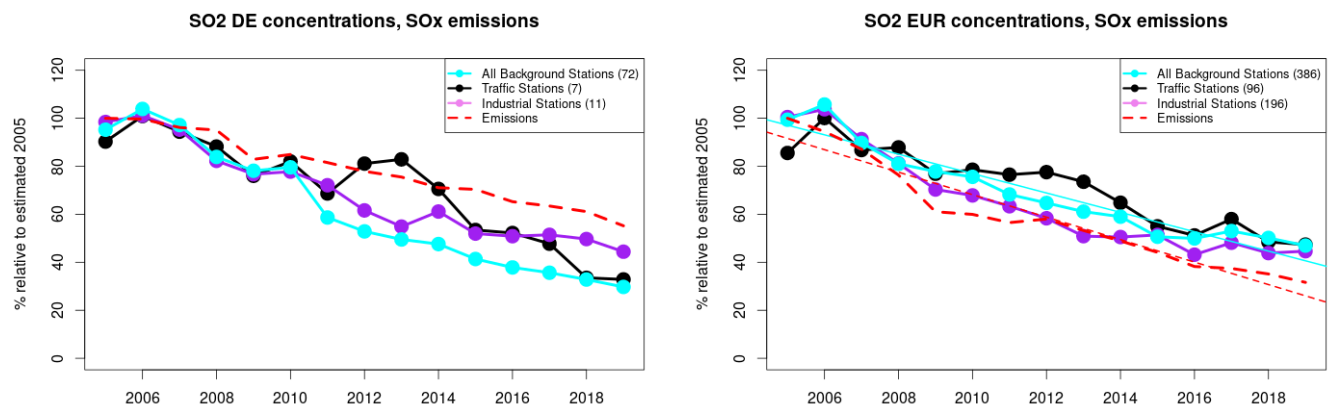


Figure S.112: Time series of 2005-2019 (left) and European (right) median SO₂ observed at traffic (black), industrial (violet) and background (cyan) sites (solid lines), and corresponding SO_x emissions (dashed line) normalised to estimated 2000 levels (%). The median is taken over where more than 5 stations of each typology is available. The total number of stations included is provided in brackets. In the European composite, straight lines are the linear fits over the whole period.

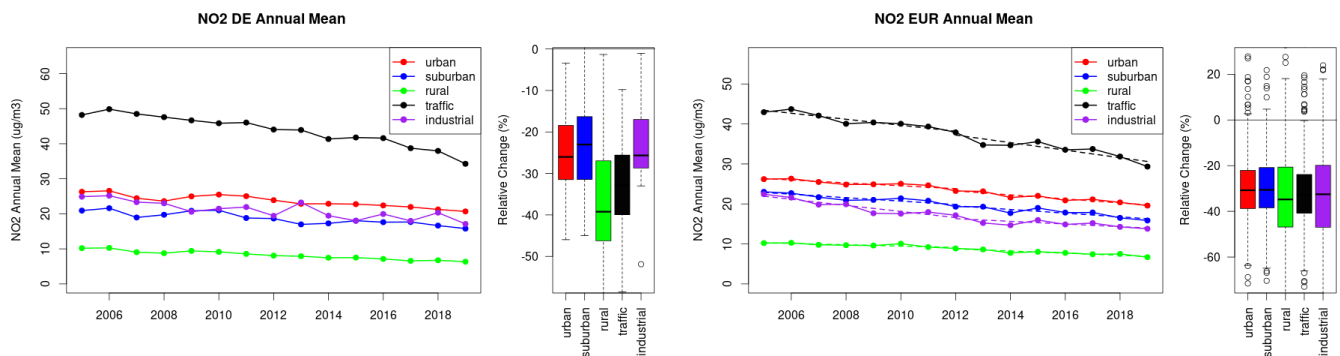


Figure S.113: Time series of the Germany (left) and European-wide composite (median) of annual mean NO₂ (ug/m³) per station type and area (red: urban background, blue suburban background, green: rural background, black: traffic, violet: industrial) between 2005 and 2019. In the European composite, the dashed lines show the linear fit between 2005 & 2012 and between 2012 & 2019. The boxplots on the right-hand side show the distribution of relative changes (%) between 2005 and 2019 for all stations of each typology in Germany and in Europe.

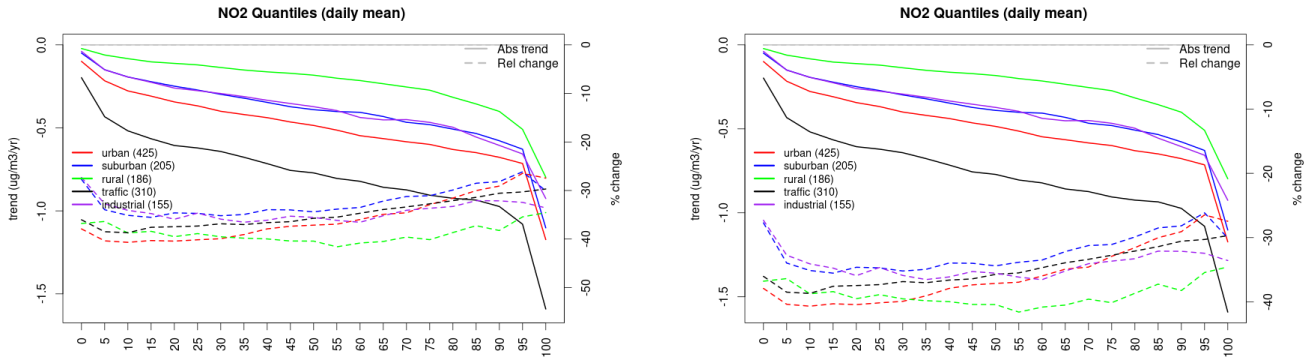


Figure S.114: For NO₂ in Germany (left) and Europe, and for each typology of station: absolute trend (solid lines, left y-axis) and relative change (dashed lines, right y-axis) of the percentiles of daily means.

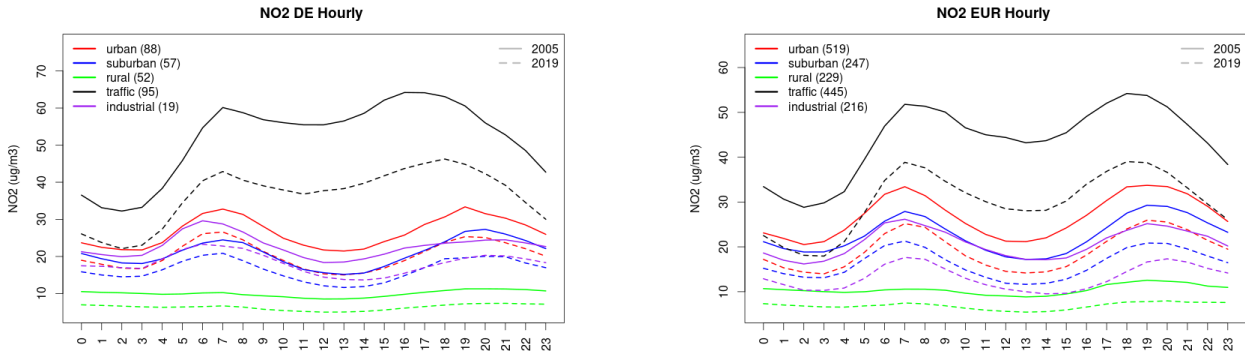


Figure S.115: Diurnal cycle of daily mean NO₂ for Germany (left) and Europe (right) at various station types estimated from the whole time series in 2005 (solid lines) and 2019

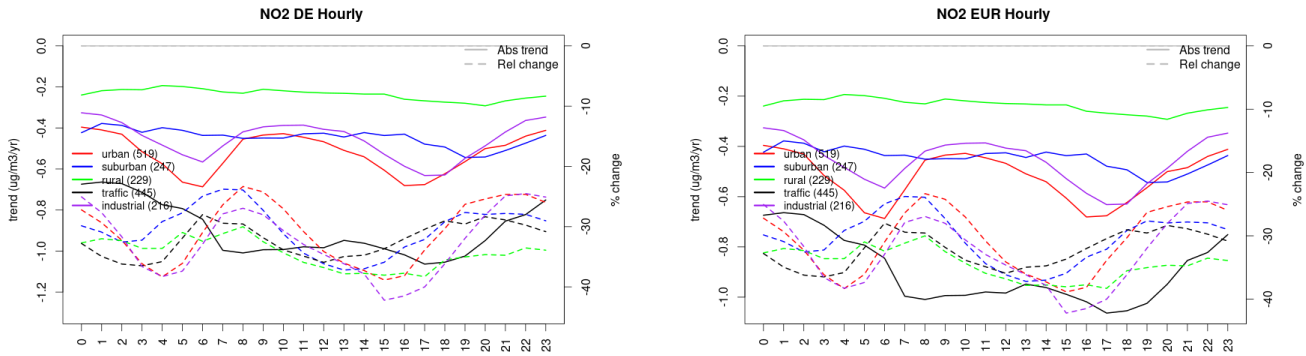


Figure S.116: Absolute (solid lines, left axis) and relative (dashed lines, right axis) trends in the diurnal cycle for Germany (left) and Europe (right) of NO₂ at various station type.

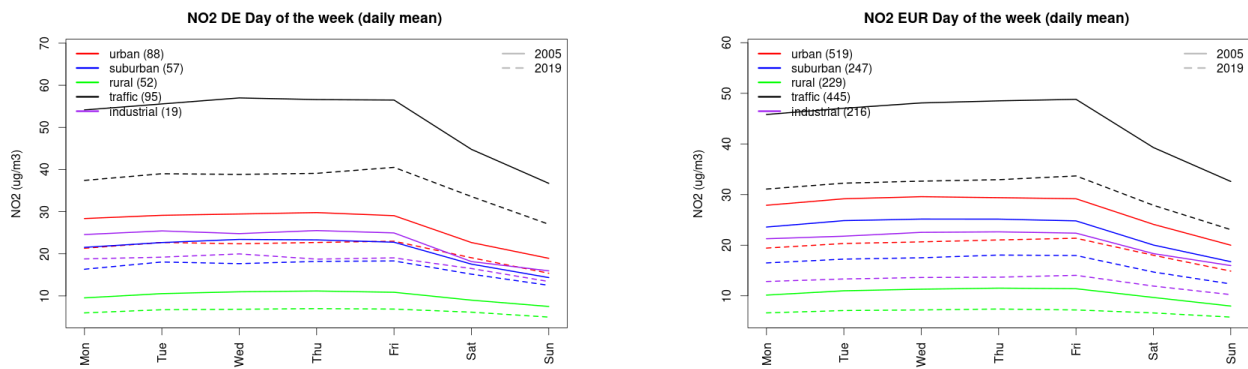


Figure S.117: Weekly cycle of daily mean NO₂ for Germany (left) and Europe (right) at various station types estimated from the whole time series in 2005 (solid lines) and 2019

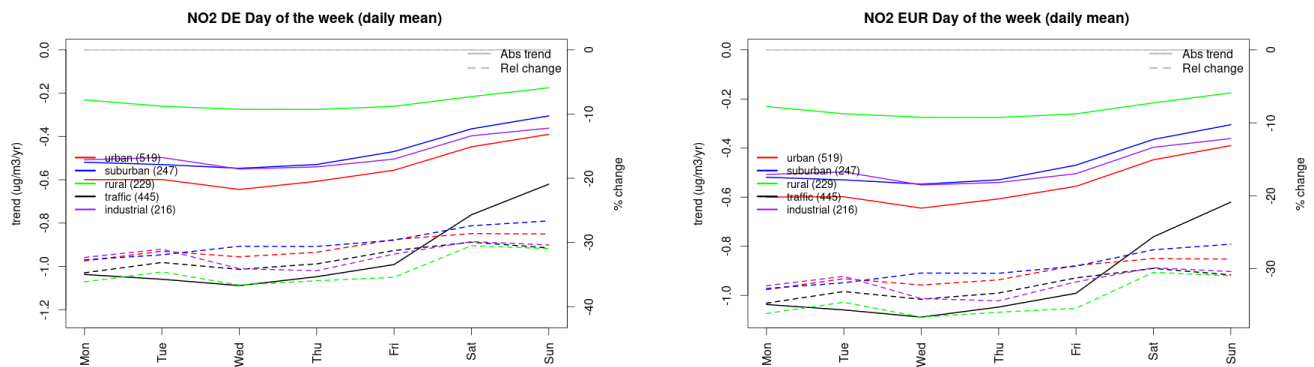


Figure S.118: Absolute (solid lines, left axis) and relative (dashed lines, right axis) trends in the weekly cycle for Germany (left) and Europe (right) of NO₂ at various station type.

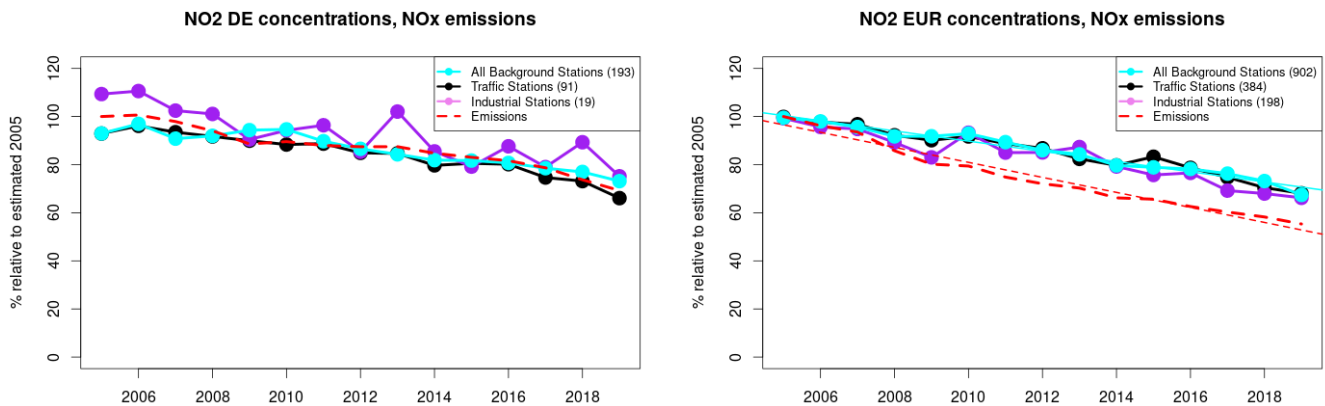


Figure S.119: Time series of 2005-2019 (left) and European (right) median NO₂ observed at traffic (black), industrial (violet) and background (cyan) sites (solid lines), and corresponding NO_x emissions (dashed line) normalised to estimated 2000 levels (%). The median is taken over where more than 5 stations of each typology is available. The total number of stations included is provided in brackets. In the European composite, straight lines are the linear fits over the whole period.

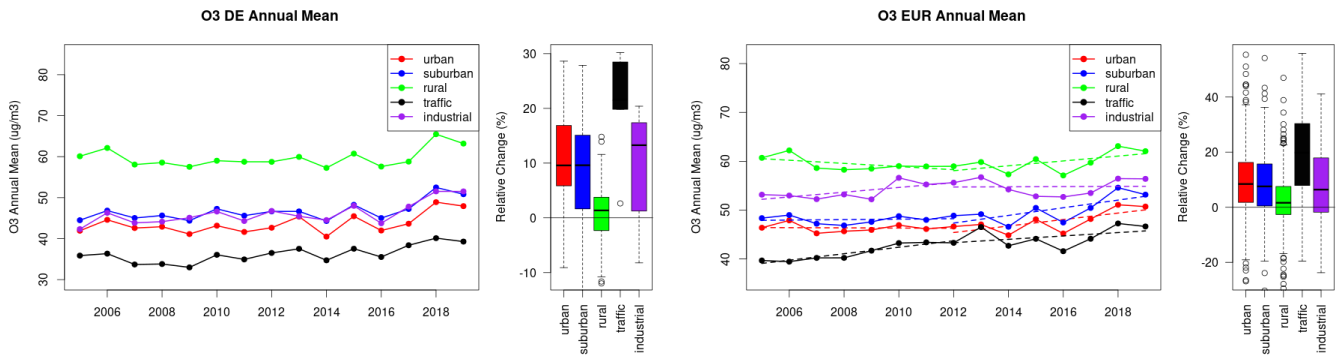


Figure S.120: Time series of the Germany (left) and European-wide composite (median) of annual mean ozone ($\mu\text{g}/\text{m}^3$) per station type and area (red: urban background, blue suburban background, green: rural background, black: traffic, violet: industrial) between 2005 and 2019. In the European composite, the dashed lines show the linear fit between 2005 & 2012 and between 2012 & 2019. The boxplots on the right-hand side show the distribution of relative changes (%) between 2005 and 2019 for all stations of each typology in Germany and in Europe.

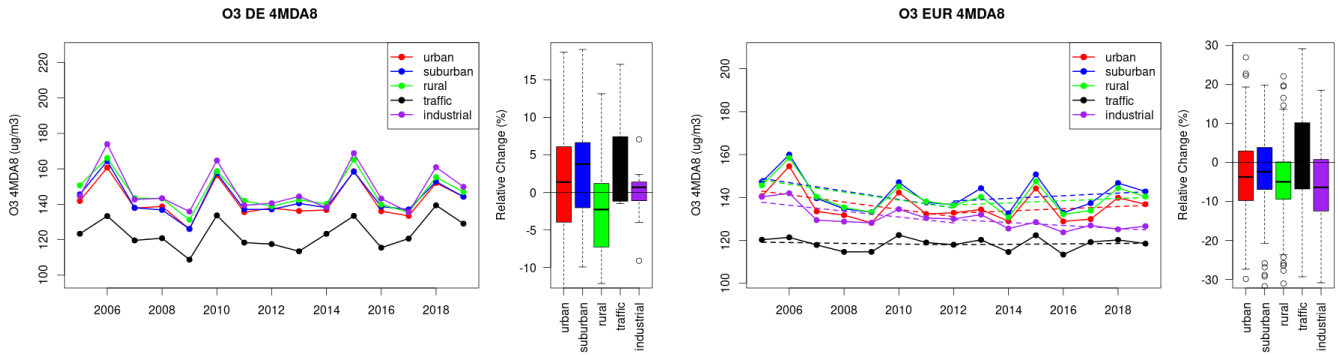


Figure S.121: Time series of the Germany (left) and European-wide composite (median) of O3 fourth highest daily peak (4MDA8, $\mu\text{g}/\text{m}^3$) per station type and area (red: urban background, blue suburban background, green: rural background, black: traffic, violet: industrial) between 2005 and 2019. In the European composite, the dashed lines show the linear fit between 2005 & 2012 and between 2012 & 2019. The boxplots on the right-hand side show the distribution of relative changes (%) between 2005 and 2019 for all stations of each typology in Germany and in Europe.

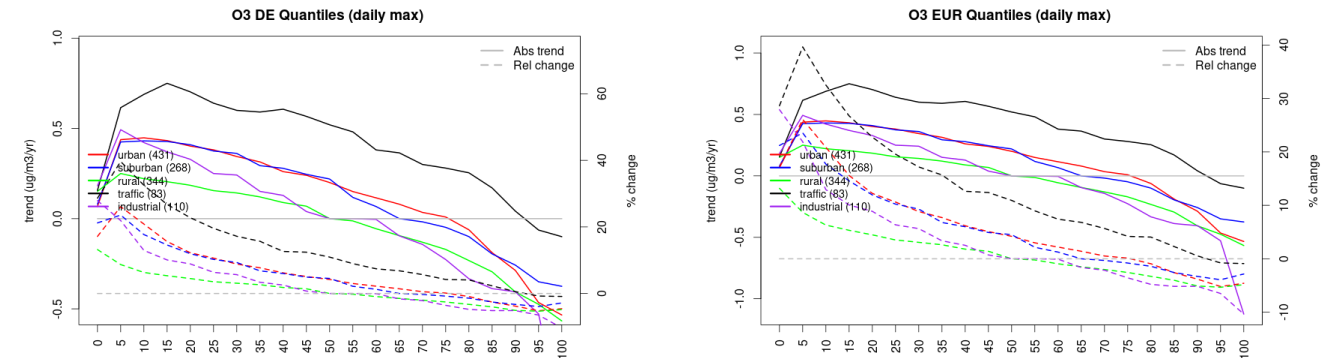


Figure S.122: For ozone in Germany (left) and Europe, and for each typology of station: absolute trend (solid lines, left y-axis) and relative change (dashed lines, right y-axis) of the percentiles of daily maxima.

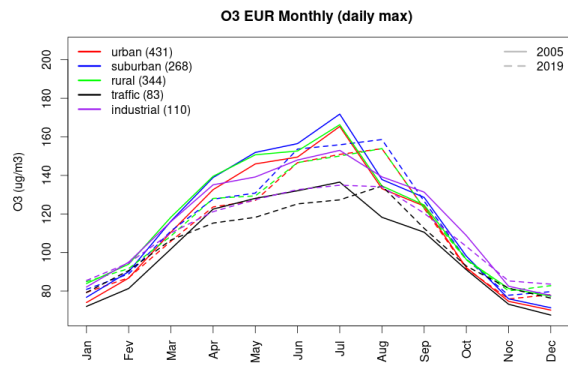
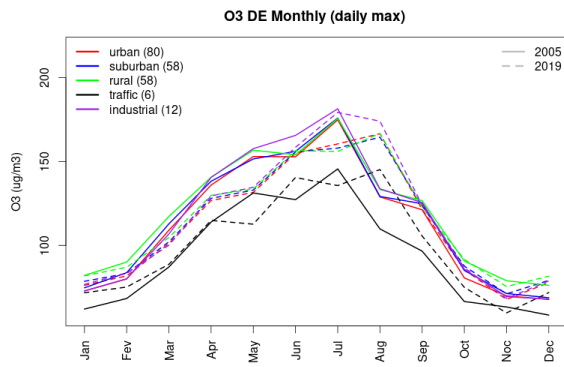


Figure S.123: Monthly cycle of daily max ozone for Germany (left) and Europe (right) at various station types estimated from the whole time series in 2005 (solid lines) and 2019

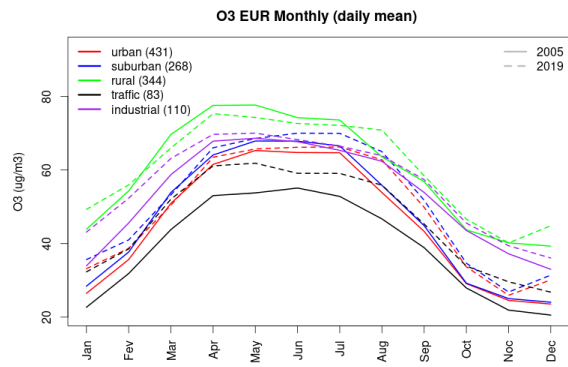
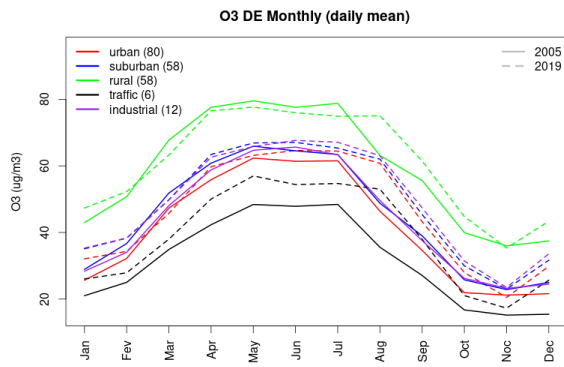


Figure S.124: Monthly cycle of daily mean ozone for Germany (left) and Europe (right) at various station types estimated from the whole time series in 2005 (solid lines) and 2019

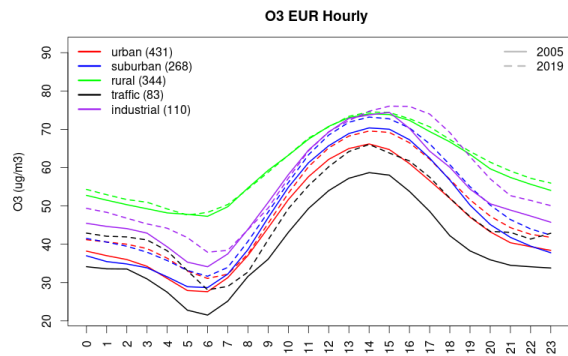
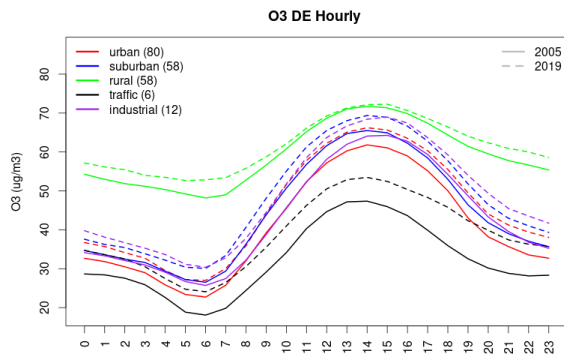


Figure S.125: Diurnal cycle of daily mean ozone for Germany (left) and Europe (right) at various station types estimated from the whole time series in 2005 (solid lines) and 2019

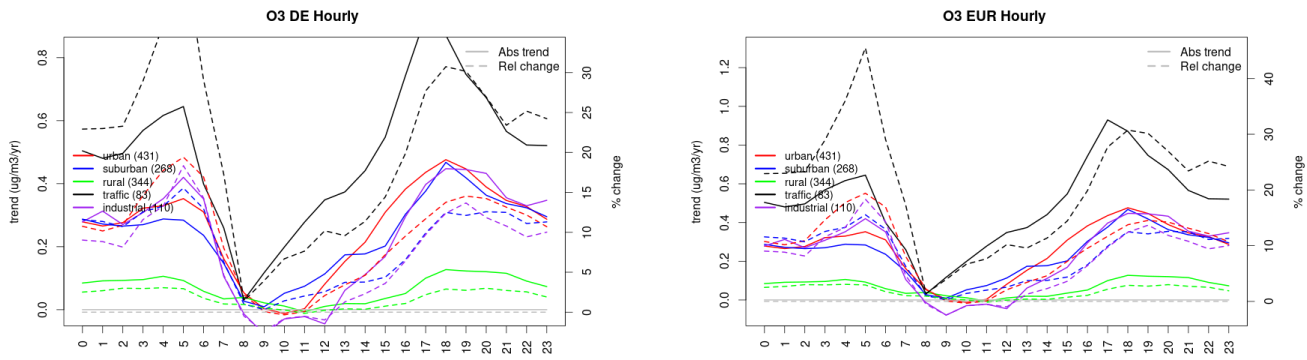


Figure S.126: Absolute (solid lines, left axis) and relative (dashed lines, right axis) trends in the diurnal cycle for Germany (left) and Europe (right) of ozone at various station type.

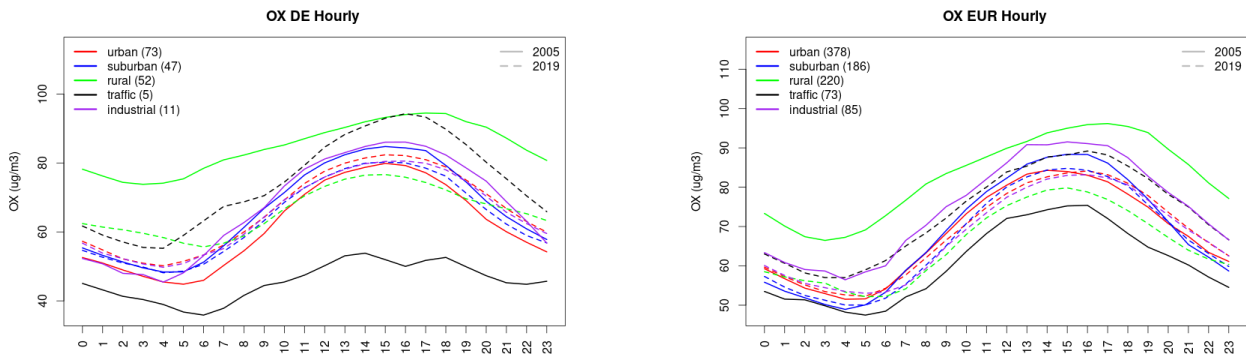


Figure S.127: Diurnal cycle of daily mean OX (as NO₂+O₃) for Germany (left) and Europe (right) at various station types estimated from the whole time series in 2005 (solid lines) and 2019 (dashed lines).

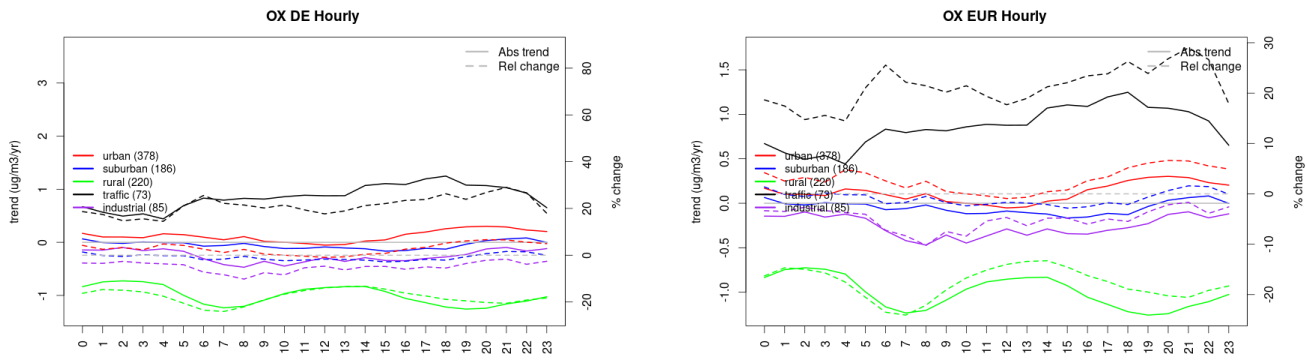


Figure S.128: Absolute (solid lines, left axis) and relative (dashed lines, right axis) trends in the diurnal cycle for Germany (left) and Europe (right) of OX (as NO₂+O₃) at various station type.

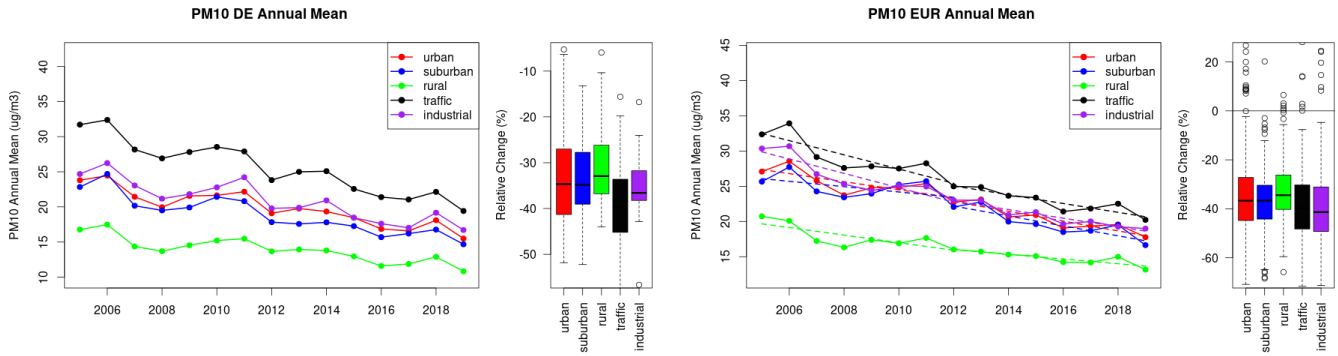


Figure S.129: Time series of the Germany (left) and European-wide composite (median) of annual mean PM10 ($\mu\text{g}/\text{m}^3$) per station type and area (red: urban background, blue suburban background, green: rural background, black: traffic, violet: industrial) between 2005 and 2019. In the European composite, the dashed lines show the linear fit between 2005 & 2012 and between 2012 & 2019. The boxplots on the right-hand side show the distribution of relative changes (%) between 2005 and 2019 for all stations of each typology in Germany and in Europe.

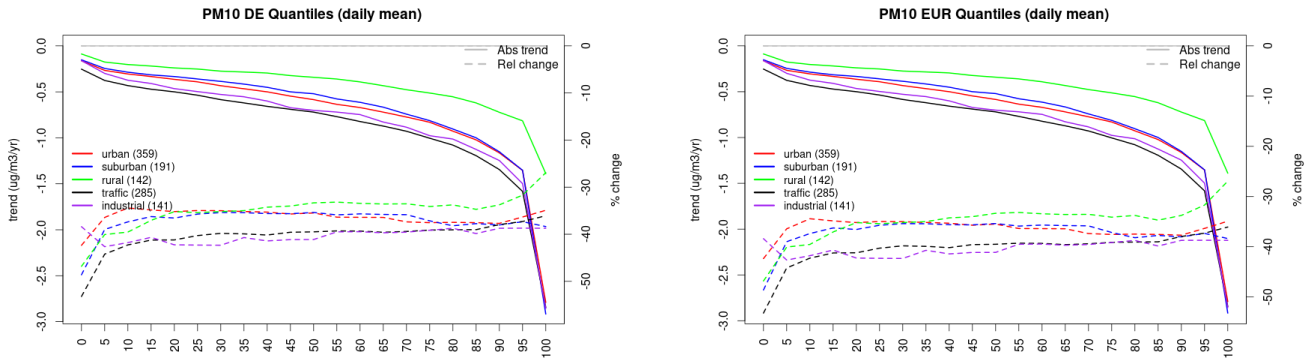


Figure S.130: For PM10 in Germany (left) and Europe, and for each typology of station: absolute trend (solid lines, left y-axis) and relative change (dashed lines, right y-axis) of the percentiles of daily means.

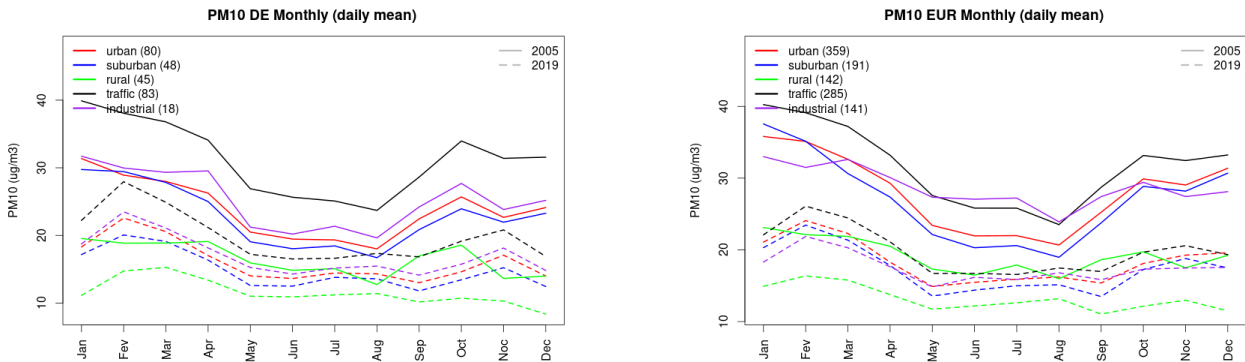


Figure S.131: Monthly cycle of daily mean PM10 for Germany (left) and Europe (right) at various station types estimated from the whole time series in 2005 (solid lines) and 2019

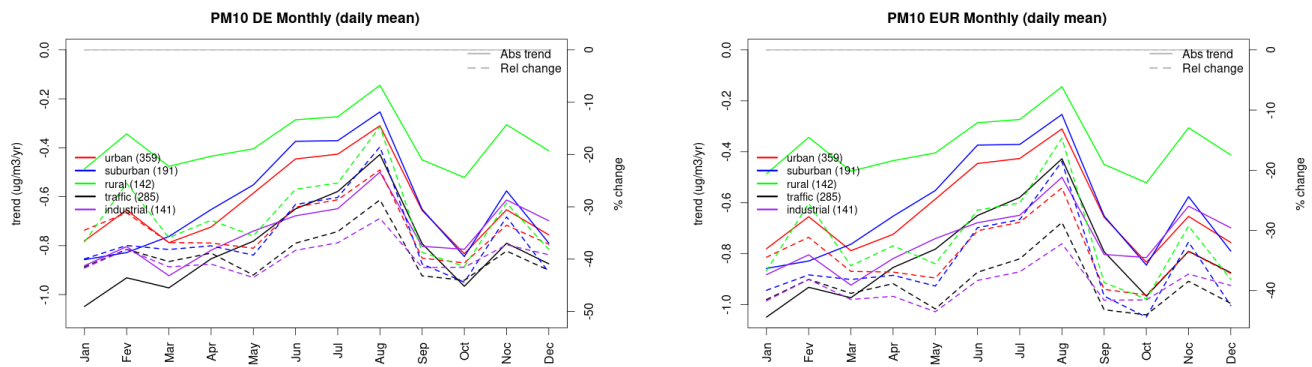


Figure S.132: Absolute (solid lines, left axis) and relative (dashed lines, right axis) trends in the monthly cycle for Germany (left) and Europe (right) of PM10 at various station type.

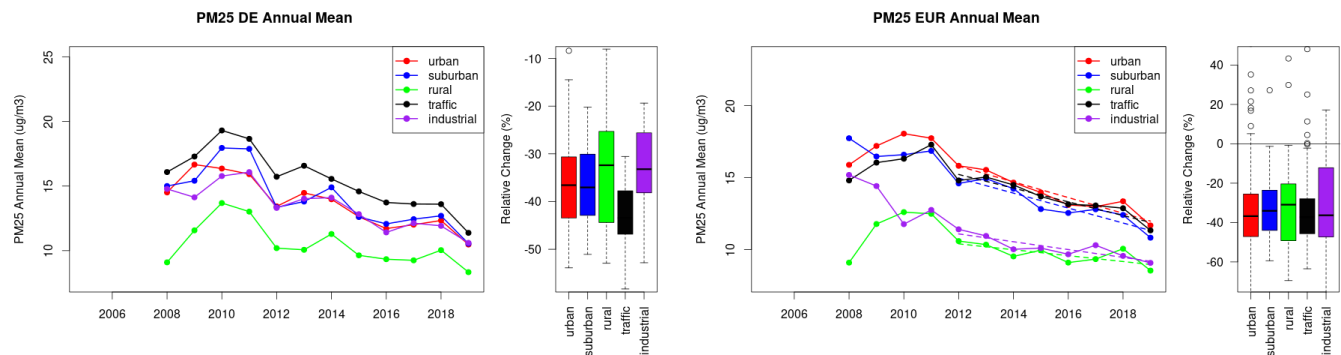


Figure S.133: Time series of the Germany (left) and European-wide composite (median) of annual mean PM25 ($\mu\text{g}/\text{m}^3$) per station type and area (red: urban background, blue suburban background, green: rural background, black: traffic, violet: industrial) between 2005 and 2019. In the European composite, the dashed lines show the linear fit between 2005 & 2012 and between 2012 & 2019. The boxplots on the right-hand side show the distribution of relative changes (%) between 2005 and 2019 for all stations of each typology in Germany and in Europe.

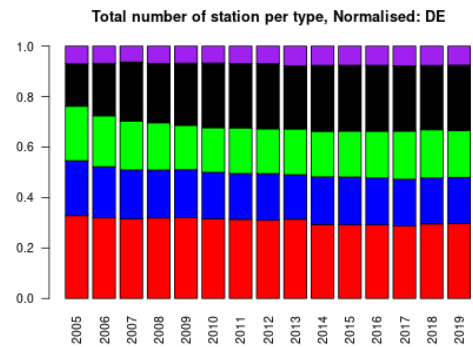
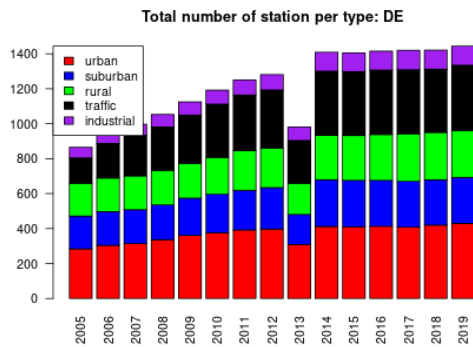
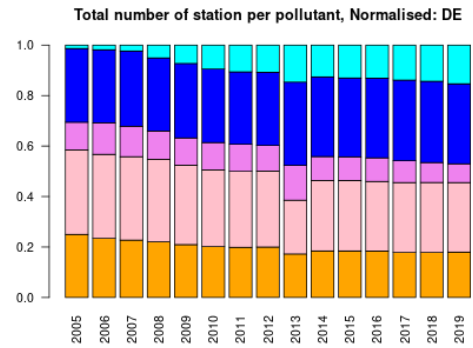
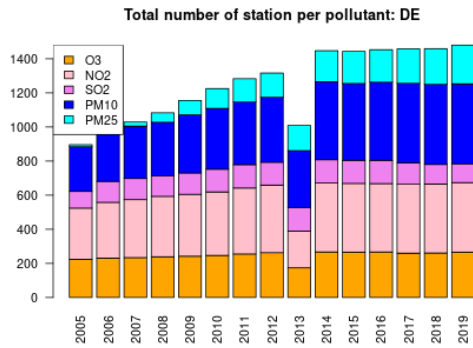
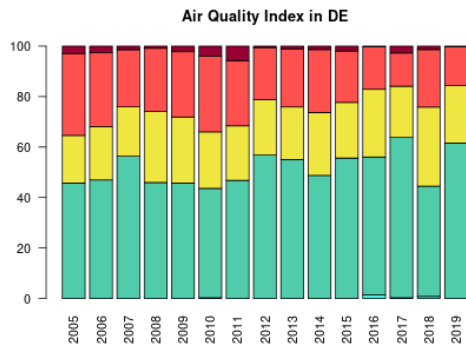


Figure S.134: For Germany: overall air quality index (percentage of days in a given year) and distribution of daily categories per pollutant (light blue: good, light green: fair, yellow: moderate, orange: poor, red: very poor, violet: extremely poor).

7 Denmark

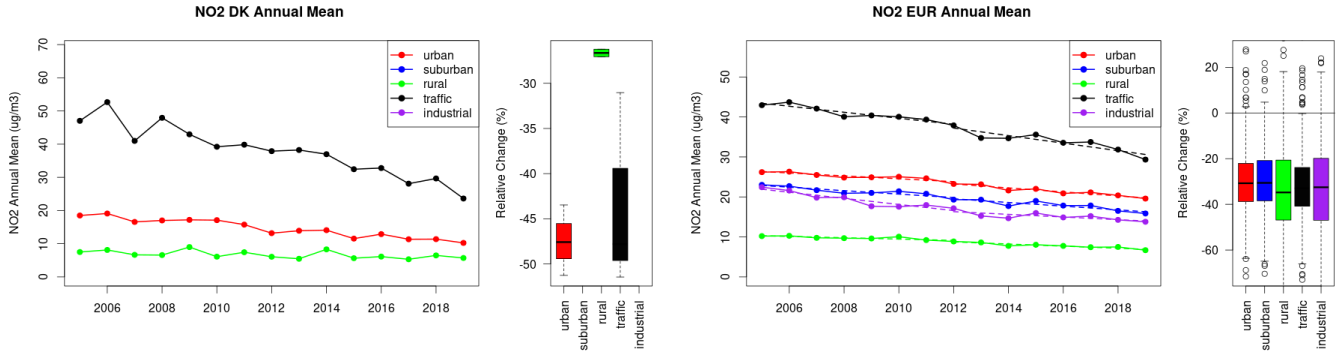


Figure S.135: Time series of the Denmark (left) and European-wide composite (median) of annual mean NO₂ (ug/m³) per station type and area (red: urban background, blue suburban background, green: rural background, black: traffic, violet: industrial) between 2005 and 2019. In the European composite, the dashed lines show the linear fit between 2005 & 2012 and between 2012 & 2019. The boxplots on the right-hand side show the distribution of relative changes (%) between 2005 and 2019 for all stations of each typology in Denmark and in Europe.

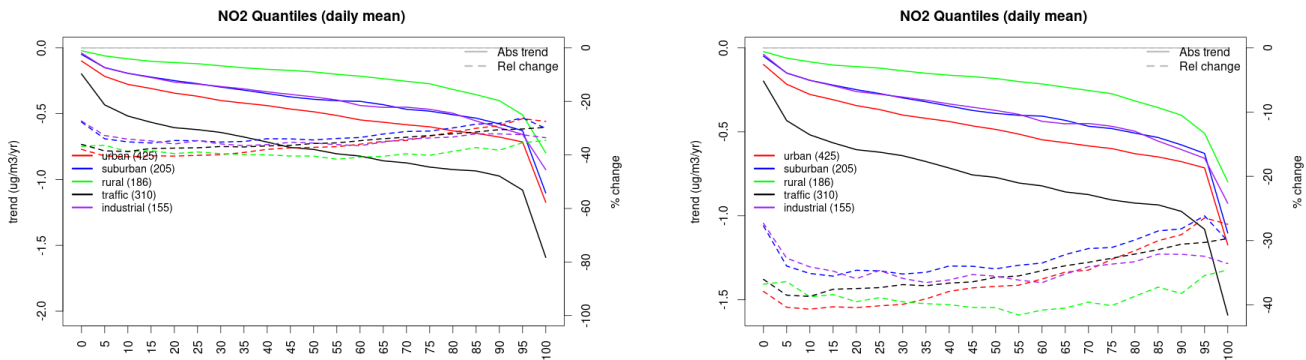


Figure S.136: For NO₂ in Denmark (left) and Europe, and for each typology of station: absolute trend (solid lines, left y-axis) and relative change (dashed lines, right y-axis) of the percentiles of daily means.

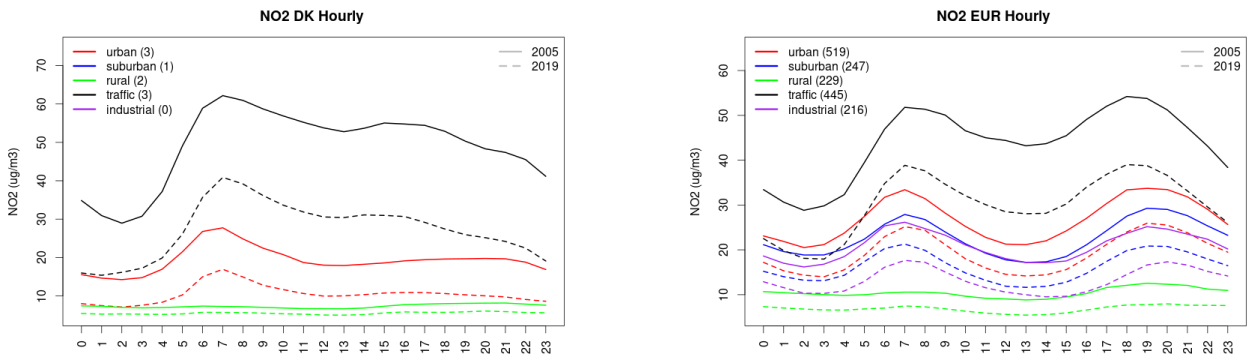


Figure S.137: Diurnal cycle of daily mean NO₂ for Denmark (left) and Europe (right) at various station types estimated from the whole time series in 2005 (solid lines) and 2019

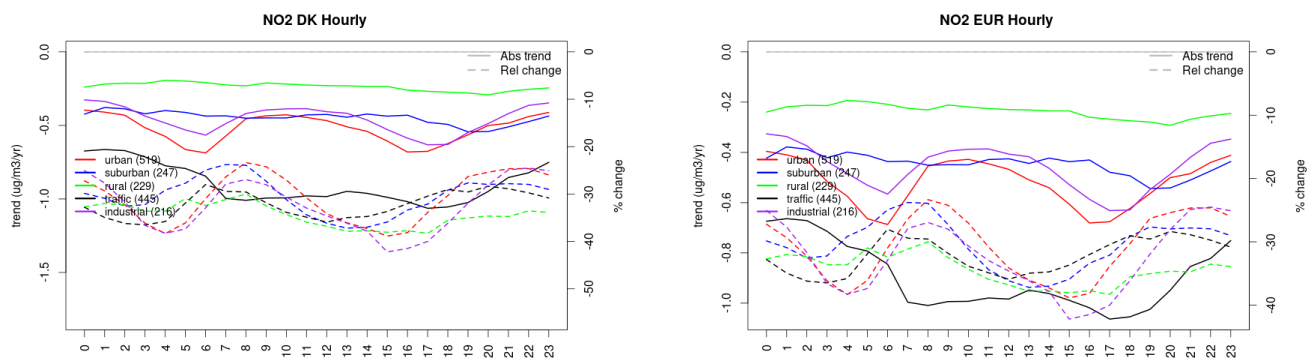


Figure S.138: Absolute (solid lines, left axis) and relative (dashed lines, right axis) trends in the diurnal cycle for Denmark (left) and Europe (right) of NO2 at various station type.

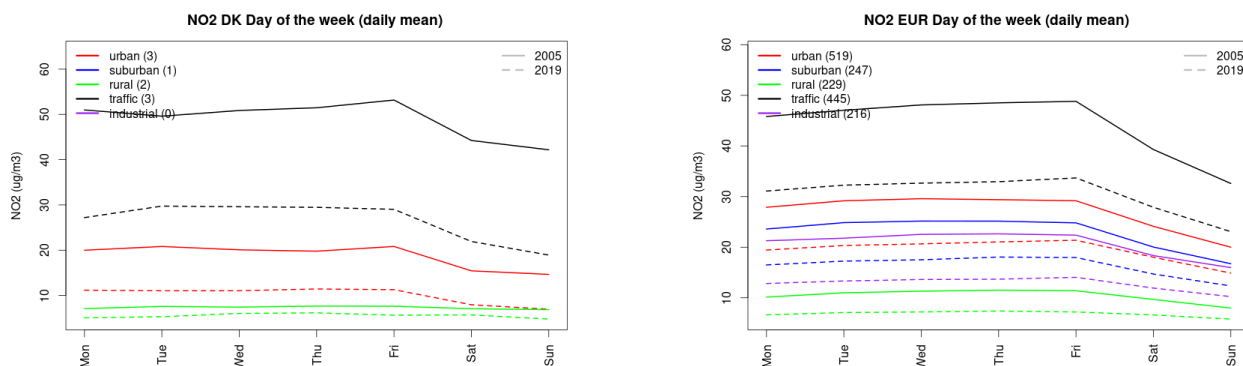


Figure S.139: Weekly cycle of daily mean NO2 for Denmark (left) and Europe (right) at various station types estimated from the whole time series in 2005 (solid lines) and 2019 (dashed lines).

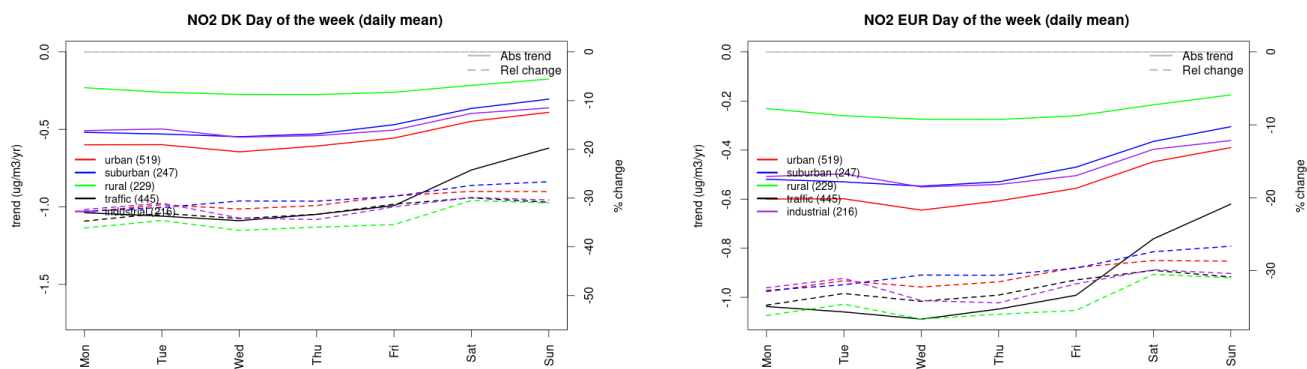


Figure S.140: Absolute (solid lines, left axis) and relative (dashed lines, right axis) trends in the weekly cycle for Denmark (left) and Europe (right) of NO2 at various station type.

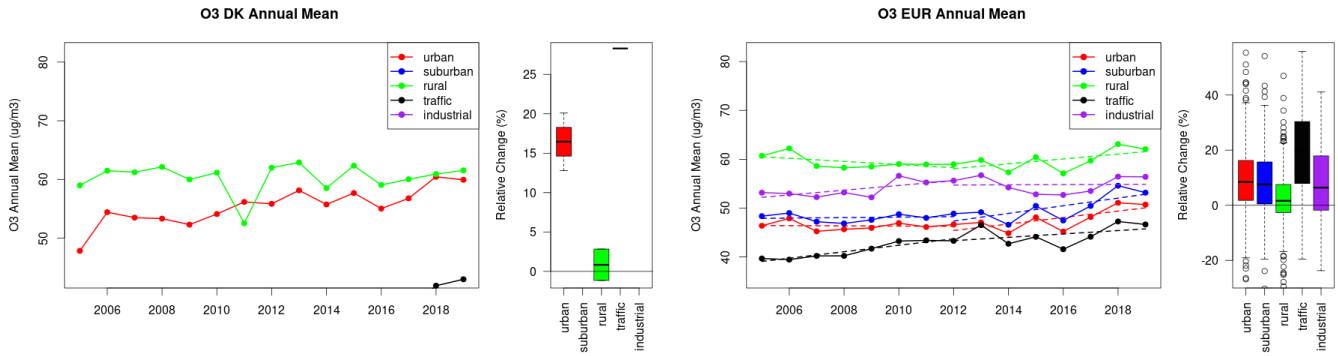


Figure S.141: Time series of the Denmark (left) and European-wide composite (median) of annual mean ozone ($\mu\text{g}/\text{m}^3$) per station type and area (red: urban background, blue suburban background, green: rural background, black: traffic, violet: industrial) between 2005 and 2019. In the European composite, the dashed lines show the linear fit between 2005 & 2012 and between 2012 & 2019. The boxplots on the right-hand side show the distribution of relative changes (%) between 2005 and 2019 for all stations of each typology in Denmark and in Europe.

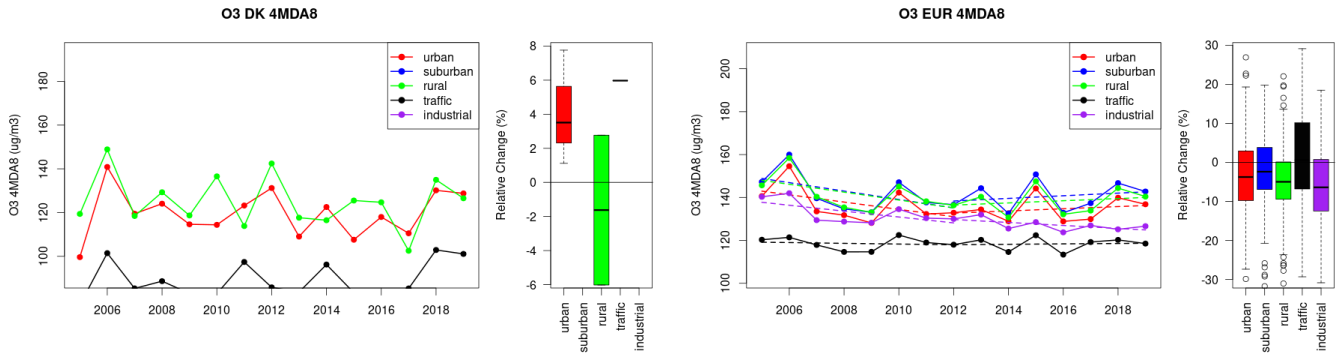


Figure S.142: Time series of the Denmark (left) and European-wide composite (median) of O3 fourth highest daily peak (4MDA8, $\mu\text{g}/\text{m}^3$) per station type and area (red: urban background, blue suburban background, green: rural background, black: traffic, violet: industrial) between 2005 and 2019. In the European composite, the dashed lines show the linear fit between 2005 & 2012 and between 2012 & 2019. The boxplots on the right-hand side show the distribution of relative changes (%) between 2005 and 2019 for all stations of each typology in Denmark and in Europe.

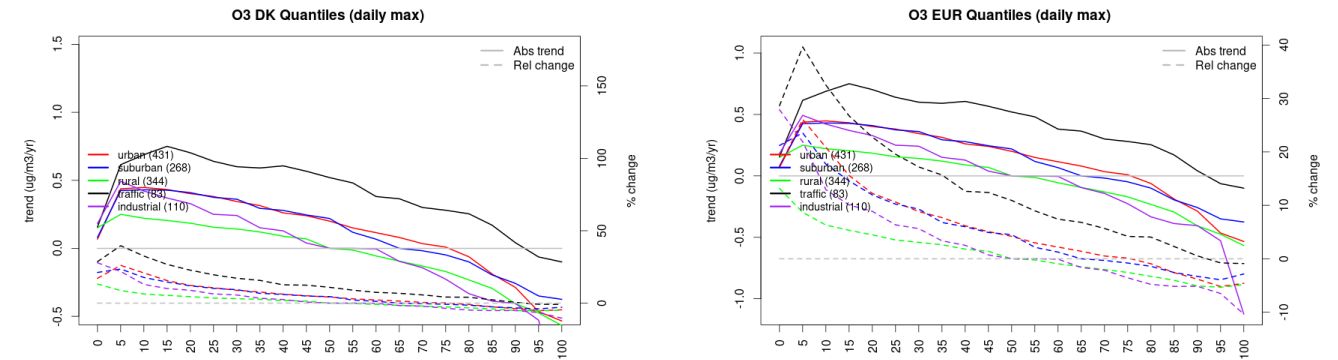


Figure S.143: For ozone in Denmark (left) and Europe, and for each typology of station: absolute trend (solid lines, left y-axis) and relative change (dashed lines, right y-axis) of the percentiles of daily maxima.

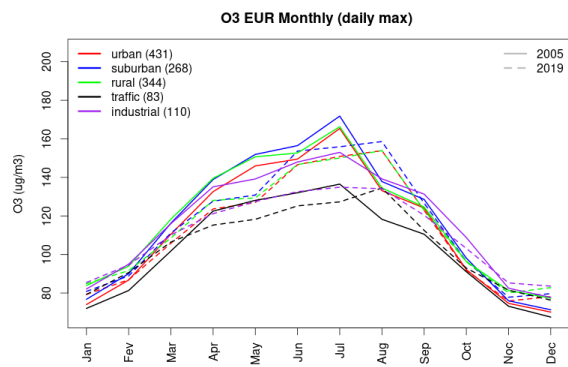
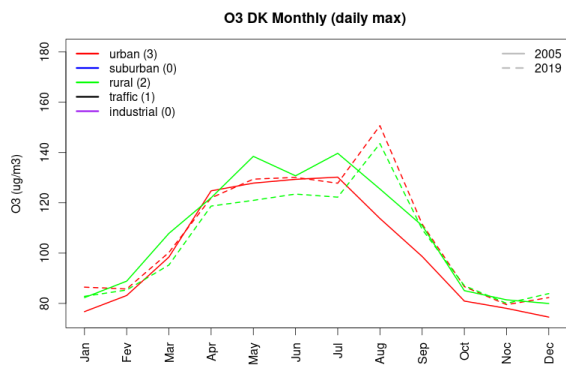


Figure S.144: Monthly cycle of daily max ozone for Denmark (left) and Europe (right) at various station types estimated from the whole time series in 2005 (solid lines) and 2019

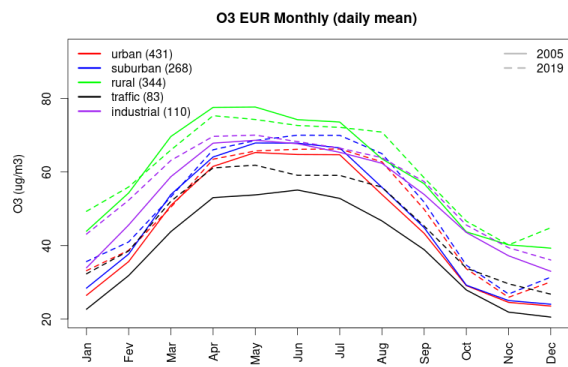
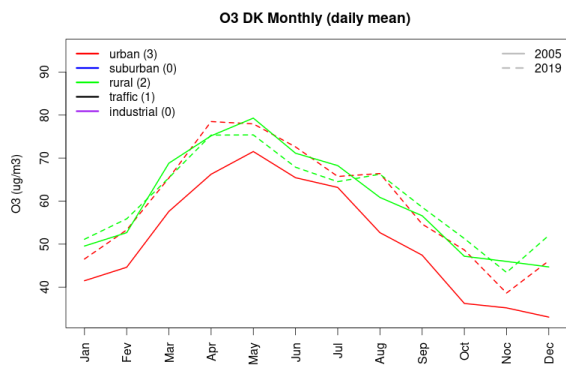


Figure S.145: Monthly cycle of daily mean ozone for Denmark (left) and Europe (right) at various station types estimated from the whole time series in 2005 (solid lines) and 2019

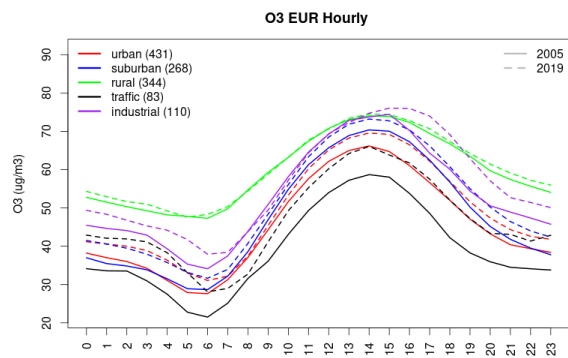
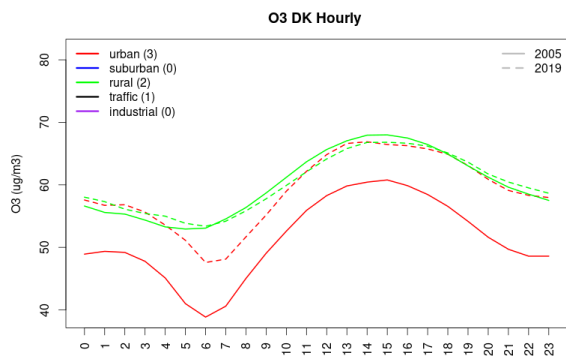


Figure S.146: Diurnal cycle of daily mean ozone for Denmark (left) and Europe (right) at various station types estimated from the whole time series in 2005 (solid lines) and 2019

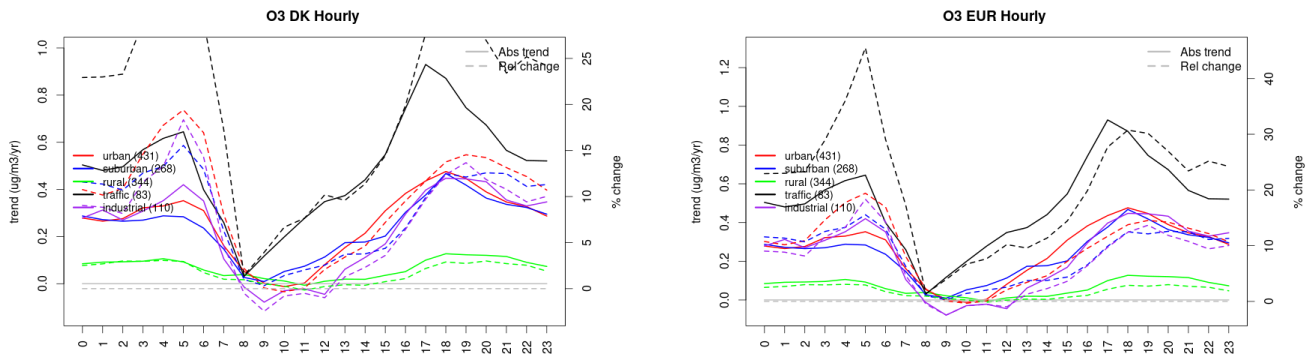


Figure S.147: Absolute (solid lines, left axis) and relative (dashed lines, right axis) trends in the diurnal cycle for Denmark (left) and Europe (right) of ozone at various station type.

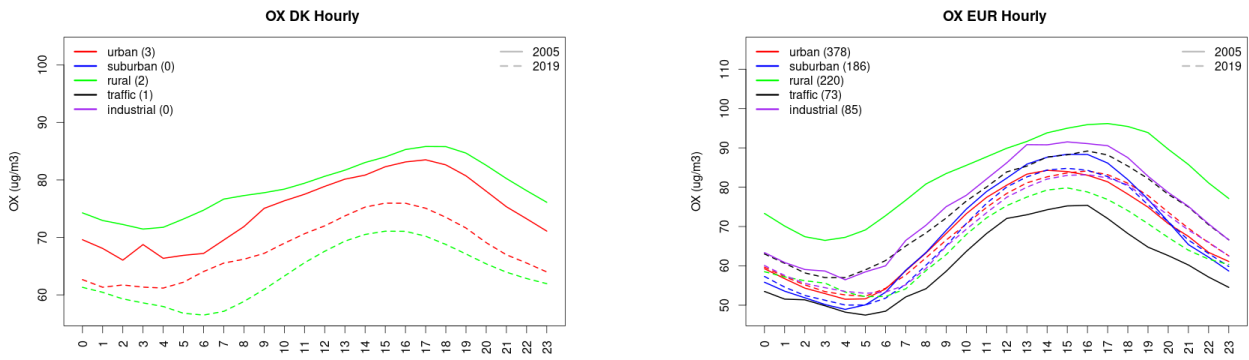


Figure S.148: Diurnal cycle of daily mean OX (as NO₂+O₃) for Denmark (left) and Europe (right) at various station types estimated from the whole time series in 2005 (solid lines) and 2019

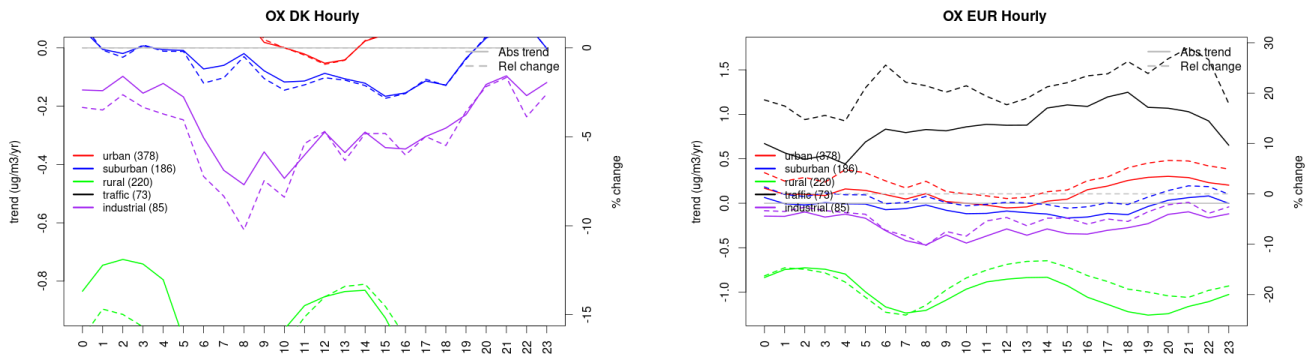


Figure S.149: Absolute (solid lines, left axis) and relative (dashed lines, right axis) trends in the diurnal cycle for Denmark (left) and Europe (right) of OX (as NO₂+O₃) at various station type.

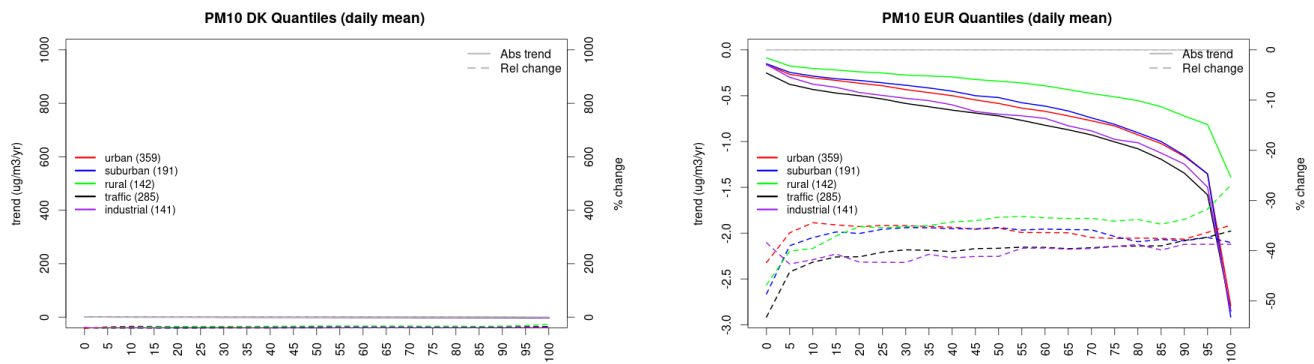


Figure S.150: For PM10 in Denmark (left) and Europe, and for each typology of station: absolute trend (solid lines, left y-axis) and relative change (dashed lines, right y-axis) of the percentiles of daily means.

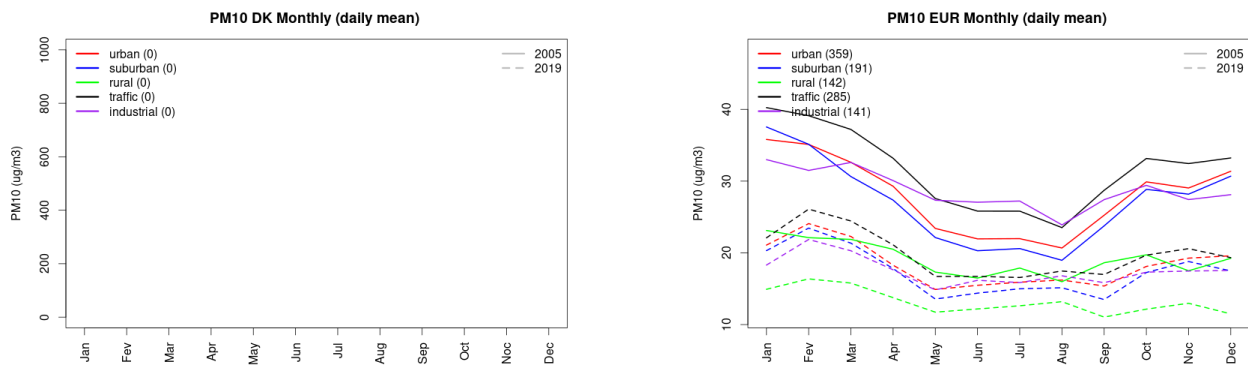


Figure S.151: Monthly cycle of daily mean PM10 for Denmark (left) and Europe (right) at various station types estimated from the whole time series in 2005 (solid lines) and 2019

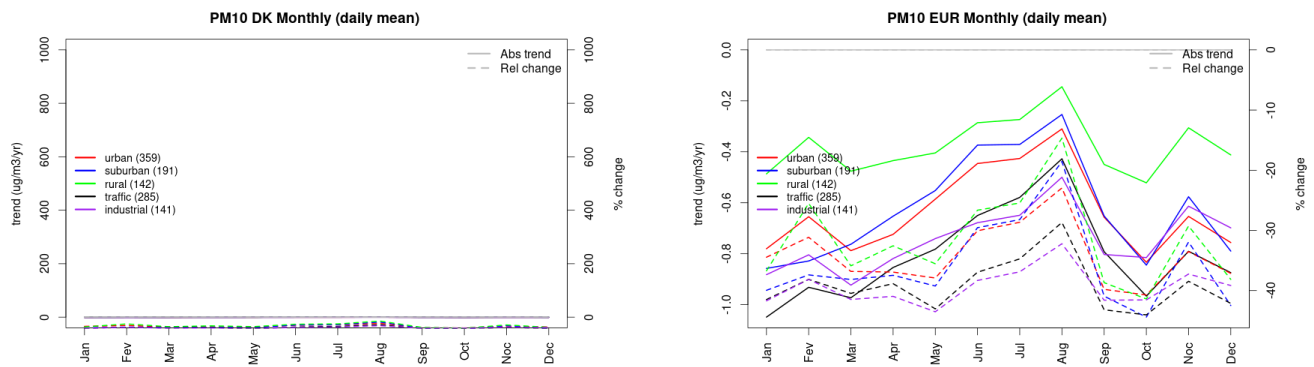


Figure S.152: Absolute (solid lines, left axis) and relative (dashed lines, right axis) trends in the monthly cycle for Denmark (left) and Europe (right) of PM10 at various station type.

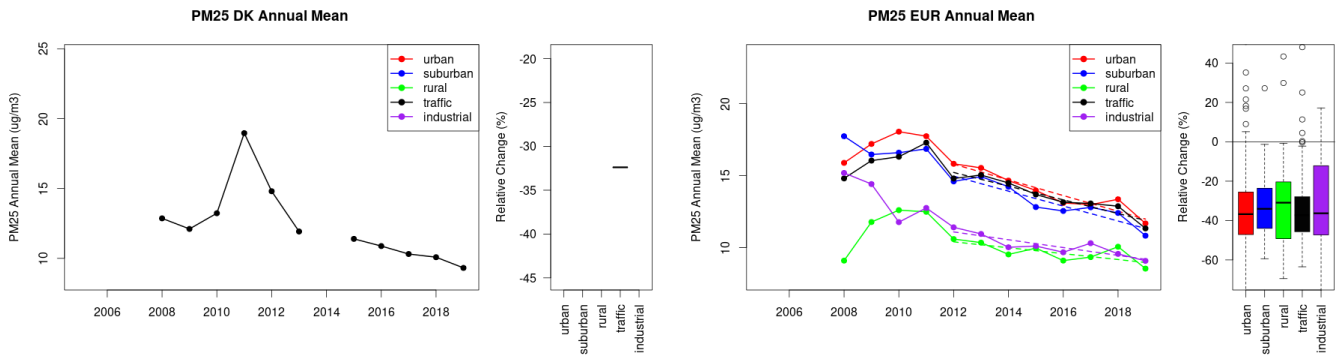


Figure S.153: Time series of the Denmark (left) and European-wide composite (median) of annual mean PM25 (ug/m³) per station type and area (red: urban background, blue suburban background, green: rural background, black: traffic, violet: industrial) between 2005 and 2019. In the European composite, the dashed lines show the linear fit between 2005 & 2012 and between 2012 & 2019. The boxplots on the right-hand side show the distribution of relative changes (%) between 2005 and 2019 for all stations of each typology in Denmark and in Europe.

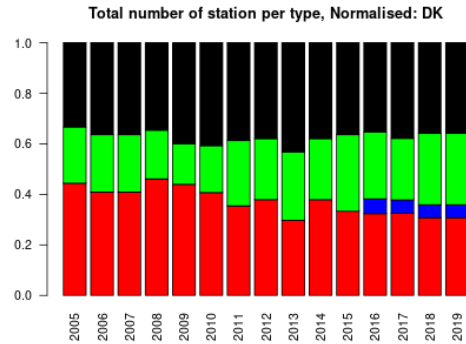
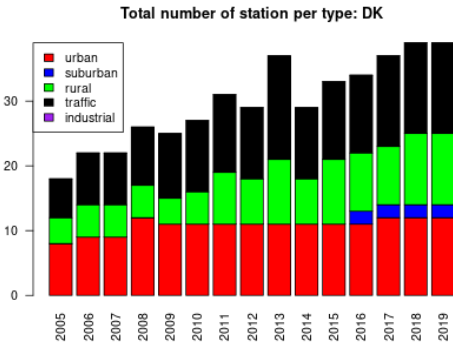
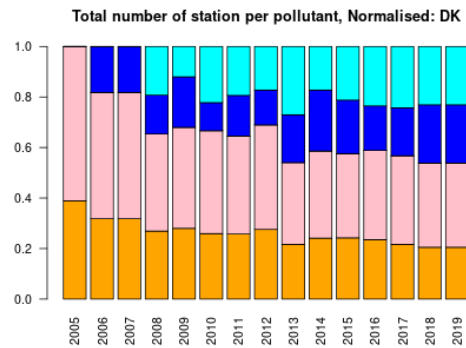
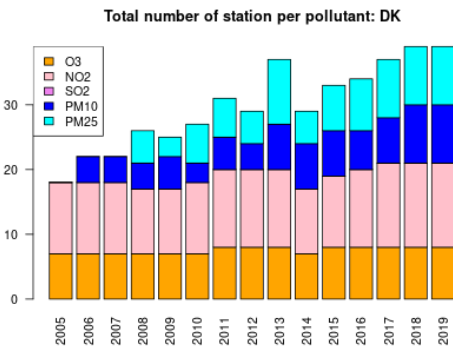
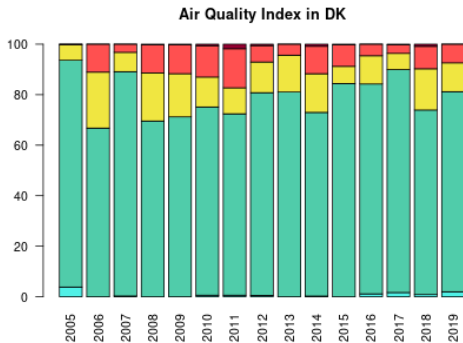


Figure S.154: For Denmark: overall air quality index (percentage of days in a given year) and distribution of daily categories per pollutant (light blue: good, light green: fair, yellow: moderate, orange: poor, red: very poor, violet: extremely poor).

8 Estonia

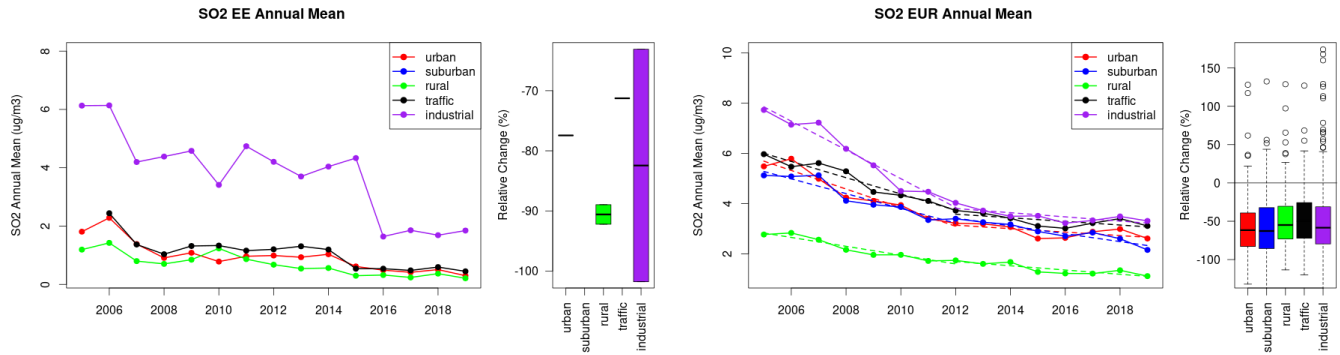


Figure S.155: Time series of the Estonia (left) and European-wide composite (median) of annual mean SO₂ (ug/m³) per station type and area (red: urban background, blue suburban background, green: rural background, black: traffic, violet: industrial) between 2005 and 2019. In the European composite, the dashed lines show the linear fit between 2005 & 2012 and between 2012 & 2019. The boxplots on the right-hand side show the distribution of relative changes (%) between 2005 and 2019 for all stations of each typology in Estonia and in Europe.

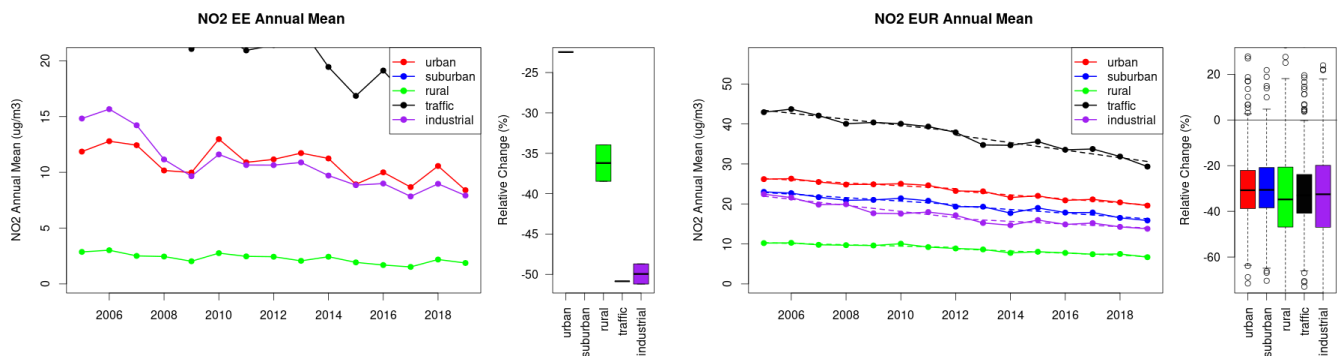


Figure S.156: Time series of the Estonia (left) and European-wide composite (median) of annual mean NO₂ (ug/m³) per station type and area (red: urban background, blue suburban background, green: rural background, black: traffic, violet: industrial) between 2005 and 2019. In the European composite, the dashed lines show the linear fit between 2005 & 2012 and between 2012 & 2019. The boxplots on the right-hand side show the distribution of relative changes (%) between 2005 and 2019 for all stations of each typology in Estonia and in Europe.

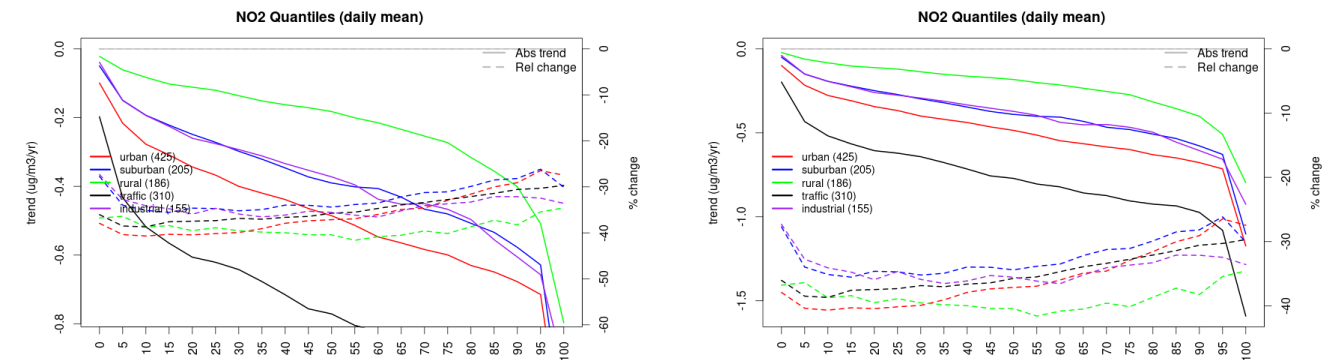


Figure S.157: For NO₂ in Estonia (left) and Europe, and for each typology of station: absolute trend (solid lines, left y-axis) and relative change (dashed lines, right y-axis) of the percentiles of daily means.

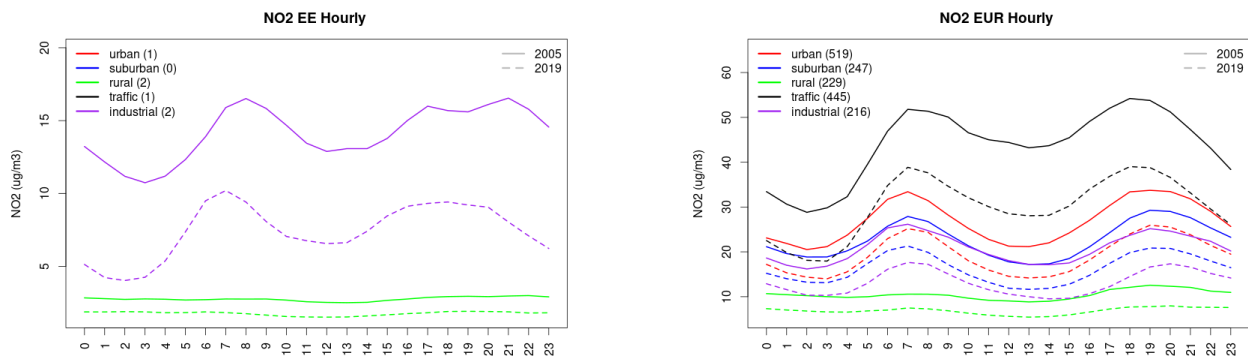


Figure S.158: Diurnal cycle of daily mean NO2 for Estonia (left) and Europe (right) at various station types estimated from the whole time series in 2005 (solid lines) and 2019

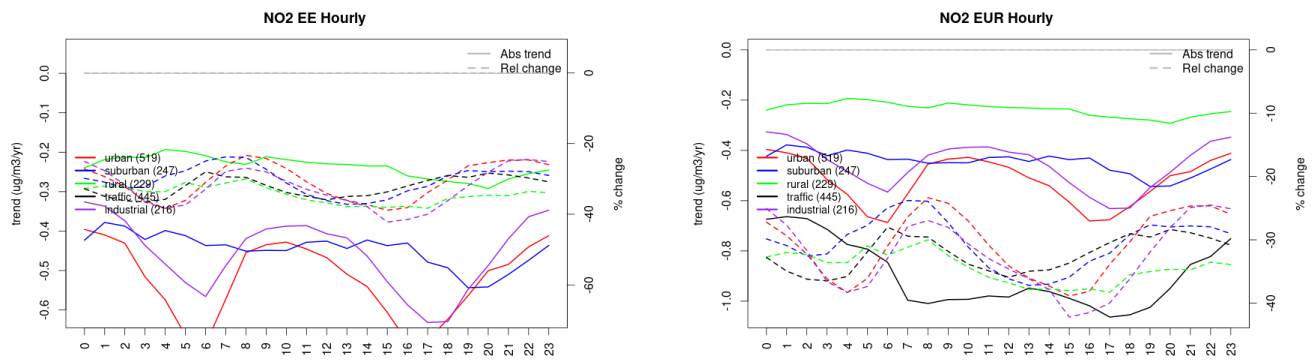


Figure S.159: Absolute (solid lines, left axis) and relative (dashed lines, right axis) trends in the diurnal cycle for Estonia (left) and Europe (right) of NO2 at various station type.

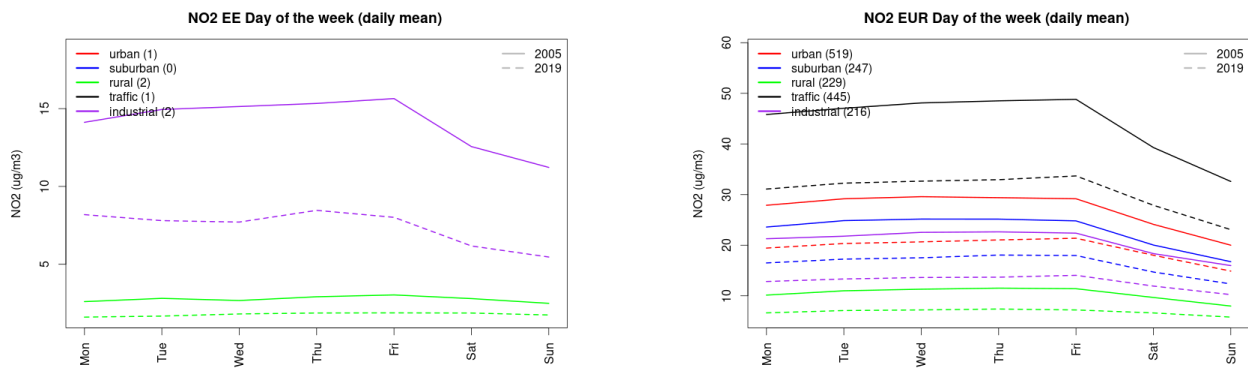


Figure S.160: Weekly cycle of daily mean NO2 for Estonia (left) and Europe (right) at various station types estimated from the whole time series in 2005 (solid lines) and 2019

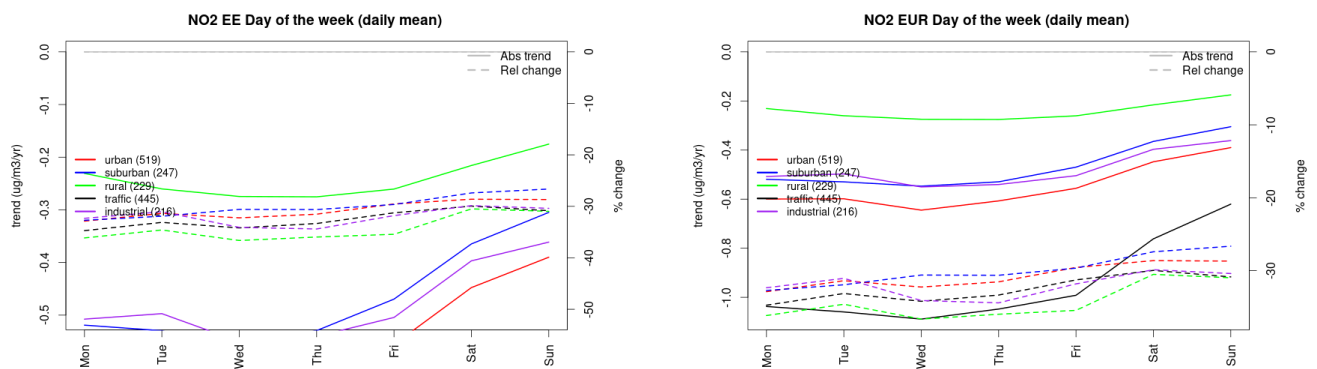


Figure S.161: Absolute (solid lines, left axis) and relative (dashed lines, right axis) trends in the weekly cycle for Estonia (left) and Europe (right) of NO₂ at various station type.

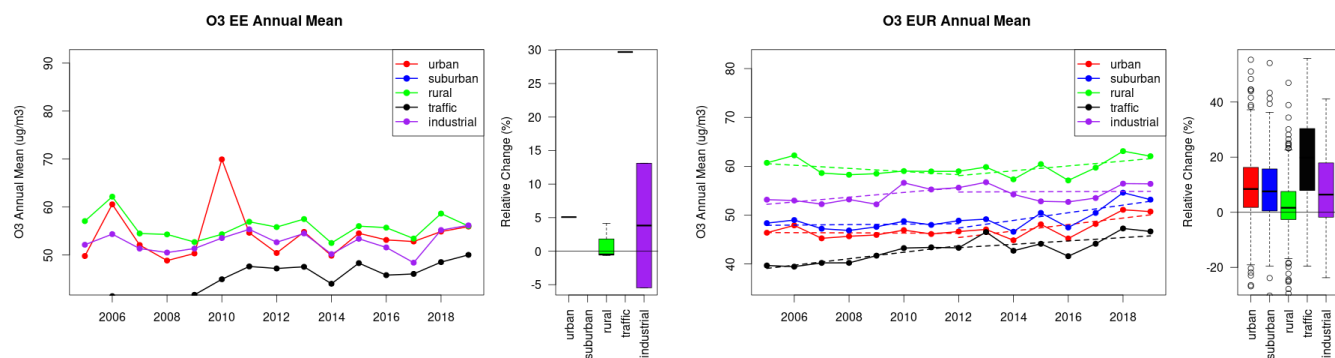


Figure S.162: Time series of the Estonia (left) and European-wide composite (median) of annual mean ozone (ug/m³) per station type and area (red: urban background, blue suburban background, green: rural background, black: traffic, violet: industrial) between 2005 and 2019. In the European composite, the dashed lines show the linear fit between 2005 & 2012 and between 2012 & 2019. The boxplots on the right-hand side show the distribution of relative changes (%) between 2005 and 2019 for all stations of each typology in Estonia and in Europe.

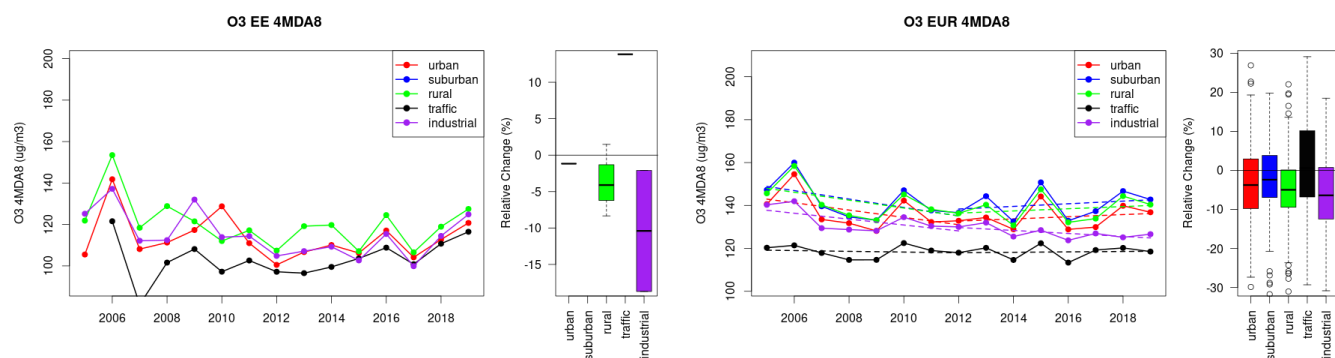


Figure S.163: Time series of the Estonia (left) and European-wide composite (median) of O₃ fourth highest daily peak (4MDA8, ug/m³) per station type and area (red: urban background, blue suburban background, green: rural background, black: traffic, violet: industrial) between 2005 and 2019. In the European composite, the dashed lines show the linear fit between 2005 & 2012 and between 2012 & 2019. The boxplots on the right-hand side show the distribution of relative changes (%) between 2005 and 2019 for all stations of each typology in Estonia and in Europe.

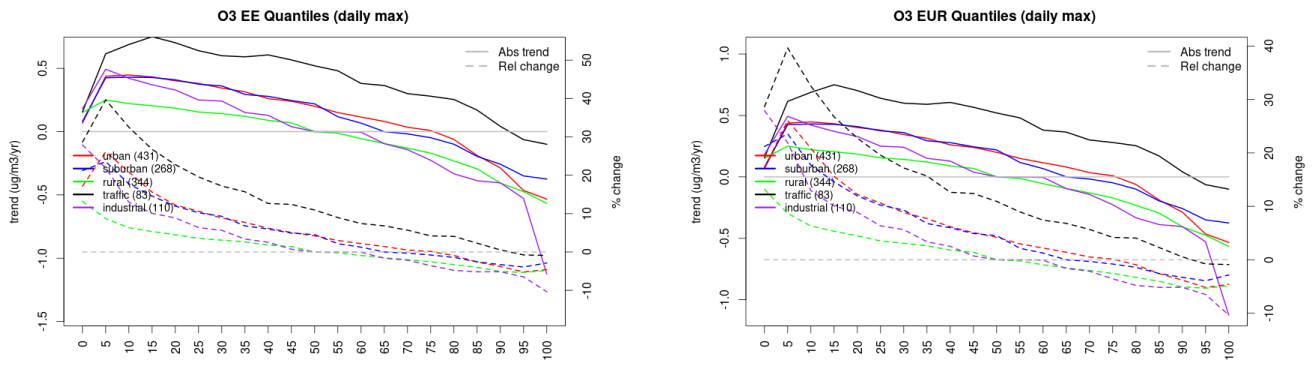


Figure S.164: For ozone in Estonia (left) and Europe, and for each typology of station: absolute trend (solid lines, left y-axis) and relative change (dashed lines, right y-axis) of the percentiles of daily maxima.

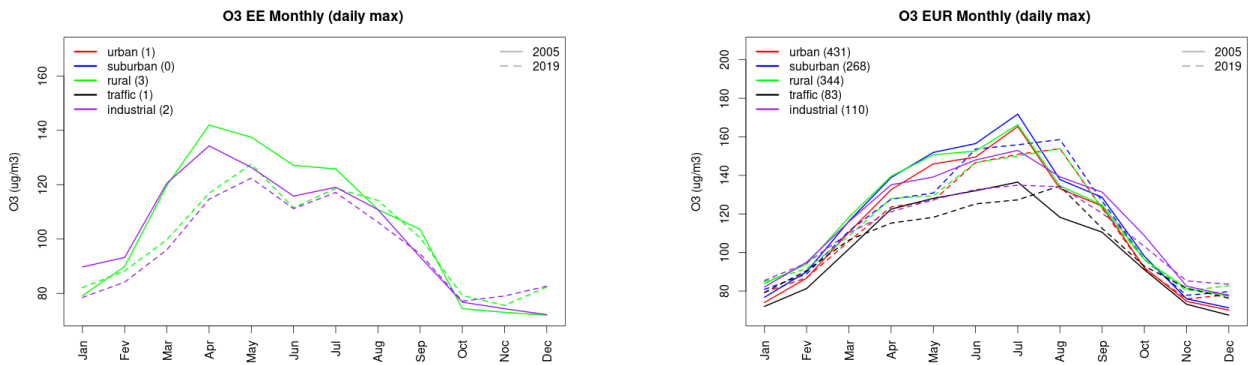


Figure S.165: Monthly cycle of daily max ozone for Estonia (left) and Europe (right) at various station types estimated from the whole time series in 2005 (solid lines) and 2019

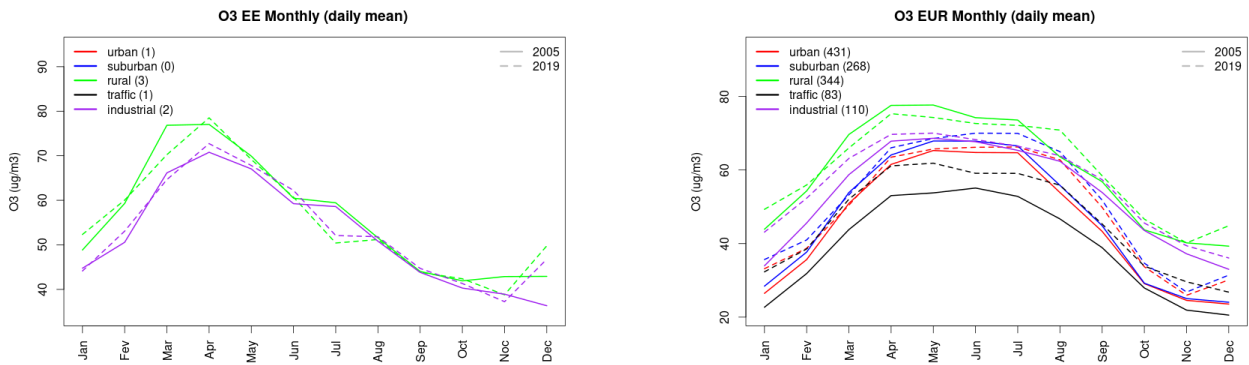


Figure S.166: Monthly cycle of daily mean ozone for Estonia (left) and Europe (right) at various station types estimated from the whole time series in 2005 (solid lines) and 2019

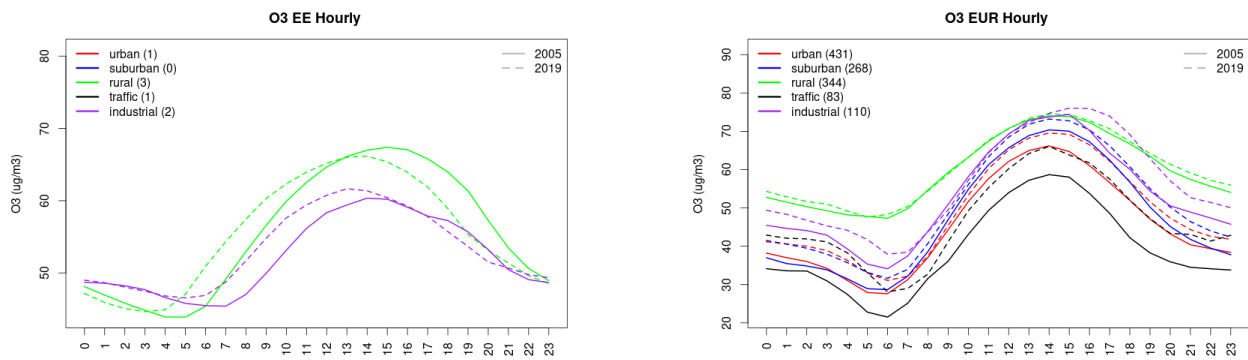


Figure S.167: Diurnal cycle of daily mean ozone for Estonia (left) and Europe (right) at various station types estimated from the whole time series in 2005 (solid lines) and 2019

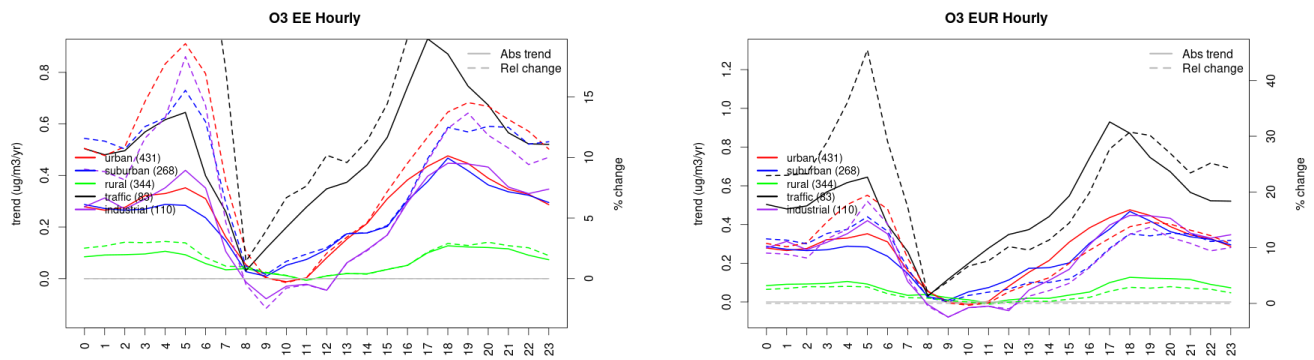


Figure S.168: Absolute (solid lines, left axis) and relative (dashed lines, right axis) trends in the diurnal cycle for Estonia (left) and Europe (right) of ozone at various station type.

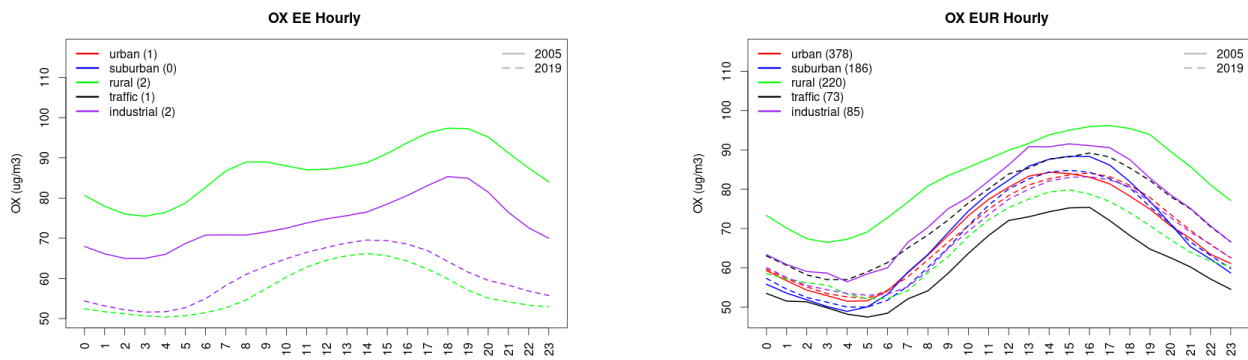


Figure S.169: Diurnal cycle of daily mean OX (as NO₂+O₃) for Estonia (left) and Europe (right) at various station types estimated from the whole time series in 2005 (solid lines) and 2019

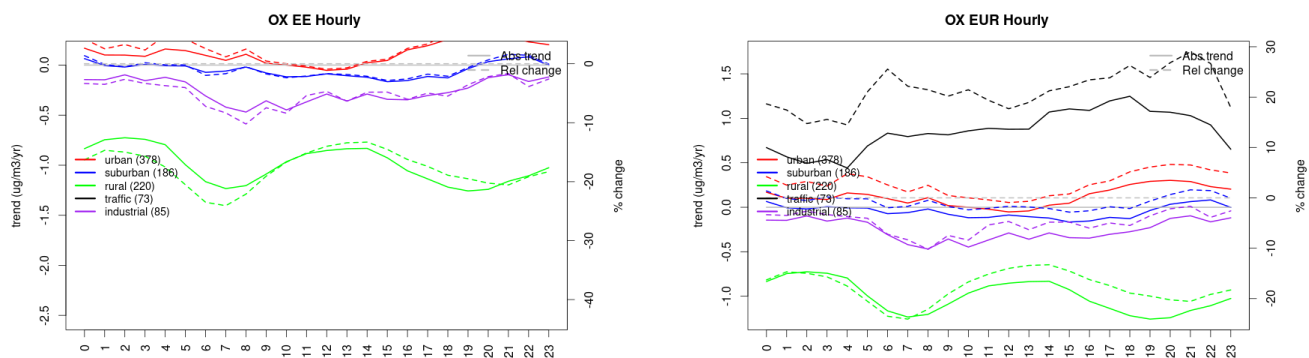


Figure S.170: Absolute (solid lines, left axis) and relative (dashed lines, right axis) trends in the diurnal cycle for Estonia (left) and Europe (right) of OX (as NO₂+O₃) at various station type.

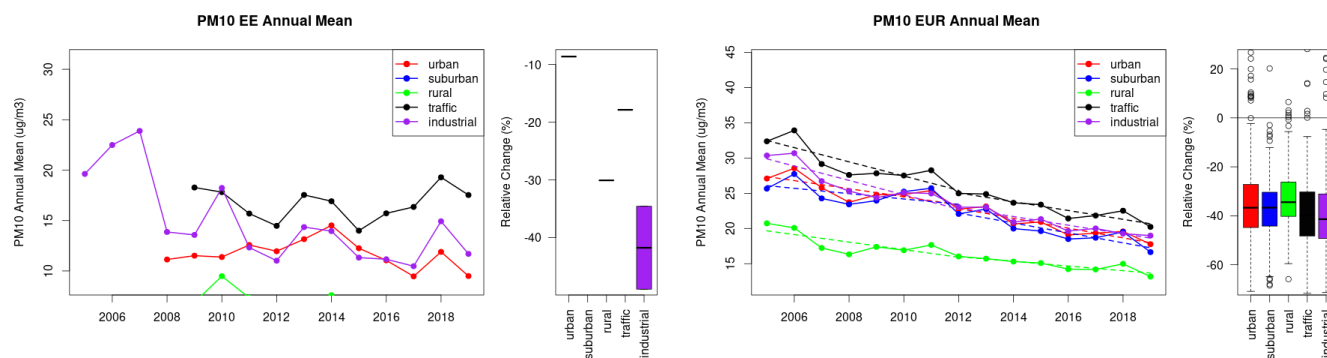


Figure S.171: Time series of the Estonia (left) and European-wide composite (median) of annual mean PM₁₀ (ug/m³) per station type and area (red: urban background, blue suburban background, green: rural background, black: traffic, violet: industrial) between 2005 and 2019. In the European composite, the dashed lines show the linear fit between 2005 & 2012 and between 2012 & 2019. The boxplots on the right-hand side show the distribution of relative changes (%) between 2005 and 2019 for all stations of each typology in Estonia and in Europe.

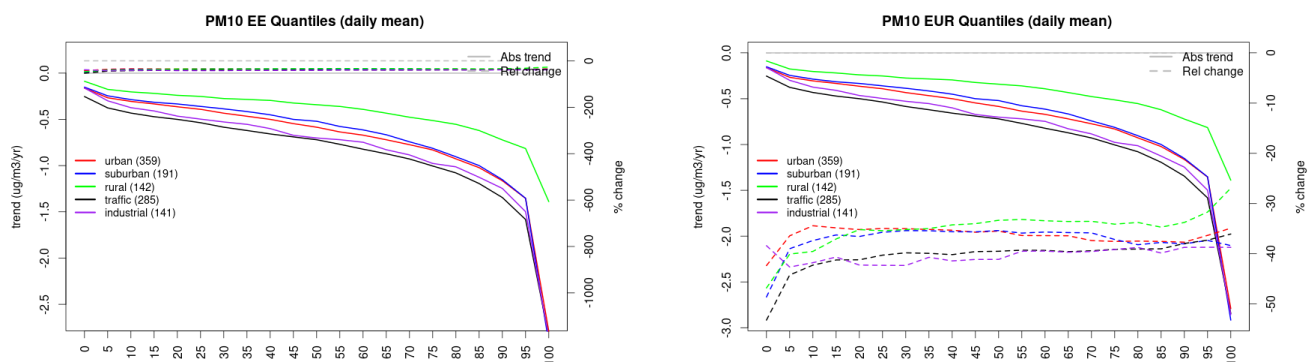


Figure S.172: For PM₁₀ in Estonia (left) and Europe, and for each typology of station: absolute trend (solid lines, left y-axis) and relative change (dashed lines, right y-axis) of the percentiles of daily means.

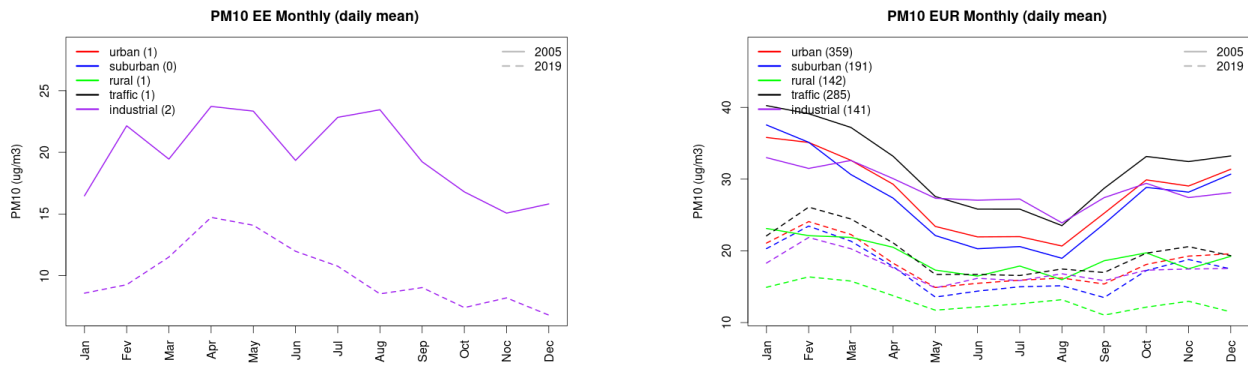


Figure S.173: Monthly cycle of daily mean PM10 for Estonia (left) and Europe (right) at various station types estimated from the whole time series in 2005 (solid lines) and 2019

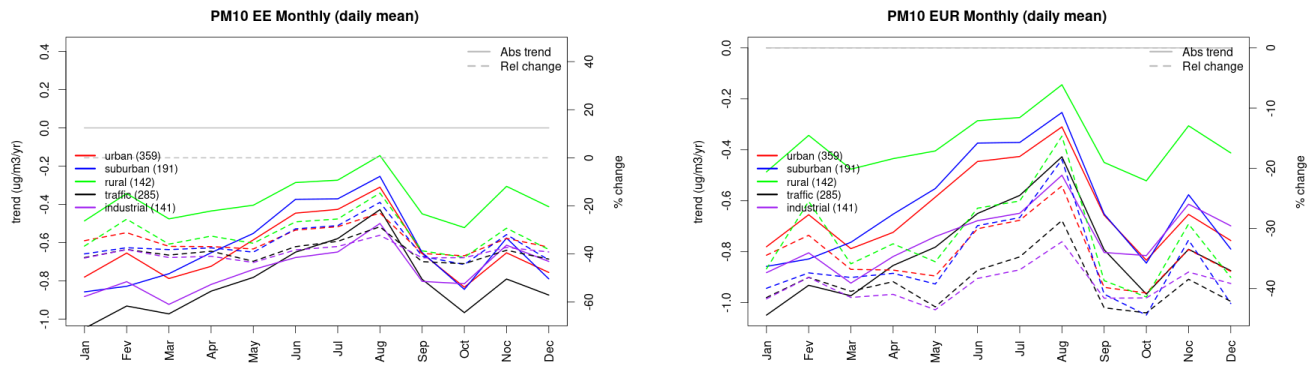


Figure S.174: Absolute (solid lines, left axis) and relative (dashed lines, right axis) trends in the monthly cycle for Estonia (left) and Europe (right) of PM10 at various station type.

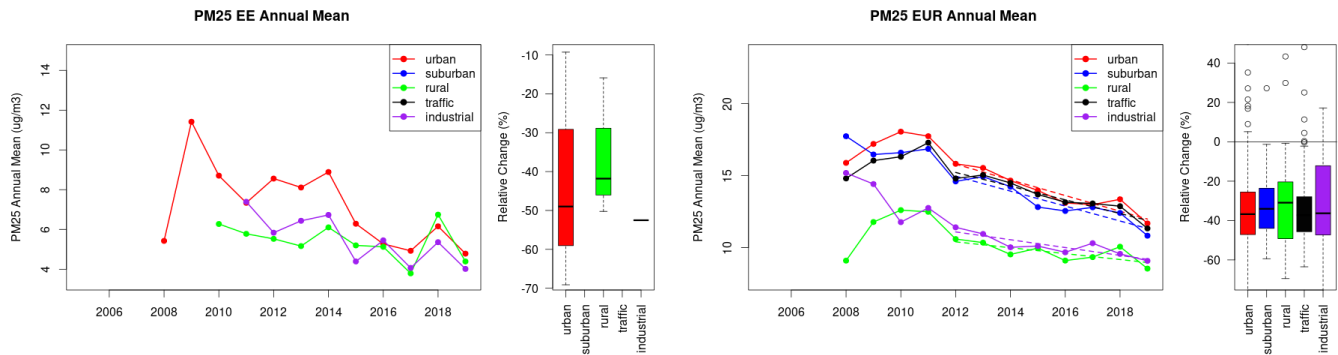


Figure S.175: Time series of the Estonia (left) and European-wide composite (median) of annual mean PM25 ($\mu\text{g}/\text{m}^3$) per station type and area (red: urban background, blue suburban background, green: rural background, black: traffic, violet: industrial) between 2005 and 2019. In the European composite, the dashed lines show the linear fit between 2005 & 2012 and between 2012 & 2019. The boxplots on the right-hand side show the distribution of relative changes (%) between 2005 and 2019 for all stations of each typology in Estonia and in Europe.

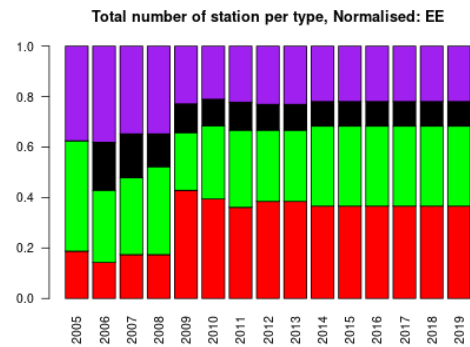
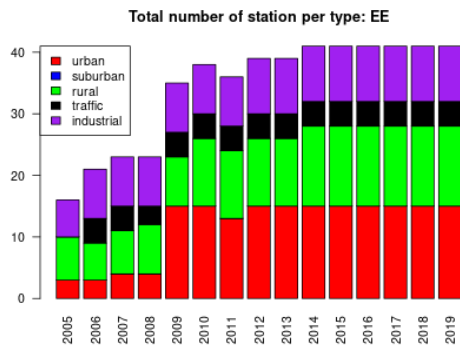
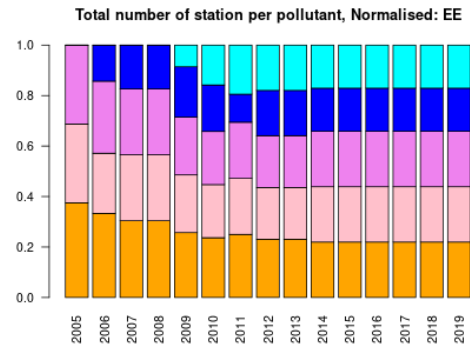
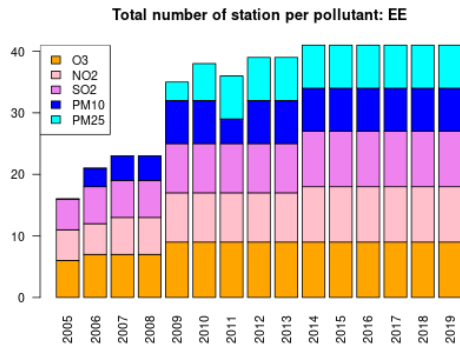
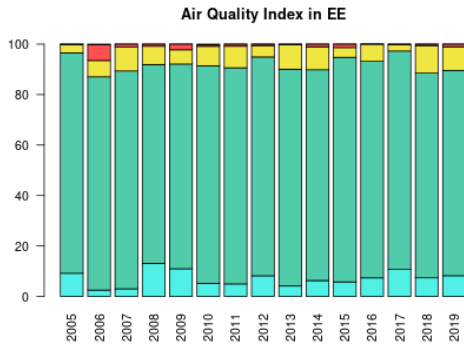


Figure S.176: For Estonia: overall air quality index (percentage of days in a given year) and distribution of daily categories per pollutant (light blue: good, light green: fair, yellow: moderate, orange: poor, red: very poor, violet: extremely poor).

9 Spain

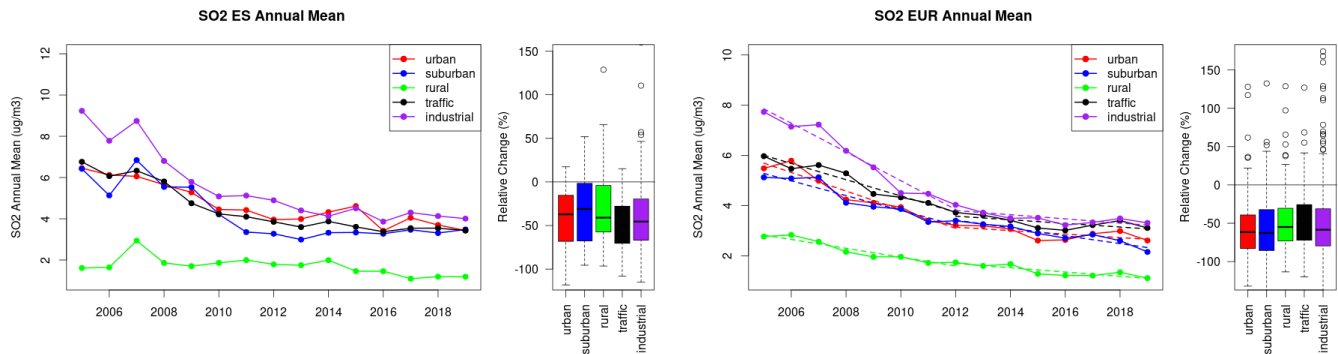


Figure S.177: Time series of the Spain (left) and European-wide composite (median) of annual mean SO₂ (ug/m³) per station type and area (red: urban background, blue suburban background, green: rural background, black: traffic, violet: industrial) between 2005 and 2019. In the European composite, the dashed lines show the linear fit between 2005 & 2012 and between 2012 & 2019. The boxplots on the right-hand side show the distribution of relative changes (%) between 2005 and 2019 for all stations of each typology in Spain and in Europe.

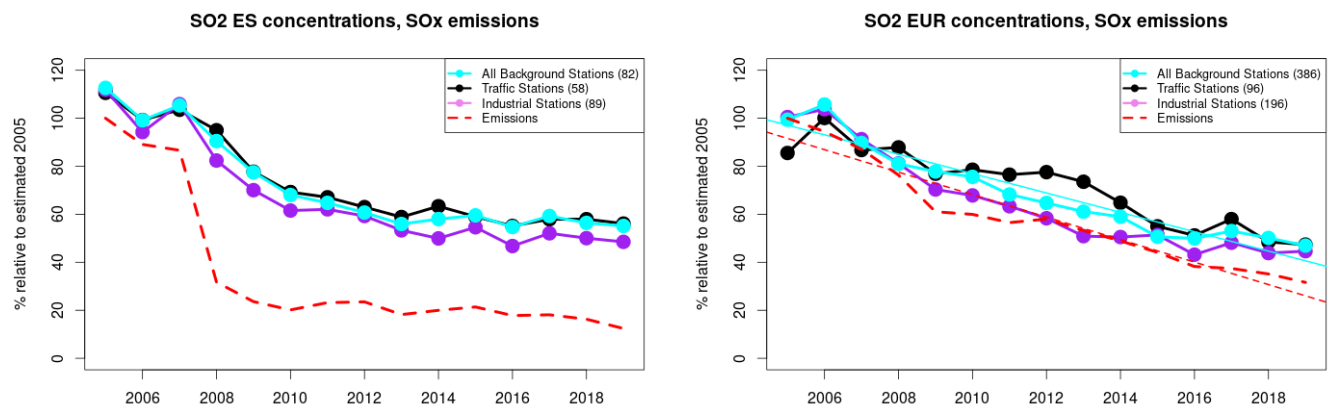


Figure S.178: Time series of 2005-2019 (left) and European (right) median SO₂ observed at traffic (black), industrial (violet) and background (cyan) sites (solid lines), and corresponding SO_x emissions (dashed line) normalised to estimated 2000 levels (%). The median is taken over where more than 5 stations of each typology is available. The total number of stations included is provided in brackets. In the European composite, straight lines are the linear fits over the whole period.

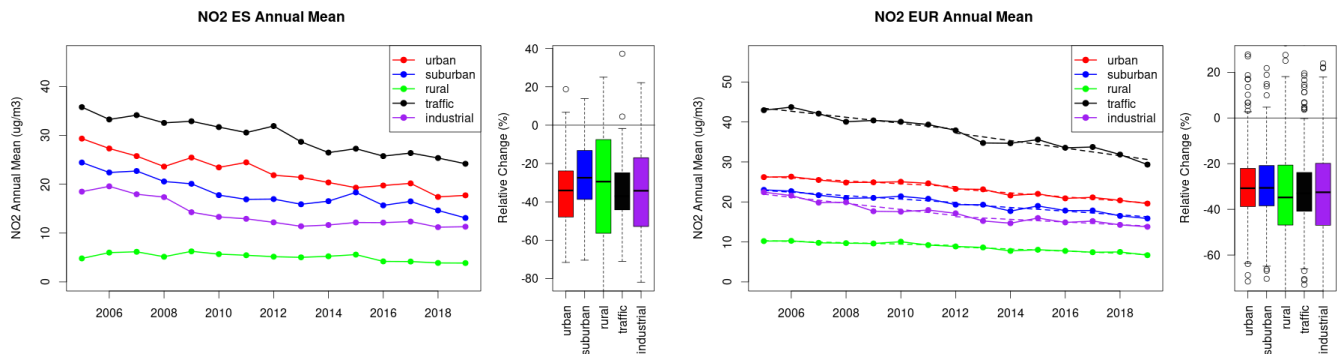


Figure S.179: Time series of the Spain (left) and European-wide composite (median) of annual mean NO₂ (ug/m³) per station type and area (red: urban background, blue suburban background, green: rural background, black: traffic, violet: industrial) between 2005 and 2019. In the European composite, the dashed lines show the linear fit between 2005 & 2012 and between 2012 & 2019. The boxplots on the right-hand side show the distribution of relative changes (%) between 2005 and 2019 for all stations of each typology in Spain and in Europe.

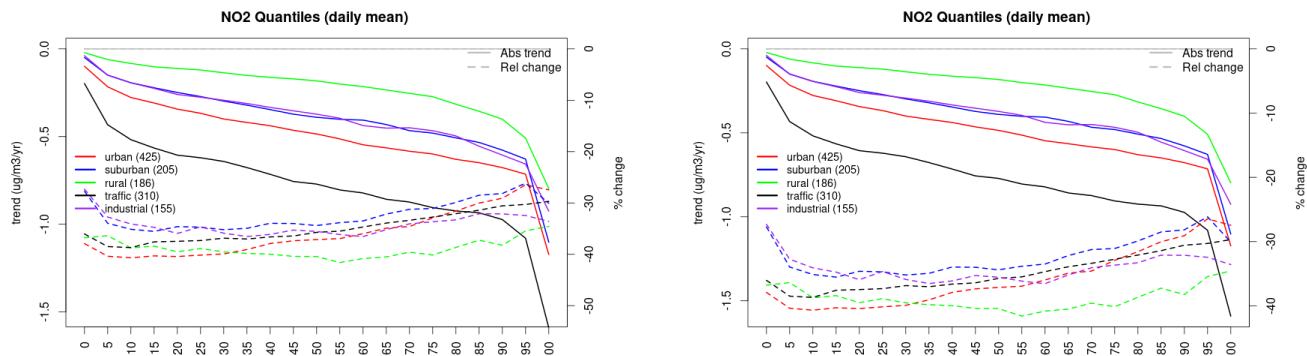


Figure S.180: For NO₂ in Spain (left) and Europe, and for each typology of station: absolute trend (solid lines, left y-axis) and relative change (dashed lines, right y-axis) of the percentiles of daily means.

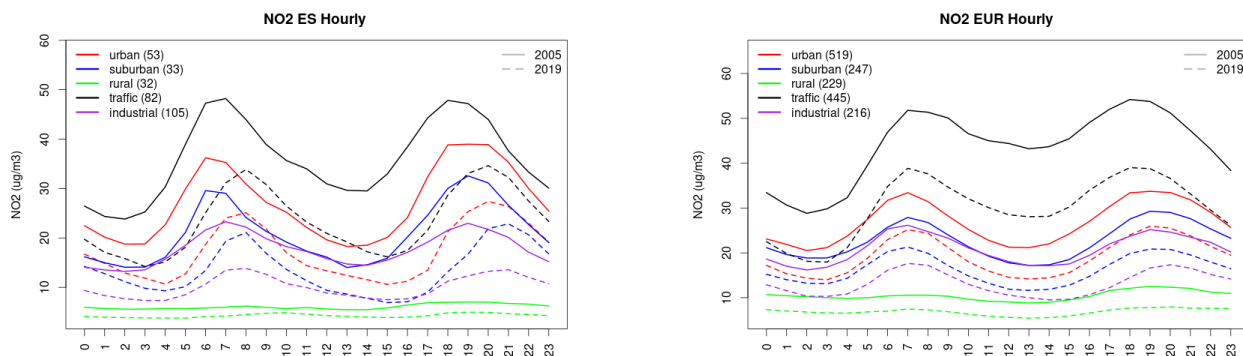


Figure S.181: Diurnal cycle of daily mean NO₂ for Spain (left) and Europe (right) at various station types estimated from the whole time series in 2005 (solid lines) and 2019

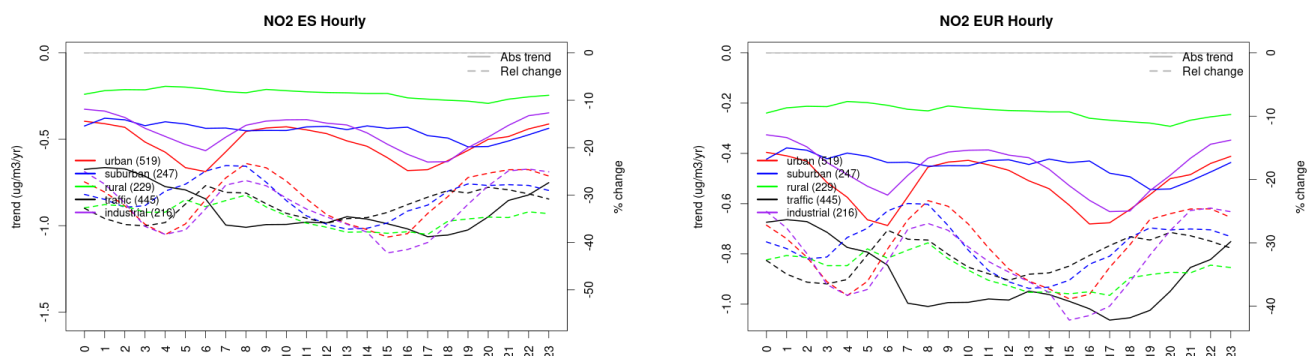


Figure S.182: Absolute (solid lines, left axis) and relative (dashed lines, right axis) trends in the diurnal cycle for Spain (left) and Europe (right) of NO₂ at various station type.

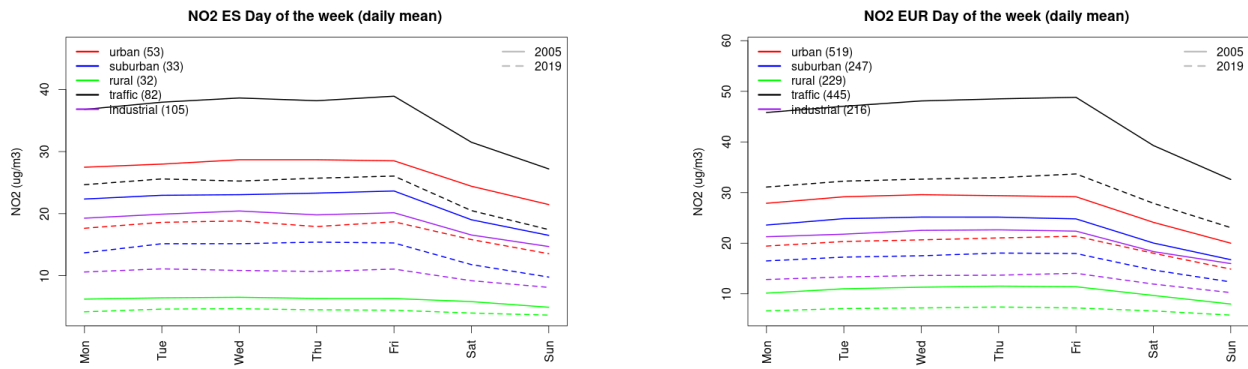


Figure S.183: Weekly cycle of daily mean NO₂ for Spain (left) and Europe (right) at various station types estimated from the whole time series in 2005 (solid lines) and 2019

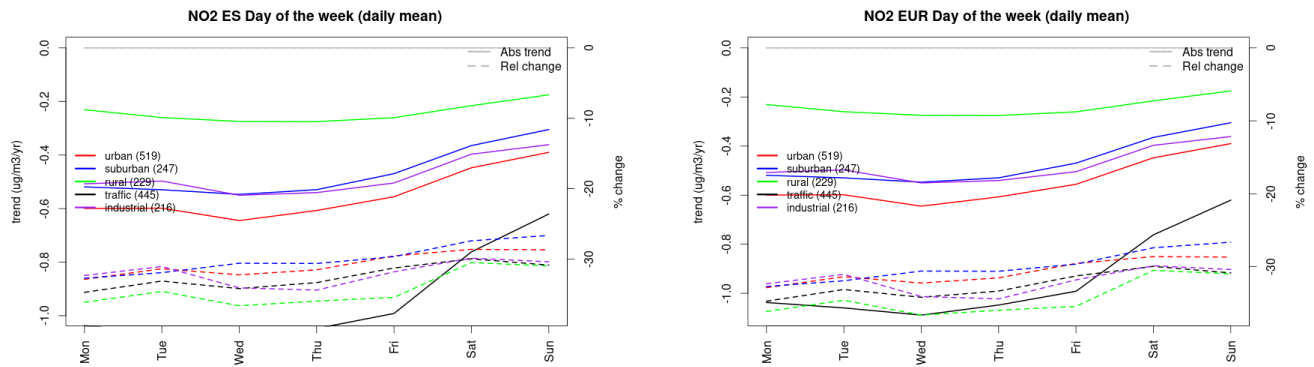


Figure S.184: Absolute (solid lines, left axis) and relative (dashed lines, right axis) trends in the weekly cycle for Spain (left) and Europe (right) of NO₂ at various station type.

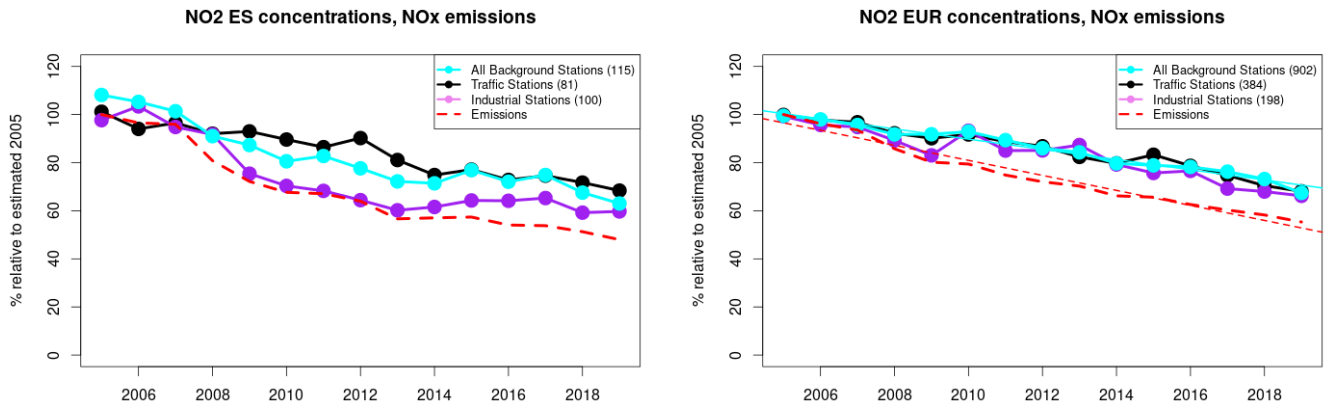


Figure S.185: Time series of 2005-2019 (left) and European (right) median NO₂ observed at traffic (black), industrial (violet) and background (cyan) sites (solid lines), and corresponding NO_x emissions (dashed line) normalised to estimated 2000 levels (%). The median is taken over where more than 5 stations of each typology is available. The total number of stations included is provided in brackets. In the European composite, straight lines are the linear fits over the whole period.

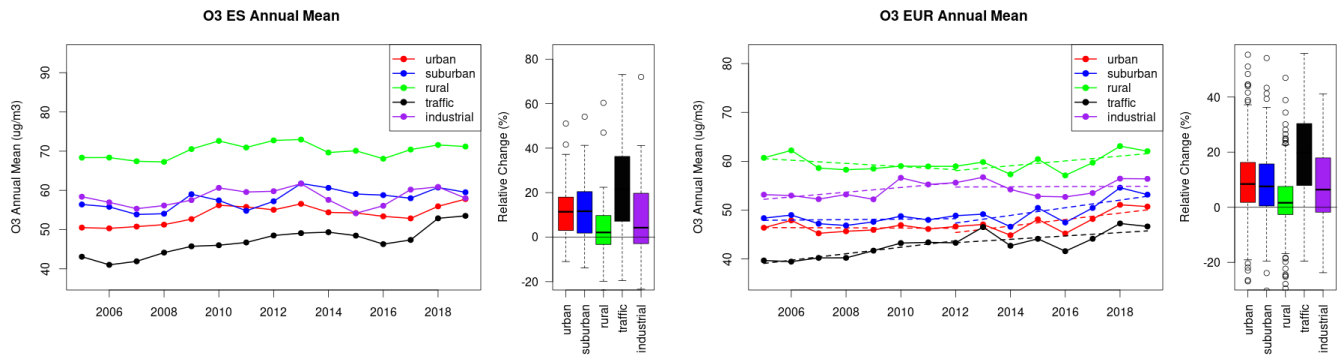


Figure S.186: Time series of the Spain (left) and European-wide composite (median) of annual mean ozone (ug/m³) per station type and area (red: urban background, blue suburban background, green: rural background, black: traffic, violet: industrial) between 2005 and 2019. In the European composite, the dashed lines show the linear fit between 2005 & 2012 and between 2012 & 2019. The boxplots on the right-hand side show the distribution of relative changes (%) between 2005 and 2019 for all stations of each typology in Spain and in Europe.

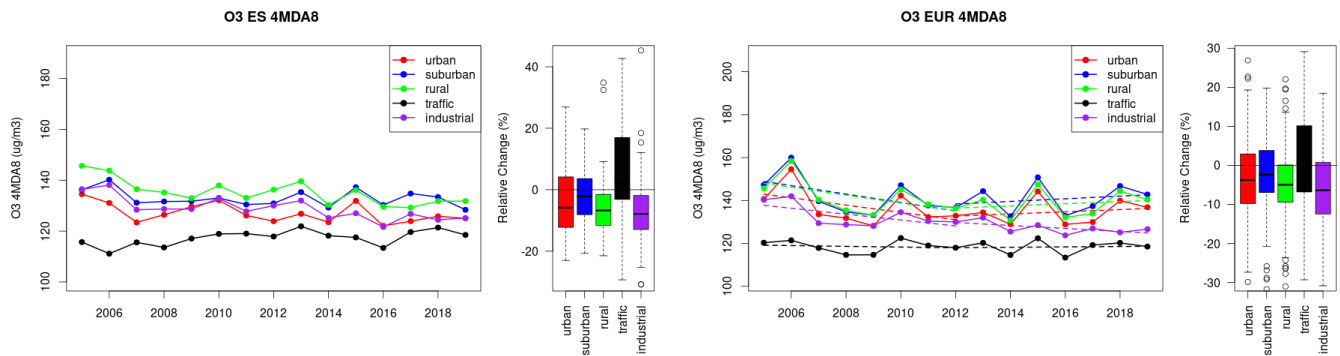


Figure S.187: Time series of the Spain (left) and European-wide composite (median) of O₃ fourth highest daily peak (4MDA8, ug/m³) per station type and area (red: urban background, blue suburban background, green: rural background, black: traffic, violet: industrial) between 2005 and 2019. In the European composite, the dashed lines show the linear fit between 2005 & 2012 and between 2012 & 2019. The boxplots on the right-hand side show the distribution of relative changes (%) between 2005 and 2019 for all stations of each typology in Spain and in Europe.

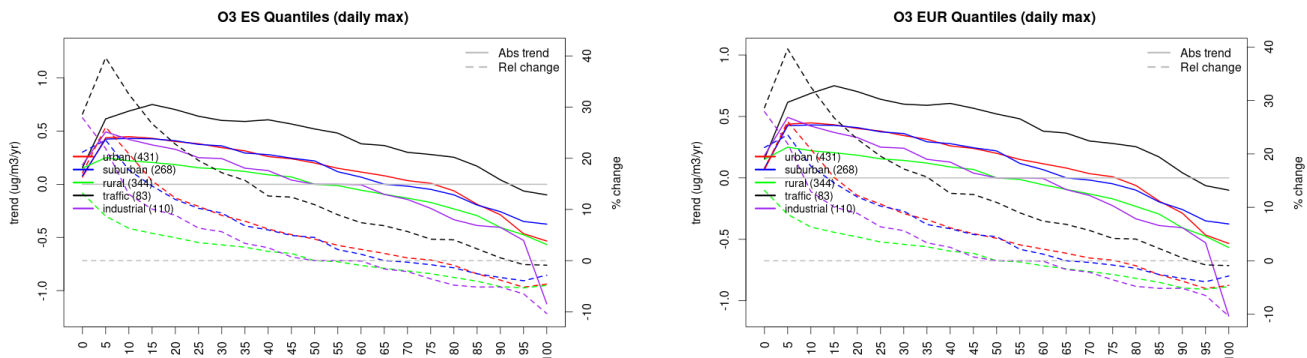


Figure S.188: For ozone in Spain (left) and Europe, and for each typology of station: absolute trend (solid lines, left y-axis) and relative change (dashed lines, right y-axis) of the percentiles of daily maxima.

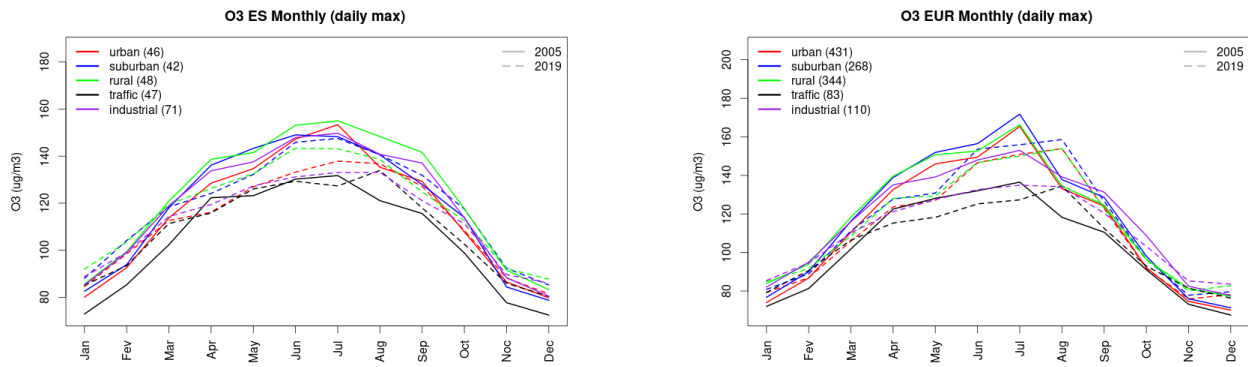


Figure S.189: Monthly cycle of daily max ozone for Spain (left) and Europe (right) at various station types estimated from the whole time series in 2005 (solid lines) and 2019

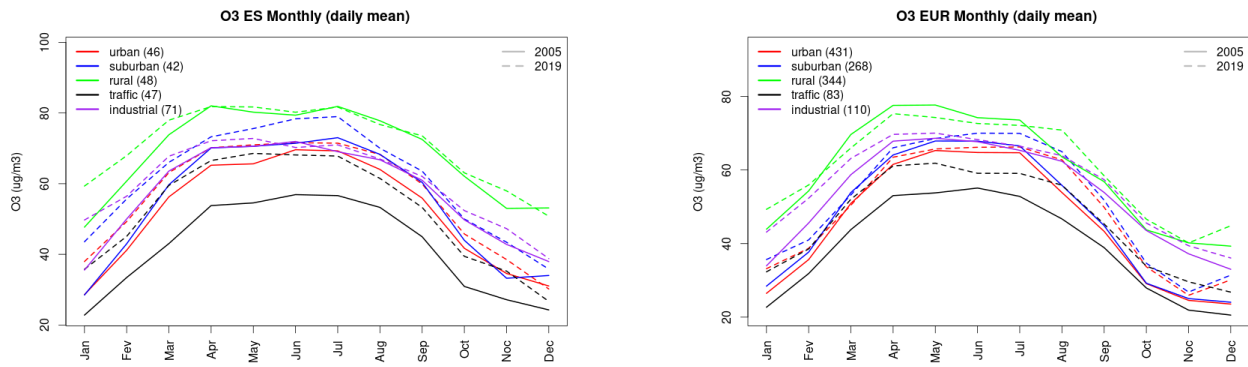


Figure S.190: Monthly cycle of daily mean ozone for Spain (left) and Europe (right) at various station types estimated from the whole time series in 2005 (solid lines) and 2019

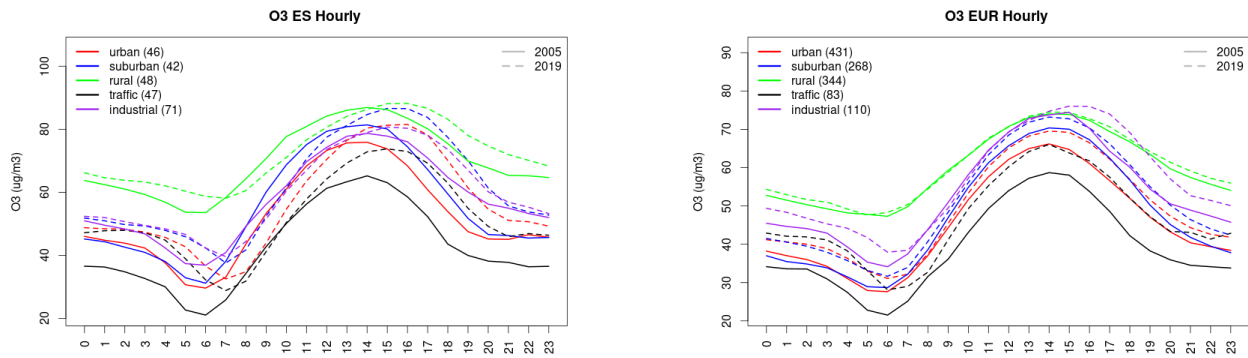


Figure S.191: Diurnal cycle of daily mean ozone for Spain (left) and Europe (right) at various station types estimated from the whole time series in 2005 (solid lines) and 2019

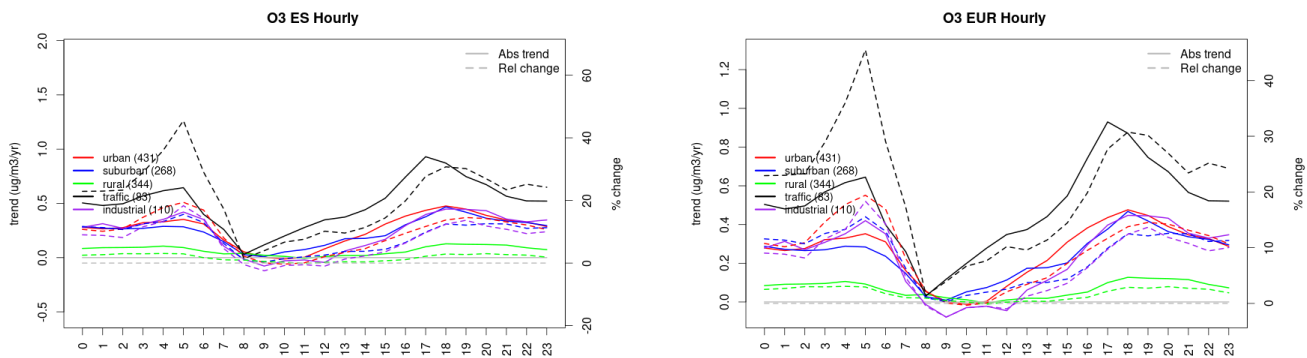


Figure S.192: Absolute (solid lines, left axis) and relative (dashed lines, right axis) trends in the diurnal cycle for Spain (left) and Europe (right) of ozone at various station type.

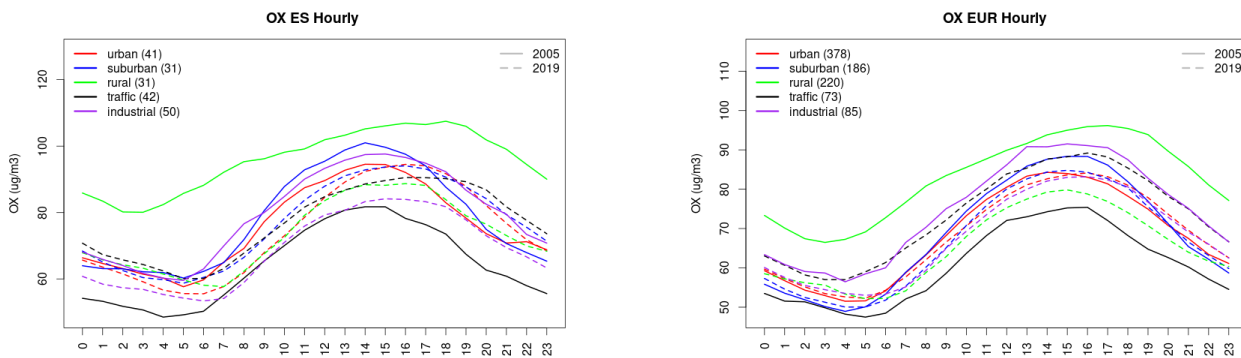


Figure S.193: Diurnal cycle of daily mean OX (as NO₂+O₃) for Spain (left) and Europe (right) at various station types estimated from the whole time series in 2005 (solid lines) and 2019 (dashed lines).

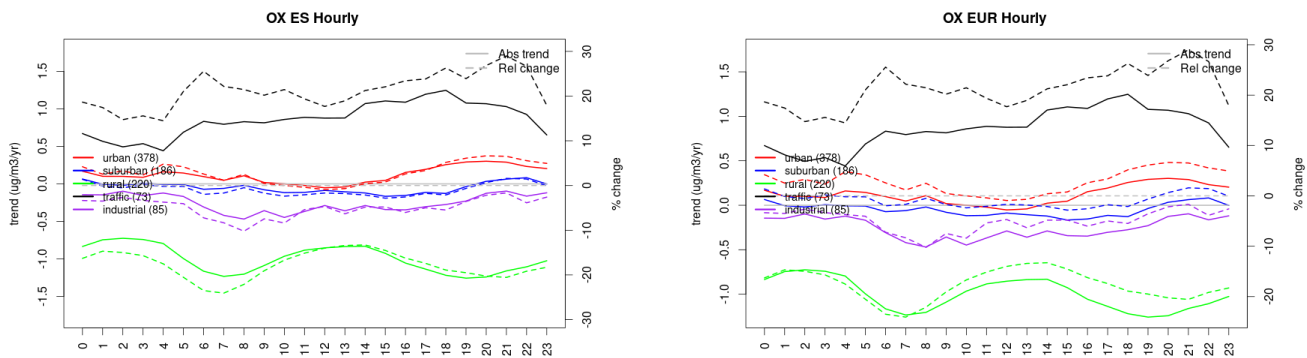


Figure S.194: Absolute (solid lines, left axis) and relative (dashed lines, right axis) trends in the diurnal cycle for Spain (left) and Europe (right) of OX (as NO₂+O₃) at various station type.

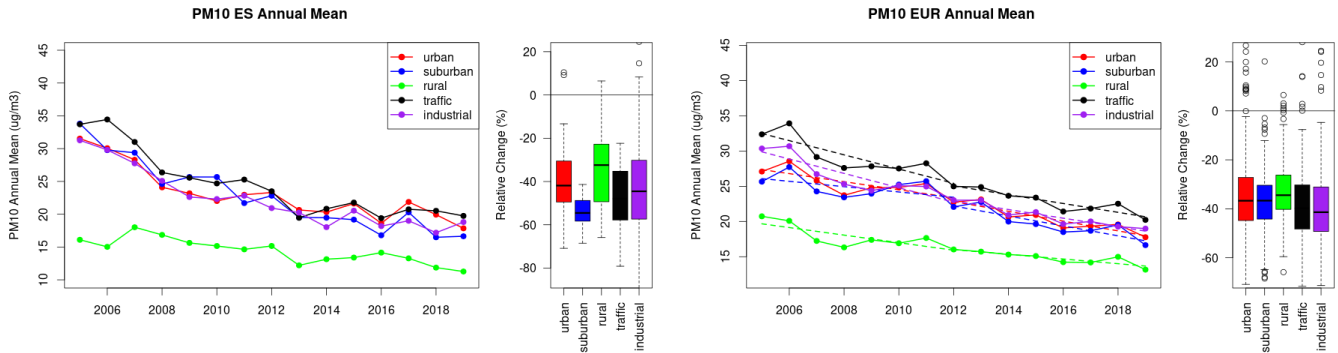


Figure S.195: Time series of the Spain (left) and European-wide composite (median) of annual mean PM10 ($\mu\text{g}/\text{m}^3$) per station type and area (red: urban background, blue suburban background, green: rural background, black: traffic, violet: industrial) between 2005 and 2019. In the European composite, the dashed lines show the linear fit between 2005 & 2012 and between 2012 & 2019. The boxplots on the right-hand side show the distribution of relative changes (%) between 2005 and 2019 for all stations of each typology in Spain and in Europe.

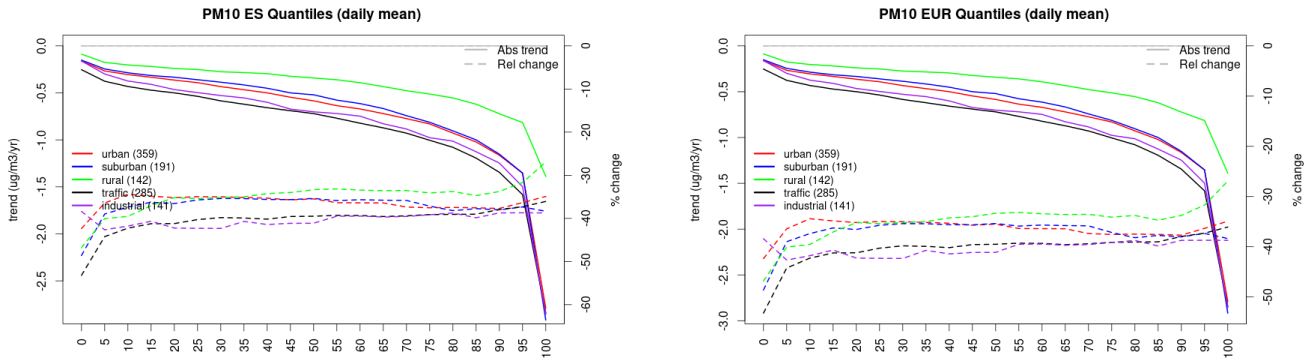


Figure S.196: For PM10 in Spain (left) and Europe, and for each typology of station: absolute trend (solid lines, left y-axis) and relative change (dashed lines, right y-axis) of the percentiles of daily means.

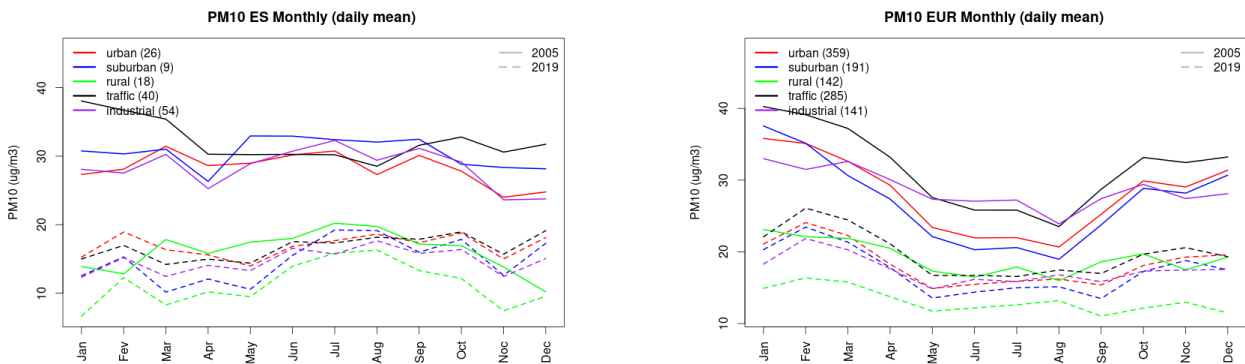


Figure S.197: Monthly cycle of daily mean PM10 for Spain (left) and Europe (right) at various station types estimated from the whole time series in 2005 (solid lines) and 2019

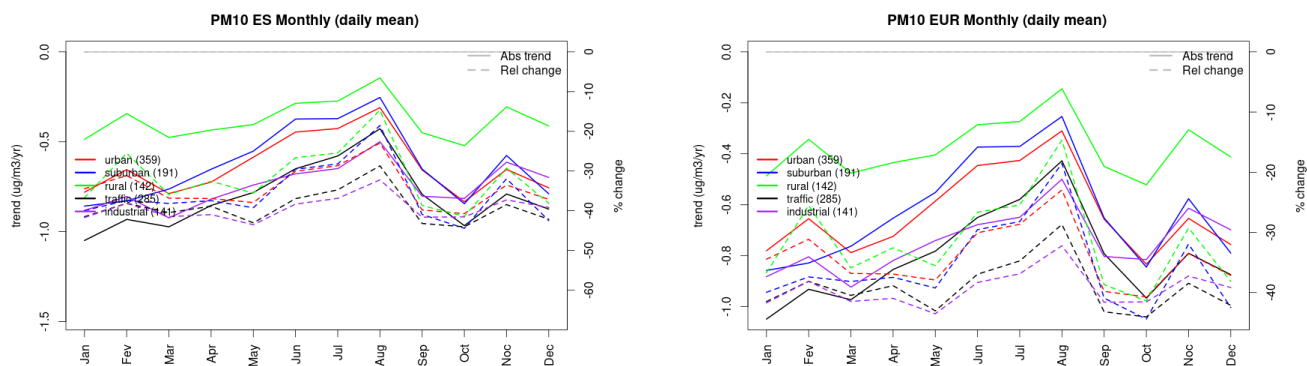


Figure S.198: Absolute (solid lines, left axis) and relative (dashed lines, right axis) trends in the monthly cycle for Spain (left) and Europe (right) of PM10 at various station type.

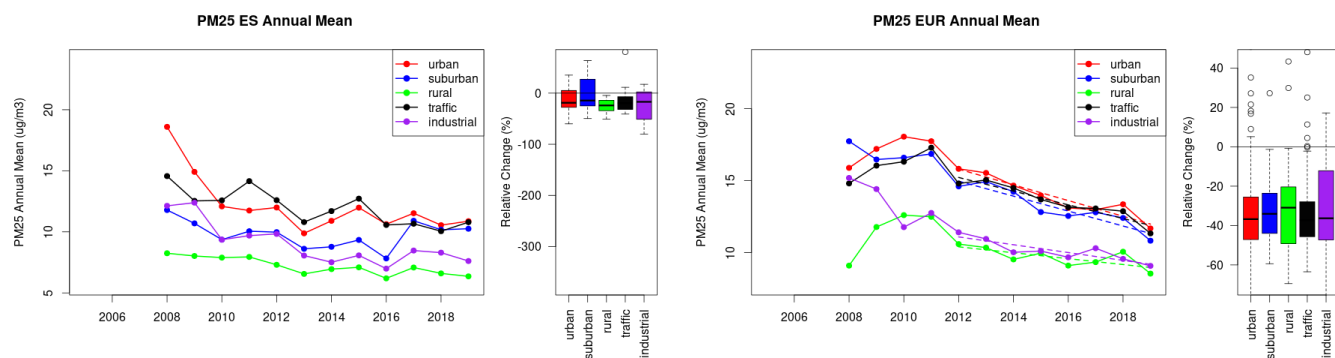


Figure S.199: Time series of the Spain (left) and European-wide composite (median) of annual mean PM25 ($\mu\text{g}/\text{m}^3$) per station type and area (red: urban background, blue suburban background, green: rural background, black: traffic, violet: industrial) between 2005 and 2019. In the European composite, the dashed lines show the linear fit between 2005 & 2012 and between 2012 & 2019. The boxplots on the right-hand side show the distribution of relative changes (%) between 2005 and 2019 for all stations of each typology in Spain and in Europe.

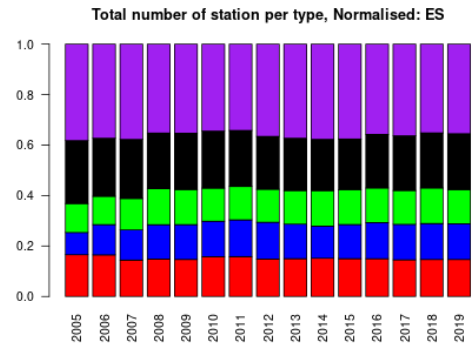
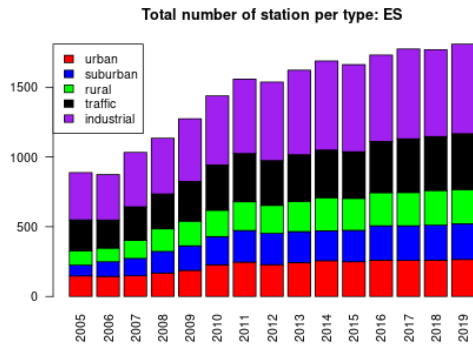
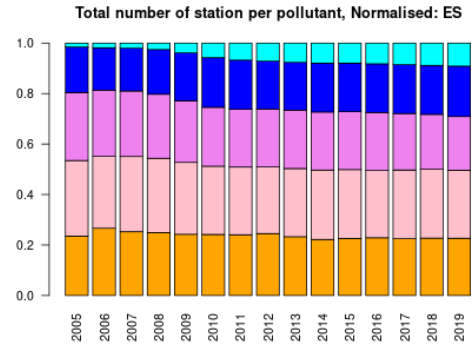
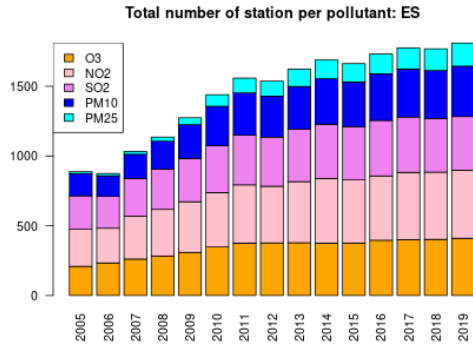
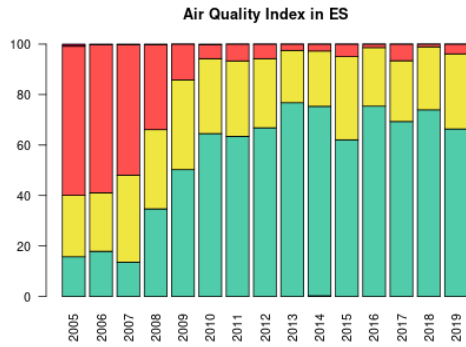


Figure S.200: For Spain: overall air quality index (percentage of days in a given year) and distribution of daily categories per pollutant (light blue: good, light green: fair, yellow: moderate, orange: poor, red: very poor, violet: extremely poor).

10 Finland

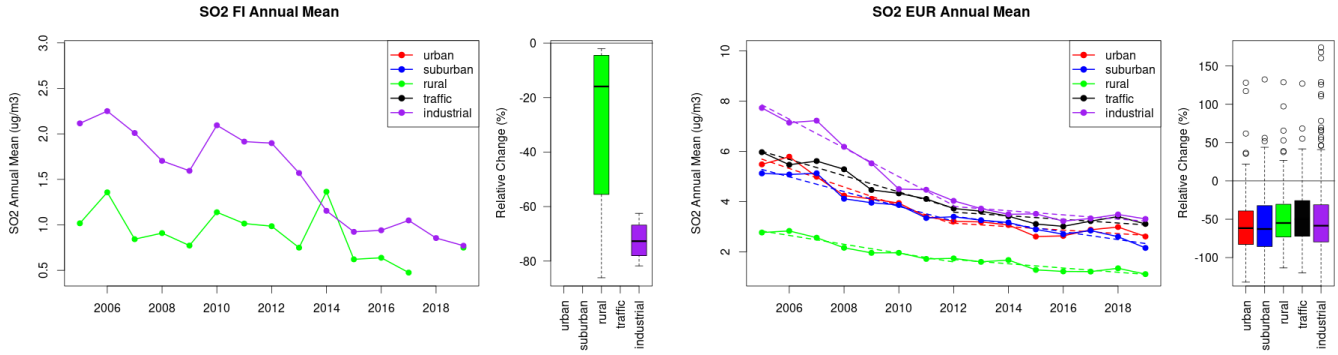


Figure S.201: Time series of the Finland (left) and European-wide composite (median) of annual mean SO₂ (ug/m³) per station type and area (red: urban background, blue suburban background, green: rural background, black: traffic, violet: industrial) between 2005 and 2019. In the European composite, the dashed lines show the linear fit between 2005 & 2012 and between 2012 & 2019. The boxplots on the right-hand side show the distribution of relative changes (%) between 2005 and 2019 for all stations of each typology in Finland and in Europe.

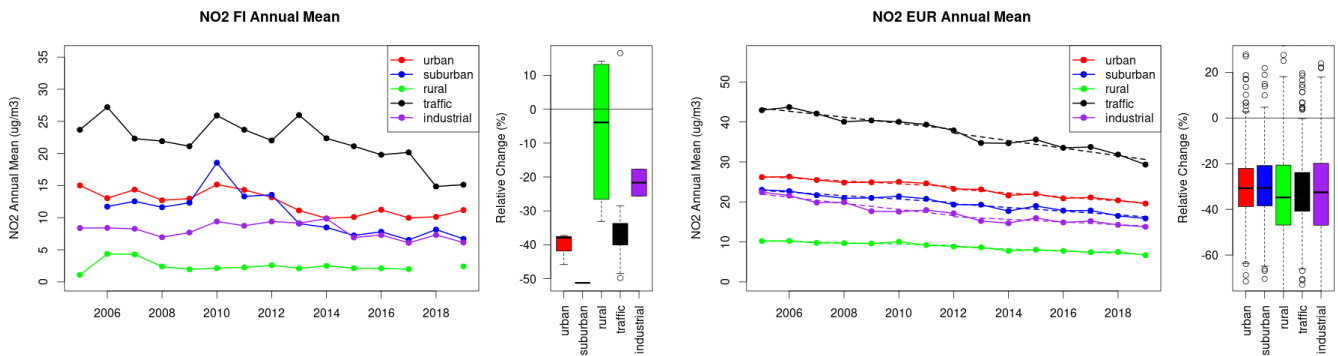


Figure S.202: Time series of the Finland (left) and European-wide composite (median) of annual mean NO₂ (ug/m³) per station type and area (red: urban background, blue suburban background, green: rural background, black: traffic, violet: industrial) between 2005 and 2019. In the European composite, the dashed lines show the linear fit between 2005 & 2012 and between 2012 & 2019. The boxplots on the right-hand side show the distribution of relative changes (%) between 2005 and 2019 for all stations of each typology in Finland and in Europe.

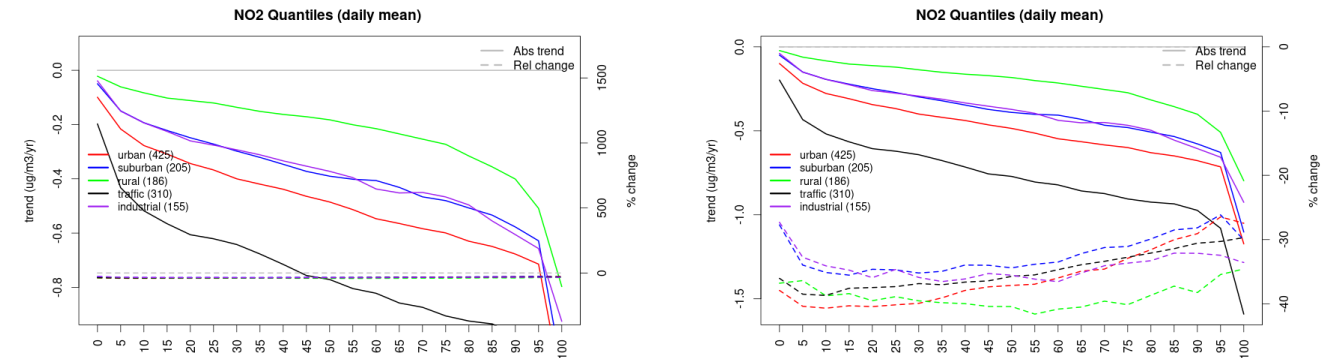


Figure S.203: For NO₂ in Finland (left) and Europe, and for each typology of station: absolute trend (solid lines, left y-axis) and relative change (dashed lines, right y-axis) of the percentiles of daily means.

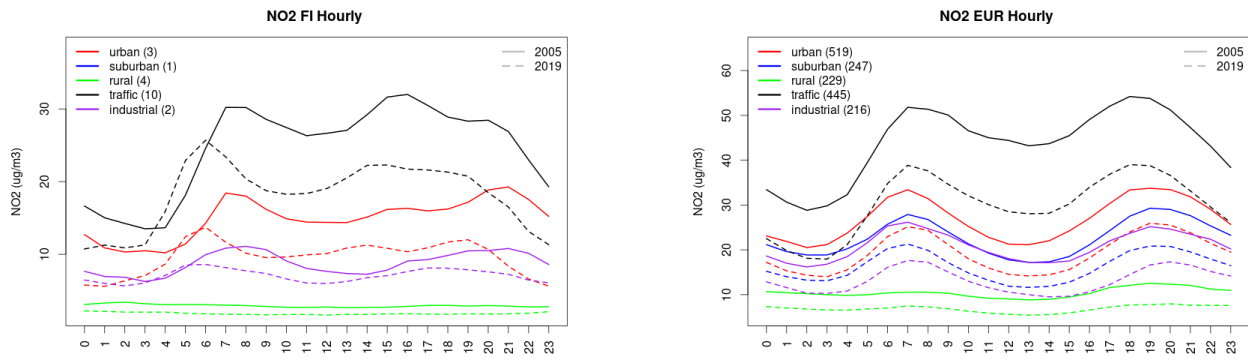


Figure S.204: Diurnal cycle of daily mean NO2 for Finland (left) and Europe (right) at various station types estimated from the whole time series in 2005 (solid lines) and 2019

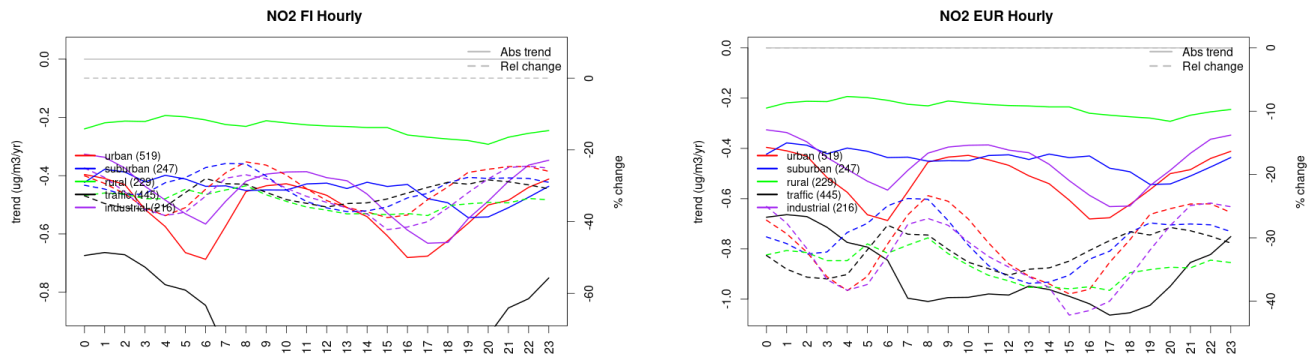


Figure S.205: Absolute (solid lines, left axis) and relative (dashed lines, right axis) trends in the diurnal cycle for Finland (left) and Europe (right) of NO2 at various station type.

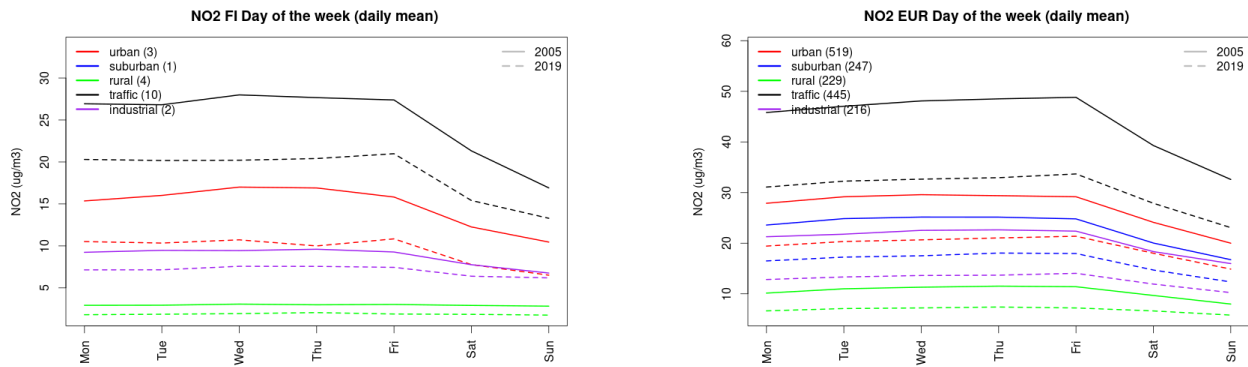


Figure S.206: Weekly cycle of daily mean NO2 for Finland (left) and Europe (right) at various station types estimated from the whole time series in 2005 (solid lines) and 2019

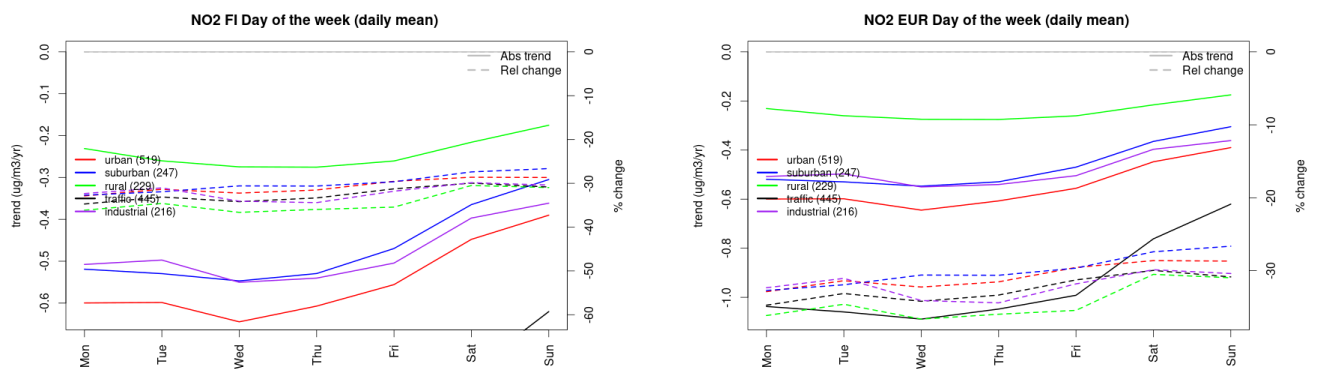


Figure S.207: Absolute (solid lines, left axis) and relative (dashed lines, right axis) trends in the weekly cycle for Finland (left) and Europe (right) of NO₂ at various station type.

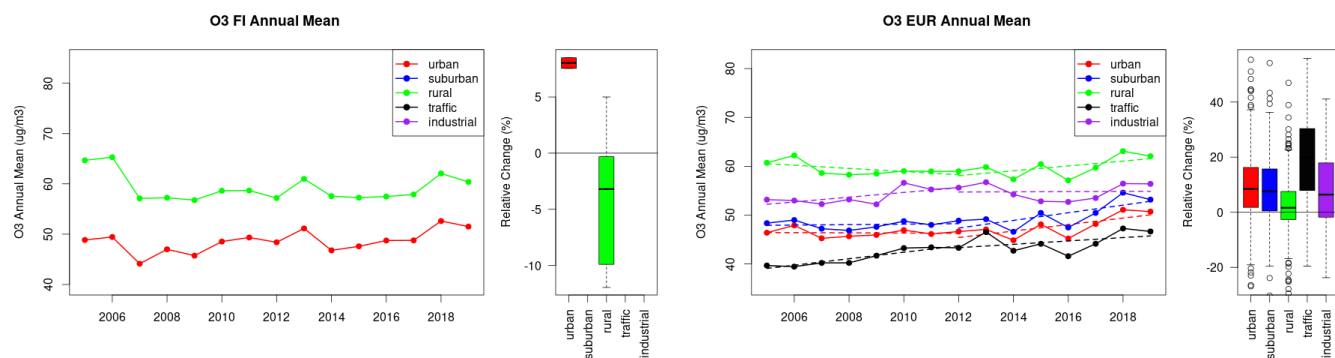


Figure S.208: Time series of the Finland (left) and European-wide composite (median) of annual mean ozone (ug/m³) per station type and area (red: urban background, blue suburban background, green: rural background, black: traffic, violet: industrial) between 2005 and 2019. In the European composite, the dashed lines show the linear fit between 2005 & 2012 and between 2012 & 2019. The boxplots on the right-hand side show the distribution of relative changes (%) between 2005 and 2019 for all stations of each typology in Finland and in Europe.

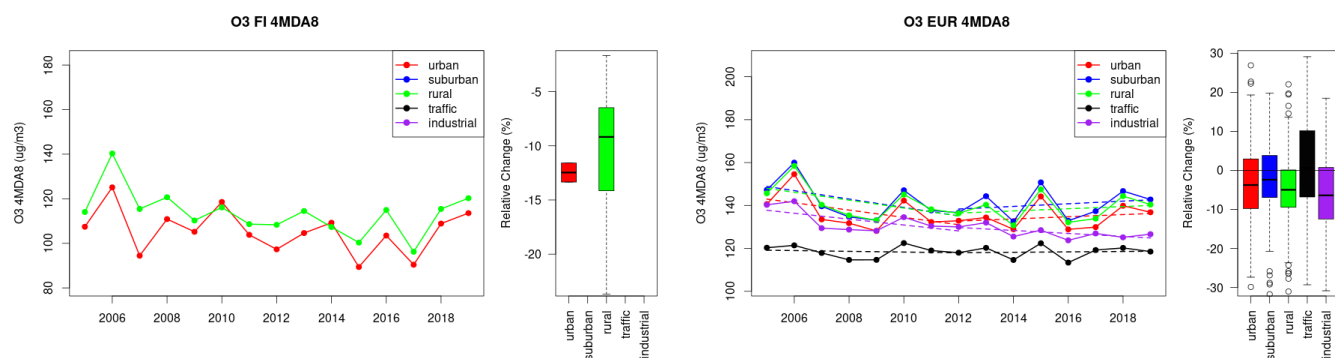


Figure S.209: Time series of the Finland (left) and European-wide composite (median) of O₃ fourth highest daily peak (4MDA8, ug/m³) per station type and area (red: urban background, blue suburban background, green: rural background, black: traffic, violet: industrial) between 2005 and 2019. In the European composite, the dashed lines show the linear fit between 2005 & 2012 and between 2012 & 2019. The boxplots on the right-hand side show the distribution of relative changes (%) between 2005 and 2019 for all stations of each typology in Finland and in Europe.

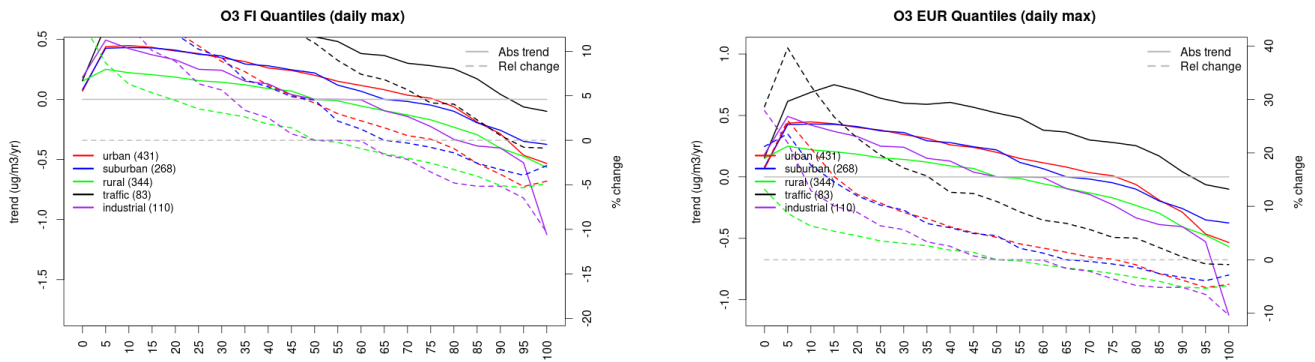


Figure S.210: For ozone in Finland (left) and Europe, and for each typology of station: absolute trend (solid lines, left y-axis) and relative change (dashed lines, right y-axis) of the percentiles of daily maxima.

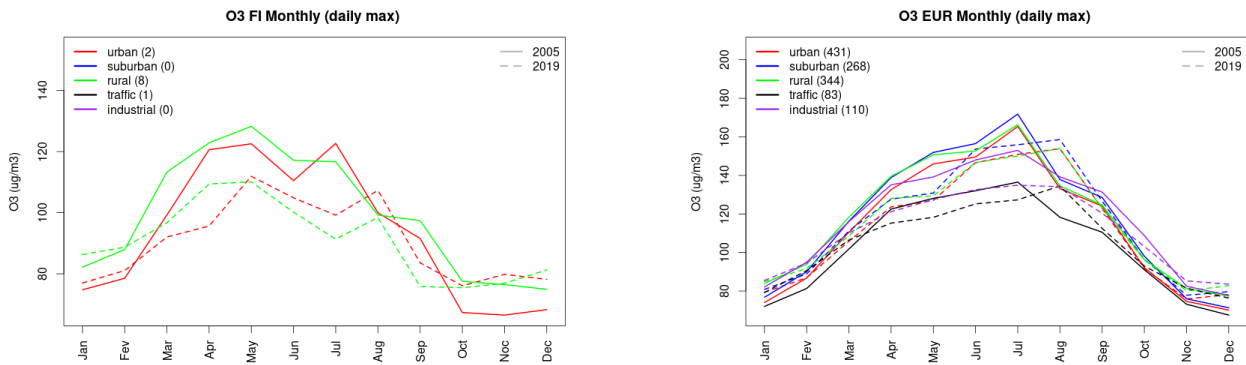


Figure S.211: Monthly cycle of daily max ozone for Finland (left) and Europe (right) at various station types estimated from the whole time series in 2005 (solid lines) and 2019

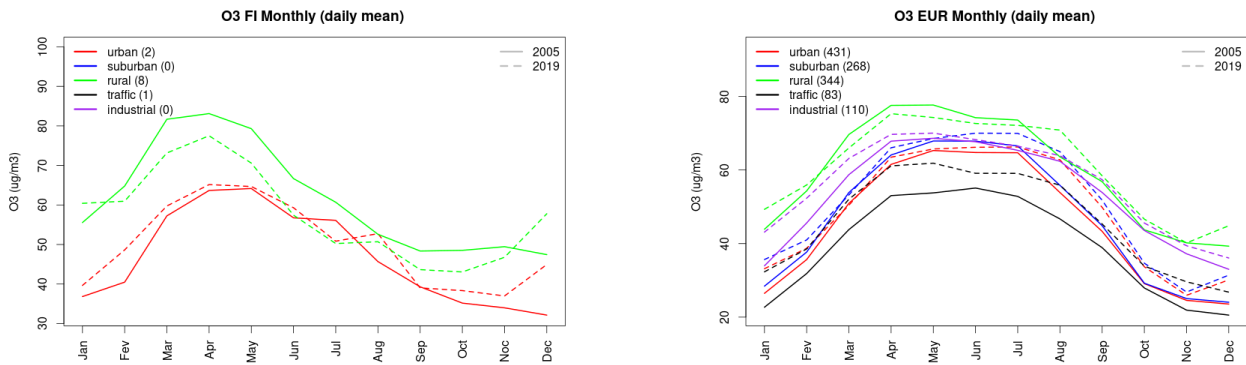


Figure S.212: Monthly cycle of daily mean ozone for Finland (left) and Europe (right) at various station types estimated from the whole time series in 2005 (solid lines) and 2019

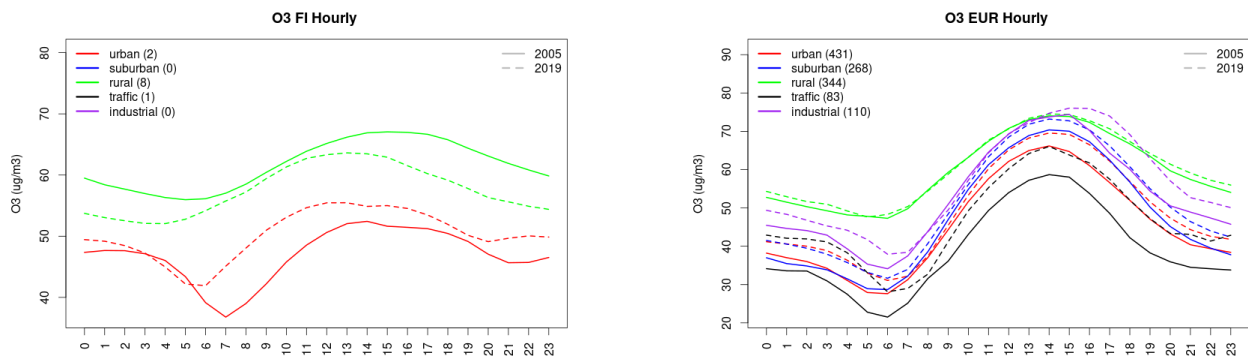


Figure S.213: Diurnal cycle of daily mean ozone for Finland (left) and Europe (right) at various station types estimated from the whole time series in 2005 (solid lines) and 2019

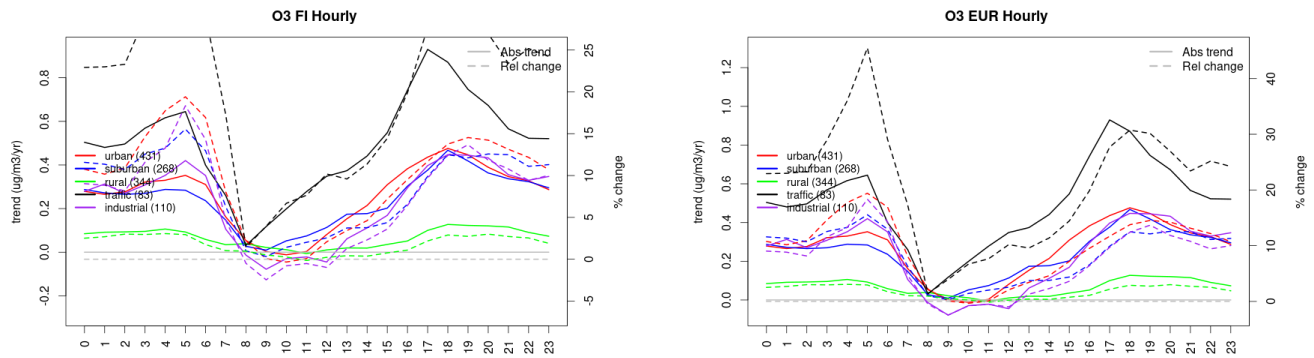


Figure S.214: Absolute (solid lines, left axis) and relative (dashed lines, right axis) trends in the diurnal cycle for Finland (left) and Europe (right) of ozone at various station type.

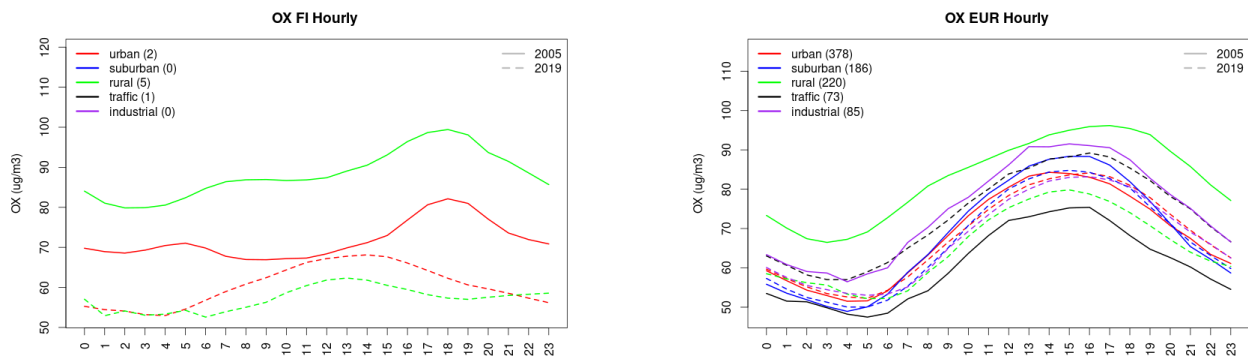


Figure S.215: Diurnal cycle of daily mean OX (as NO2+O3) for Finland (left) and Europe (right) at various station types estimated from the whole time series in 2005 (solid lines) and 2019

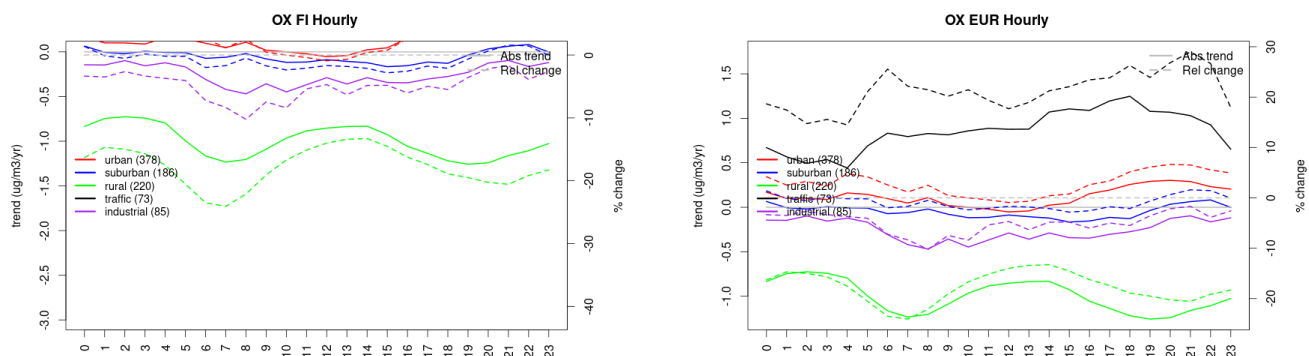


Figure S.216: Absolute (solid lines, left axis) and relative (dashed lines, right axis) trends in the diurnal cycle for Finland (left) and Europe (right) of OX (as NO₂+O₃) at various station type.

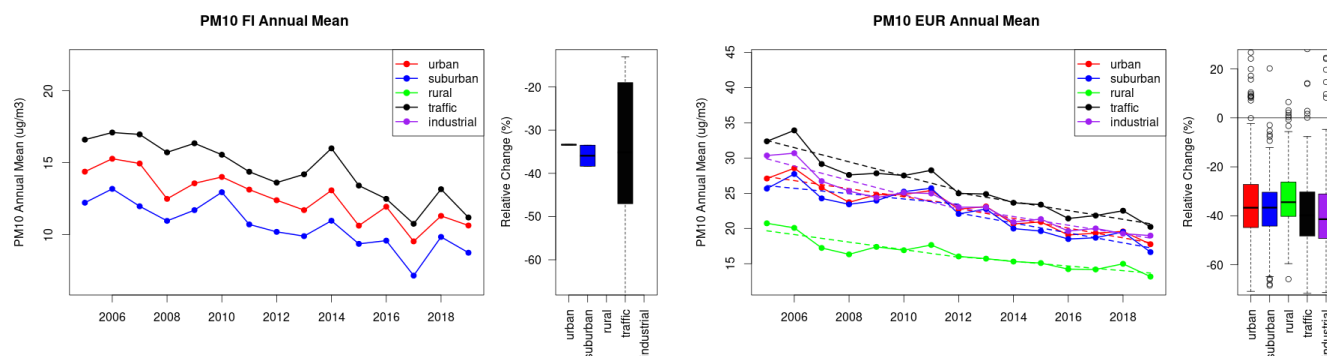


Figure S.217: Time series of the Finland (left) and European-wide composite (median) of annual mean PM₁₀ (ug/m³) per station type and area (red: urban background, blue suburban background, green: rural background, black: traffic, violet: industrial) between 2005 and 2019. In the European composite, the dashed lines show the linear fit between 2005 & 2012 and between 2012 & 2019. The boxplots on the right-hand side show the distribution of relative changes (%) between 2005 and 2019 for all stations of each typology in Finland and in Europe.

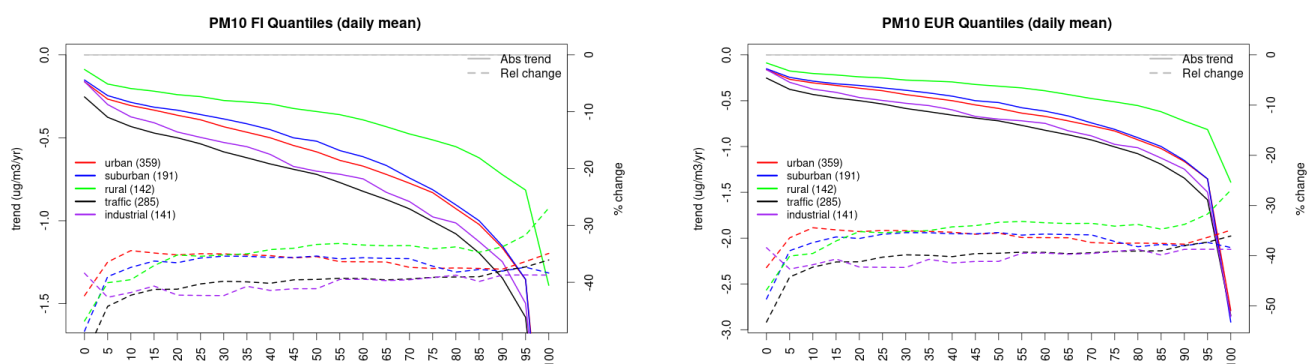


Figure S.218: For PM₁₀ in Finland (left) and Europe, and for each typology of station: absolute trend (solid lines, left y-axis) and relative change (dashed lines, right y-axis) of the percentiles of daily means.

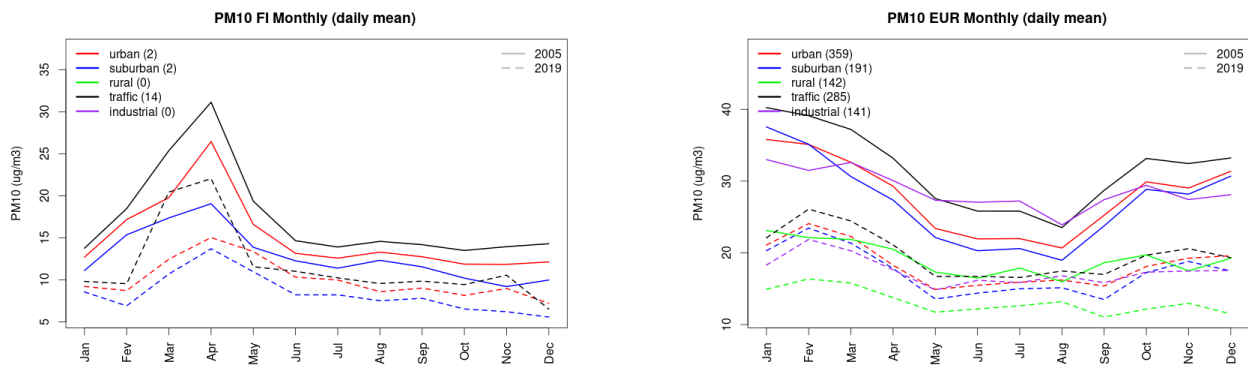


Figure S.219: Monthly cycle of daily mean PM10 for Finland (left) and Europe (right) at various station types estimated from the whole time series in 2005 (solid lines) and 2019

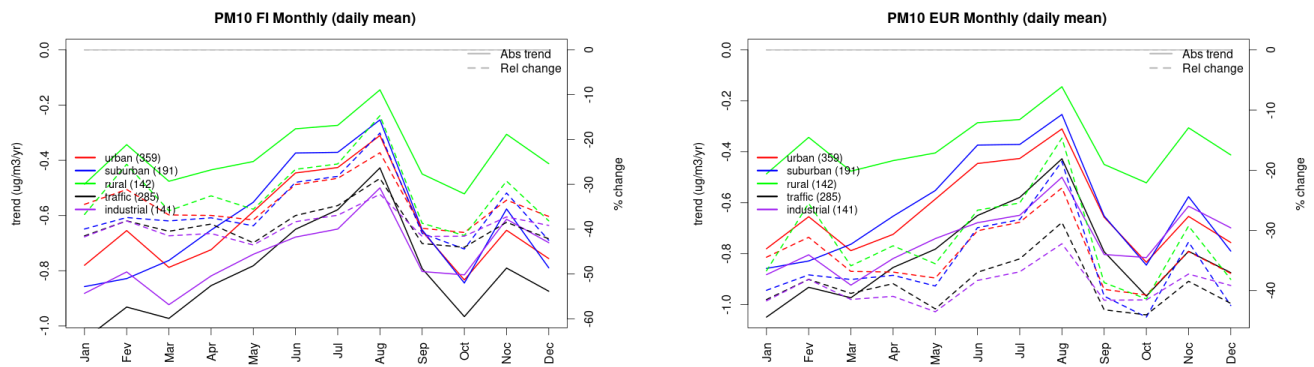


Figure S.220: Absolute (solid lines, left axis) and relative (dashed lines, right axis) trends in the monthly cycle for Finland (left) and Europe (right) of PM10 at various station type.

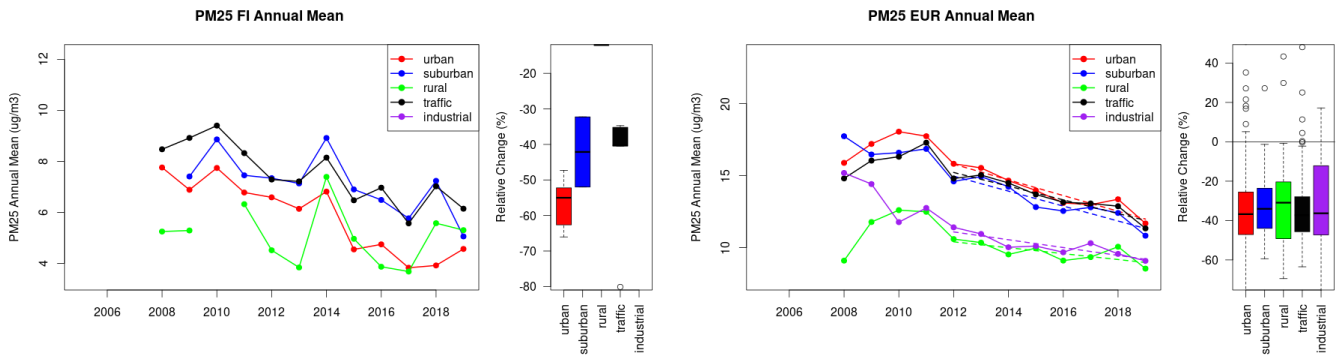


Figure S.221: Time series of the Finland (left) and European-wide composite (median) of annual mean PM25 ($\mu\text{g}/\text{m}^3$) per station type and area (red: urban background, blue suburban background, green: rural background, black: traffic, violet: industrial) between 2005 and 2019. In the European composite, the dashed lines show the linear fit between 2005 & 2012 and between 2012 & 2019. The boxplots on the right-hand side show the distribution of relative changes (%) between 2005 and 2019 for all stations of each typology in Finland and in Europe.

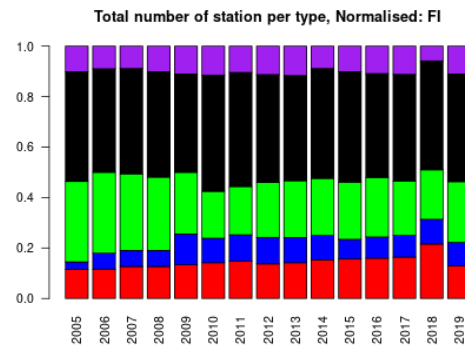
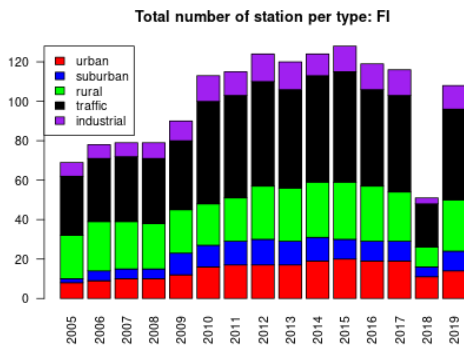
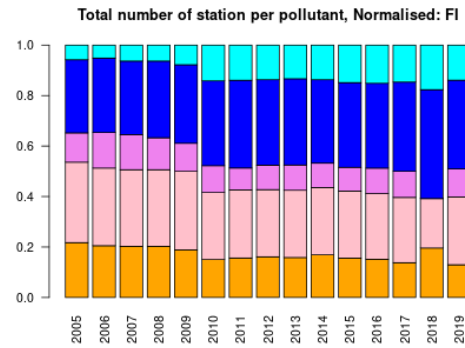
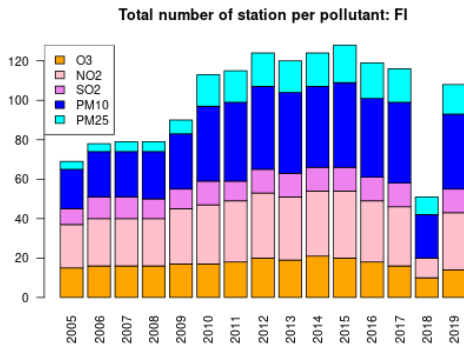
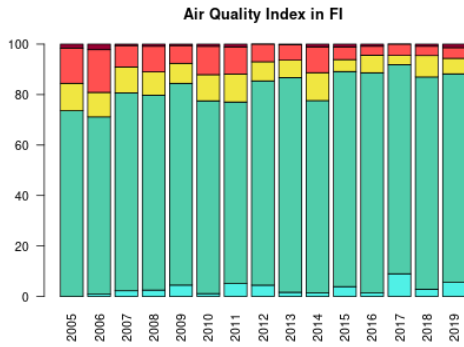


Figure S.222: For Finland: overall air quality index (percentage of days in a given year) and distribution of daily categories per pollutant (light blue: good, light green: fair, yellow: moderate, orange: poor, red: very poor, violet: extremely poor).

11 France

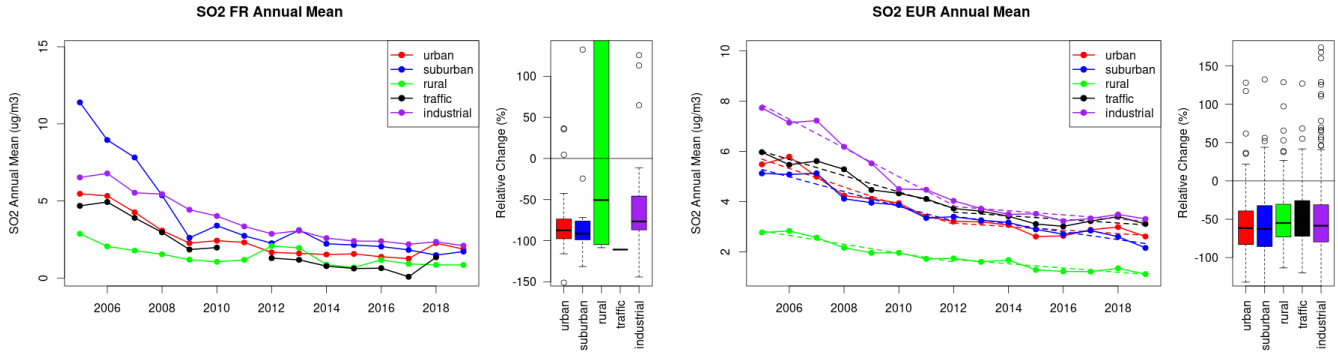


Figure S.223: Time series of the France (left) and European-wide composite (median) of annual mean SO₂ (ug/m³) per station type and area (red: urban background, blue suburban background, green: rural background, black: traffic, violet: industrial) between 2005 and 2019. In the European composite, the dashed lines show the linear fit between 2005 & 2012 and between 2012 & 2019. The boxplots on the right-hand side show the distribution of relative changes (%) between 2005 and 2019 for all stations of each typology in France and in Europe.

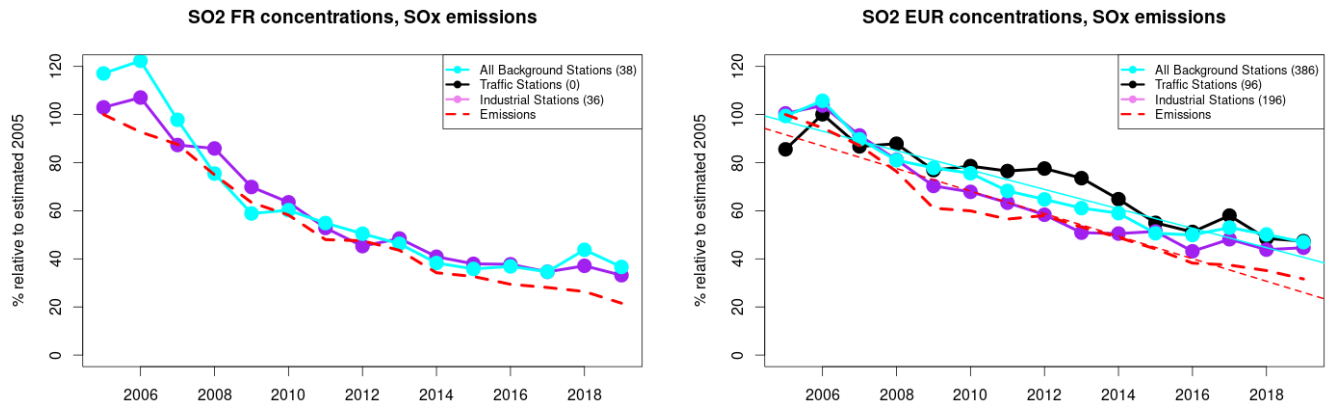


Figure S.224: Time series of 2005-2019 (left) and European (right) median SO₂ observed at traffic (black), industrial (violet) and background (cyan) sites (solid lines), and corresponding SO_x emissions (dashed line) normalised to estimated 2000 levels (%). The median is taken over where more than 5 stations of each typology is available. The total number of stations included is provided in brackets. In the European composite, straight lines are the linear fits over the whole period.

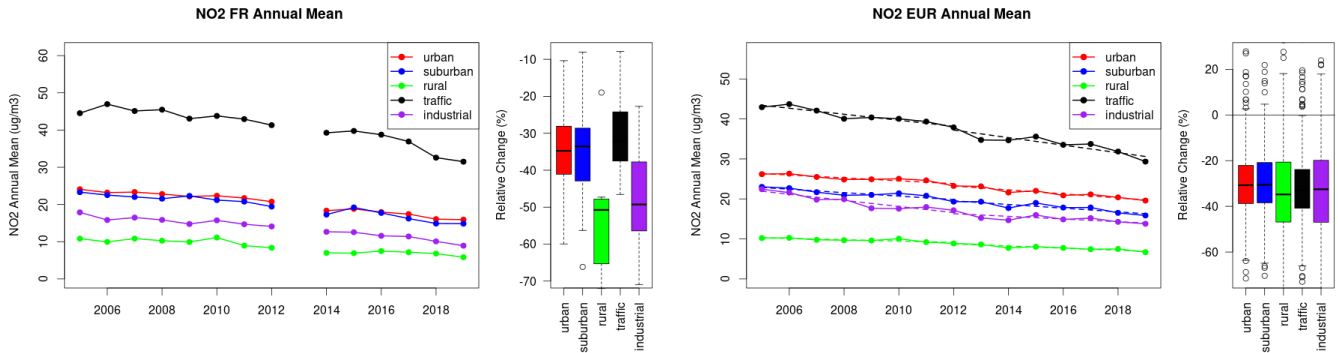


Figure S.225: Time series of the France (left) and European-wide composite (median) of annual mean NO₂ (ug/m³) per station type and area (red: urban background, blue suburban background, green: rural background, black: traffic, violet: industrial) between 2005 and 2019. In the European composite, the dashed lines show the linear fit between 2005 & 2012 and between 2012 & 2019. The boxplots on the right-hand side show the distribution of relative changes (%) between 2005 and 2019 for all stations of each typology in France and in Europe.

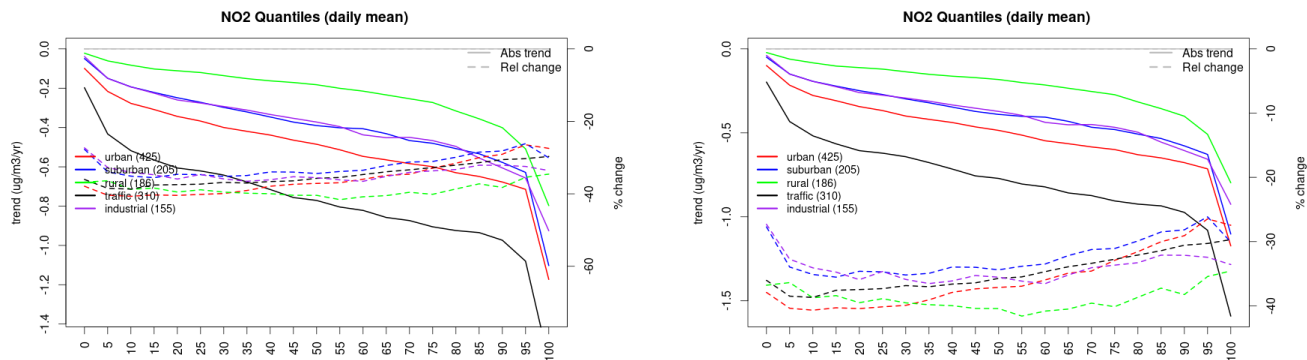


Figure S.226: For NO₂ in France (left) and Europe, and for each typology of station: absolute trend (solid lines, left y-axis) and relative change (dashed lines, right y-axis) of the percentiles of daily means.

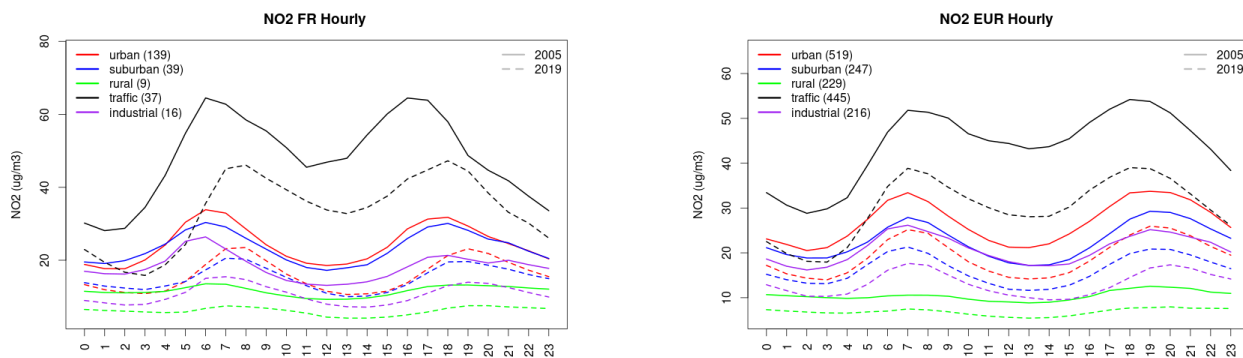


Figure S.227: Diurnal cycle of daily mean NO₂ for France (left) and Europe (right) at various station types estimated from the whole time series in 2005 (solid lines) and 2019

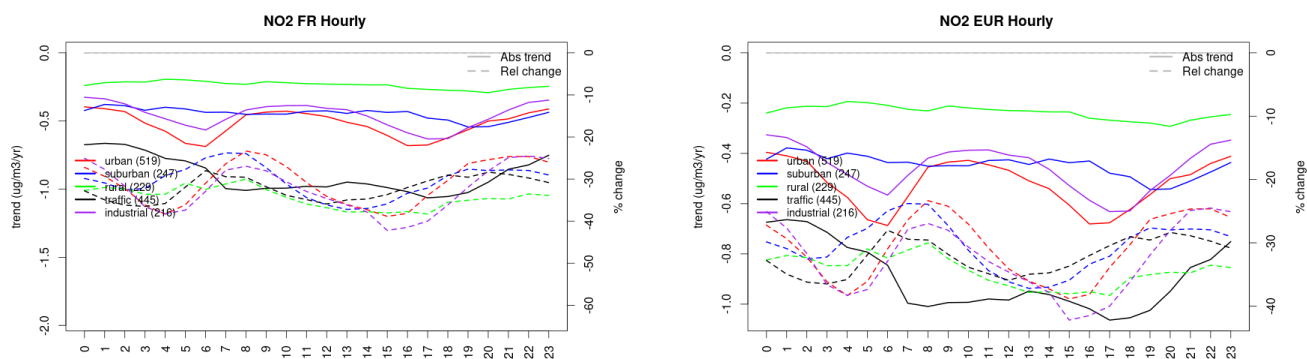


Figure S.228: Absolute (solid lines, left axis) and relative (dashed lines, right axis) trends in the diurnal cycle for France (left) and Europe (right) of NO₂ at various station type.

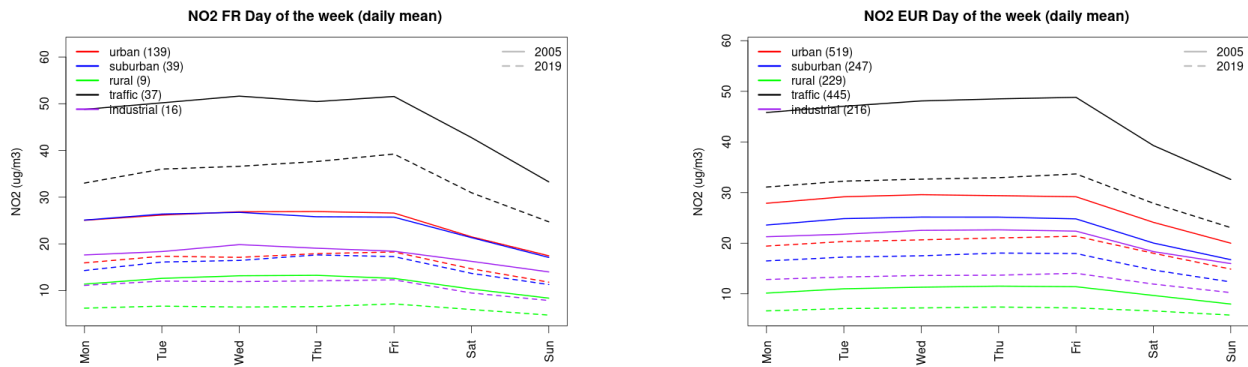


Figure S.229: Weekly cycle of daily mean NO2 for France (left) and Europe (right) at various station types estimated from the whole time series in 2005 (solid lines) and 2019

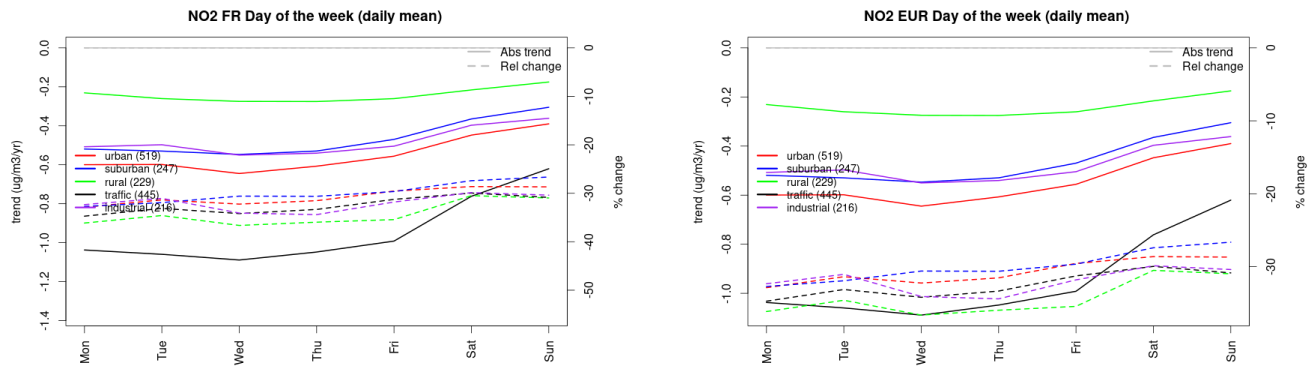


Figure S.230: Absolute (solid lines, left axis) and relative (dashed lines, right axis) trends in the weekly cycle for France (left) and Europe (right) of NO2 at various station type.

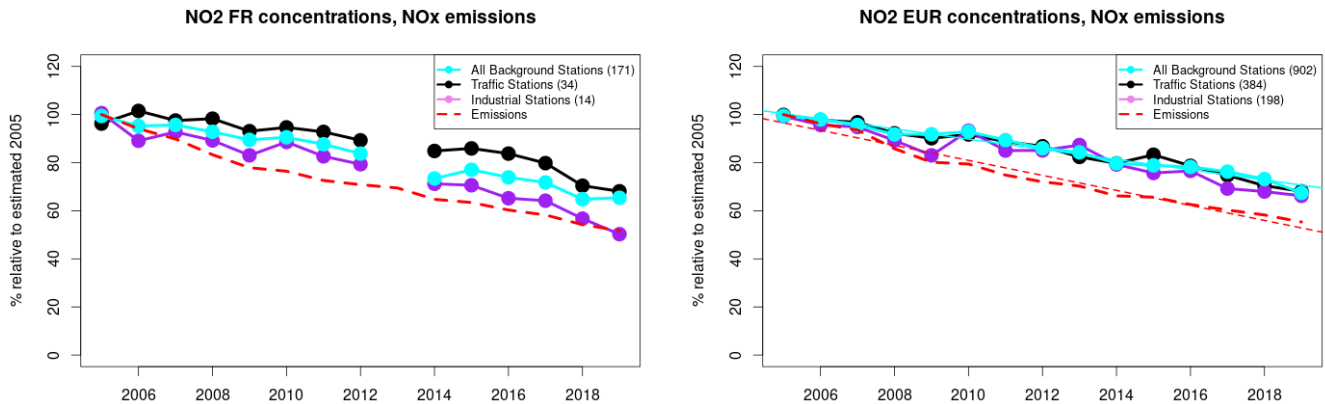


Figure S.231: Time series of 2005-2019 (left) and European (right) median NO2 observed at traffic (black), industrial (violet) and background (cyan) sites (solid lines), and corresponding NOx emissions (dashed line) normalised to estimated 2000 levels (%). The median is taken over where more than 5 stations of each typology is available. The total number of stations included is provided in brackets. In the European composite, straight lines are the linear fits over the whole period.

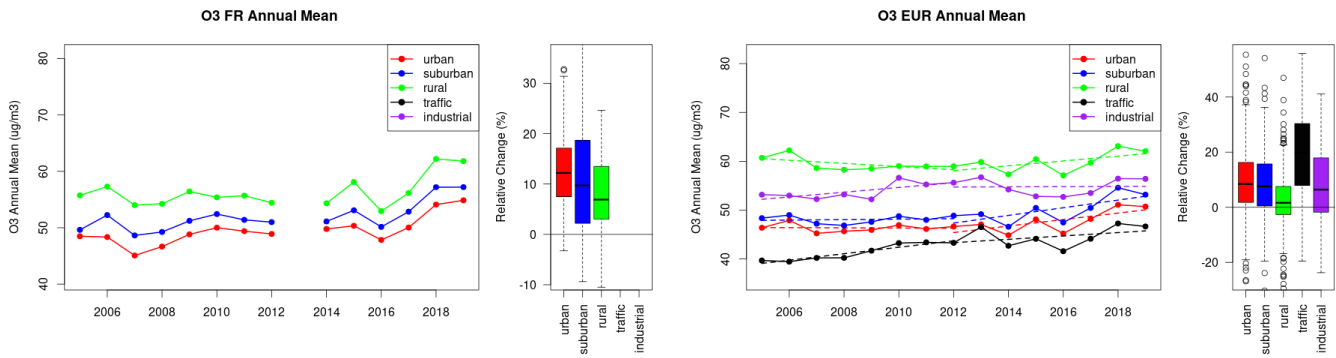


Figure S.232: Time series of the France (left) and European-wide composite (median) of annual mean ozone (ug/m³) per station type and area (red: urban background, blue suburban background, green: rural background, black: traffic, violet: industrial) between 2005 and 2019. In the European composite, the dashed lines show the linear fit between 2005 & 2012 and between 2012 & 2019. The boxplots on the right-hand side show the distribution of relative changes (%) between 2005 and 2019 for all stations of each typology in France and in Europe.

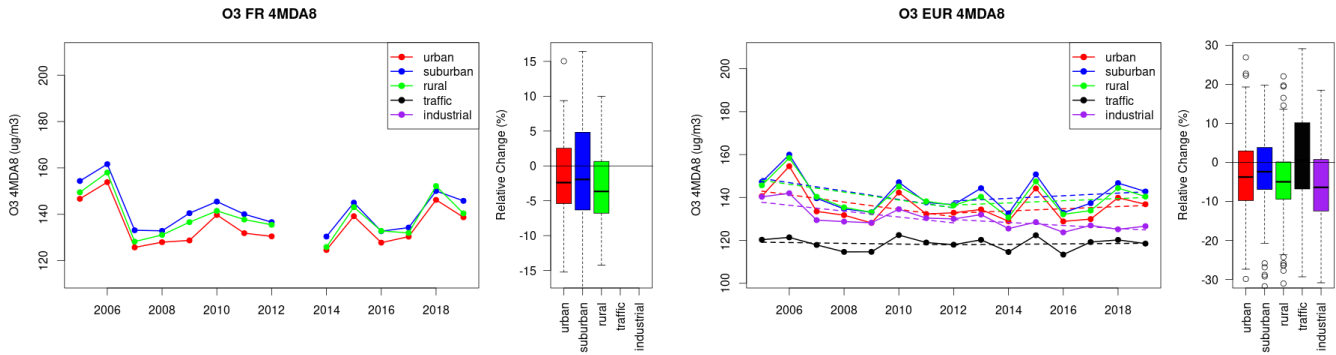


Figure S.233: Time series of the France (left) and European-wide composite (median) of O₃ fourth highest daily peak (4MDA8, ug/m³) per station type and area (red: urban background, blue suburban background, green: rural background, black: traffic, violet: industrial) between 2005 and 2019. In the European composite, the dashed lines show the linear fit between 2005 & 2012 and between 2012 & 2019. The boxplots on the right-hand side show the distribution of relative changes (%) between 2005 and 2019 for all stations of each typology in France and in Europe.

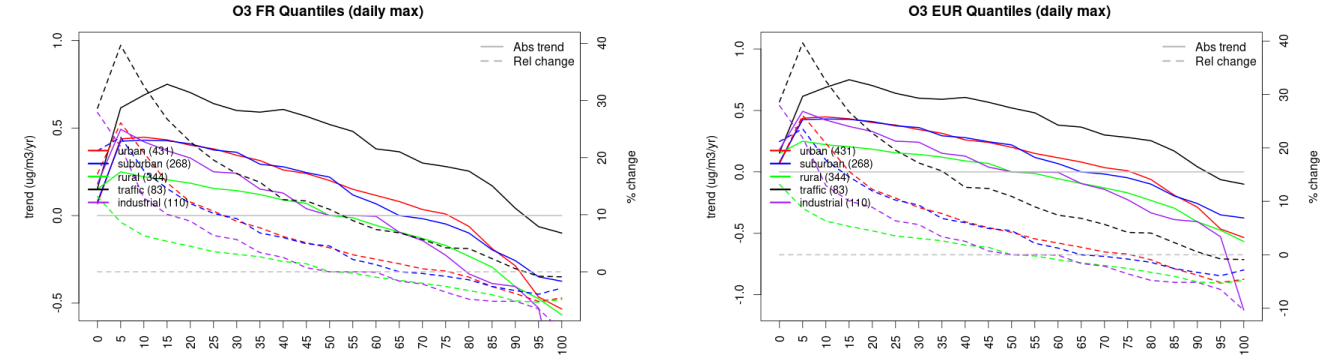


Figure S.234: For ozone in France (left) and Europe, and for each typology of station: absolute trend (solid lines, left y-axis) and relative change (dashed lines, right y-axis) of the percentiles of daily maxima.

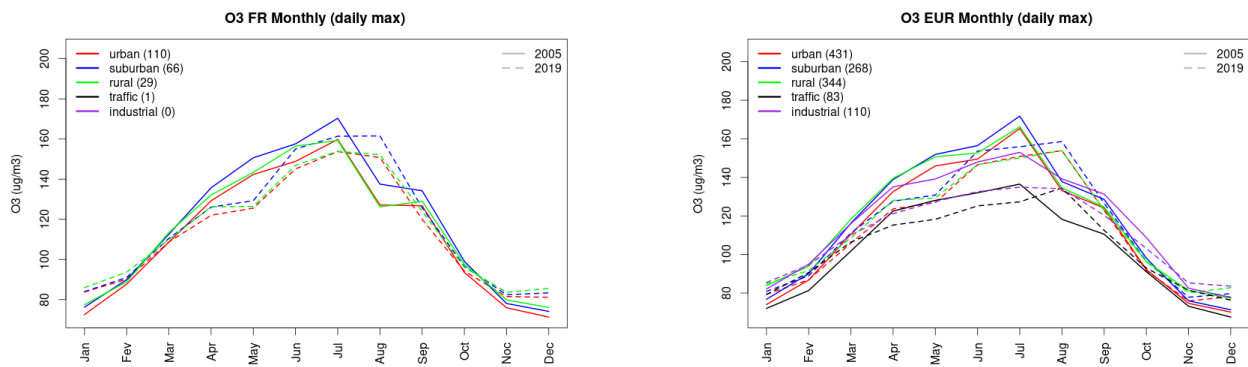


Figure S.235: Monthly cycle of daily max ozone for France (left) and Europe (right) at various station types estimated from the whole time series in 2005 (solid lines) and 2019

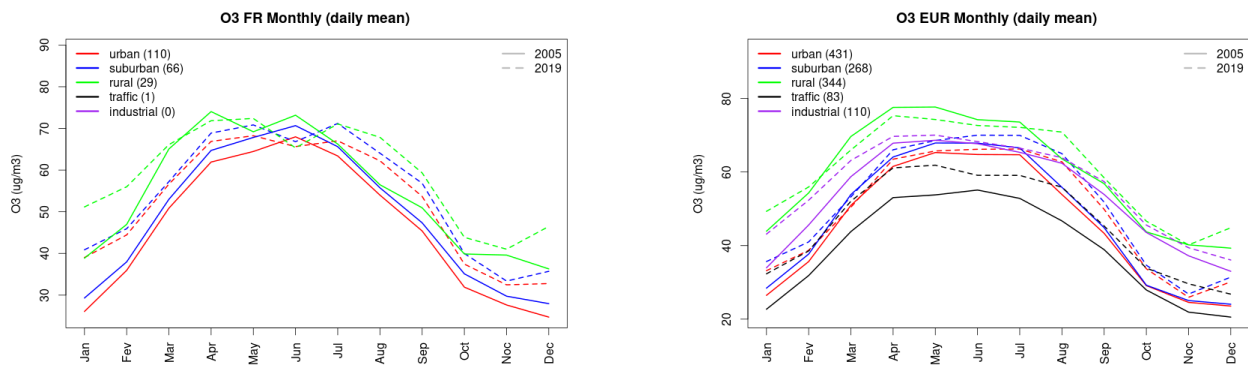


Figure S.236: Monthly cycle of daily mean ozone for France (left) and Europe (right) at various station types estimated from the whole time series in 2005 (solid lines) and 2019

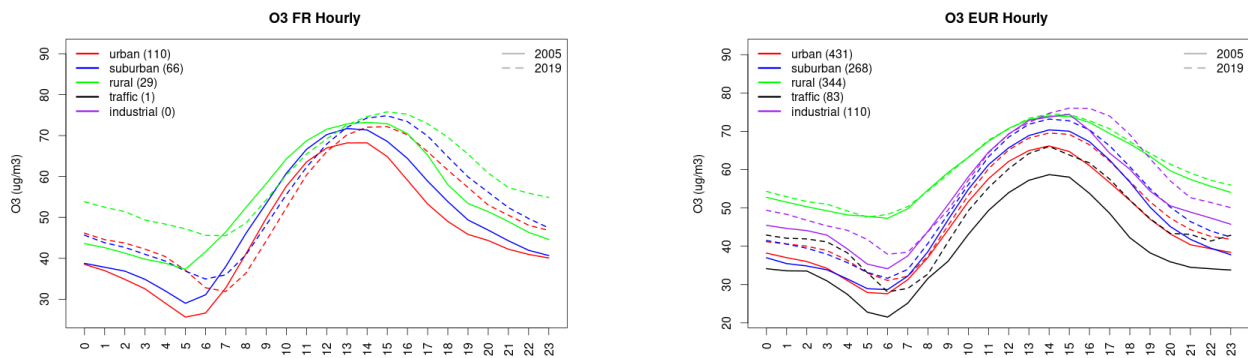


Figure S.237: Diurnal cycle of daily mean ozone for France (left) and Europe (right) at various station types estimated from the whole time series in 2005 (solid lines) and 2019

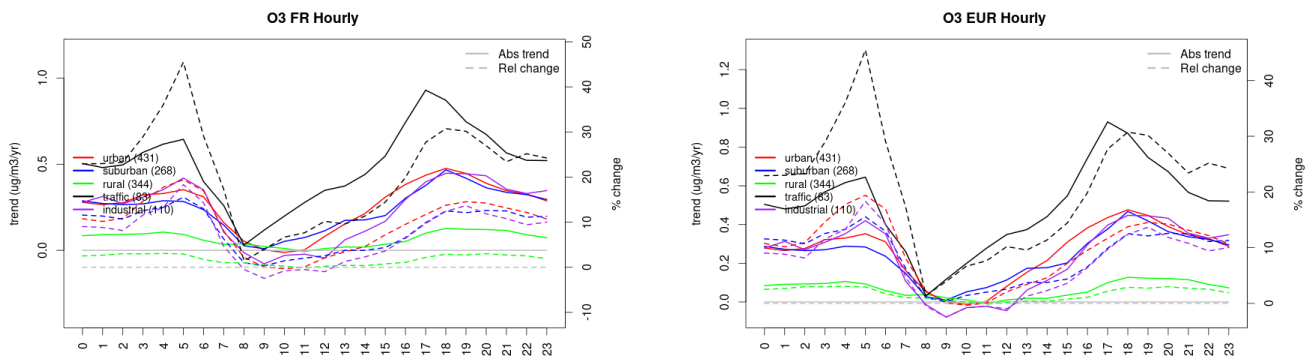


Figure S.238: Absolute (solid lines, left axis) and relative (dashed lines, right axis) trends in the diurnal cycle for France (left) and Europe (right) of ozone at various station type.

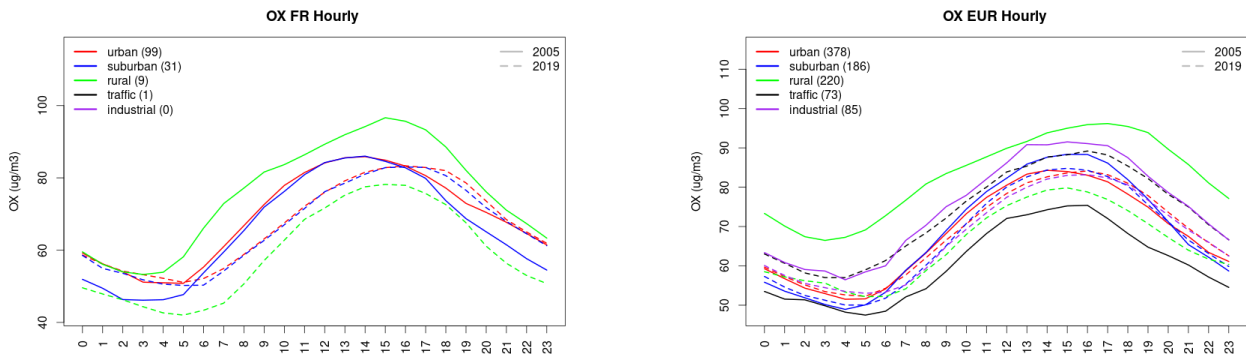


Figure S.239: Diurnal cycle of daily mean OX (as NO₂+O₃) for France (left) and Europe (right) at various station types estimated from the whole time series in 2005 (solid lines) and 2019

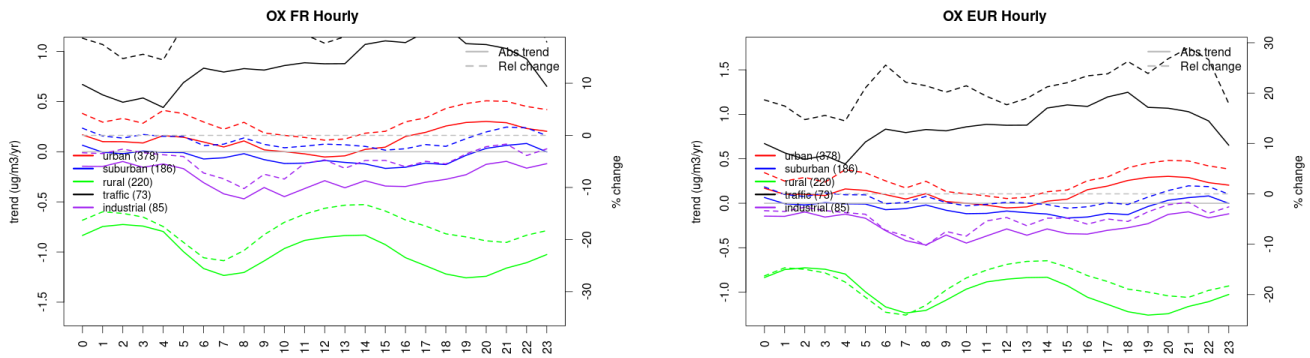


Figure S.240: Absolute (solid lines, left axis) and relative (dashed lines, right axis) trends in the diurnal cycle for France (left) and Europe (right) of OX (as NO₂+O₃) at various station type.

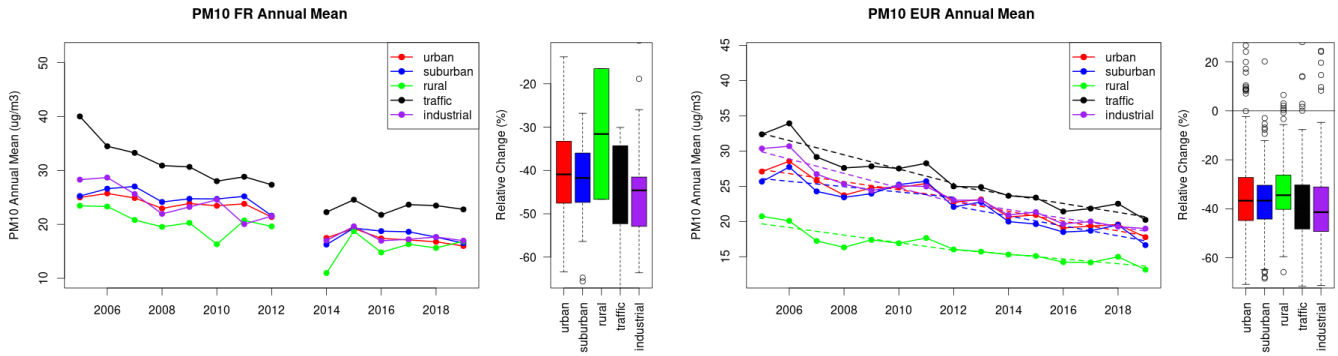


Figure S.241: Time series of the France (left) and European-wide composite (median) of annual mean PM10 ($\mu\text{g}/\text{m}^3$) per station type and area (red: urban background, blue suburban background, green: rural background, black: traffic, violet: industrial) between 2005 and 2019. In the European composite, the dashed lines show the linear fit between 2005 & 2012 and between 2012 & 2019. The boxplots on the right-hand side show the distribution of relative changes (%) between 2005 and 2019 for all stations of each typology in France and in Europe.

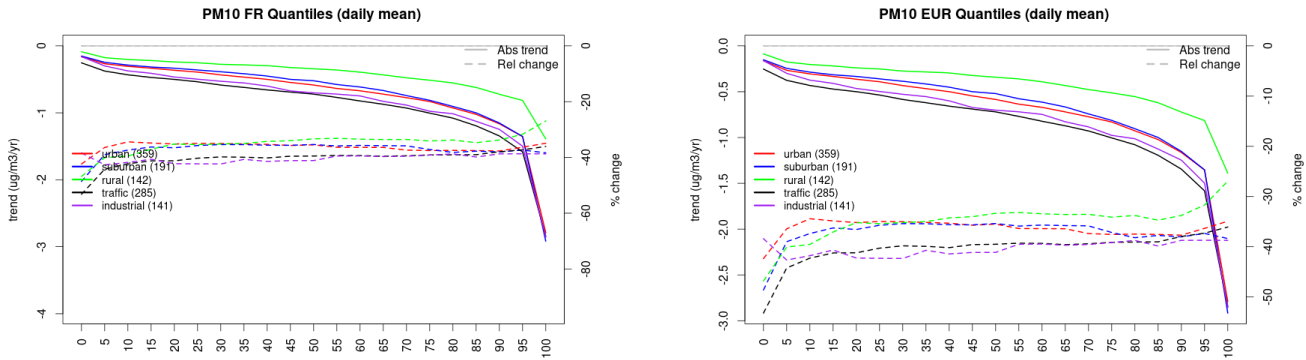


Figure S.242: For PM10 in France (left) and Europe, and for each typology of station: absolute trend (solid lines, left y-axis) and relative change (dashed lines, right y-axis) of the percentiles of daily means.

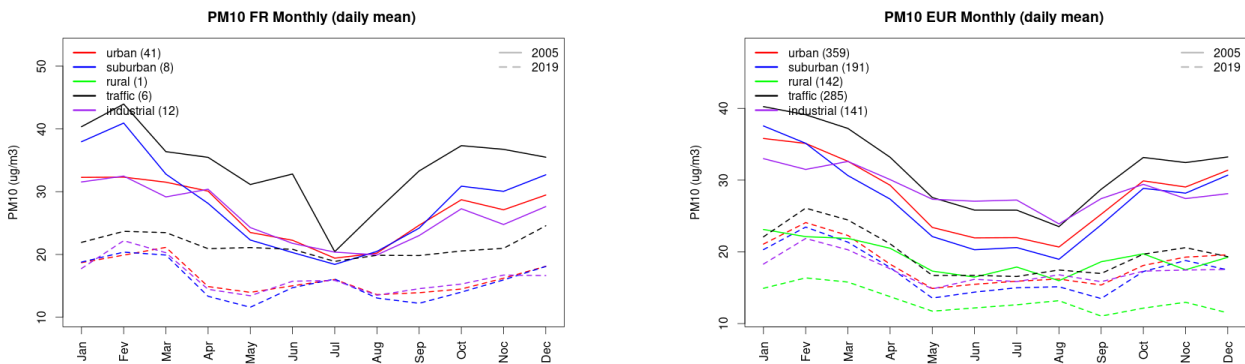


Figure S.243: Monthly cycle of daily mean PM10 for France (left) and Europe (right) at various station types estimated from the whole time series in 2005 (solid lines) and 2019 (dashed lines).

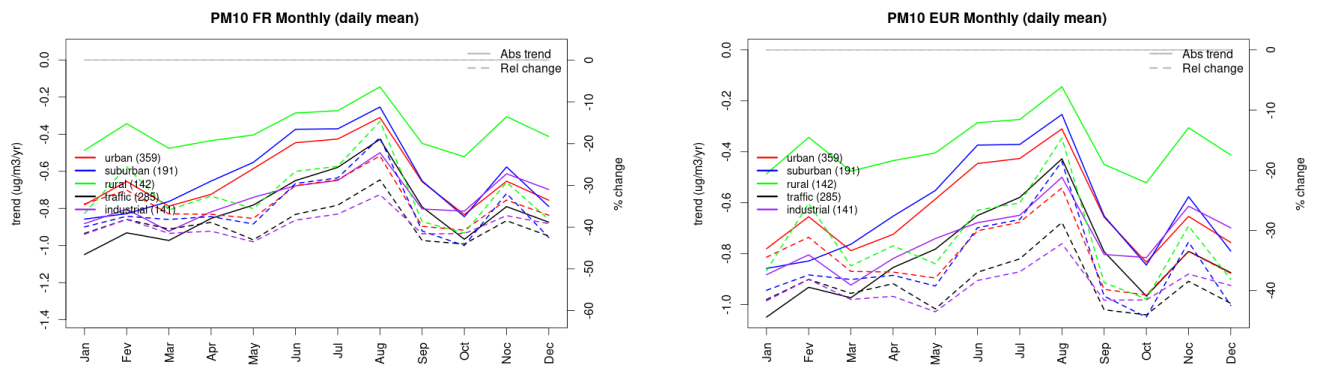


Figure S.244: Absolute (solid lines, left axis) and relative (dashed lines, right axis) trends in the monthly cycle for France (left) and Europe (right) of PM10 at various station type.

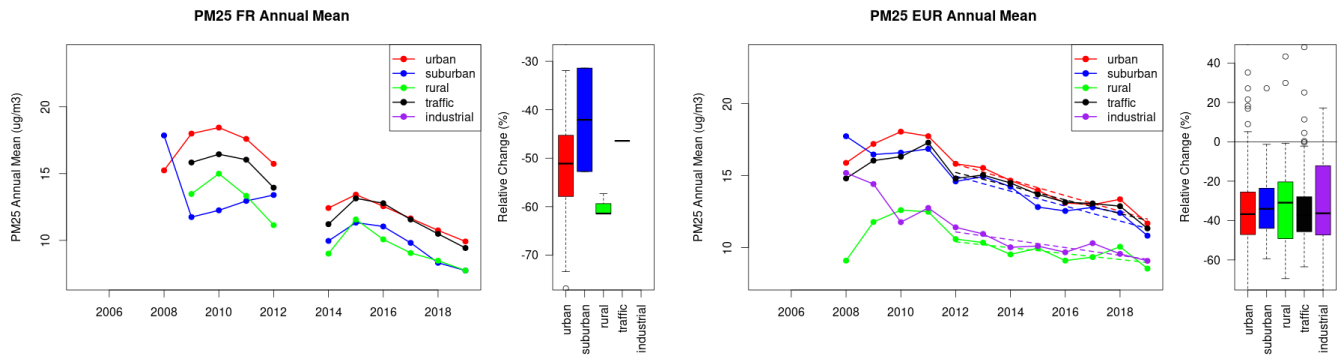


Figure S.245: Time series of the France (left) and European-wide composite (median) of annual mean PM25 ($\mu\text{g}/\text{m}^3$) per station type and area (red: urban background, blue suburban background, green: rural background, black: traffic, violet: industrial) between 2005 and 2019. In the European composite, the dashed lines show the linear fit between 2005 & 2012 and between 2012 & 2019. The boxplots on the right-hand side show the distribution of relative changes (%) between 2005 and 2019 for all stations of each typology in France and in Europe.

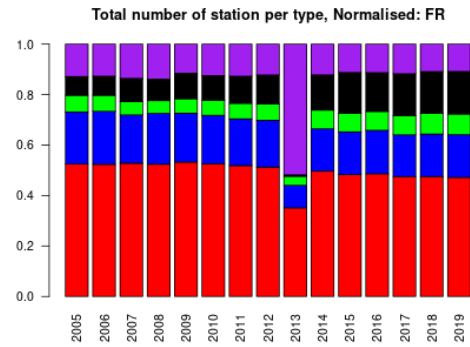
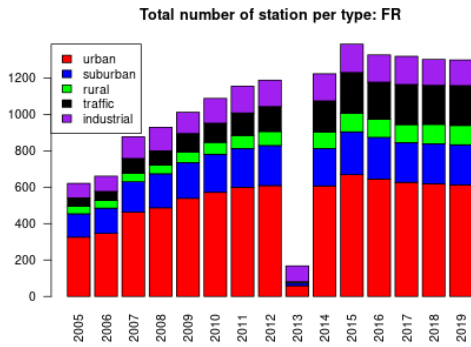
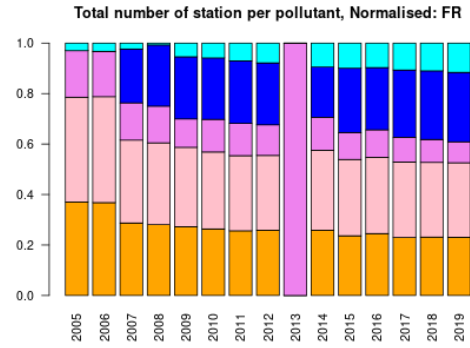
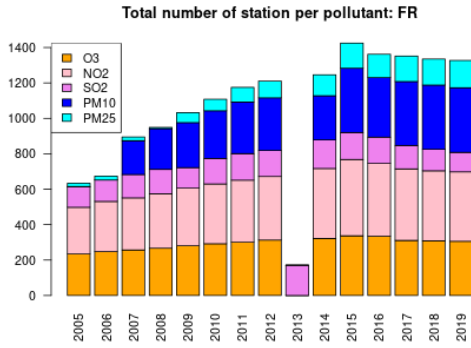
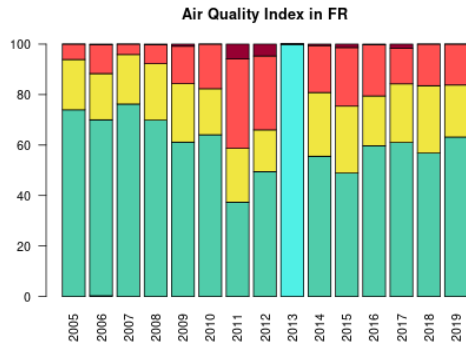


Figure S.246: For France: overall air quality index (percentage of days in a given year) and distribution of daily categories per pollutant (light blue: good, light green: fair, yellow: moderate, orange: poor, red: very poor, violet: extremely poor).

12 Great Britain

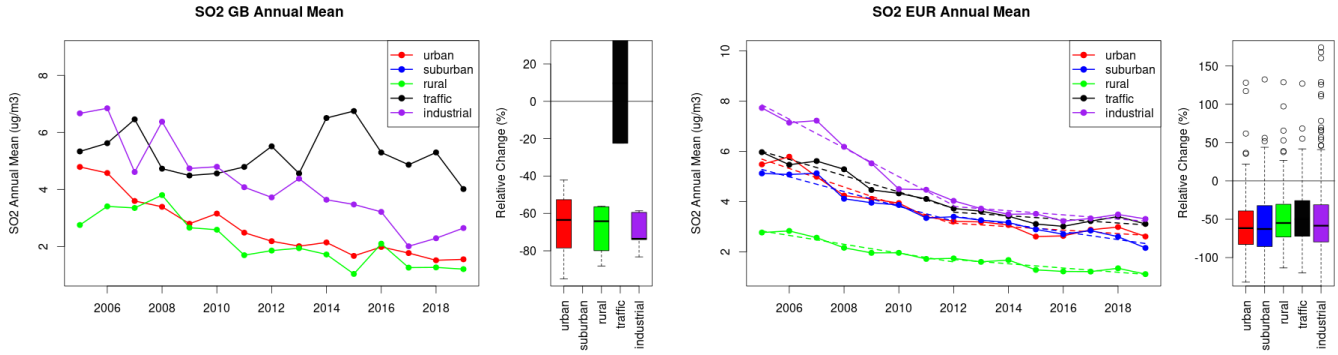


Figure S.247: Time series of the Great Britain (left) and European-wide composite (median) of annual mean SO₂ (ug/m³) per station type and area (red: urban background, blue suburban background, green: rural background, black: traffic, violet: industrial) between 2005 and 2019. In the European composite, the dashed lines show the linear fit between 2005 & 2012 and between 2012 & 2019. The boxplots on the right-hand side show the distribution of relative changes (%) between 2005 and 2019 for all stations of each typology in Great Britain and in Europe.

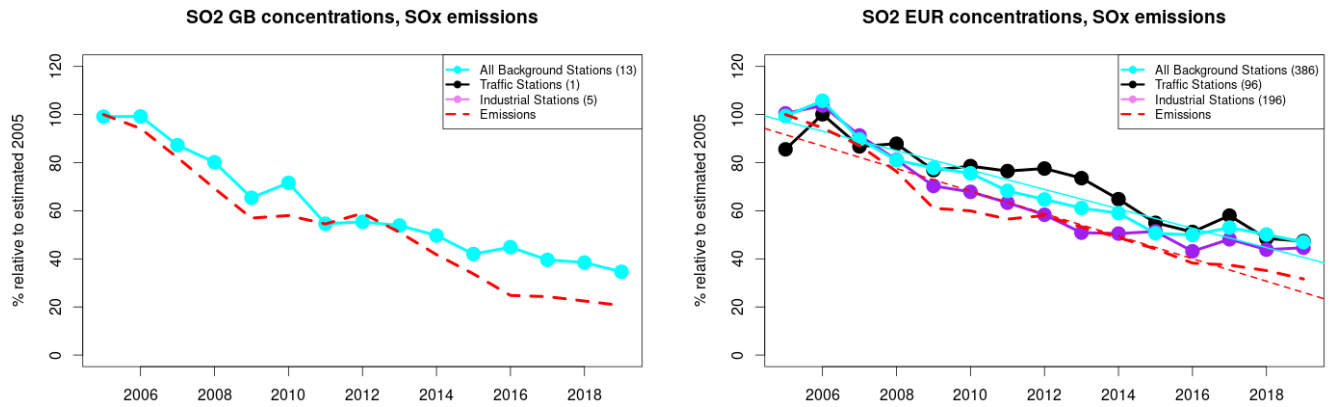


Figure S.248: Time series of 2005-2019 (left) and European (right) median SO₂ observed at traffic (black), industrial (violet) and background (cyan) sites (solid lines), and corresponding SO_x emissions (dashed line) normalised to estimated 2000 levels (%). The median is taken over where more than 5 stations of each typology is available. The total number of stations included is provided in brackets. In the European composite, straight lines are the linear fits over the whole period.

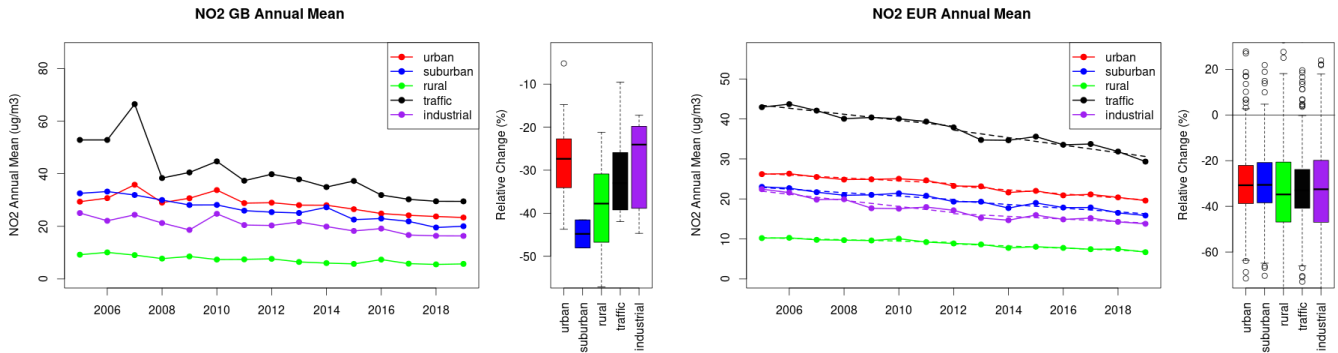


Figure S.249: Time series of the Great Britain (left) and European-wide composite (median) of annual mean NO₂ (ug/m³) per station type and area (red: urban background, blue suburban background, green: rural background, black: traffic, violet: industrial) between 2005 and 2019. In the European composite, the dashed lines show the linear fit between 2005 & 2012 and between 2012 & 2019. The boxplots on the right-hand side show the distribution of relative changes (%) between 2005 and 2019 for all stations of each typology in Great Britain and in Europe.

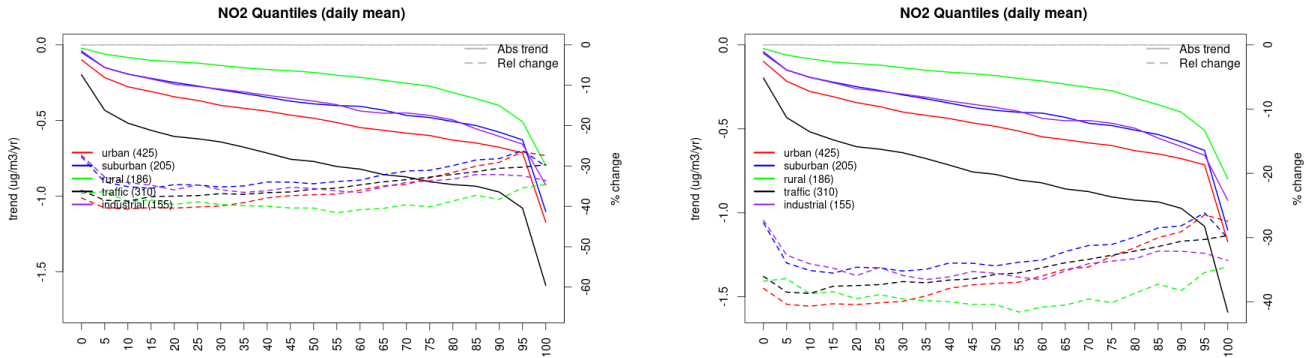


Figure S.250: For NO₂ in Great Britain (left) and Europe, and for each typology of station: absolute trend (solid lines, left y-axis) and relative change (dashed lines, right y-axis) of the percentiles of daily means.

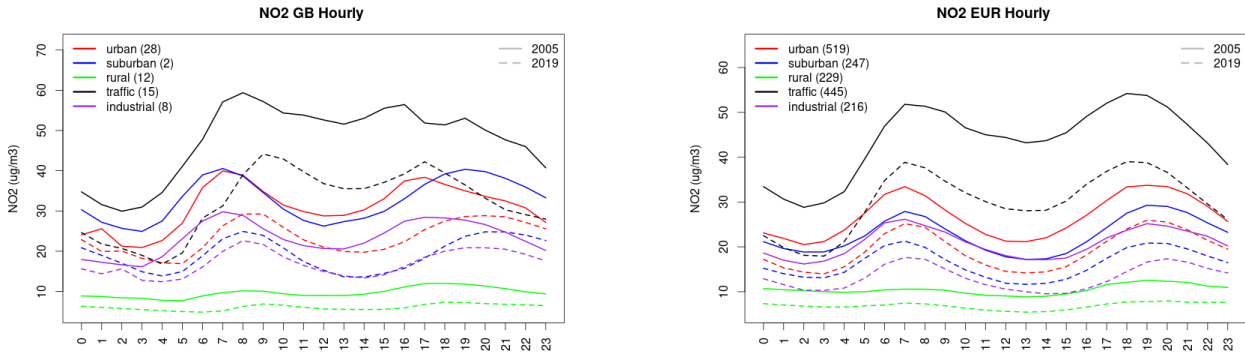


Figure S.251: Diurnal cycle of daily mean NO₂ for Great Britain (left) and Europe (right) at various station types estimated from the whole time series in 2005 (solid lines) and 2019

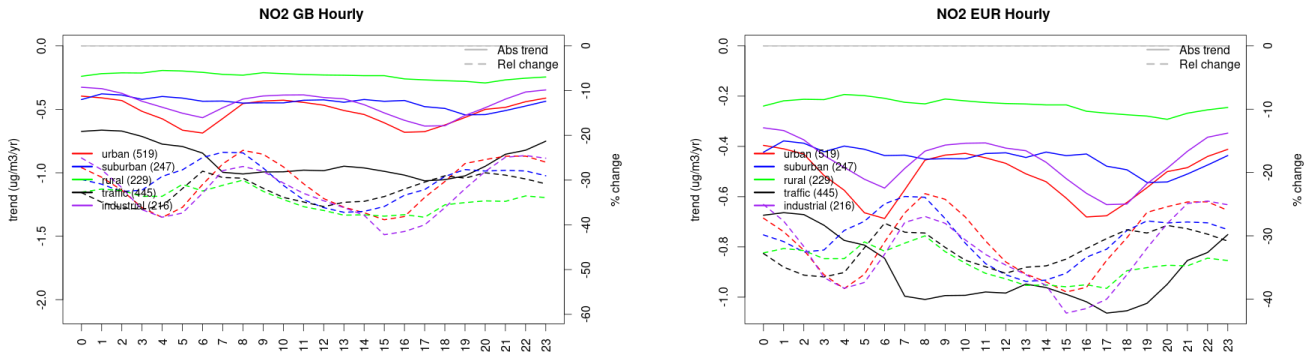


Figure S.252: Absolute (solid lines, left axis) and relative (dashed lines, right axis) trends in the diurnal cycle for Great Britain (left) and Europe (right) of NO₂ at various station type.

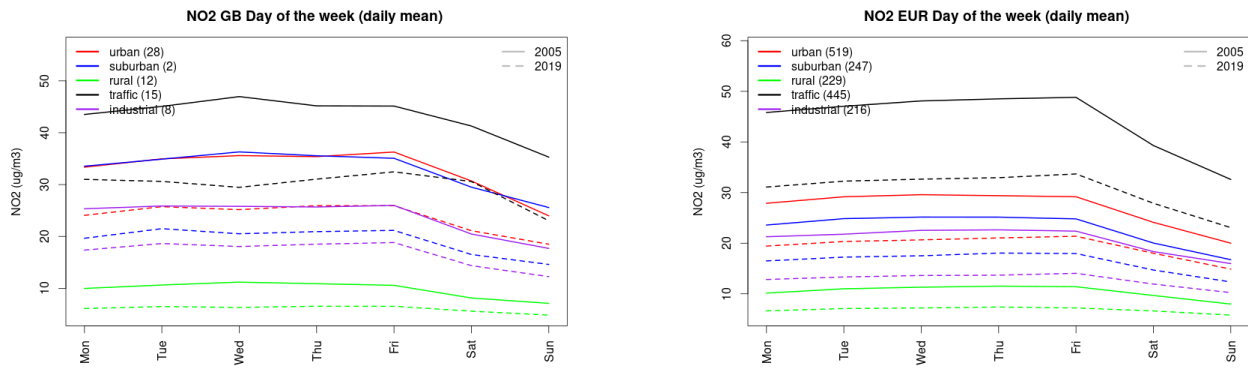


Figure S.253: Weekly cycle of daily mean NO2 for Great Britain (left) and Europe (right) at various station types estimated from the whole time series in 2005 (solid lines) and 2019

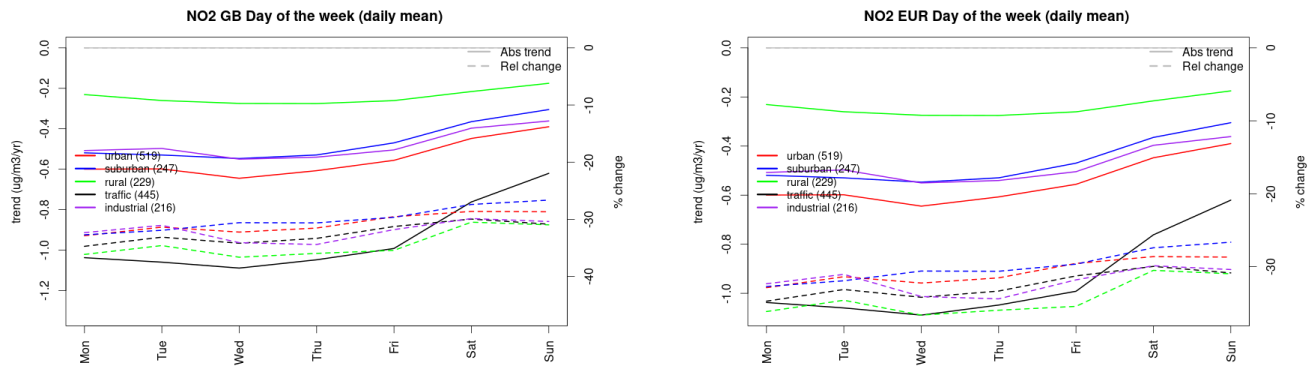


Figure S.254: Absolute (solid lines, left axis) and relative (dashed lines, right axis) trends in the weekly cycle for Great Britain (left) and Europe (right) of NO2 at various station type.

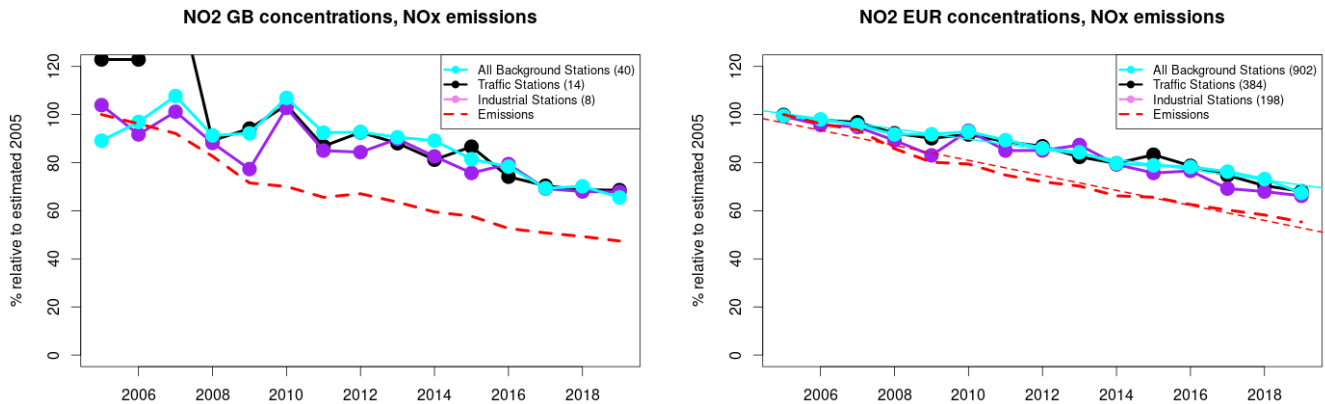


Figure S.255: Time series of 2005-2019 (left) and European (right) median NO2 observed at traffic (black), industrial (violet) and background (cyan) sites (solid lines), and corresponding NOx emissions (dashed line) normalised to estimated 2000 levels (%). The median is taken over where more than 5 stations of each typology is available. The total number of stations included is provided in brackets. In the European composite, straight lines are the linear fits over the whole period.

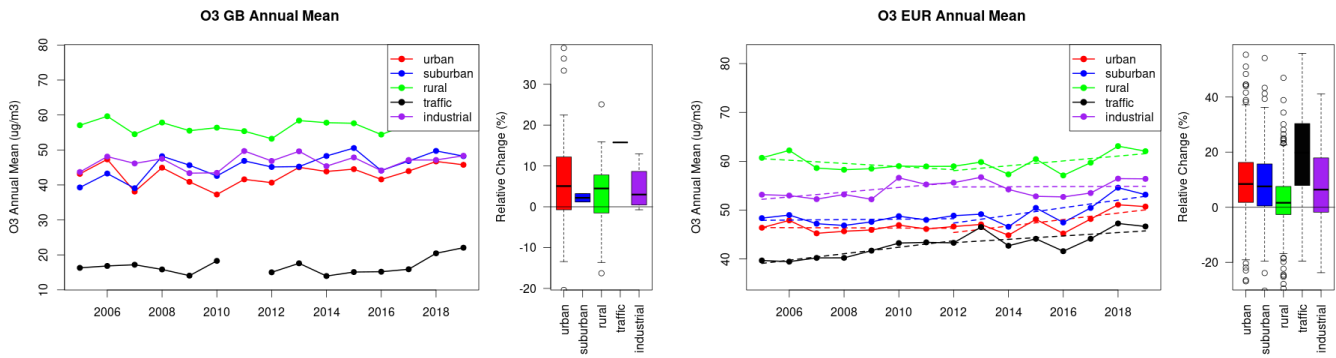


Figure S.256: Time series of the Great Britain (left) and European-wide composite (median) of annual mean ozone ($\mu\text{g}/\text{m}^3$) per station type and area (red: urban background, blue suburban background, green: rural background, black: traffic, violet: industrial) between 2005 and 2019. In the European composite, the dashed lines show the linear fit between 2005 & 2012 and between 2012 & 2019. The boxplots on the right-hand side show the distribution of relative changes (%) between 2005 and 2019 for all stations of each typology in Great Britain and in Europe.

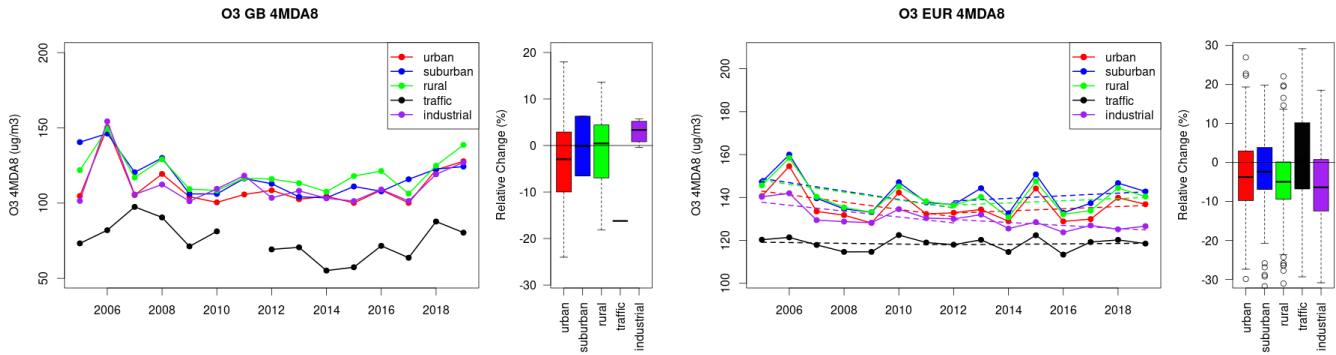


Figure S.257: Time series of the Great Britain (left) and European-wide composite (median) of O3 fourth highest daily peak (4MDA8, $\mu\text{g}/\text{m}^3$) per station type and area (red: urban background, blue suburban background, green: rural background, black: traffic, violet: industrial) between 2005 and 2019. In the European composite, the dashed lines show the linear fit between 2005 & 2012 and between 2012 & 2019. The boxplots on the right-hand side show the distribution of relative changes (%) between 2005 and 2019 for all stations of each typology in Great Britain and in Europe.

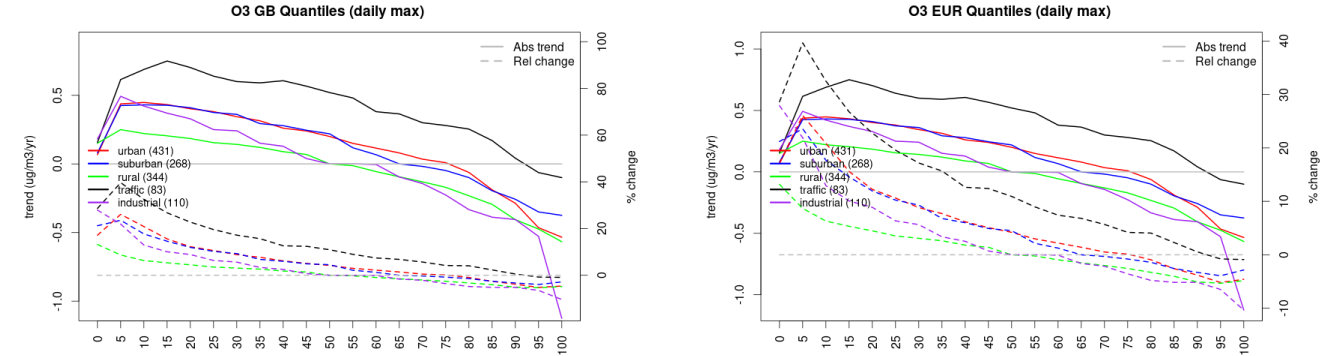


Figure S.258: For ozone in Great Britain (left) and Europe, and for each typology of station: absolute trend (solid lines, left y-axis) and relative change (dashed lines, right y-axis) of the percentiles of daily maxima.

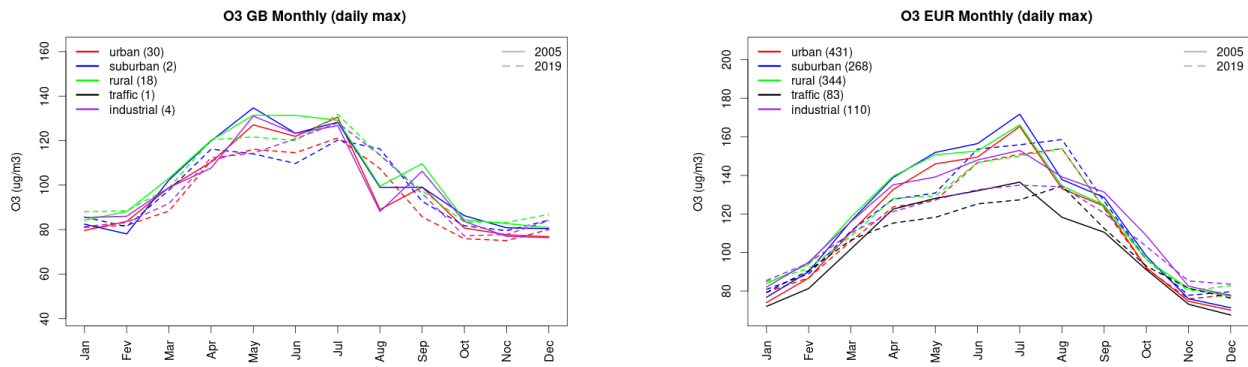


Figure S.259: Monthly cycle of daily max ozone for Great Britain (left) and Europe (right) at various station types estimated from the whole time series in 2005 (solid lines) and 2019

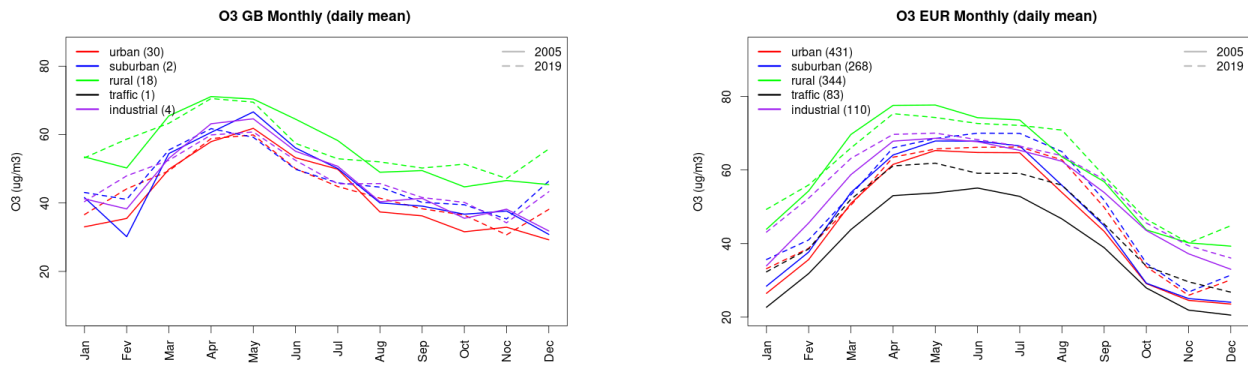


Figure S.260: Monthly cycle of daily mean ozone for Great Britain (left) and Europe (right) at various station types estimated from the whole time series in 2005 (solid lines) and 2019

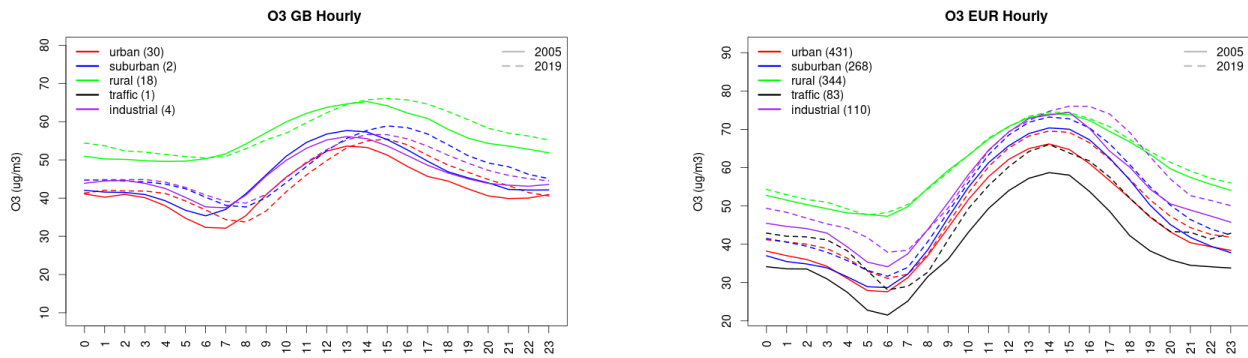


Figure S.261: Diurnal cycle of daily mean ozone for Great Britain (left) and Europe (right) at various station types estimated from the whole time series in 2005 (solid lines) and 2019

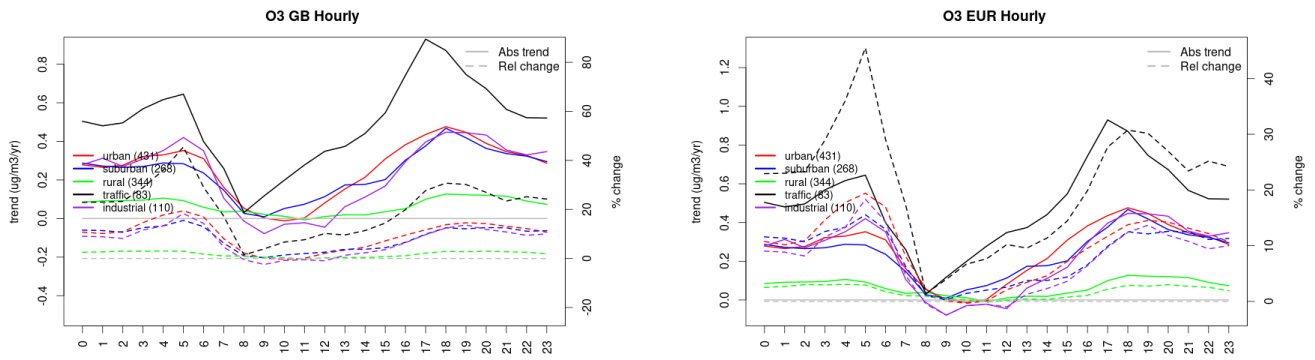


Figure S.262: Absolute (solid lines, left axis) and relative (dashed lines, right axis) trends in the diurnal cycle for Great Britain (left) and Europe (right) of ozone at various station type.

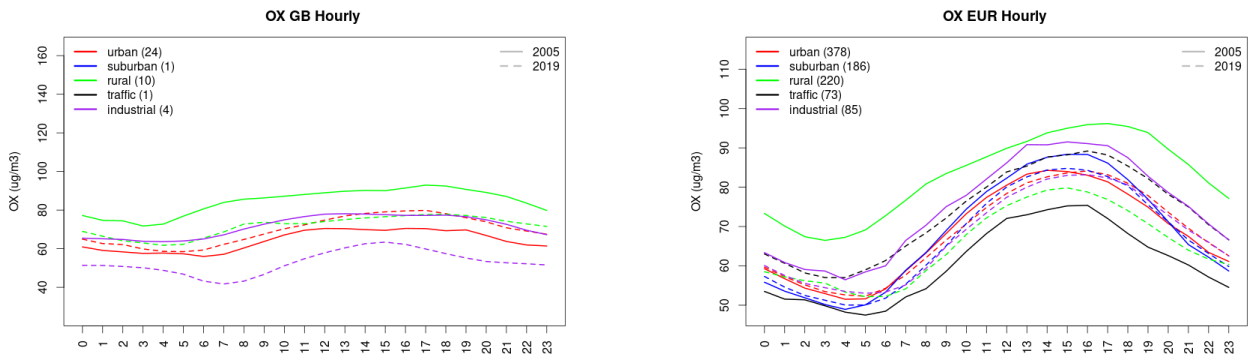


Figure S.263: Diurnal cycle of daily mean OX (as NO₂+O₃) for Great Britain (left) and Europe (right) at various station types estimated from the whole time series in 2005 (solid lines) and 2019

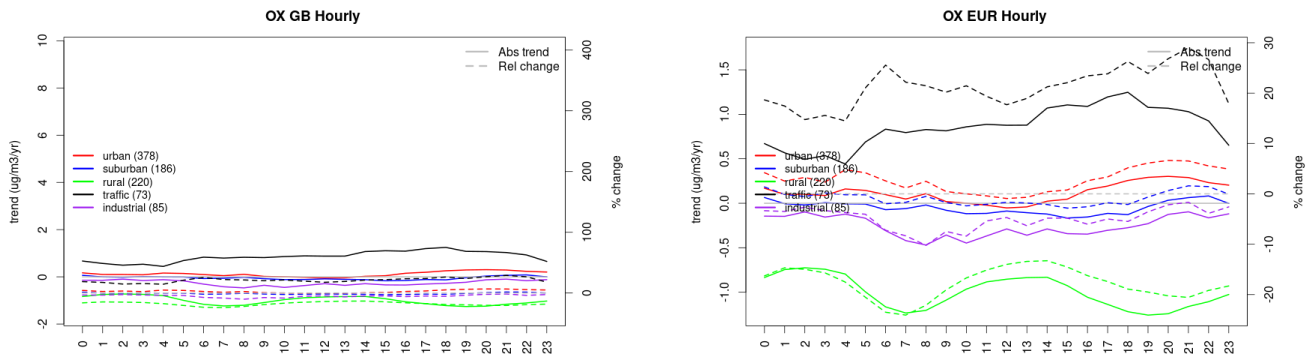


Figure S.264: Absolute (solid lines, left axis) and relative (dashed lines, right axis) trends in the diurnal cycle for Great Britain (left) and Europe (right) of OX (as NO₂+O₃) at various station type.

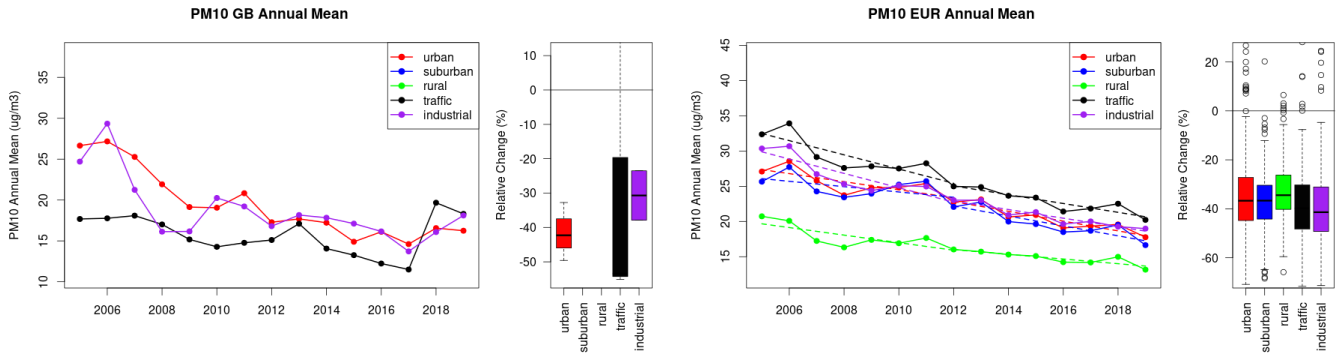


Figure S.265: Time series of the Great Britain (left) and European-wide composite (median) of annual mean PM10 ($\mu\text{g}/\text{m}^3$) per station type and area (red: urban background, blue suburban background, green: rural background, black: traffic, violet: industrial) between 2005 and 2019. In the European composite, the dashed lines show the linear fit between 2005 & 2012 and between 2012 & 2019. The boxplots on the right-hand side show the distribution of relative changes (%) between 2005 and 2019 for all stations of each typology in Great Britain and in Europe.

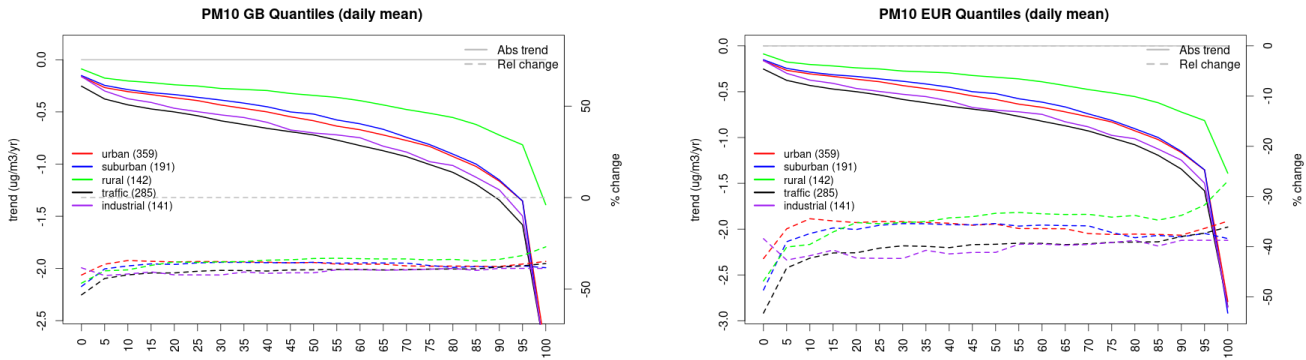


Figure S.266: For PM10 in Great Britain (left) and Europe, and for each typology of station: absolute trend (solid lines, left y-axis) and relative change (dashed lines, right y-axis) of the percentiles of daily means.

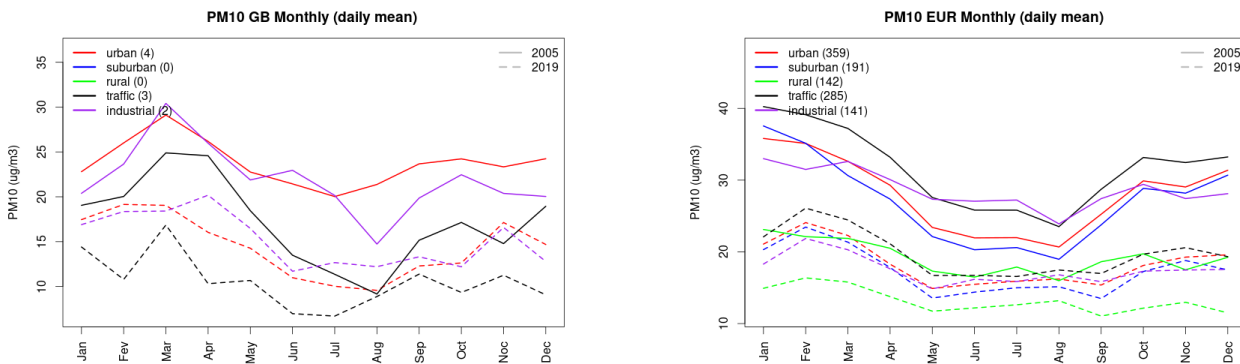


Figure S.267: Monthly cycle of daily mean PM10 for Great Britain (left) and Europe (right) at various station types estimated from the whole time series in 2005 (solid lines) and 2019

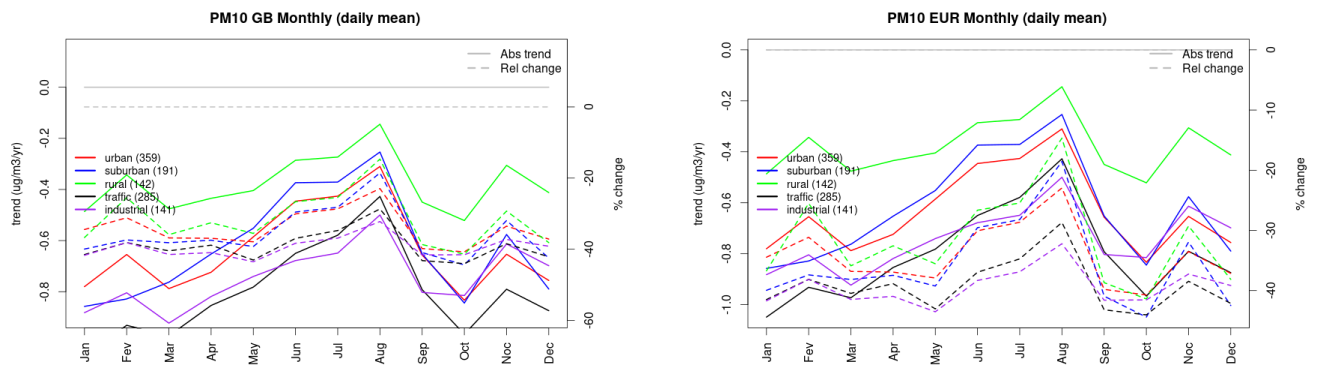


Figure S.268: Absolute (solid lines, left axis) and relative (dashed lines, right axis) trends in the monthly cycle for Great Britain (left) and Europe (right) of PM10 at various station type.

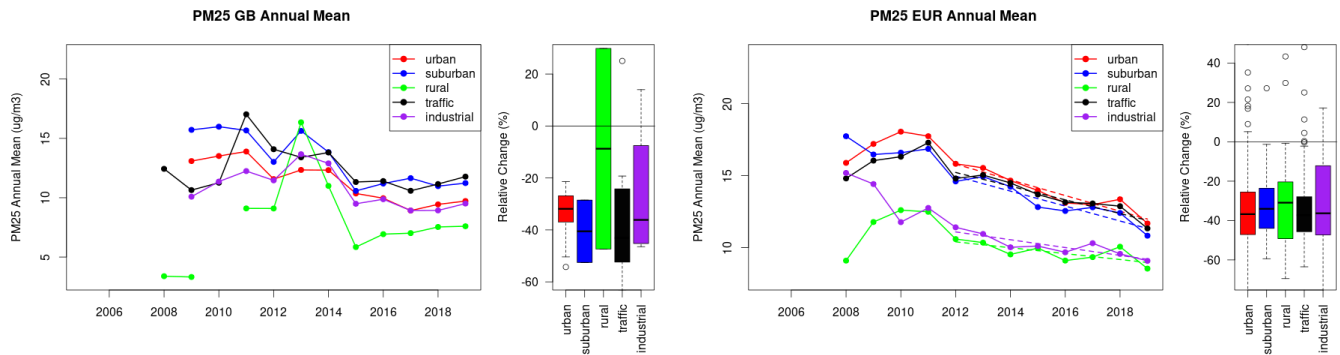


Figure S.269: Time series of the Great Britain (left) and European-wide composite (median) of annual mean PM25 ($\mu\text{g}/\text{m}^3$) per station type and area (red: urban background, blue suburban background, green: rural background, black: traffic, violet: industrial) between 2005 and 2019. In the European composite, the dashed lines show the linear fit between 2005 & 2012 and between 2012 & 2019. The boxplots on the right-hand side show the distribution of relative changes (%) between 2005 and 2019 for all stations of each typology in Great Britain and in Europe.

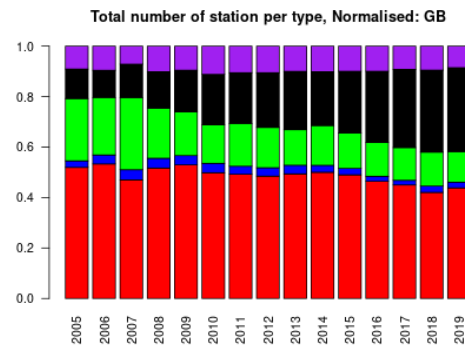
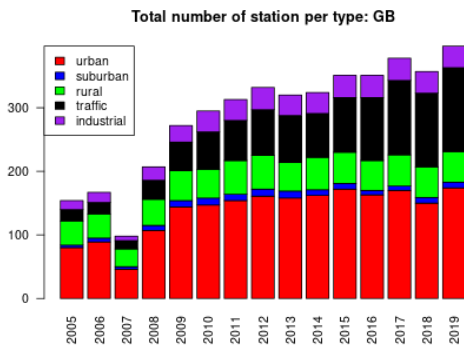
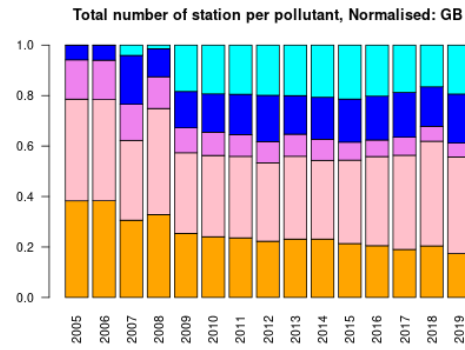
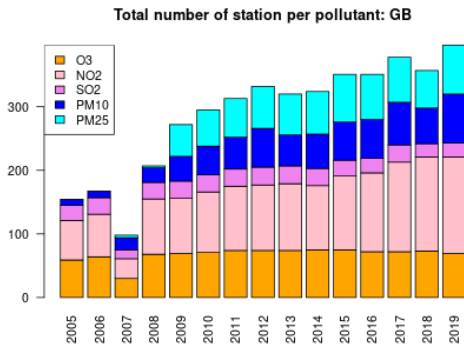
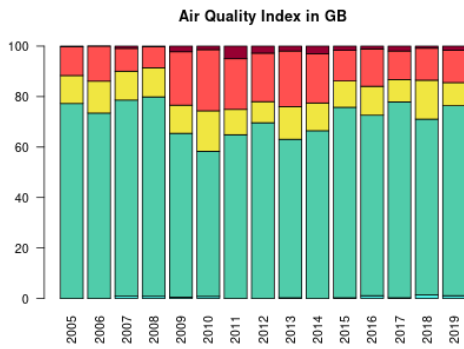


Figure S.270: For Great Britain: overall air quality index (percentage of days in a given year) and distribution of daily categories per pollutant (light blue: good, light green: fair, yellow: moderate, orange: poor, red: very poor, violet: extremely poor).

13 Greece

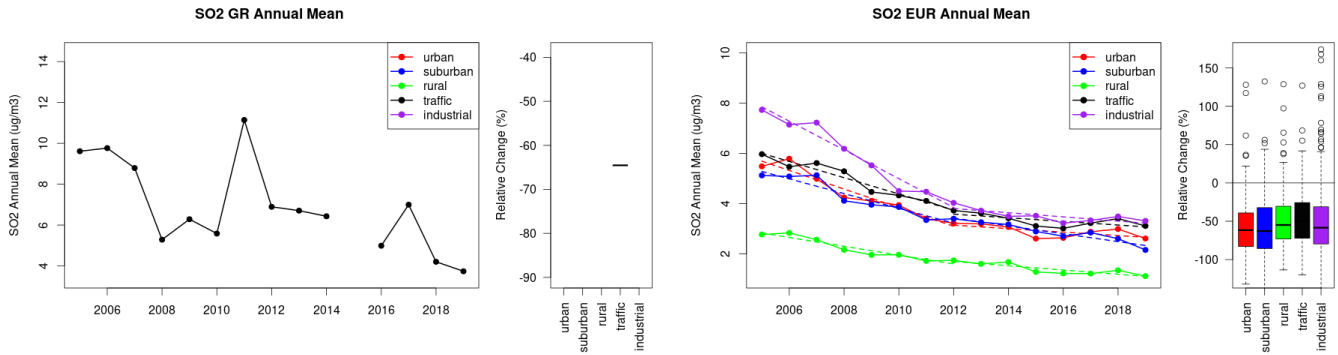


Figure S.271: Time series of the Greece (left) and European-wide composite (median) of annual mean SO2 (ug/m3) per station type and area (red: urban background, blue suburban background, green: rural background, black: traffic, violet: industrial) between 2005 and 2019. In the European composite, the dashed lines show the linear fit between 2005 & 2012 and between 2012 & 2019. The boxplots on the right-hand side show the distribution of relative changes (%) between 2005 and 2019 for all stations of each typology in Greece and in Europe.

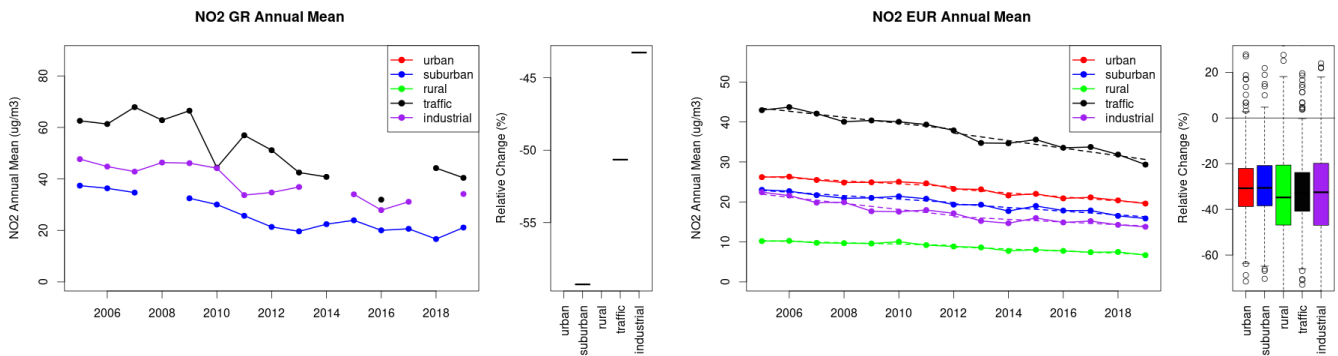


Figure S.272: Time series of the Greece (left) and European-wide composite (median) of annual mean NO2 (ug/m3) per station type and area (red: urban background, blue suburban background, green: rural background, black: traffic, violet: industrial) between 2005 and 2019. In the European composite, the dashed lines show the linear fit between 2005 & 2012 and between 2012 & 2019. The boxplots on the right-hand side show the distribution of relative changes (%) between 2005 and 2019 for all stations of each typology in Greece and in Europe.

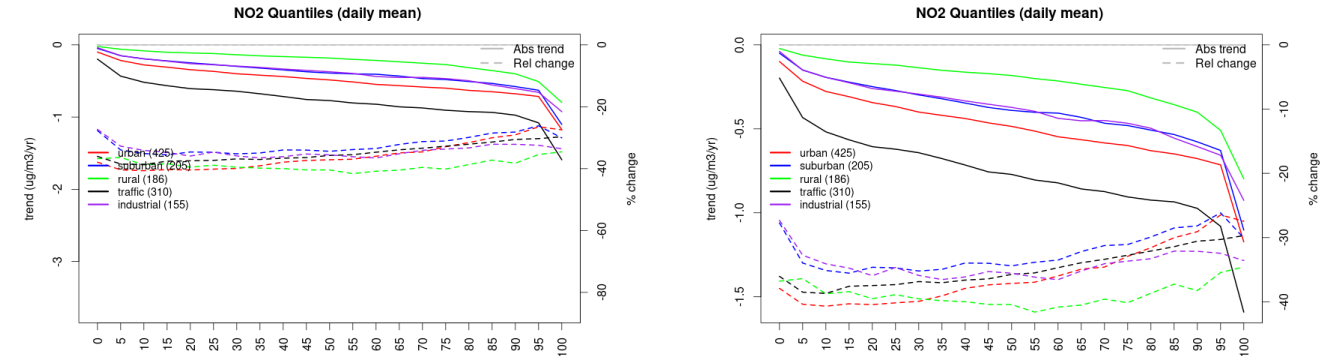


Figure S.273: For NO2 in Greece (left) and Europe, and for each typology of station: absolute trend (solid lines, left y-axis) and relative change (dashed lines, right y-axis) of the percentiles of daily means.

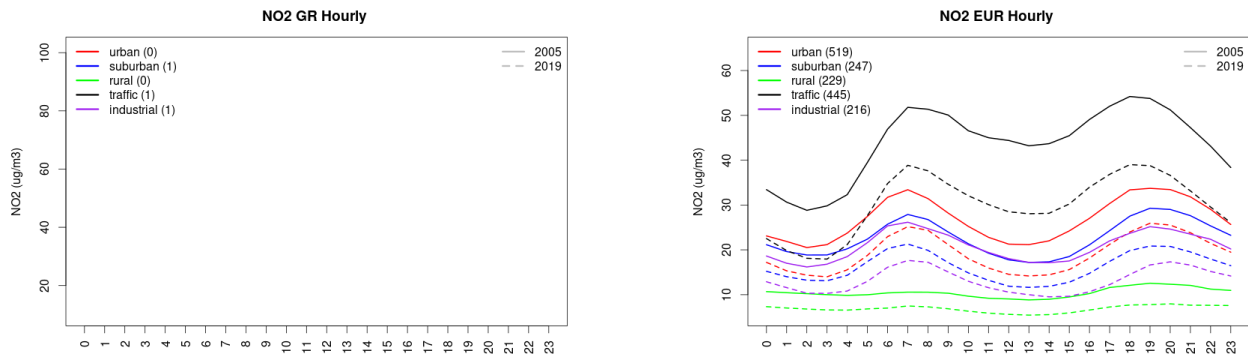


Figure S.274: Diurnal cycle of daily mean NO2 for Greece (left) and Europe (right) at various station types estimated from the whole time series in 2005 (solid lines) and 2019

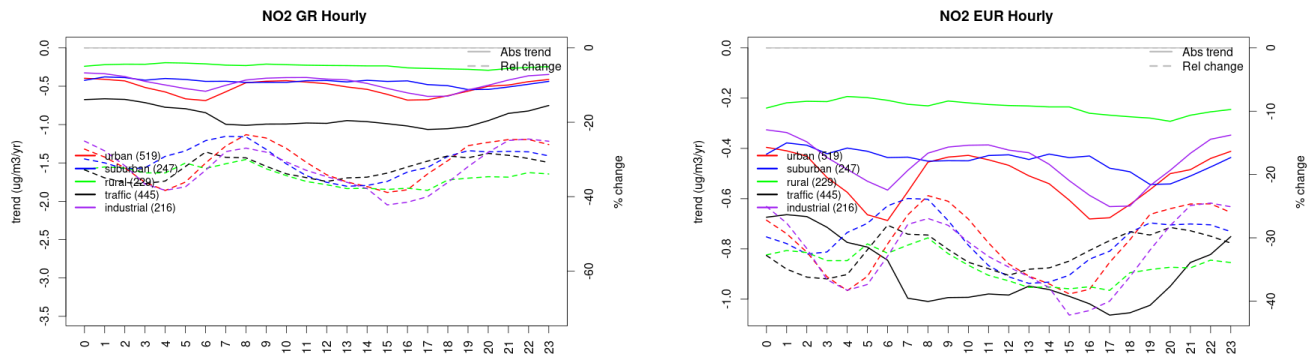


Figure S.275: Absolute (solid lines, left axis) and relative (dashed lines, right axis) trends in the diurnal cycle for Greece (left) and Europe (right) of NO2 at various station type.

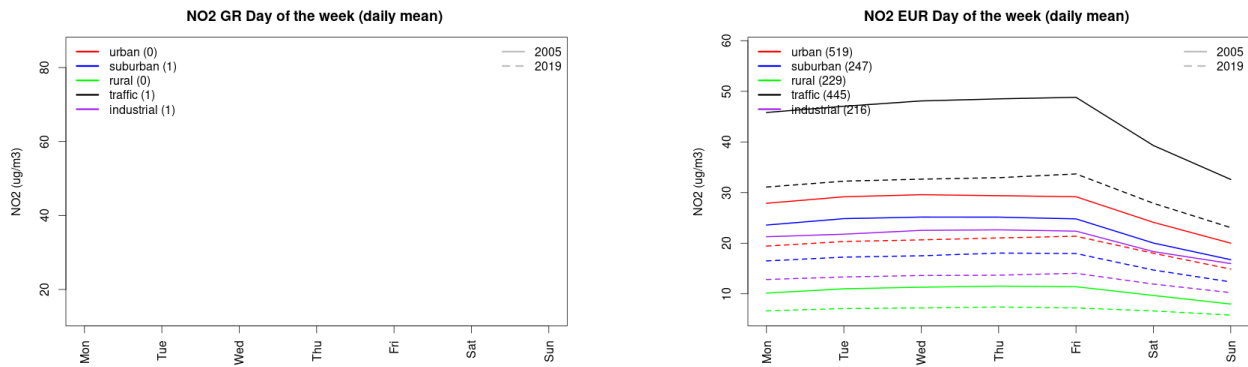


Figure S.276: Weekly cycle of daily mean NO2 for Greece (left) and Europe (right) at various station types estimated from the whole time series in 2005 (solid lines) and 2019

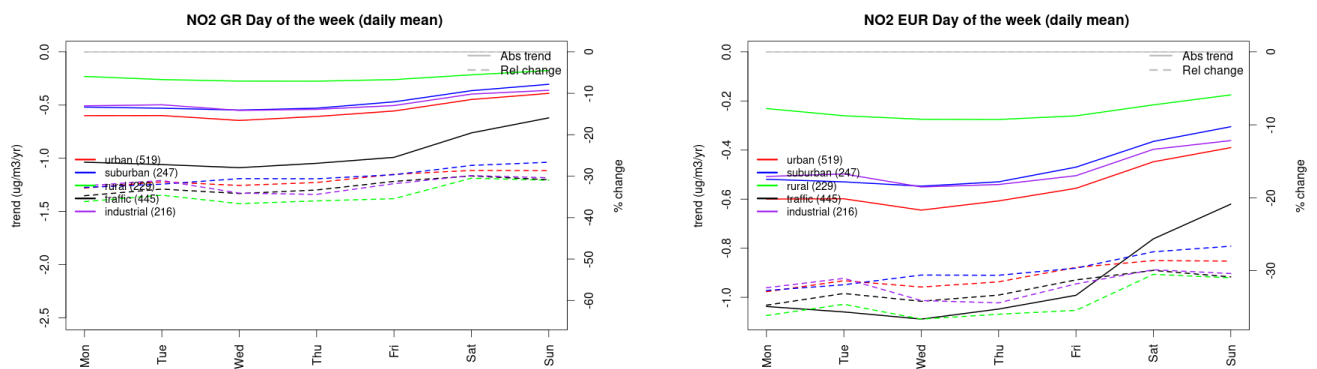


Figure S.277: Absolute (solid lines, left axis) and relative (dashed lines, right axis) trends in the weekly cycle for Greece (left) and Europe (right) of NO₂ at various station type.

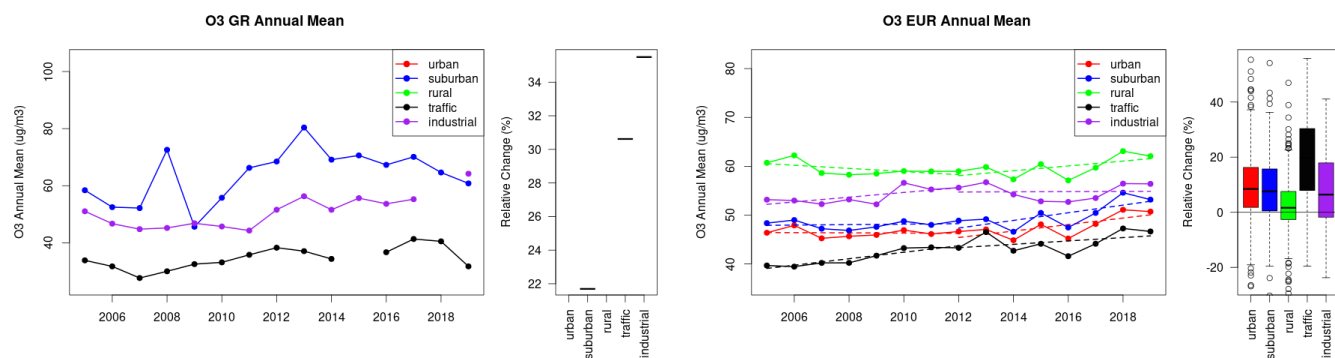


Figure S.278: Time series of the Greece (left) and European-wide composite (median) of annual mean ozone (ug/m³) per station type and area (red: urban background, blue suburban background, green: rural background, black: traffic, violet: industrial) between 2005 and 2019. In the European composite, the dashed lines show the linear fit between 2005 & 2012 and between 2012 & 2019. The boxplots on the right-hand side show the distribution of relative changes (%) between 2005 and 2019 for all stations of each typology in Greece and in Europe.

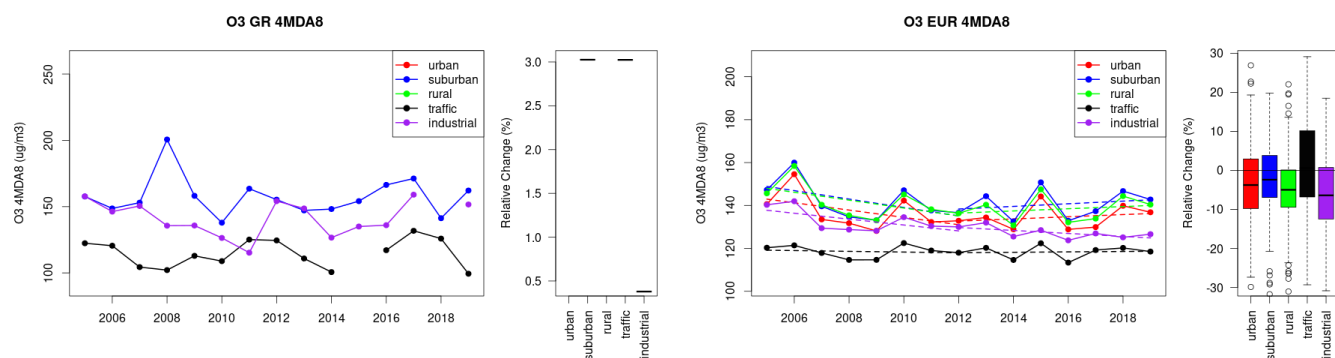


Figure S.279: Time series of the Greece (left) and European-wide composite (median) of O₃ fourth highest daily peak (4MDA8, ug/m³) per station type and area (red: urban background, blue suburban background, green: rural background, black: traffic, violet: industrial) between 2005 and 2019. In the European composite, the dashed lines show the linear fit between 2005 & 2012 and between 2012 & 2019. The boxplots on the right-hand side show the distribution of relative changes (%) between 2005 and 2019 for all stations of each typology in Greece and in Europe.

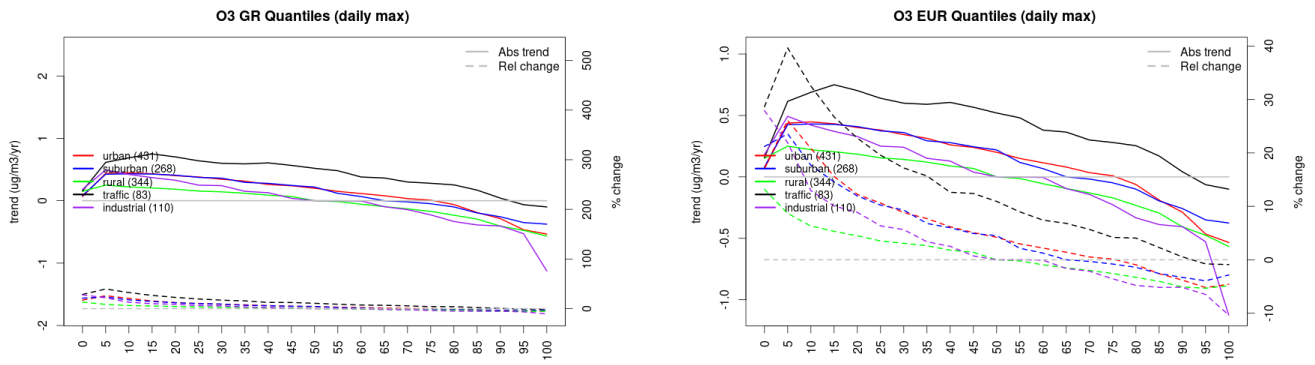


Figure S.280: For ozone in Greece (left) and Europe, and for each typology of station: absolute trend (solid lines, left y-axis) and relative change (dashed lines, right y-axis) of the percentiles of daily maxima.

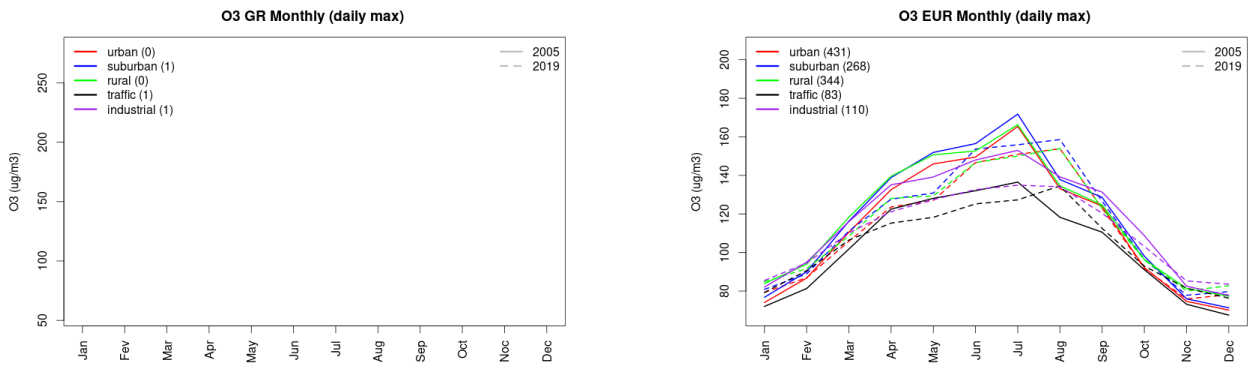


Figure S.281: Monthly cycle of daily max ozone for Greece (left) and Europe (right) at various station types estimated from the whole time series in 2005 (solid lines) and 2019

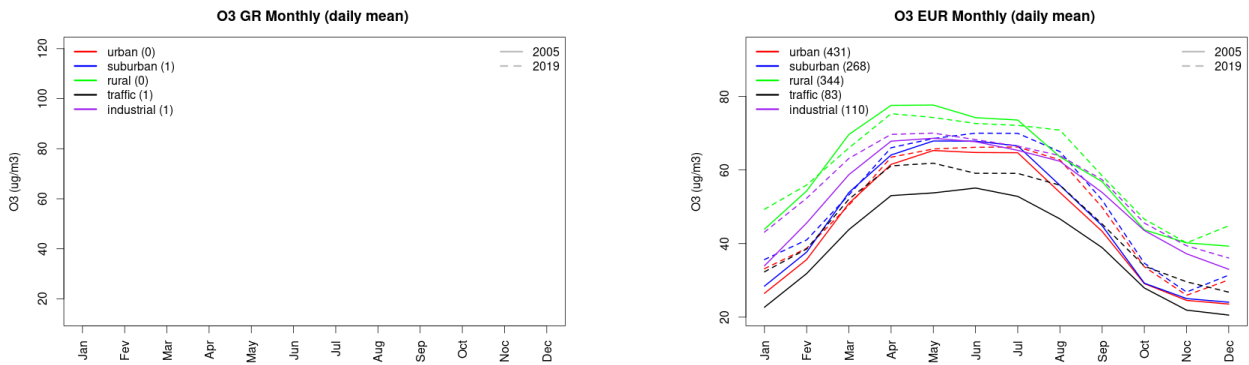


Figure S.282: Monthly cycle of daily mean ozone for Greece (left) and Europe (right) at various station types estimated from the whole time series in 2005 (solid lines) and 2019

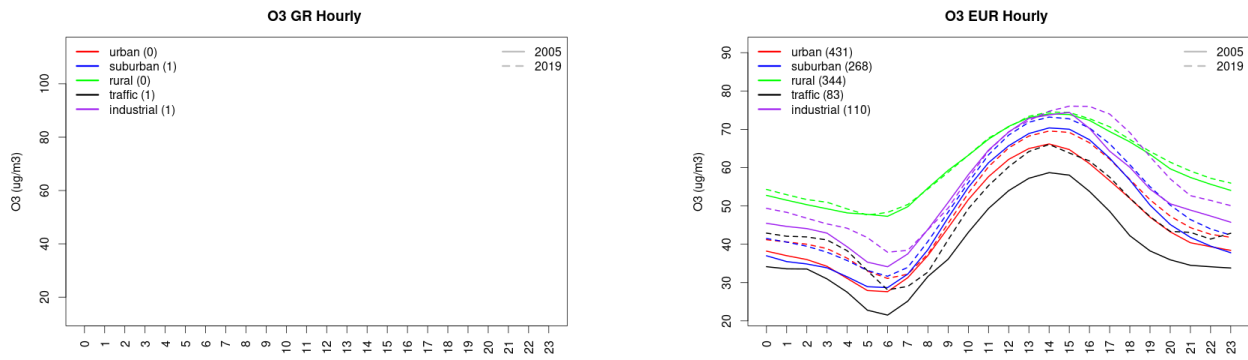


Figure S.283: Diurnal cycle of daily mean ozone for Greece (left) and Europe (right) at various station types estimated from the whole time series in 2005 (solid lines) and 2019

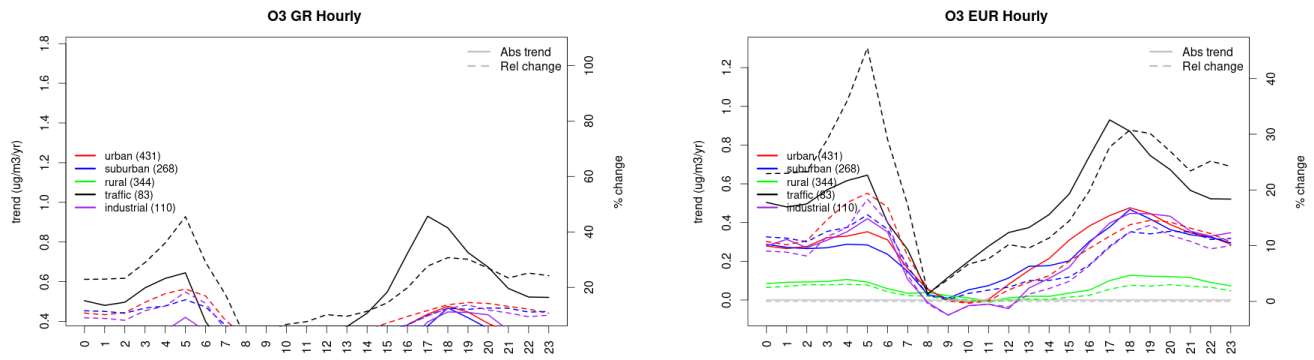


Figure S.284: Absolute (solid lines, left axis) and relative (dashed lines, right axis) trends in the diurnal cycle for Greece (left) and Europe (right) of ozone at various station type.

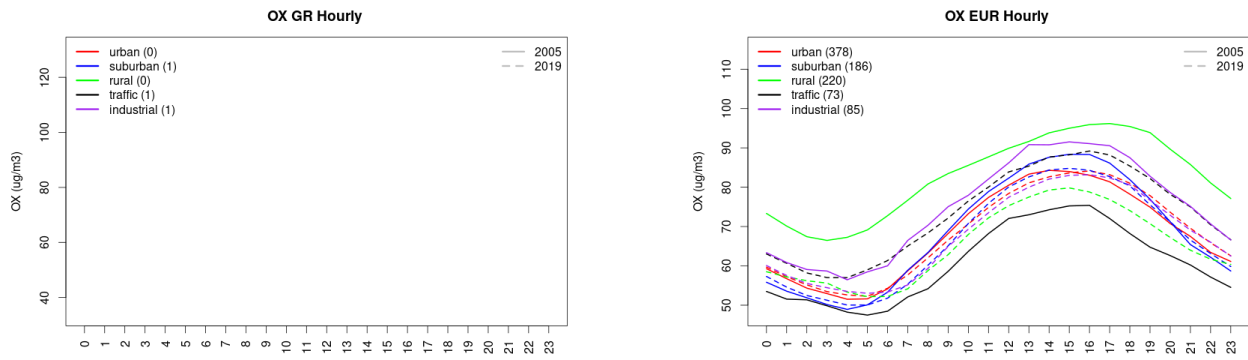


Figure S.285: Diurnal cycle of daily mean OX (as $\text{NO}_2 + \text{O}_3$) for Greece (left) and Europe (right) at various station types estimated from the whole time series in 2005 (solid lines) and 2019

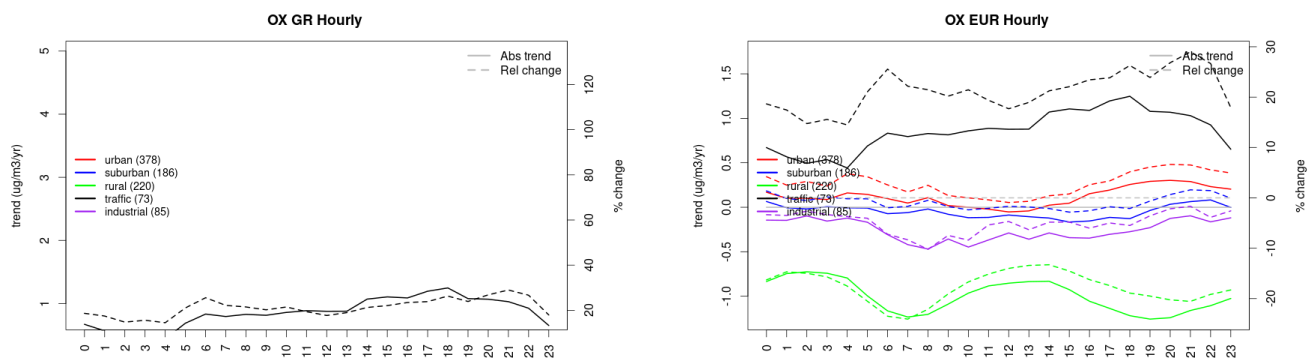


Figure S.286: Absolute (solid lines, left axis) and relative (dashed lines, right axis) trends in the diurnal cycle for Greece (left) and Europe (right) of OX (as NO₂+O₃) at various station type.

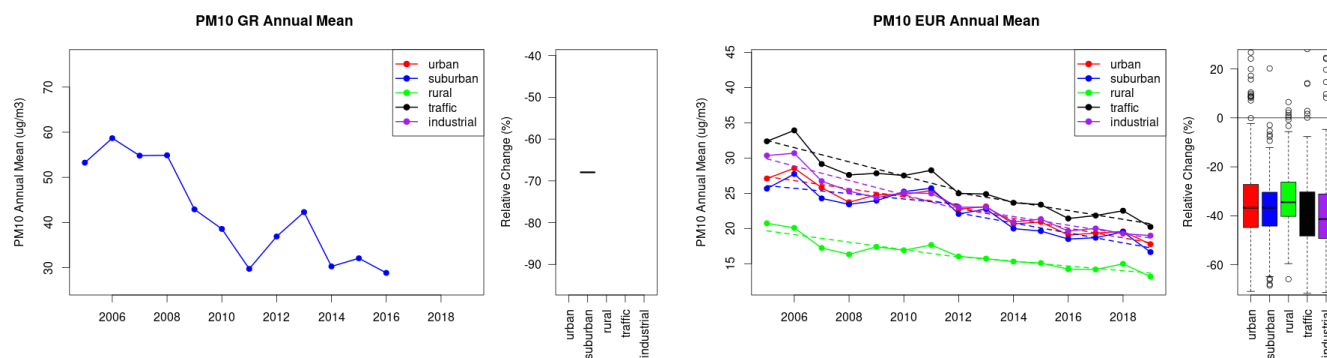


Figure S.287: Time series of the Greece (left) and European-wide composite (median) of annual mean PM₁₀ (ug/m³) per station type and area (red: urban background, blue suburban background, green: rural background, black: traffic, violet: industrial) between 2005 and 2019. In the European composite, the dashed lines show the linear fit between 2005 & 2012 and between 2012 & 2019. The boxplots on the right-hand side show the distribution of relative changes (%) between 2005 and 2019 for all stations of each typology in Greece and in Europe.

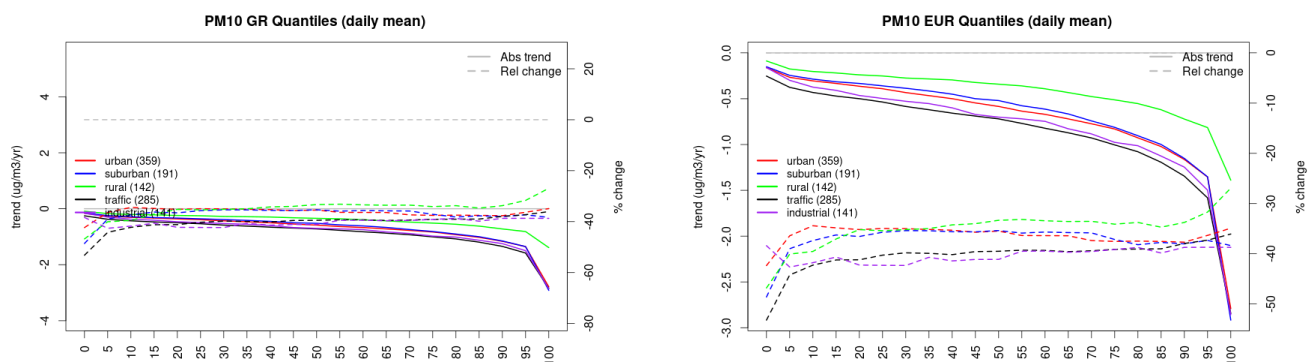


Figure S.288: For PM₁₀ in Greece (left) and Europe, and for each typology of station: absolute trend (solid lines, left y-axis) and relative change (dashed lines, right y-axis) of the percentiles of daily means.

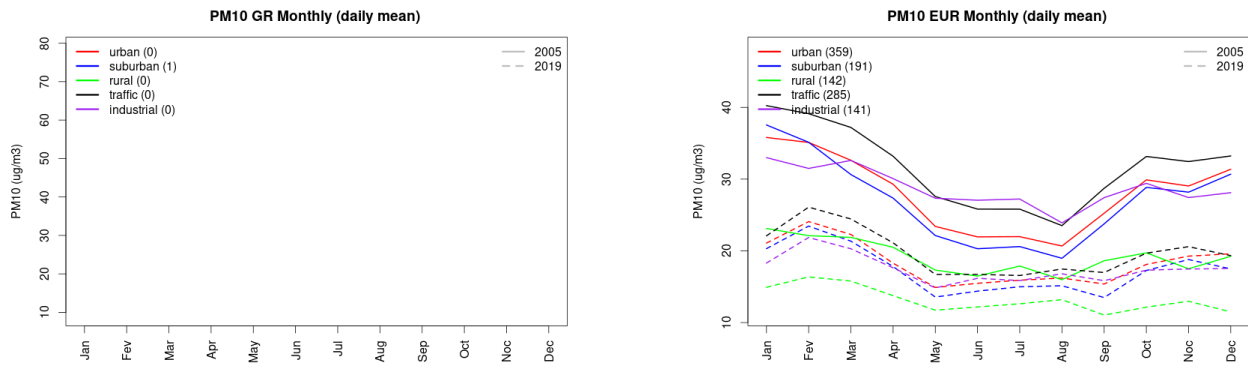


Figure S.289: Monthly cycle of daily mean PM10 for Greece (left) and Europe (right) at various station types estimated from the whole time series in 2005 (solid lines) and 2019

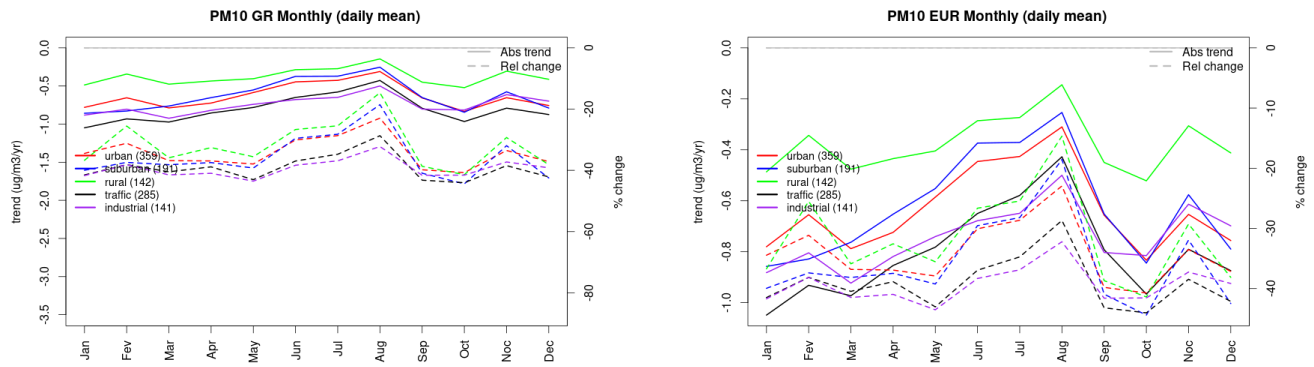


Figure S.290: Absolute (solid lines, left axis) and relative (dashed lines, right axis) trends in the monthly cycle for Greece (left) and Europe (right) of PM10 at various station type.

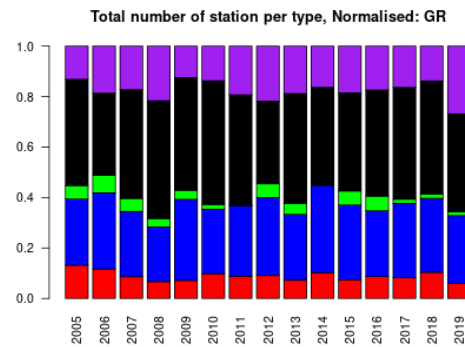
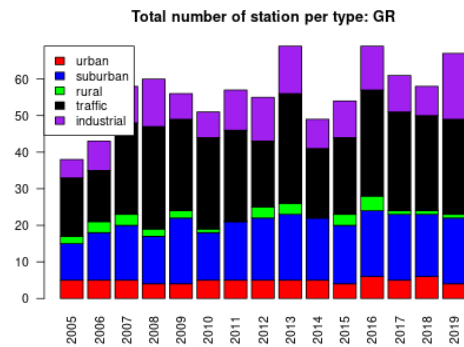
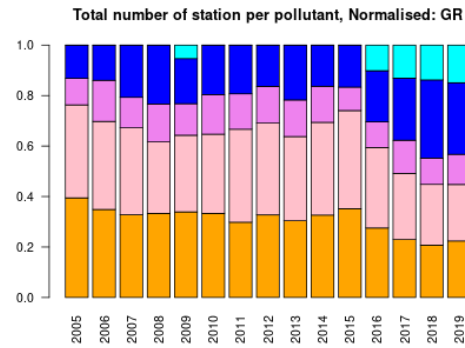
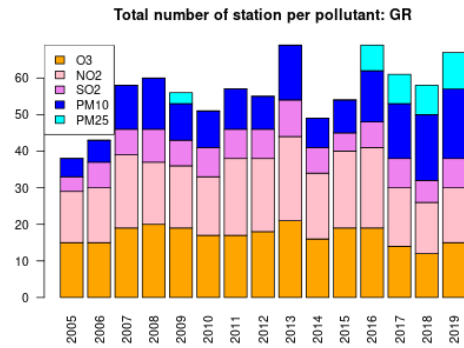
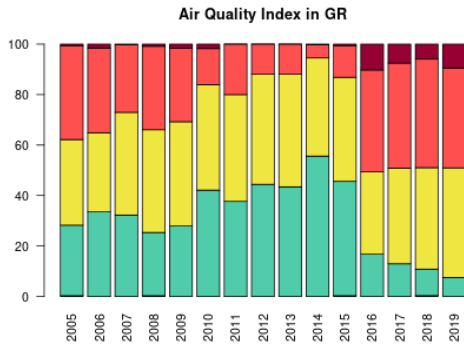


Figure S.291: For Greece: overall air quality index (percentage of days in a given year) and distribution of daily categories per pollutant (light blue: good, light green: fair, yellow: moderate, orange: poor, red: very poor, violet: extremely poor).

14 Croatia

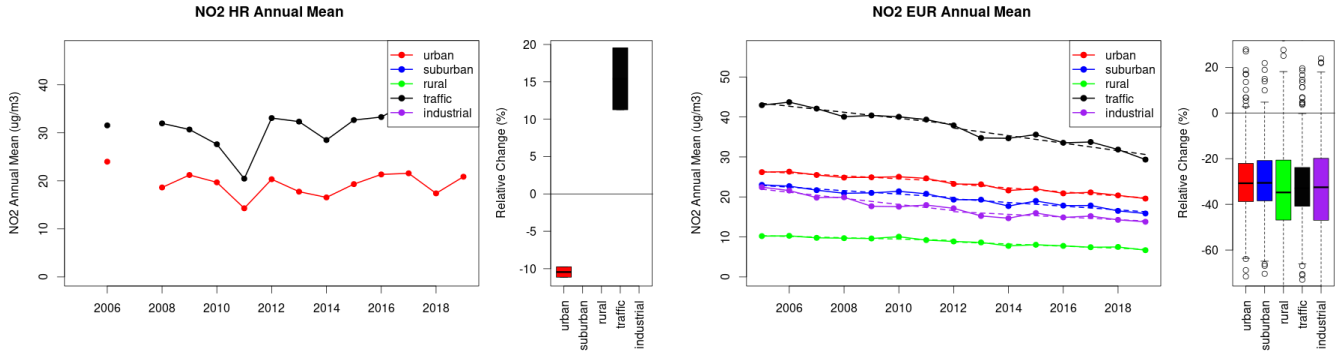


Figure S.292: Time series of the Croatia (left) and European-wide composite (median) of annual mean NO₂ (ug/m³) per station type and area (red: urban background, blue suburban background, green: rural background, black: traffic, violet: industrial) between 2005 and 2019. In the European composite, the dashed lines show the linear fit between 2005 & 2012 and between 2012 & 2019. The boxplots on the right-hand side show the distribution of relative changes (%) between 2005 and 2019 for all stations of each typology in Croatia and in Europe.

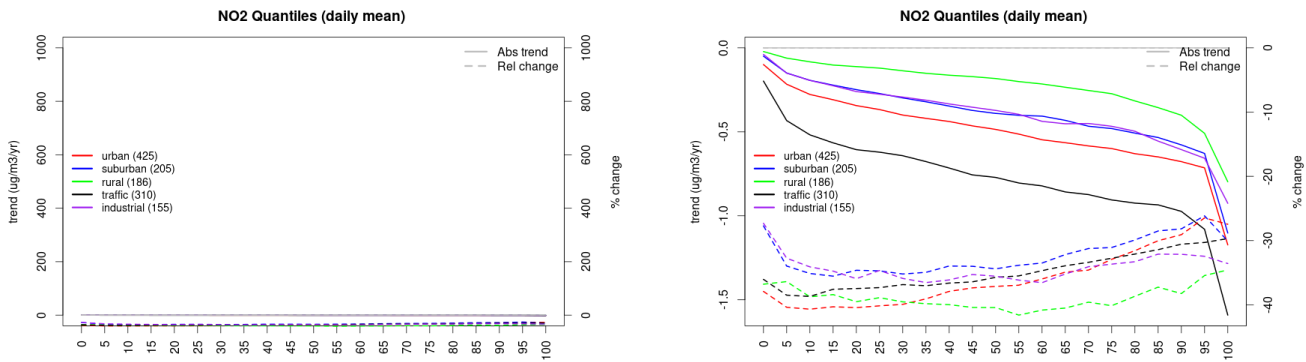


Figure S.293: For NO₂ in Croatia (left) and Europe, and for each typology of station: absolute trend (solid lines, left y-axis) and relative change (dashed lines, right y-axis) of the percentiles of daily means.

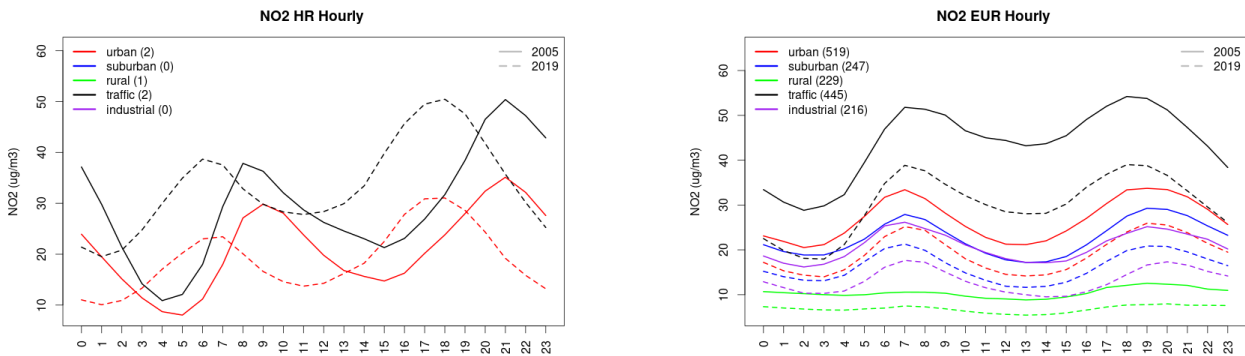


Figure S.294: Diurnal cycle of daily mean NO₂ for Croatia (left) and Europe (right) at various station types estimated from the whole time series in 2005 (solid lines) and 2019

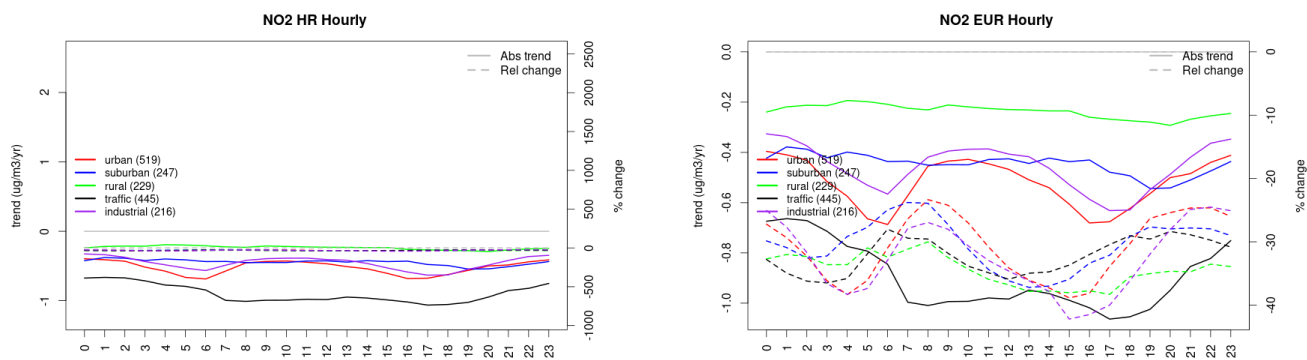


Figure S.295: Absolute (solid lines, left axis) and relative (dashed lines, right axis) trends in the diurnal cycle for Croatia (left) and Europe (right) of NO2 at various station type.

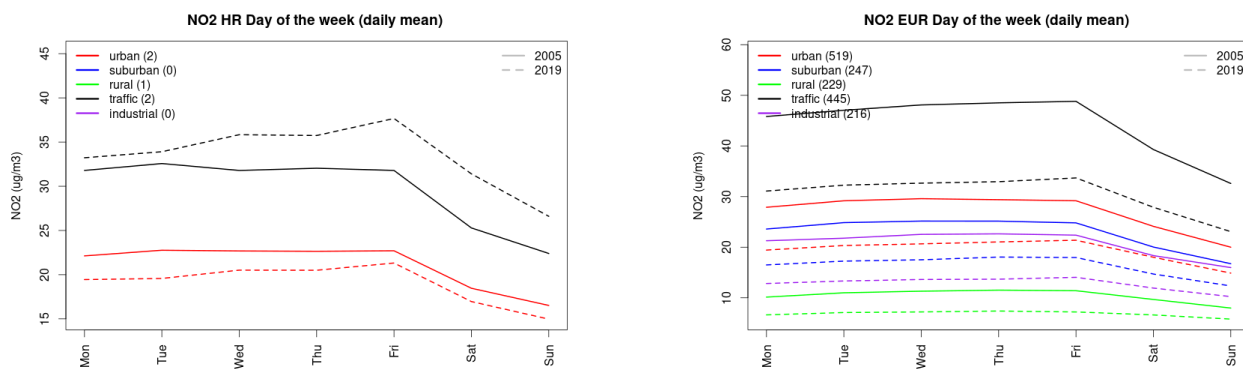


Figure S.296: Weekly cycle of daily mean NO2 for Croatia (left) and Europe (right) at various station types estimated from the whole time series in 2005 (solid lines) and 2019

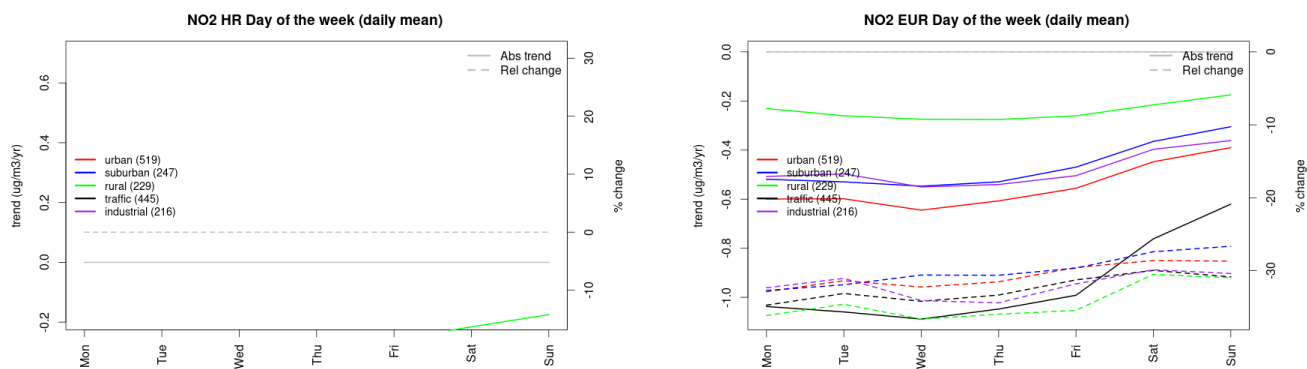


Figure S.297: Absolute (solid lines, left axis) and relative (dashed lines, right axis) trends in the weekly cycle for Croatia (left) and Europe (right) of NO2 at various station type.

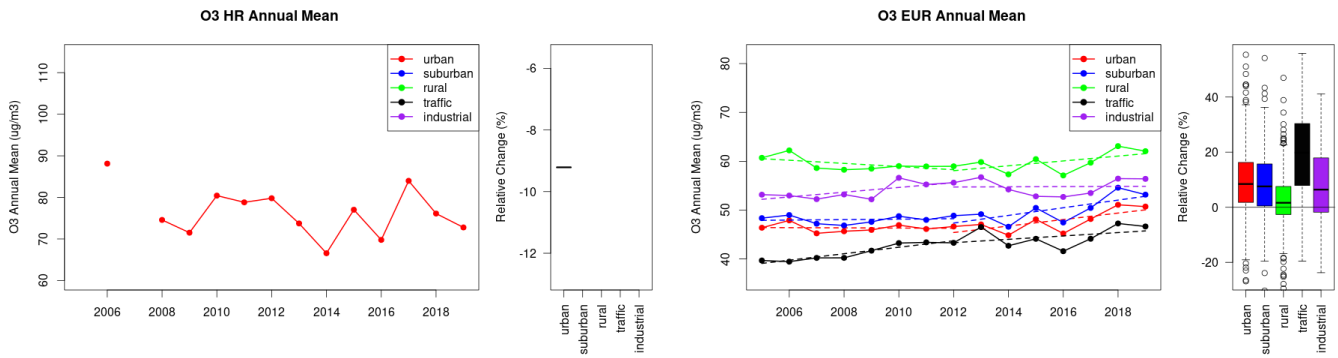


Figure S.298: Time series of the Croatia (left) and European-wide composite (median) of annual mean ozone ($\mu\text{g}/\text{m}^3$) per station type and area (red: urban background, blue suburban background, green: rural background, black: traffic, violet: industrial) between 2005 and 2019. In the European composite, the dashed lines show the linear fit between 2005 & 2012 and between 2012 & 2019. The boxplots on the right-hand side show the distribution of relative changes (%) between 2005 and 2019 for all stations of each typology in Croatia and in Europe.

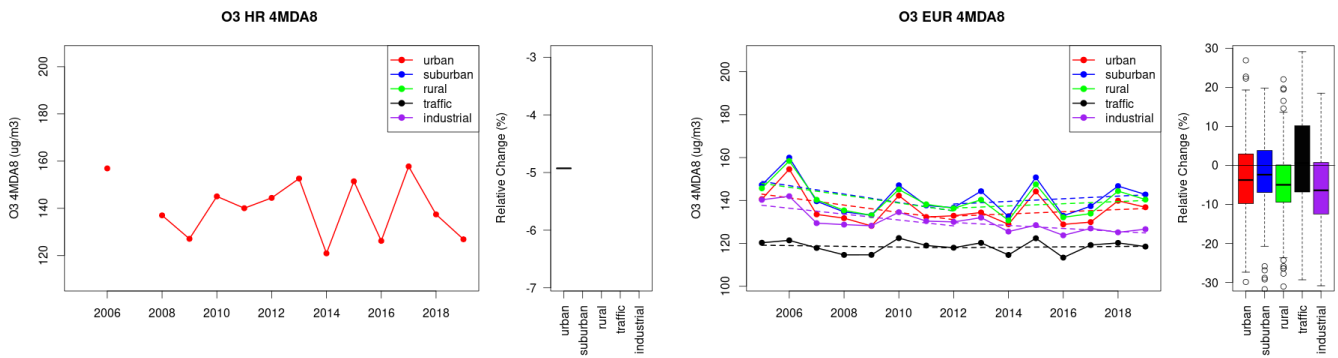


Figure S.299: Time series of the Croatia (left) and European-wide composite (median) of O3 fourth highest daily peak (4MDA8, $\mu\text{g}/\text{m}^3$) per station type and area (red: urban background, blue suburban background, green: rural background, black: traffic, violet: industrial) between 2005 and 2019. In the European composite, the dashed lines show the linear fit between 2005 & 2012 and between 2012 & 2019. The boxplots on the right-hand side show the distribution of relative changes (%) between 2005 and 2019 for all stations of each typology in Croatia and in Europe.

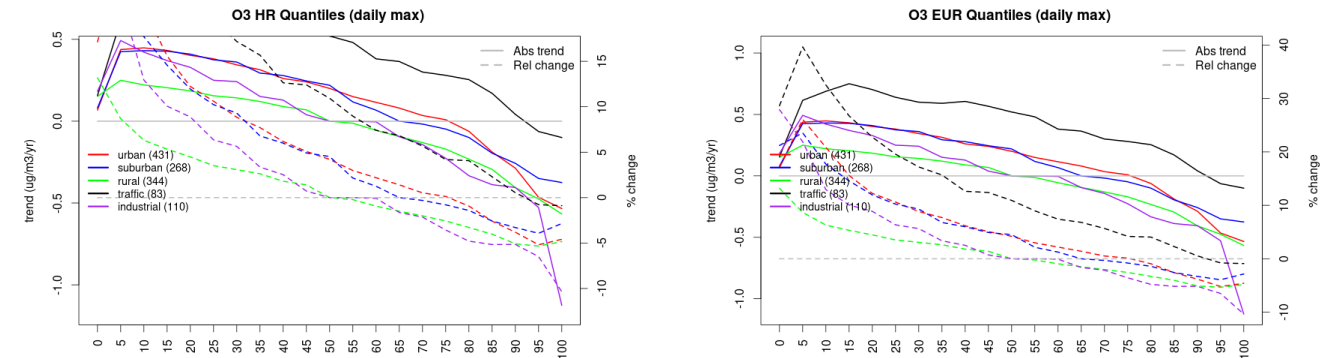


Figure S.300: For ozone in Croatia (left) and Europe, and for each typology of station: absolute trend (solid lines, left y-axis) and relative change (dashed lines, right y-axis) of the percentiles of daily maxima.

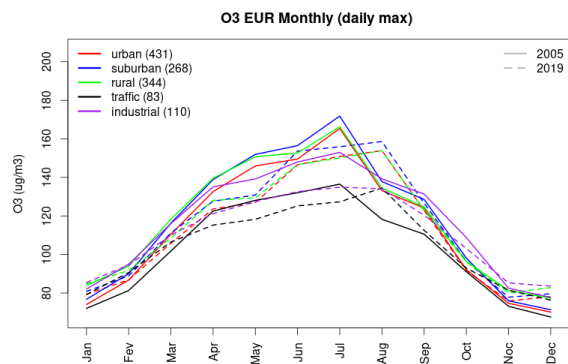
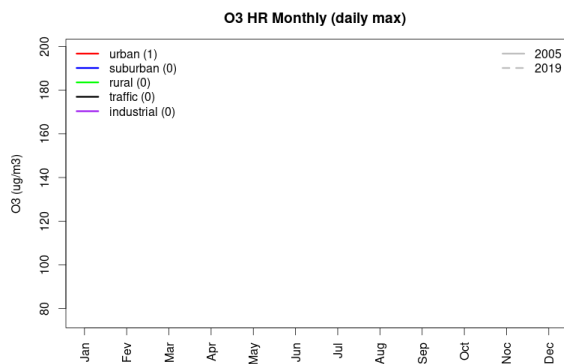


Figure S.301: Monthly cycle of daily max ozone for Croatia (left) and Europe (right) at various station types estimated from the whole time series in 2005 (solid lines) and 2019

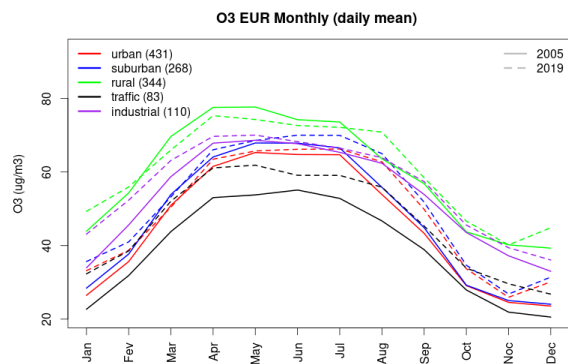
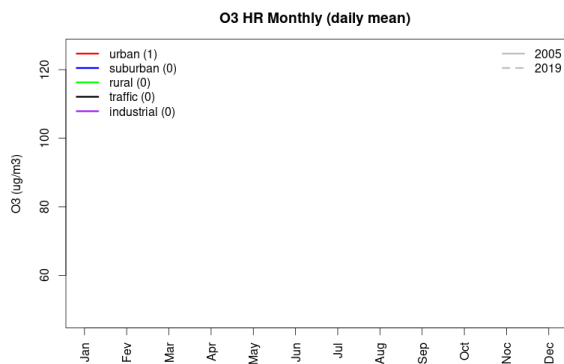


Figure S.302: Monthly cycle of daily mean ozone for Croatia (left) and Europe (right) at various station types estimated from the whole time series in 2005 (solid lines) and 2019

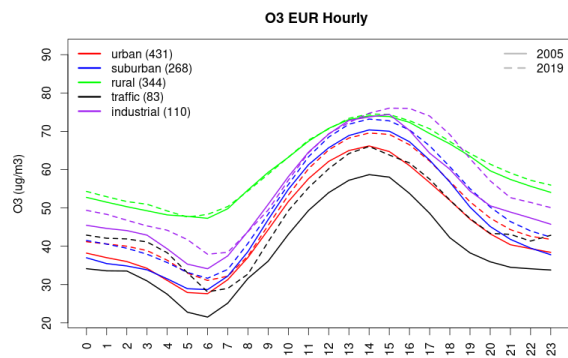
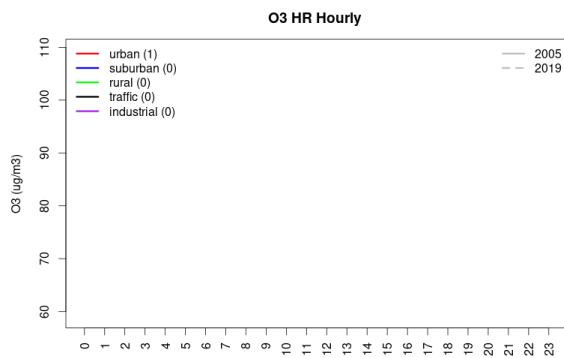


Figure S.303: Diurnal cycle of daily mean ozone for Croatia (left) and Europe (right) at various station types estimated from the whole time series in 2005 (solid lines) and 2019

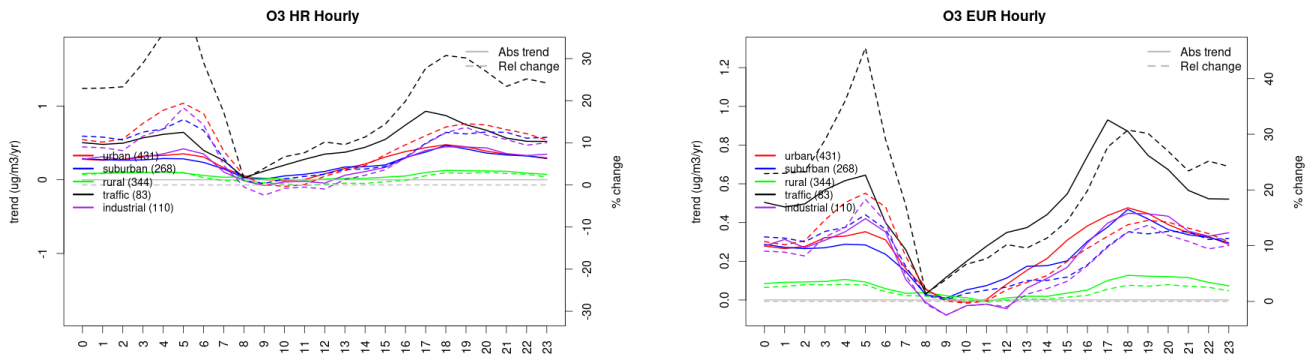


Figure S.304: Absolute (solid lines, left axis) and relative (dashed lines, right axis) trends in the diurnal cycle for Croatia (left) and Europe (right) of ozone at various station type.

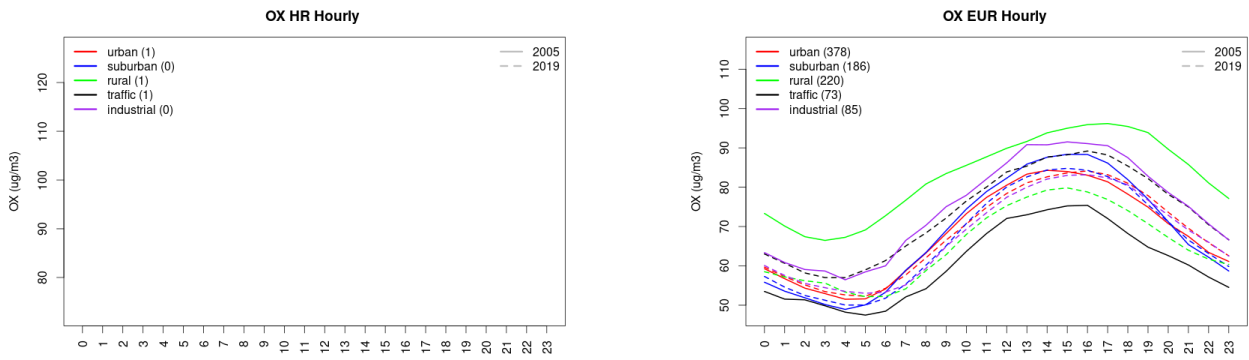


Figure S.305: Diurnal cycle of daily mean OX (as NO₂+O₃) for Croatia (left) and Europe (right) at various station types estimated from the whole time series in 2005 (solid lines) and 2019

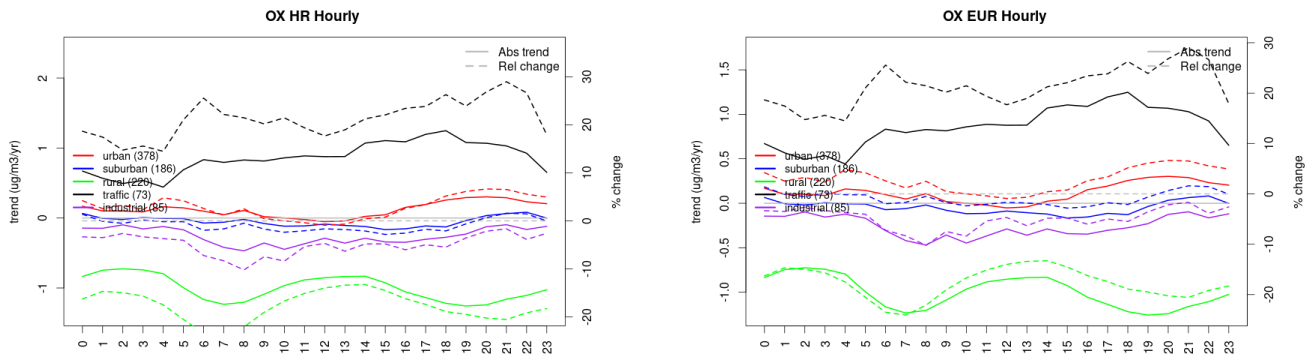


Figure S.306: Absolute (solid lines, left axis) and relative (dashed lines, right axis) trends in the diurnal cycle for Croatia (left) and Europe (right) of OX (as NO₂+O₃) at various station type.

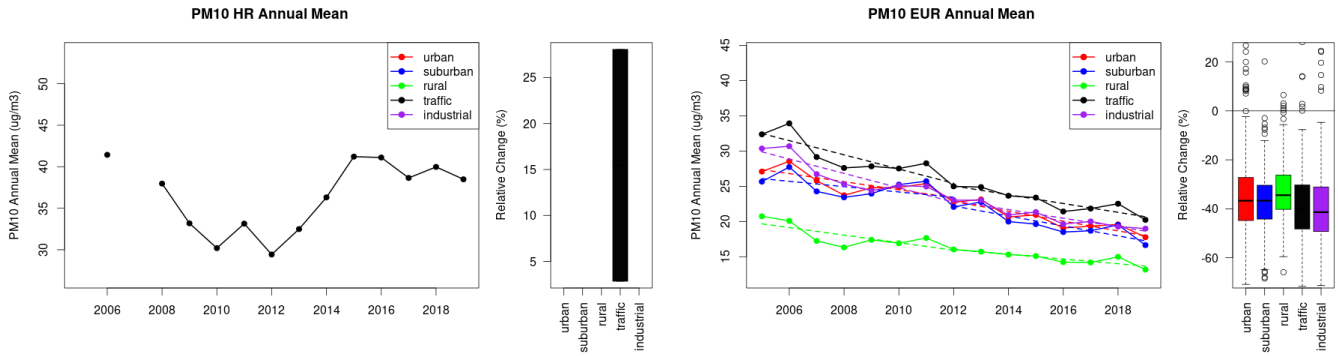


Figure S.307: Time series of the Croatia (left) and European-wide composite (median) of annual mean PM10 ($\mu\text{g}/\text{m}^3$) per station type and area (red: urban background, blue suburban background, green: rural background, black: traffic, violet: industrial) between 2005 and 2019. In the European composite, the dashed lines show the linear fit between 2005 & 2012 and between 2012 & 2019. The boxplots on the right-hand side show the distribution of relative changes (%) between 2005 and 2019 for all stations of each typology in Croatia and in Europe.

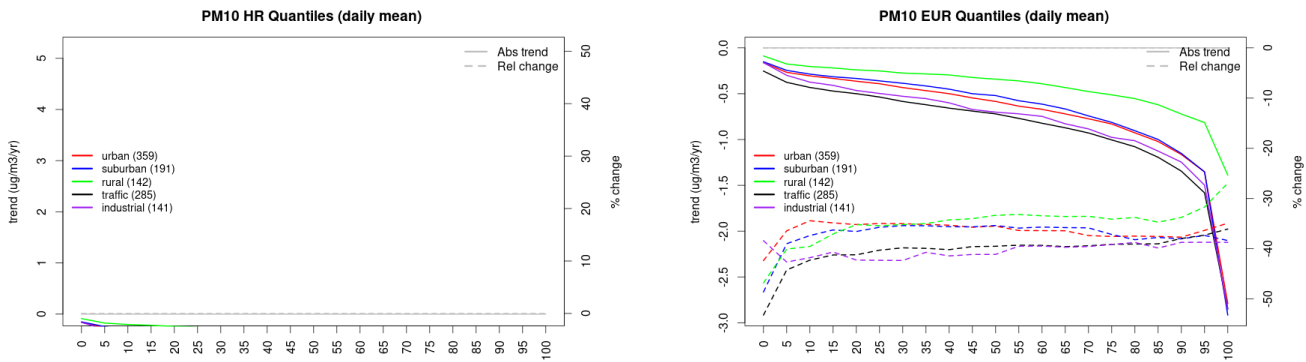


Figure S.308: For PM10 in Croatia (left) and Europe, and for each typology of station: absolute trend (solid lines, left y-axis) and relative change (dashed lines, right y-axis) of the percentiles of daily means.

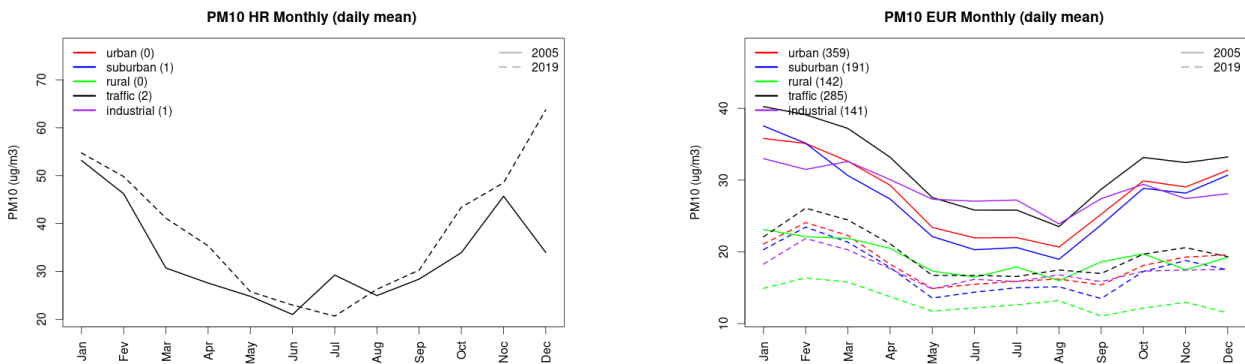


Figure S.309: Monthly cycle of daily mean PM10 for Croatia (left) and Europe (right) at various station types estimated from the whole time series in 2005 (solid lines) and 2019

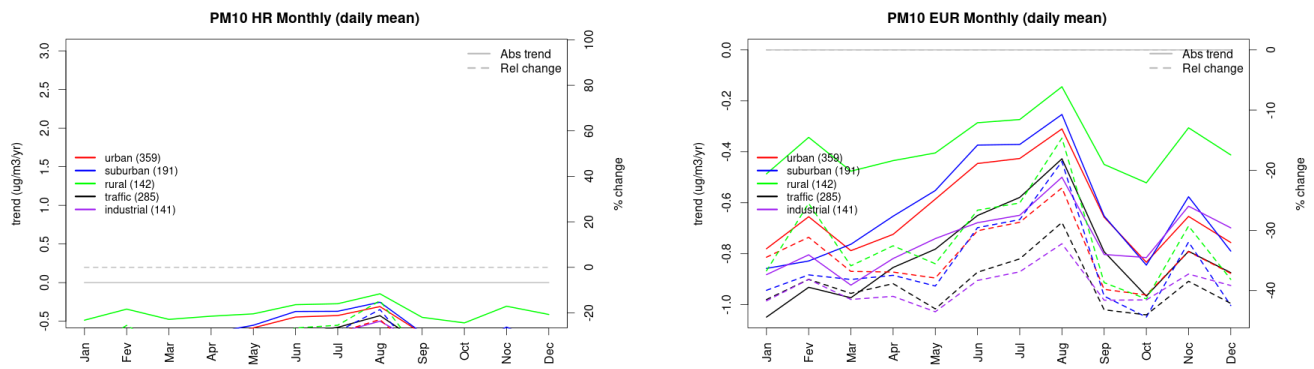


Figure S.310: Absolute (solid lines, left axis) and relative (dashed lines, right axis) trends in the monthly cycle for Croatia (left) and Europe (right) of PM10 at various station type.

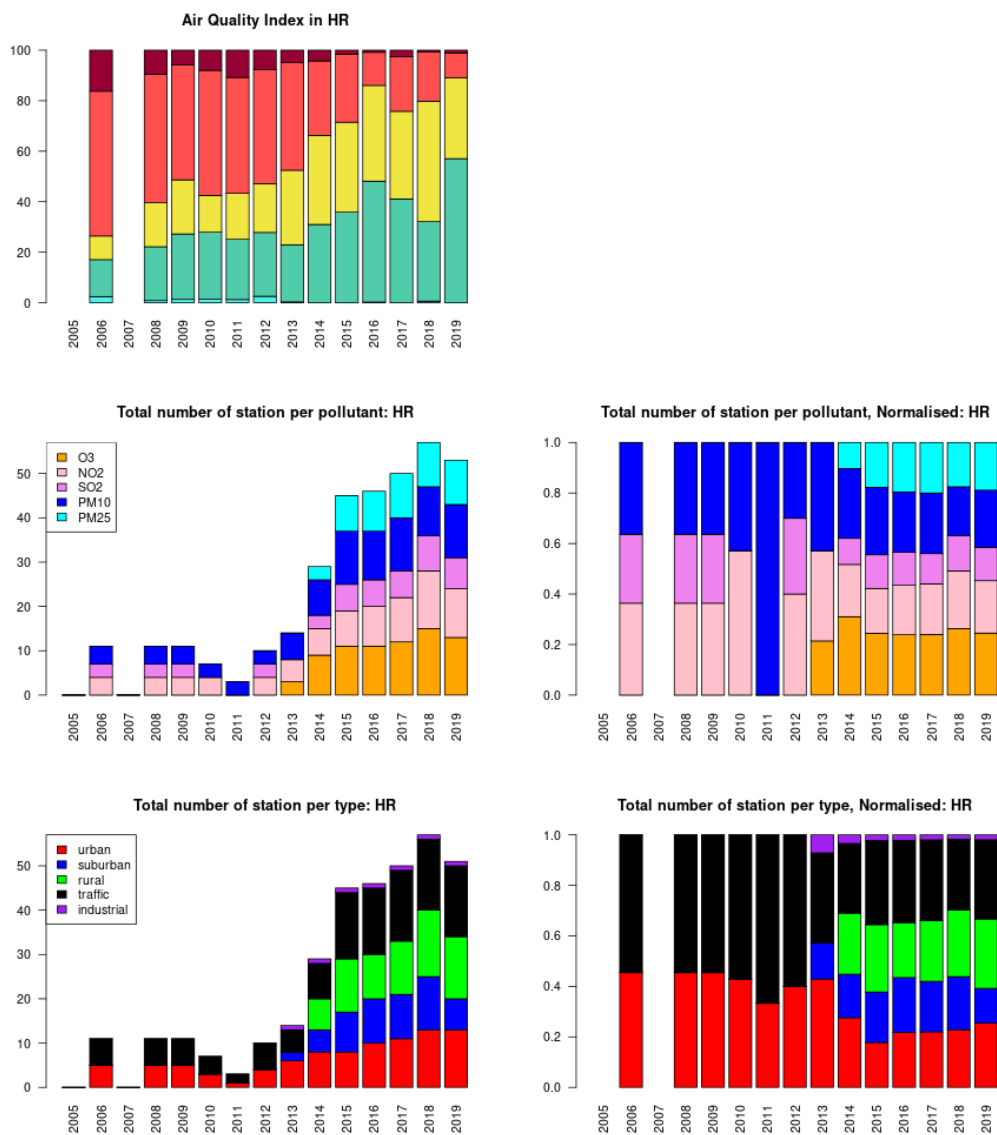


Figure S.311: For Croatia: overall air quality index (percentage of days in a given year) and distribution of daily categories per pollutant (light blue: good, light green: fair, yellow: moderate, orange: poor, red: very poor, violet: extremely poor).

15 Hungary

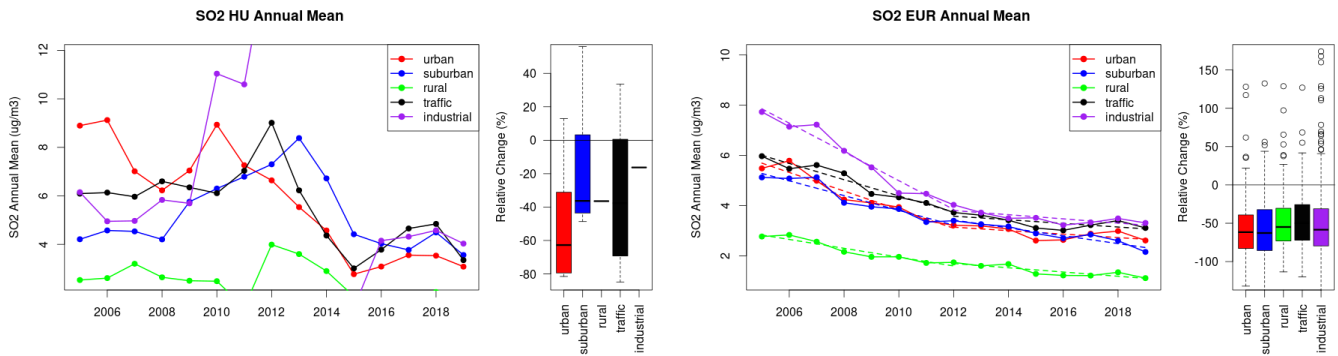


Figure S.312: Time series of the Hungary (left) and European-wide composite (median) of annual mean SO₂ (ug/m³) per station type and area (red: urban background, blue suburban background, green: rural background, black: traffic, violet: industrial) between 2005 and 2019. In the European composite, the dashed lines show the linear fit between 2005 & 2012 and between 2012 & 2019. The boxplots on the right-hand side show the distribution of relative changes (%) between 2005 and 2019 for all stations of each typology in Hungary and in Europe.

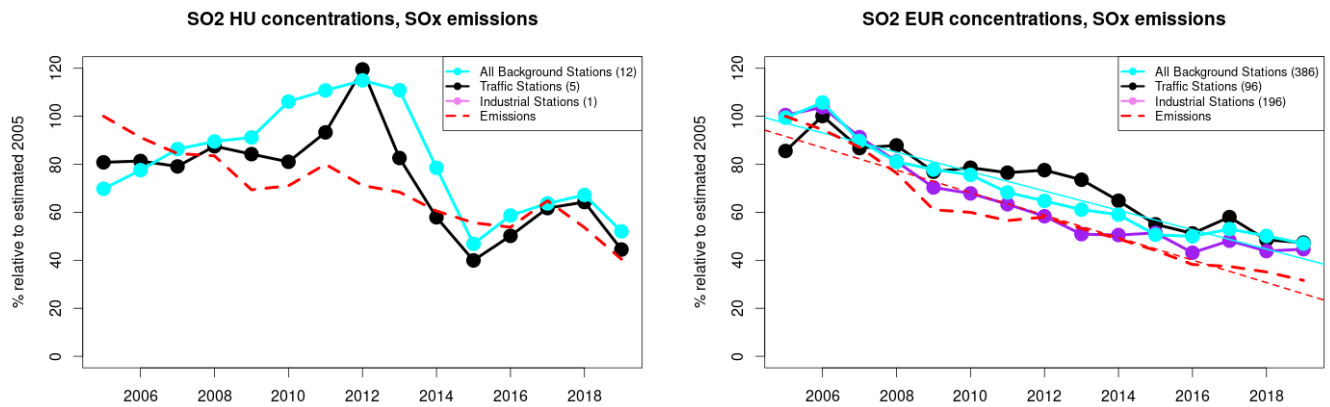


Figure S.313: Time series of 2005-2019 (left) and European (right) median SO₂ observed at traffic (black), industrial (violet) and background (cyan) sites (solid lines), and corresponding SO_x emissions (dashed line) normalised to estimated 2000 levels (%). The median is taken over where more than 5 stations of each typology is available. The total number of stations included is provided in brackets. In the European composite, straight lines are the linear fits over the whole period.

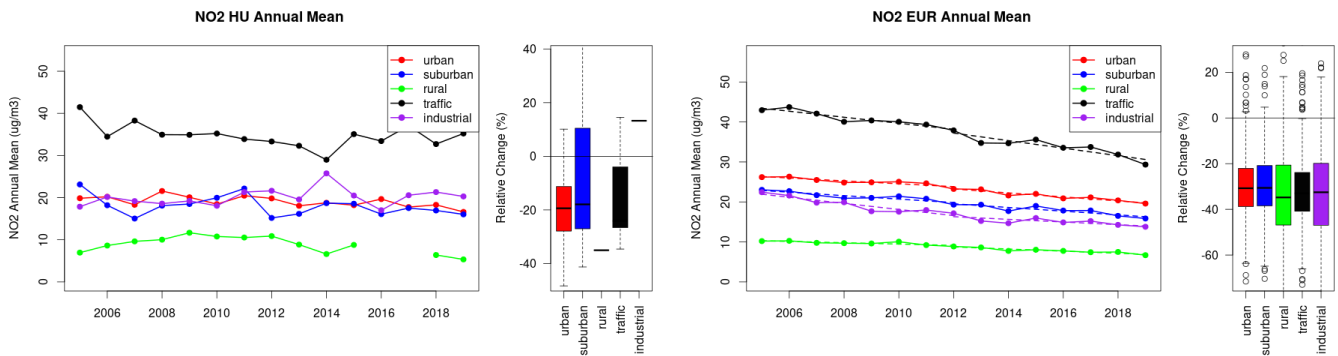


Figure S.314: Time series of the Hungary (left) and European-wide composite (median) of annual mean NO₂ (ug/m³) per station type and area (red: urban background, blue suburban background, green: rural background, black: traffic, violet: industrial) between 2005 and 2019. In the European composite, the dashed lines show the linear fit between 2005 & 2012 and between 2012 & 2019. The boxplots on the right-hand side show the distribution of relative changes (%) between 2005 and 2019 for all stations of each typology in Hungary and in Europe.

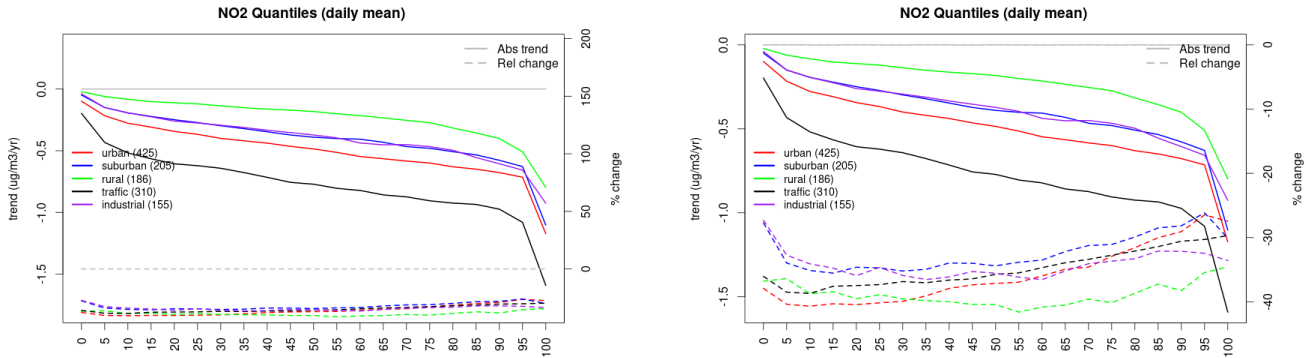


Figure S.315: For NO₂ in Hungary (left) and Europe, and for each typology of station: absolute trend (solid lines, left y-axis) and relative change (dashed lines, right y-axis) of the percentiles of daily means.

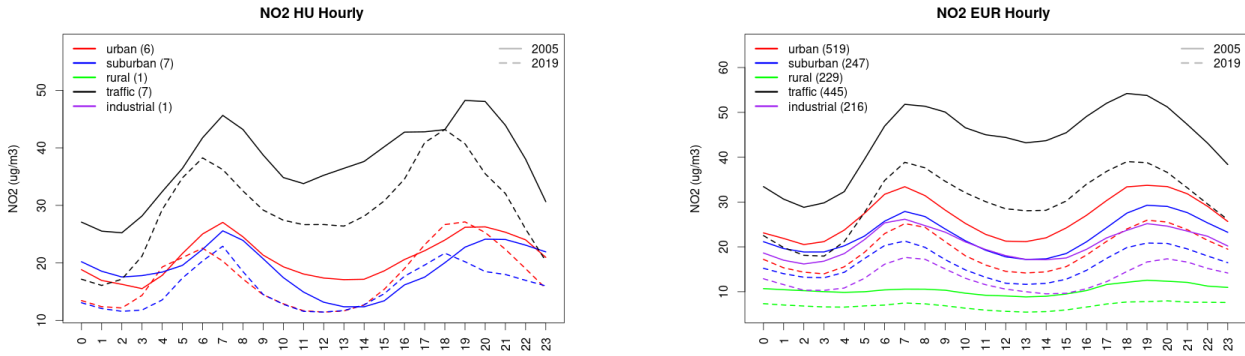


Figure S.316: Diurnal cycle of daily mean NO₂ for Hungary (left) and Europe (right) at various station types estimated from the whole time series in 2005 (solid lines) and 2019

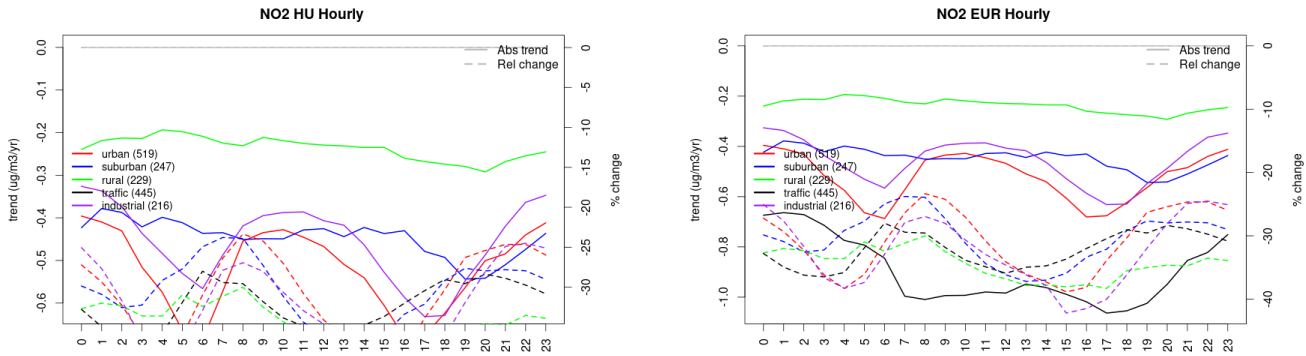


Figure S.317: Absolute (solid lines, left axis) and relative (dashed lines, right axis) trends in the diurnal cycle for Hungary (left) and Europe (right) of NO₂ at various station type.

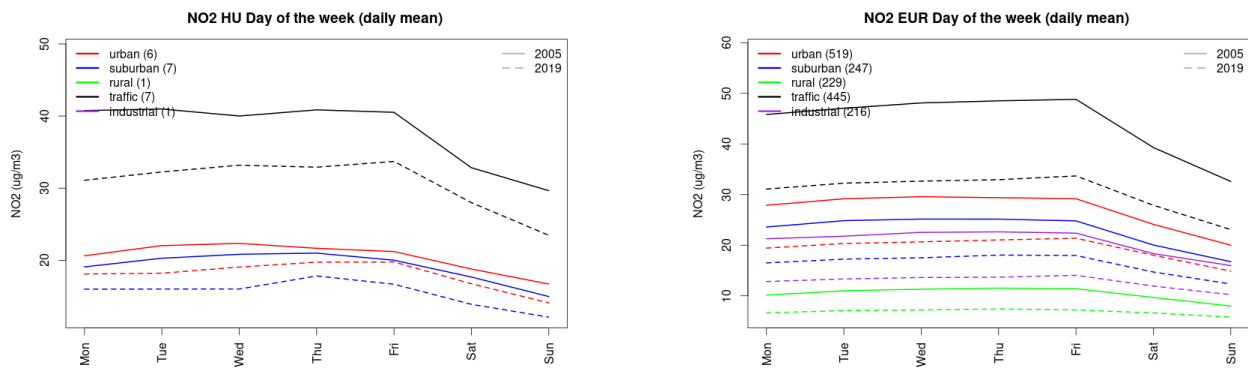


Figure S.318: Weekly cycle of daily mean NO2 for Hungary (left) and Europe (right) at various station types estimated from the whole time series in 2005 (solid lines) and 2019

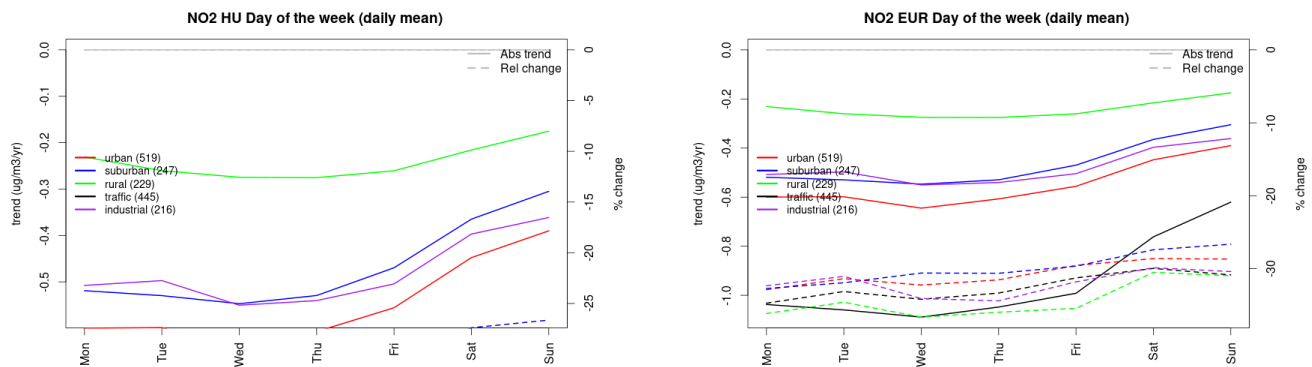


Figure S.319: Absolute (solid lines, left axis) and relative (dashed lines, right axis) trends in the weekly cycle for Hungary (left) and Europe (right) of NO2 at various station type.

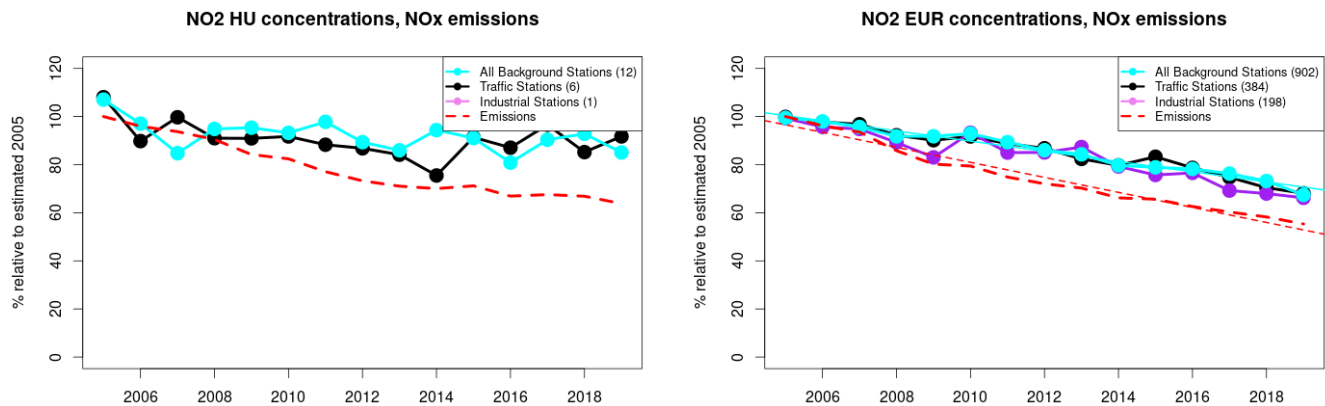


Figure S.320: Time series of 2005-2019 (left) and European (right) median NO2 observed at traffic (black), industrial (violet) and background (cyan) sites (solid lines), and corresponding NOx emissions (dashed line) normalised to estimated 2000 levels (%). The median is taken over where more than 5 stations of each typology is available. The total number of stations included is provided in brackets. In the European composite, straight lines are the linear fits over the whole period.

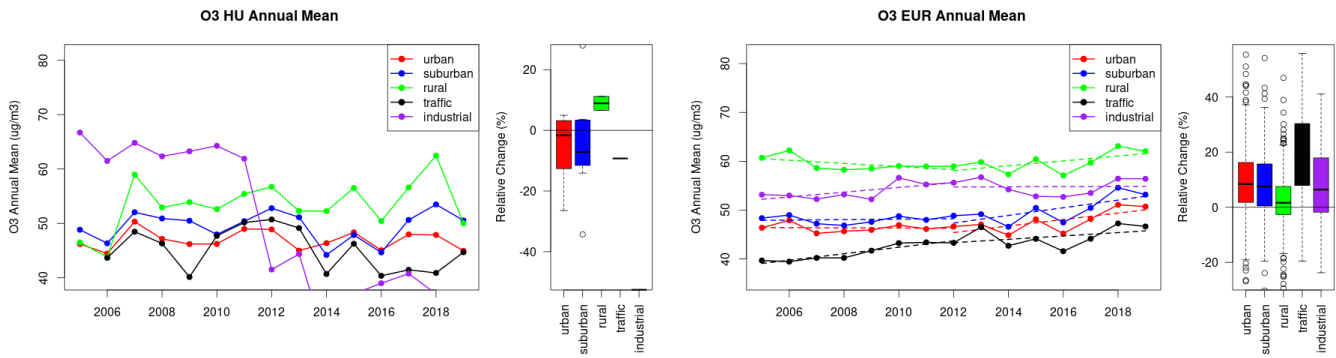


Figure S.321: Time series of the Hungary (left) and European-wide composite (median) of annual mean ozone ($\mu\text{g}/\text{m}^3$) per station type and area (red: urban background, blue suburban background, green: rural background, black: traffic, violet: industrial) between 2005 and 2019. In the European composite, the dashed lines show the linear fit between 2005 & 2012 and between 2012 & 2019. The boxplots on the right-hand side show the distribution of relative changes (%) between 2005 and 2019 for all stations of each typology in Hungary and in Europe.

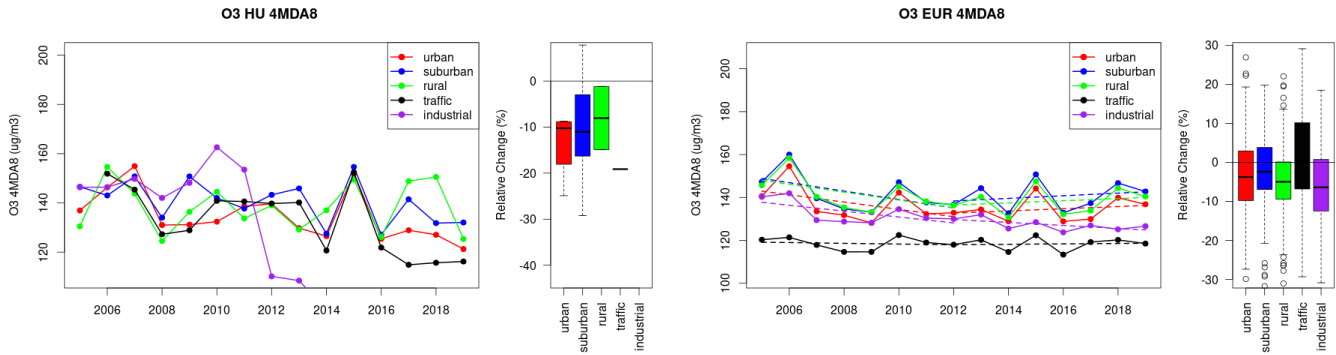


Figure S.322: Time series of the Hungary (left) and European-wide composite (median) of O3 fourth highest daily peak (4MDA8, $\mu\text{g}/\text{m}^3$) per station type and area (red: urban background, blue suburban background, green: rural background, black: traffic, violet: industrial) between 2005 and 2019. In the European composite, the dashed lines show the linear fit between 2005 & 2012 and between 2012 & 2019. The boxplots on the right-hand side show the distribution of relative changes (%) between 2005 and 2019 for all stations of each typology in Hungary and in Europe.

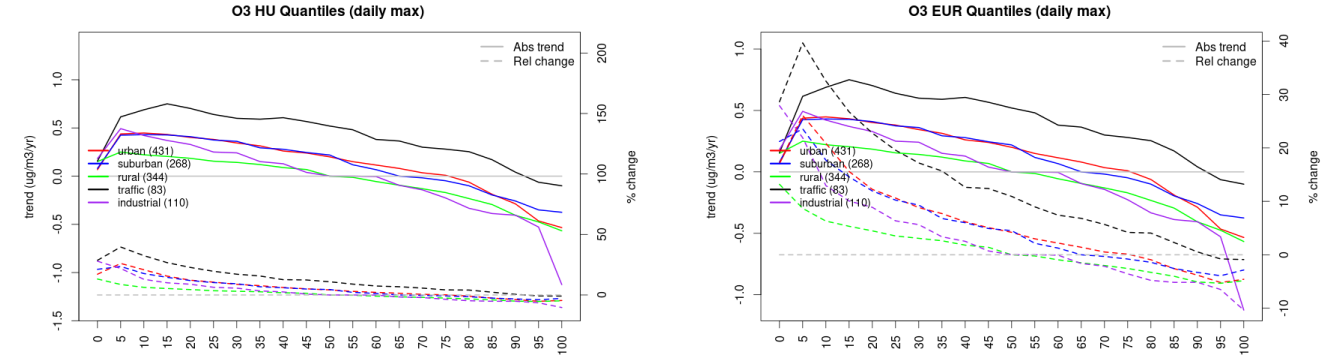


Figure S.323: For ozone in Hungary (left) and Europe, and for each typology of station: absolute trend (solid lines, left y-axis) and relative change (dashed lines, right y-axis) of the percentiles of daily maxima.

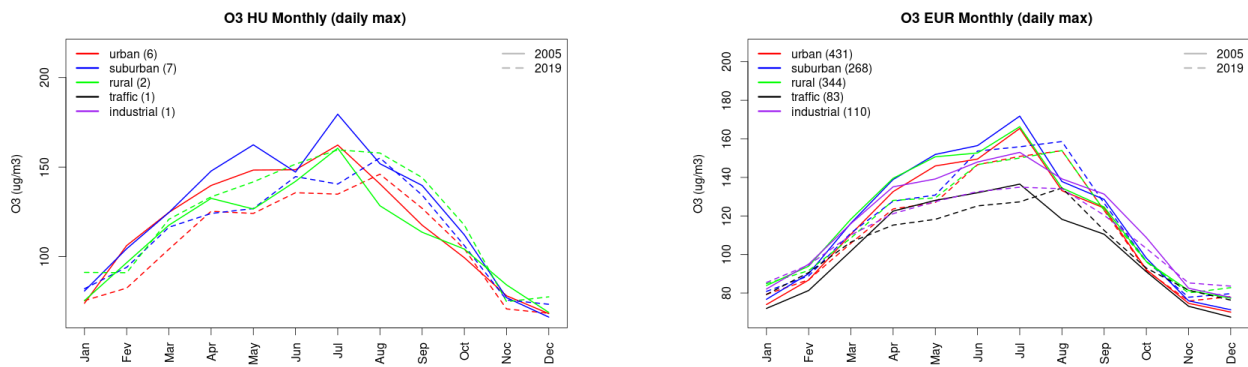


Figure S.324: Monthly cycle of daily max ozone for Hungary (left) and Europe (right) at various station types estimated from the whole time series in 2005 (solid lines) and 2019

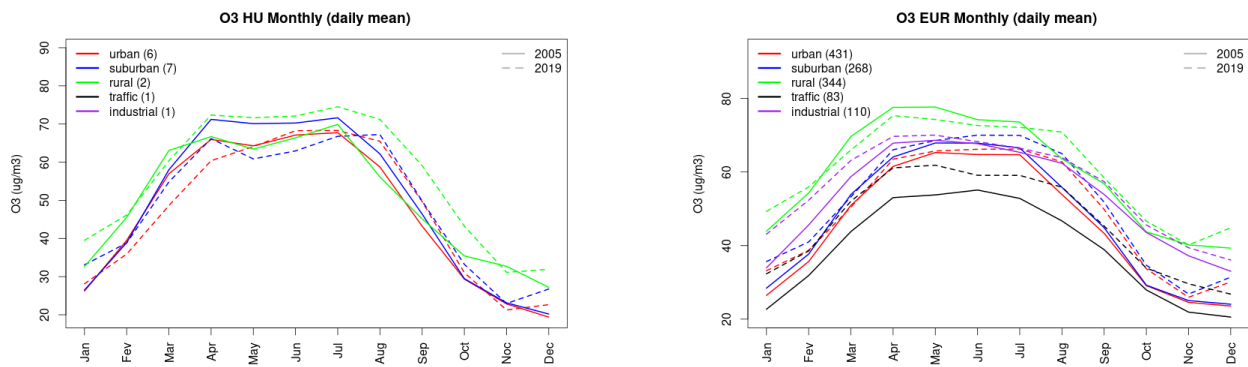


Figure S.325: Monthly cycle of daily mean ozone for Hungary (left) and Europe (right) at various station types estimated from the whole time series in 2005 (solid lines) and 2019

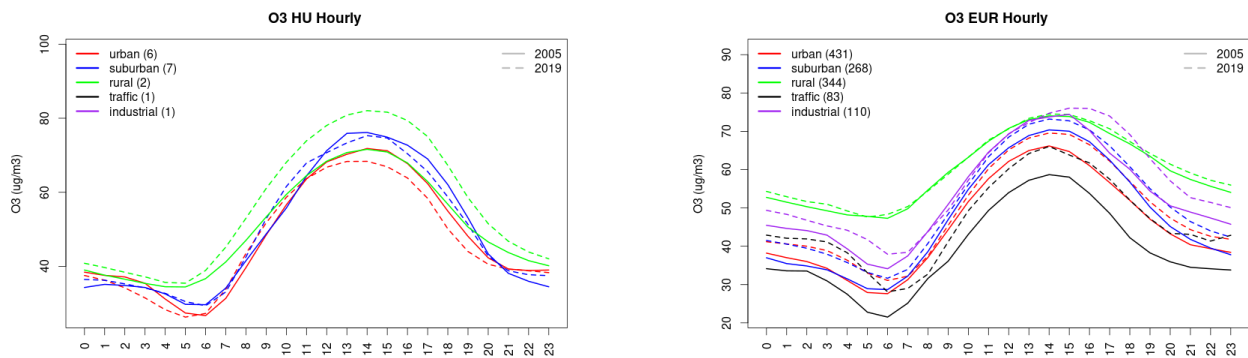


Figure S.326: Diurnal cycle of daily mean ozone for Hungary (left) and Europe (right) at various station types estimated from the whole time series in 2005 (solid lines) and 2019

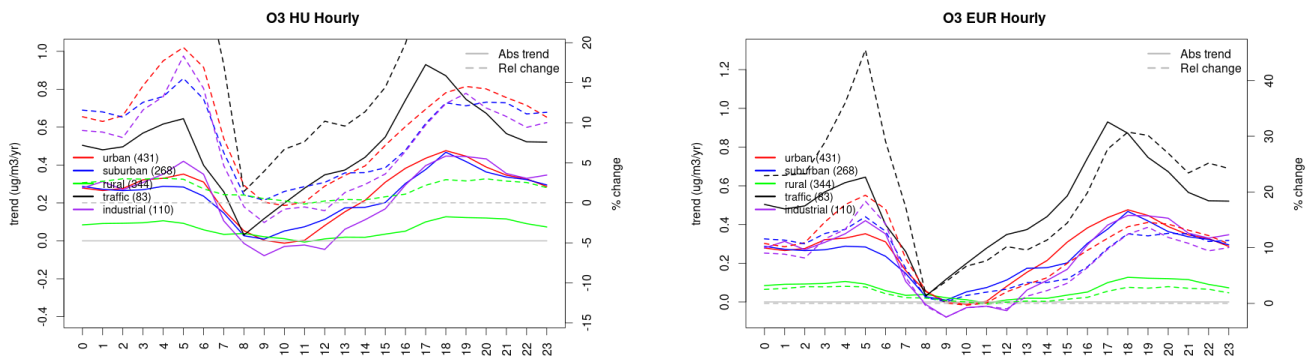


Figure S.327: Absolute (solid lines, left axis) and relative (dashed lines, right axis) trends in the diurnal cycle for Hungary (left) and Europe (right) of ozone at various station type.

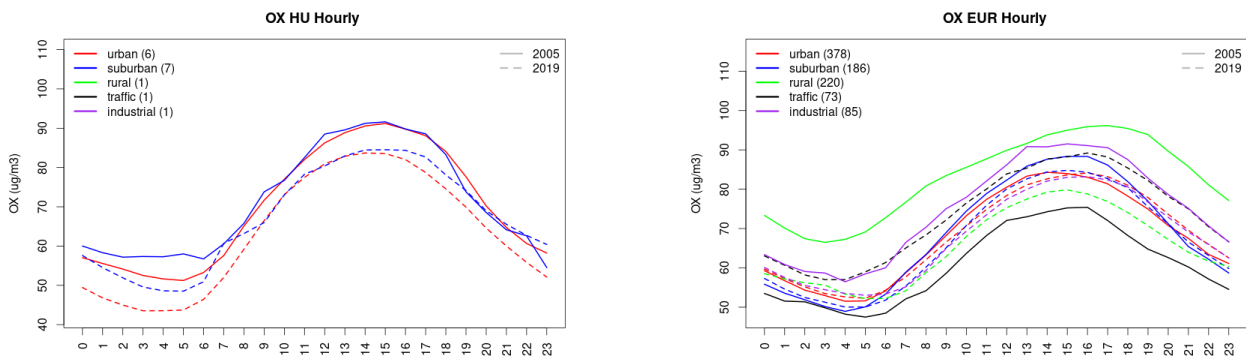


Figure S.328: Diurnal cycle of daily mean OX (as NO₂+O₃) for Hungary (left) and Europe (right) at various station types estimated from the whole time series in 2005 (solid lines) and 2019

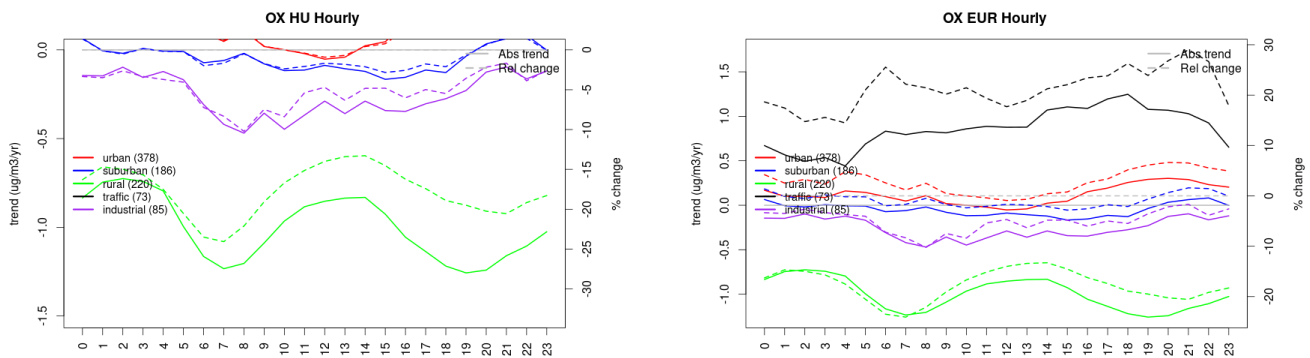


Figure S.329: Absolute (solid lines, left axis) and relative (dashed lines, right axis) trends in the diurnal cycle for Hungary (left) and Europe (right) of OX (as NO₂+O₃) at various station type.

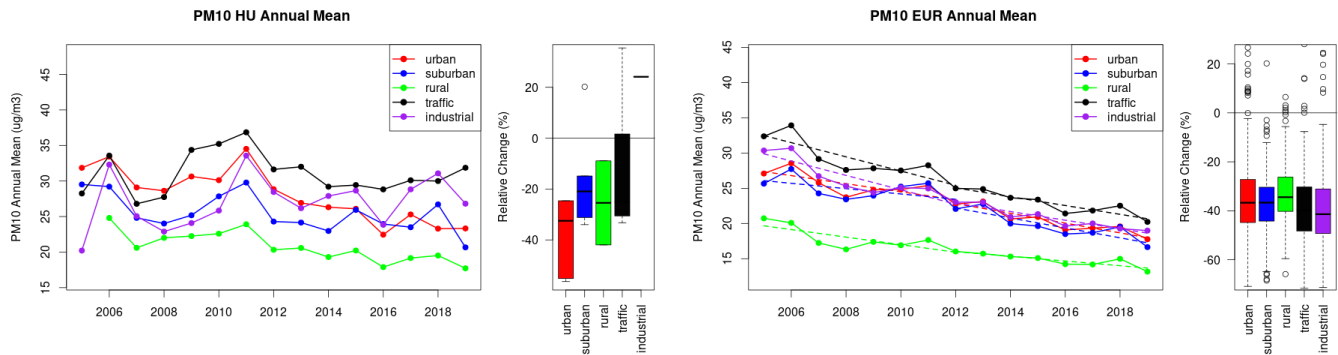


Figure S.330: Time series of the Hungary (left) and European-wide composite (median) of annual mean PM10 ($\mu\text{g}/\text{m}^3$) per station type and area (red: urban background, blue suburban background, green: rural background, black: traffic, violet: industrial) between 2005 and 2019. In the European composite, the dashed lines show the linear fit between 2005 & 2012 and between 2012 & 2019. The boxplots on the right-hand side show the distribution of relative changes (%) between 2005 and 2019 for all stations of each typology in Hungary and in Europe.

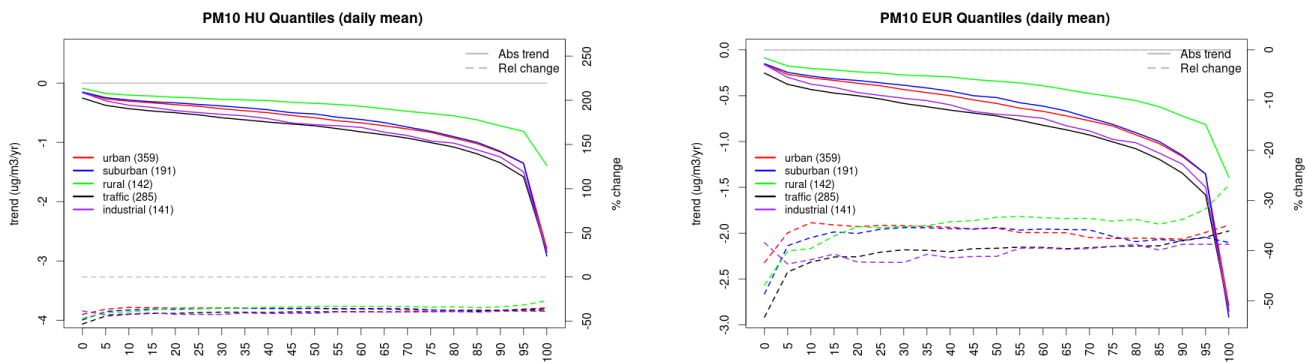


Figure S.331: For PM10 in Hungary (left) and Europe, and for each typology of station: absolute trend (solid lines, left y-axis) and relative change (dashed lines, right y-axis) of the percentiles of daily means.

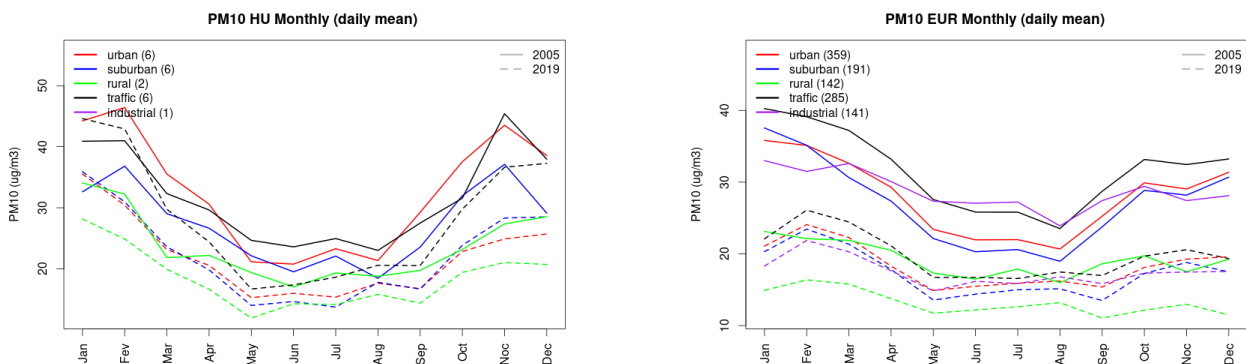


Figure S.332: Monthly cycle of daily mean PM10 for Hungary (left) and Europe (right) at various station types estimated from the whole time series in 2005 (solid lines) and 2019 (dashed lines)

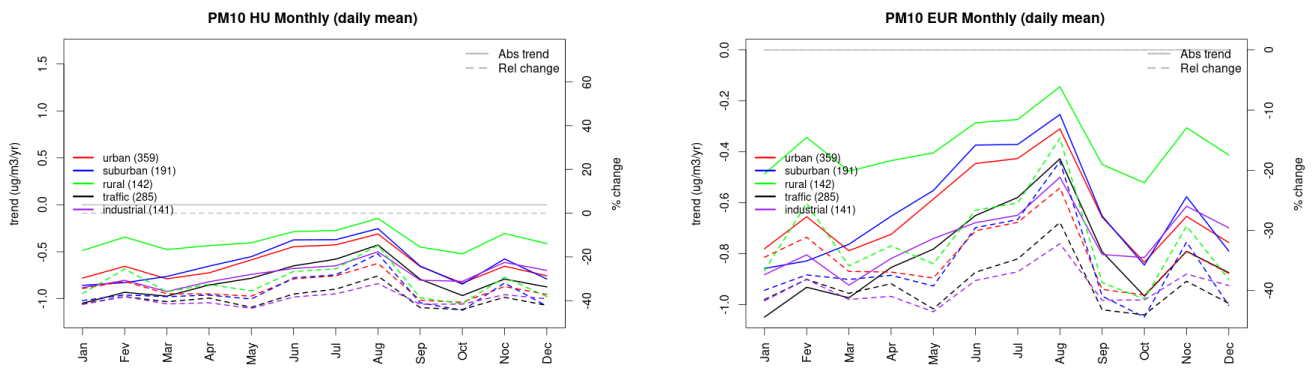


Figure S.333: Absolute (solid lines, left axis) and relative (dashed lines, right axis) trends in the monthly cycle for Hungary (left) and Europe (right) of PM10 at various station type.

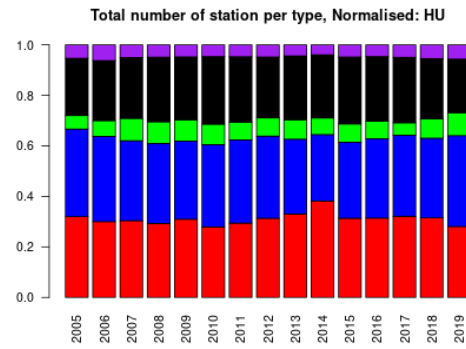
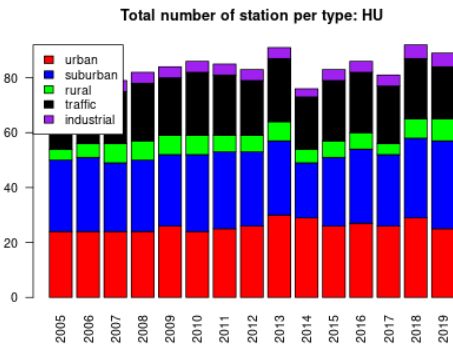
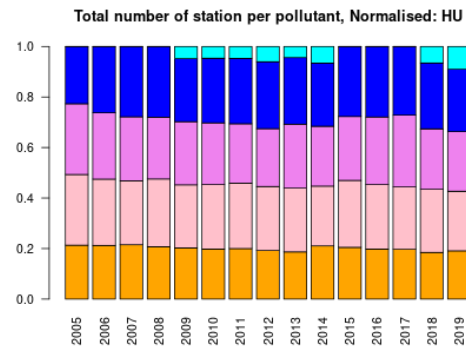
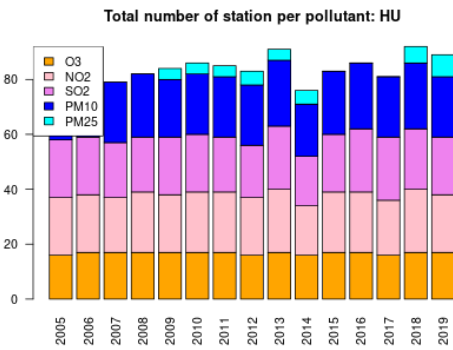
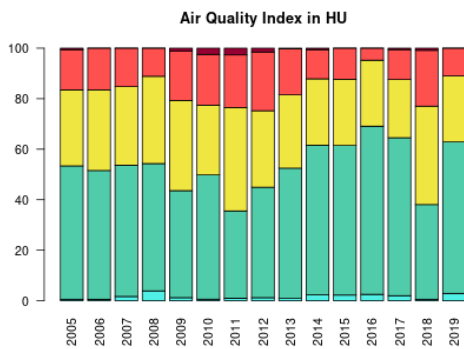


Figure S.334: For Hungary: overall air quality index (percentage of days in a given year) and distribution of daily categories per pollutant (light blue: good, light green: fair, yellow: moderate, orange: poor, red: very poor, violet: extremely poor).

16 Ireland

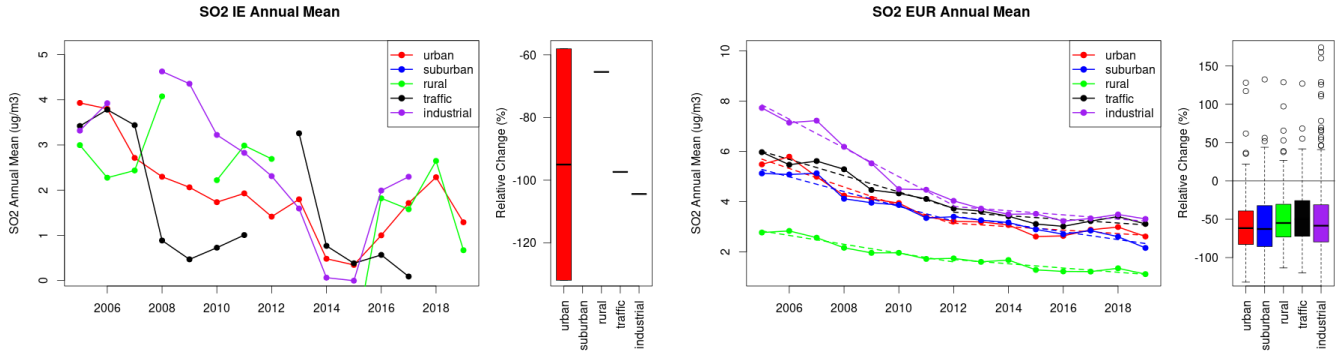


Figure S.335: Time series of the Ireland (left) and European-wide composite (median) of annual mean SO₂ (ug/m³) per station type and area (red: urban background, blue suburban background, green: rural background, black: traffic, violet: industrial) between 2005 and 2019. In the European composite, the dashed lines show the linear fit between 2005 & 2012 and between 2012 & 2019. The boxplots on the right-hand side show the distribution of relative changes (%) between 2005 and 2019 for all stations of each typology in Ireland and in Europe.

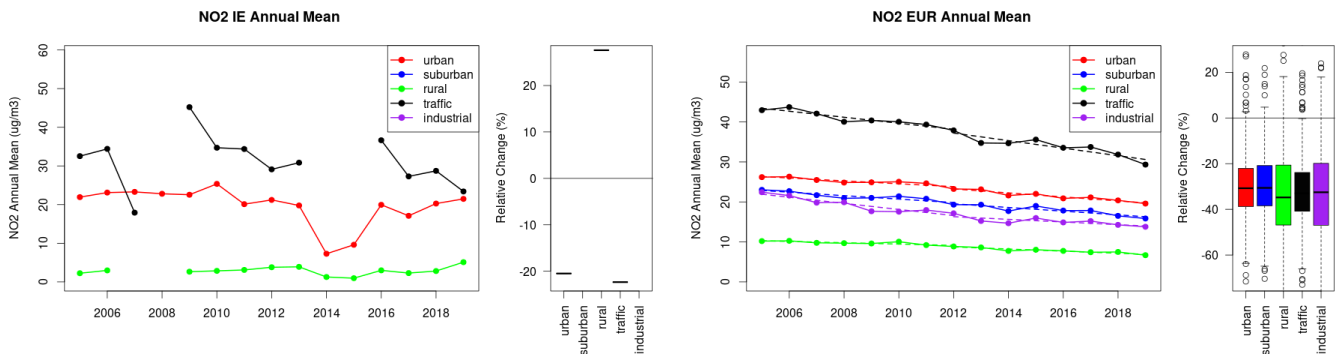


Figure S.336: Time series of the Ireland (left) and European-wide composite (median) of annual mean NO₂ (ug/m³) per station type and area (red: urban background, blue suburban background, green: rural background, black: traffic, violet: industrial) between 2005 and 2019. In the European composite, the dashed lines show the linear fit between 2005 & 2012 and between 2012 & 2019. The boxplots on the right-hand side show the distribution of relative changes (%) between 2005 and 2019 for all stations of each typology in Ireland and in Europe.

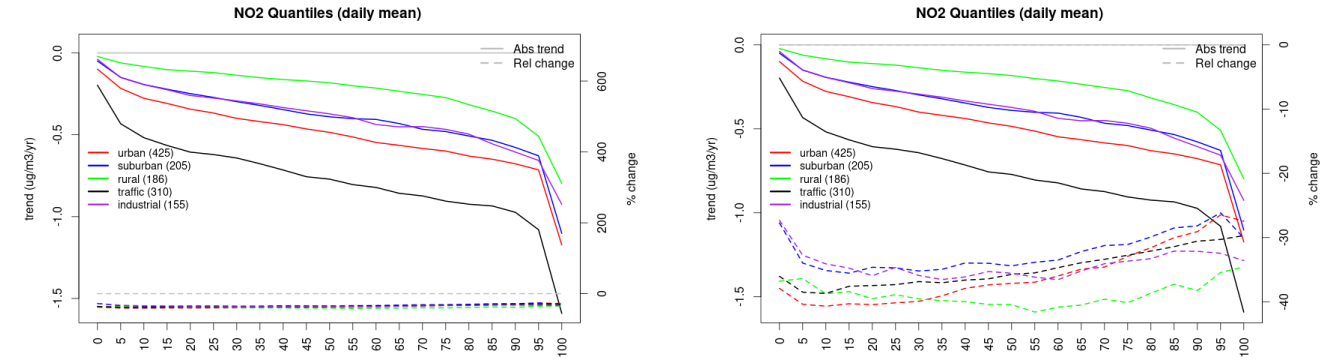


Figure S.337: For NO₂ in Ireland (left) and Europe, and for each typology of station: absolute trend (solid lines, left y-axis) and relative change (dashed lines, right y-axis) of the percentiles of daily means.

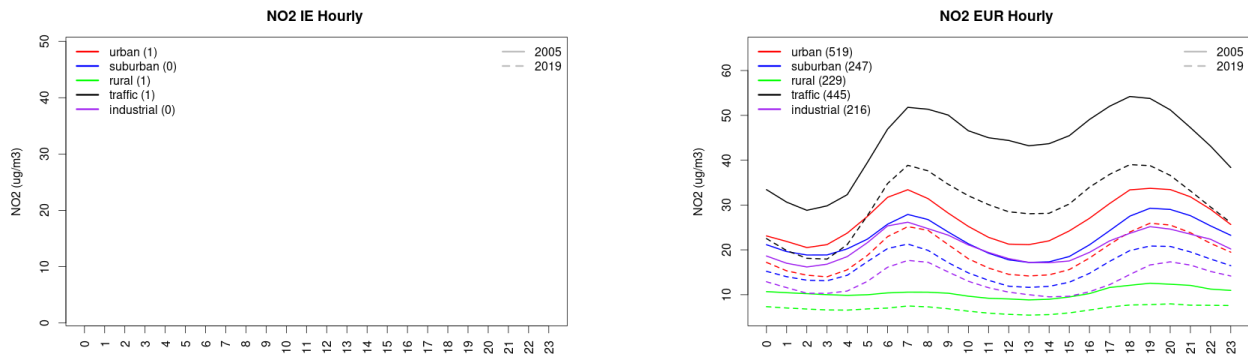


Figure S.338: Diurnal cycle of daily mean NO2 for Ireland (left) and Europe (right) at various station types estimated from the whole time series in 2005 (solid lines) and 2019

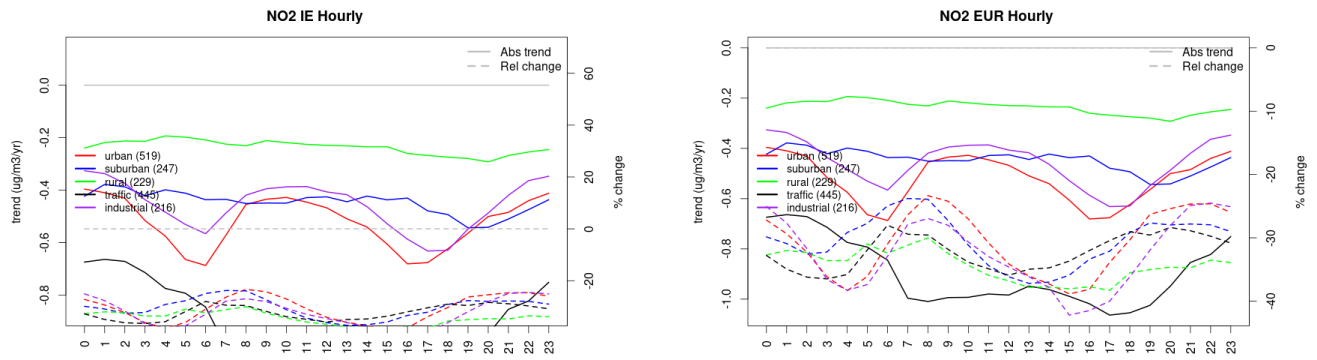


Figure S.339: Absolute (solid lines, left axis) and relative (dashed lines, right axis) trends in the diurnal cycle for Ireland (left) and Europe (right) of NO2 at various station type.

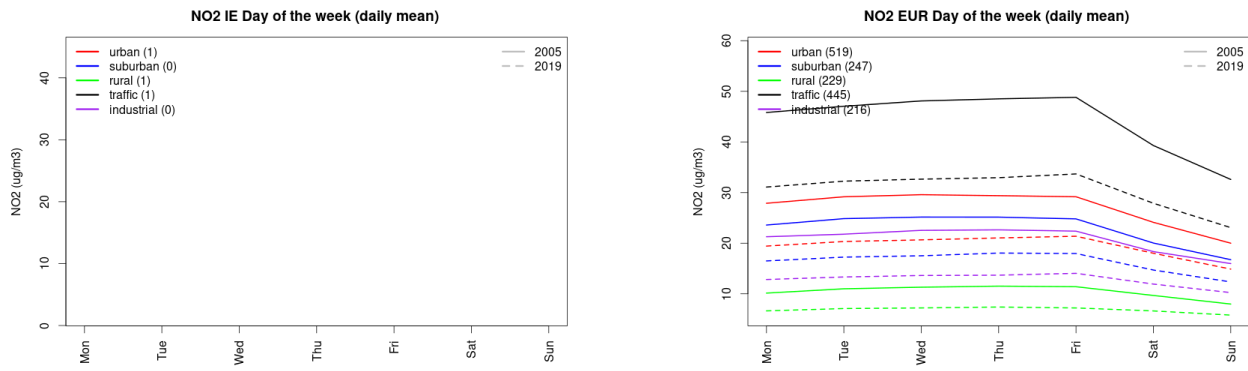


Figure S.340: Weekly cycle of daily mean NO2 for Ireland (left) and Europe (right) at various station types estimated from the whole time series in 2005 (solid lines) and 2019

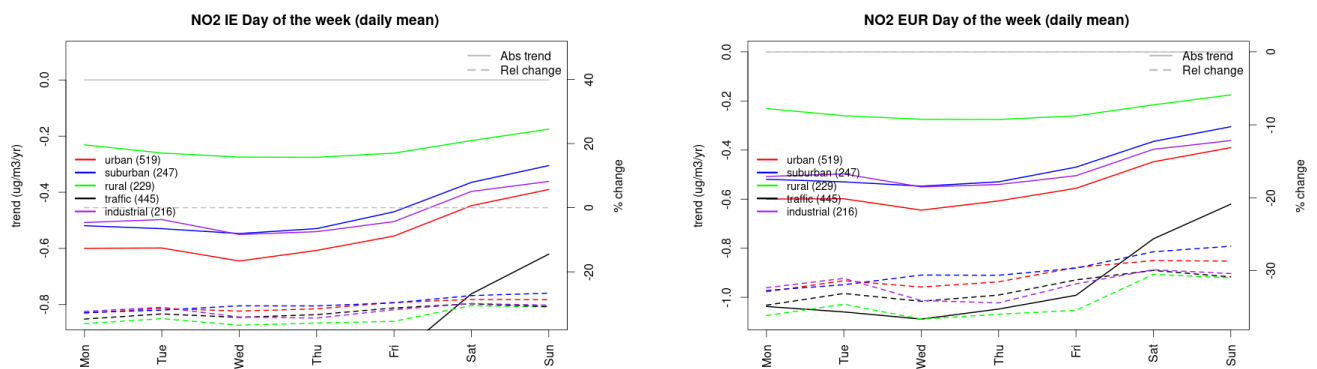


Figure S.341: Absolute (solid lines, left axis) and relative (dashed lines, right axis) trends in the weekly cycle for Ireland (left) and Europe (right) of NO₂ at various station type.

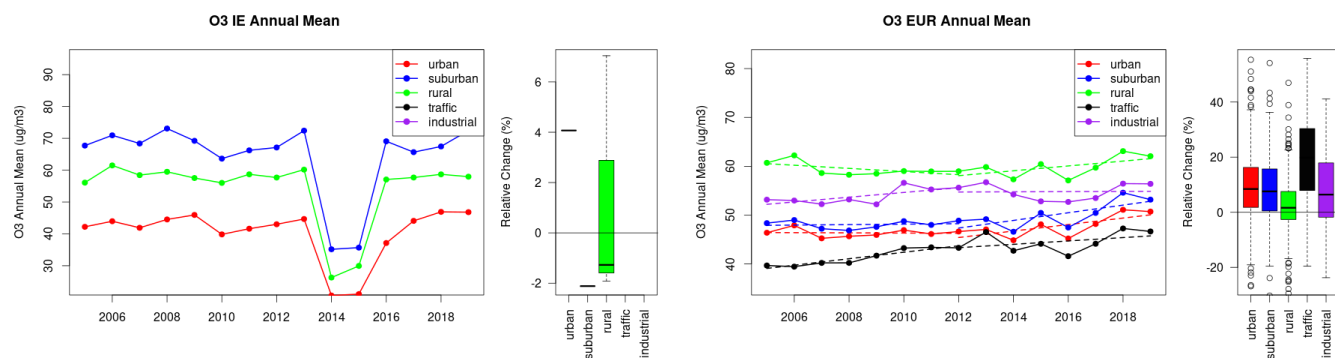


Figure S.342: Time series of the Ireland (left) and European-wide composite (median) of annual mean ozone (ug/m³) per station type and area (red: urban background, blue suburban background, green: rural background, black: traffic, violet: industrial) between 2005 and 2019. In the European composite, the dashed lines show the linear fit between 2005 & 2012 and between 2012 & 2019. The boxplots on the right-hand side show the distribution of relative changes (%) between 2005 and 2019 for all stations of each typology in Ireland and in Europe.

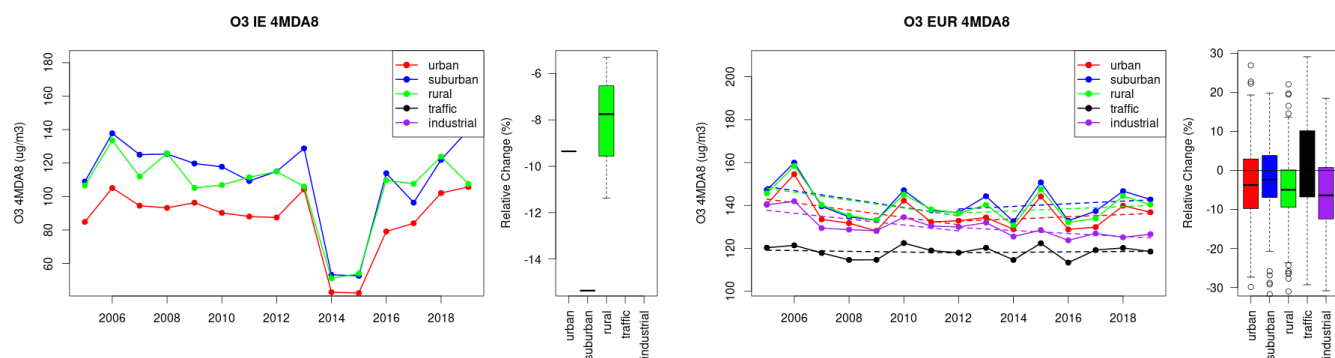


Figure S.343: Time series of the Ireland (left) and European-wide composite (median) of O₃ fourth highest daily peak (4MDA8, ug/m³) per station type and area (red: urban background, blue suburban background, green: rural background, black: traffic, violet: industrial) between 2005 and 2019. In the European composite, the dashed lines show the linear fit between 2005 & 2012 and between 2012 & 2019. The boxplots on the right-hand side show the distribution of relative changes (%) between 2005 and 2019 for all stations of each typology in Ireland and in Europe.

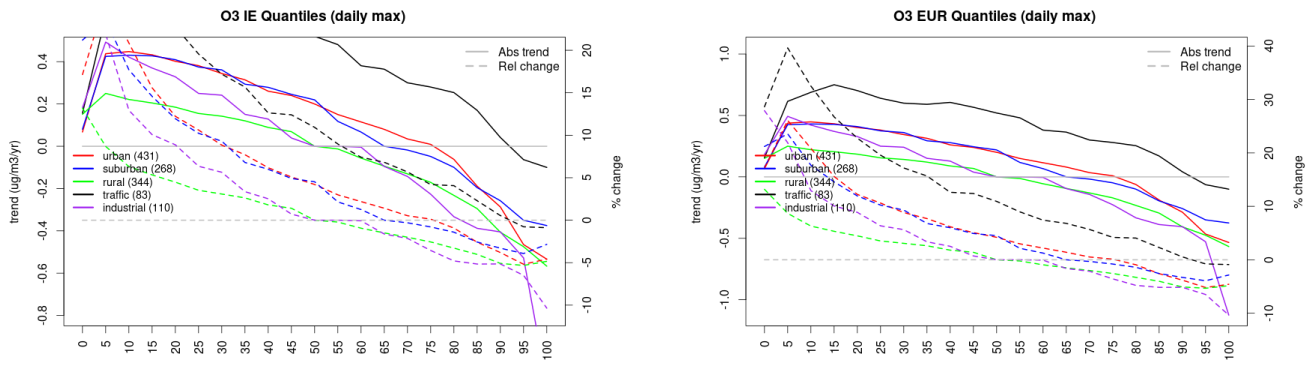


Figure S.344: For ozone in Ireland (left) and Europe, and for each typology of station: absolute trend (solid lines, left y-axis) and relative change (dashed lines, right y-axis) of the percentiles of daily maxima.

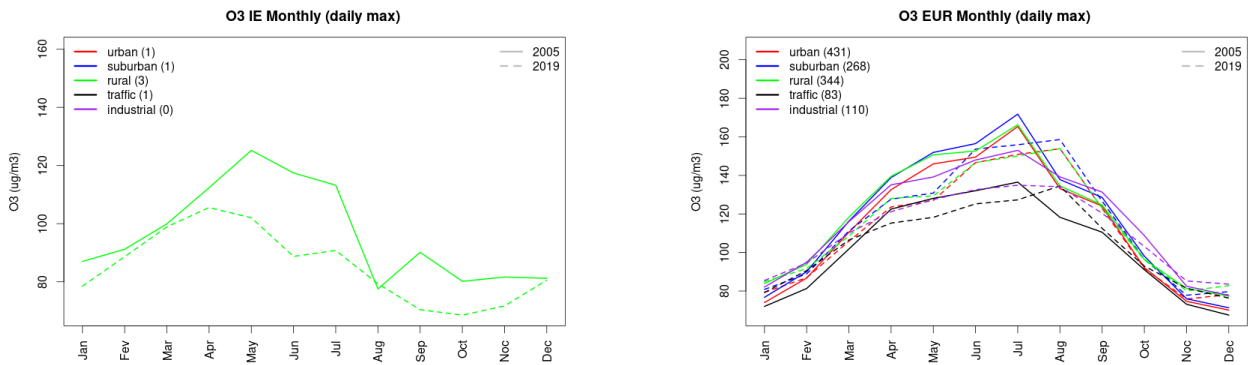


Figure S.345: Monthly cycle of daily max ozone for Ireland (left) and Europe (right) at various station types estimated from the whole time series in 2005 (solid lines) and 2019

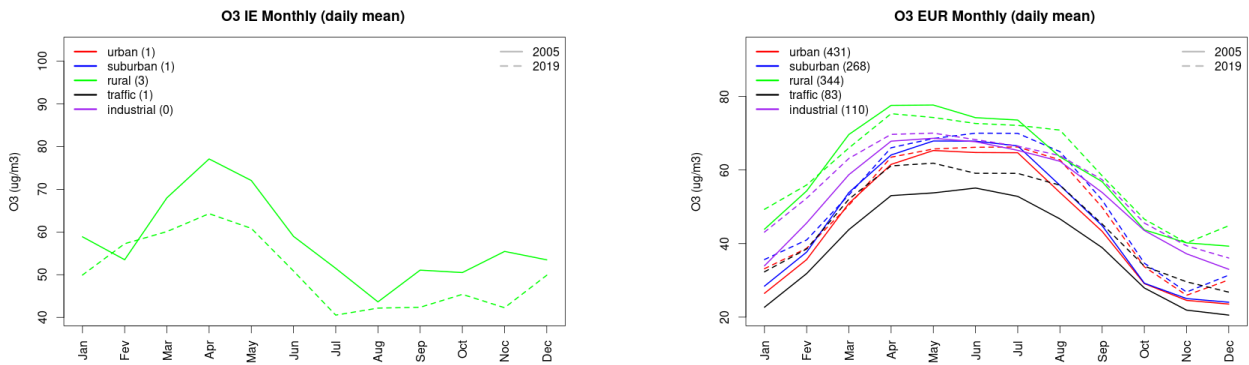


Figure S.346: Monthly cycle of daily mean ozone for Ireland (left) and Europe (right) at various station types estimated from the whole time series in 2005 (solid lines) and 2019

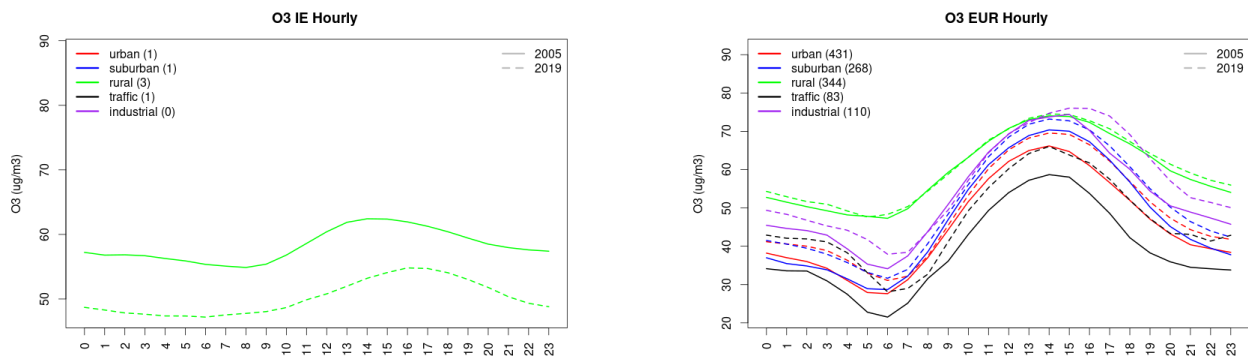


Figure S.347: Diurnal cycle of daily mean ozone for Ireland (left) and Europe (right) at various station types estimated from the whole time series in 2005 (solid lines) and 2019

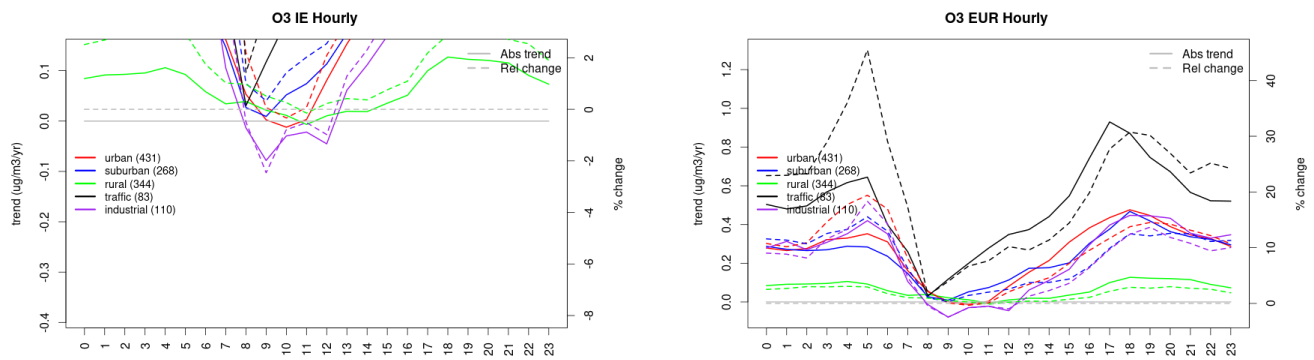


Figure S.348: Absolute (solid lines, left axis) and relative (dashed lines, right axis) trends in the diurnal cycle for Ireland (left) and Europe (right) of ozone at various station type.

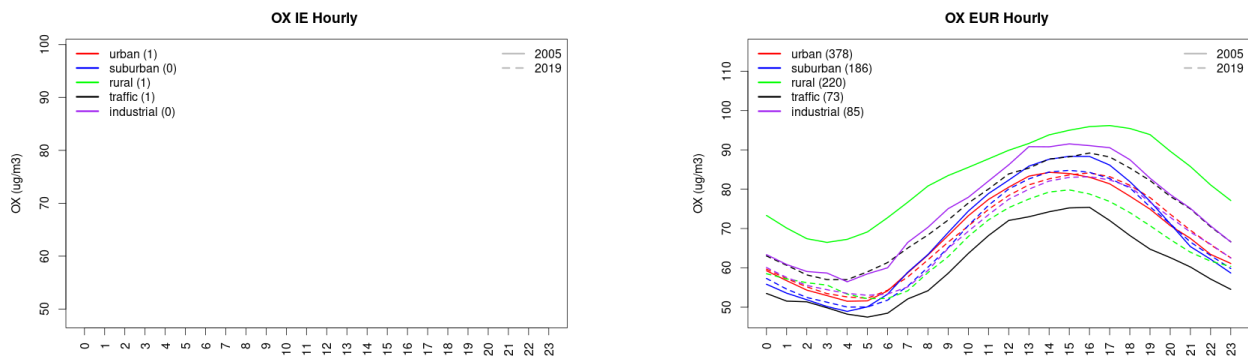


Figure S.349: Diurnal cycle of daily mean OX (as $\text{NO}_2 + \text{O}_3$) for Ireland (left) and Europe (right) at various station types estimated from the whole time series in 2005 (solid lines) and 2019

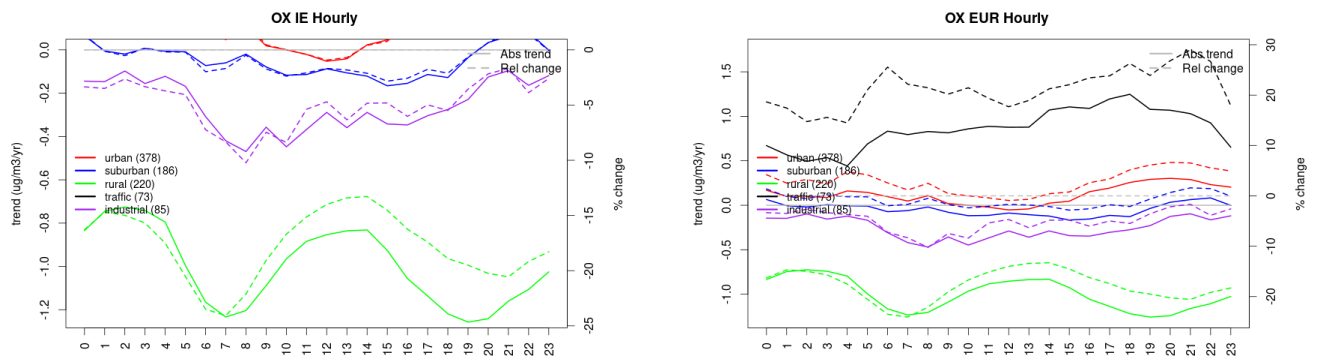


Figure S.350: Absolute (solid lines, left axis) and relative (dashed lines, right axis) trends in the diurnal cycle for Ireland (left) and Europe (right) of OX (as NO₂+O₃) at various station type.

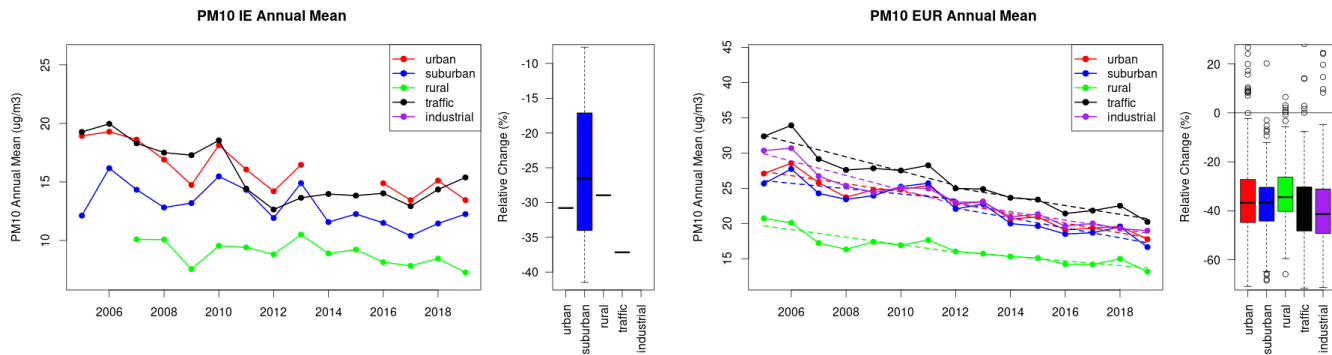


Figure S.351: Time series of the Ireland (left) and European-wide composite (median) of annual mean PM₁₀ (ug/m³) per station type and area (red: urban background, blue suburban background, green: rural background, black: traffic, violet: industrial) between 2005 and 2019. In the European composite, the dashed lines show the linear fit between 2005 & 2012 and between 2012 & 2019. The boxplots on the right-hand side show the distribution of relative changes (%) between 2005 and 2019 for all stations of each typology in Ireland and in Europe.

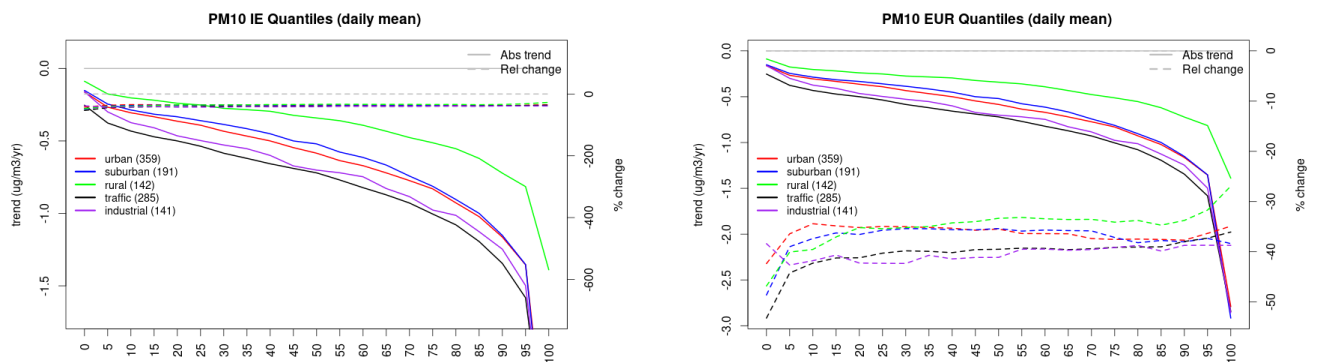


Figure S.352: For PM₁₀ in Ireland (left) and Europe, and for each typology of station: absolute trend (solid lines, left y-axis) and relative change (dashed lines, right y-axis) of the percentiles of daily means.

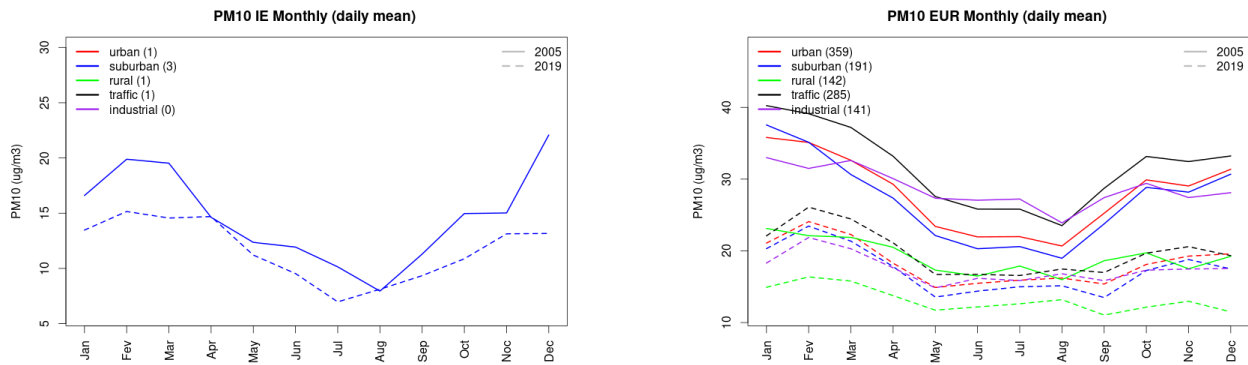


Figure S.353: Monthly cycle of daily mean PM10 for Ireland (left) and Europe (right) at various station types estimated from the whole time series in 2005 (solid lines) and 2019

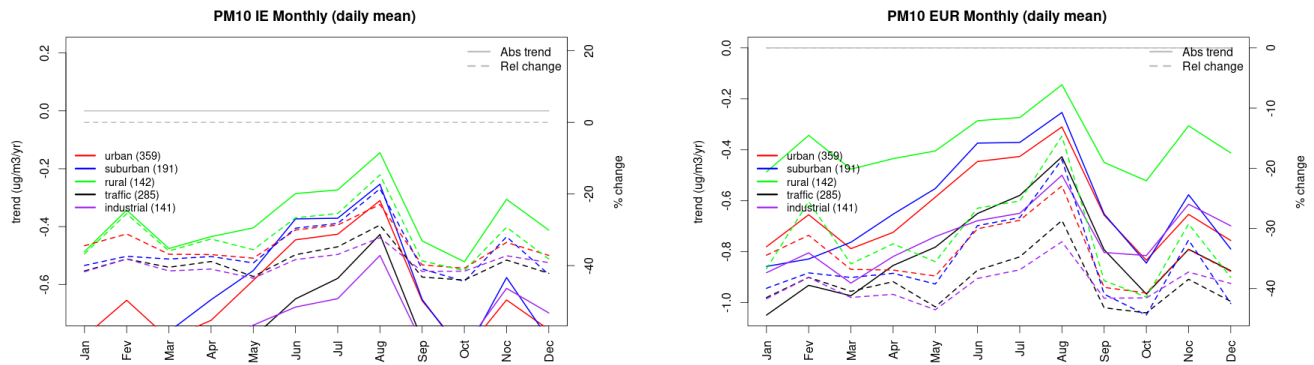


Figure S.354: Absolute (solid lines, left axis) and relative (dashed lines, right axis) trends in the monthly cycle for Ireland (left) and Europe (right) of PM10 at various station type.

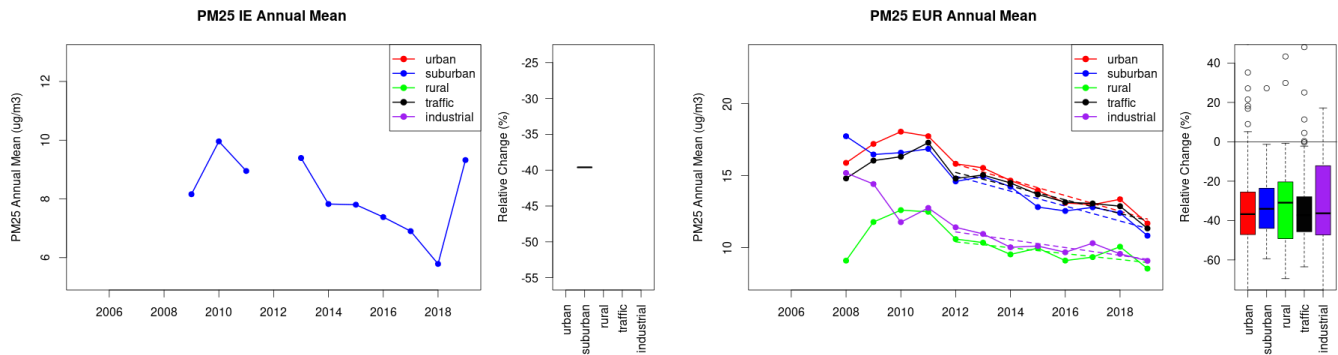


Figure S.355: Time series of the Ireland (left) and European-wide composite (median) of annual mean PM25 ($\mu\text{g}/\text{m}^3$) per station type and area (red: urban background, blue suburban background, green: rural background, black: traffic, violet: industrial) between 2005 and 2019. In the European composite, the dashed lines show the linear fit between 2005 & 2012 and between 2012 & 2019. The boxplots on the right-hand side show the distribution of relative changes (%) between 2005 and 2019 for all stations of each typology in Ireland and in Europe.

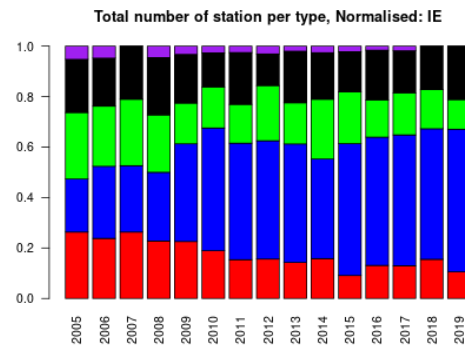
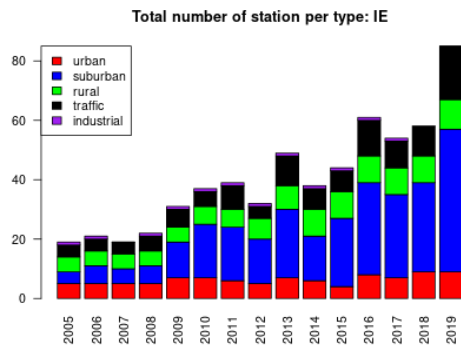
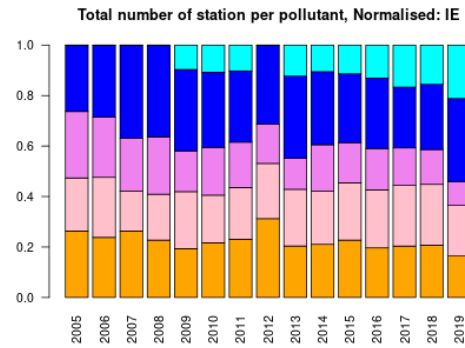
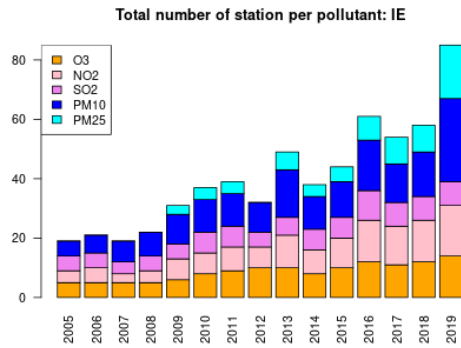
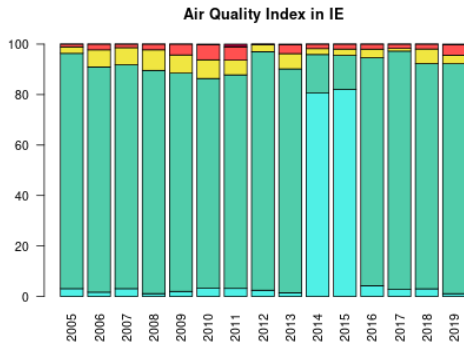


Figure S.356: For Ireland: overall air quality index (percentage of days in a given year) and distribution of daily categories per pollutant (light blue: good, light green: fair, yellow: moderate, orange: poor, red: very poor, violet: extremely poor).

17 Italy

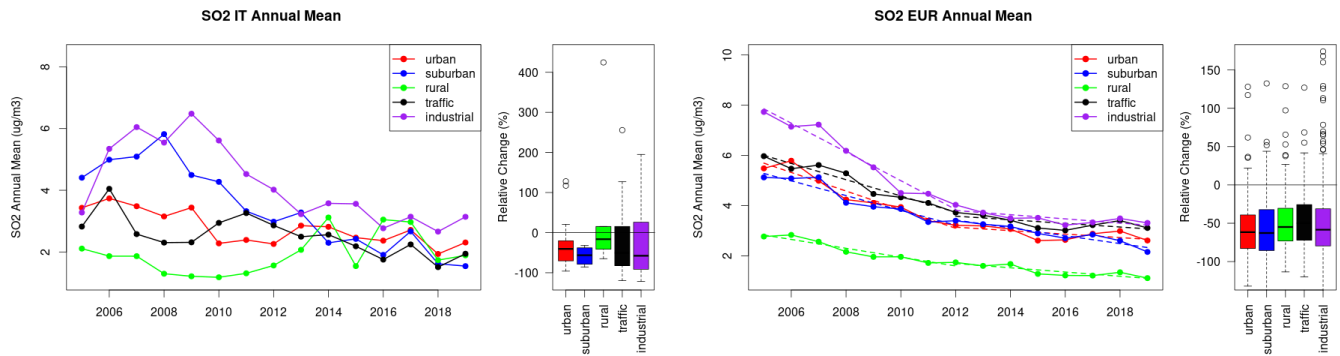


Figure S.357: Time series of the Italy (left) and European-wide composite (median) of annual mean SO₂ (ug/m³) per station type and area (red: urban background, blue suburban background, green: rural background, black: traffic, violet: industrial) between 2005 and 2019. In the European composite, the dashed lines show the linear fit between 2005 & 2012 and between 2012 & 2019. The boxplots on the right-hand side show the distribution of relative changes (%) between 2005 and 2019 for all stations of each typology in Italy and in Europe.

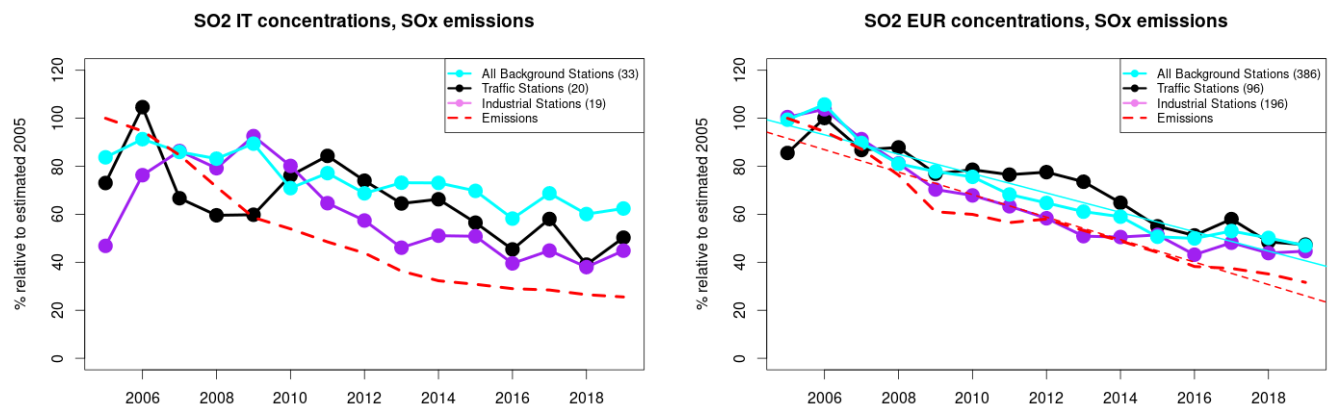


Figure S.358: Time series of 2005-2019 (left) and European (right) median SO₂ observed at traffic (black), industrial (violet) and background (cyan) sites (solid lines), and corresponding SO_x emissions (dashed line) normalised to estimated 2000 levels (%). The median is taken over where more than 5 stations of each typology is available. The total number of stations included is provided in brackets. In the European composite, straight lines are the linear fits over the whole period.

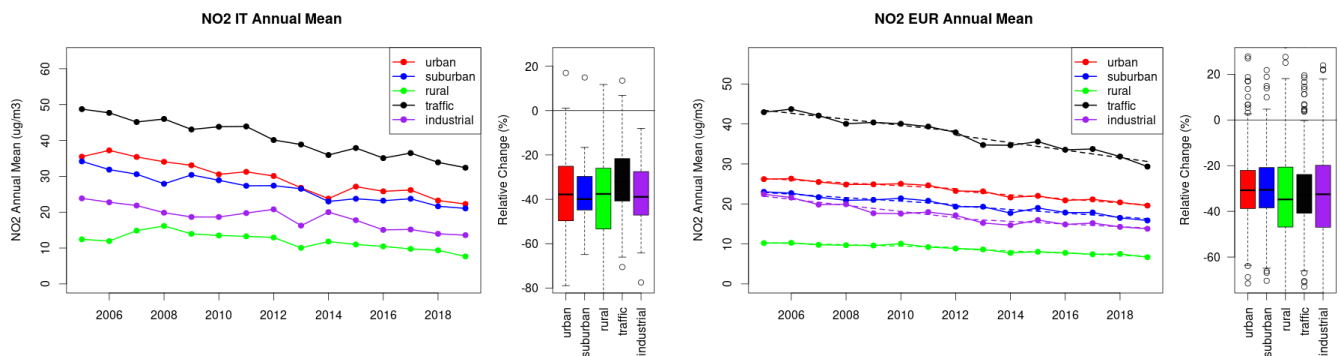


Figure S.359: Time series of the Italy (left) and European-wide composite (median) of annual mean NO₂ (ug/m³) per station type and area (red: urban background, blue suburban background, green: rural background, black: traffic, violet: industrial) between 2005 and 2019. In the European composite, the dashed lines show the linear fit between 2005 & 2012 and between 2012 & 2019. The boxplots on the right-hand side show the distribution of relative changes (%) between 2005 and 2019 for all stations of each typology in Italy and in Europe.

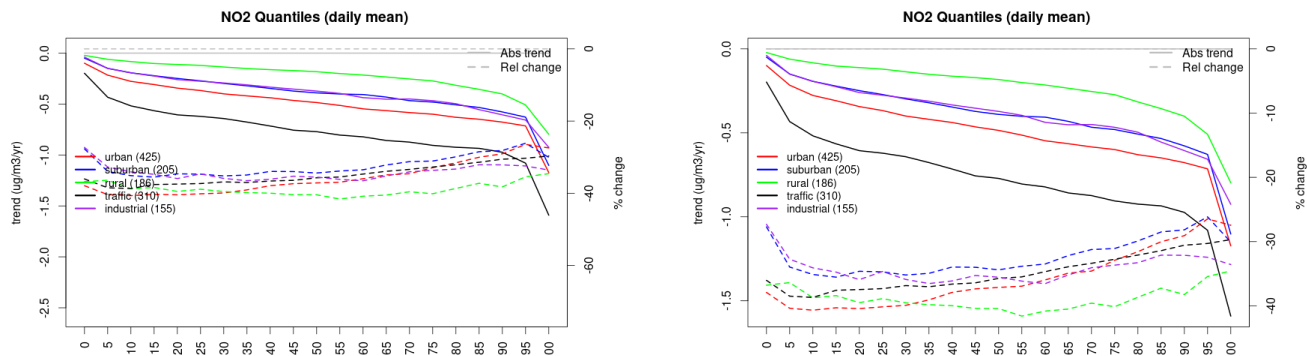


Figure S.360: For NO₂ in Italy (left) and Europe, and for each typology of station: absolute trend (solid lines, left y-axis) and relative change (dashed lines, right y-axis) of the percentiles of daily means.

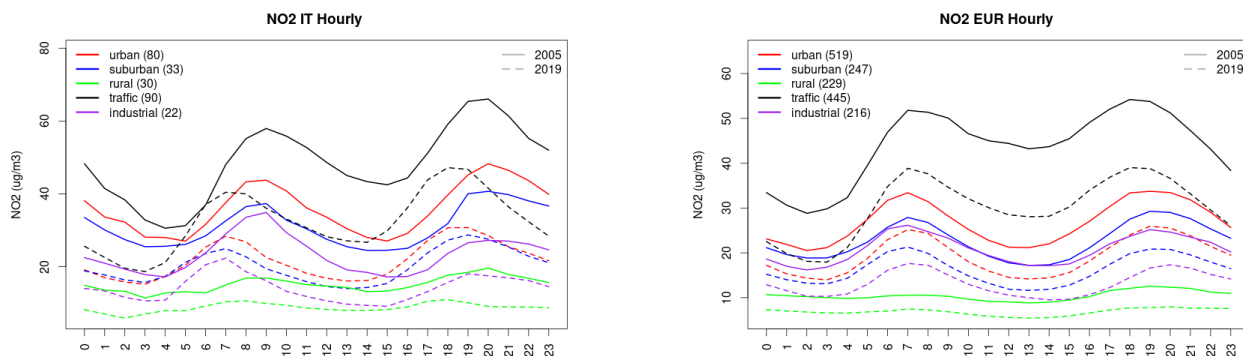


Figure S.361: Diurnal cycle of daily mean NO₂ for Italy (left) and Europe (right) at various station types estimated from the whole time series in 2005 (solid lines) and 2019

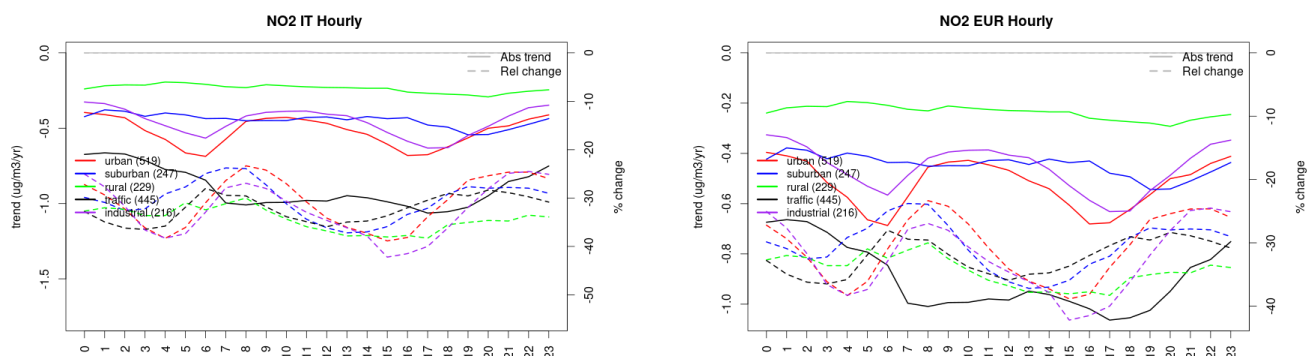


Figure S.362: Absolute (solid lines, left axis) and relative (dashed lines, right axis) trends in the diurnal cycle for Italy (left) and Europe (right) of NO₂ at various station type.

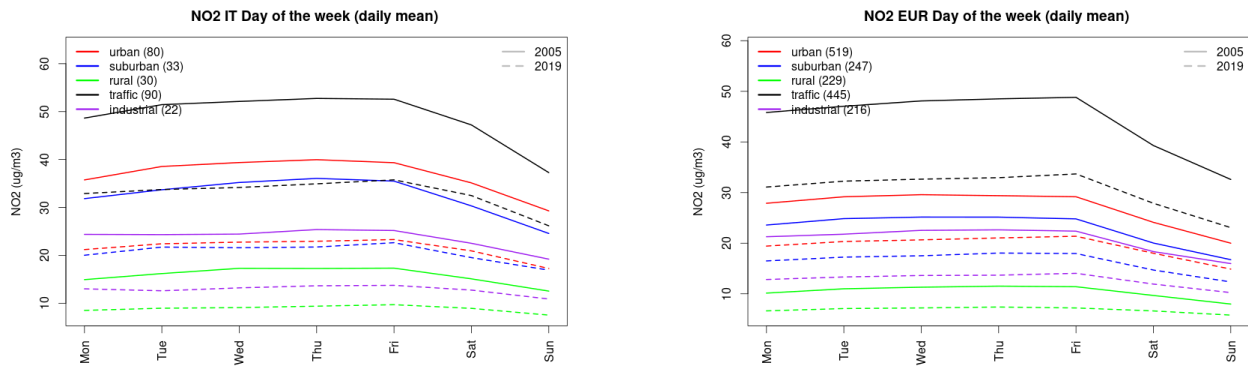


Figure S.363: Weekly cycle of daily mean NO₂ for Italy (left) and Europe (right) at various station types estimated from the whole time series in 2005 (solid lines) and 2019

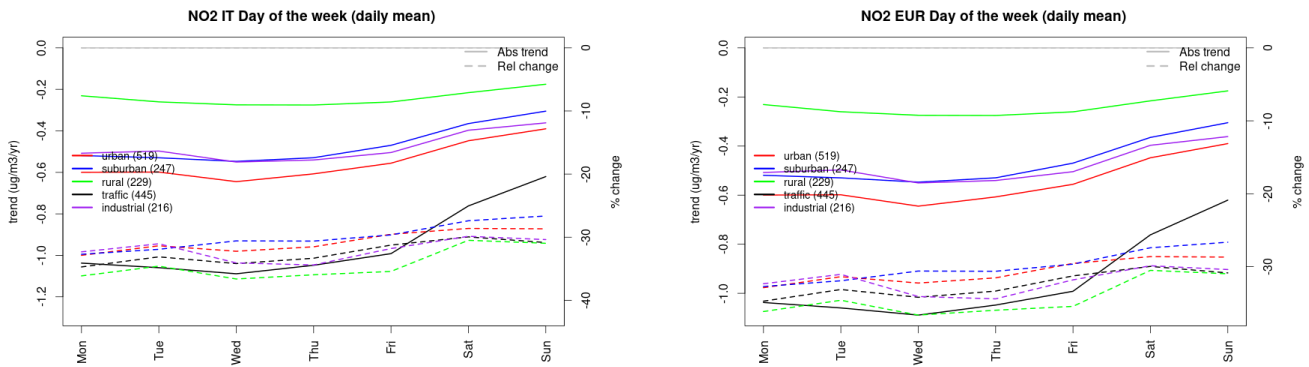


Figure S.364: Absolute (solid lines, left axis) and relative (dashed lines, right axis) trends in the weekly cycle for Italy (left) and Europe (right) of NO₂ at various station type.

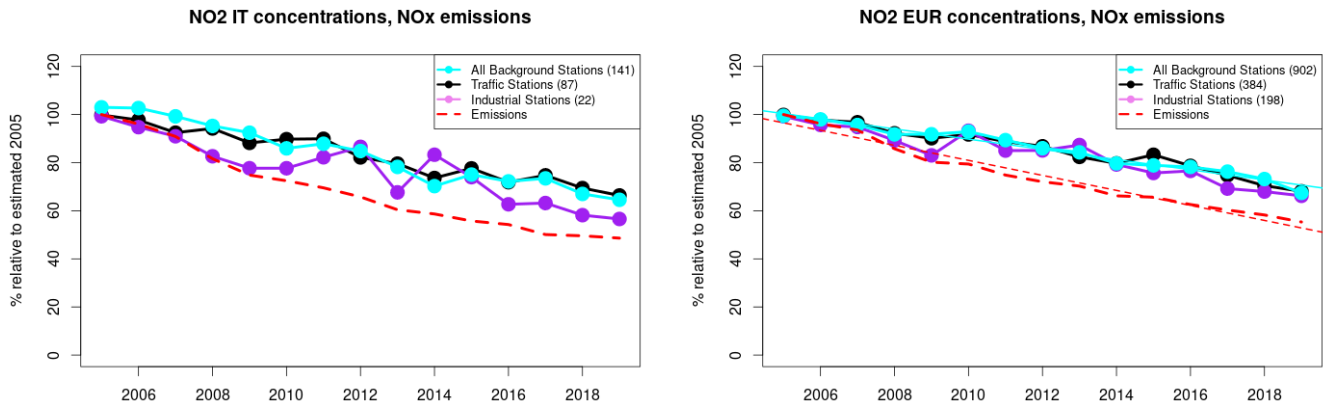


Figure S.365: Time series of 2005-2019 (left) and European (right) median NO₂ observed at traffic (black), industrial (violet) and background (cyan) sites (solid lines), and corresponding NO_x emissions (dashed line) normalised to estimated 2000 levels (%). The median is taken over where more than 5 stations of each typology is available. The total number of stations included is provided in brackets. In the European composite, straight lines are the linear fits over the whole period.

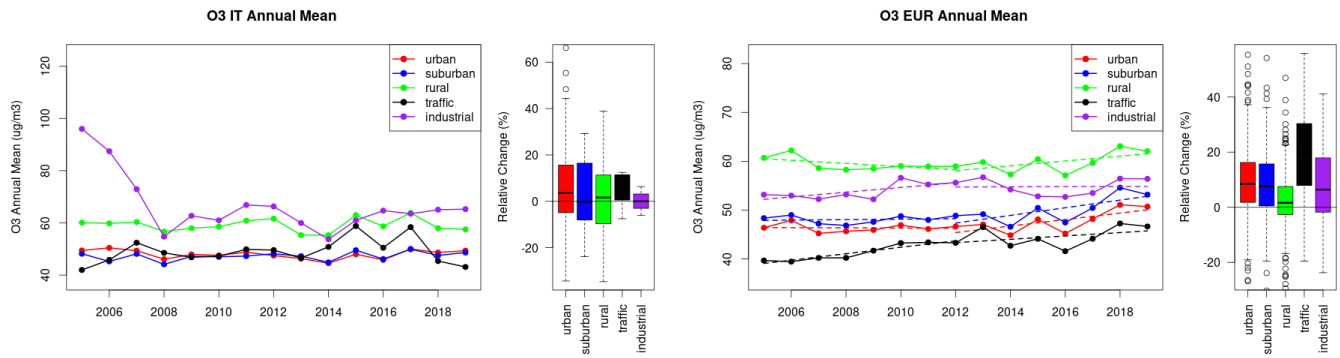


Figure S.366: Time series of the Italy (left) and European-wide composite (median) of annual mean ozone (ug/m³) per station type and area (red: urban background, blue suburban background, green: rural background, black: traffic, violet: industrial) between 2005 and 2019. In the European composite, the dashed lines show the linear fit between 2005 & 2012 and between 2012 & 2019. The boxplots on the right-hand side show the distribution of relative changes (%) between 2005 and 2019 for all stations of each typology in Italy and in Europe.

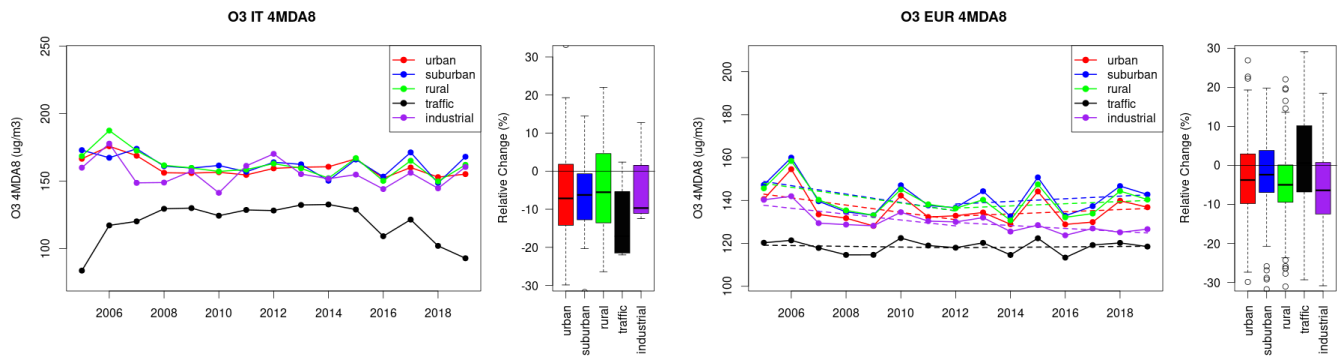


Figure S.367: Time series of the Italy (left) and European-wide composite (median) of O₃ fourth highest daily peak (4MDA₈, ug/m³) per station type and area (red: urban background, blue suburban background, green: rural background, black: traffic, violet: industrial) between 2005 and 2019. In the European composite, the dashed lines show the linear fit between 2005 & 2012 and between 2012 & 2019. The boxplots on the right-hand side show the distribution of relative changes (%) between 2005 and 2019 for all stations of each typology in Italy and in Europe.

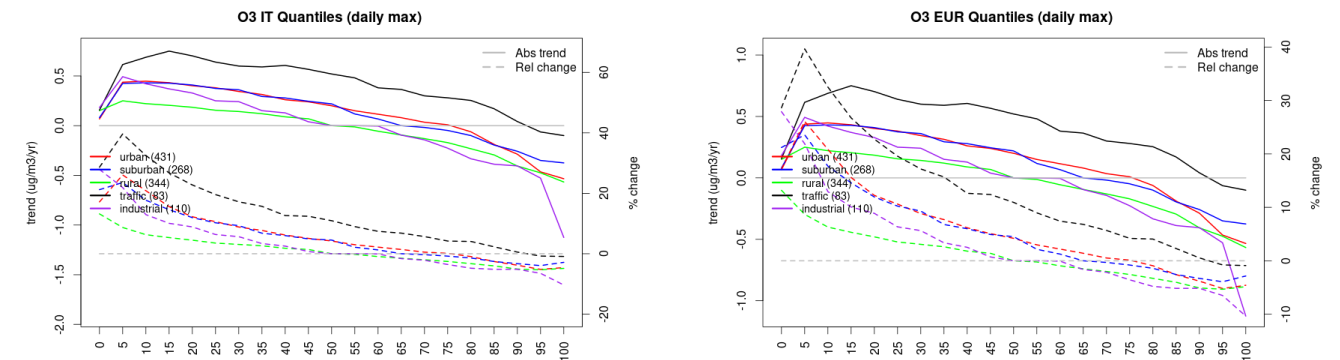


Figure S.368: For ozone in Italy (left) and Europe, and for each typology of station: absolute trend (solid lines, left y-axis) and relative change (dashed lines, right y-axis) of the percentiles of daily maxima.

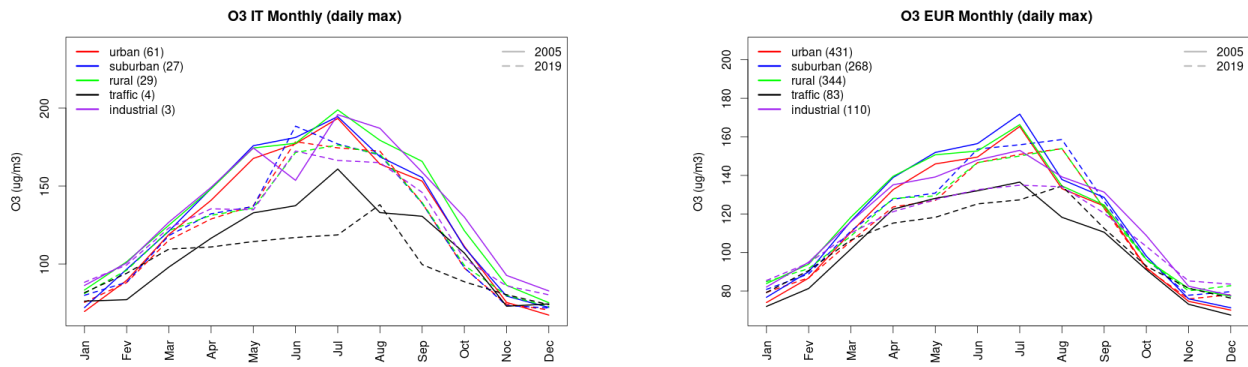


Figure S.369: Monthly cycle of daily max ozone for Italy (left) and Europe (right) at various station types estimated from the whole time series in 2005 (solid lines) and 2019

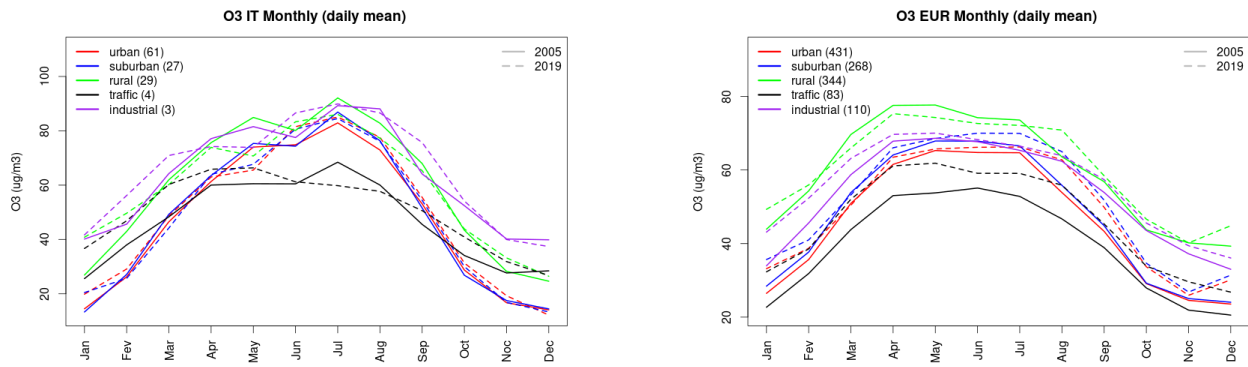


Figure S.370: Monthly cycle of daily mean ozone for Italy (left) and Europe (right) at various station types estimated from the whole time series in 2005 (solid lines) and 2019

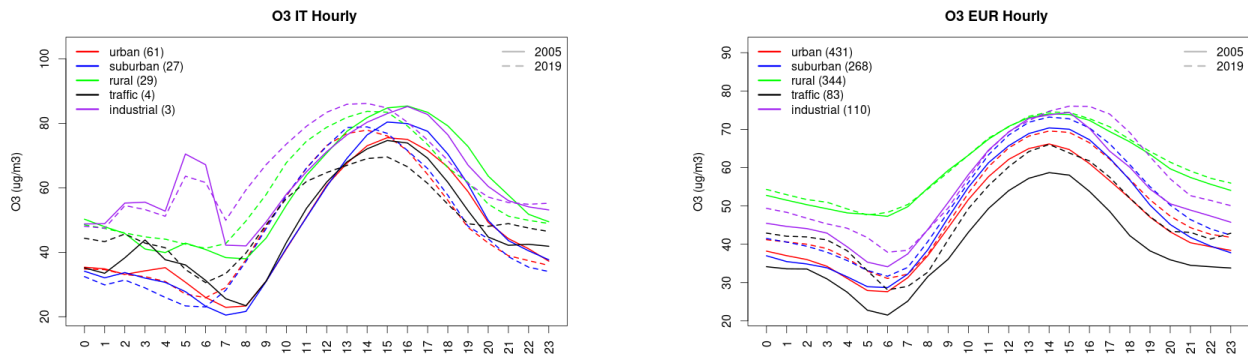


Figure S.371: Diurnal cycle of daily mean ozone for Italy (left) and Europe (right) at various station types estimated from the whole time series in 2005 (solid lines) and 2019

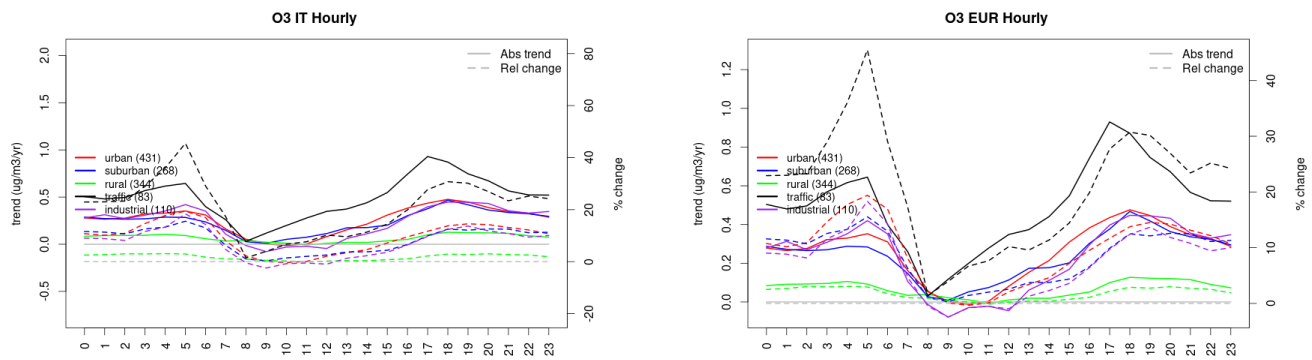


Figure S.372: Absolute (solid lines, left axis) and relative (dashed lines, right axis) trends in the diurnal cycle for Italy (left) and Europe (right) of ozone at various station type.

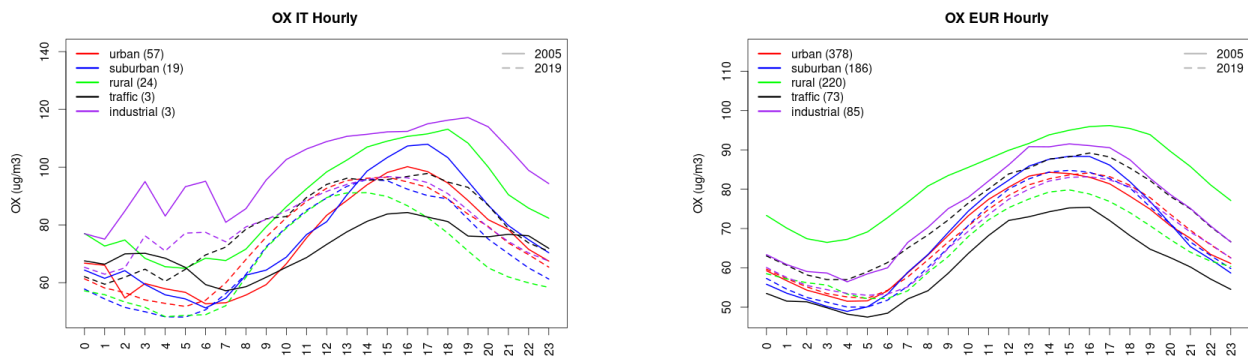


Figure S.373: Diurnal cycle of daily mean OX (as NO₂+O₃) for Italy (left) and Europe (right) at various station types estimated from the whole time series in 2005 (solid lines) and 2019

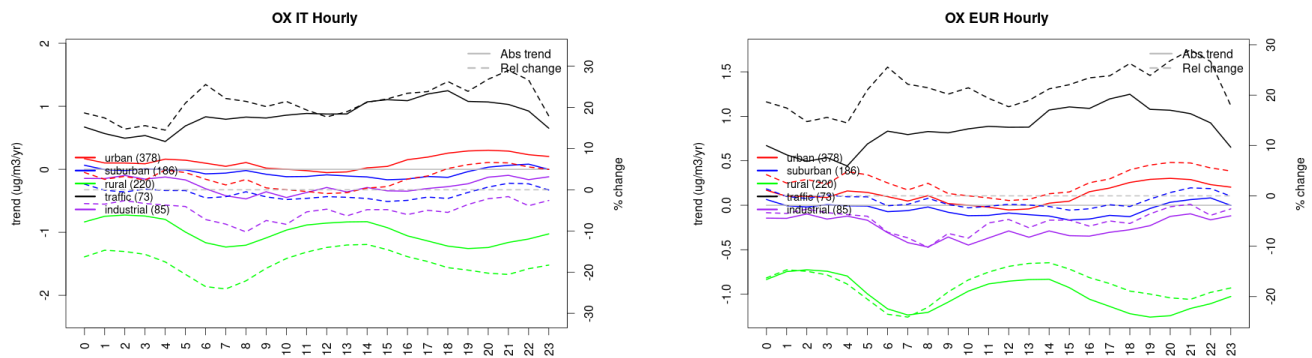


Figure S.374: Absolute (solid lines, left axis) and relative (dashed lines, right axis) trends in the diurnal cycle for Italy (left) and Europe (right) of OX (as NO₂+O₃) at various station type.

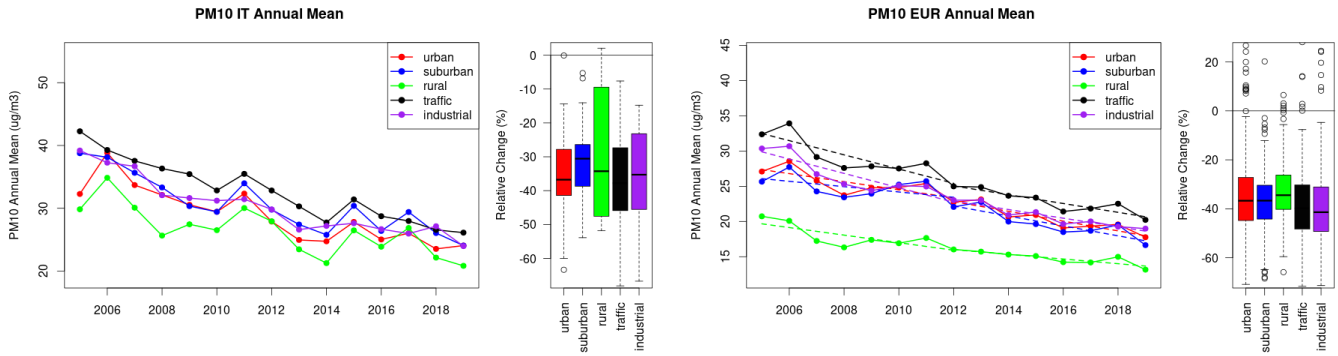


Figure S.375: Time series of the Italy (left) and European-wide composite (median) of annual mean PM10 (ug/m³) per station type and area (red: urban background, blue suburban background, green: rural background, black: traffic, violet: industrial) between 2005 and 2019. In the European composite, the dashed lines show the linear fit between 2005 & 2012 and between 2012 & 2019. The boxplots on the right-hand side show the distribution of relative changes (%) between 2005 and 2019 for all stations of each typology in Italy and in Europe.

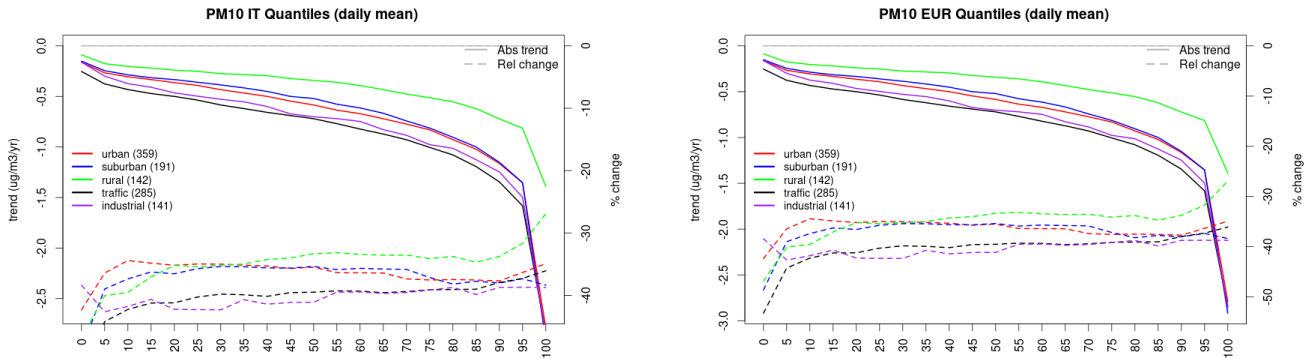


Figure S.376: For PM10 in Italy (left) and Europe, and for each typology of station: absolute trend (solid lines, left y-axis) and relative change (dashed lines, right y-axis) of the percentiles of daily means.

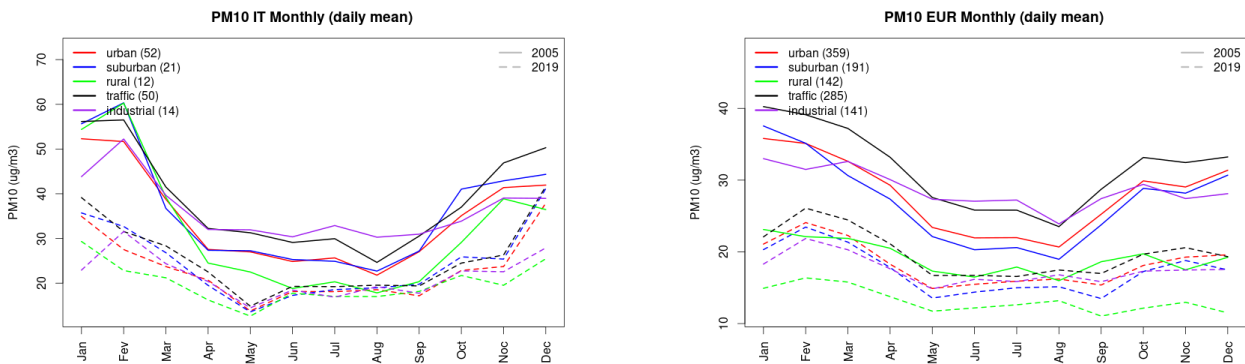


Figure S.377: Monthly cycle of daily mean PM10 for Italy (left) and Europe (right) at various station types estimated from the whole time series in 2005 (solid lines) and 2019 (dashed lines).

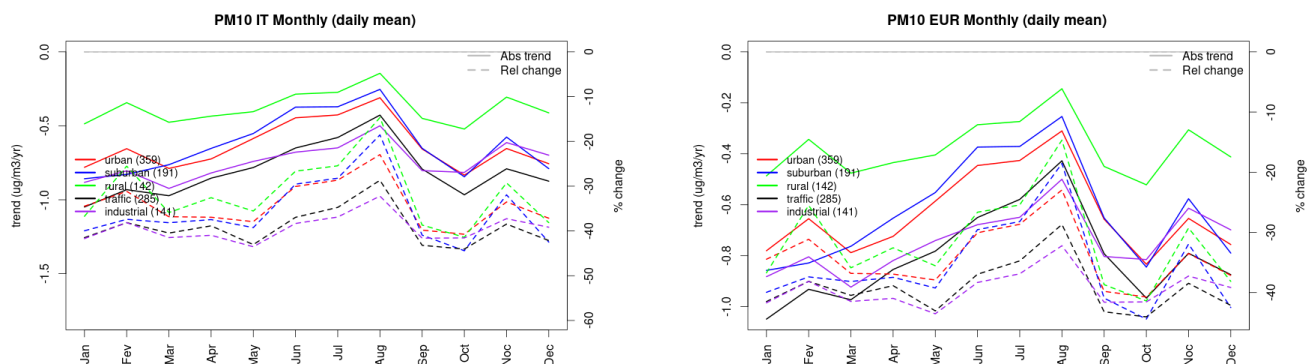


Figure S.378: Absolute (solid lines, left axis) and relative (dashed lines, right axis) trends in the monthly cycle for Italy (left) and Europe (right) of PM10 at various station type.

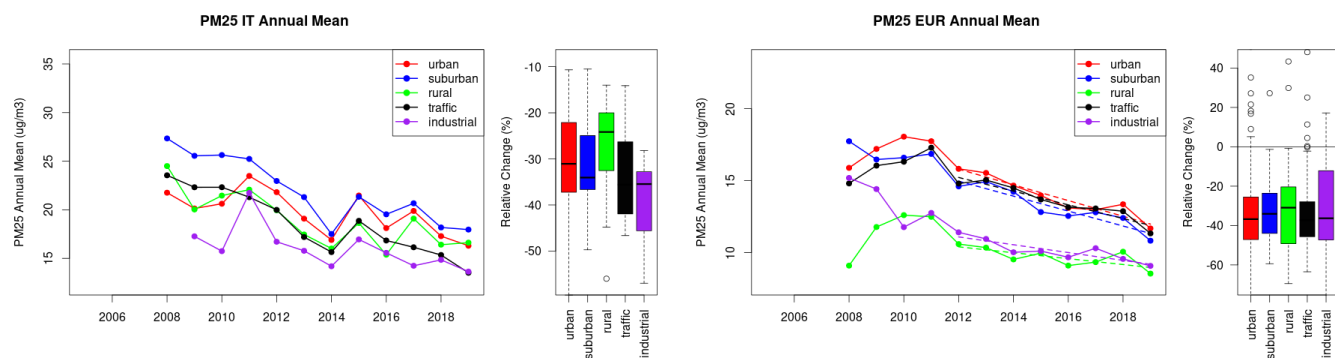


Figure S.379: Time series of the Italy (left) and European-wide composite (median) of annual mean PM25 ($\mu\text{g}/\text{m}^3$) per station type and area (red: urban background, blue suburban background, green: rural background, black: traffic, violet: industrial) between 2005 and 2019. In the European composite, the dashed lines show the linear fit between 2005 & 2012 and between 2012 & 2019. The boxplots on the right-hand side show the distribution of relative changes (%) between 2005 and 2019 for all stations of each typology in Italy and in Europe.

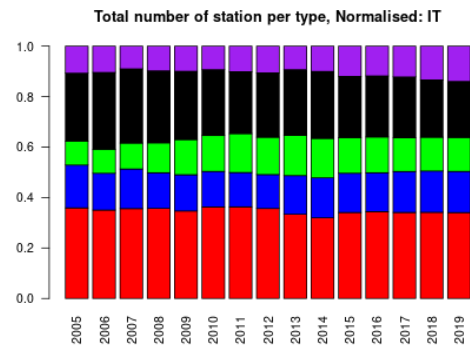
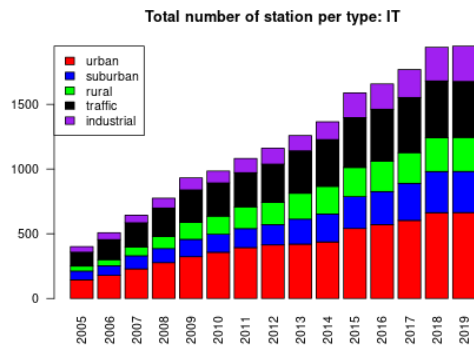
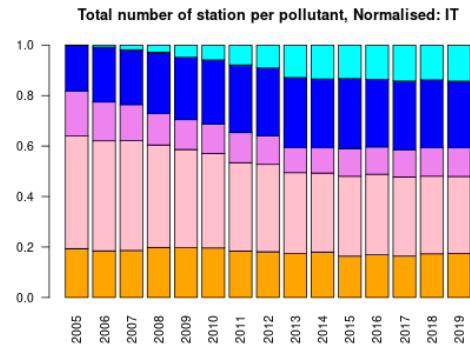
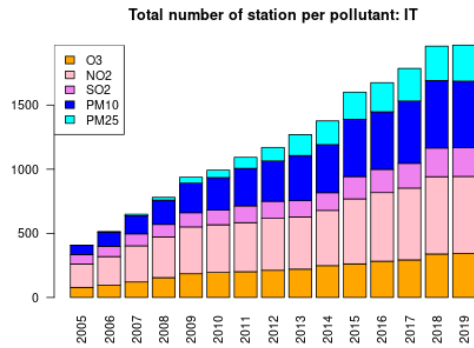
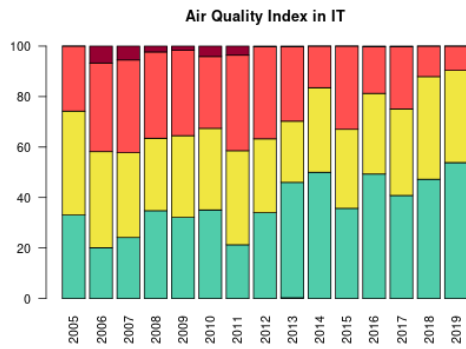


Figure S.380: For Italy: overall air quality index (percentage of days in a given year) and distribution of daily categories per pollutant (light blue: good, light green: fair, yellow: moderate, orange: poor, red: very poor, violet: extremely poor).

18 Lithuania

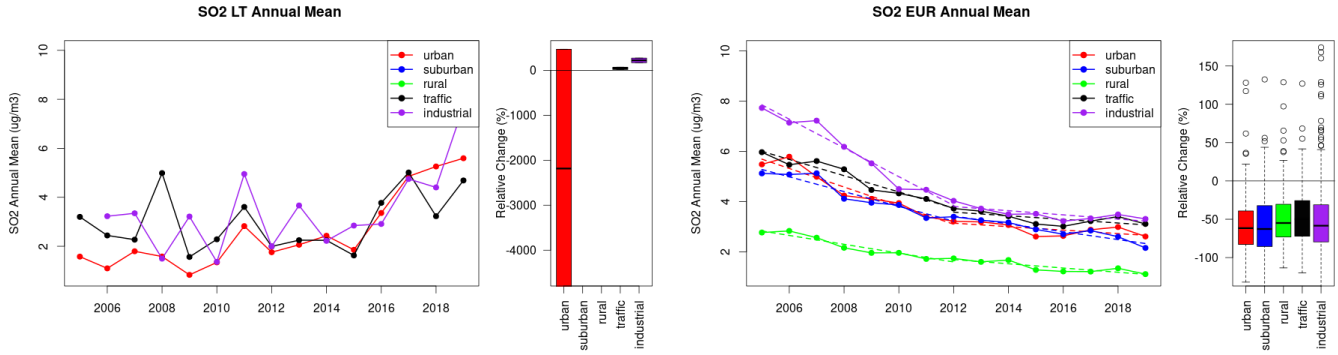


Figure S.381: Time series of the Lithuania (left) and European-wide composite (median) of annual mean SO₂ (ug/m³) per station type and area (red: urban background, blue suburban background, green: rural background, black: traffic, violet: industrial) between 2005 and 2019. In the European composite, the dashed lines show the linear fit between 2005 & 2012 and between 2012 & 2019. The boxplots on the right-hand side show the distribution of relative changes (%) between 2005 and 2019 for all stations of each typology in Lithuania and in Europe.

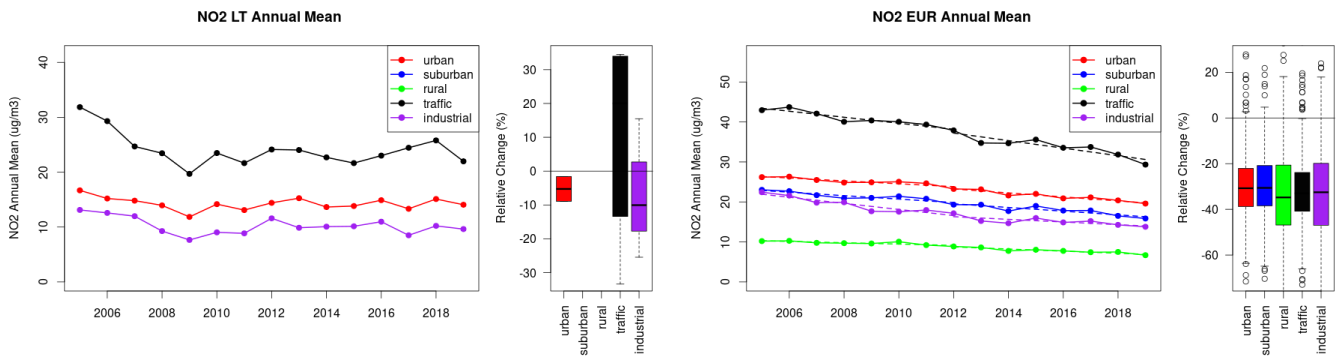


Figure S.382: Time series of the Lithuania (left) and European-wide composite (median) of annual mean NO₂ (ug/m³) per station type and area (red: urban background, blue suburban background, green: rural background, black: traffic, violet: industrial) between 2005 and 2019. In the European composite, the dashed lines show the linear fit between 2005 & 2012 and between 2012 & 2019. The boxplots on the right-hand side show the distribution of relative changes (%) between 2005 and 2019 for all stations of each typology in Lithuania and in Europe.

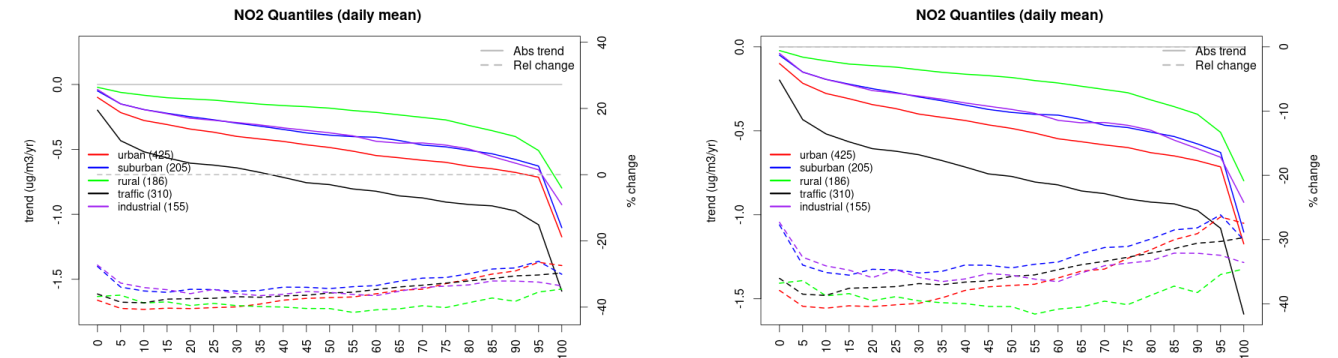


Figure S.383: For NO₂ in Lithuania (left) and Europe, and for each typology of station: absolute trend (solid lines, left y-axis) and relative change (dashed lines, right y-axis) of the percentiles of daily means.

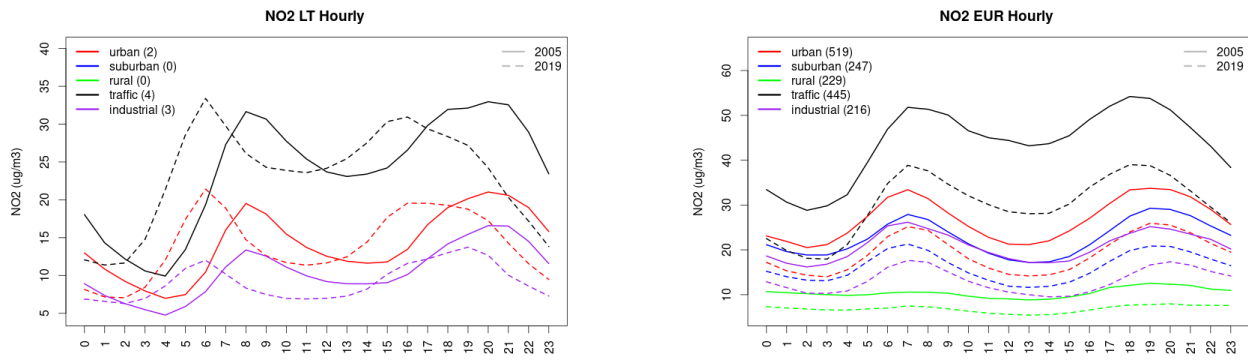


Figure S.384: Diurnal cycle of daily mean NO2 for Lithuania (left) and Europe (right) at various station types estimated from the whole time series in 2005 (solid lines) and 2019

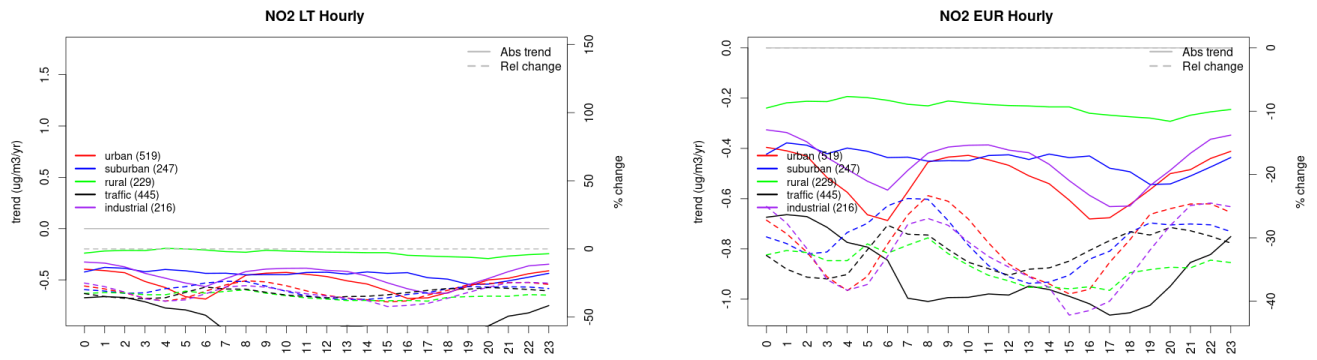


Figure S.385: Absolute (solid lines, left axis) and relative (dashed lines, right axis) trends in the diurnal cycle for Lithuania (left) and Europe (right) of NO2 at various station type.

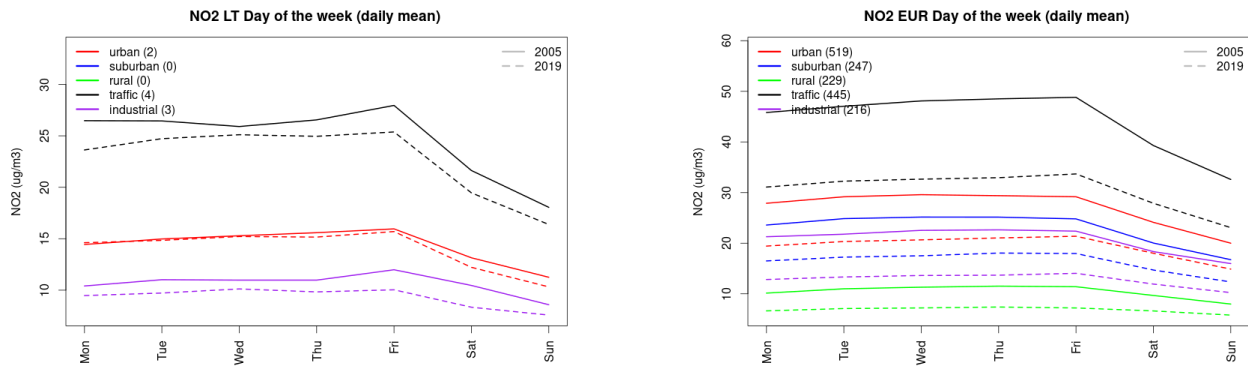


Figure S.386: Weekly cycle of daily mean NO2 for Lithuania (left) and Europe (right) at various station types estimated from the whole time series in 2005 (solid lines) and 2019

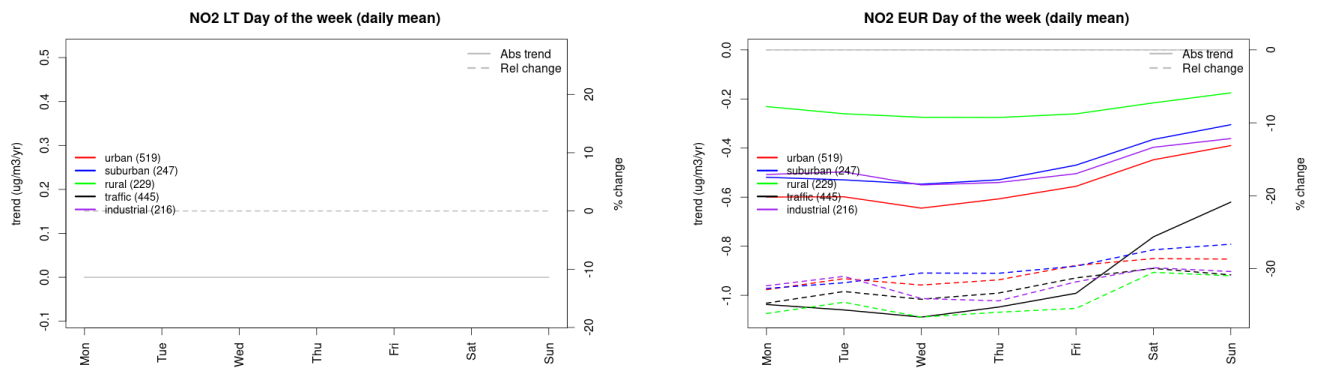


Figure S.387: Absolute (solid lines, left axis) and relative (dashed lines, right axis) trends in the weekly cycle for Lithuania (left) and Europe (right) of NO₂ at various station type.

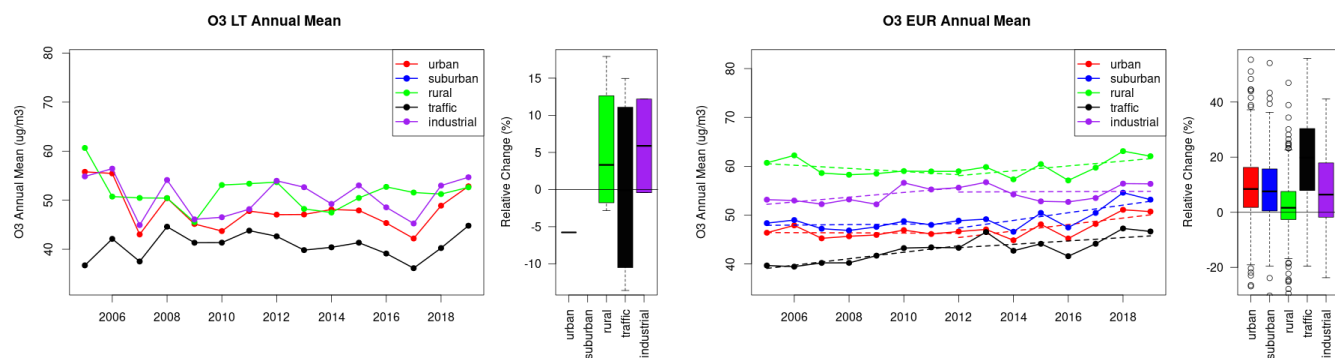


Figure S.388: Time series of the Lithuania (left) and European-wide composite (median) of annual mean ozone (ug/m³) per station type and area (red: urban background, blue suburban background, green: rural background, black: traffic, violet: industrial) between 2005 and 2019. In the European composite, the dashed lines show the linear fit between 2005 & 2012 and between 2012 & 2019. The boxplots on the right-hand side show the distribution of relative changes (%) between 2005 and 2019 for all stations of each typology in Lithuania and in Europe.

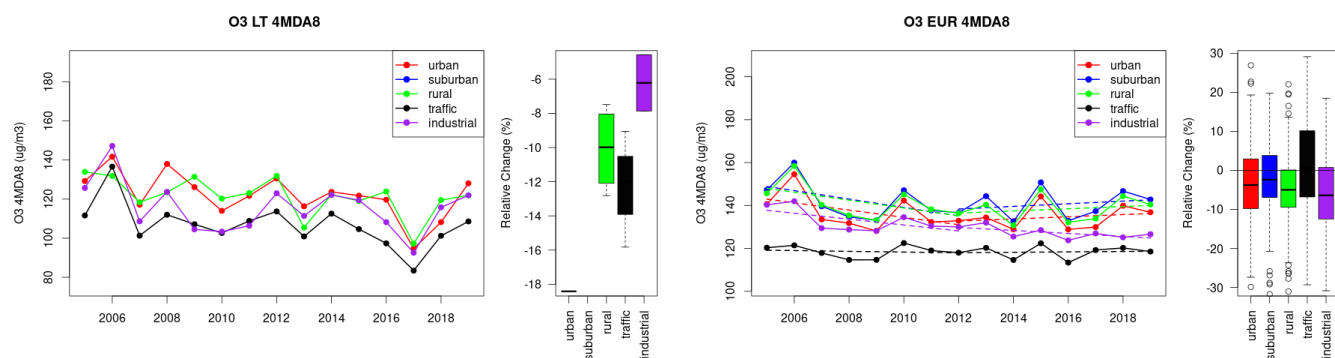


Figure S.389: Time series of the Lithuania (left) and European-wide composite (median) of O₃ fourth highest daily peak (4MDA8, ug/m³) per station type and area (red: urban background, blue suburban background, green: rural background, black: traffic, violet: industrial) between 2005 and 2019. In the European composite, the dashed lines show the linear fit between 2005 & 2012 and between 2012 & 2019. The boxplots on the right-hand side show the distribution of relative changes (%) between 2005 and 2019 for all stations of each typology in Lithuania and in Europe.

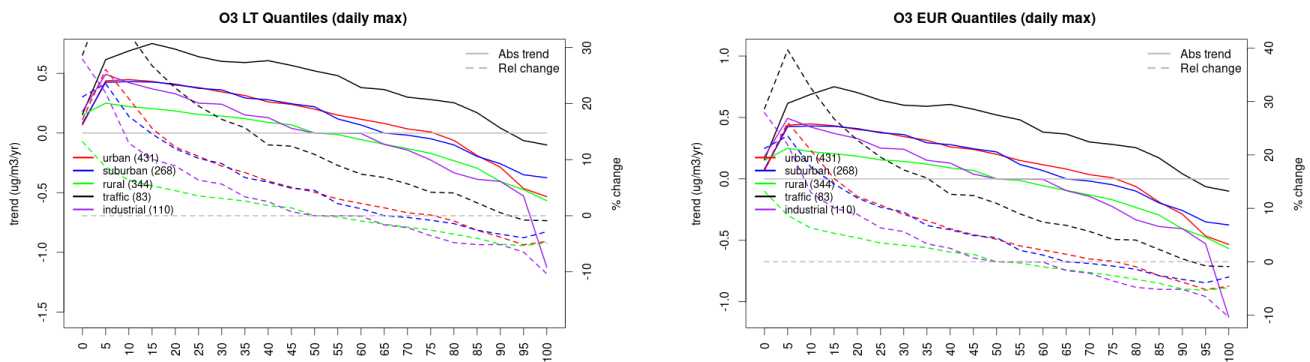


Figure S.390: For ozone in Lithuania (left) and Europe, and for each typology of station: absolute trend (solid lines, left y-axis) and relative change (dashed lines, right y-axis) of the percentiles of daily maxima.

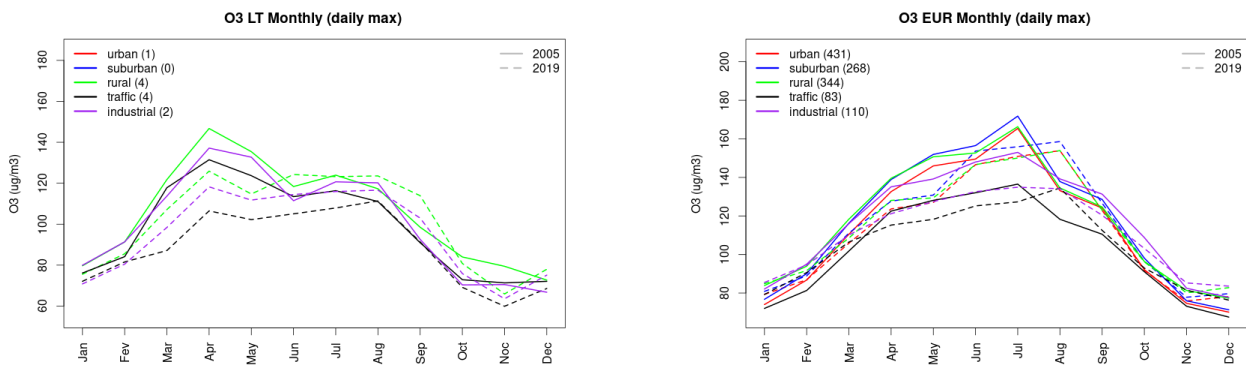


Figure S.391: Monthly cycle of daily max ozone for Lithuania (left) and Europe (right) at various station types estimated from the whole time series in 2005 (solid lines) and 2019

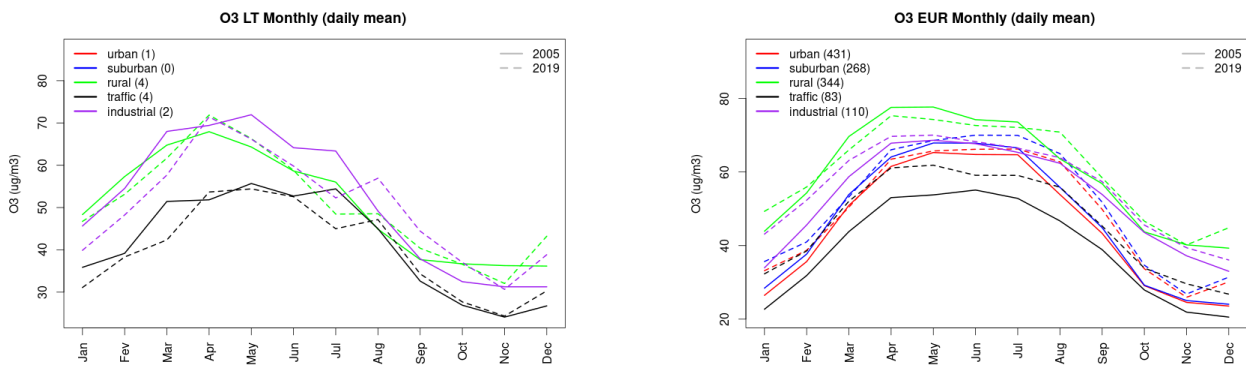


Figure S.392: Monthly cycle of daily mean ozone for Lithuania (left) and Europe (right) at various station types estimated from the whole time series in 2005 (solid lines) and 2019

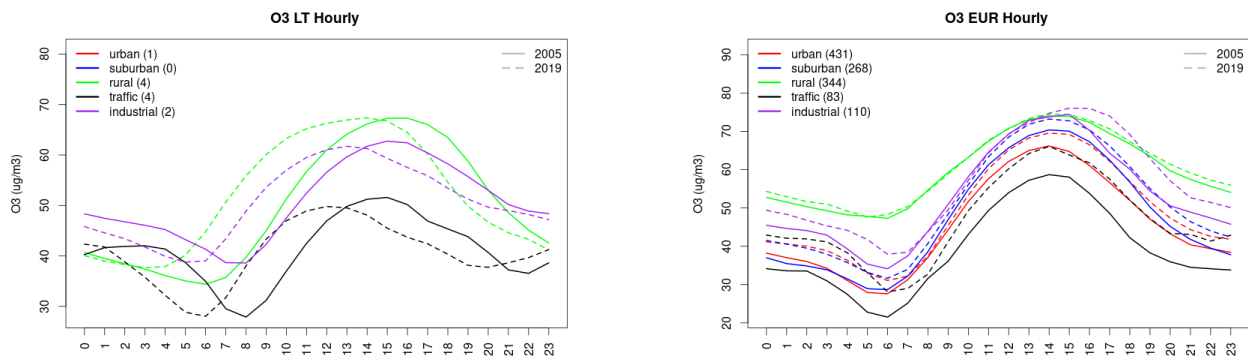


Figure S.393: Diurnal cycle of daily mean ozone for Lithuania (left) and Europe (right) at various station types estimated from the whole time series in 2005 (solid lines) and 2019

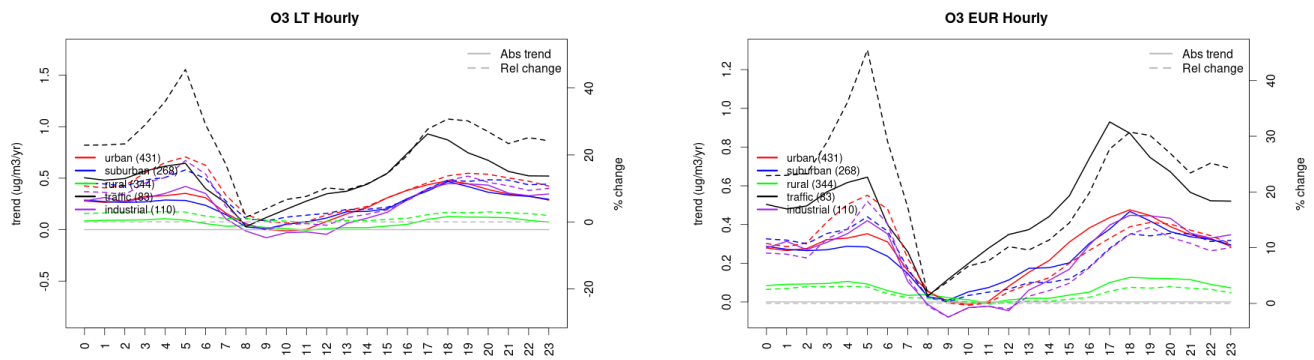


Figure S.394: Absolute (solid lines, left axis) and relative (dashed lines, right axis) trends in the diurnal cycle for Lithuania (left) and Europe (right) of ozone at various station type.

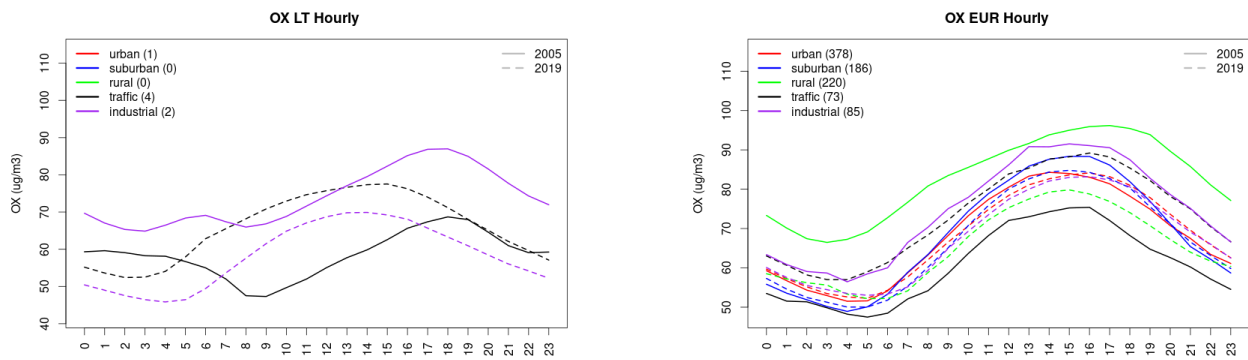


Figure S.395: Diurnal cycle of daily mean OX (as $\text{NO}_2 + \text{O}_3$) for Lithuania (left) and Europe (right) at various station types estimated from the whole time series in 2005 (solid lines) and 2019

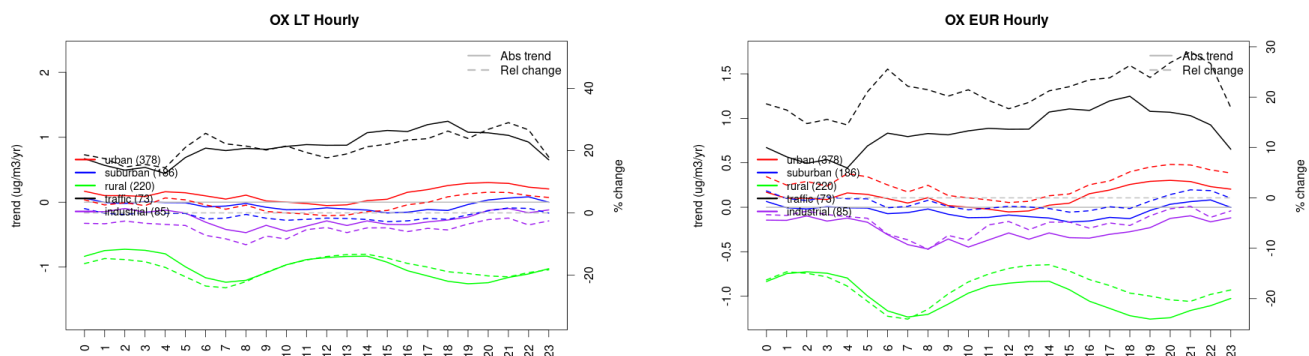


Figure S.396: Absolute (solid lines, left axis) and relative (dashed lines, right axis) trends in the diurnal cycle for Lithuania (left) and Europe (right) of OX (as NO₂+O₃) at various station type.

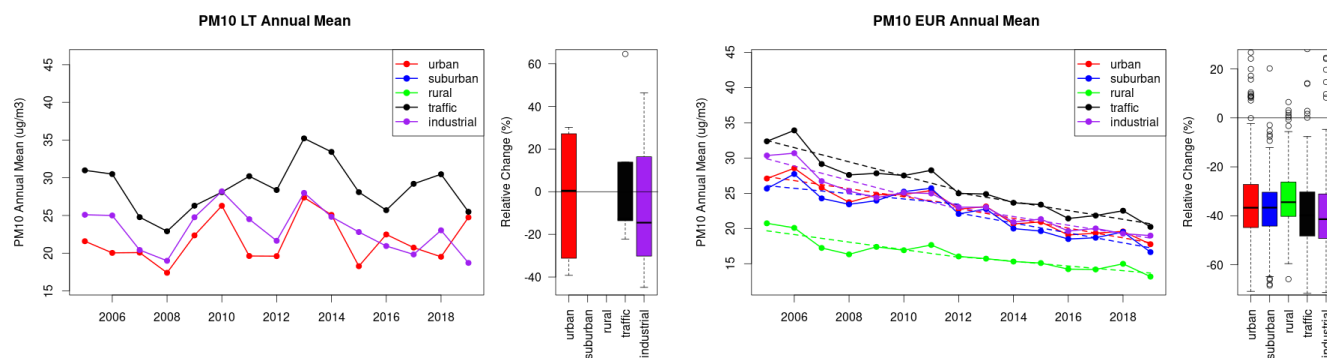


Figure S.397: Time series of the Lithuania (left) and European-wide composite (median) of annual mean PM₁₀ (ug/m³) per station type and area (red: urban background, blue suburban background, green: rural background, black: traffic, violet: industrial) between 2005 and 2019. In the European composite, the dashed lines show the linear fit between 2005 & 2012 and between 2012 & 2019. The boxplots on the right-hand side show the distribution of relative changes (%) between 2005 and 2019 for all stations of each typology in Lithuania and in Europe.

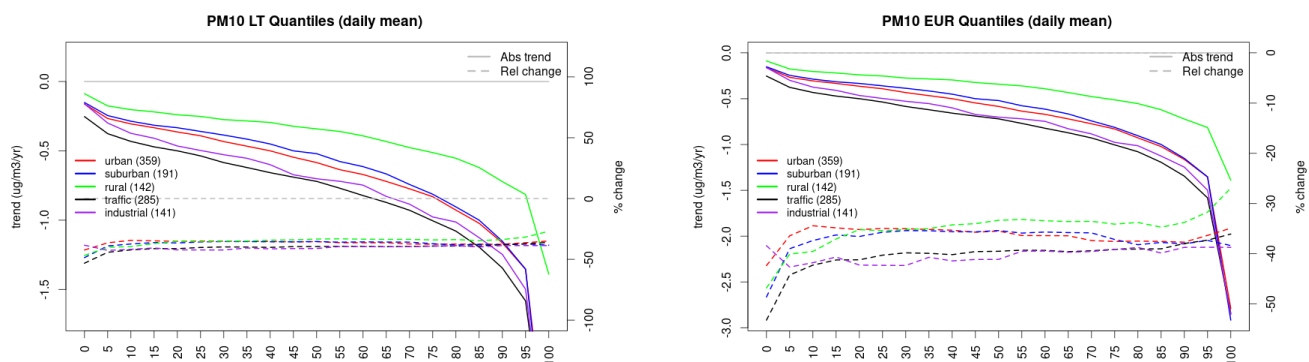


Figure S.398: For PM₁₀ in Lithuania (left) and Europe, and for each typology of station: absolute trend (solid lines, left y-axis) and relative change (dashed lines, right y-axis) of the percentiles of daily means.

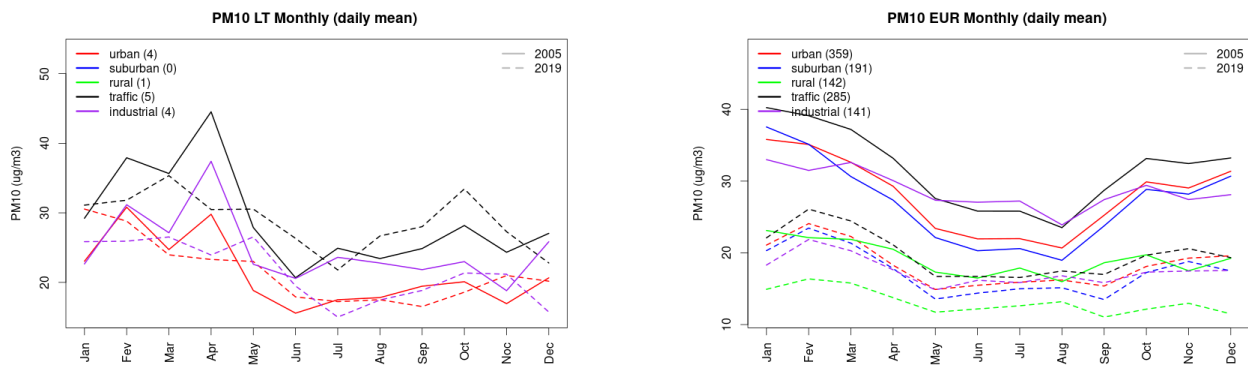


Figure S.399: Monthly cycle of daily mean PM10 for Lithuania (left) and Europe (right) at various station types estimated from the whole time series in 2005 (solid lines) and 2019

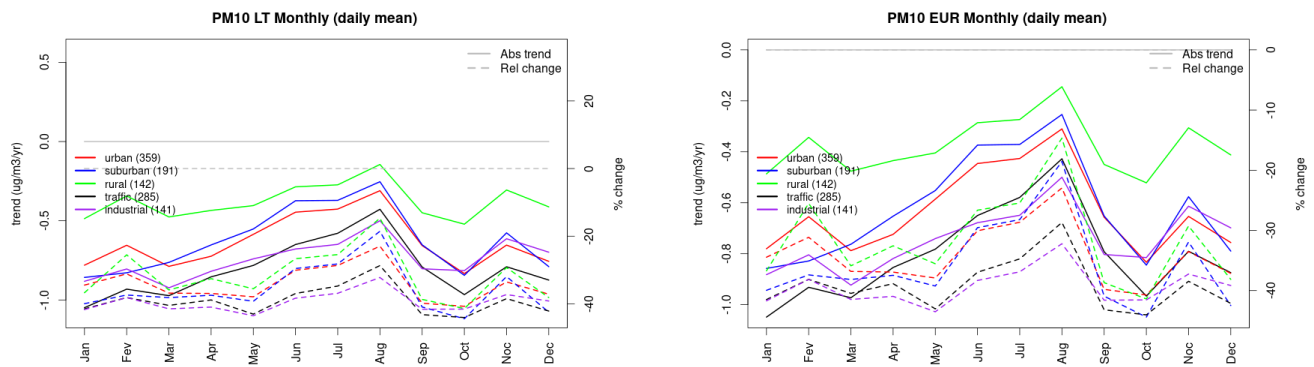


Figure S.400: Absolute (solid lines, left axis) and relative (dashed lines, right axis) trends in the monthly cycle for Lithuania (left) and Europe (right) of PM10 at various station type.

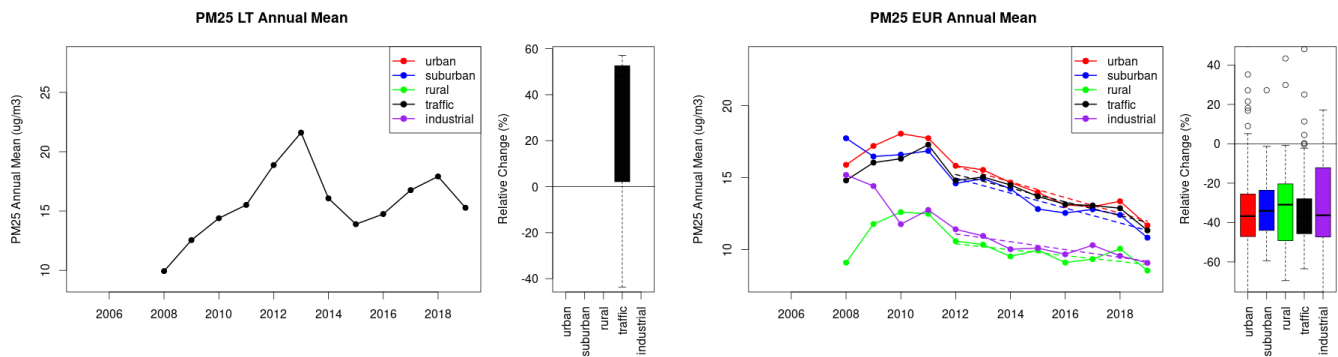


Figure S.401: Time series of the Lithuania (left) and European-wide composite (median) of annual mean PM25 ($\mu\text{g}/\text{m}^3$) per station type and area (red: urban background, blue suburban background, green: rural background, black: traffic, violet: industrial) between 2005 and 2019. In the European composite, the dashed lines show the linear fit between 2005 & 2012 and between 2012 & 2019. The boxplots on the right-hand side show the distribution of relative changes (%) between 2005 and 2019 for all stations of each typology in Lithuania and in Europe.

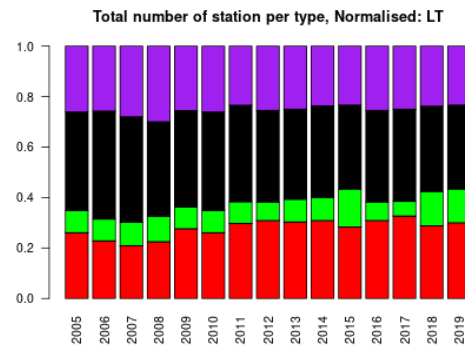
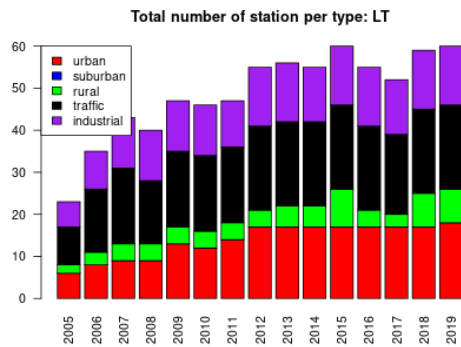
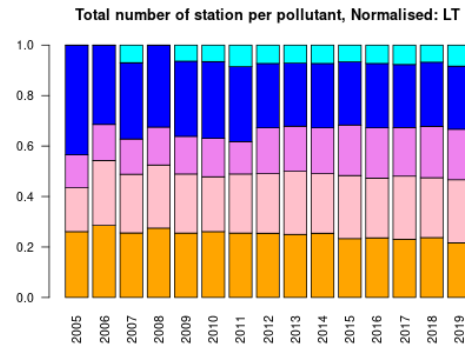
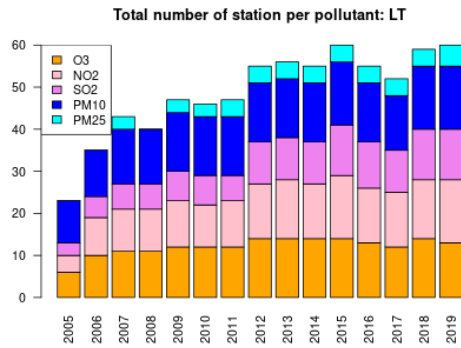
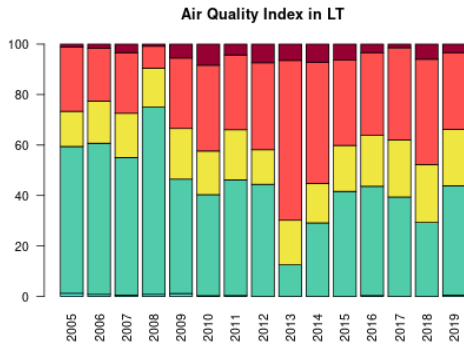


Figure S.402: For Lithuania: overall air quality index (percentage of days in a given year) and distribution of daily categories per pollutant (light blue: good, light green: fair, yellow: moderate, orange: poor, red: very poor, violet: extremely poor).

19 Luxembourg

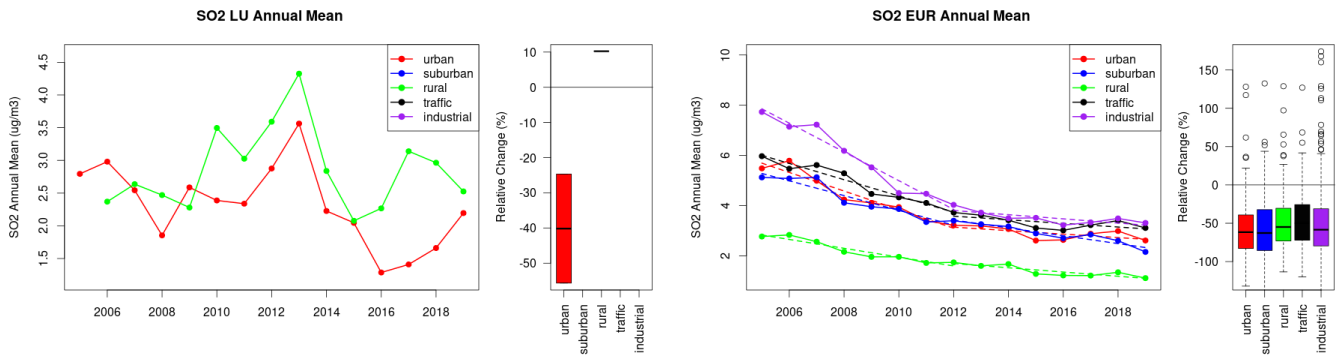


Figure S.403: Time series of the Luxembourg (left) and European-wide composite (median) of annual mean SO₂ (ug/m³) per station type and area (red: urban background, blue suburban background, green: rural background, black: traffic, violet: industrial) between 2005 and 2019. In the European composite, the dashed lines show the linear fit between 2005 & 2012 and between 2012 & 2019. The boxplots on the right-hand side show the distribution of relative changes (%) between 2005 and 2019 for all stations of each typology in Luxembourg and in Europe.

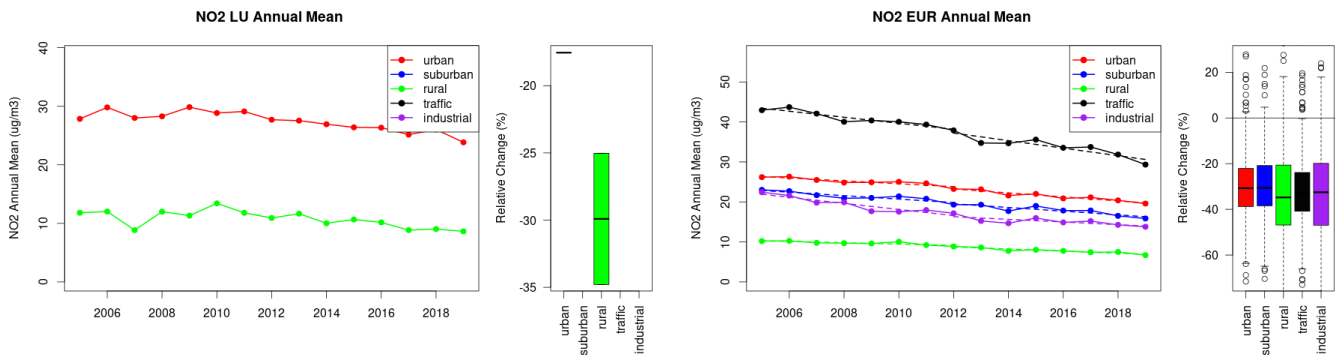


Figure S.404: Time series of the Luxembourg (left) and European-wide composite (median) of annual mean NO₂ (ug/m³) per station type and area (red: urban background, blue suburban background, green: rural background, black: traffic, violet: industrial) between 2005 and 2019. In the European composite, the dashed lines show the linear fit between 2005 & 2012 and between 2012 & 2019. The boxplots on the right-hand side show the distribution of relative changes (%) between 2005 and 2019 for all stations of each typology in Luxembourg and in Europe.

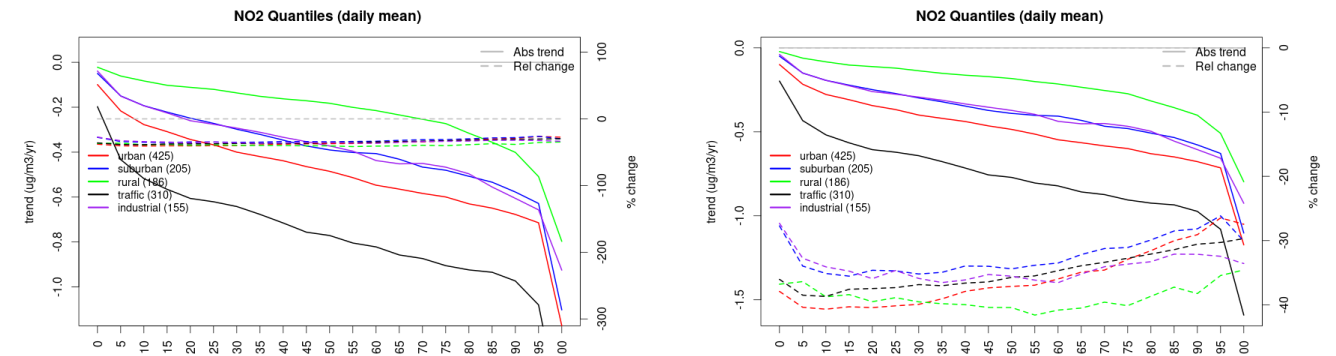


Figure S.405: For NO₂ in Luxembourg (left) and Europe, and for each typology of station: absolute trend (solid lines, left y-axis) and relative change (dashed lines, right y-axis) of the percentiles of daily means.

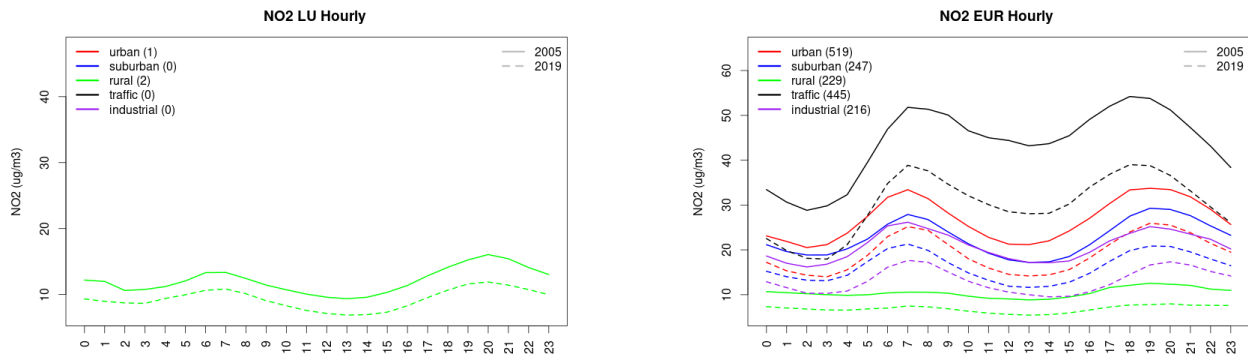


Figure S.406: Diurnal cycle of daily mean NO2 for Luxembourg (left) and Europe (right) at various station types estimated from the whole time series in 2005 (solid lines) and 2019

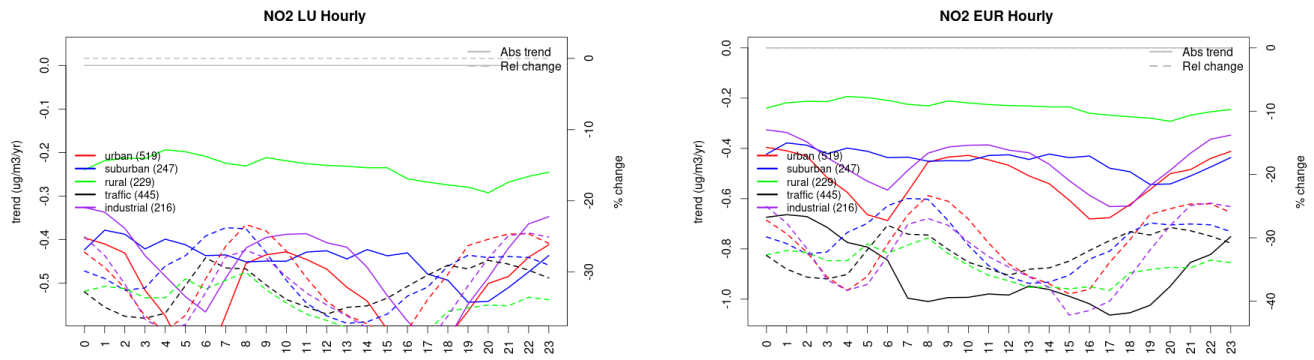


Figure S.407: Absolute (solid lines, left axis) and relative (dashed lines, right axis) trends in the diurnal cycle for Luxembourg (left) and Europe (right) of NO2 at various station type.

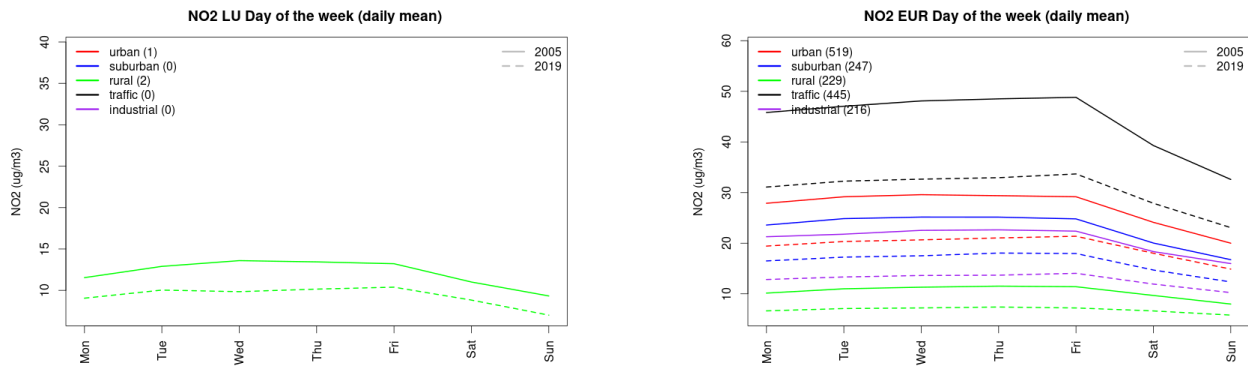


Figure S.408: Weekly cycle of daily mean NO2 for Luxembourg (left) and Europe (right) at various station types estimated from the whole time series in 2005 (solid lines) and 2019

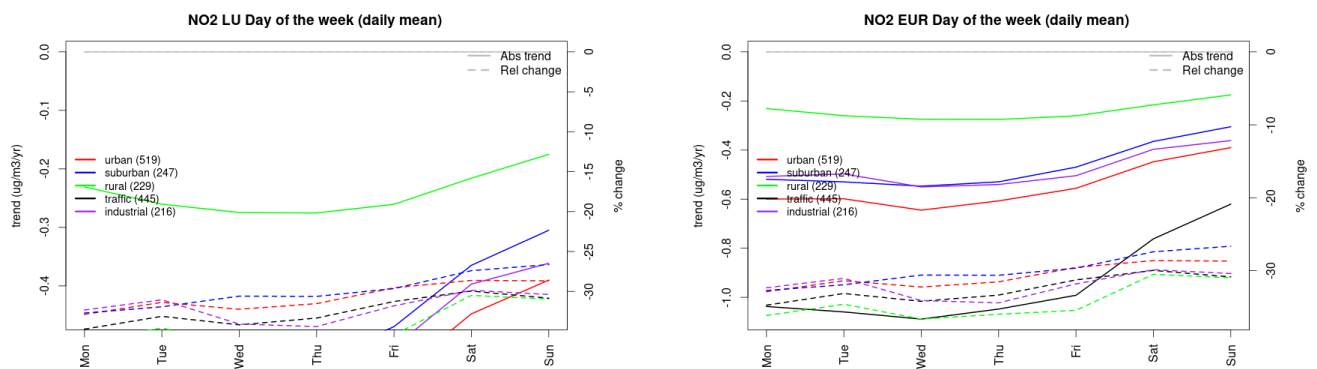


Figure S.409: Absolute (solid lines, left axis) and relative (dashed lines, right axis) trends in the weekly cycle for Luxembourg (left) and Europe (right) of NO₂ at various station type.

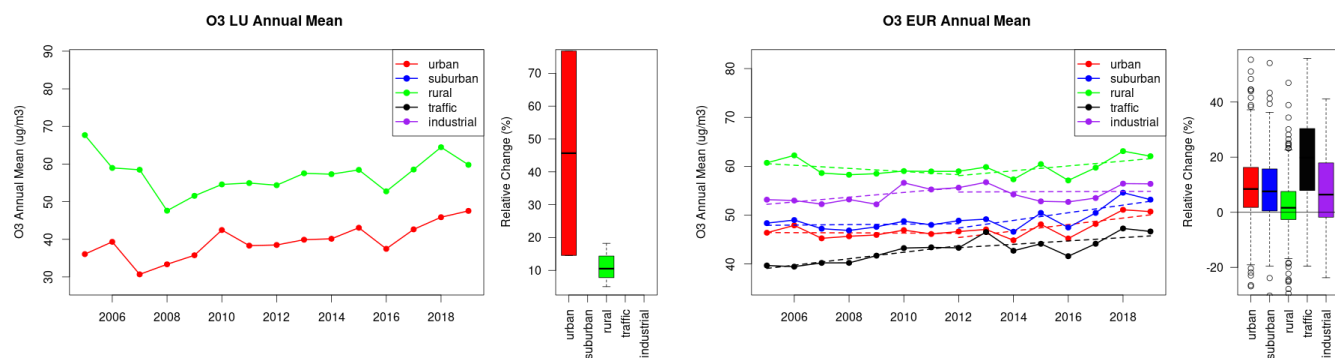


Figure S.410: Time series of the Luxembourg (left) and European-wide composite (median) of annual mean ozone (ug/m³) per station type and area (red: urban background, blue suburban background, green: rural background, black: traffic, violet: industrial) between 2005 and 2019. In the European composite, the dashed lines show the linear fit between 2005 & 2012 and between 2012 & 2019. The boxplots on the right-hand side show the distribution of relative changes (%) between 2005 and 2019 for all stations of each typology in Luxembourg and in Europe.

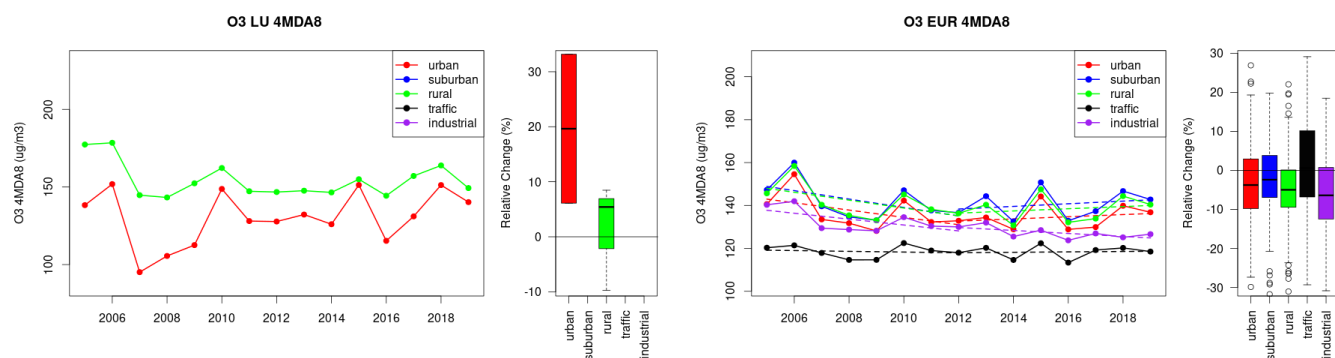


Figure S.411: Time series of the Luxembourg (left) and European-wide composite (median) of O₃ fourth highest daily peak (4MDA8, ug/m³) per station type and area (red: urban background, blue suburban background, green: rural background, black: traffic, violet: industrial) between 2005 and 2019. In the European composite, the dashed lines show the linear fit between 2005 & 2012 and between 2012 & 2019. The boxplots on the right-hand side show the distribution of relative changes (%) between 2005 and 2019 for all stations of each typology in Luxembourg and in Europe.

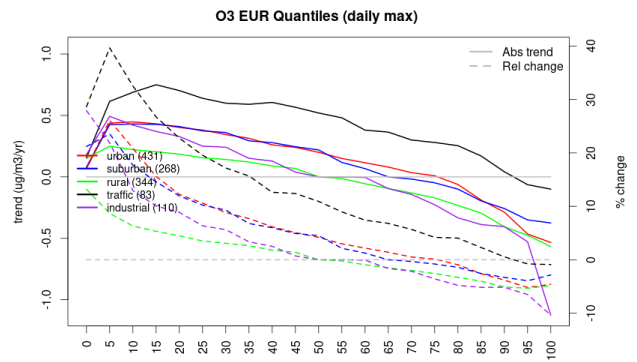
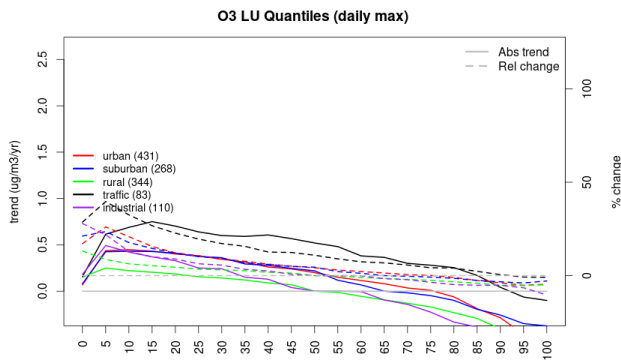


Figure S.412: For ozone in Luxembourg (left) and Europe, and for each typology of station: absolute trend (solid lines, left y-axis) and relative change (dashed lines, right y-axis) of the percentiles of daily maxima.

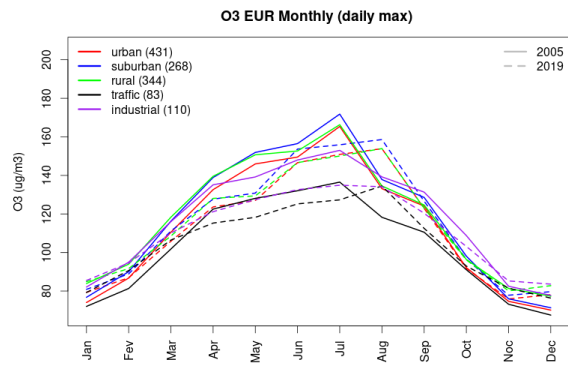
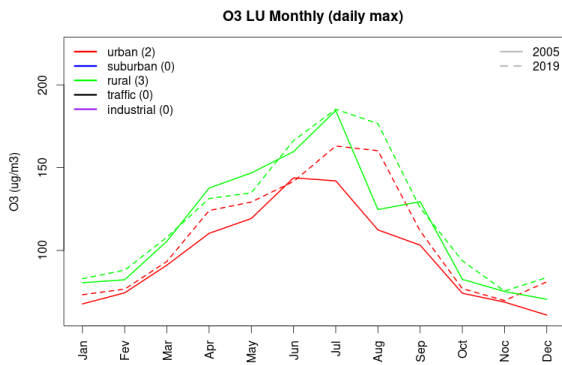


Figure S.413: Monthly cycle of daily max ozone for Luxembourg (left) and Europe (right) at various station types estimated from the whole time series in 2005 (solid lines) and 2019

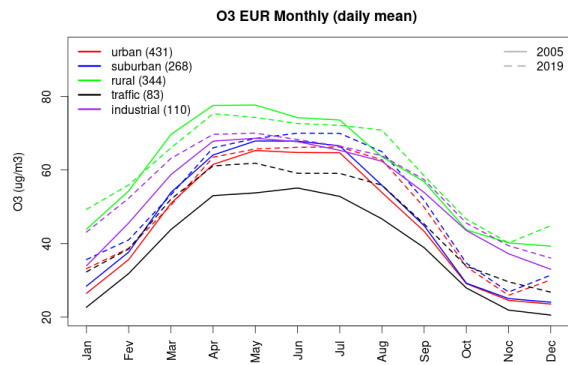
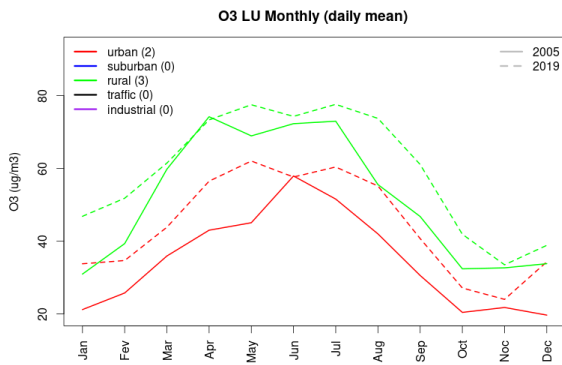


Figure S.414: Monthly cycle of daily mean ozone for Luxembourg (left) and Europe (right) at various station types estimated from the whole time series in 2005 (solid lines) and 2019

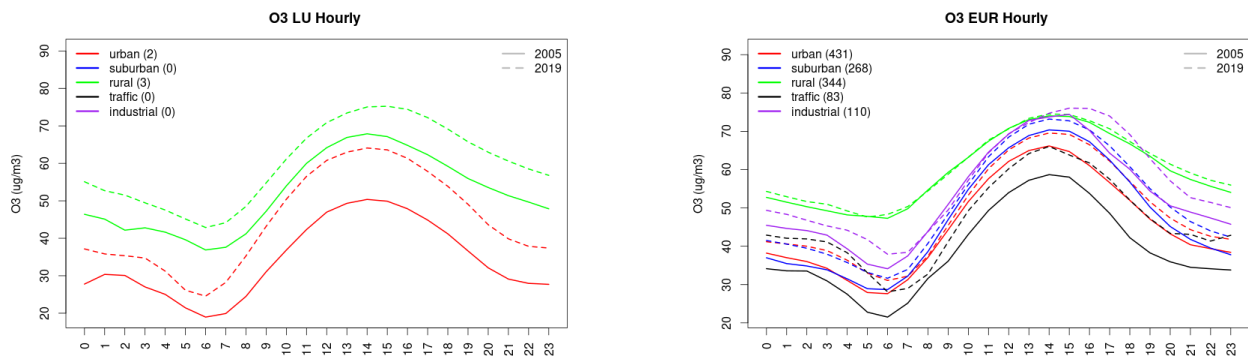


Figure S.415: Diurnal cycle of daily mean ozone for Luxembourg (left) and Europe (right) at various station types estimated from the whole time series in 2005 (solid lines) and 2019

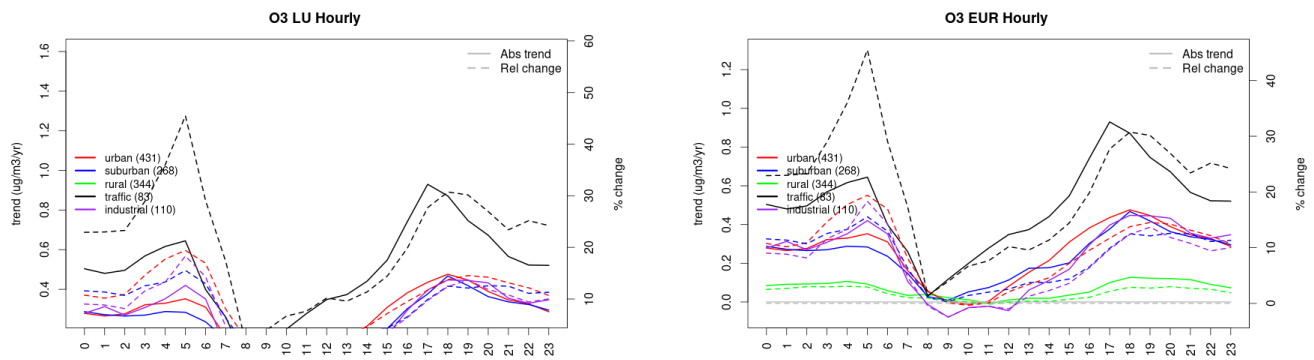


Figure S.416: Absolute (solid lines, left axis) and relative (dashed lines, right axis) trends in the diurnal cycle for Luxembourg (left) and Europe (right) of ozone at various station type.

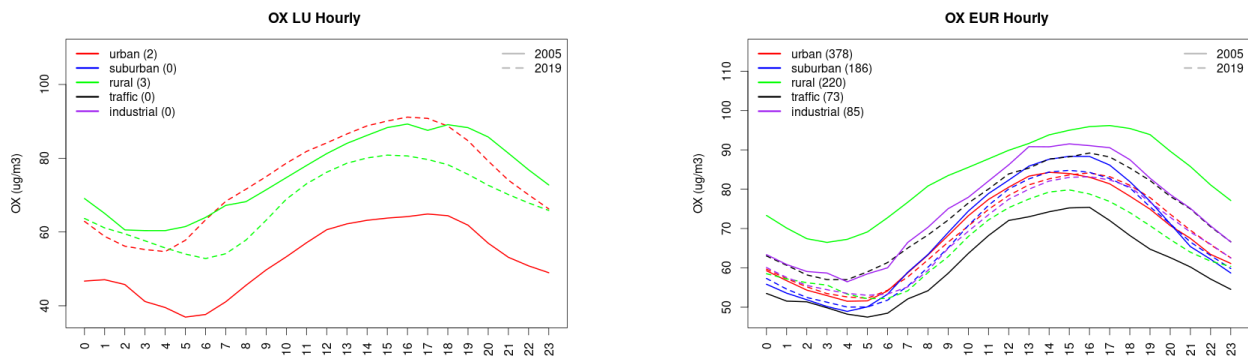


Figure S.417: Diurnal cycle of daily mean OX (as $\text{NO}_2 + \text{O}_3$) for Luxembourg (left) and Europe (right) at various station types estimated from the whole time series in 2005 (solid lines) and 2019

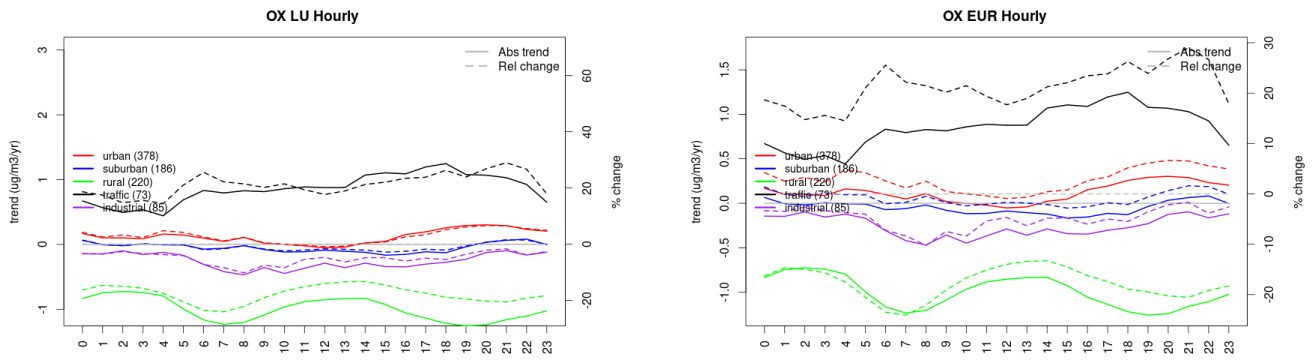


Figure S.418: Absolute (solid lines, left axis) and relative (dashed lines, right axis) trends in the diurnal cycle for Luxembourg (left) and Europe (right) of OX (as NO₂+O₃) at various station type.

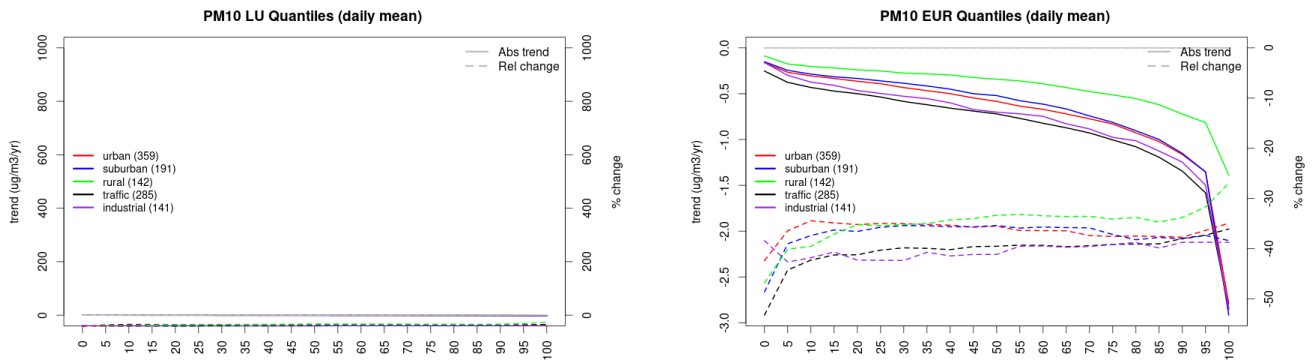


Figure S.419: For PM₁₀ in Luxembourg (left) and Europe, and for each typology of station: absolute trend (solid lines, left y-axis) and relative change (dashed lines, right y-axis) of the percentiles of daily means.

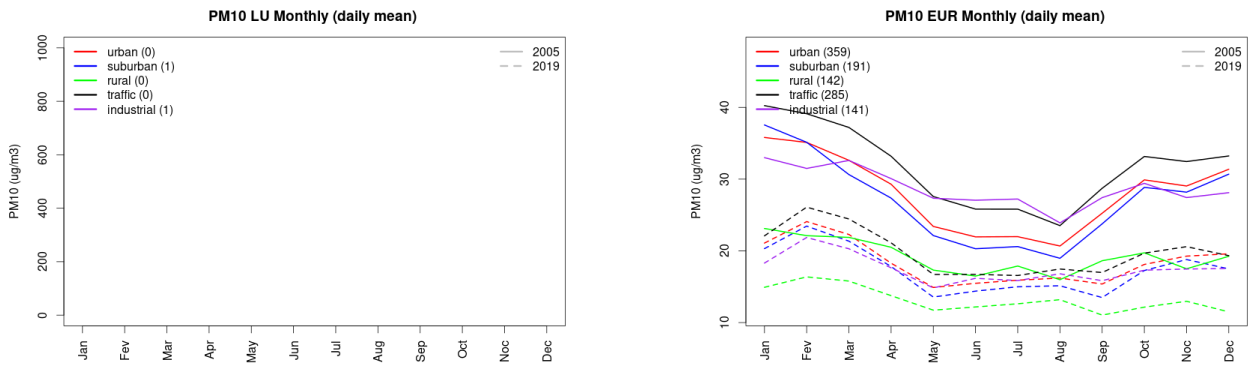


Figure S.420: Monthly cycle of daily mean PM₁₀ for Luxembourg (left) and Europe (right) at various station types estimated from the whole time series in 2005 (solid lines) and 2019

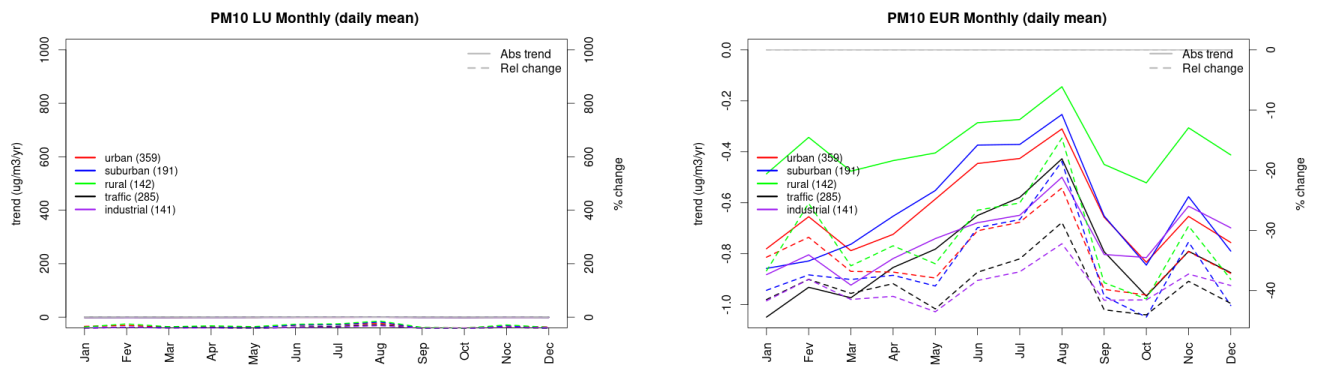


Figure S.421: Absolute (solid lines, left axis) and relative (dashed lines, right axis) trends in the monthly cycle for Luxembourg (left) and Europe (right) of PM10 at various station type.

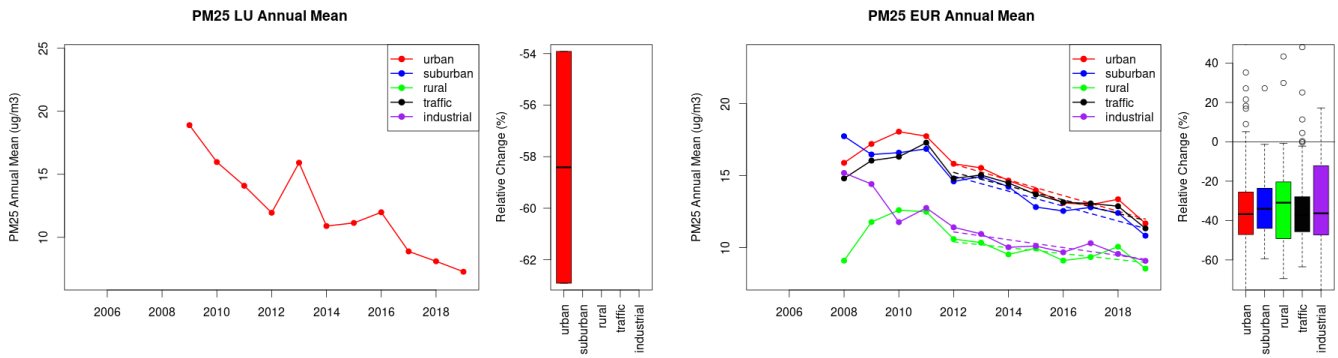


Figure S.422: Time series of the Luxembourg (left) and European-wide composite (median) of annual mean PM25 ($\mu\text{g}/\text{m}^3$) per station type and area (red: urban background, blue suburban background, green: rural background, black: traffic, violet: industrial) between 2005 and 2019. In the European composite, the dashed lines show the linear fit between 2005 & 2012 and between 2012 & 2019. The boxplots on the right-hand side show the distribution of relative changes (%) between 2005 and 2019 for all stations of each typology in Luxembourg and in Europe.

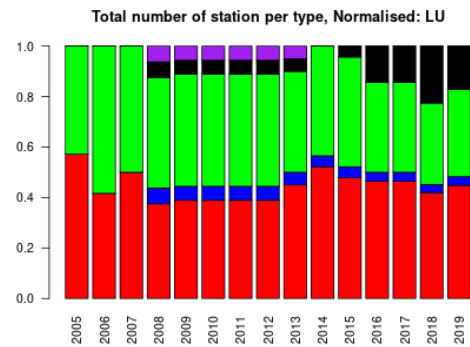
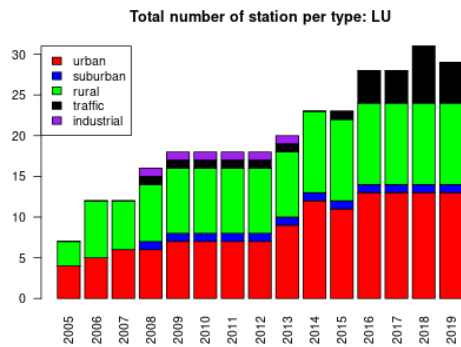
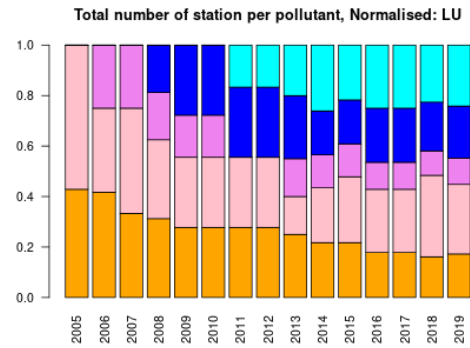
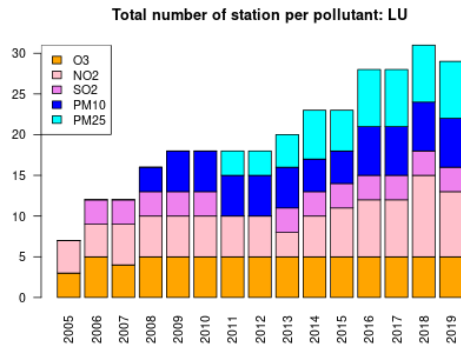
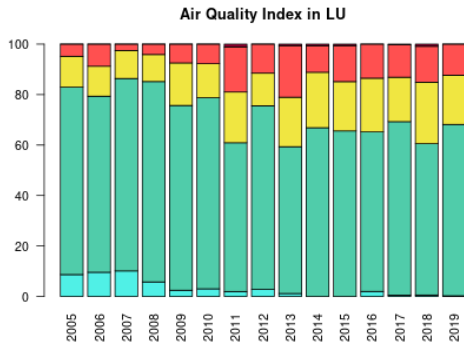


Figure S.423: For Luxembourg: overall air quality index (percentage of days in a given year) and distribution of daily categories per pollutant (light blue: good, light green: fair, yellow: moderate, orange: poor, red: very poor, violet: extremely poor).

20 Republic of North Macedonia

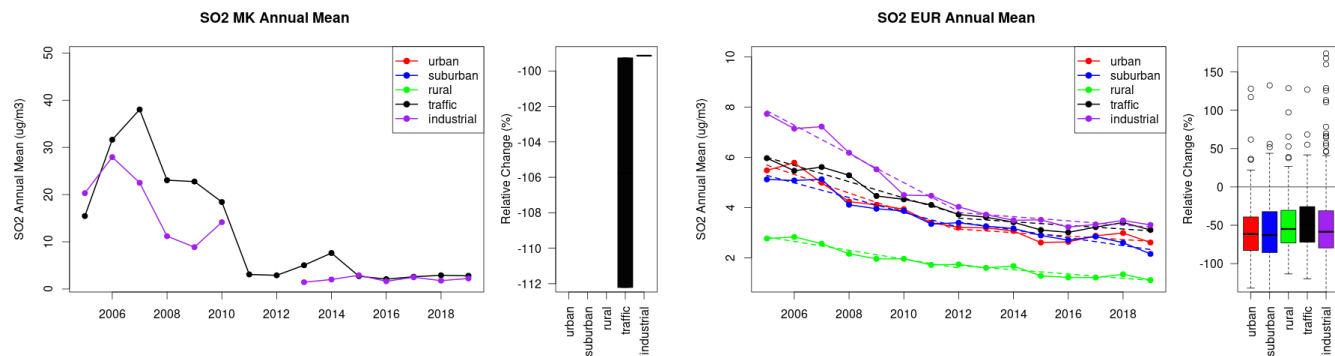


Figure S.424: Time series of the Republic of North Macedonia (left) and European-wide composite (median) of annual mean SO₂ (ug/m³) per station type and area (red: urban background, blue suburban background, green: rural background, black: traffic, violet: industrial) between 2005 and 2019. In the European composite, the dashed lines show the linear fit between 2005 & 2012 and between 2012 & 2019. The boxplots on the right-hand side show the distribution of relative changes (%) between 2005 and 2019 for all stations of each typology in Republic of North Macedonia and in Europe.

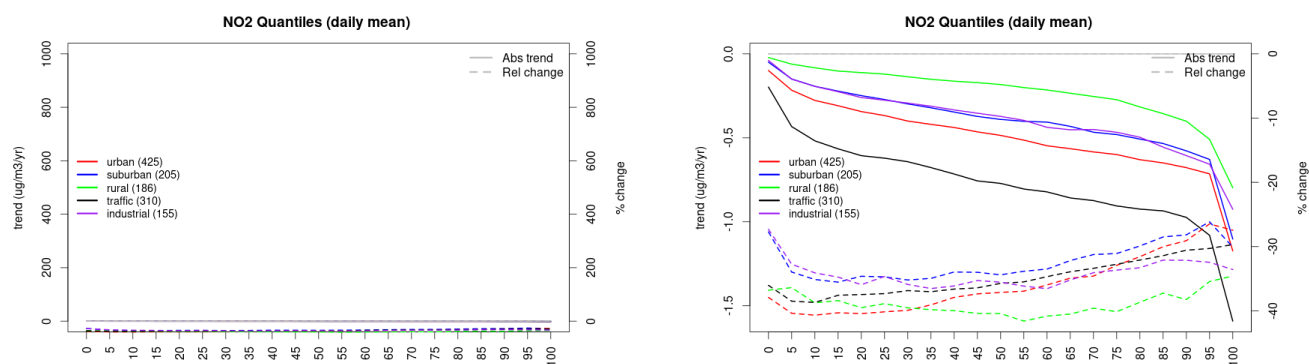


Figure S.425: For NO₂ in Republic of North Macedonia (left) and Europe, and for each typology of station: absolute trend (solid lines, left y-axis) and relative change (dashed lines, right y-axis) of the percentiles of daily means.

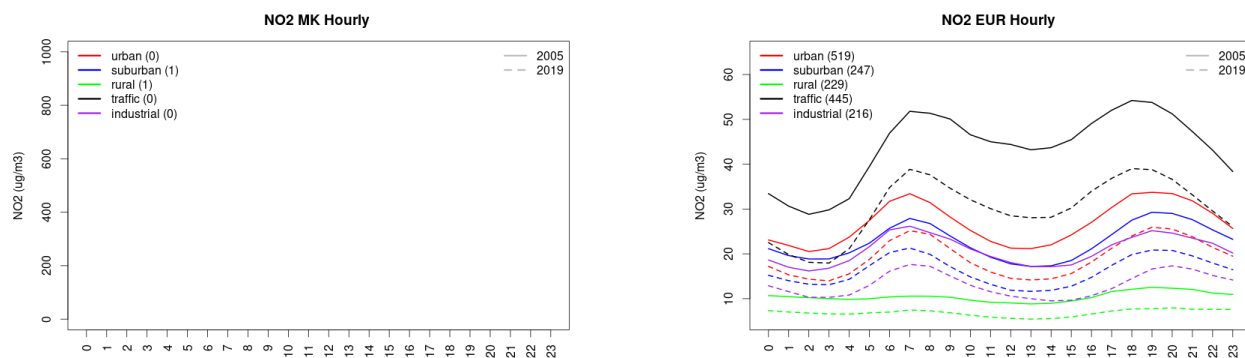


Figure S.426: Diurnal cycle of daily mean NO₂ for Republic of North Macedonia (left) and Europe (right) at various station types estimated from the whole time series in 2005 (solid lines) and 2019

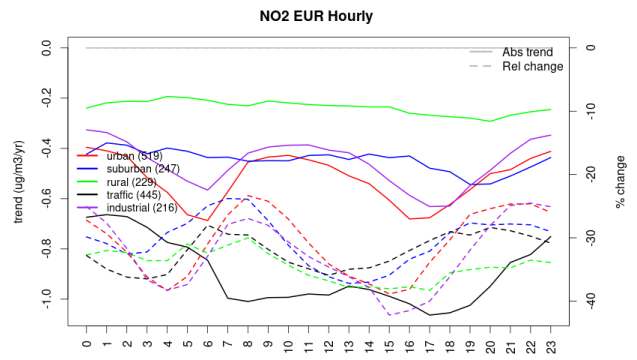
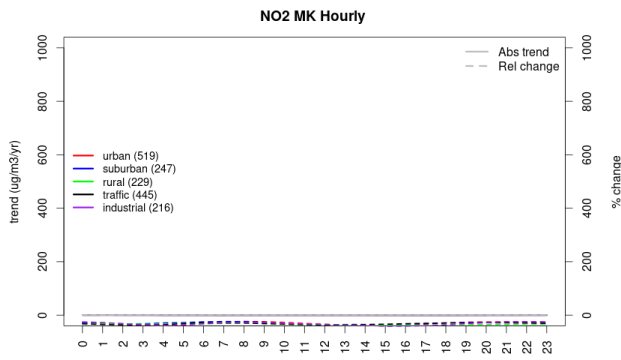


Figure S.427: Absolute (solid lines, left axis) and relative (dashed lines, right axis) trends in the diurnal cycle for Republic of North Macedonia (left) and Europe (right) of NO2 at various station type.

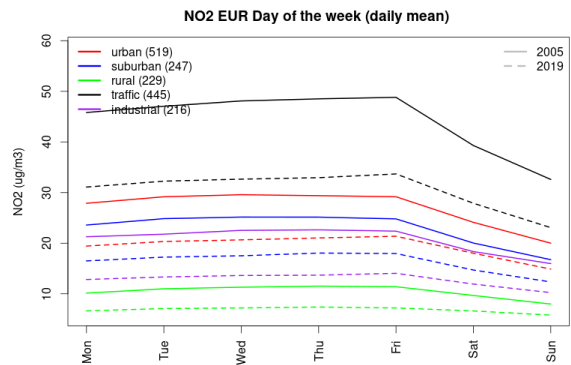
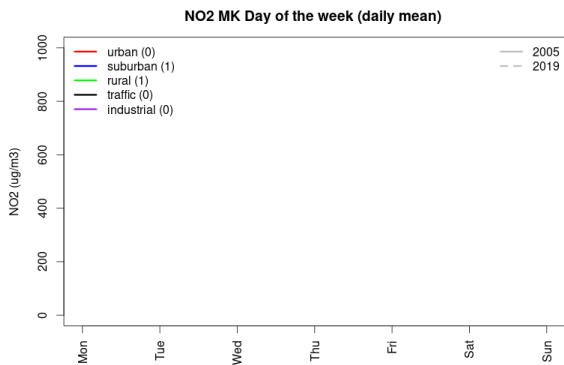


Figure S.428: Weekly cycle of daily mean NO2 for Republic of North Macedonia (left) and Europe (right) at various station types estimated from the whole time series in 2005 (solid lines) and 2019 (dashed lines).

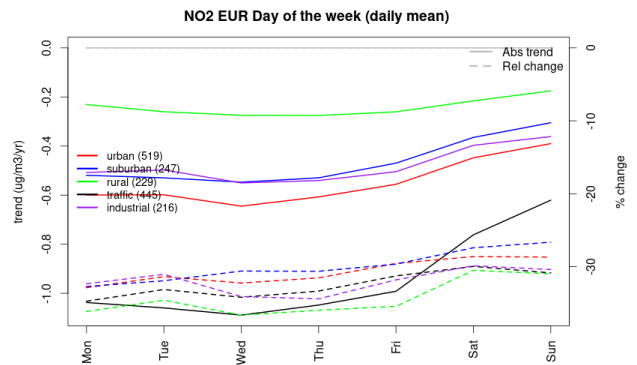
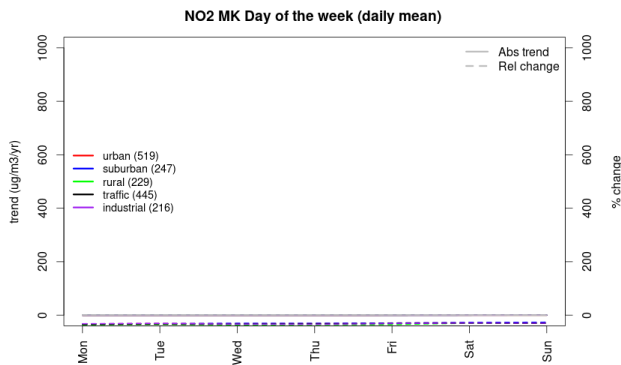


Figure S.429: Absolute (solid lines, left axis) and relative (dashed lines, right axis) trends in the weekly cycle for Republic of North Macedonia (left) and Europe (right) of NO2 at various station type.

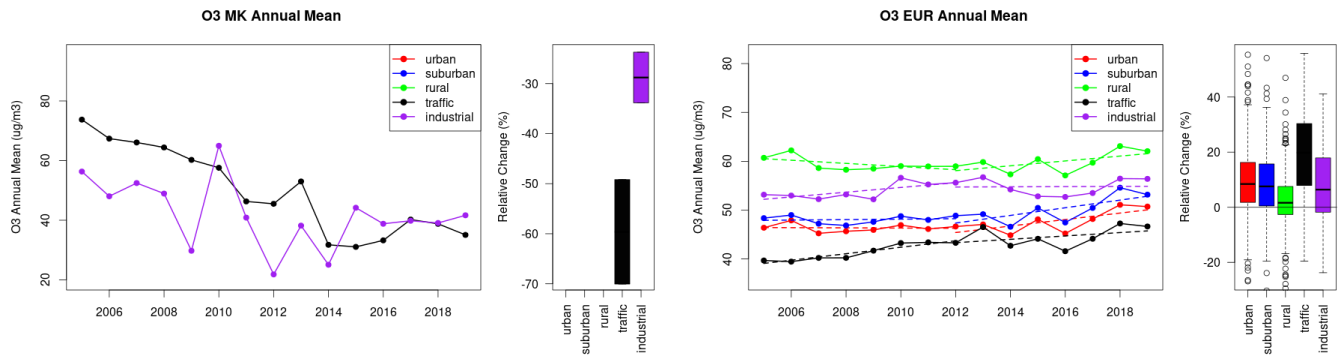


Figure S.430: Time series of the Republic of North Macedonia (left) and European-wide composite (median) of annual mean ozone ($\mu\text{g}/\text{m}^3$) per station type and area (red: urban background, blue suburban background, green: rural background, black: traffic, violet: industrial) between 2005 and 2019. In the European composite, the dashed lines show the linear fit between 2005 & 2012 and between 2012 & 2019. The boxplots on the right-hand side show the distribution of relative changes (%) between 2005 and 2019 for all stations of each typology in Republic of North Macedonia and in Europe.

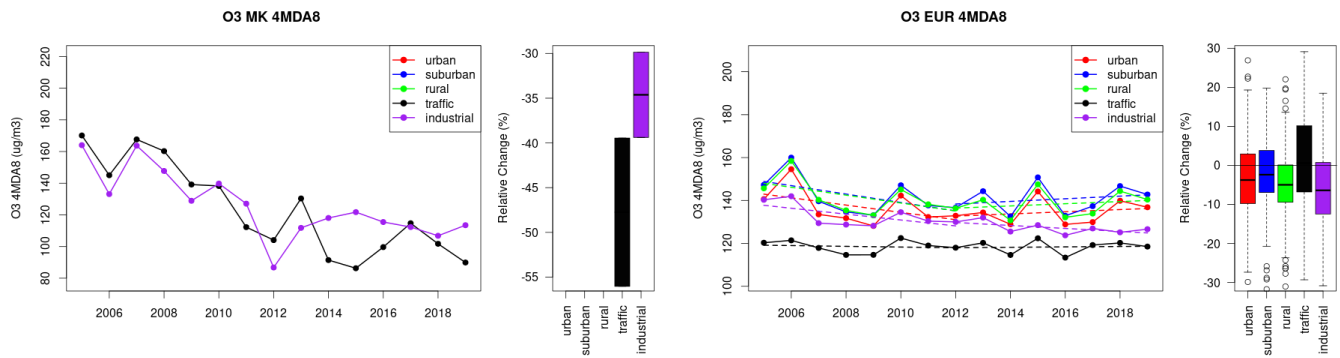


Figure S.431: Time series of the Republic of North Macedonia (left) and European-wide composite (median) of O3 fourth highest daily peak (4MDA8, $\mu\text{g}/\text{m}^3$) per station type and area (red: urban background, blue suburban background, green: rural background, black: traffic, violet: industrial) between 2005 and 2019. In the European composite, the dashed lines show the linear fit between 2005 & 2012 and between 2012 & 2019. The boxplots on the right-hand side show the distribution of relative changes (%) between 2005 and 2019 for all stations of each typology in Republic of North Macedonia and in Europe.

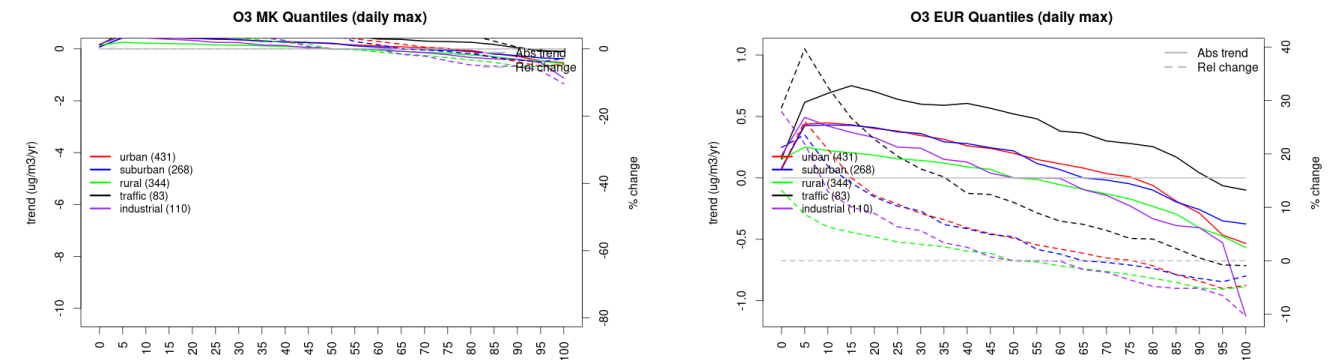


Figure S.432: For ozone in Republic of North Macedonia (left) and Europe, and for each typology of station: absolute trend (solid lines, left y-axis) and relative change (dashed lines, right y-axis) of the percentiles of daily maxima.

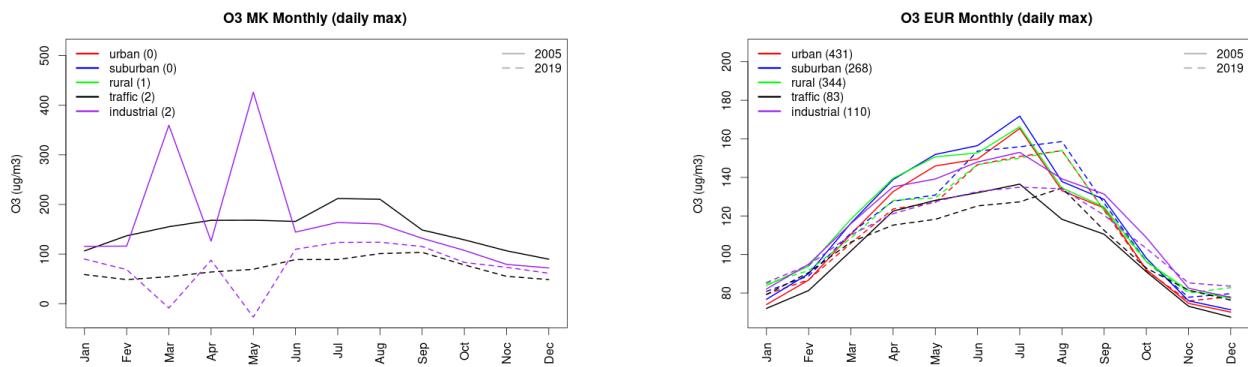


Figure S.433: Monthly cycle of daily max ozone for Republic of North Macedonia (left) and Europe (right) at various station types estimated from the whole time series in 2005 (solid lines) and 2019

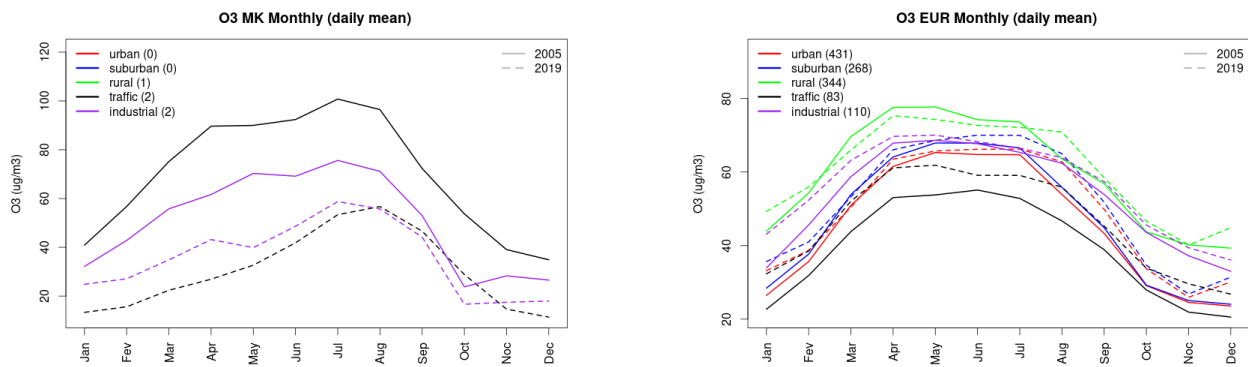


Figure S.434: Monthly cycle of daily mean ozone for Republic of North Macedonia (left) and Europe (right) at various station types estimated from the whole time series in 2005 (solid lines) and 2019

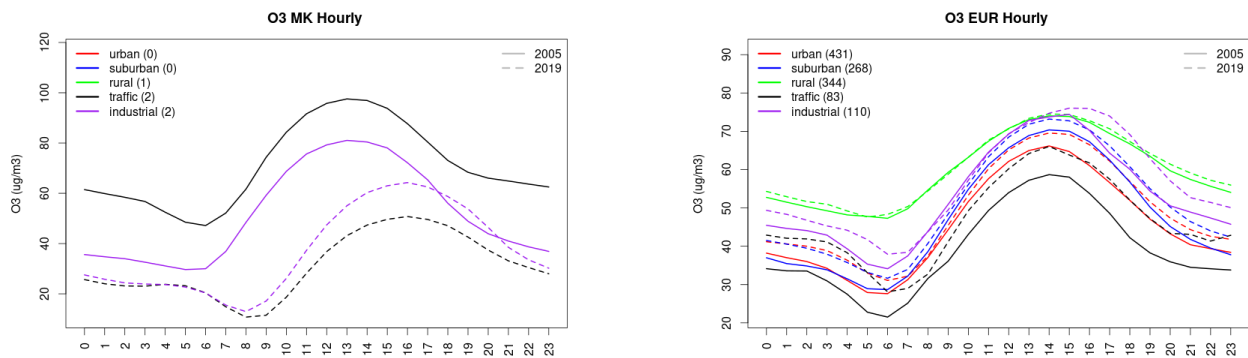


Figure S.435: Diurnal cycle of daily mean ozone for Republic of North Macedonia (left) and Europe (right) at various station types estimated from the whole time series in 2005 (solid lines) and 2019

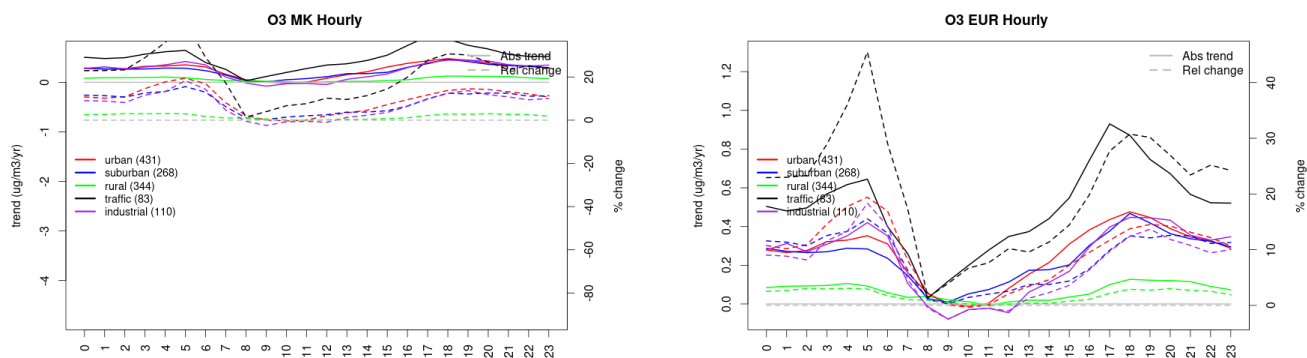


Figure S.436: Absolute (solid lines, left axis) and relative (dashed lines, right axis) trends in the diurnal cycle for Republic of North Macedonia (left) and Europe (right) of ozone at various station type.

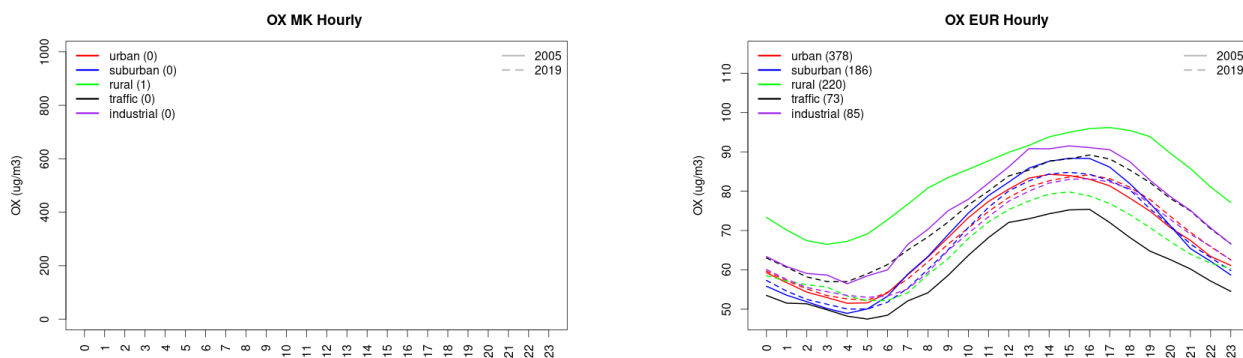


Figure S.437: Diurnal cycle of daily mean OX (as NO₂+O₃) for Republic of North Macedonia (left) and Europe (right) at various station types estimated from the whole time series in 2005 (solid lines) and 2019 (dashed lines).

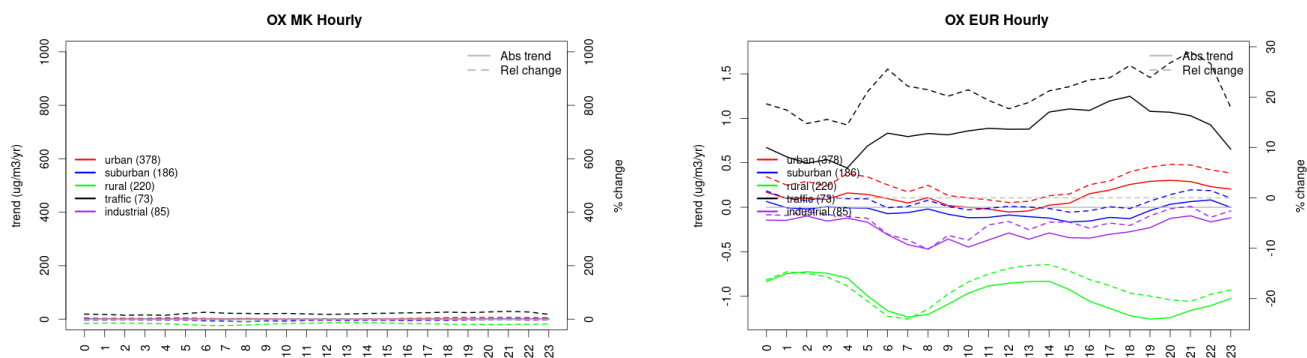


Figure S.438: Absolute (solid lines, left axis) and relative (dashed lines, right axis) trends in the diurnal cycle for Republic of North Macedonia (left) and Europe (right) of OX (as NO₂+O₃) at various station type.

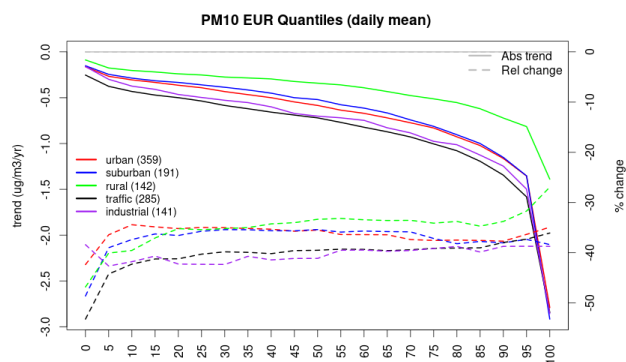
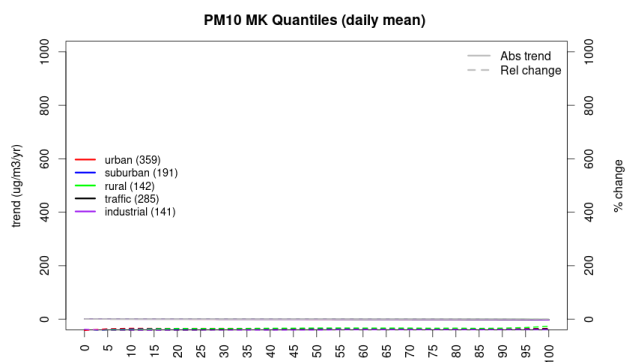


Figure S.439: For PM10 in Republic of North Macedonia (left) and Europe, and for each typology of station: absolute trend (solid lines, left y-axis) and relative change (dashed lines, right y-axis) of the percentiles of daily means.

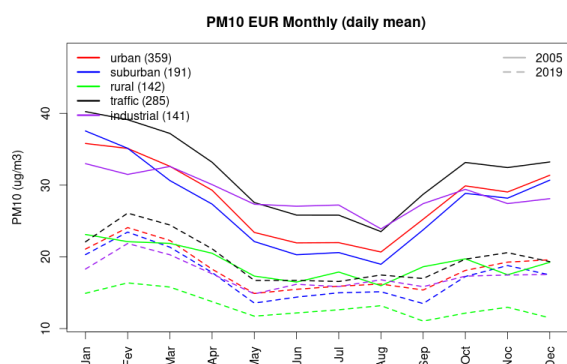
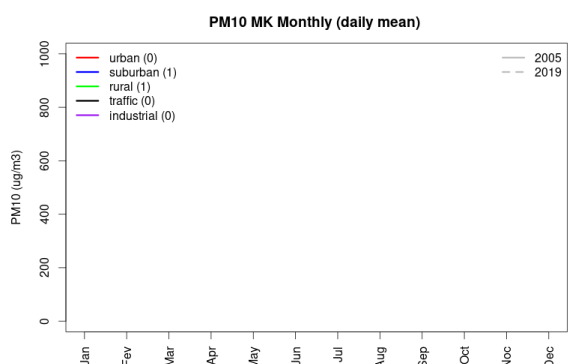


Figure S.440: Monthly cycle of daily mean PM10 for Republic of North Macedonia (left) and Europe (right) at various station types estimated from the whole time series in 2005 (solid lines) and 2019

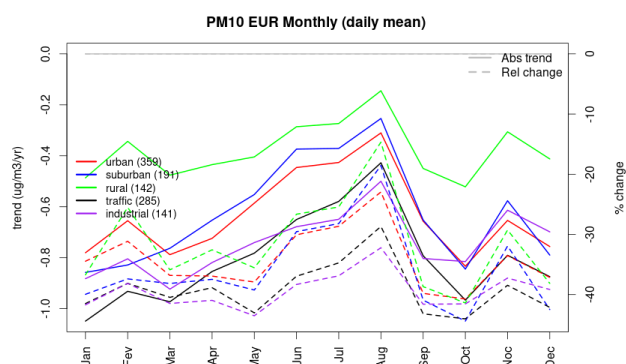
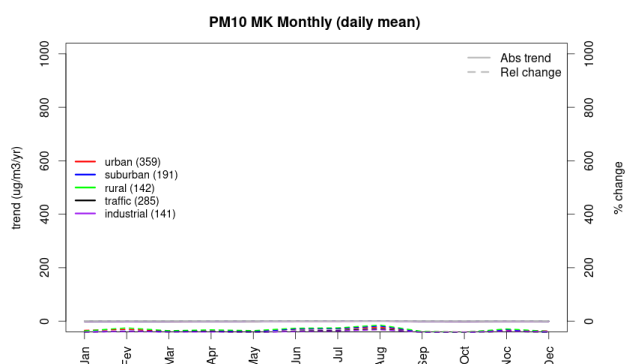


Figure S.441: Absolute (solid lines, left axis) and relative (dashed lines, right axis) trends in the monthly cycle for Republic of North Macedonia (left) and Europe (right) of PM10 at various station type.

21 Netherlands

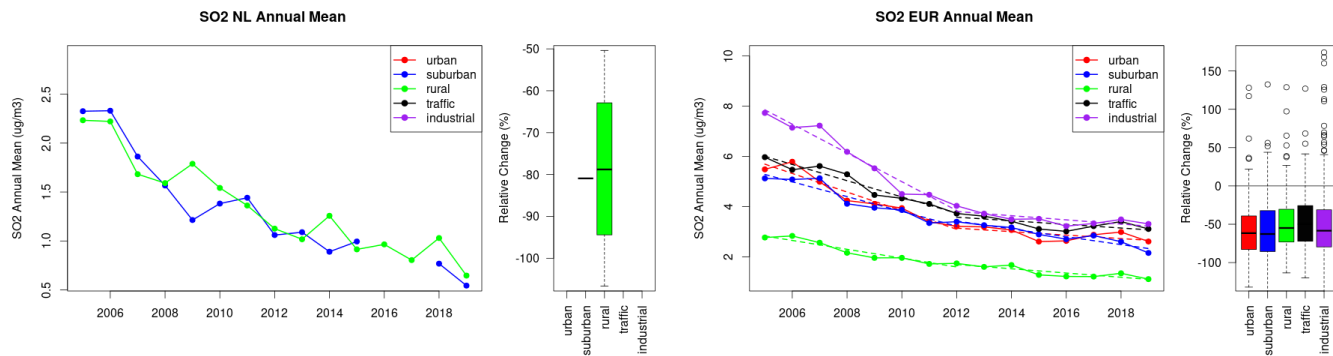


Figure S.442: Time series of the Netherlands (left) and European-wide composite (median) of annual mean SO₂ (ug/m³) per station type and area (red: urban background, blue suburban background, green: rural background, black: traffic, violet: industrial) between 2005 and 2019. In the European composite, the dashed lines show the linear fit between 2005 & 2012 and between 2012 & 2019. The boxplots on the right-hand side show the distribution of relative changes (%) between 2005 and 2019 for all stations of each typology in Netherlands and in Europe.

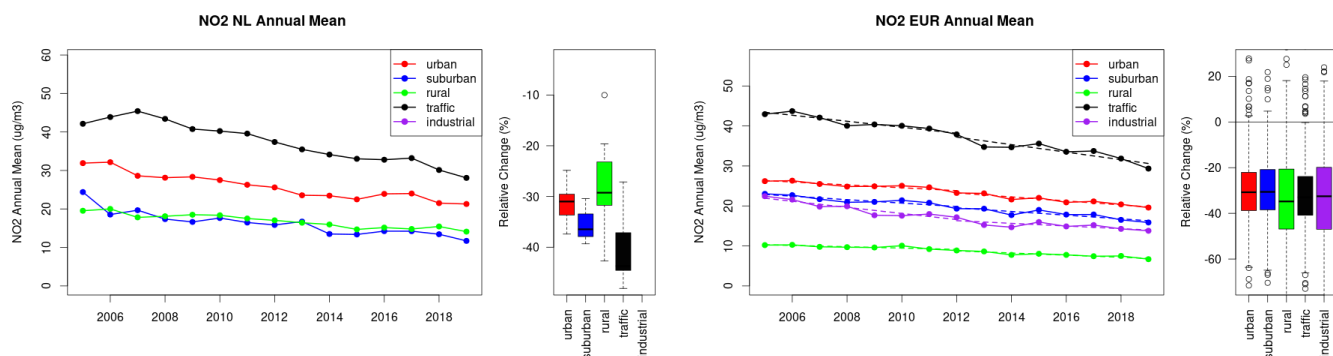


Figure S.443: Time series of the Netherlands (left) and European-wide composite (median) of annual mean NO₂ (ug/m³) per station type and area (red: urban background, blue suburban background, green: rural background, black: traffic, violet: industrial) between 2005 and 2019. In the European composite, the dashed lines show the linear fit between 2005 & 2012 and between 2012 & 2019. The boxplots on the right-hand side show the distribution of relative changes (%) between 2005 and 2019 for all stations of each typology in Netherlands and in Europe.

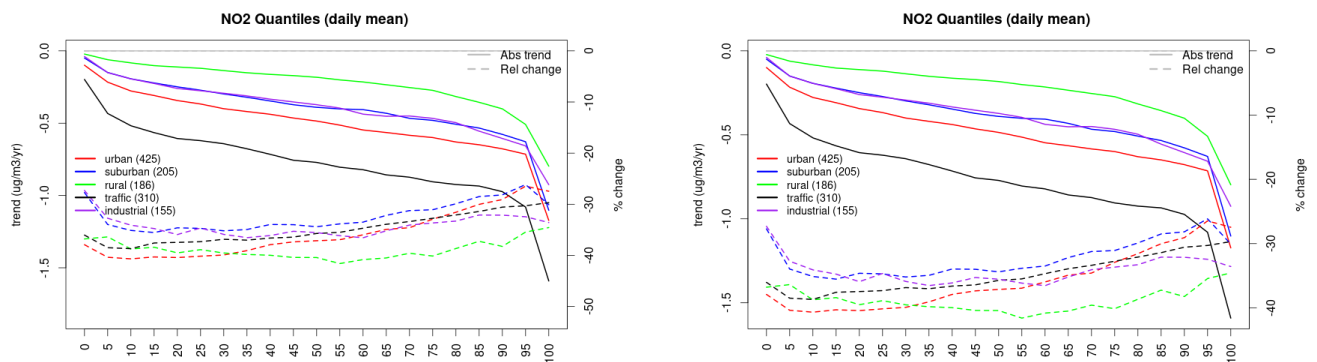


Figure S.444: For NO₂ in Netherlands (left) and Europe, and for each typology of station: absolute trend (solid lines, left y-axis) and relative change (dashed lines, right y-axis) of the percentiles of daily means.

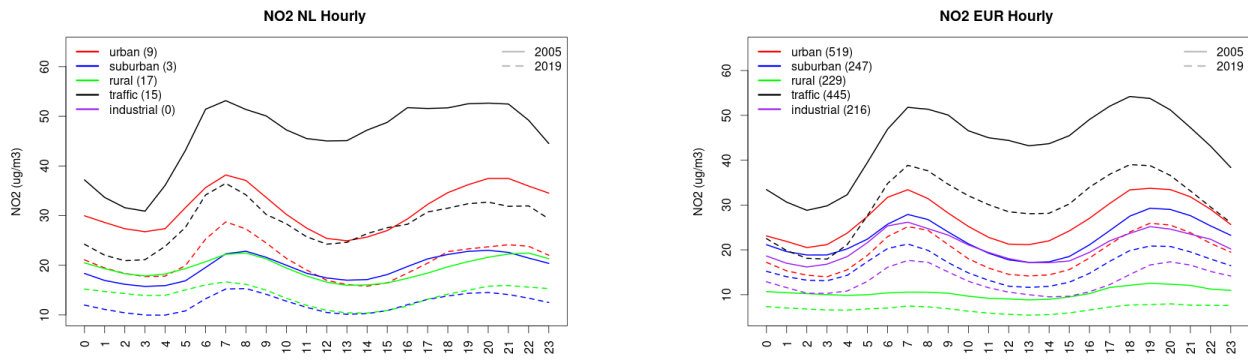


Figure S.445: Diurnal cycle of daily mean NO₂ for Netherlands (left) and Europe (right) at various station types estimated from the whole time series in 2005 (solid lines) and 2019

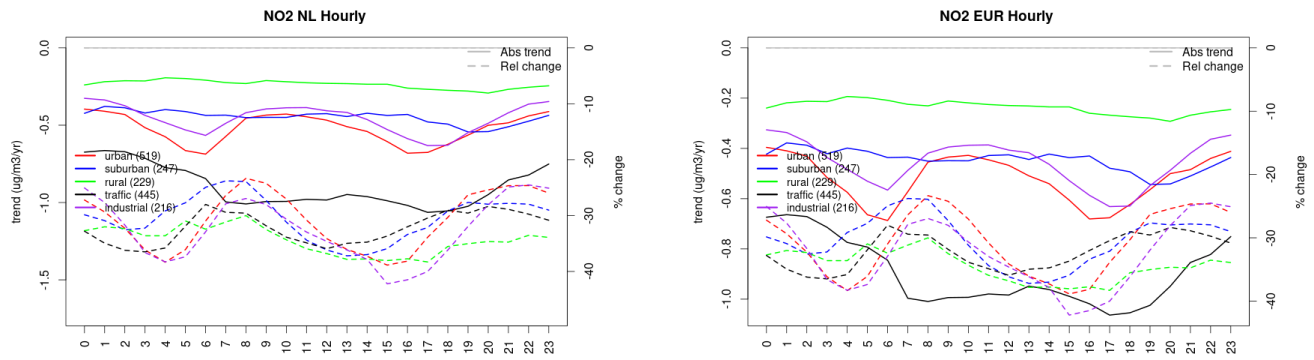


Figure S.446: Absolute (solid lines, left axis) and relative (dashed lines, right axis) trends in the diurnal cycle for Netherlands (left) and Europe (right) of NO₂ at various station type.

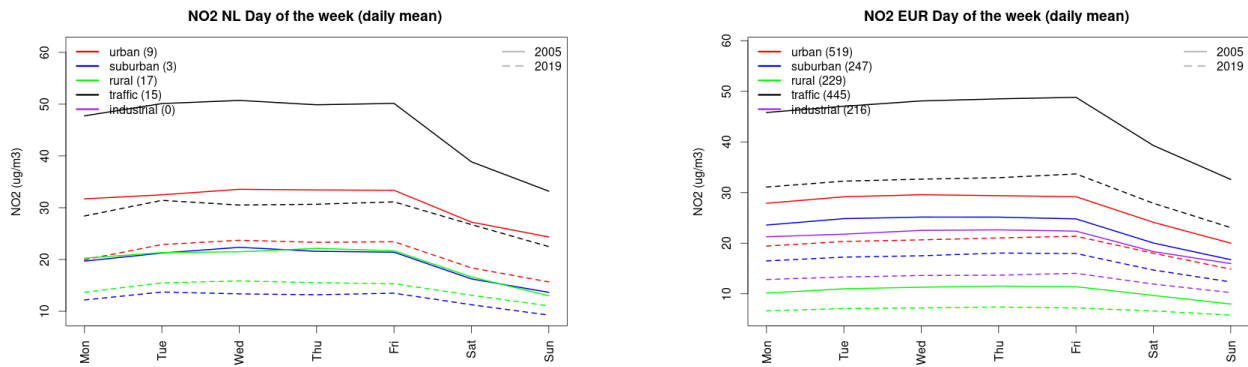


Figure S.447: Weekly cycle of daily mean NO₂ for Netherlands (left) and Europe (right) at various station types estimated from the whole time series in 2005 (solid lines) and 2019

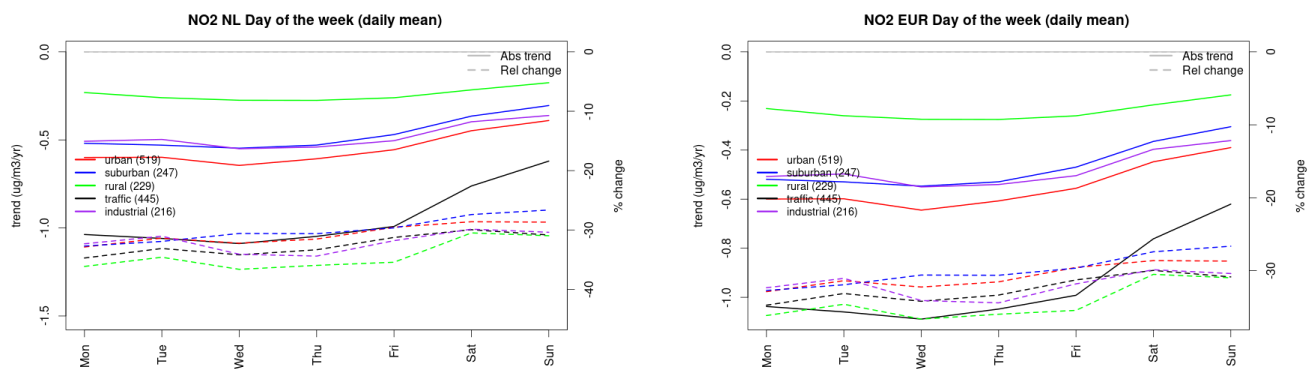


Figure S.448: Absolute (solid lines, left axis) and relative (dashed lines, right axis) trends in the weekly cycle for Netherlands (left) and Europe (right) of NO2 at various station type.

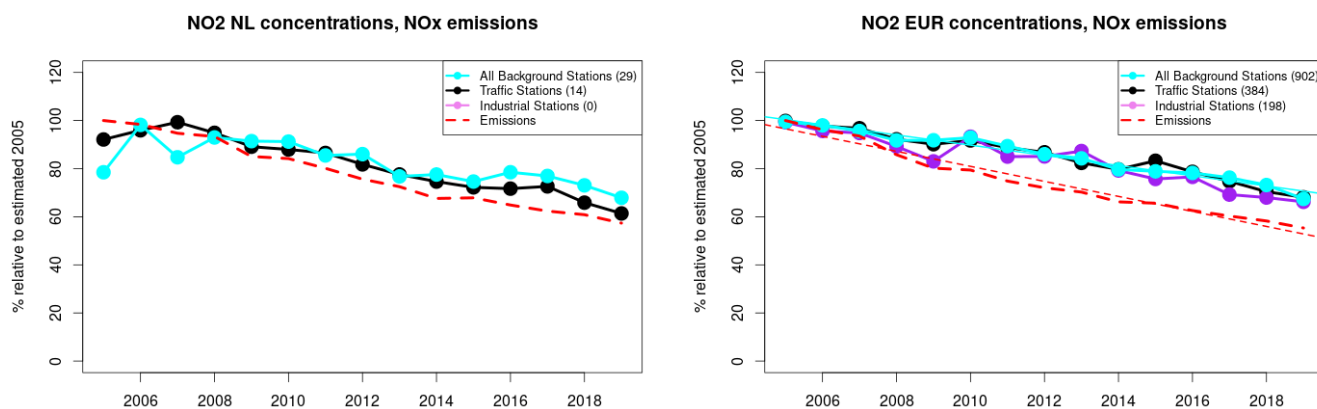


Figure S.449: Time series of 2005-2019 (left) and European (right) median NO2 observed at traffic (black), industrial (violet) and background (cyan) sites (solid lines), and corresponding NOx emissions (dashed line) normalised to estimated 2000 levels (%). The median is taken over where more than 5 stations of each typology is available. The total number of stations included is provided in brackets. In the European composite, straight lines are the linear fits over the whole period.

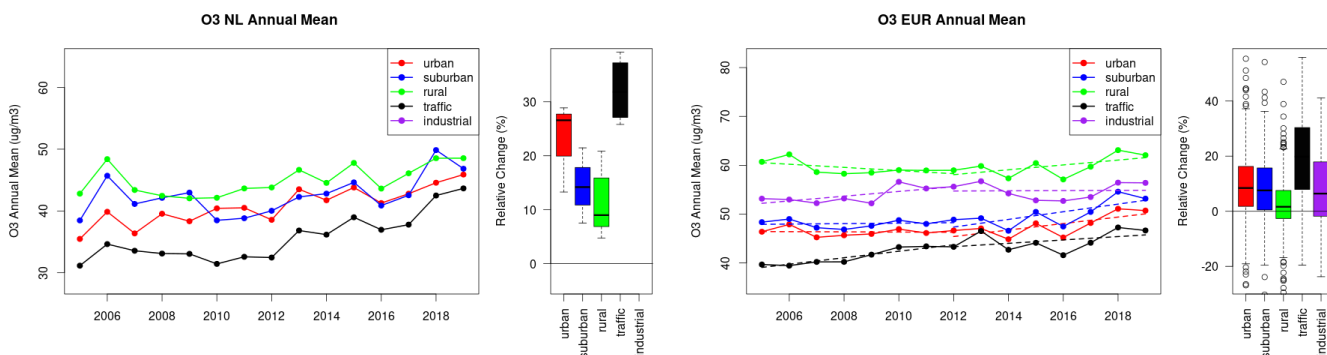


Figure S.450: Time series of the Netherlands (left) and European-wide composite (median) of annual mean ozone ($\mu\text{g}/\text{m}^3$) per station type and area (red: urban background, blue suburban background, green: rural background, black: traffic, violet: industrial) between 2005 and 2019. In the European composite, the dashed lines show the linear fit between 2005 & 2012 and between 2012 & 2019. The boxplots on the right-hand side show the distribution of relative changes (%) between 2005 and 2019 for all stations of each typology in Netherlands and in Europe.

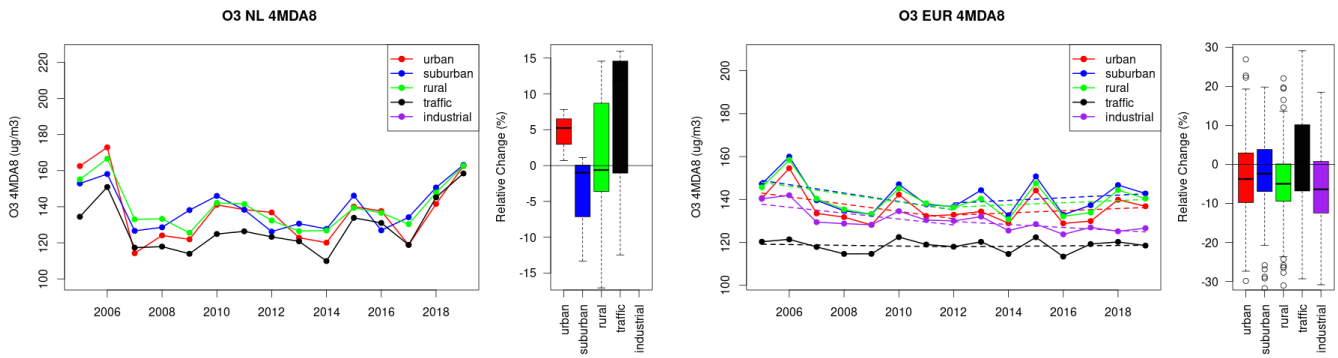


Figure S.451: Time series of the Netherlands (left) and European-wide composite (median) of O₃ fourth highest daily peak (4MDA8, ug/m³) per station type and area (red: urban background, blue suburban background, green: rural background, black: traffic, violet: industrial) between 2005 and 2019. In the European composite, the dashed lines show the linear fit between 2005 & 2012 and between 2012 & 2019. The boxplots on the right-hand side show the distribution of relative changes (%) between 2005 and 2019 for all stations of each typology in Netherlands and in Europe.

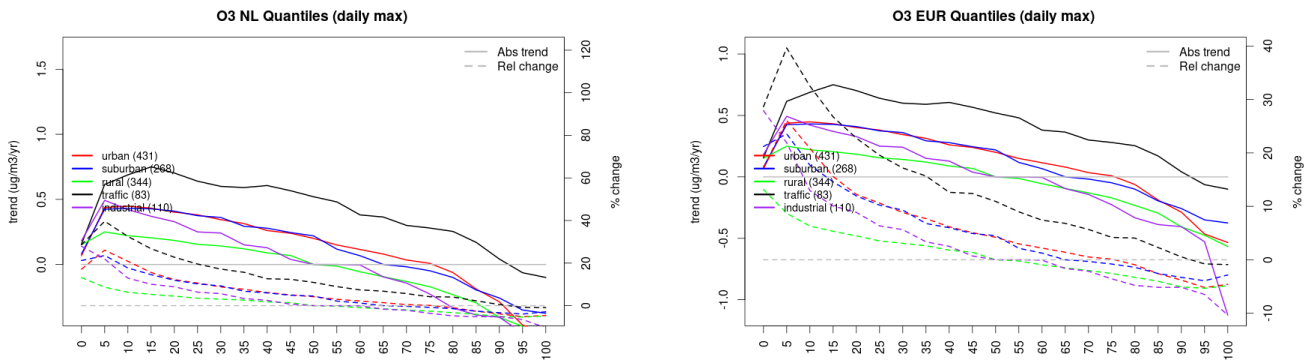


Figure S.452: For ozone in Netherlands (left) and Europe, and for each typology of station: absolute trend (solid lines, left y-axis) and relative change (dashed lines, right y-axis) of the percentiles of daily maxima.

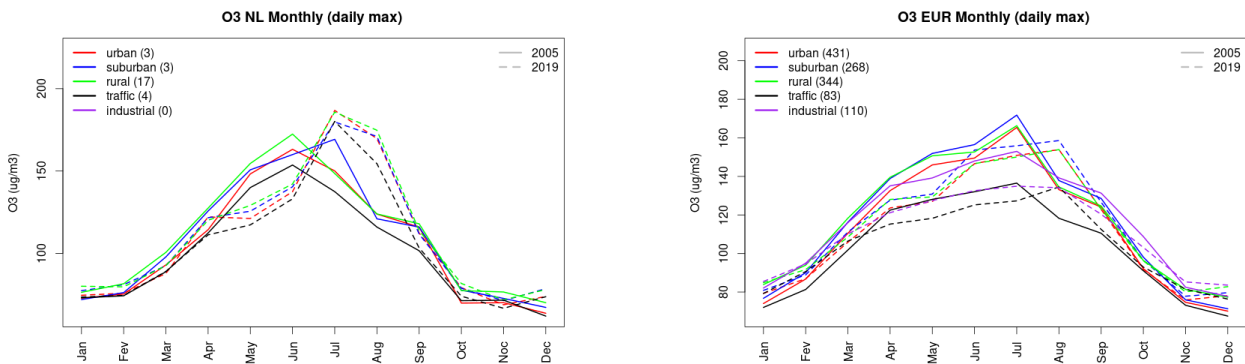


Figure S.453: Monthly cycle of daily max ozone for Netherlands (left) and Europe (right) at various station types estimated from the whole time series in 2005 (solid lines) and 2019 (dashed lines)

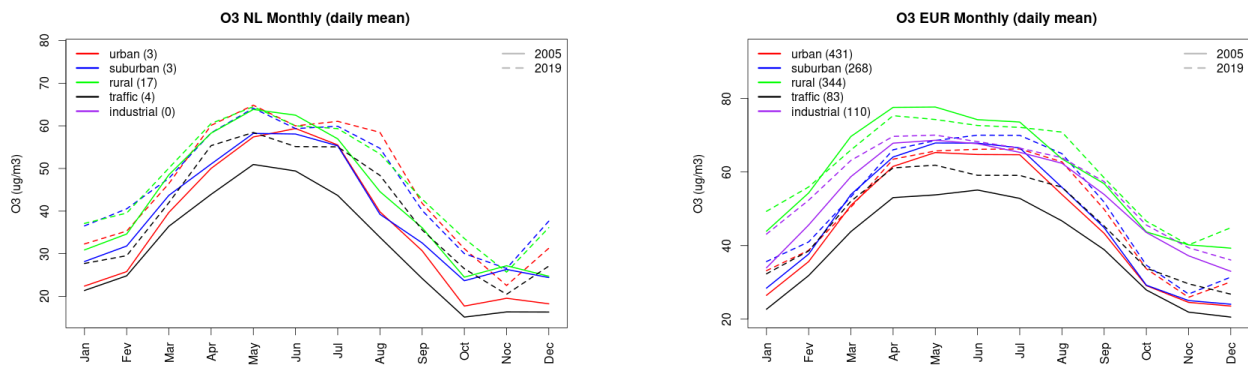


Figure S.454: Monthly cycle of daily mean ozone for Netherlands (left) and Europe (right) at various station types estimated from the whole time series in 2005 (solid lines) and 2019

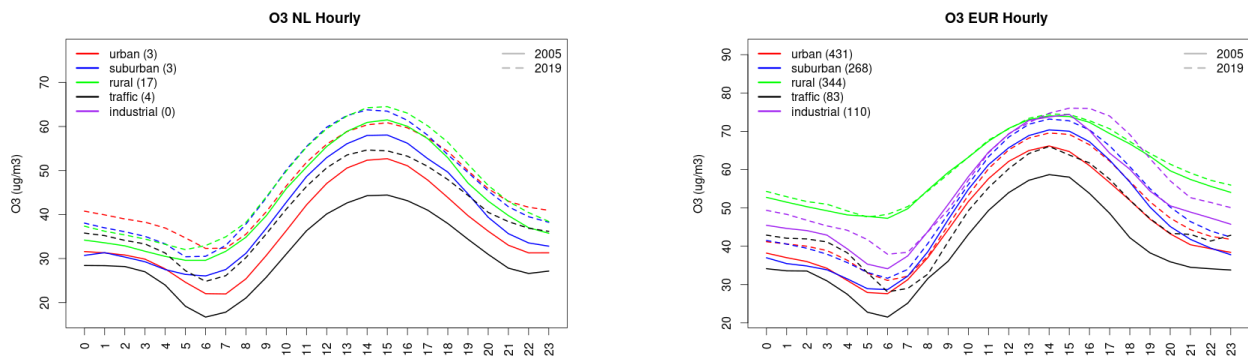


Figure S.455: Diurnal cycle of daily mean ozone for Netherlands (left) and Europe (right) at various station types estimated from the whole time series in 2005 (solid lines) and 2019

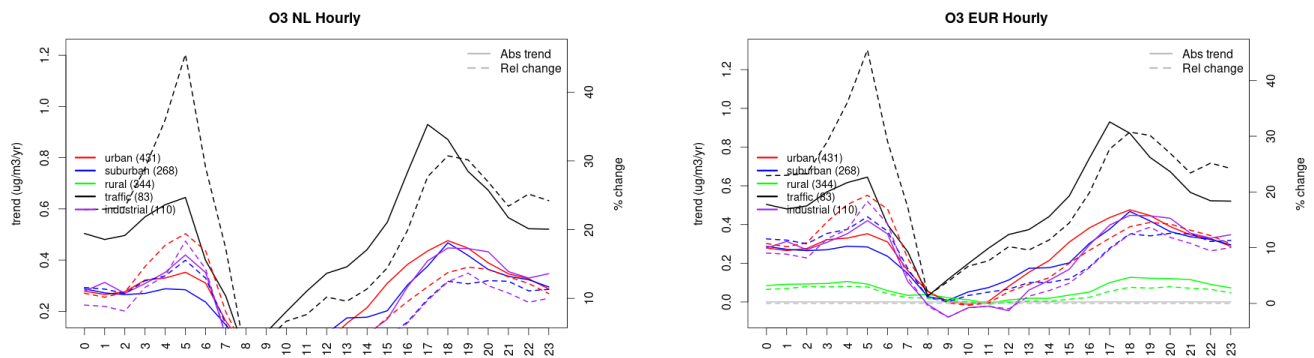


Figure S.456: Absolute (solid lines, left axis) and relative (dashed lines, right axis) trends in the diurnal cycle for Netherlands (left) and Europe (right) of ozone at various station type.

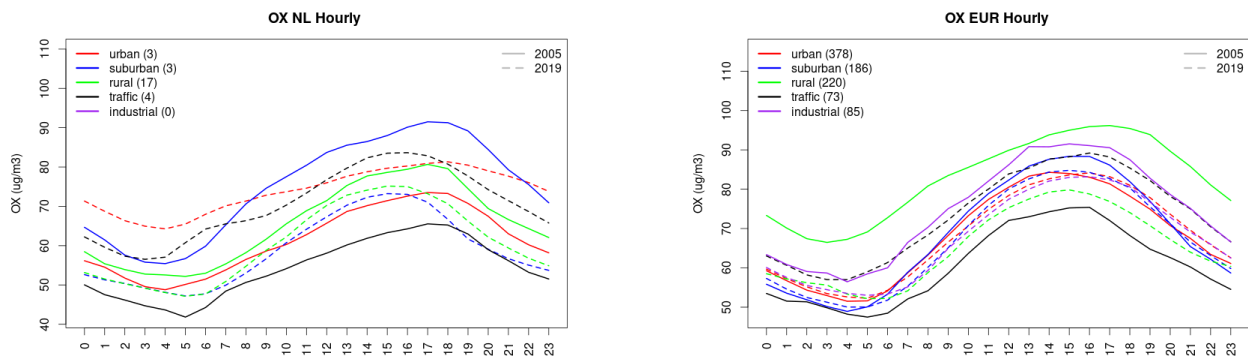


Figure S.457: Diurnal cycle of daily mean OX (as NO₂+O₃) for Netherlands (left) and Europe (right) at various station types estimated from the whole time series in 2005 (solid lines) and 2019

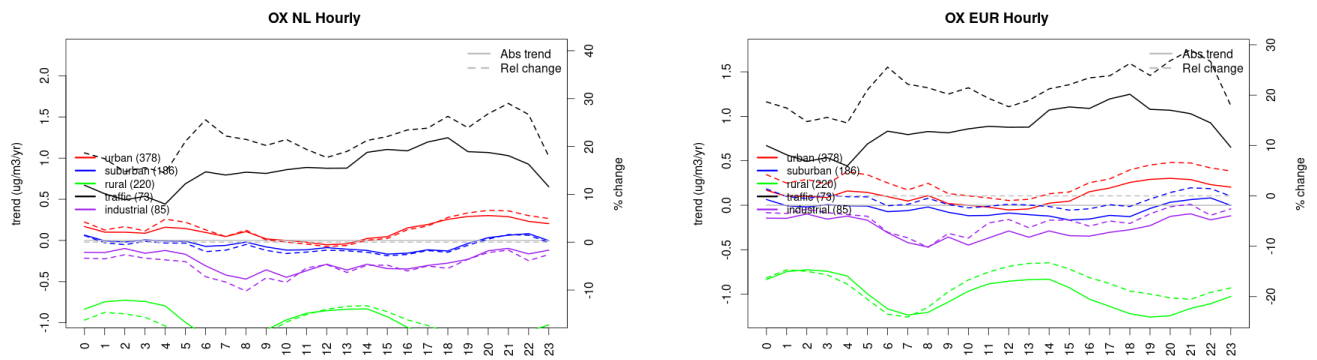


Figure S.458: Absolute (solid lines, left axis) and relative (dashed lines, right axis) trends in the diurnal cycle for Netherlands (left) and Europe (right) of OX (as NO₂+O₃) at various station type.

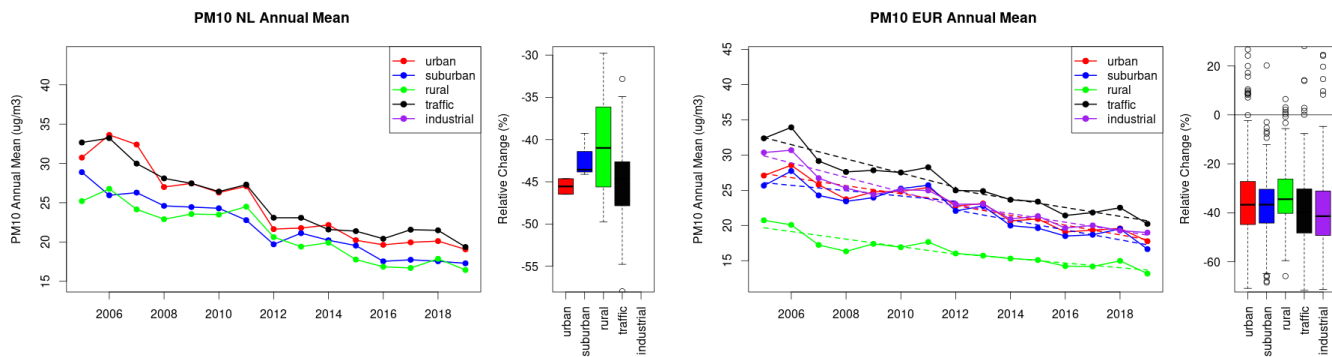


Figure S.459: Time series of the Netherlands (left) and European-wide composite (median) of annual mean PM₁₀ (ug/m³) per station type and area (red: urban background, blue suburban background, green: rural background, black: traffic, violet: industrial) between 2005 and 2019. In the European composite, the dashed lines show the linear fit between 2005 & 2012 and between 2012 & 2019. The boxplots on the right-hand side show the distribution of relative changes (%) between 2005 and 2019 for all stations of each typology in Netherlands and in Europe.

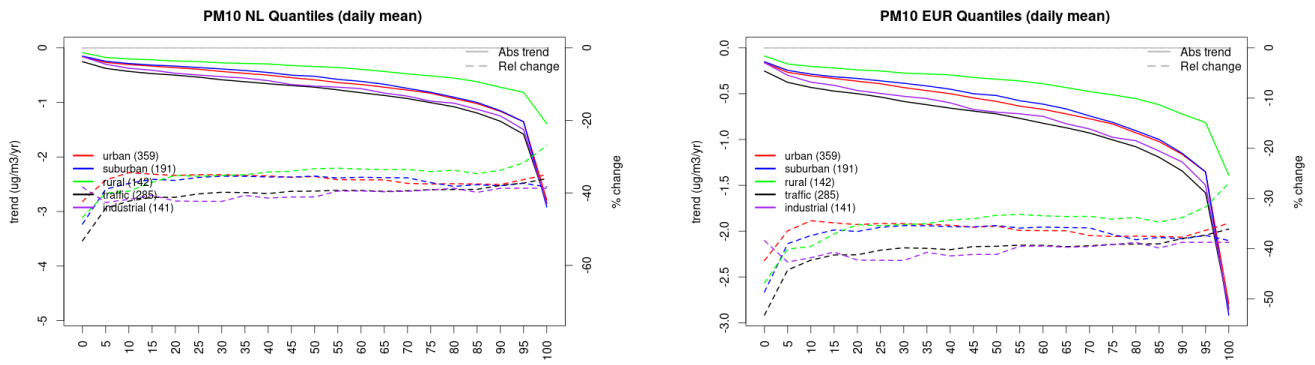


Figure S.460: For PM10 in Netherlands (left) and Europe, and for each typology of station: absolute trend (solid lines, left y-axis) and relative change (dashed lines, right y-axis) of the percentiles of daily means.

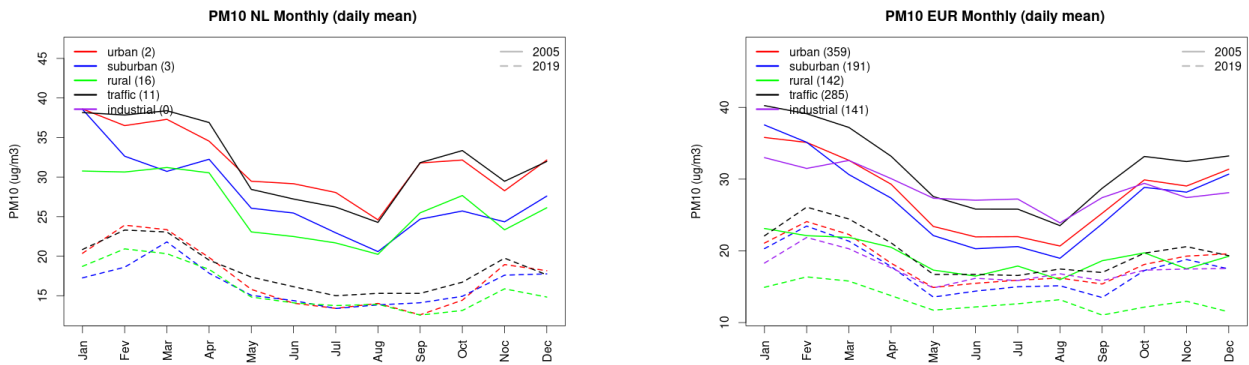


Figure S.461: Monthly cycle of daily mean PM10 for Netherlands (left) and Europe (right) at various station types estimated from the whole time series in 2005 (solid lines) and 2019

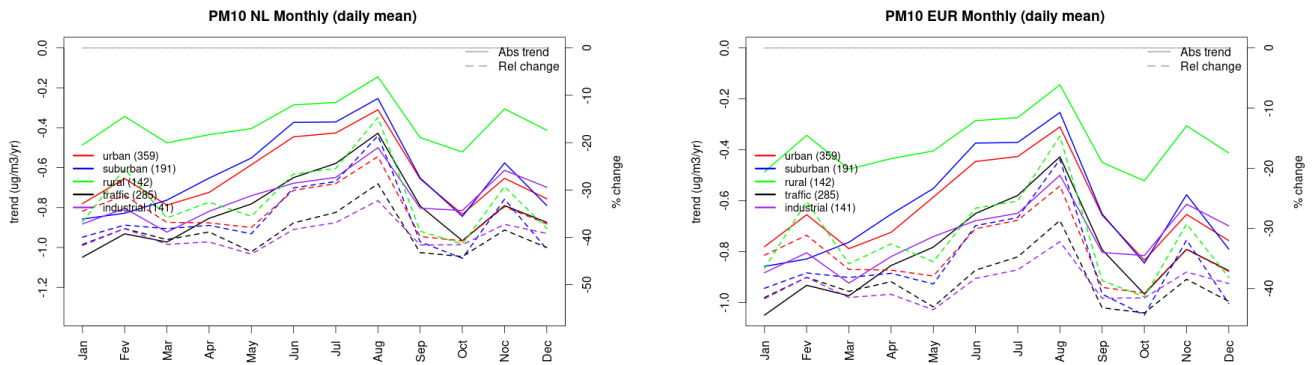


Figure S.462: Absolute (solid lines, left axis) and relative (dashed lines, right axis) trends in the monthly cycle for Netherlands (left) and Europe (right) of PM10 at various station type.

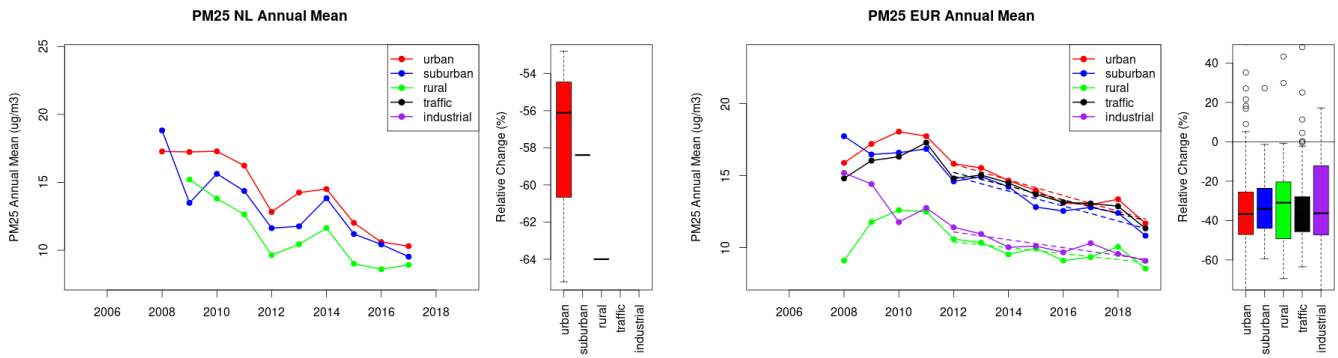


Figure S.463: Time series of the Netherlands (left) and European-wide composite (median) of annual mean PM25 (ug/m3) per station type and area (red: urban background, blue suburban background, green: rural background, black: traffic, violet: industrial) between 2005 and 2019. In the European composite, the dashed lines show the linear fit between 2005 & 2012 and between 2012 & 2019. The boxplots on the right-hand side show the distribution of relative changes (%) between 2005 and 2019 for all stations of each typology in Netherlands and in Europe.

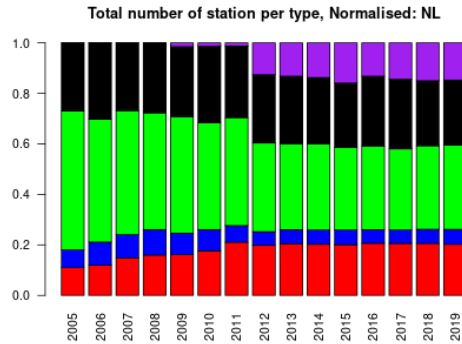
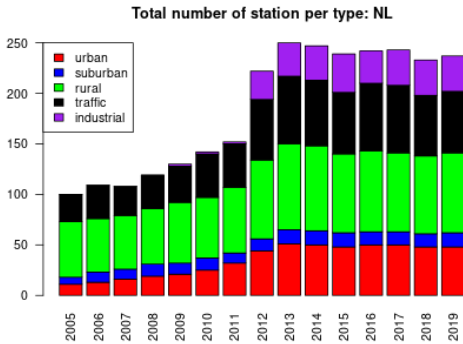
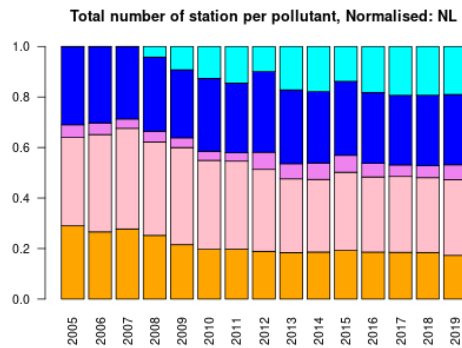
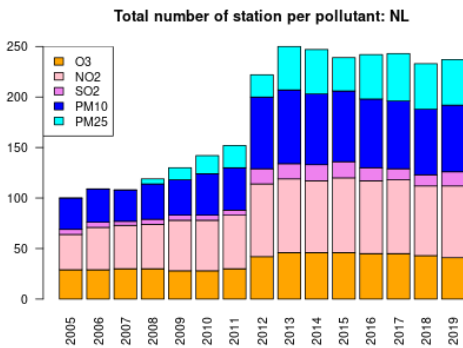
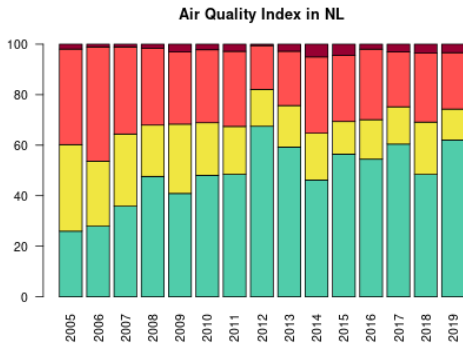


Figure S.464: For Netherlands: overall air quality index (percentage of days in a given year) and distribution of daily categories per pollutant (light blue: good, light green: fair, yellow: moderate, orange: poor, red: very poor, violet: extremely poor).

22 Norway

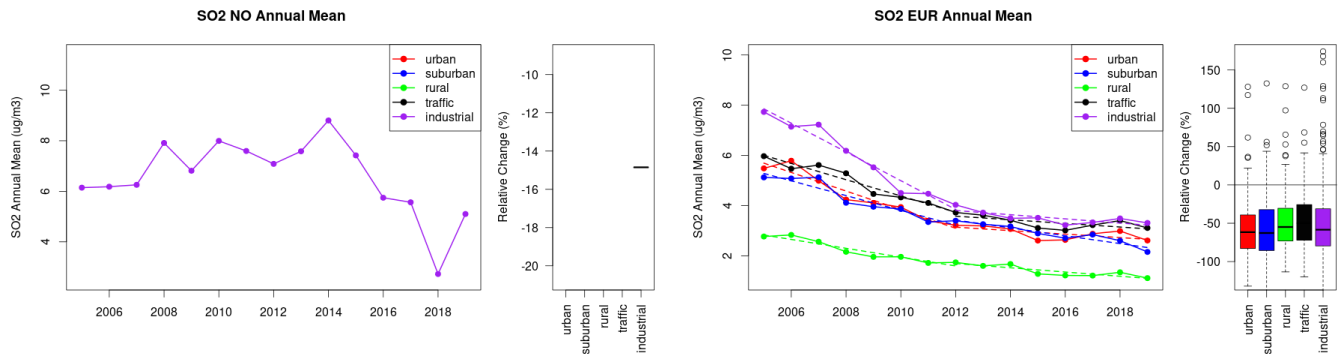


Figure S.465: Time series of the Norway (left) and European-wide composite (median) of annual mean SO₂ (ug/m³) per station type and area (red: urban background, blue suburban background, green: rural background, black: traffic, violet: industrial) between 2005 and 2019. In the European composite, the dashed lines show the linear fit between 2005 & 2012 and between 2012 & 2019. The boxplots on the right-hand side show the distribution of relative changes (%) between 2005 and 2019 for all stations of each typology in Norway and in Europe.

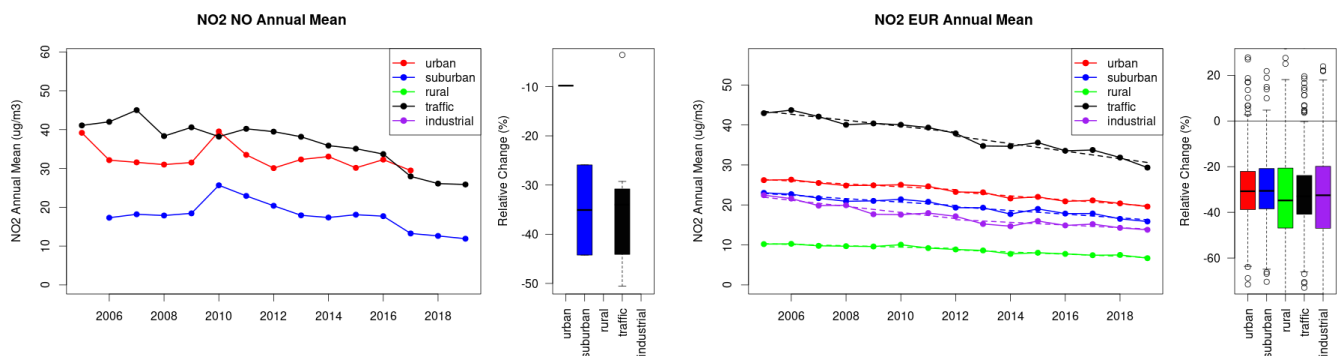


Figure S.466: Time series of the Norway (left) and European-wide composite (median) of annual mean NO₂ (ug/m³) per station type and area (red: urban background, blue suburban background, green: rural background, black: traffic, violet: industrial) between 2005 and 2019. In the European composite, the dashed lines show the linear fit between 2005 & 2012 and between 2012 & 2019. The boxplots on the right-hand side show the distribution of relative changes (%) between 2005 and 2019 for all stations of each typology in Norway and in Europe.

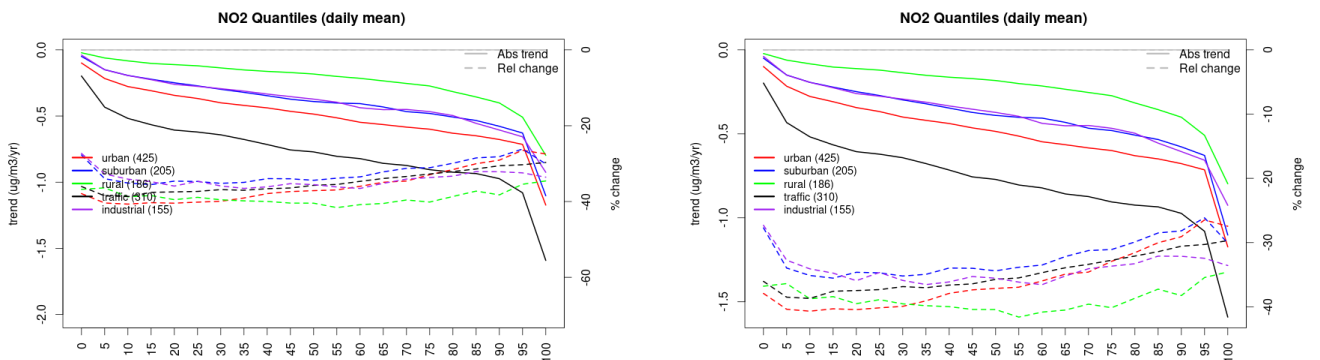


Figure S.467: For NO₂ in Norway (left) and Europe, and for each typology of station: absolute trend (solid lines, left y-axis) and relative change (dashed lines, right y-axis) of the percentiles of daily means.

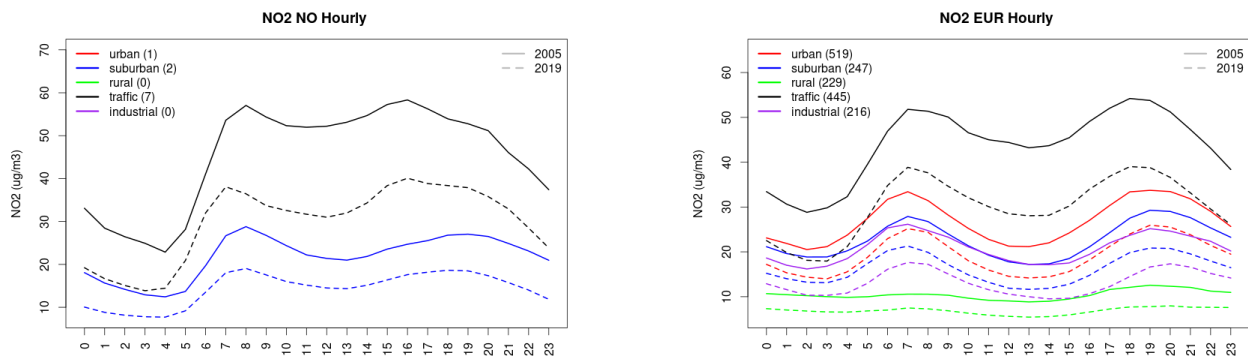


Figure S.468: Diurnal cycle of daily mean NO2 for Norway (left) and Europe (right) at various station types estimated from the whole time series in 2005 (solid lines) and 2019

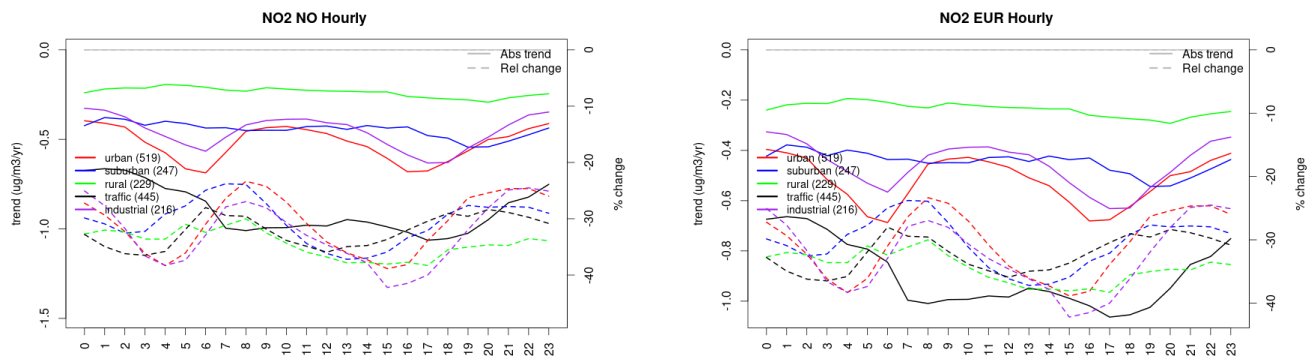


Figure S.469: Absolute (solid lines, left axis) and relative (dashed lines, right axis) trends in the diurnal cycle for Norway (left) and Europe (right) of NO2 at various station type.

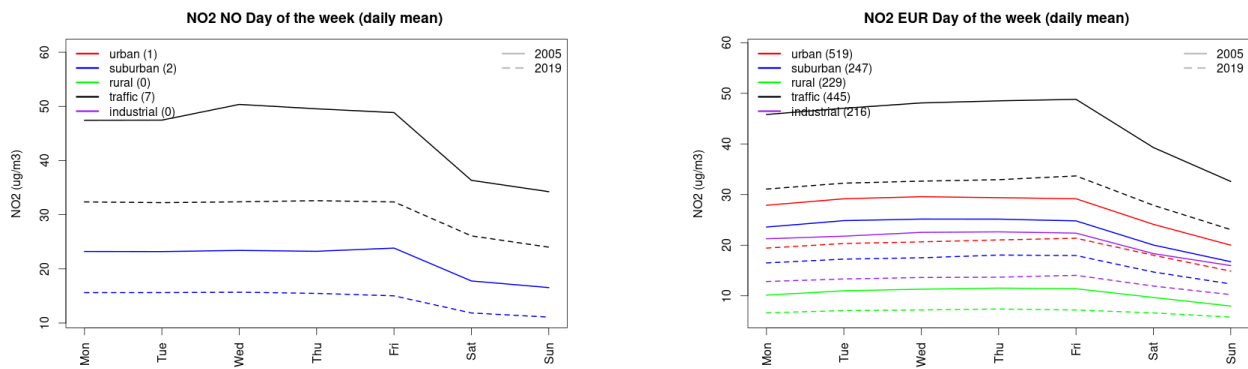


Figure S.470: Weekly cycle of daily mean NO2 for Norway (left) and Europe (right) at various station types estimated from the whole time series in 2005 (solid lines) and 2019

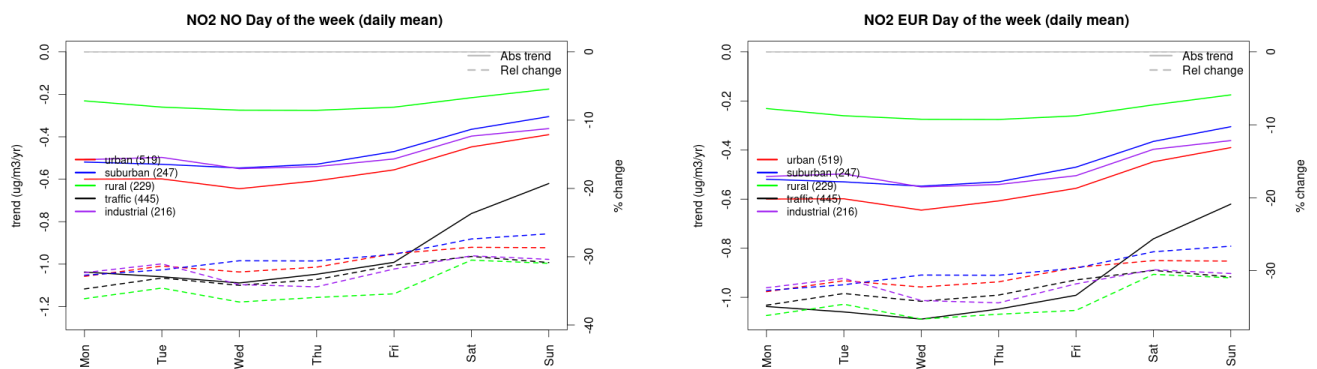


Figure S.471: Absolute (solid lines, left axis) and relative (dashed lines, right axis) trends in the weekly cycle for Norway (left) and Europe (right) of NO₂ at various station type.

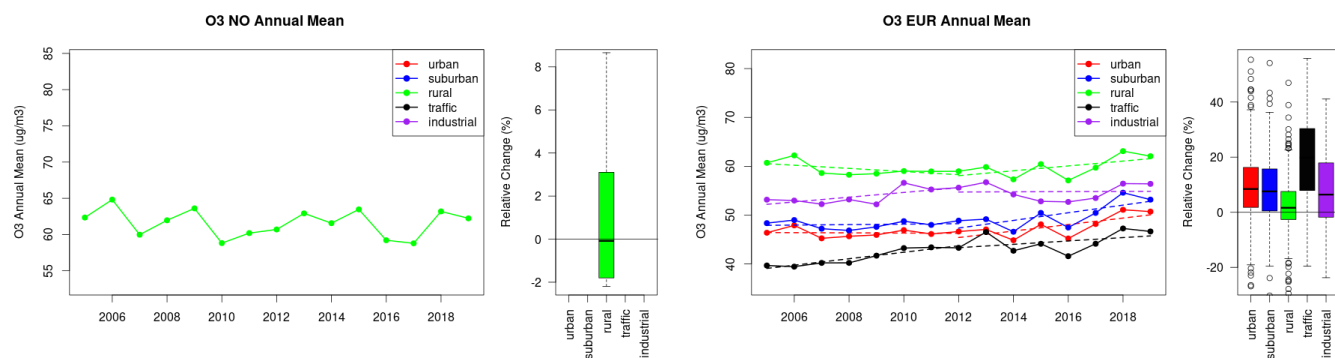


Figure S.472: Time series of the Norway (left) and European-wide composite (median) of annual mean ozone (ug/m³) per station type and area (red: urban background, blue suburban background, green: rural background, black: traffic, violet: industrial) between 2005 and 2019. In the European composite, the dashed lines show the linear fit between 2005 & 2012 and between 2012 & 2019. The boxplots on the right-hand side show the distribution of relative changes (%) between 2005 and 2019 for all stations of each typology in Norway and in Europe.

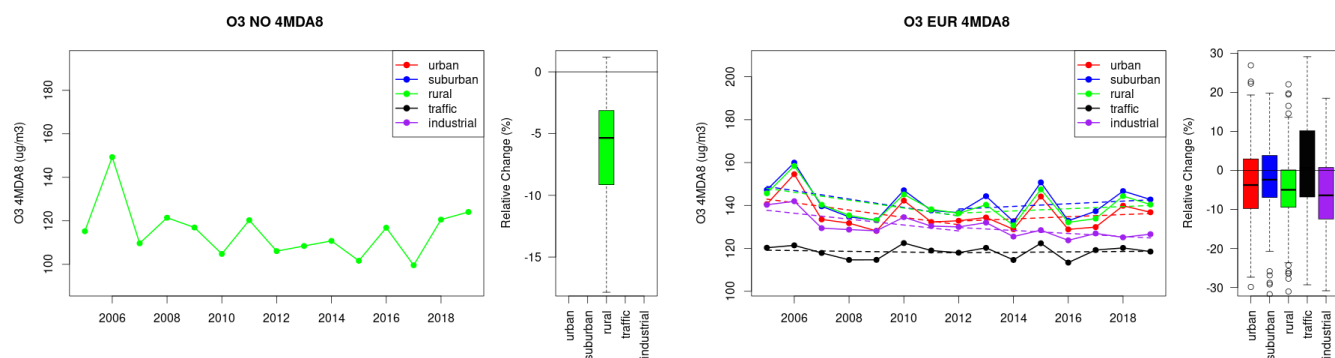


Figure S.473: Time series of the Norway (left) and European-wide composite (median) of O₃ fourth highest daily peak (4MDA8, ug/m³) per station type and area (red: urban background, blue suburban background, green: rural background, black: traffic, violet: industrial) between 2005 and 2019. In the European composite, the dashed lines show the linear fit between 2005 & 2012 and between 2012 & 2019. The boxplots on the right-hand side show the distribution of relative changes (%) between 2005 and 2019 for all stations of each typology in Norway and in Europe.

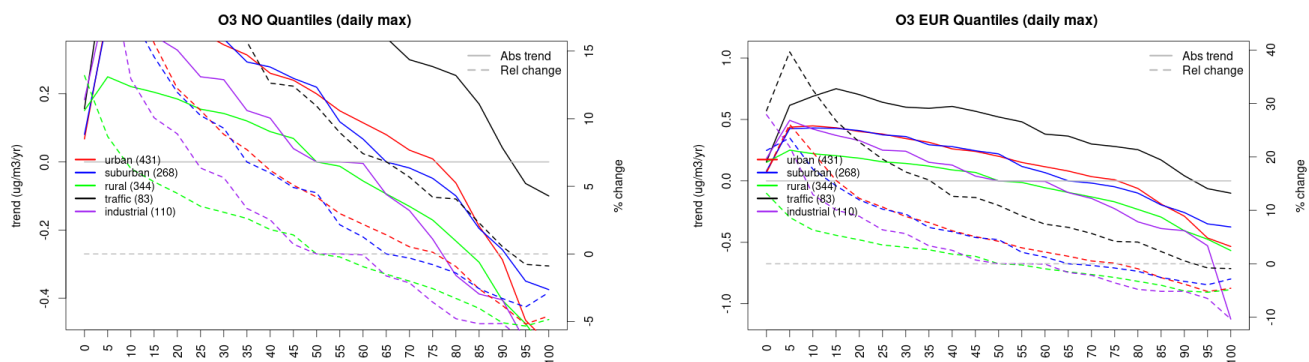


Figure S.474: For ozone in Norway (left) and Europe, and for each typology of station: absolute trend (solid lines, left y-axis) and relative change (dashed lines, right y-axis) of the percentiles of daily maxima.

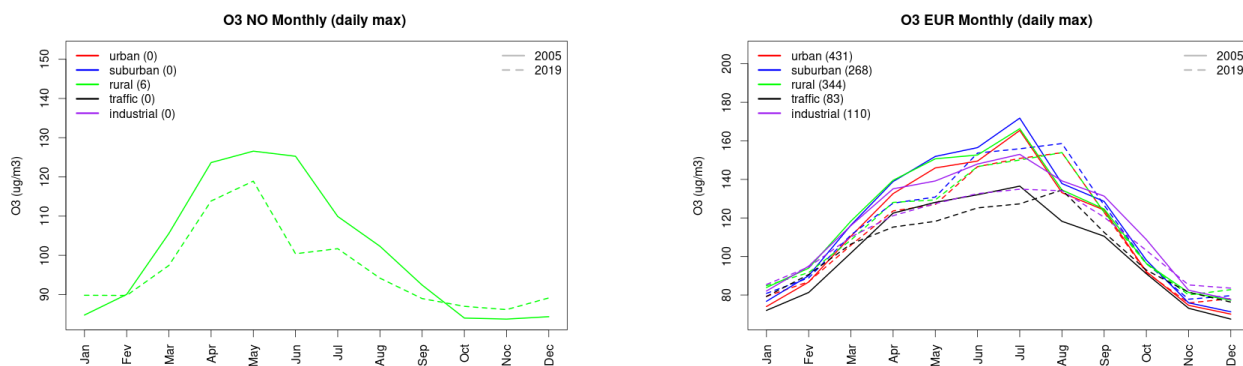


Figure S.475: Monthly cycle of daily max ozone for Norway (left) and Europe (right) at various station types estimated from the whole time series in 2005 (solid lines) and 2019

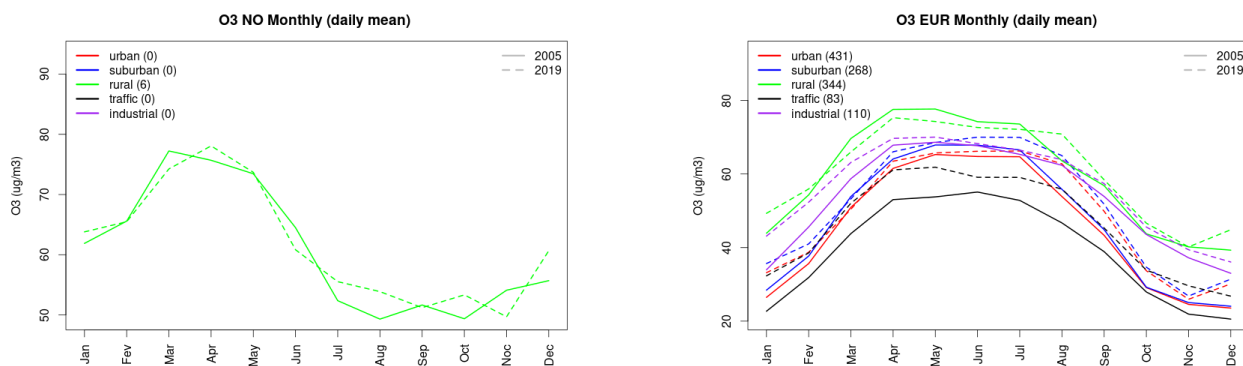


Figure S.476: Monthly cycle of daily mean ozone for Norway (left) and Europe (right) at various station types estimated from the whole time series in 2005 (solid lines) and 2019

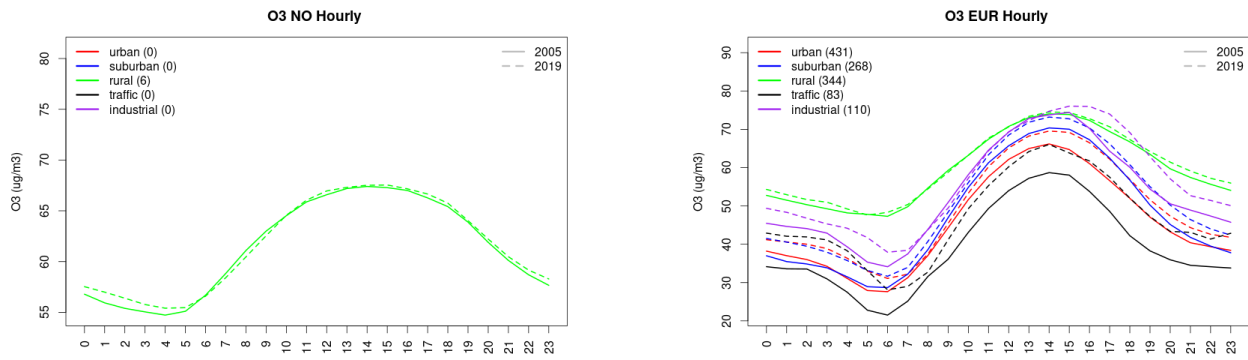


Figure S.477: Diurnal cycle of daily mean ozone for Norway (left) and Europe (right) at various station types estimated from the whole time series in 2005 (solid lines) and 2019

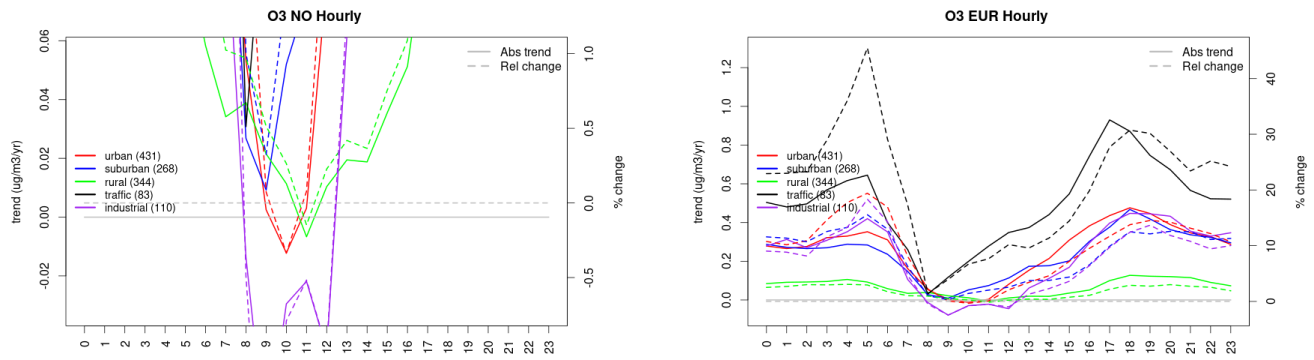


Figure S.478: Absolute (solid lines, left axis) and relative (dashed lines, right axis) trends in the diurnal cycle for Norway (left) and Europe (right) of ozone at various station type.

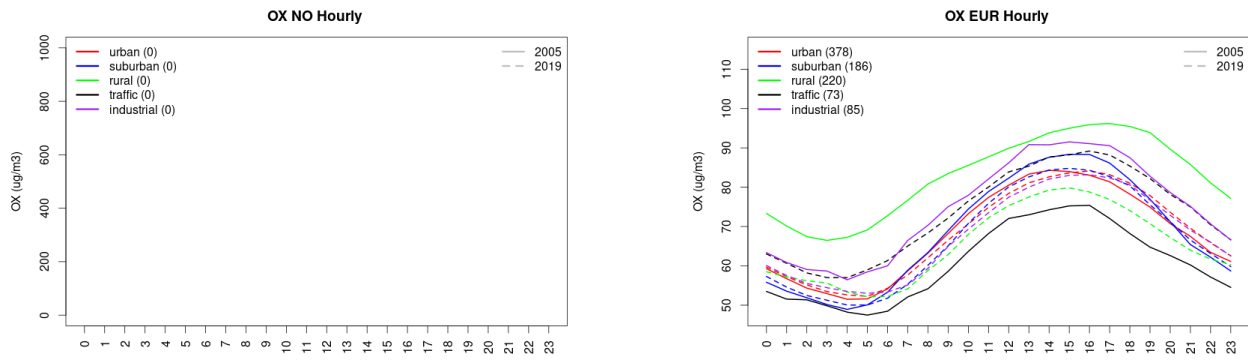


Figure S.479: Diurnal cycle of daily mean OX (as $\text{NO}_2 + \text{O}_3$) for Norway (left) and Europe (right) at various station types estimated from the whole time series in 2005 (solid lines) and 2019

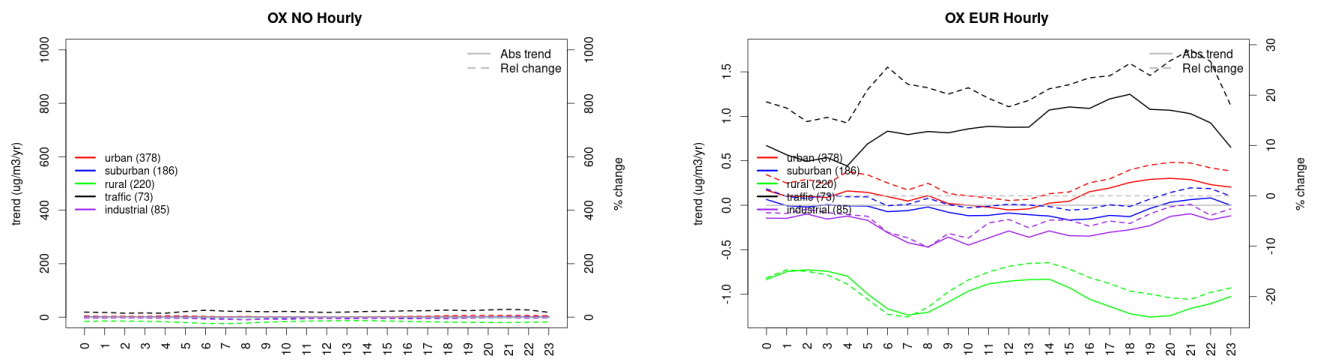


Figure S.480: Absolute (solid lines, left axis) and relative (dashed lines, right axis) trends in the diurnal cycle for Norway (left) and Europe (right) of OX (as NO₂+O₃) at various station type.

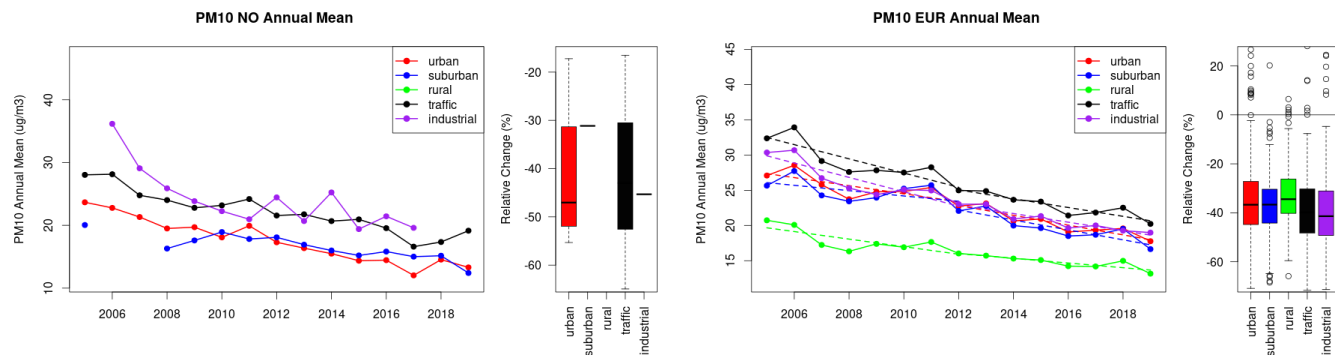


Figure S.481: Time series of the Norway (left) and European-wide composite (median) of annual mean PM₁₀ (ug/m³) per station type and area (red: urban background, blue suburban background, green: rural background, black: traffic, violet: industrial) between 2005 and 2019. In the European composite, the dashed lines show the linear fit between 2005 & 2012 and between 2012 & 2019. The boxplots on the right-hand side show the distribution of relative changes (%) between 2005 and 2019 for all stations of each typology in Norway and in Europe.

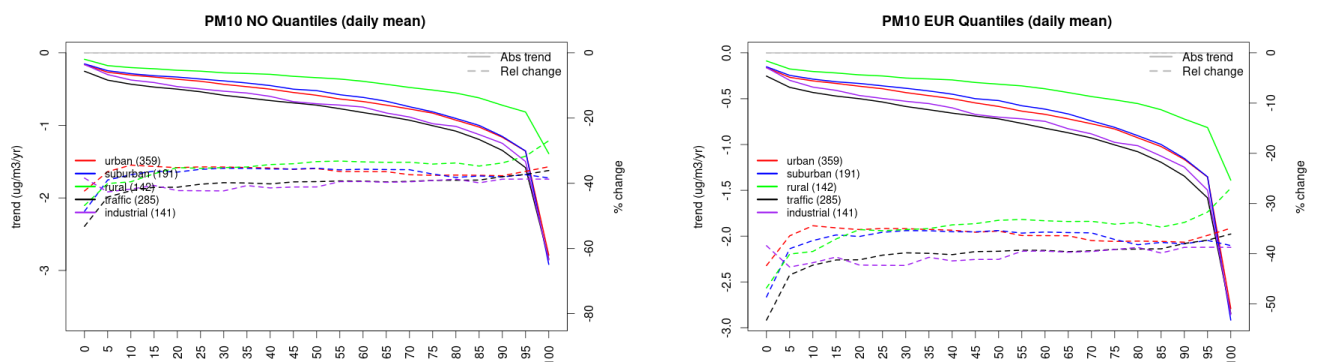


Figure S.482: For PM₁₀ in Norway (left) and Europe, and for each typology of station: absolute trend (solid lines, left y-axis) and relative change (dashed lines, right y-axis) of the percentiles of daily means.

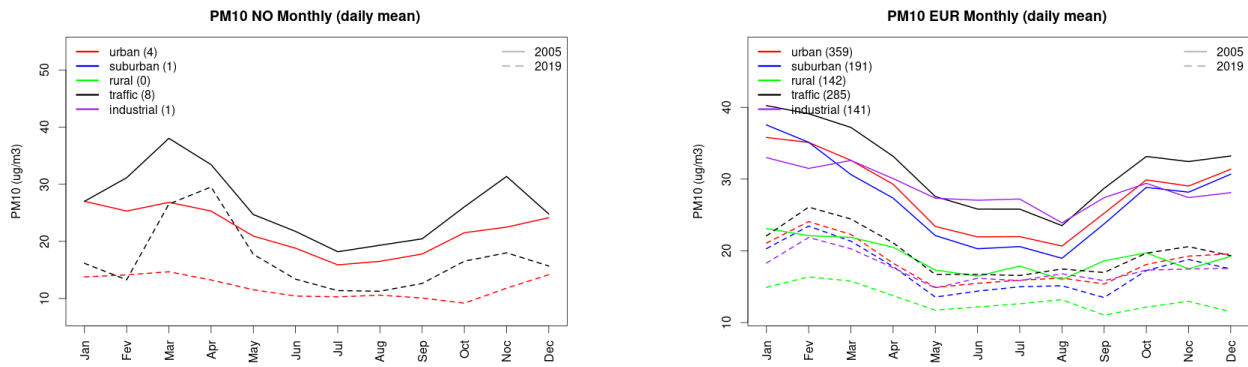


Figure S.483: Monthly cycle of daily mean PM10 for Norway (left) and Europe (right) at various station types estimated from the whole time series in 2005 (solid lines) and 2019

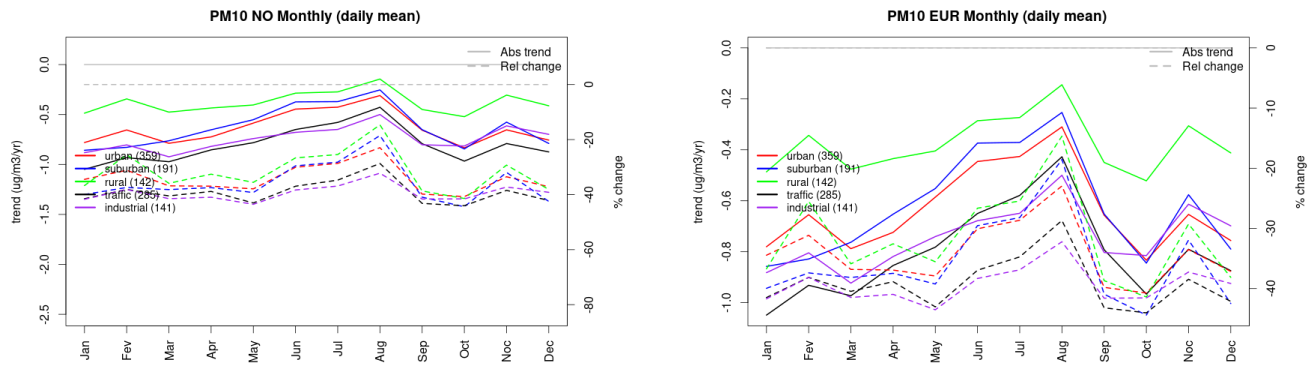


Figure S.484: Absolute (solid lines, left axis) and relative (dashed lines, right axis) trends in the monthly cycle for Norway (left) and Europe (right) of PM10 at various station type.

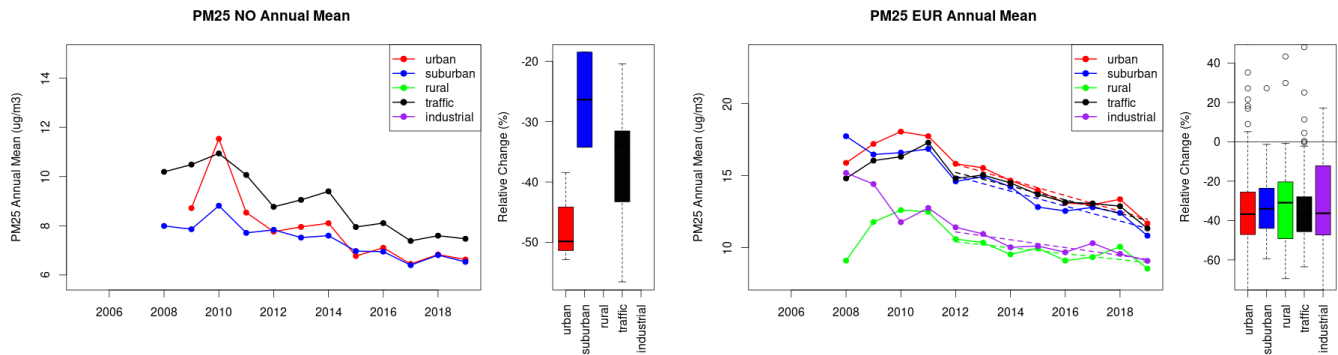


Figure S.485: Time series of the Norway (left) and European-wide composite (median) of annual mean PM25 ($\mu\text{g}/\text{m}^3$) per station type and area (red: urban background, blue suburban background, green: rural background, black: traffic, violet: industrial) between 2005 and 2019. In the European composite, the dashed lines show the linear fit between 2005 & 2012 and between 2012 & 2019. The boxplots on the right-hand side show the distribution of relative changes (%) between 2005 and 2019 for all stations of each typology in Norway and in Europe.

23 Poland

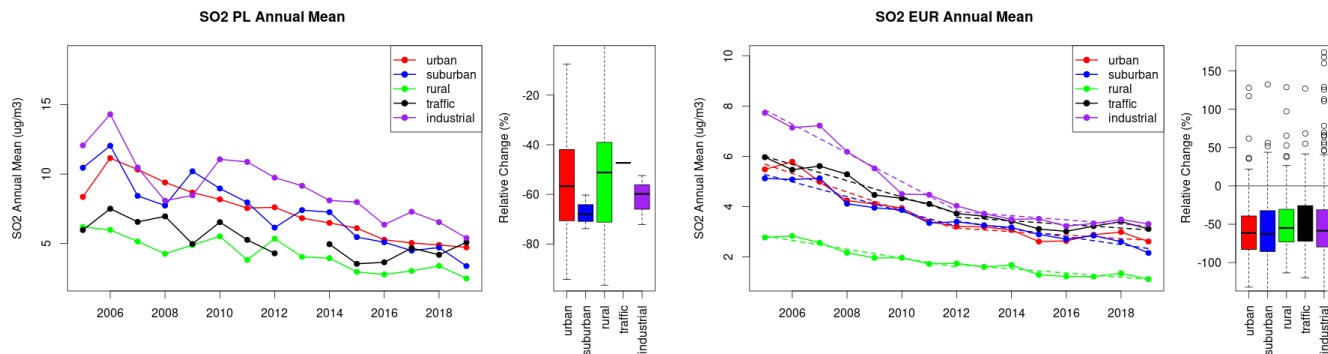


Figure S.486: Time series of the Poland (left) and European-wide composite (median) of annual mean SO₂ (ug/m³) per station type and area (red: urban background, blue suburban background, green: rural background, black: traffic, violet: industrial) between 2005 and 2019. In the European composite, the dashed lines show the linear fit between 2005 & 2012 and between 2012 & 2019. The boxplots on the right-hand side show the distribution of relative changes (%) between 2005 and 2019 for all stations of each typology in Poland and in Europe.

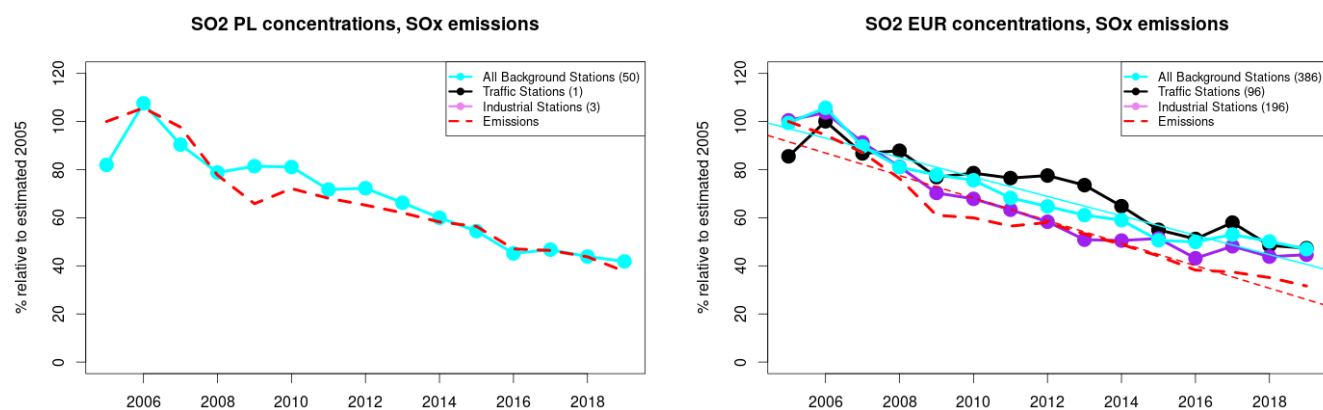


Figure S.487: Time series of 2005-2019 (left) and European (right) median SO₂ observed at traffic (black), industrial (violet) and background (cyan) sites (solid lines), and corresponding SO_x emissions (dashed line) normalised to estimated 2000 levels (%). The median is taken over where more than 5 stations of each typology is available. The total number of stations included is provided in brackets. In the European composite, straight lines are the linear fits over the whole period.

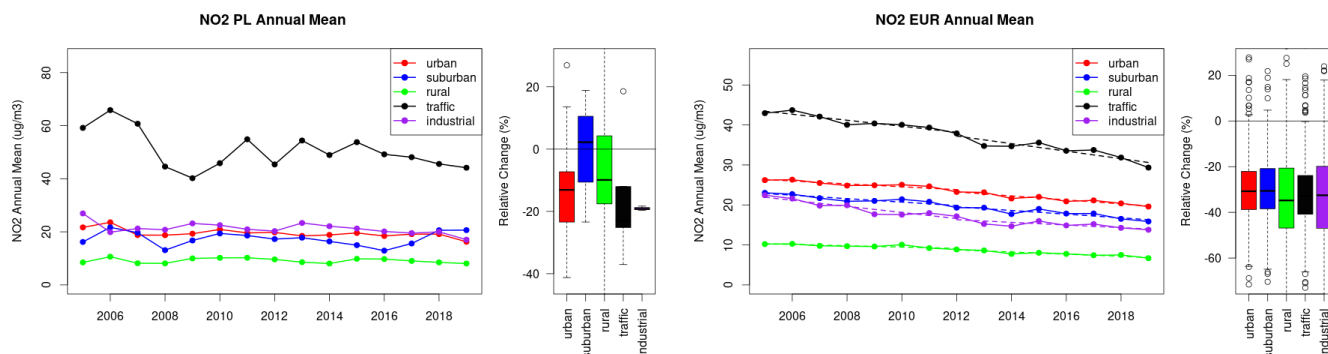


Figure S.488: Time series of the Poland (left) and European-wide composite (median) of annual mean NO₂ (ug/m³) per station type and area (red: urban background, blue suburban background, green: rural background, black: traffic, violet: industrial) between 2005 and 2019. In the European composite, the dashed lines show the linear fit between 2005 & 2012 and between 2012 & 2019. The boxplots on the right-hand side show the distribution of relative changes (%) between 2005 and 2019 for all stations of each typology in Poland and in Europe.

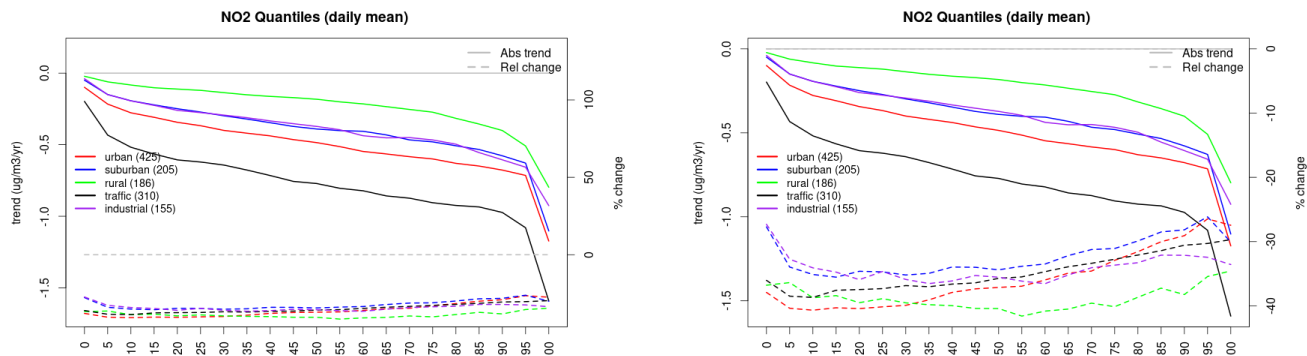


Figure S.489: For NO₂ in Poland (left) and Europe, and for each typology of station: absolute trend (solid lines, left y-axis) and relative change (dashed lines, right y-axis) of the percentiles of daily means.

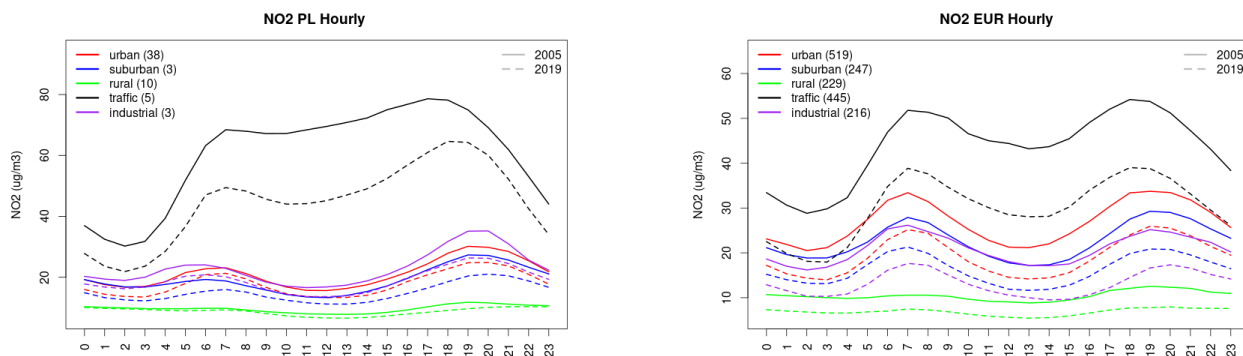


Figure S.490: Diurnal cycle of daily mean NO₂ for Poland (left) and Europe (right) at various station types estimated from the whole time series in 2005 (solid lines) and 2019

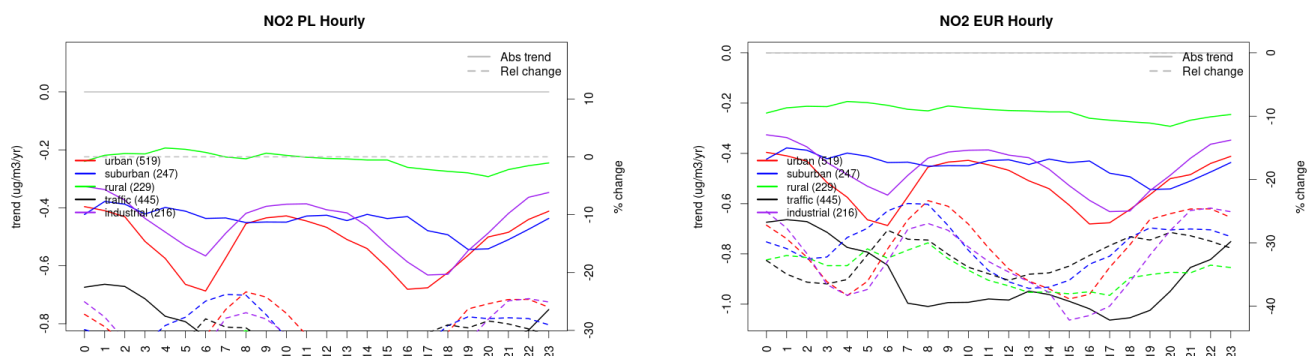


Figure S.491: Absolute (solid lines, left axis) and relative (dashed lines, right axis) trends in the diurnal cycle for Poland (left) and Europe (right) of NO₂ at various station type.

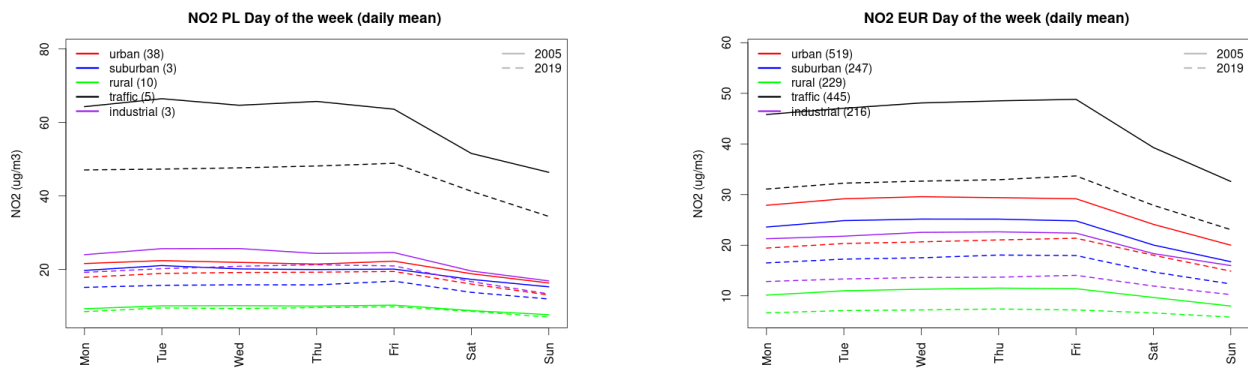


Figure S.492: Weekly cycle of daily mean NO₂ for Poland (left) and Europe (right) at various station types estimated from the whole time series in 2005 (solid lines) and 2019

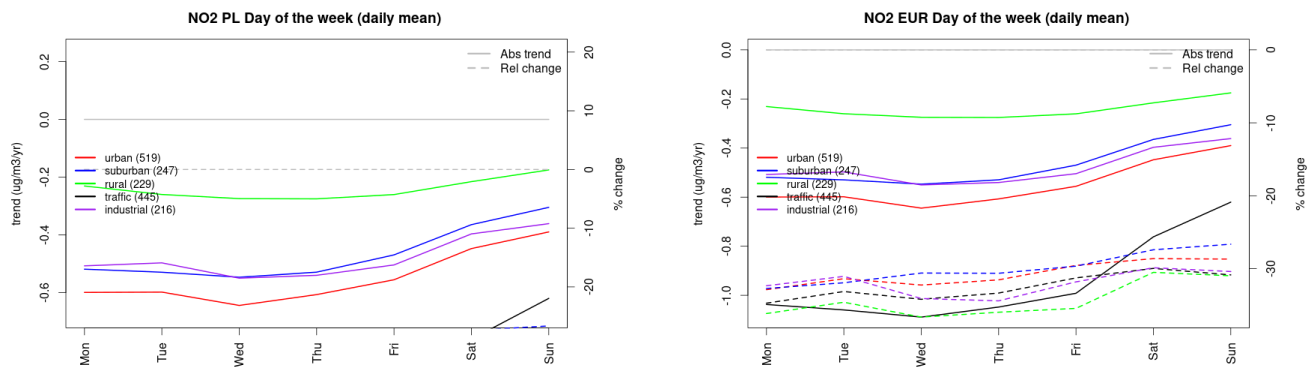


Figure S.493: Absolute (solid lines, left axis) and relative (dashed lines, right axis) trends in the weekly cycle for Poland (left) and Europe (right) of NO₂ at various station type.

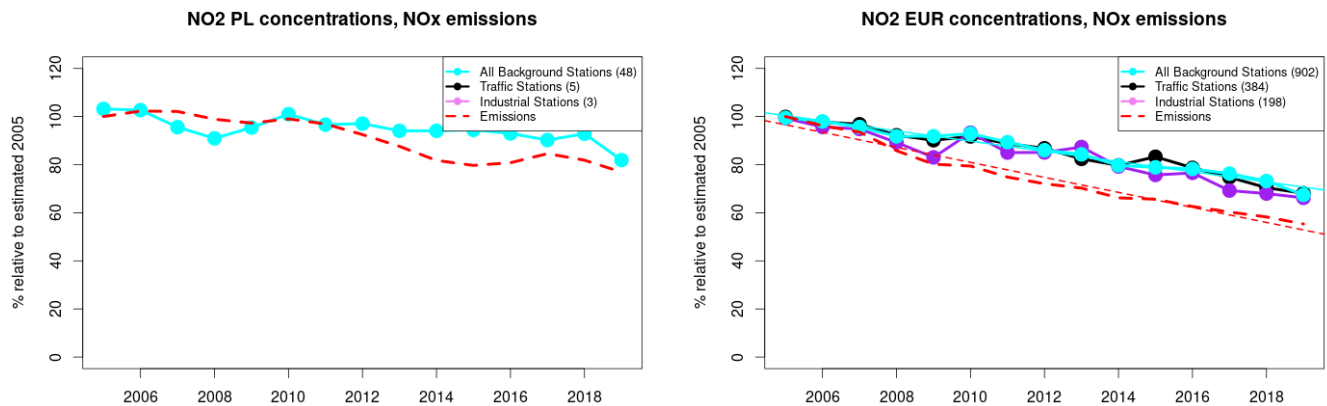


Figure S.494: Time series of 2005-2019 (left) and European (right) median NO₂ observed at traffic (black), industrial (violet) and background (cyan) sites (solid lines), and corresponding NO_x emissions (dashed line) normalised to estimated 2000 levels (%). The median is taken over where more than 5 stations of each typology is available. The total number of stations included is provided in brackets. In the European composite, straight lines are the linear fits over the whole period.

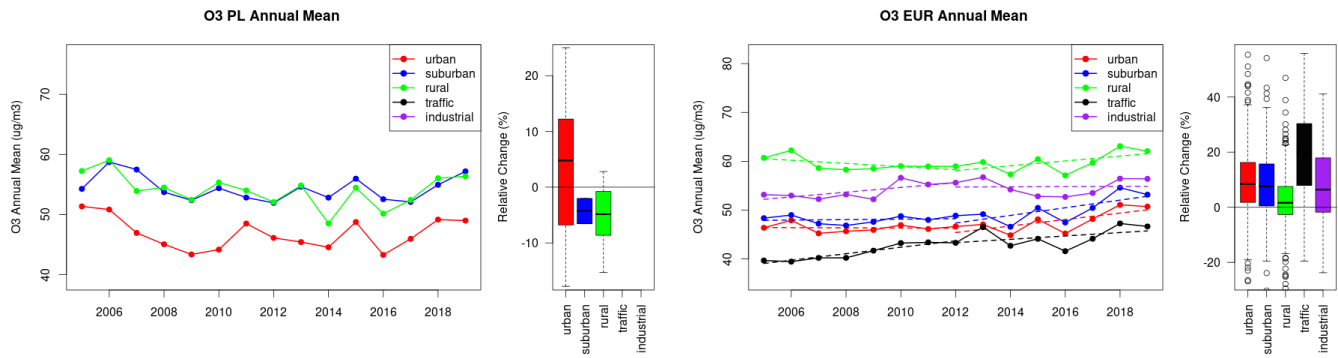


Figure S.495: Time series of the Poland (left) and European-wide composite (median) of annual mean ozone ($\mu\text{g}/\text{m}^3$) per station type and area (red: urban background, blue suburban background, green: rural background, black: traffic, violet: industrial) between 2005 and 2019. In the European composite, the dashed lines show the linear fit between 2005 & 2012 and between 2012 & 2019. The boxplots on the right-hand side show the distribution of relative changes (%) between 2005 and 2019 for all stations of each typology in Poland and in Europe.

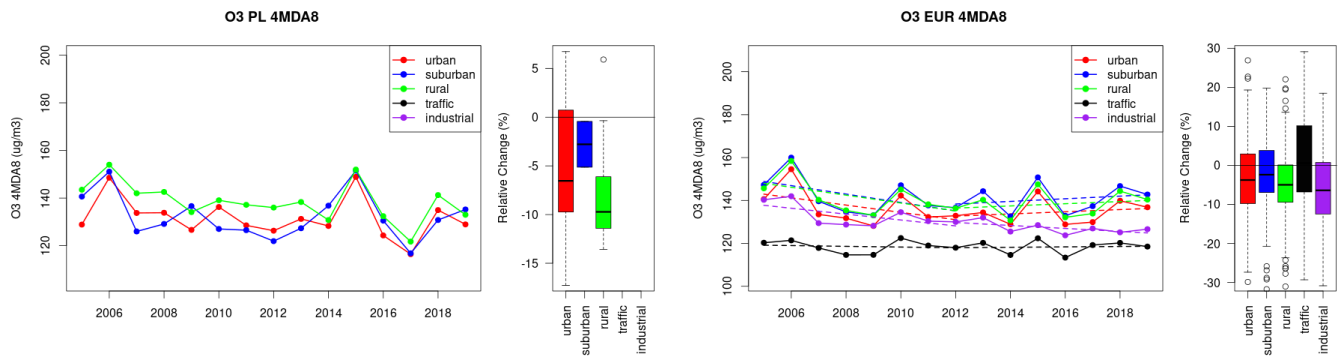


Figure S.496: Time series of the Poland (left) and European-wide composite (median) of O3 fourth highest daily peak (4MDA8, $\mu\text{g}/\text{m}^3$) per station type and area (red: urban background, blue suburban background, green: rural background, black: traffic, violet: industrial) between 2005 and 2019. In the European composite, the dashed lines show the linear fit between 2005 & 2012 and between 2012 & 2019. The boxplots on the right-hand side show the distribution of relative changes (%) between 2005 and 2019 for all stations of each typology in Poland and in Europe.

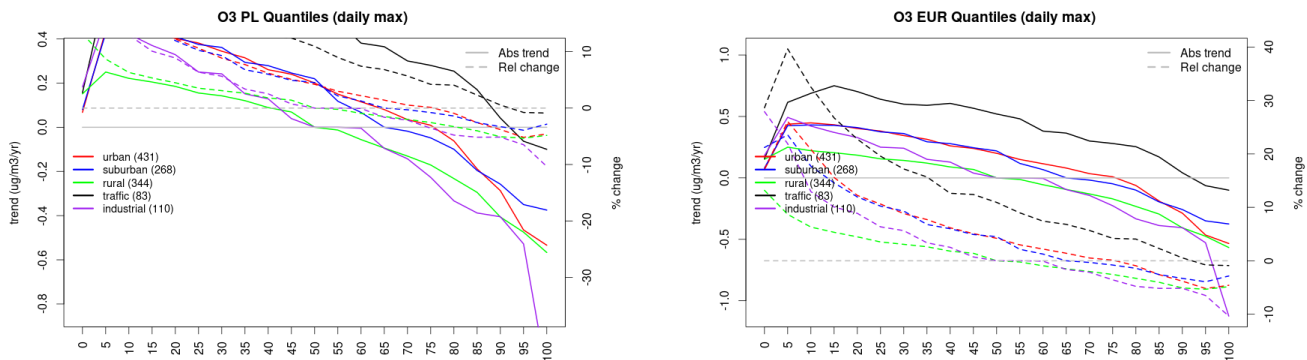


Figure S.497: For ozone in Poland (left) and Europe, and for each typology of station: absolute trend (solid lines, left y-axis) and relative change (dashed lines, right y-axis) of the percentiles of daily maxima.

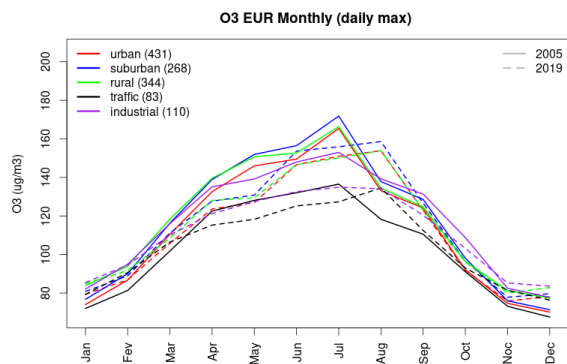
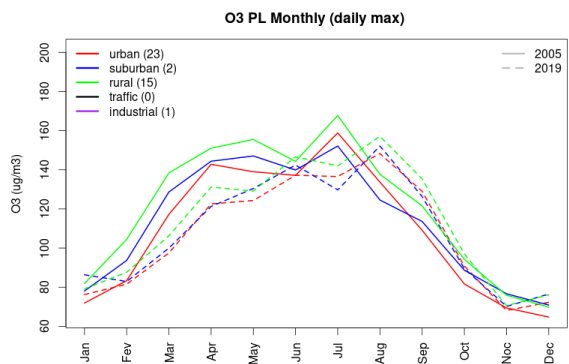


Figure S.498: Monthly cycle of daily max ozone for Poland (left) and Europe (right) at various station types estimated from the whole time series in 2005 (solid lines) and 2019

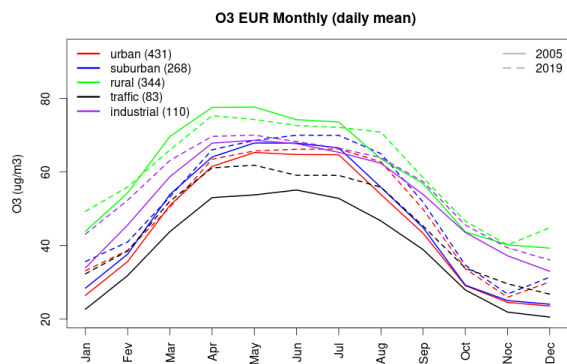
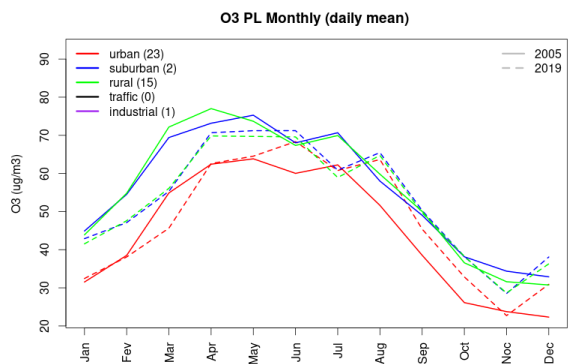


Figure S.499: Monthly cycle of daily mean ozone for Poland (left) and Europe (right) at various station types estimated from the whole time series in 2005 (solid lines) and 2019

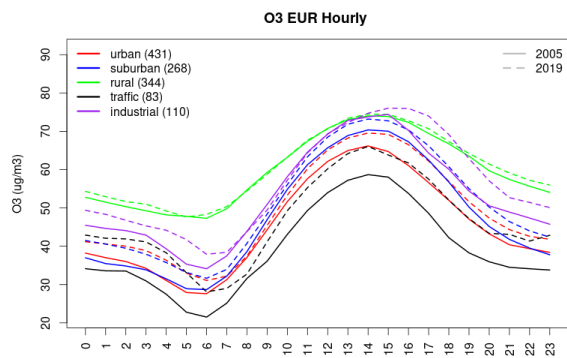
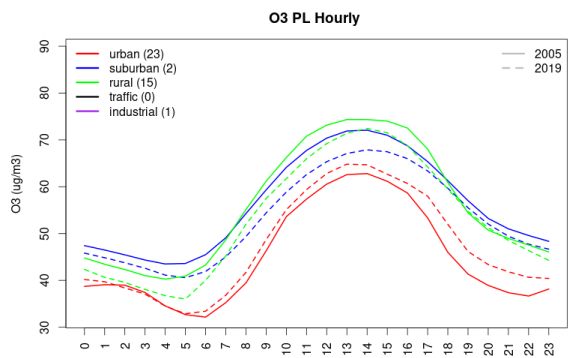


Figure S.500: Diurnal cycle of daily mean ozone for Poland (left) and Europe (right) at various station types estimated from the whole time series in 2005 (solid lines) and 2019

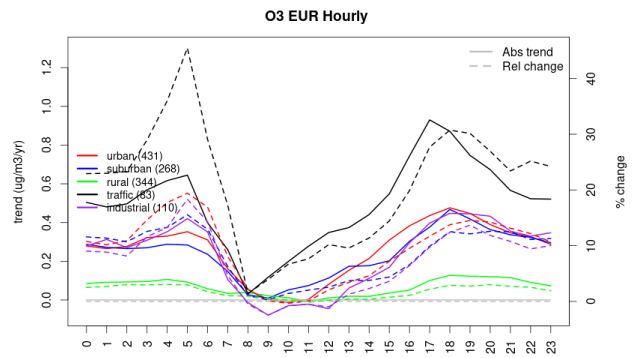
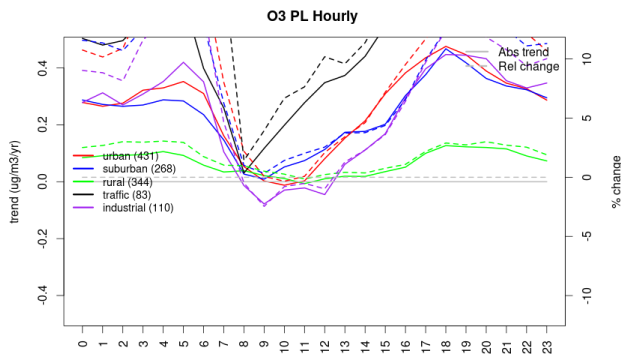


Figure S.501: Absolute (solid lines, left axis) and relative (dashed lines, right axis) trends in the diurnal cycle for Poland (left) and Europe (right) of ozone at various station type.

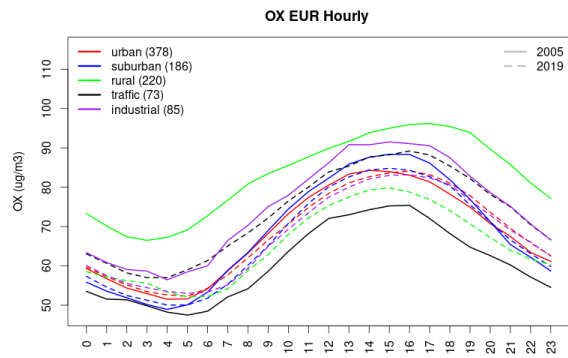
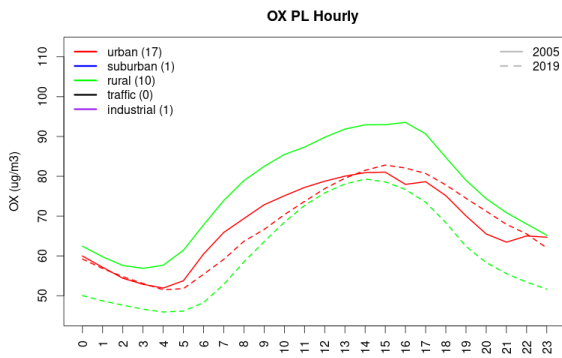


Figure S.502: Diurnal cycle of daily mean OX (as NO₂+O₃) for Poland (left) and Europe (right) at various station types estimated from the whole time series in 2005 (solid lines) and 2019

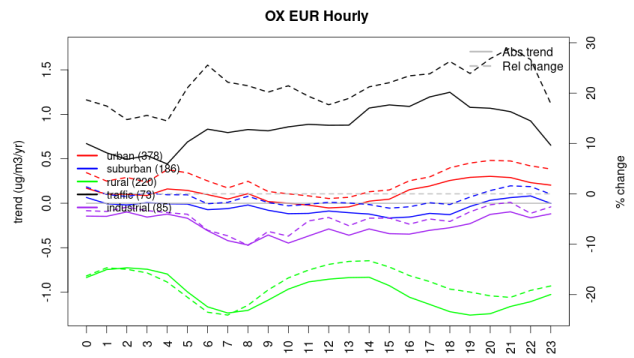
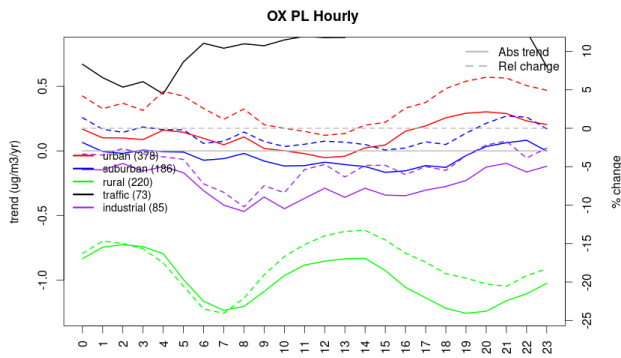


Figure S.503: Absolute (solid lines, left axis) and relative (dashed lines, right axis) trends in the diurnal cycle for Poland (left) and Europe (right) of OX (as NO₂+O₃) at various station type.

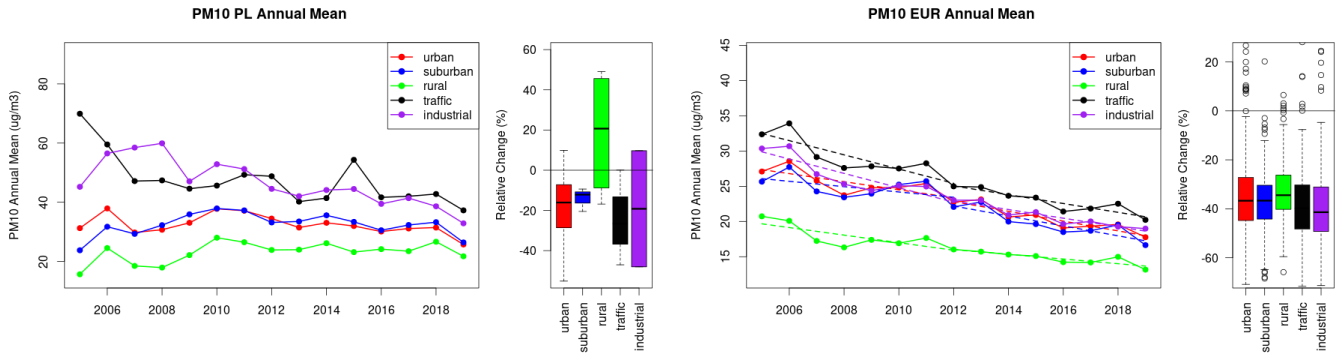


Figure S.504: Time series of the Poland (left) and European-wide composite (median) of annual mean PM10 ($\mu\text{g}/\text{m}^3$) per station type and area (red: urban background, blue suburban background, green: rural background, black: traffic, violet: industrial) between 2005 and 2019. In the European composite, the dashed lines show the linear fit between 2005 & 2012 and between 2012 & 2019. The boxplots on the right-hand side show the distribution of relative changes (%) between 2005 and 2019 for all stations of each typology in Poland and in Europe.

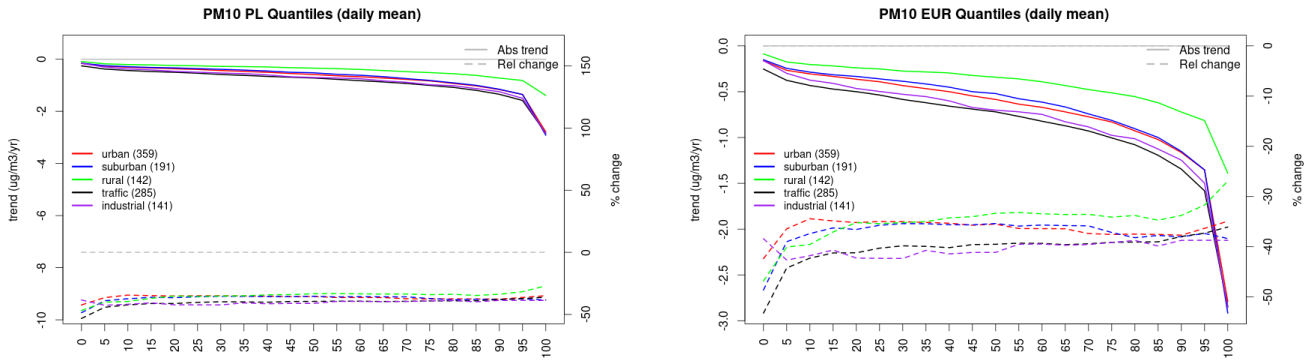


Figure S.505: For PM10 in Poland (left) and Europe, and for each typology of station: absolute trend (solid lines, left y-axis) and relative change (dashed lines, right y-axis) of the percentiles of daily means.

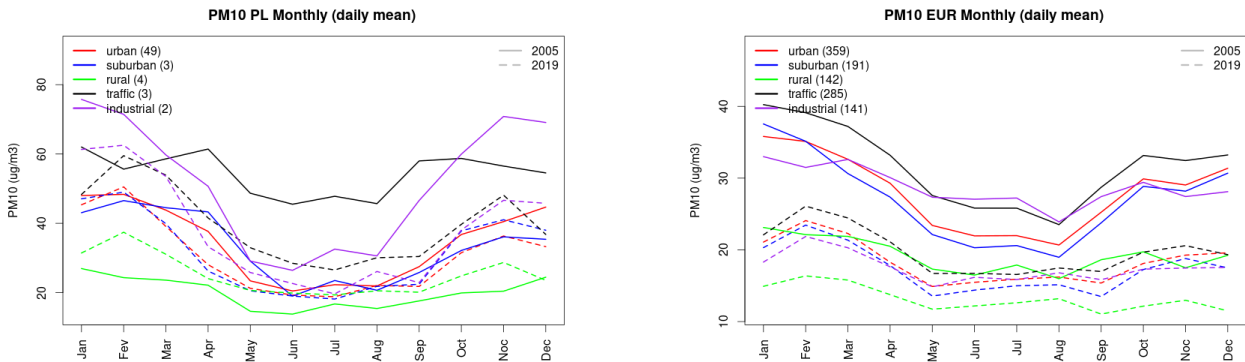


Figure S.506: Monthly cycle of daily mean PM10 for Poland (left) and Europe (right) at various station types estimated from the whole time series in 2005 (solid lines) and 2019 (dashed lines).

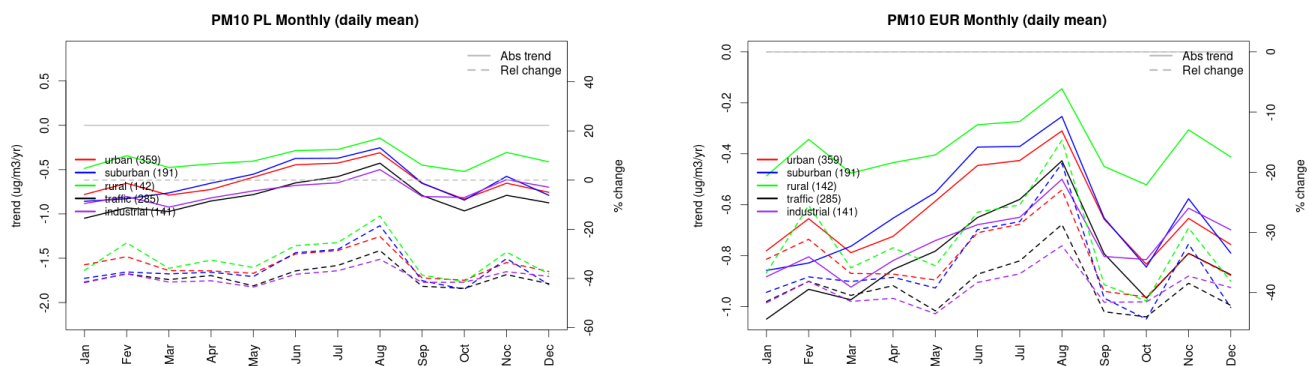


Figure S.507: Absolute (solid lines, left axis) and relative (dashed lines, right axis) trends in the monthly cycle for Poland (left) and Europe (right) of PM10 at various station type.

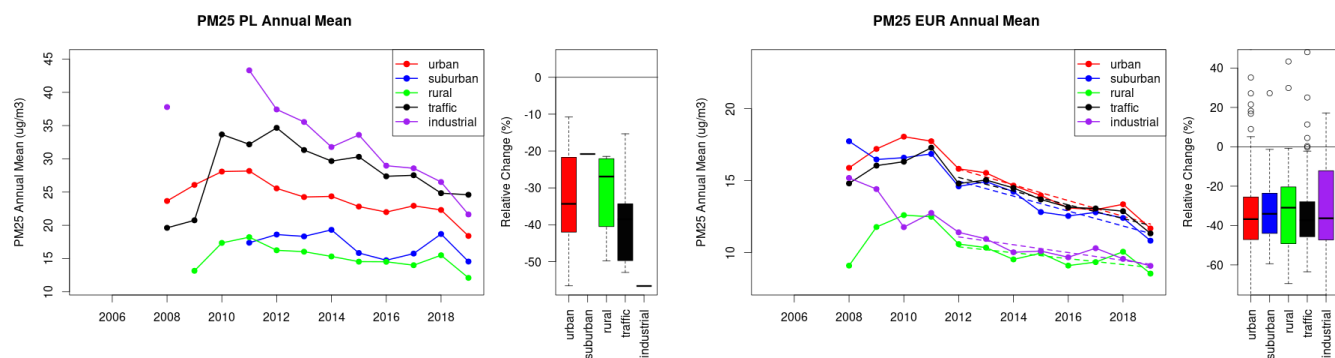


Figure S.508: Time series of the Poland (left) and European-wide composite (median) of annual mean PM25 ($\mu\text{g}/\text{m}^3$) per station type and area (red: urban background, blue suburban background, green: rural background, black: traffic, violet: industrial) between 2005 and 2019. In the European composite, the dashed lines show the linear fit between 2005 & 2012 and between 2012 & 2019. The boxplots on the right-hand side show the distribution of relative changes (%) between 2005 and 2019 for all stations of each typology in Poland and in Europe.

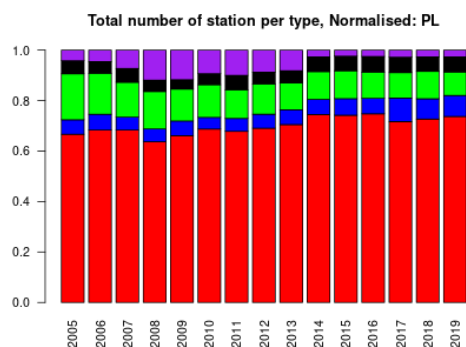
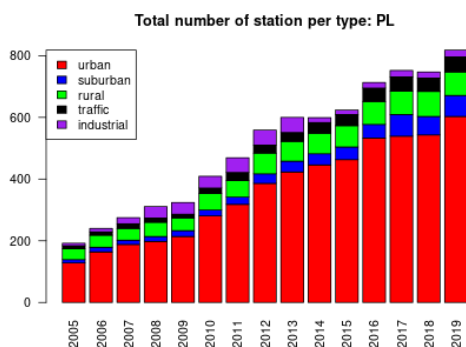
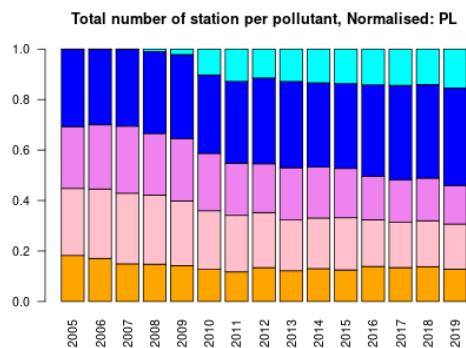
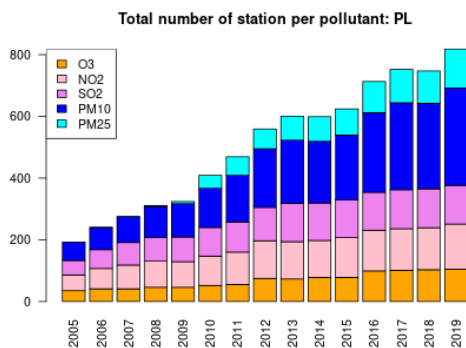
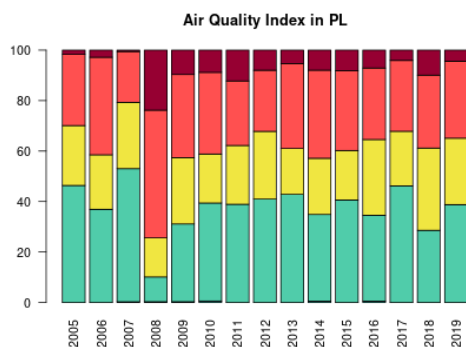


Figure S.509: For Poland: overall air quality index (percentage of days in a given year) and distribution of daily categories per pollutant (light blue: good, light green: fair, yellow: moderate, orange: poor, red: very poor, violet: extremely poor).

24 Portugal

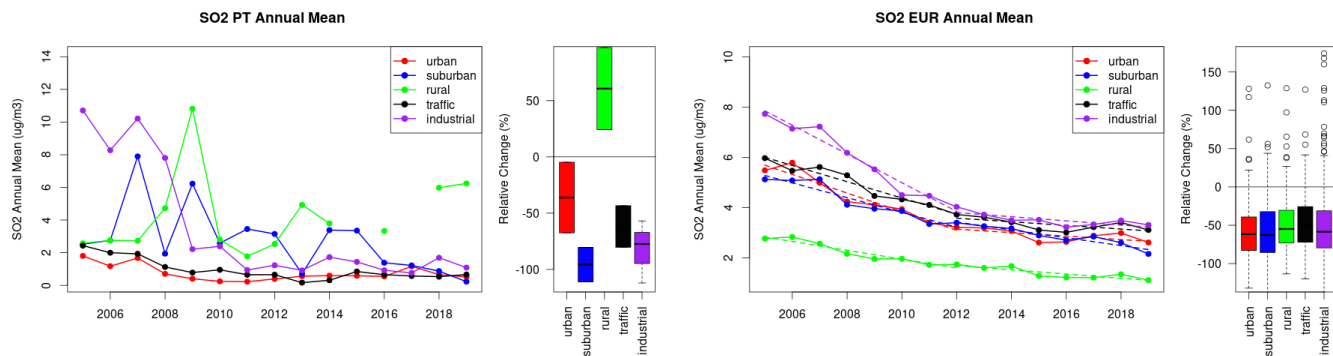


Figure S.510: Time series of the Portugal (left) and European-wide composite (median) of annual mean SO₂ (ug/m³) per station type and area (red: urban background, blue suburban background, green: rural background, black: traffic, violet: industrial) between 2005 and 2019. In the European composite, the dashed lines show the linear fit between 2005 & 2012 and between 2012 & 2019. The boxplots on the right-hand side show the distribution of relative changes (%) between 2005 and 2019 for all stations of each typology in Portugal and in Europe.

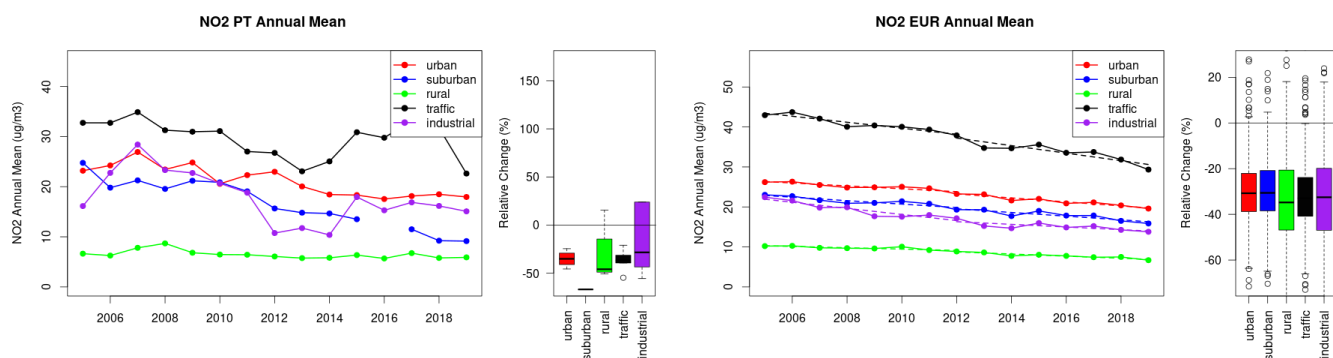


Figure S.511: Time series of the Portugal (left) and European-wide composite (median) of annual mean NO₂ (ug/m³) per station type and area (red: urban background, blue suburban background, green: rural background, black: traffic, violet: industrial) between 2005 and 2019. In the European composite, the dashed lines show the linear fit between 2005 & 2012 and between 2012 & 2019. The boxplots on the right-hand side show the distribution of relative changes (%) between 2005 and 2019 for all stations of each typology in Portugal and in Europe.

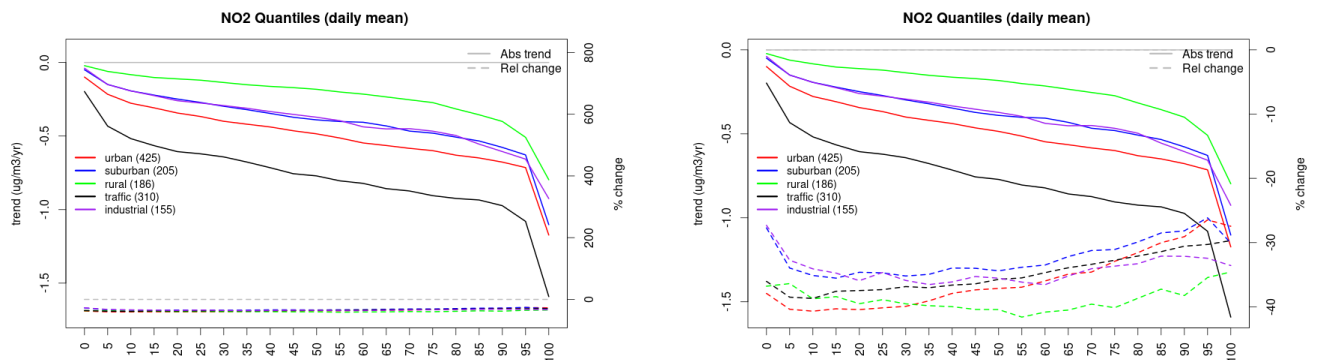


Figure S.512: For NO₂ in Portugal (left) and Europe, and for each typology of station: absolute trend (solid lines, left y-axis) and relative change (dashed lines, right y-axis) of the percentiles of daily means.

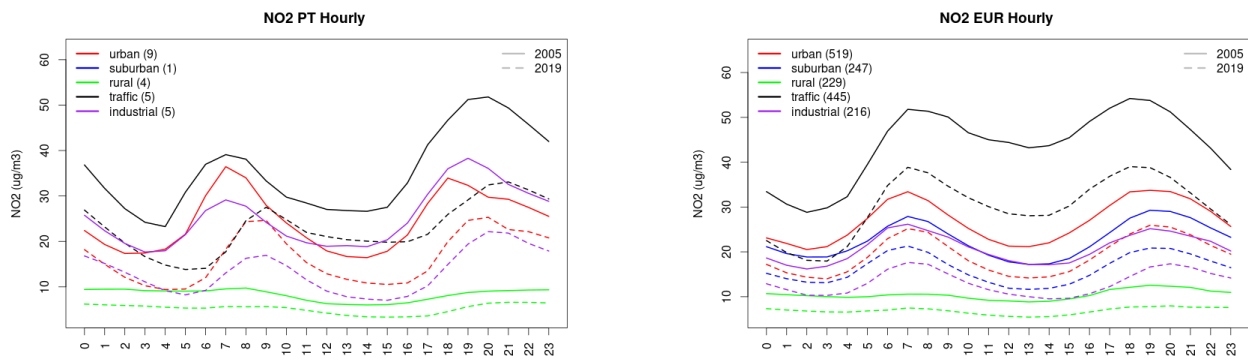


Figure S.513: Diurnal cycle of daily mean NO₂ for Portugal (left) and Europe (right) at various station types estimated from the whole time series in 2005 (solid lines) and 2019

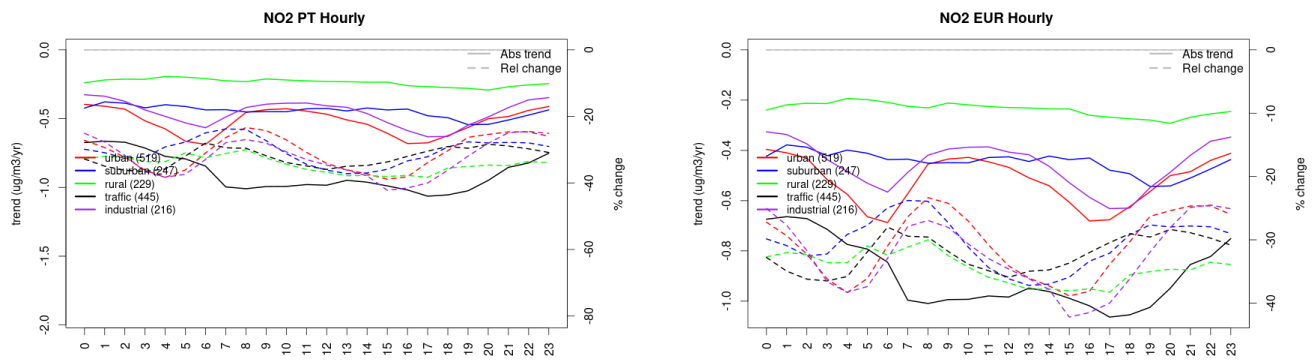


Figure S.514: Absolute (solid lines, left axis) and relative (dashed lines, right axis) trends in the diurnal cycle for Portugal (left) and Europe (right) of NO₂ at various station type.

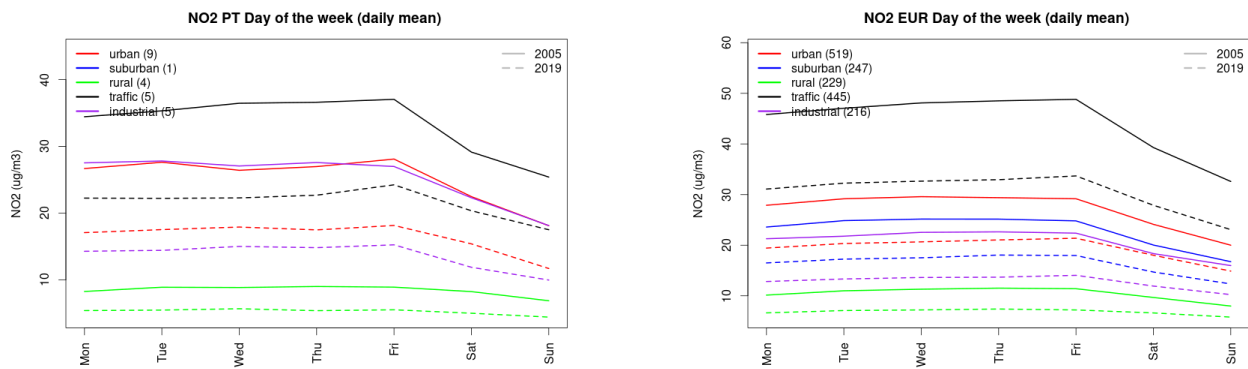


Figure S.515: Weekly cycle of daily mean NO₂ for Portugal (left) and Europe (right) at various station types estimated from the whole time series in 2005 (solid lines) and 2019

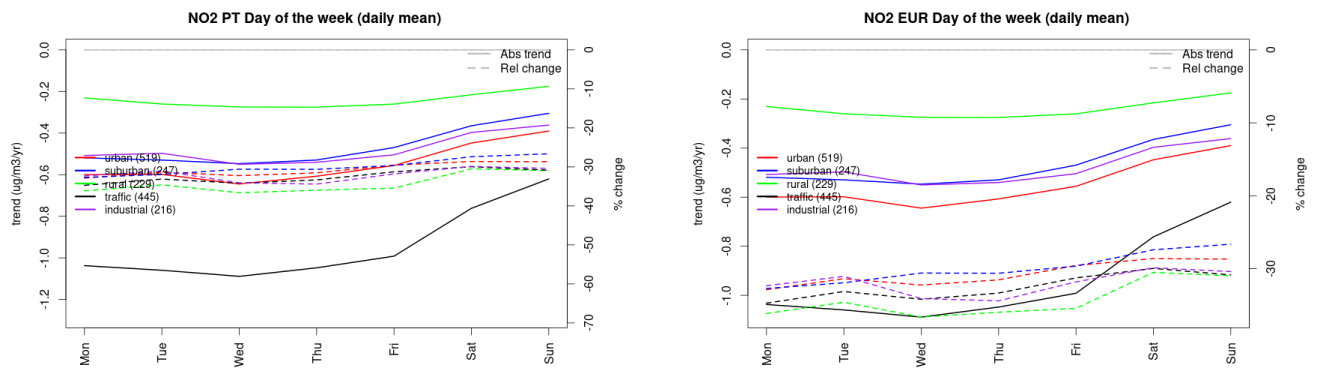


Figure S.516: Absolute (solid lines, left axis) and relative (dashed lines, right axis) trends in the weekly cycle for Portugal (left) and Europe (right) of NO₂ at various station type.

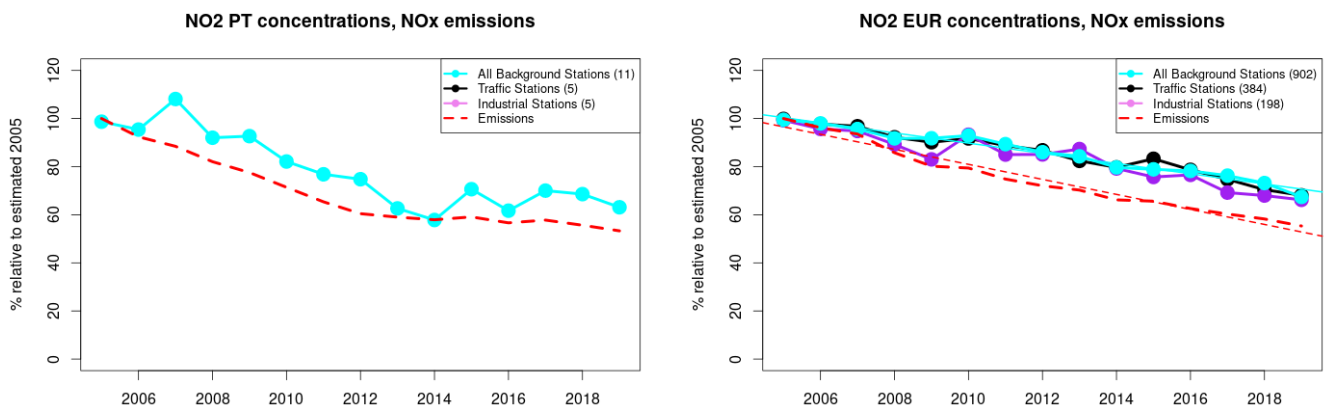


Figure S.517: Time series of 2005-2019 (left) and European (right) median NO₂ observed at traffic (black), industrial (violet) and background (cyan) sites (solid lines), and corresponding NO_x emissions (dashed line) normalised to estimated 2000 levels (%). The median is taken over where more than 5 stations of each typology is available. The total number of stations included is provided in brackets. In the European composite, straight lines are the linear fits over the whole period.

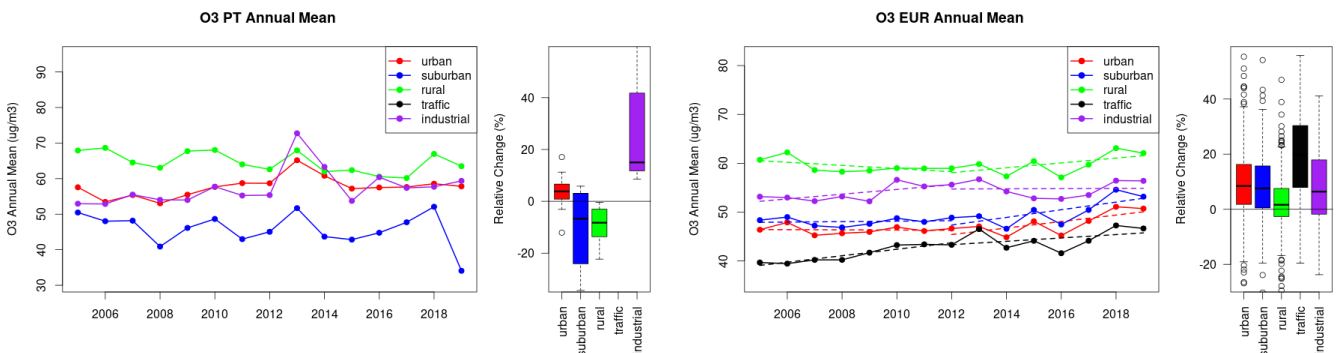


Figure S.518: Time series of the Portugal (left) and European-wide composite (median) of annual mean ozone (ug/m³) per station type and area (red: urban background, blue suburban background, green: rural background, black: traffic, violet: industrial) between 2005 and 2019. In the European composite, the dashed lines show the linear fit between 2005 & 2012 and between 2012 & 2019. The boxplots on the right-hand side show the distribution of relative changes (%) between 2005 and 2019 for all stations of each typology in Portugal and in Europe.

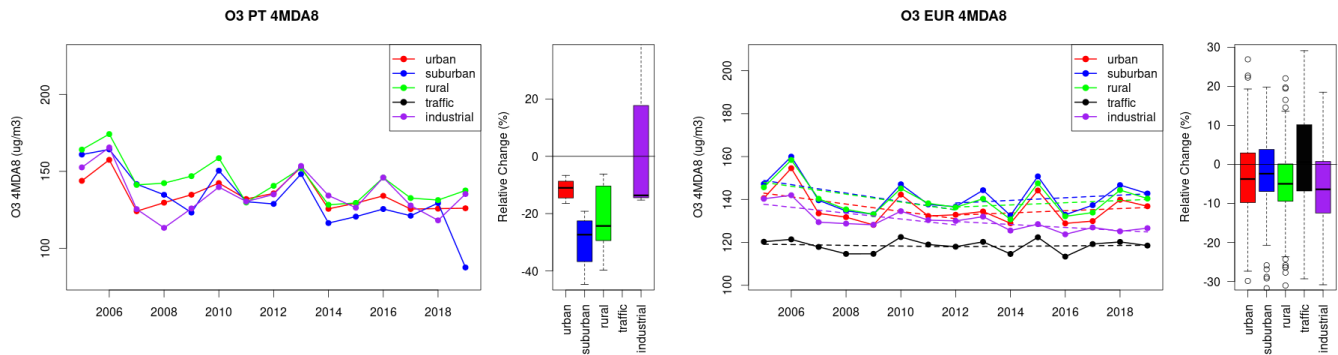


Figure S.519: Time series of the Portugal (left) and European-wide composite (median) of O3 fourth highest daily peak (4MDA8, ug/m³) per station type and area (red: urban background, blue suburban background, green: rural background, black: traffic, violet: industrial) between 2005 and 2019. In the European composite, the dashed lines show the linear fit between 2005 & 2012 and between 2012 & 2019. The boxplots on the right-hand side show the distribution of relative changes (%) between 2005 and 2019 for all stations of each typology in Portugal and in Europe.

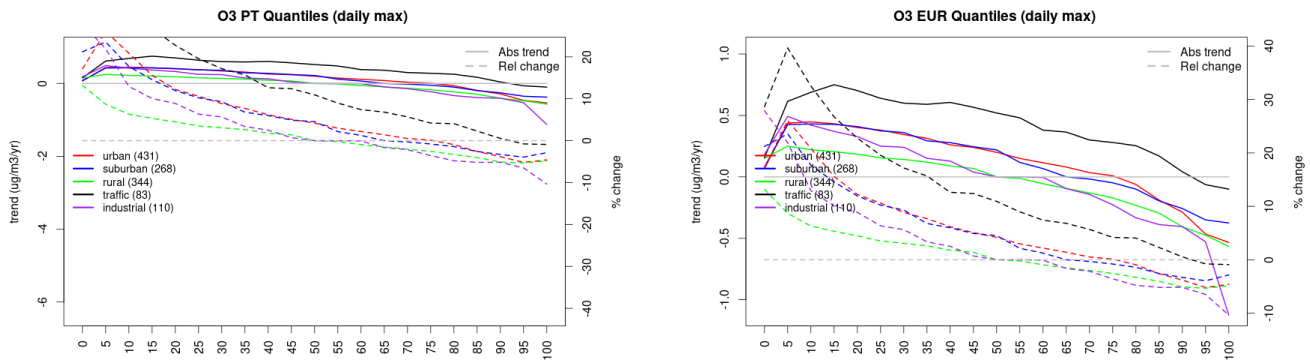


Figure S.520: For ozone in Portugal (left) and Europe, and for each typology of station: absolute trend (solid lines, left y-axis) and relative change (dashed lines, right y-axis) of the percentiles of daily maxima.

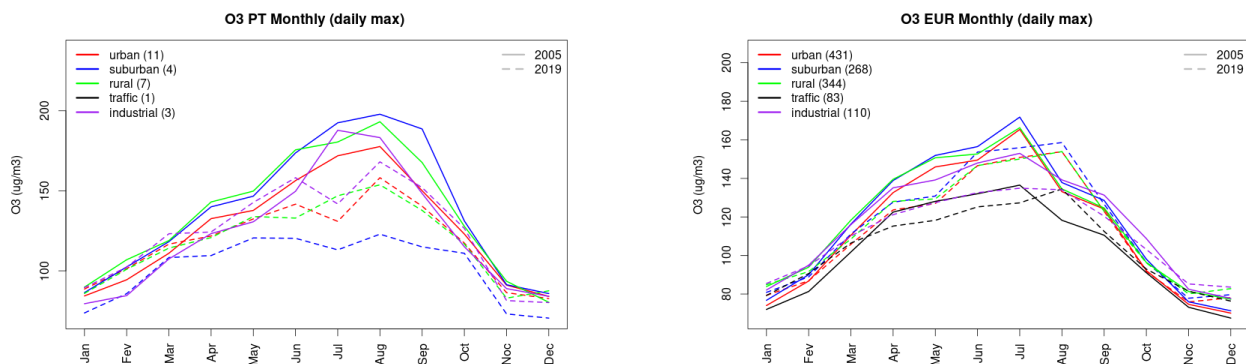


Figure S.521: Monthly cycle of daily max ozone for Portugal (left) and Europe (right) at various station types estimated from the whole time series in 2005 (solid lines) and 2019

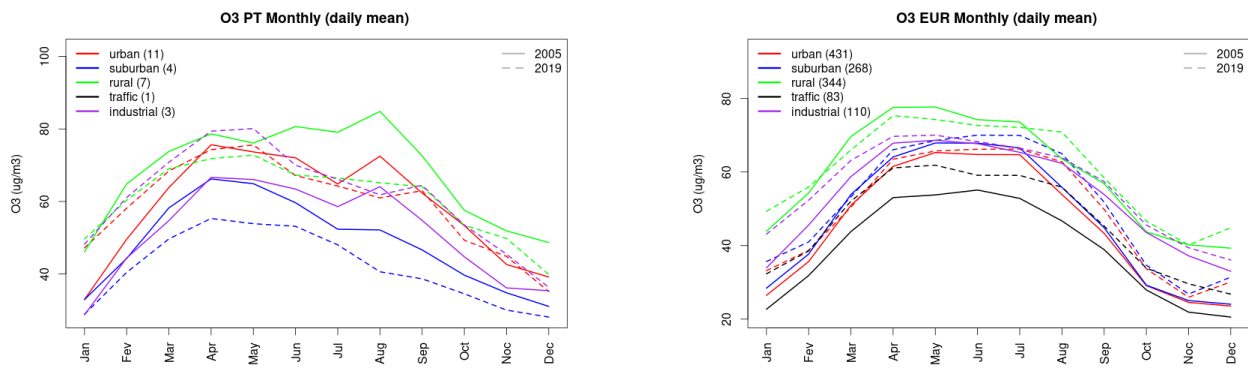


Figure S.522: Monthly cycle of daily mean ozone for Portugal (left) and Europe (right) at various station types estimated from the whole time series in 2005 (solid lines) and 2019

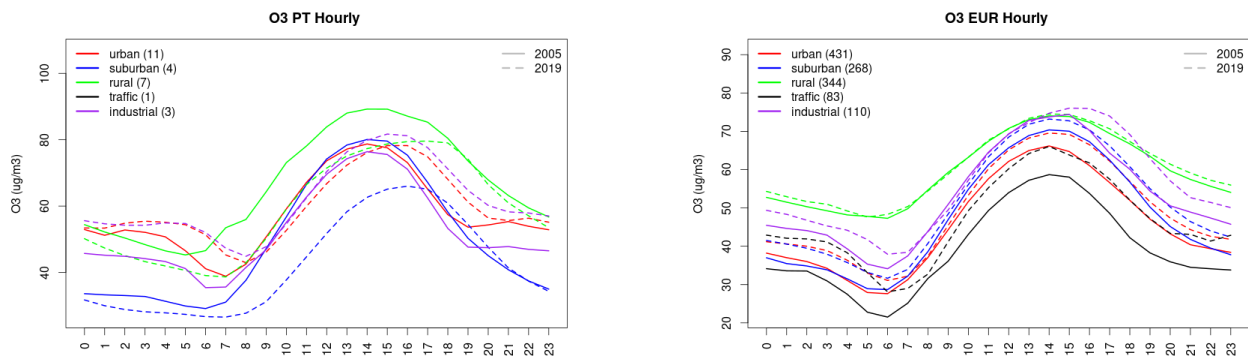


Figure S.523: Diurnal cycle of daily mean ozone for Portugal (left) and Europe (right) at various station types estimated from the whole time series in 2005 (solid lines) and 2019

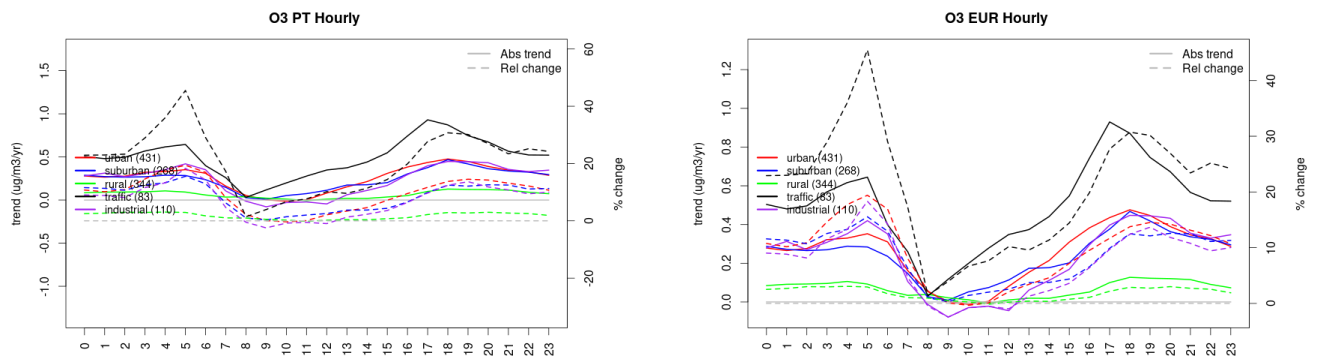


Figure S.524: Absolute (solid lines, left axis) and relative (dashed lines, right axis) trends in the diurnal cycle for Portugal (left) and Europe (right) of ozone at various station type.

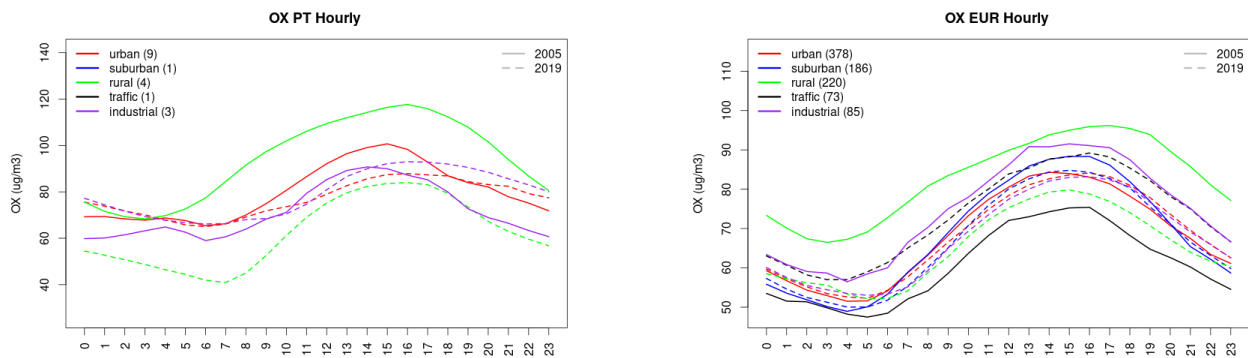


Figure S.525: Diurnal cycle of daily mean OX (as NO₂+O₃) for Portugal (left) and Europe (right) at various station types estimated from the whole time series in 2005 (solid lines) and 2019 (dashed lines)

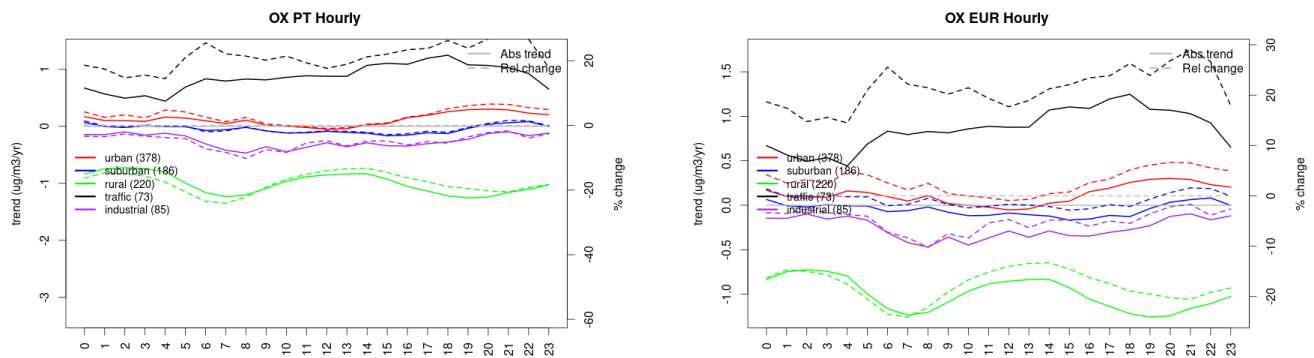


Figure S.526: Absolute (solid lines, left axis) and relative (dashed lines, right axis) trends in the diurnal cycle for Portugal (left) and Europe (right) of OX (as NO₂+O₃) at various station type.

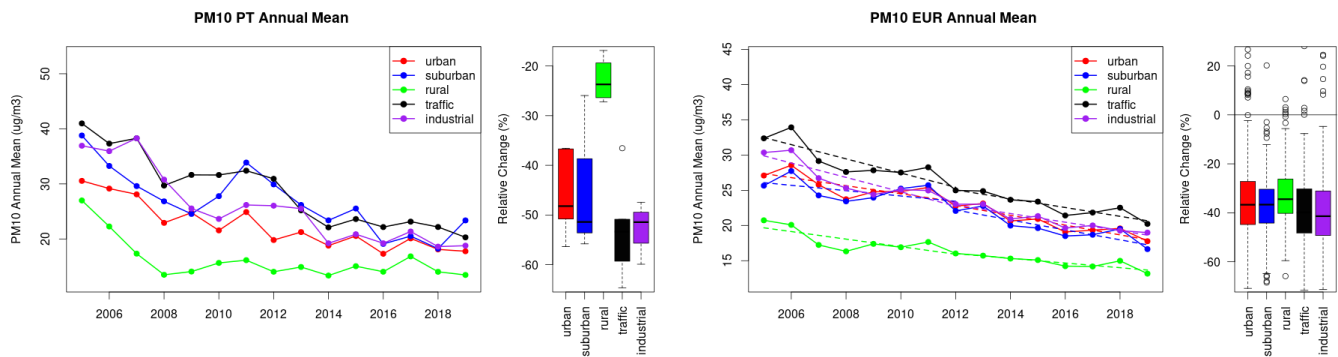


Figure S.527: Time series of the Portugal (left) and European-wide composite (median) of annual mean PM₁₀ (ug/m³) per station type and area (red: urban background, blue suburban background, green: rural background, black: traffic, violet: industrial) between 2005 and 2019. In the European composite, the dashed lines show the linear fit between 2005 & 2012 and between 2012 & 2019. The boxplots on the right-hand side show the distribution of relative changes (%) between 2005 and 2019 for all stations of each typology in Portugal and in Europe.

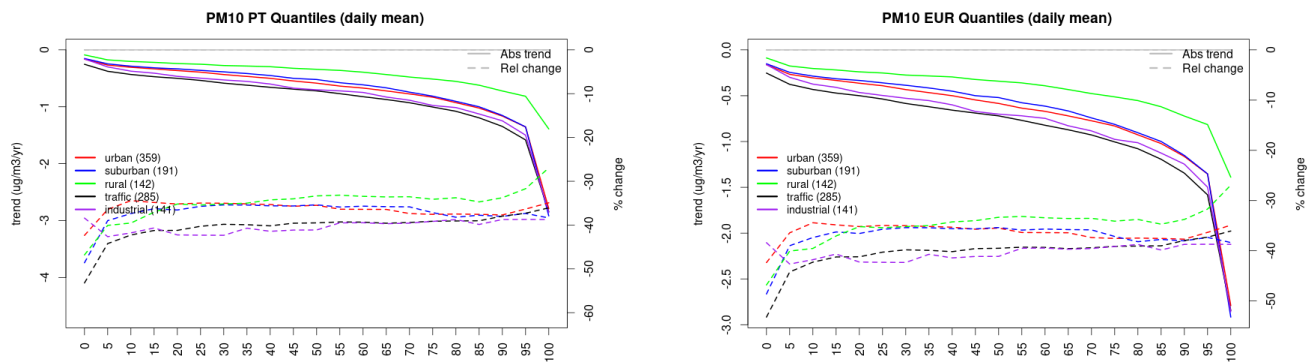


Figure S.528: For PM10 in Portugal (left) and Europe, and for each typology of station: absolute trend (solid lines, left y-axis) and relative change (dashed lines, right y-axis) of the percentiles of daily means.

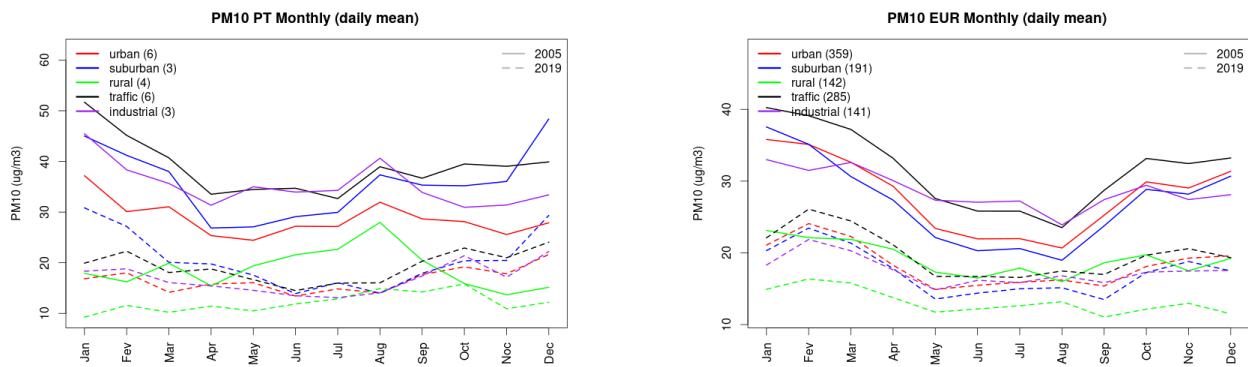


Figure S.529: Monthly cycle of daily mean PM10 for Portugal (left) and Europe (right) at various station types estimated from the whole time series in 2005 (solid lines) and 2019

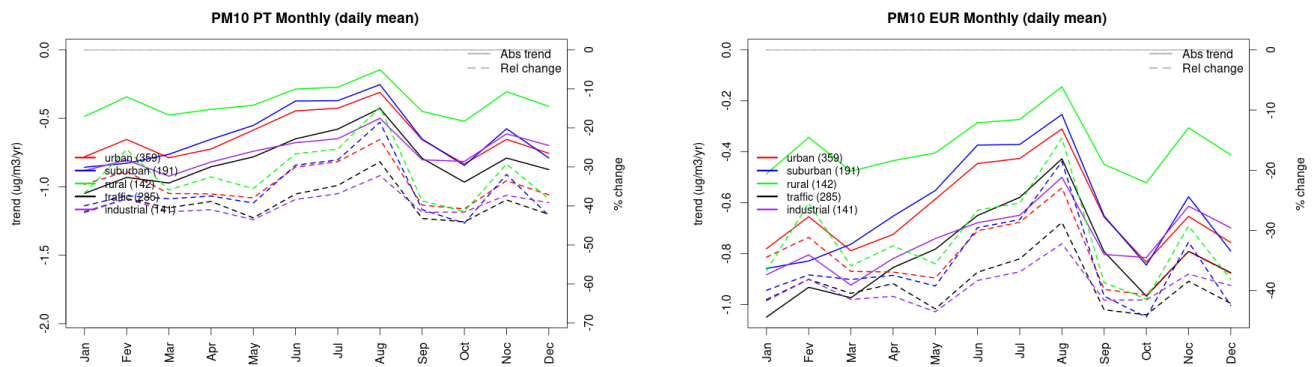


Figure S.530: Absolute (solid lines, left axis) and relative (dashed lines, right axis) trends in the monthly cycle for Portugal (left) and Europe (right) of PM10 at various station type.

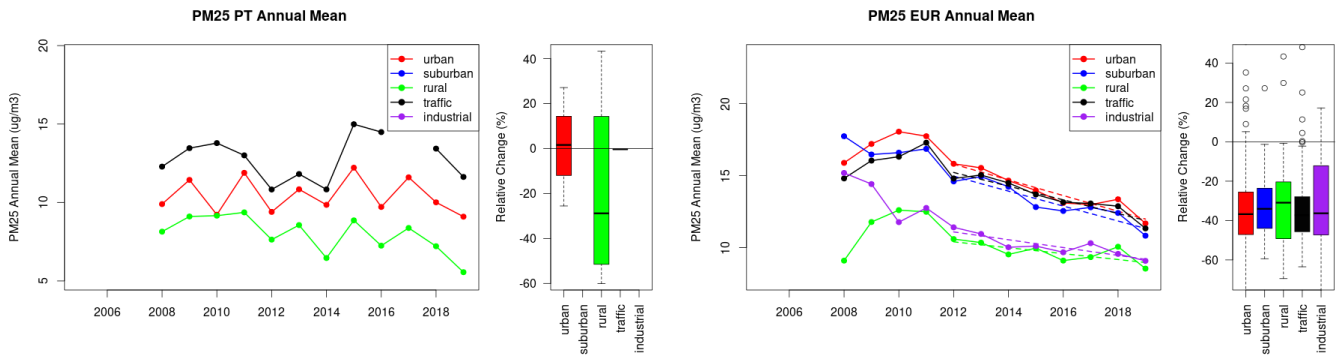


Figure S.531: Time series of the Portugal (left) and European-wide composite (median) of annual mean PM25 (ug/m3) per station type and area (red: urban background, blue suburban background, green: rural background, black: traffic, violet: industrial) between 2005 and 2019. In the European composite, the dashed lines show the linear fit between 2005 & 2012 and between 2012 & 2019. The boxplots on the right-hand side show the distribution of relative changes (%) between 2005 and 2019 for all stations of each typology in Portugal and in Europe.

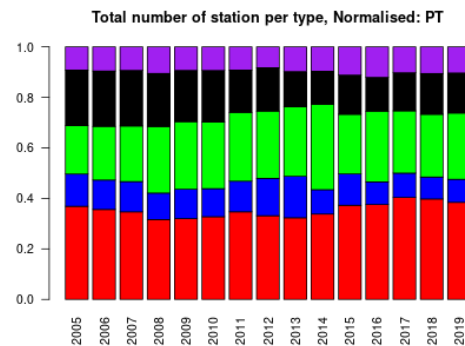
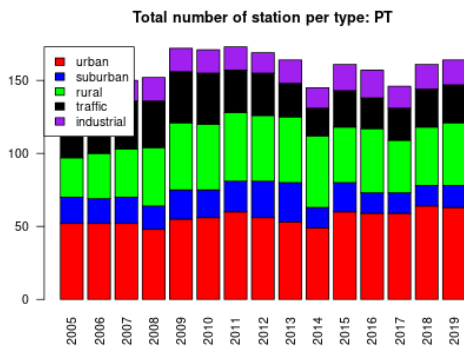
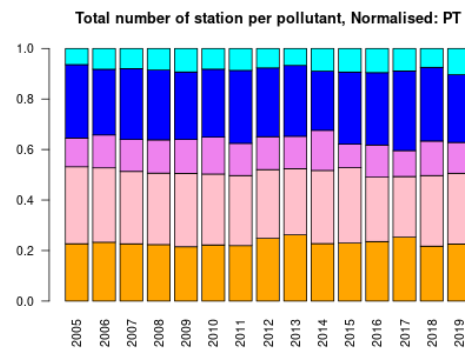
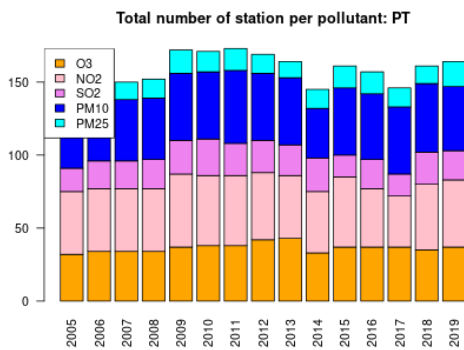
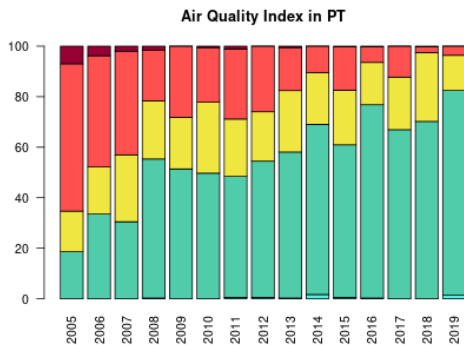


Figure S.532: For Portugal: overall air quality index (percentage of days in a given year) and distribution of daily categories per pollutant (light blue: good, light green: fair, yellow: moderate, orange: poor, red: very poor, violet: extremely poor).

25 Romania

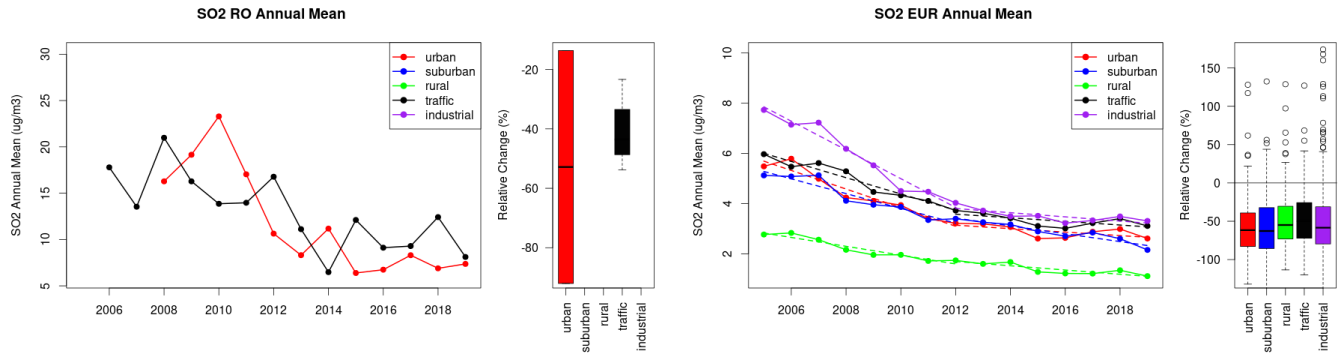


Figure S.533: Time series of the Romania (left) and European-wide composite (median) of annual mean SO₂ (ug/m³) per station type and area (red: urban background, blue suburban background, green: rural background, black: traffic, violet: industrial) between 2005 and 2019. In the European composite, the dashed lines show the linear fit between 2005 & 2012 and between 2012 & 2019. The boxplots on the right-hand side show the distribution of relative changes (%) between 2005 and 2019 for all stations of each typology in Romania and in Europe.

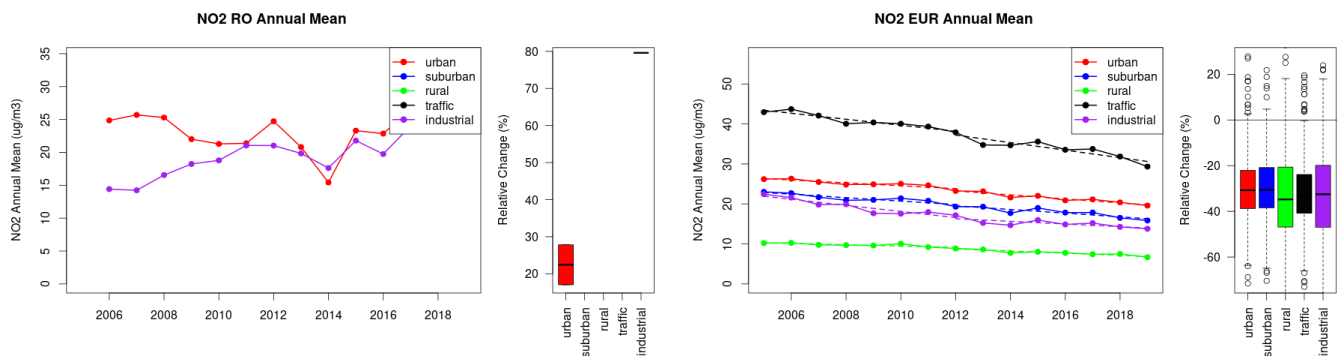


Figure S.534: Time series of the Romania (left) and European-wide composite (median) of annual mean NO₂ (ug/m³) per station type and area (red: urban background, blue suburban background, green: rural background, black: traffic, violet: industrial) between 2005 and 2019. In the European composite, the dashed lines show the linear fit between 2005 & 2012 and between 2012 & 2019. The boxplots on the right-hand side show the distribution of relative changes (%) between 2005 and 2019 for all stations of each typology in Romania and in Europe.

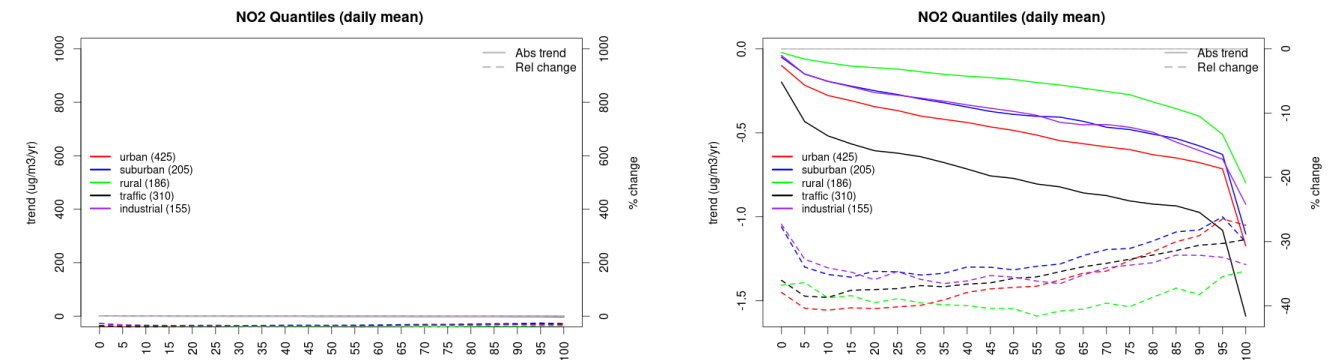


Figure S.535: For NO₂ in Romania (left) and Europe, and for each typology of station: absolute trend (solid lines, left y-axis) and relative change (dashed lines, right y-axis) of the percentiles of daily means.

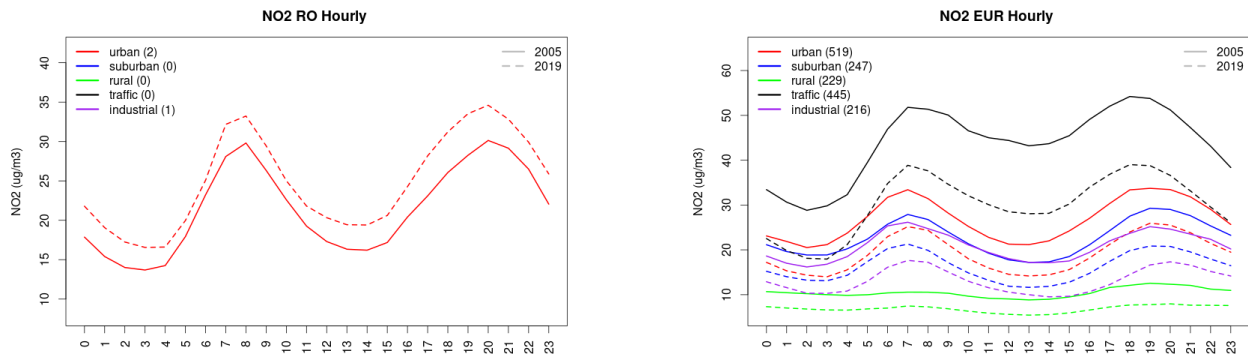


Figure S.536: Diurnal cycle of daily mean NO2 for Romania (left) and Europe (right) at various station types estimated from the whole time series in 2005 (solid lines) and 2019

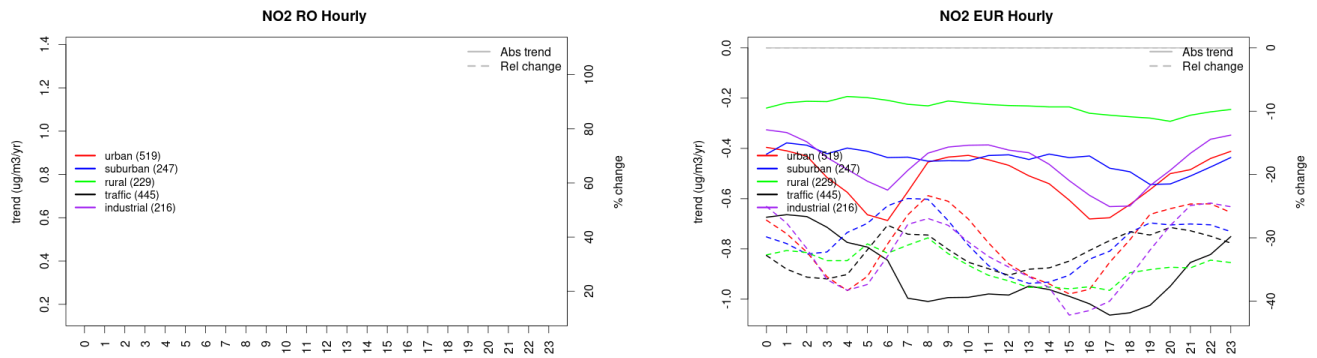


Figure S.537: Absolute (solid lines, left axis) and relative (dashed lines, right axis) trends in the diurnal cycle for Romania (left) and Europe (right) of NO2 at various station type.

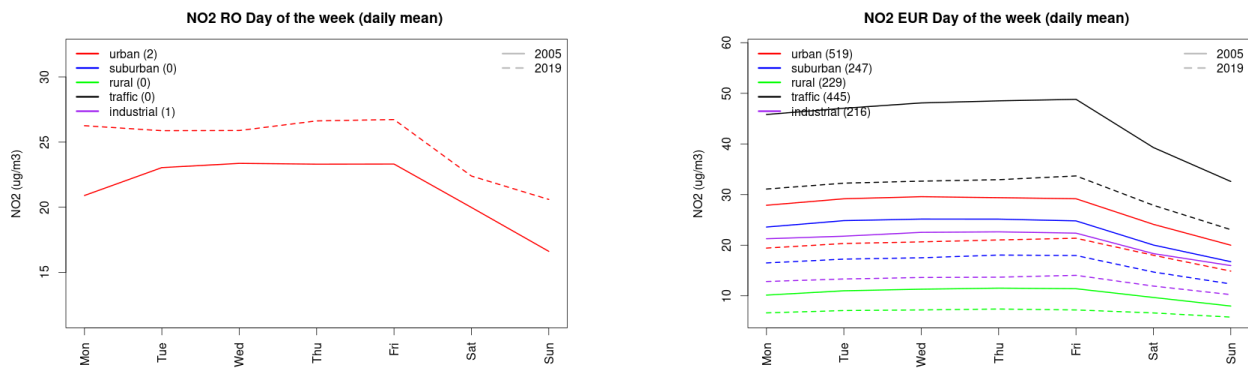


Figure S.538: Weekly cycle of daily mean NO2 for Romania (left) and Europe (right) at various station types estimated from the whole time series in 2005 (solid lines) and 2019

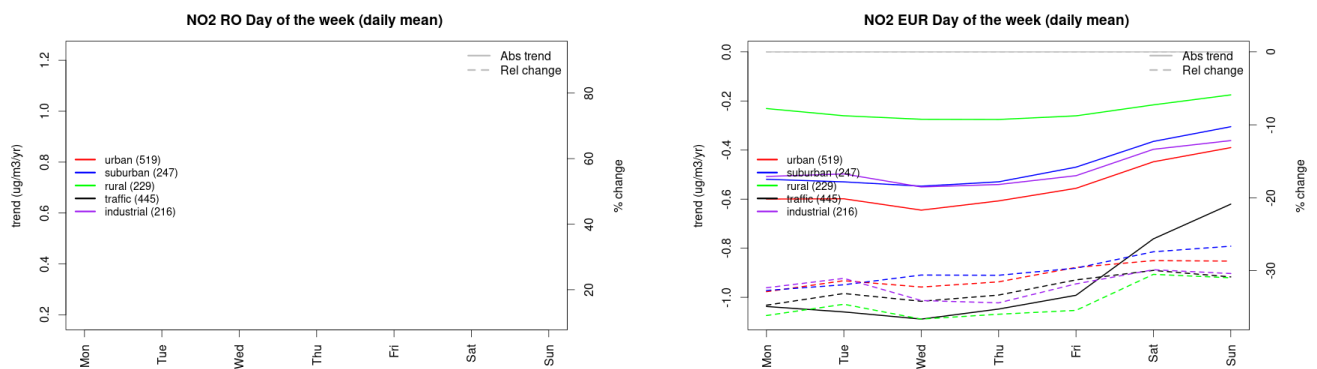


Figure S.539: Absolute (solid lines, left axis) and relative (dashed lines, right axis) trends in the weekly cycle for Romania (left) and Europe (right) of NO₂ at various station type.

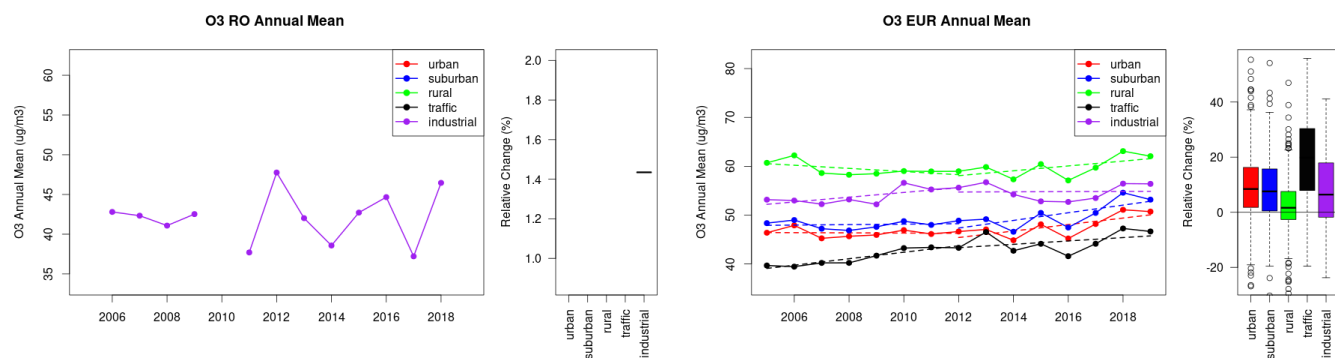


Figure S.540: Time series of the Romania (left) and European-wide composite (median) of annual mean ozone (ug/m³) per station type and area (red: urban background, blue suburban background, green: rural background, black: traffic, violet: industrial) between 2005 and 2019. In the European composite, the dashed lines show the linear fit between 2005 & 2012 and between 2012 & 2019. The boxplots on the right-hand side show the distribution of relative changes (%) between 2005 and 2019 for all stations of each typology in Romania and in Europe.

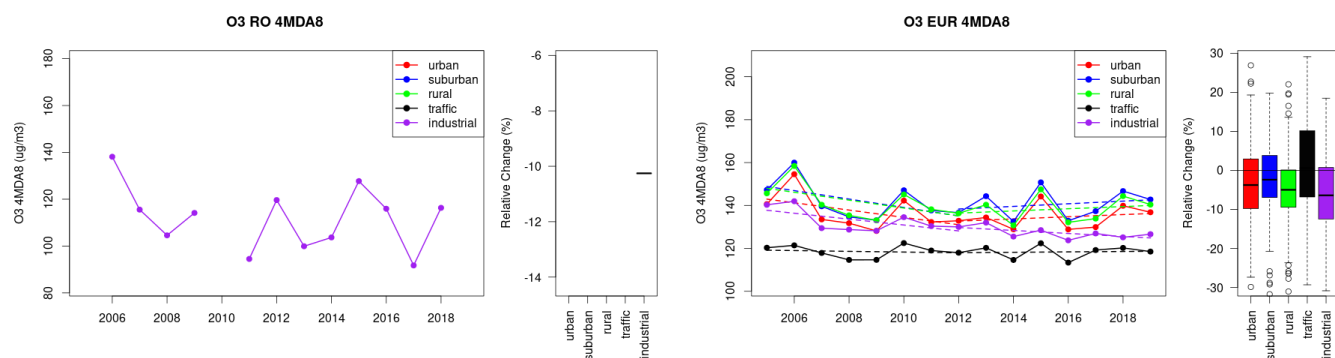


Figure S.541: Time series of the Romania (left) and European-wide composite (median) of O₃ fourth highest daily peak (4MDA8, ug/m³) per station type and area (red: urban background, blue suburban background, green: rural background, black: traffic, violet: industrial) between 2005 and 2019. In the European composite, the dashed lines show the linear fit between 2005 & 2012 and between 2012 & 2019. The boxplots on the right-hand side show the distribution of relative changes (%) between 2005 and 2019 for all stations of each typology in Romania and in Europe.

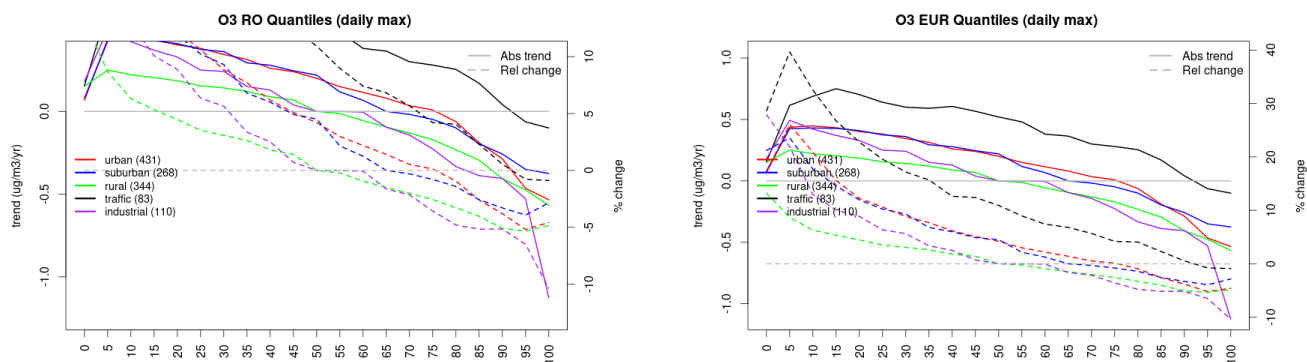


Figure S.542: For ozone in Romania (left) and Europe, and for each typology of station: absolute trend (solid lines, left y-axis) and relative change (dashed lines, right y-axis) of the percentiles of daily maxima.

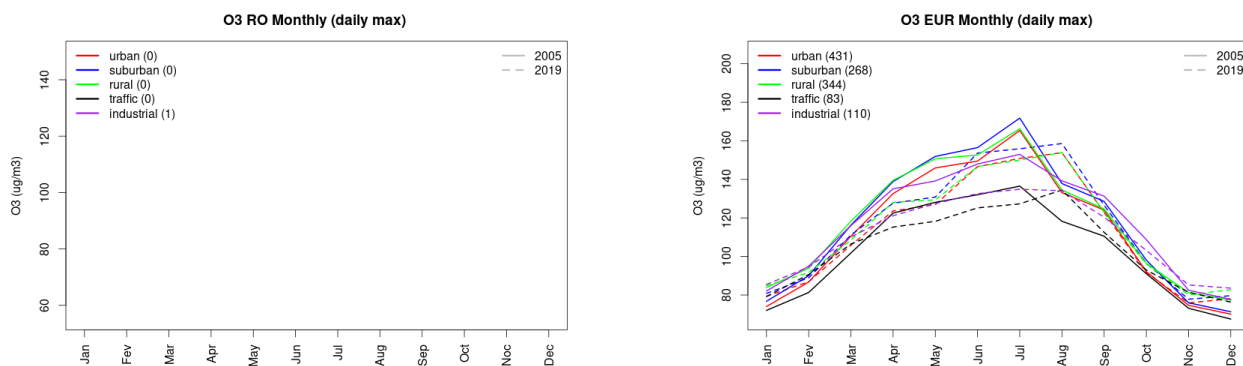


Figure S.543: Monthly cycle of daily max ozone for Romania (left) and Europe (right) at various station types estimated from the whole time series in 2005 (solid lines) and 2019

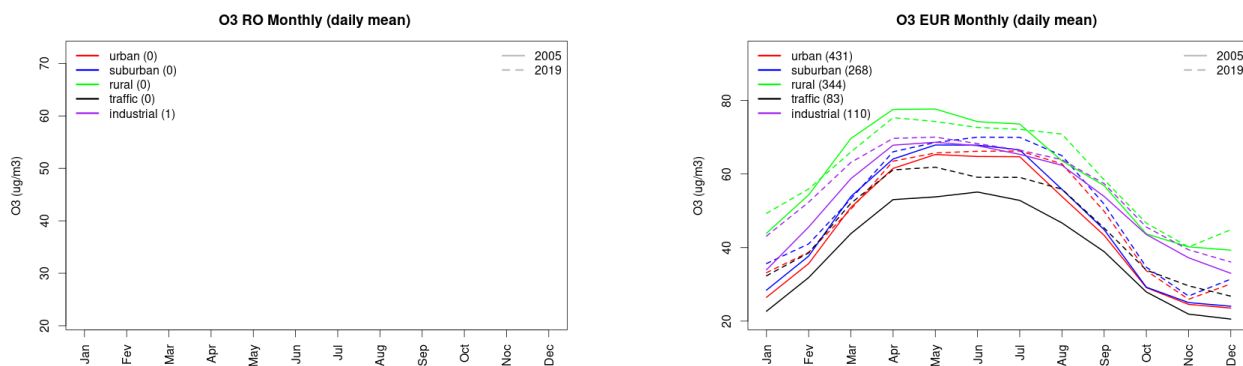


Figure S.544: Monthly cycle of daily mean ozone for Romania (left) and Europe (right) at various station types estimated from the whole time series in 2005 (solid lines) and 2019

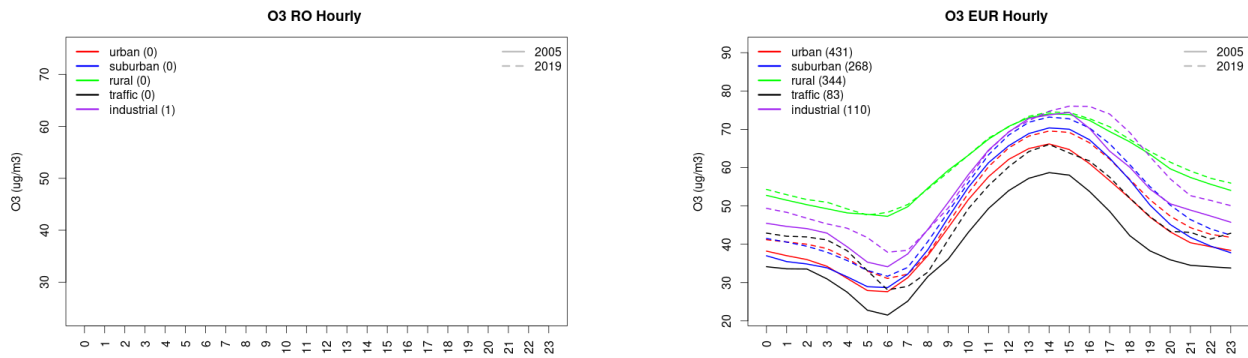


Figure S.545: Diurnal cycle of daily mean ozone for Romania (left) and Europe (right) at various station types estimated from the whole time series in 2005 (solid lines) and 2019

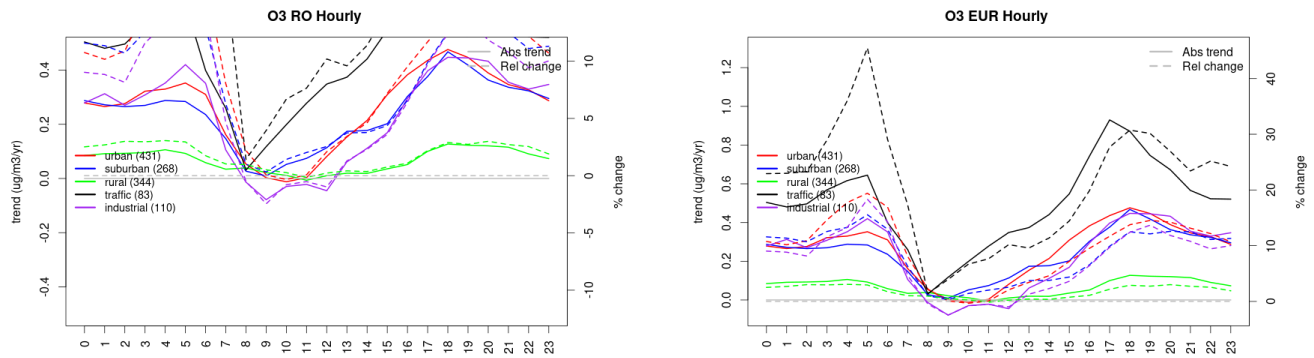


Figure S.546: Absolute (solid lines, left axis) and relative (dashed lines, right axis) trends in the diurnal cycle for Romania (left) and Europe (right) of ozone at various station type.

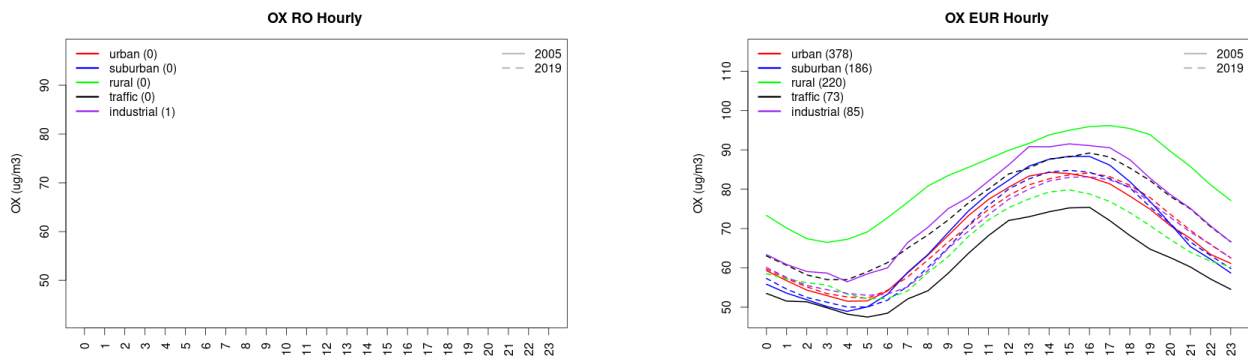


Figure S.547: Diurnal cycle of daily mean OX (as NO2+O3) for Romania (left) and Europe (right) at various station types estimated from the whole time series in 2005 (solid lines) and 2019

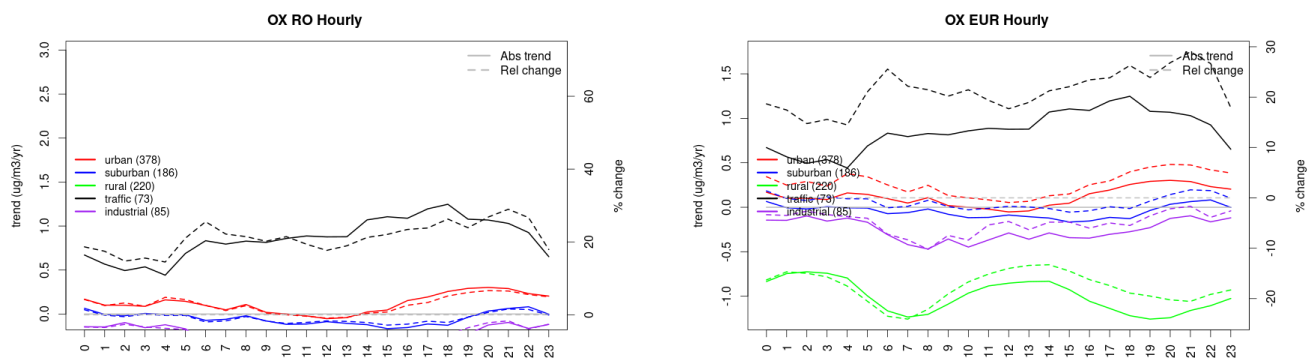


Figure S.548: Absolute (solid lines, left axis) and relative (dashed lines, right axis) trends in the diurnal cycle for Romania (left) and Europe (right) of OX (as NO₂+O₃) at various station type.

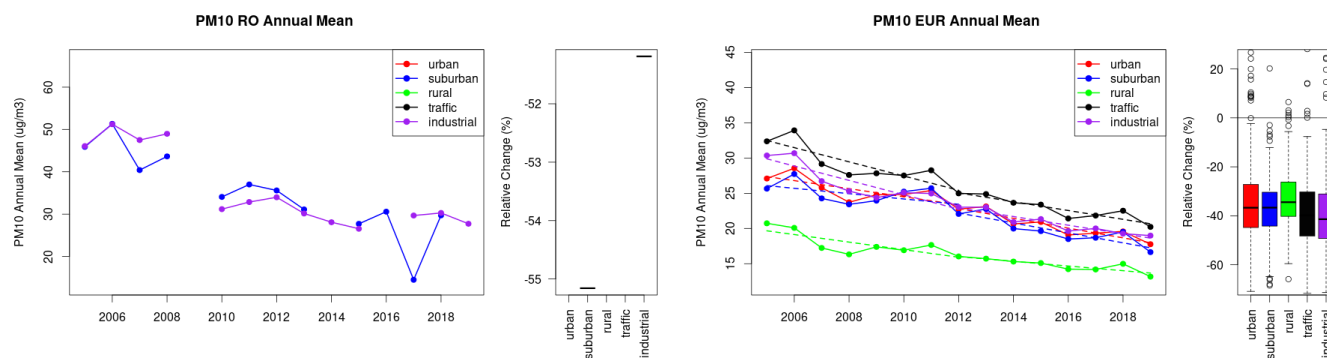


Figure S.549: Time series of the Romania (left) and European-wide composite (median) of annual mean PM₁₀ (ug/m³) per station type and area (red: urban background, blue suburban background, green: rural background, black: traffic, violet: industrial) between 2005 and 2019. In the European composite, the dashed lines show the linear fit between 2005 & 2012 and between 2012 & 2019. The boxplots on the right-hand side show the distribution of relative changes (%) between 2005 and 2019 for all stations of each typology in Romania and in Europe.

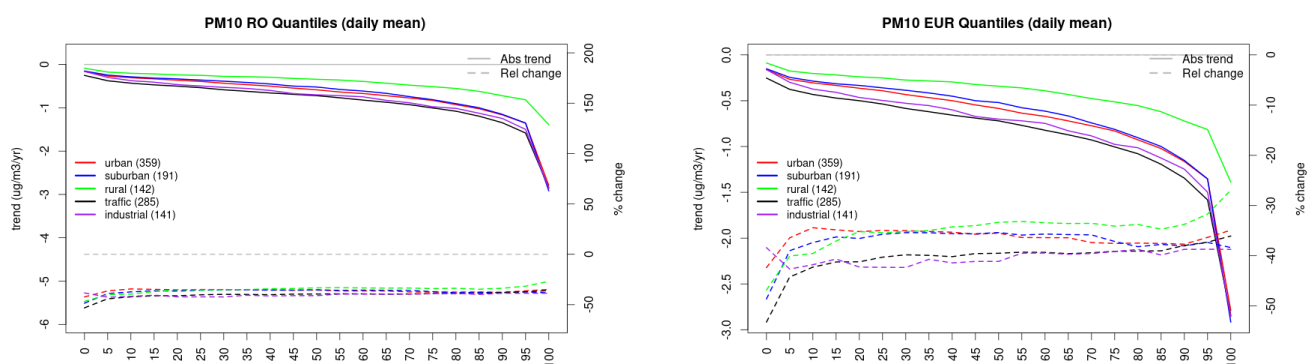


Figure S.550: For PM₁₀ in Romania (left) and Europe, and for each typology of station: absolute trend (solid lines, left y-axis) and relative change (dashed lines, right y-axis) of the percentiles of daily means.

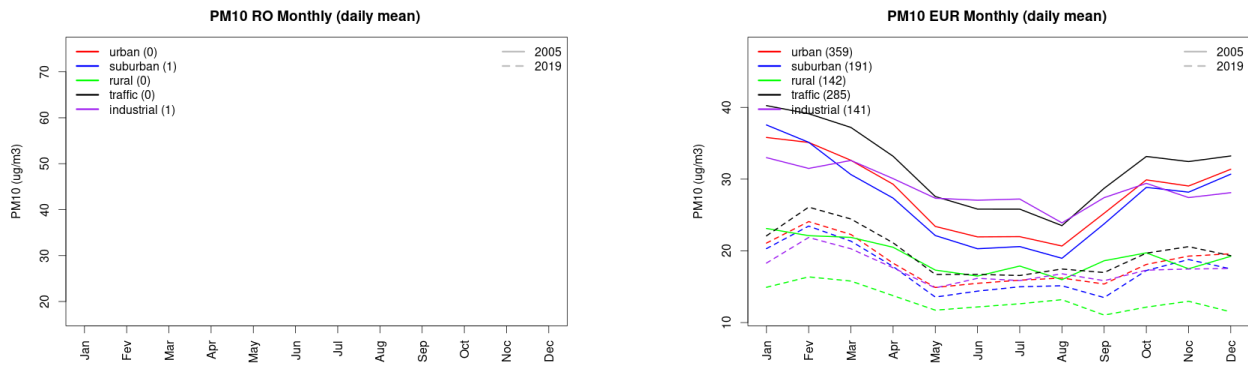


Figure S.551: Monthly cycle of daily mean PM10 for Romania (left) and Europe (right) at various station types estimated from the whole time series in 2005 (solid lines) and 2019

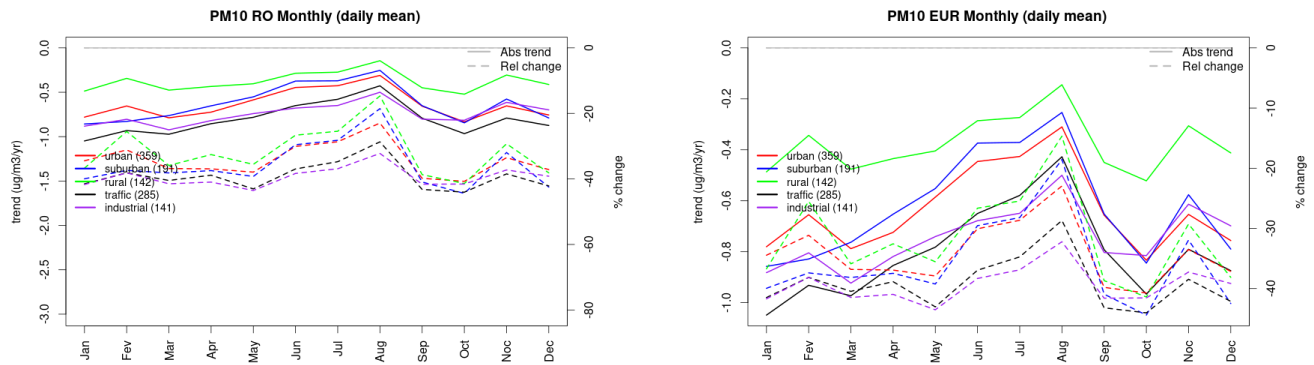


Figure S.552: Absolute (solid lines, left axis) and relative (dashed lines, right axis) trends in the monthly cycle for Romania (left) and Europe (right) of PM10 at various station type.

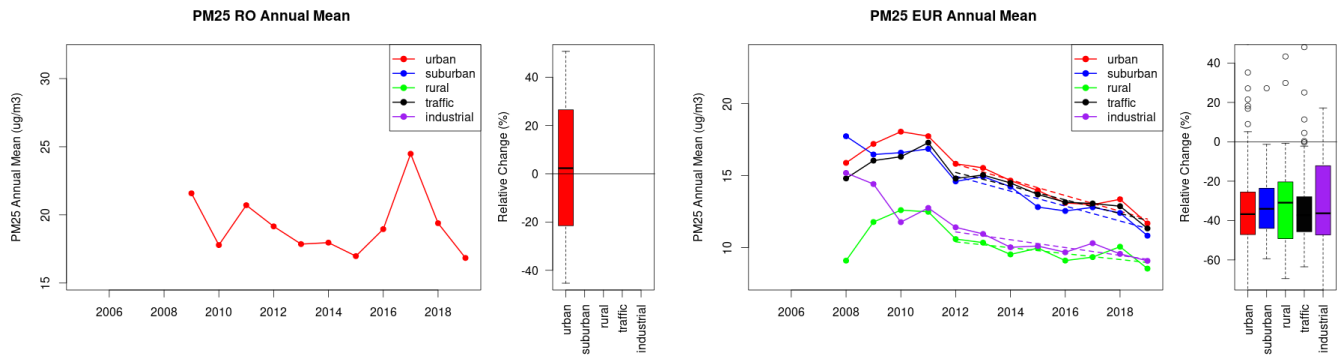


Figure S.553: Time series of the Romania (left) and European-wide composite (median) of annual mean PM25 ($\mu\text{g}/\text{m}^3$) per station type and area (red: urban background, blue suburban background, green: rural background, black: traffic, violet: industrial) between 2005 and 2019. In the European composite, the dashed lines show the linear fit between 2005 & 2012 and between 2012 & 2019. The boxplots on the right-hand side show the distribution of relative changes (%) between 2005 and 2019 for all stations of each typology in Romania and in Europe.

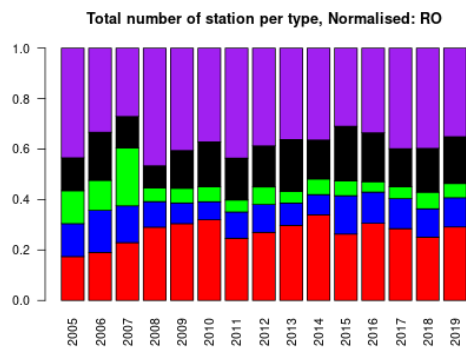
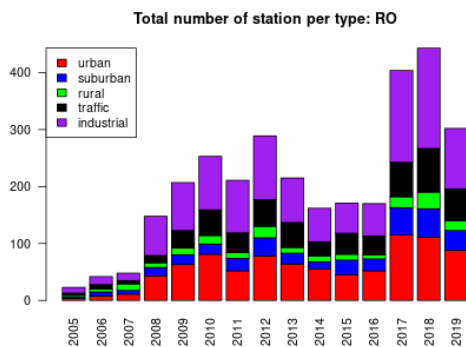
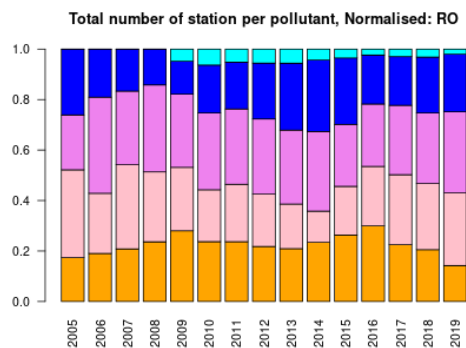
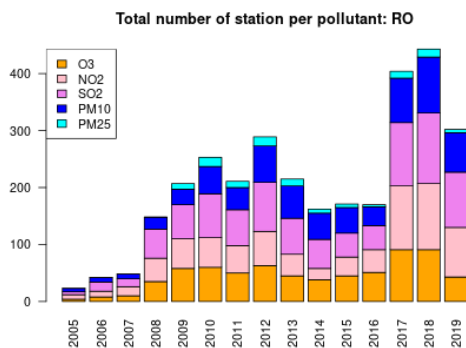
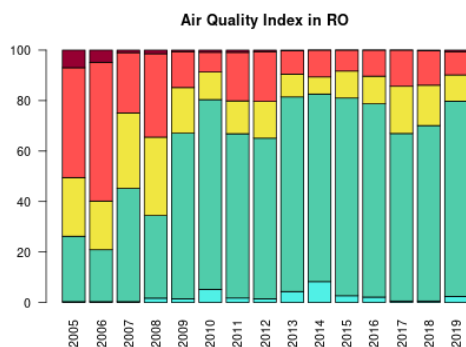


Figure S.554: For Romania: overall air quality index (percentage of days in a given year) and distribution of daily categories per pollutant (light blue: good, light green: fair, yellow: moderate, orange: poor, red: very poor, violet: extremely poor).

26 Sweden

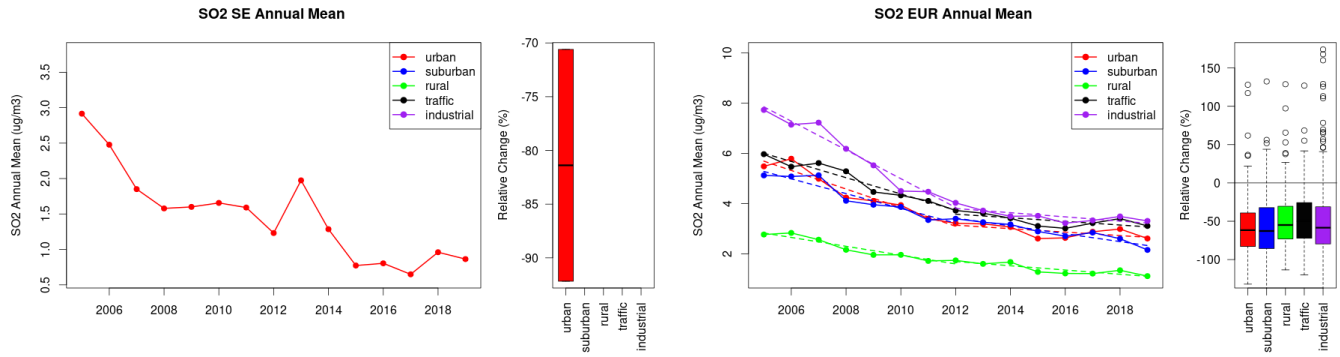


Figure S.555: Time series of the Sweden (left) and European-wide composite (median) of annual mean SO₂ (ug/m³) per station type and area (red: urban background, blue suburban background, green: rural background, black: traffic, violet: industrial) between 2005 and 2019. In the European composite, the dashed lines show the linear fit between 2005 & 2012 and between 2012 & 2019. The boxplots on the right-hand side show the distribution of relative changes (%) between 2005 and 2019 for all stations of each typology in Sweden and in Europe.

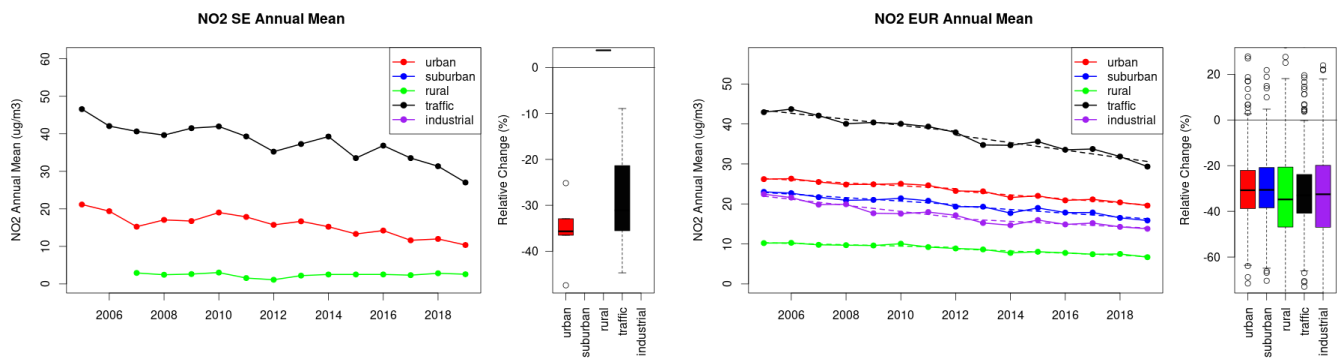


Figure S.556: Time series of the Sweden (left) and European-wide composite (median) of annual mean NO₂ (ug/m³) per station type and area (red: urban background, blue suburban background, green: rural background, black: traffic, violet: industrial) between 2005 and 2019. In the European composite, the dashed lines show the linear fit between 2005 & 2012 and between 2012 & 2019. The boxplots on the right-hand side show the distribution of relative changes (%) between 2005 and 2019 for all stations of each typology in Sweden and in Europe.

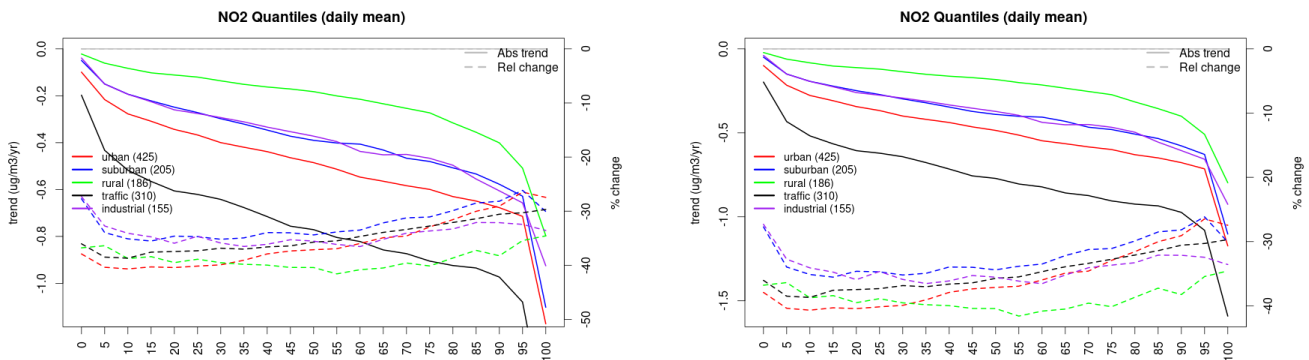


Figure S.557: For NO₂ in Sweden (left) and Europe, and for each typology of station: absolute trend (solid lines, left y-axis) and relative change (dashed lines, right y-axis) of the percentiles of daily means.

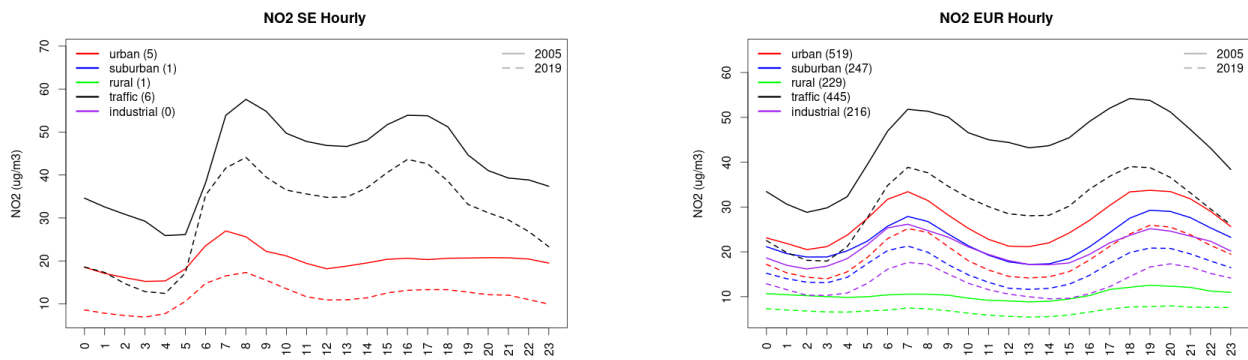


Figure S.558: Diurnal cycle of daily mean NO2 for Sweden (left) and Europe (right) at various station types estimated from the whole time series in 2005 (solid lines) and 2019

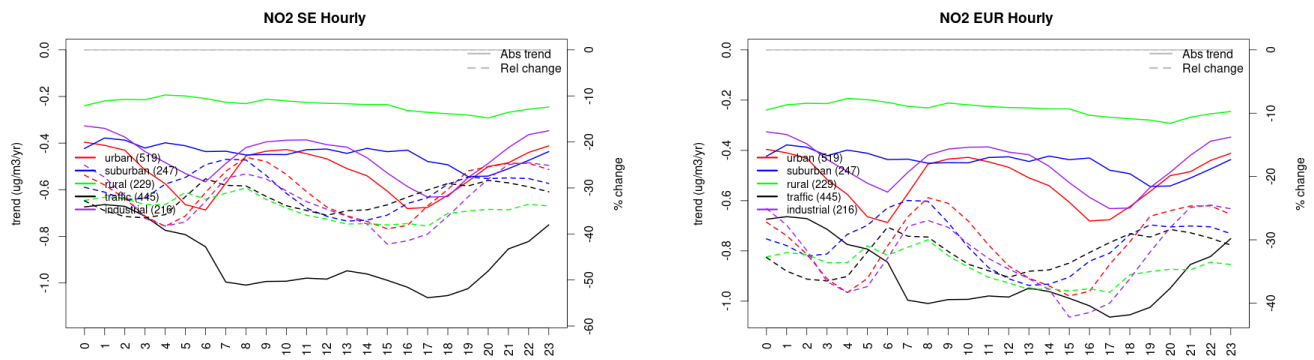


Figure S.559: Absolute (solid lines, left axis) and relative (dashed lines, right axis) trends in the diurnal cycle for Sweden (left) and Europe (right) of NO2 at various station type.

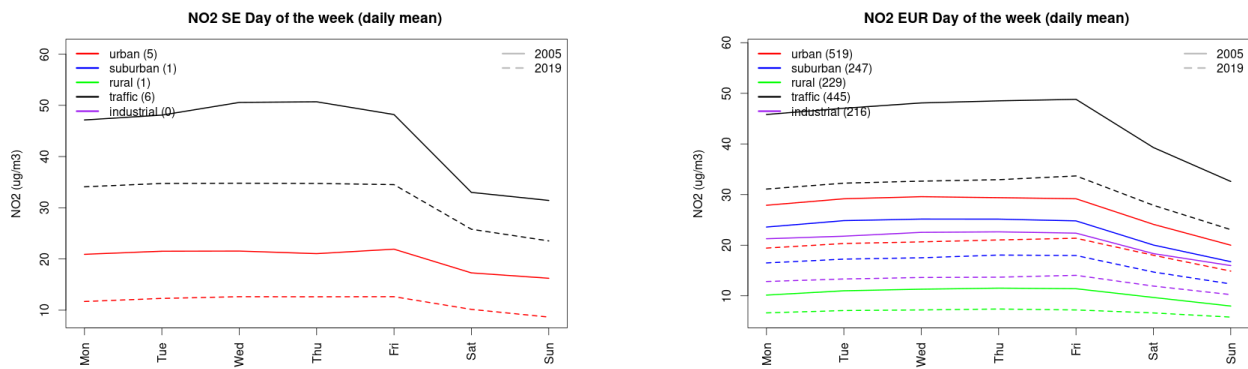


Figure S.560: Weekly cycle of daily mean NO2 for Sweden (left) and Europe (right) at various station types estimated from the whole time series in 2005 (solid lines) and 2019

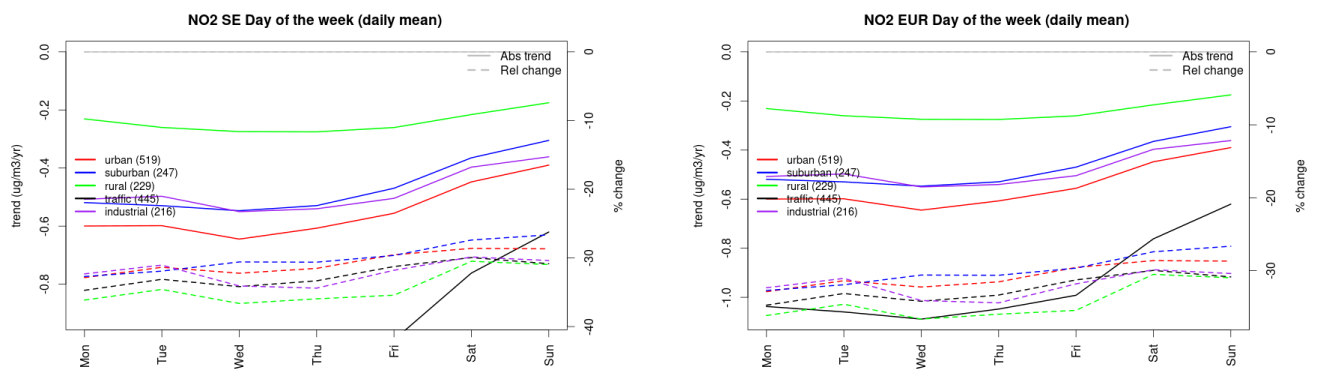


Figure S.561: Absolute (solid lines, left axis) and relative (dashed lines, right axis) trends in the weekly cycle for Sweden (left) and Europe (right) of NO₂ at various station type.

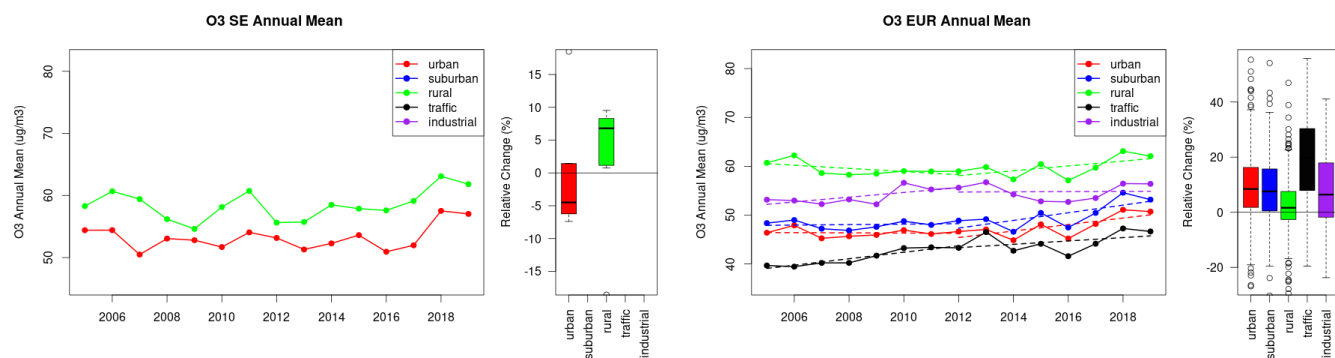


Figure S.562: Time series of the Sweden (left) and European-wide composite (median) of annual mean ozone ($\mu\text{g}/\text{m}^3$) per station type and area (red: urban background, blue suburban background, green: rural background, black: traffic, violet: industrial) between 2005 and 2019. In the European composite, the dashed lines show the linear fit between 2005 & 2012 and between 2012 & 2019. The boxplots on the right-hand side show the distribution of relative changes (%) between 2005 and 2019 for all stations of each typology in Sweden and in Europe.

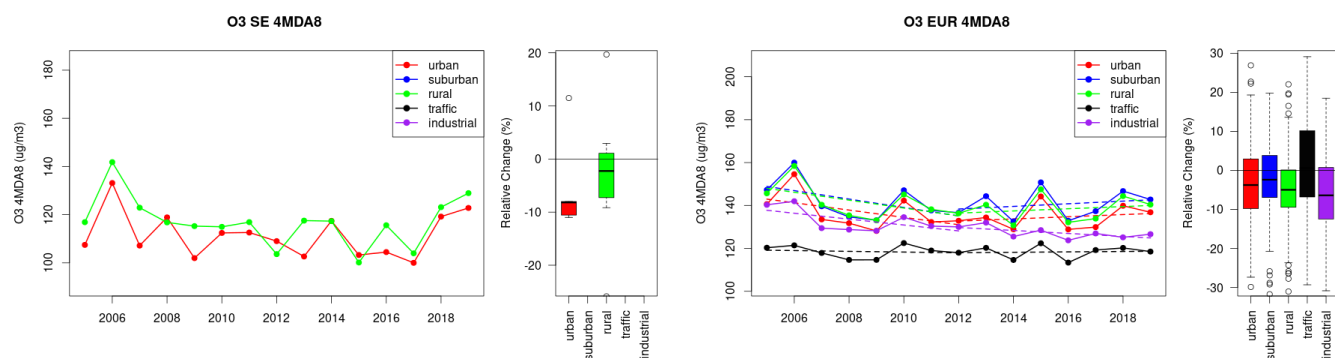


Figure S.563: Time series of the Sweden (left) and European-wide composite (median) of O₃ fourth highest daily peak (4MDA8, $\mu\text{g}/\text{m}^3$) per station type and area (red: urban background, blue suburban background, green: rural background, black: traffic, violet: industrial) between 2005 and 2019. In the European composite, the dashed lines show the linear fit between 2005 & 2012 and between 2012 & 2019. The boxplots on the right-hand side show the distribution of relative changes (%) between 2005 and 2019 for all stations of each typology in Sweden and in Europe.

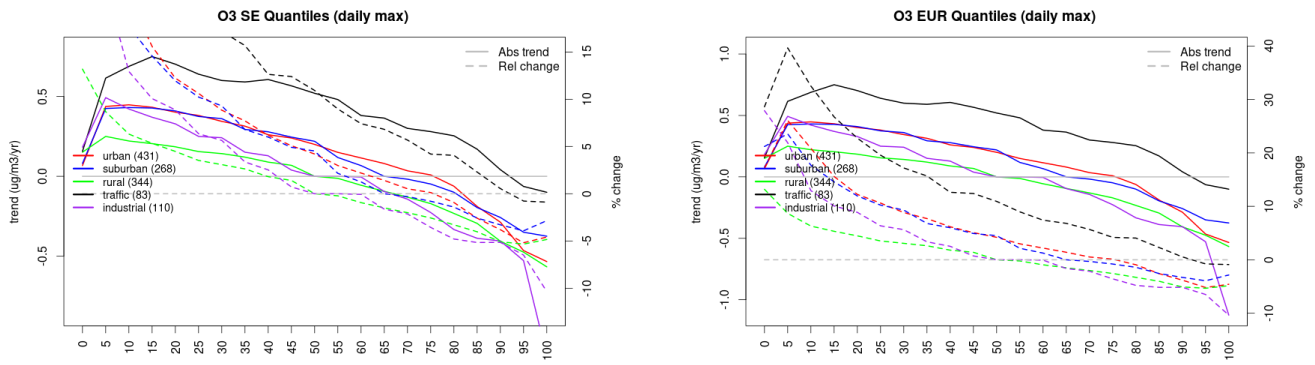


Figure S.564: For ozone in Sweden (left) and Europe, and for each typology of station: absolute trend (solid lines, left y-axis) and relative change (dashed lines, right y-axis) of the percentiles of daily maxima.

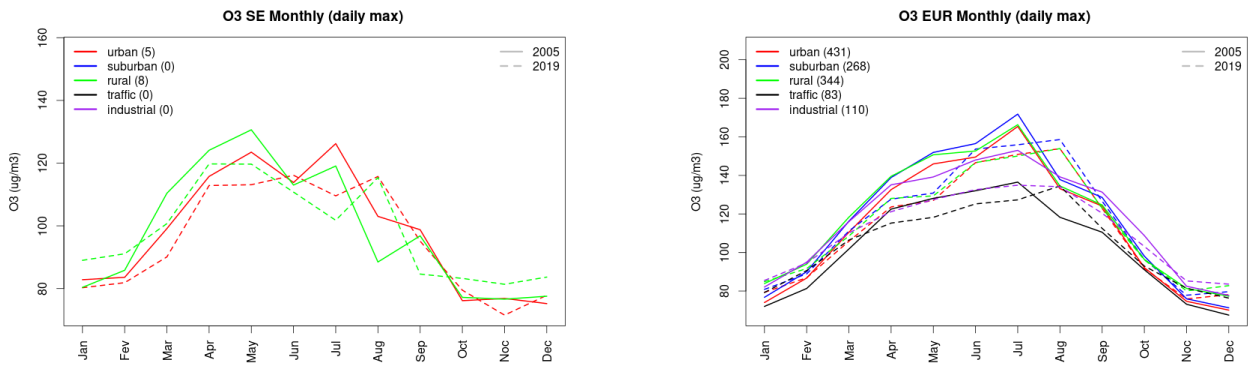


Figure S.565: Monthly cycle of daily max ozone for Sweden (left) and Europe (right) at various station types estimated from the whole time series in 2005 (solid lines) and 2019

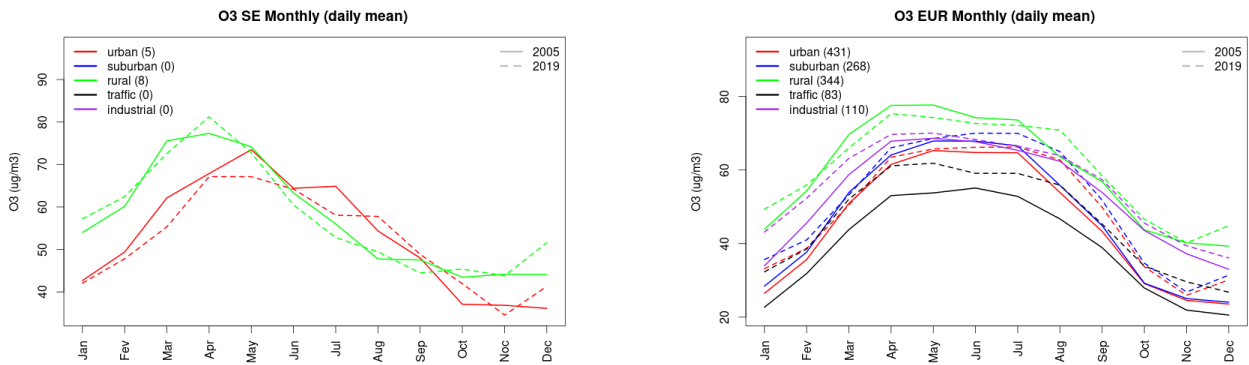


Figure S.566: Monthly cycle of daily mean ozone for Sweden (left) and Europe (right) at various station types estimated from the whole time series in 2005 (solid lines) and 2019

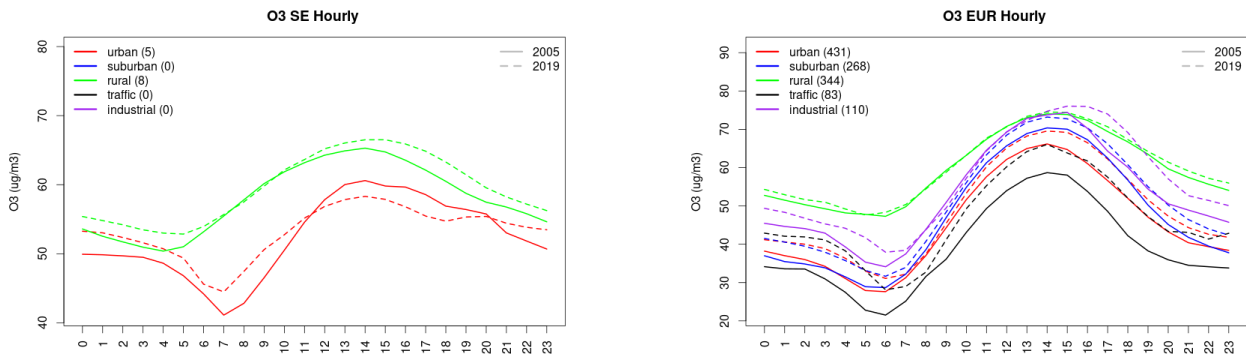


Figure S.567: Diurnal cycle of daily mean ozone for Sweden (left) and Europe (right) at various station types estimated from the whole time series in 2005 (solid lines) and 2019

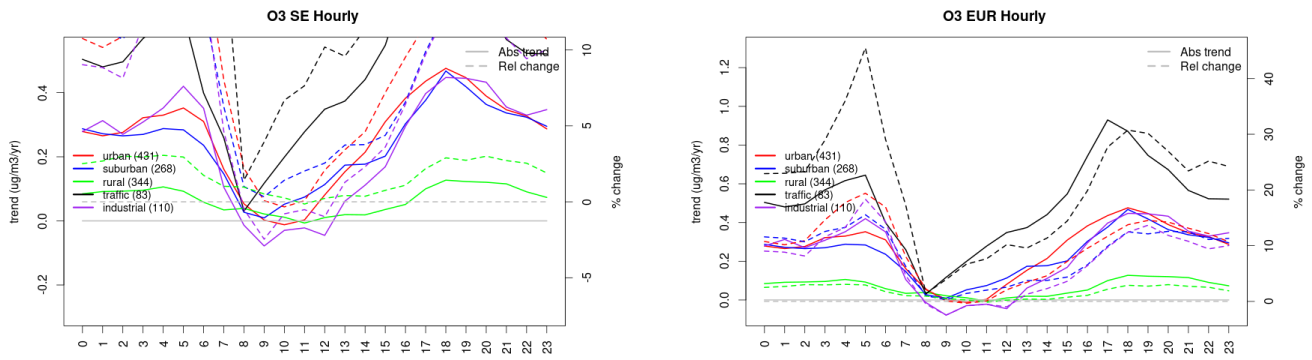


Figure S.568: Absolute (solid lines, left axis) and relative (dashed lines, right axis) trends in the diurnal cycle for Sweden (left) and Europe (right) of ozone at various station type.

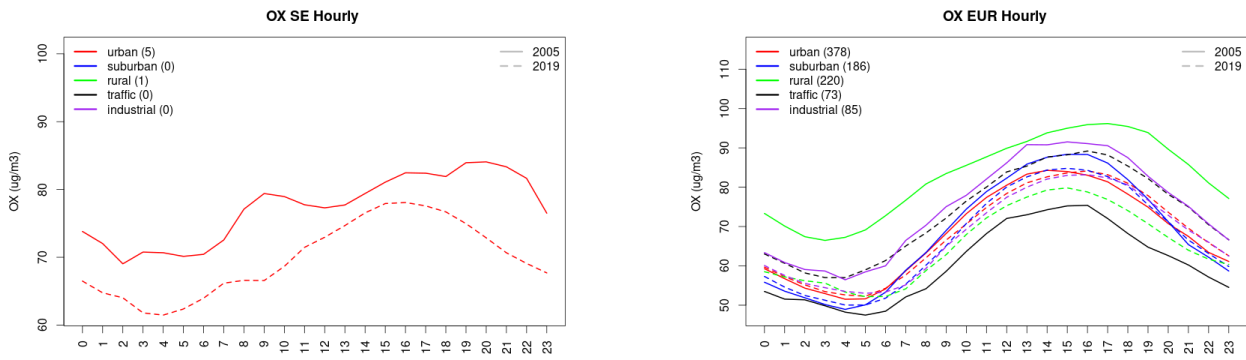


Figure S.569: Diurnal cycle of daily mean OX (as NO2+O3) for Sweden (left) and Europe (right) at various station types estimated from the whole time series in 2005 (solid lines) and 2019

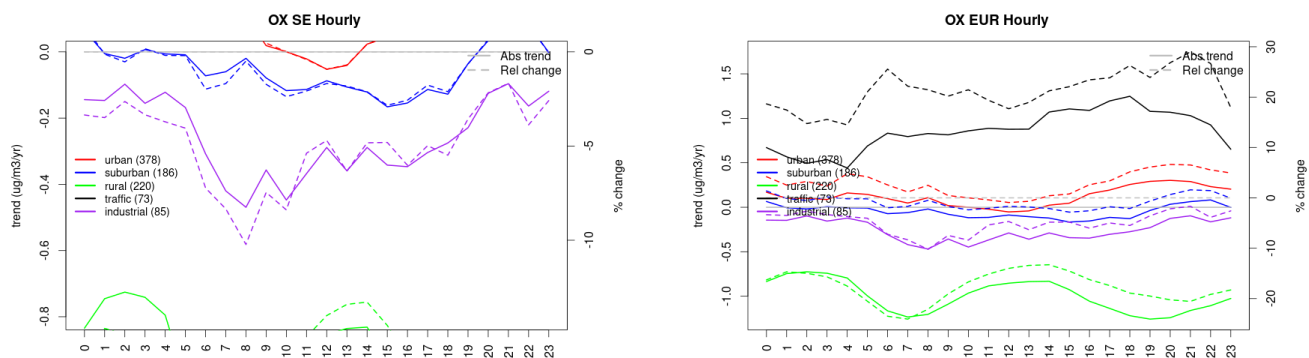


Figure S.570: Absolute (solid lines, left axis) and relative (dashed lines, right axis) trends in the diurnal cycle for Sweden (left) and Europe (right) of OX (as NO₂+O₃) at various station type.

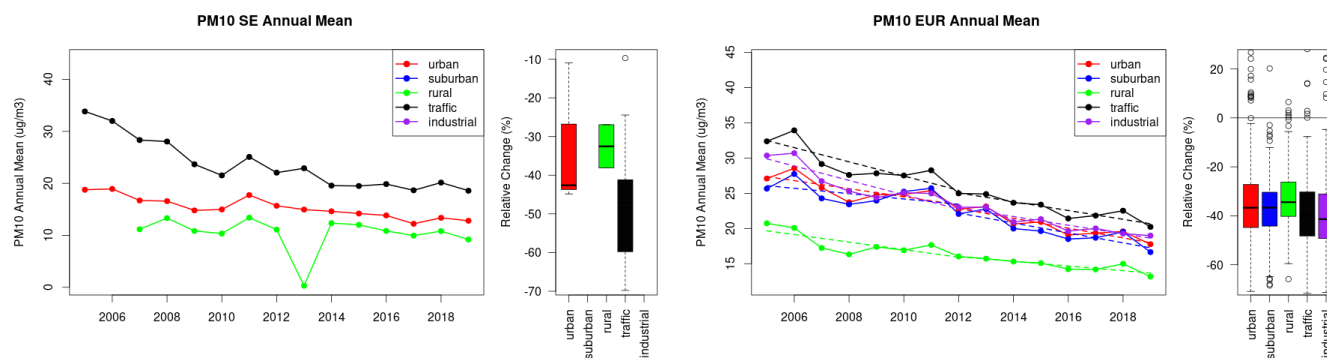


Figure S.571: Time series of the Sweden (left) and European-wide composite (median) of annual mean PM₁₀ (ug/m³) per station type and area (red: urban background, blue suburban background, green: rural background, black: traffic, violet: industrial) between 2005 and 2019. In the European composite, the dashed lines show the linear fit between 2005 & 2012 and between 2012 & 2019. The boxplots on the right-hand side show the distribution of relative changes (%) between 2005 and 2019 for all stations of each typology in Sweden and in Europe.

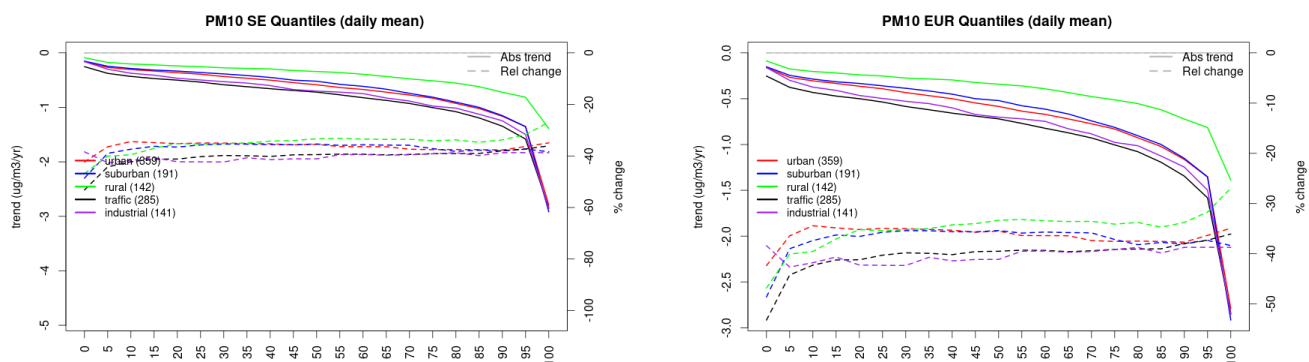


Figure S.572: For PM₁₀ in Sweden (left) and Europe, and for each typology of station: absolute trend (solid lines, left y-axis) and relative change (dashed lines, right y-axis) of the percentiles of daily means.

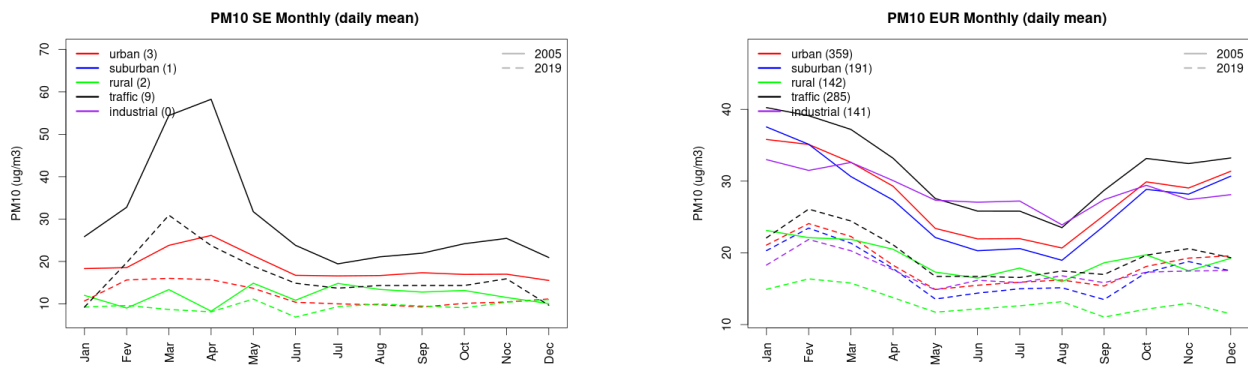


Figure S.573: Monthly cycle of daily mean PM10 for Sweden (left) and Europe (right) at various station types estimated from the whole time series in 2005 (solid lines) and 2019

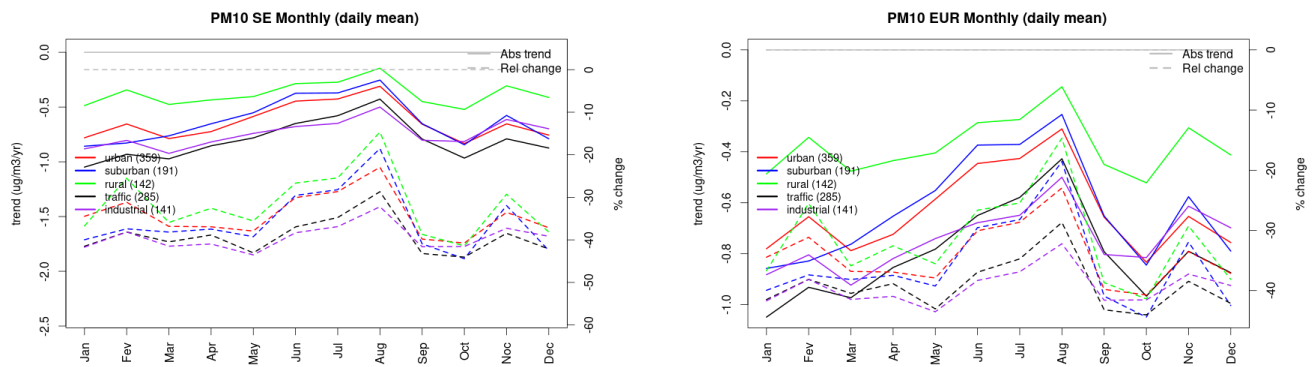


Figure S.574: Absolute (solid lines, left axis) and relative (dashed lines, right axis) trends in the monthly cycle for Sweden (left) and Europe (right) of PM10 at various station type.

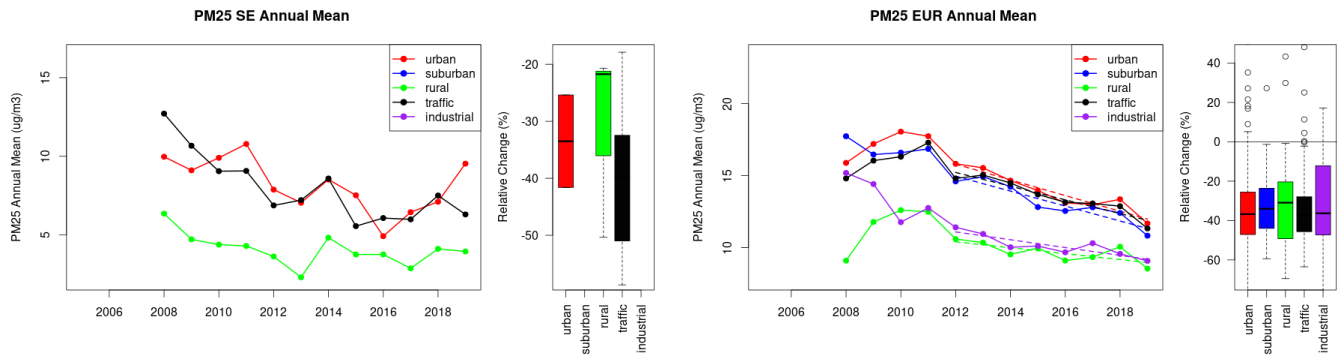


Figure S.575: Time series of the Sweden (left) and European-wide composite (median) of annual mean PM25 ($\mu\text{g}/\text{m}^3$) per station type and area (red: urban background, blue suburban background, green: rural background, black: traffic, violet: industrial) between 2005 and 2019. In the European composite, the dashed lines show the linear fit between 2005 & 2012 and between 2012 & 2019. The boxplots on the right-hand side show the distribution of relative changes (%) between 2005 and 2019 for all stations of each typology in Sweden and in Europe.

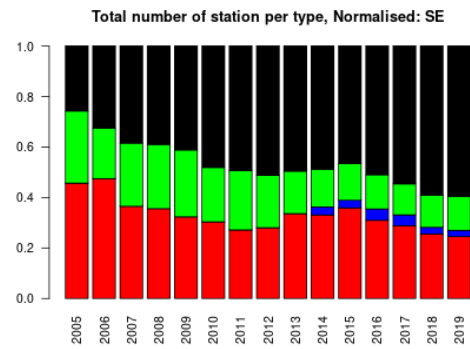
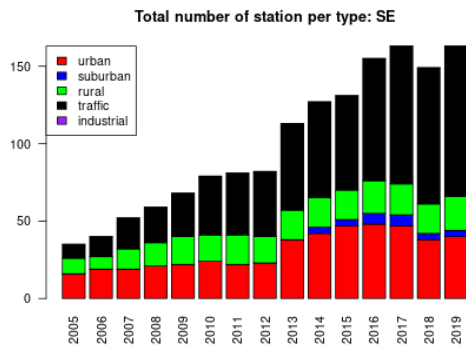
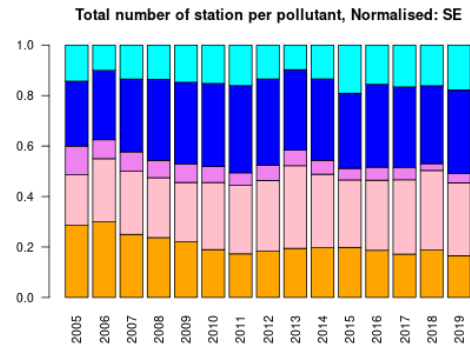
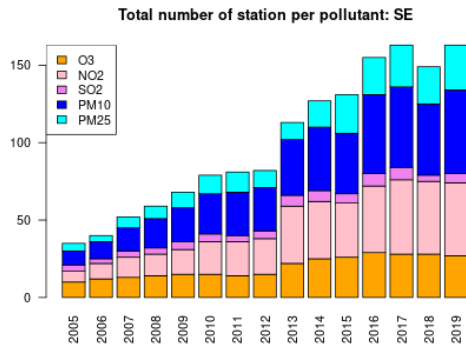
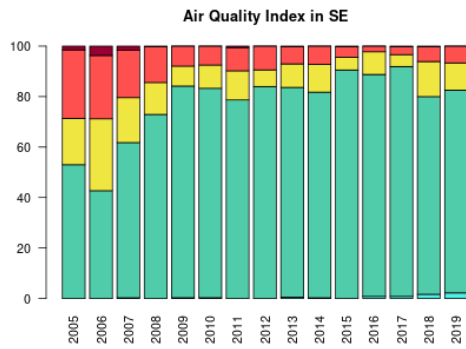


Figure S.576: For Sweden: overall air quality index (percentage of days in a given year) and distribution of daily categories per pollutant (light blue: good, light green: fair, yellow: moderate, orange: poor, red: very poor, violet: extremely poor).

27 Slovenia

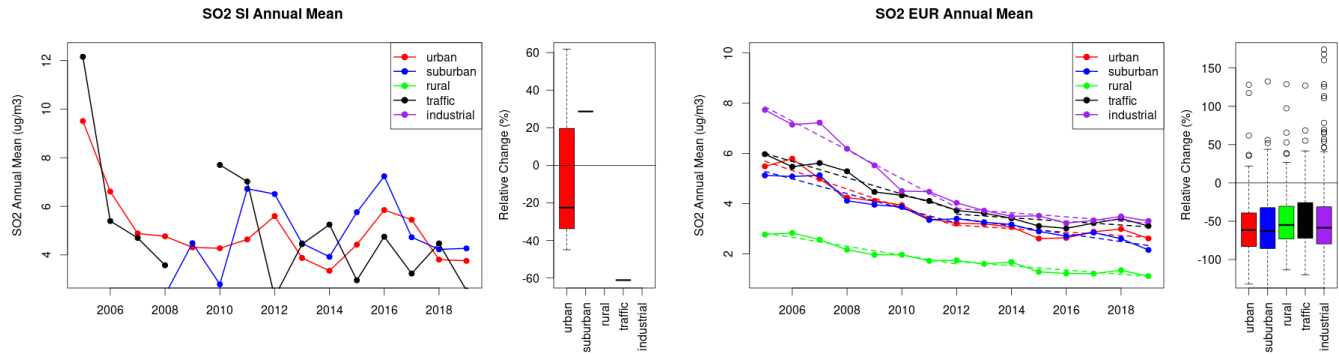


Figure S.577: Time series of the Slovenia (left) and European-wide composite (median) of annual mean SO₂ (ug/m³) per station type and area (red: urban background, blue suburban background, green: rural background, black: traffic, violet: industrial) between 2005 and 2019. In the European composite, the dashed lines show the linear fit between 2005 & 2012 and between 2012 & 2019. The boxplots on the right-hand side show the distribution of relative changes (%) between 2005 and 2019 for all stations of each typology in Slovenia and in Europe.

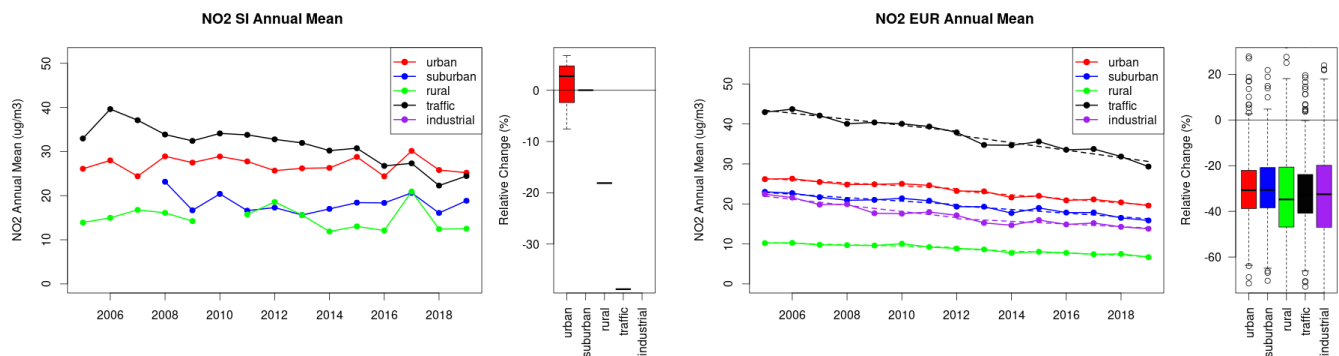


Figure S.578: Time series of the Slovenia (left) and European-wide composite (median) of annual mean NO₂ (ug/m³) per station type and area (red: urban background, blue suburban background, green: rural background, black: traffic, violet: industrial) between 2005 and 2019. In the European composite, the dashed lines show the linear fit between 2005 & 2012 and between 2012 & 2019. The boxplots on the right-hand side show the distribution of relative changes (%) between 2005 and 2019 for all stations of each typology in Slovenia and in Europe.

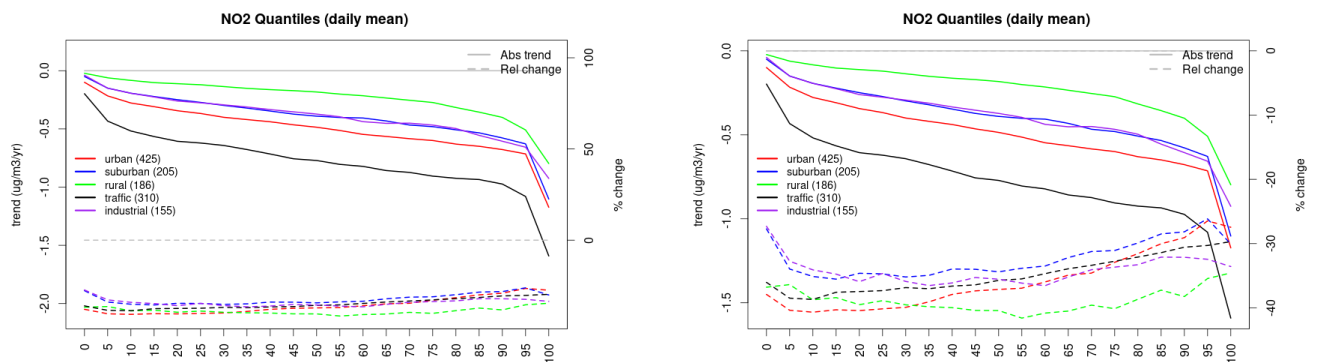


Figure S.579: For NO₂ in Slovenia (left) and Europe, and for each typology of station: absolute trend (solid lines, left y-axis) and relative change (dashed lines, right y-axis) of the percentiles of daily means.

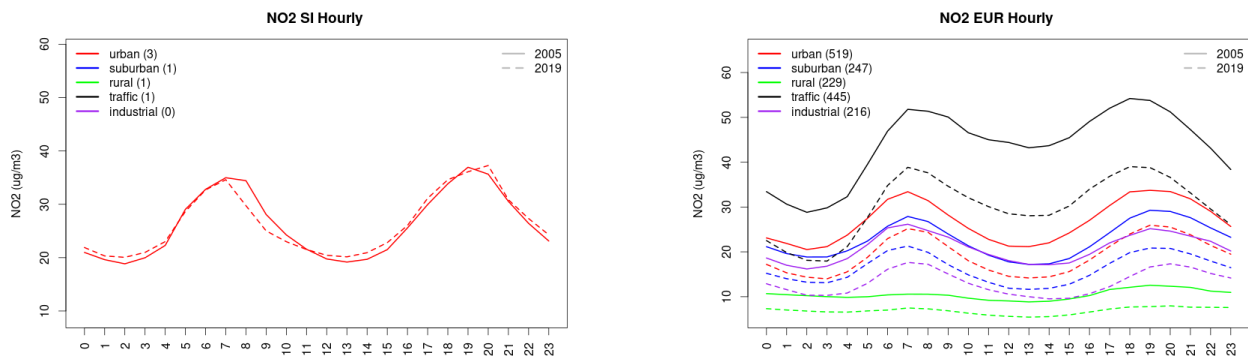


Figure S.580: Diurnal cycle of daily mean NO₂ for Slovenia (left) and Europe (right) at various station types estimated from the whole time series in 2005 (solid lines) and 2019

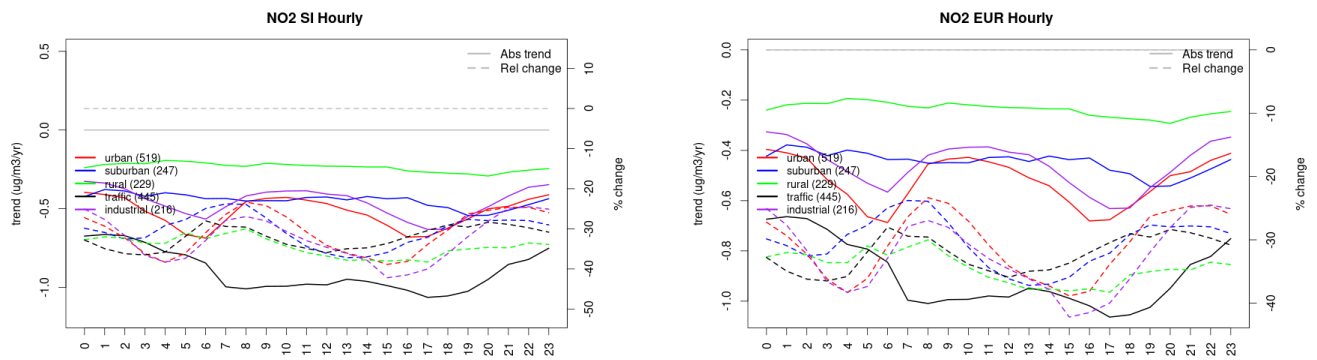


Figure S.581: Absolute (solid lines, left axis) and relative (dashed lines, right axis) trends in the diurnal cycle for Slovenia (left) and Europe (right) of NO₂ at various station type.

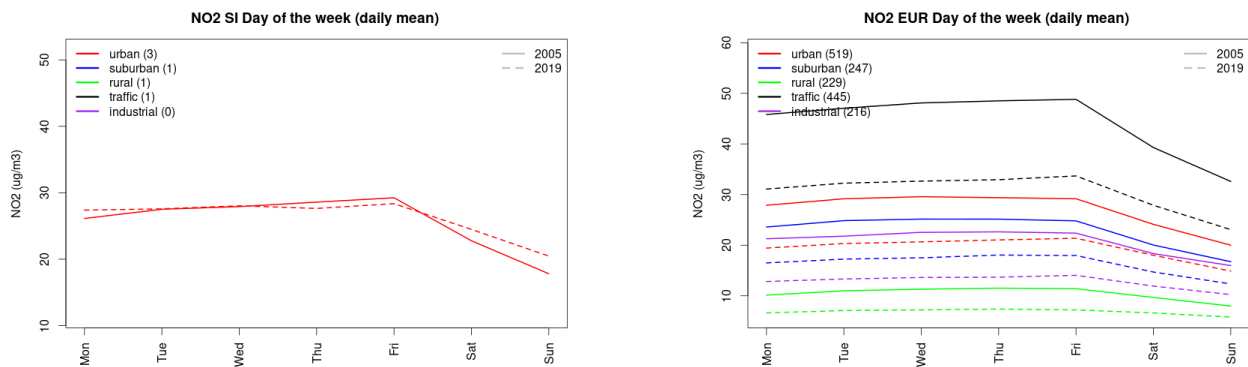


Figure S.582: Weekly cycle of daily mean NO₂ for Slovenia (left) and Europe (right) at various station types estimated from the whole time series in 2005 (solid lines) and 2019

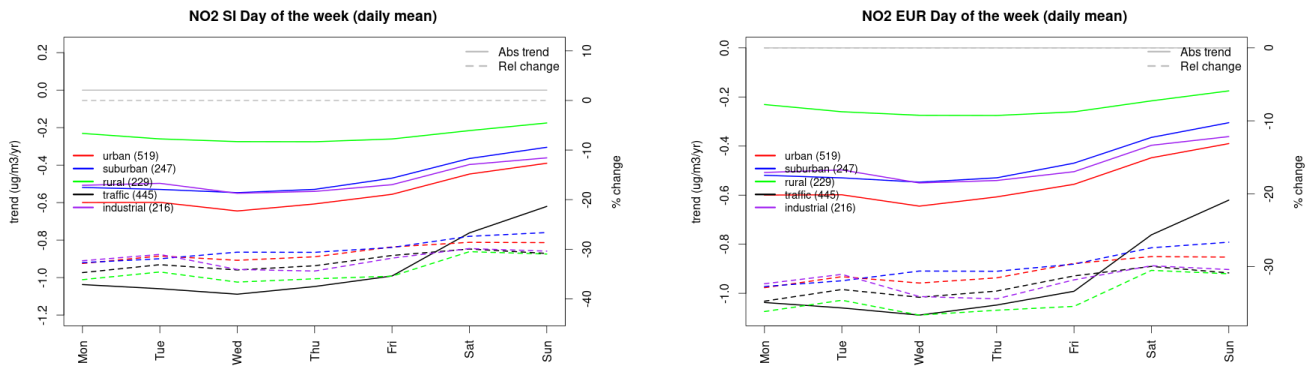


Figure S.583: Absolute (solid lines, left axis) and relative (dashed lines, right axis) trends in the weekly cycle for Slovenia (left) and Europe (right) of NO₂ at various station type.

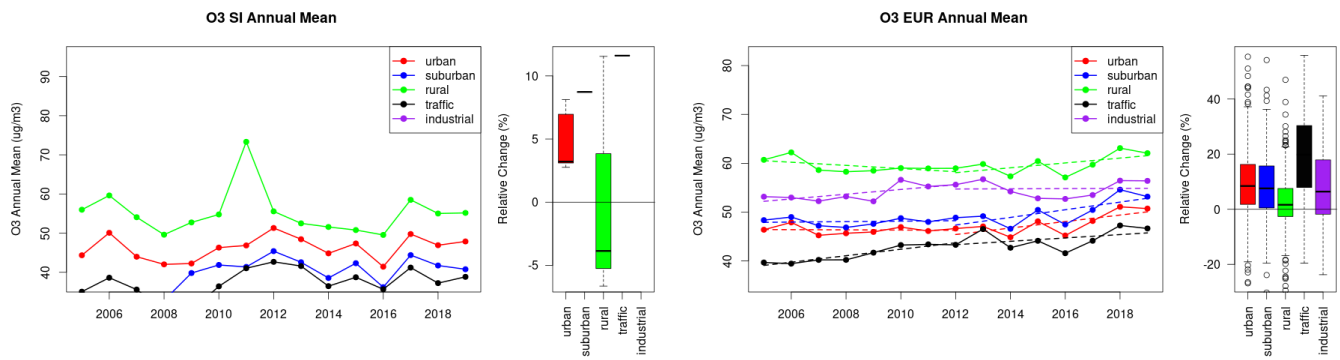


Figure S.584: Time series of the Slovenia (left) and European-wide composite (median) of annual mean ozone (ug/m³) per station type and area (red: urban background, blue suburban background, green: rural background, black: traffic, violet: industrial) between 2005 and 2019. In the European composite, the dashed lines show the linear fit between 2005 & 2012 and between 2012 & 2019. The boxplots on the right-hand side show the distribution of relative changes (%) between 2005 and 2019 for all stations of each typology in Slovenia and in Europe.

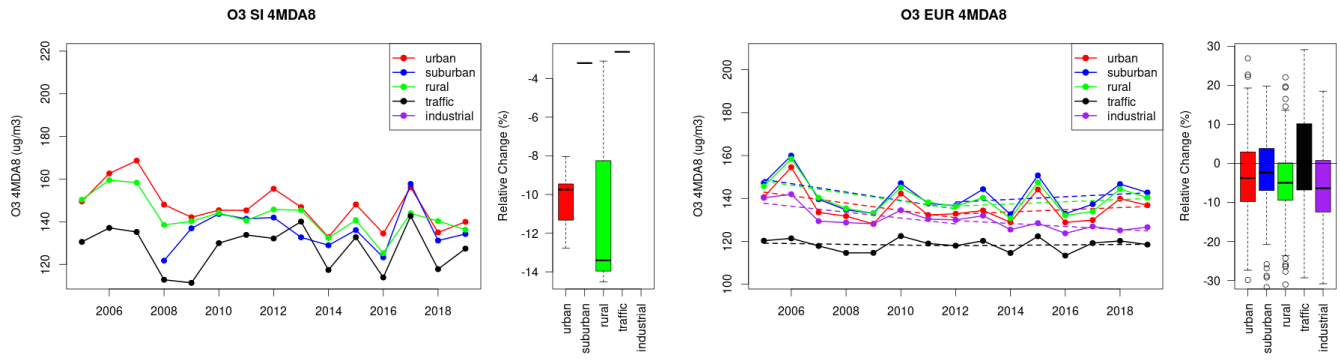


Figure S.585: Time series of the Slovenia (left) and European-wide composite (median) of O₃ fourth highest daily peak (4MDA8, ug/m³) per station type and area (red: urban background, blue suburban background, green: rural background, black: traffic, violet: industrial) between 2005 and 2019. In the European composite, the dashed lines show the linear fit between 2005 & 2012 and between 2012 & 2019. The boxplots on the right-hand side show the distribution of relative changes (%) between 2005 and 2019 for all stations of each typology in Slovenia and in Europe.

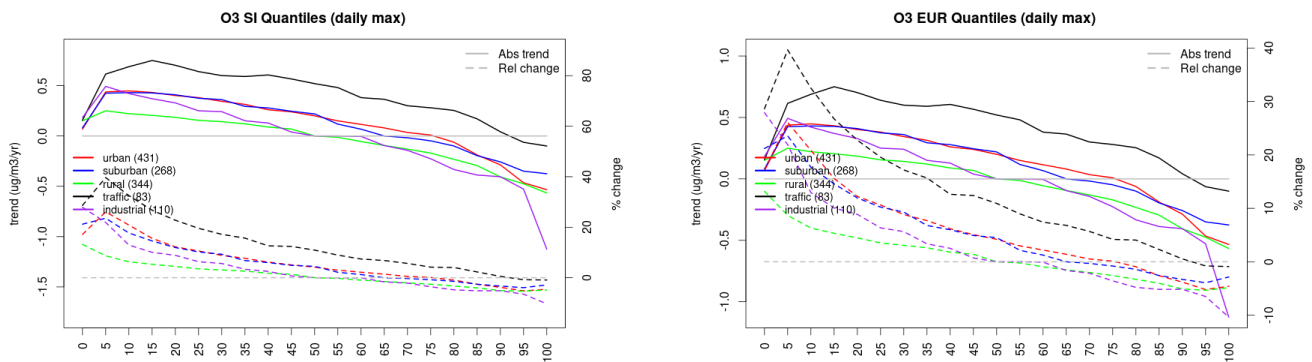


Figure S.586: For ozone in Slovenia (left) and Europe, and for each typology of station: absolute trend (solid lines, left y-axis) and relative change (dashed lines, right y-axis) of the percentiles of daily maxima.

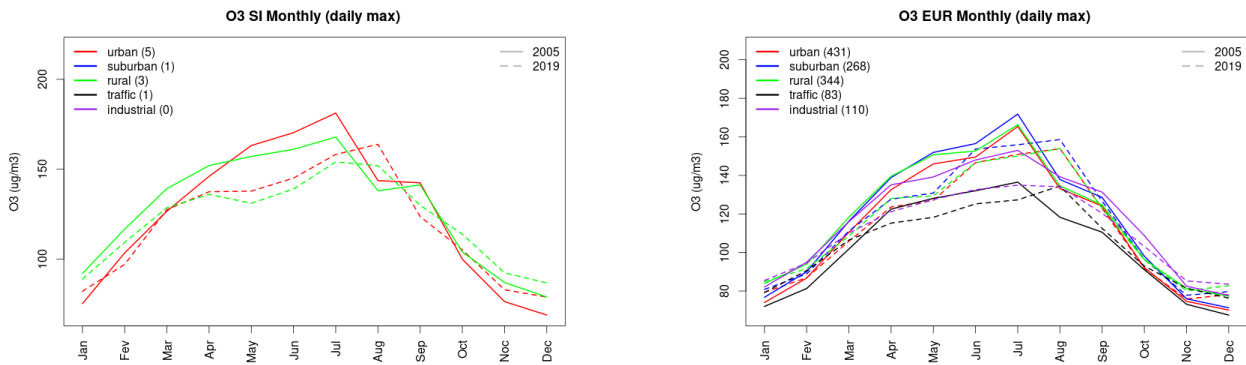


Figure S.587: Monthly cycle of daily max ozone for Slovenia (left) and Europe (right) at various station types estimated from the whole time series in 2005 (solid lines) and 2019

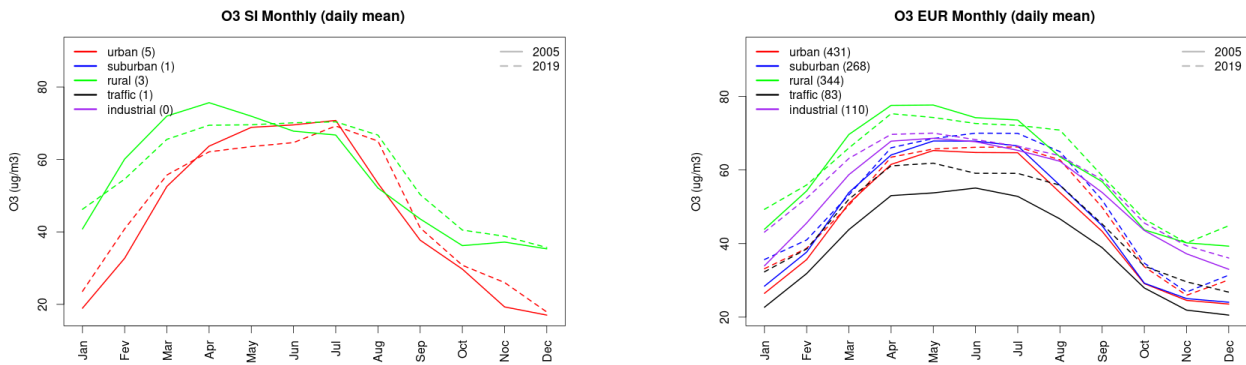


Figure S.588: Monthly cycle of daily mean ozone for Slovenia (left) and Europe (right) at various station types estimated from the whole time series in 2005 (solid lines) and 2019

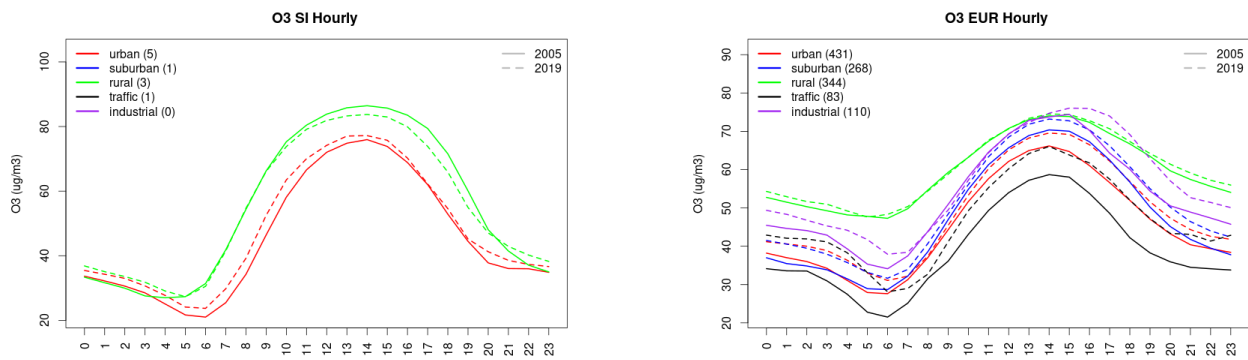


Figure S.589: Diurnal cycle of daily mean ozone for Slovenia (left) and Europe (right) at various station types estimated from the whole time series in 2005 (solid lines) and 2019

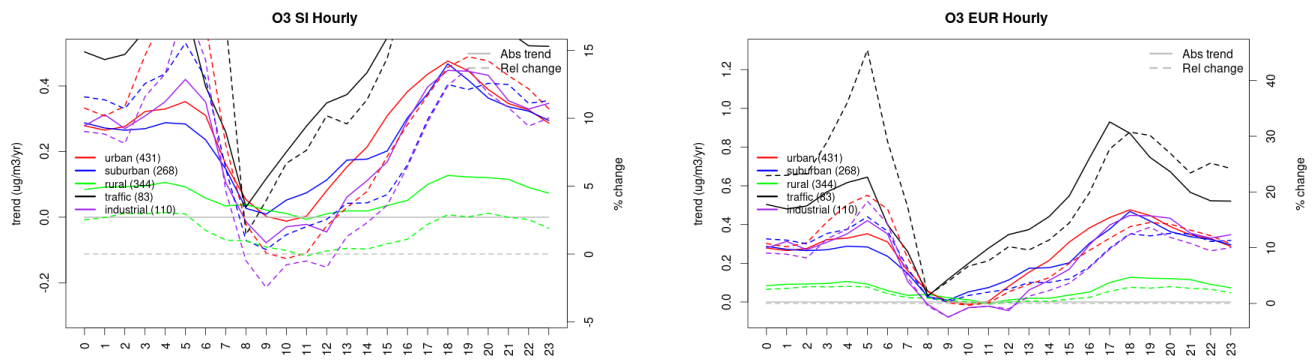


Figure S.590: Absolute (solid lines, left axis) and relative (dashed lines, right axis) trends in the diurnal cycle for Slovenia (left) and Europe (right) of ozone at various station type.

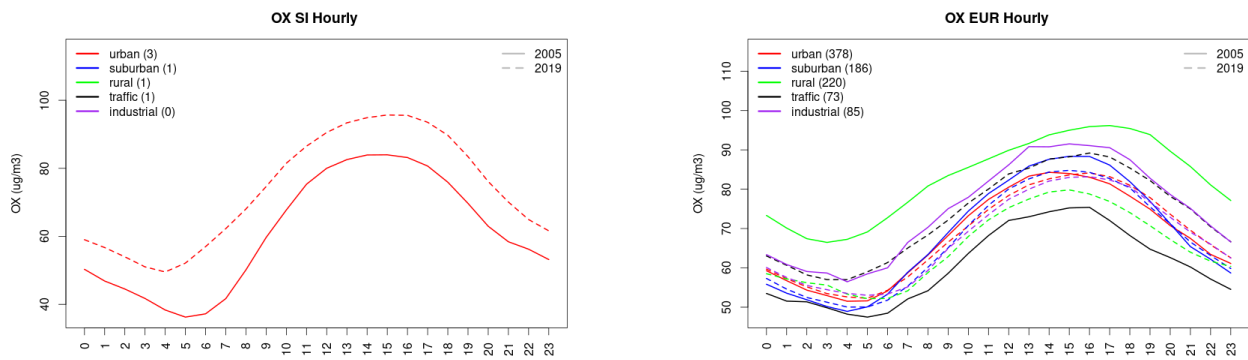


Figure S.591: Diurnal cycle of daily mean OX (as $\text{NO}_2 + \text{O}_3$) for Slovenia (left) and Europe (right) at various station types estimated from the whole time series in 2005 (solid lines) and 2019

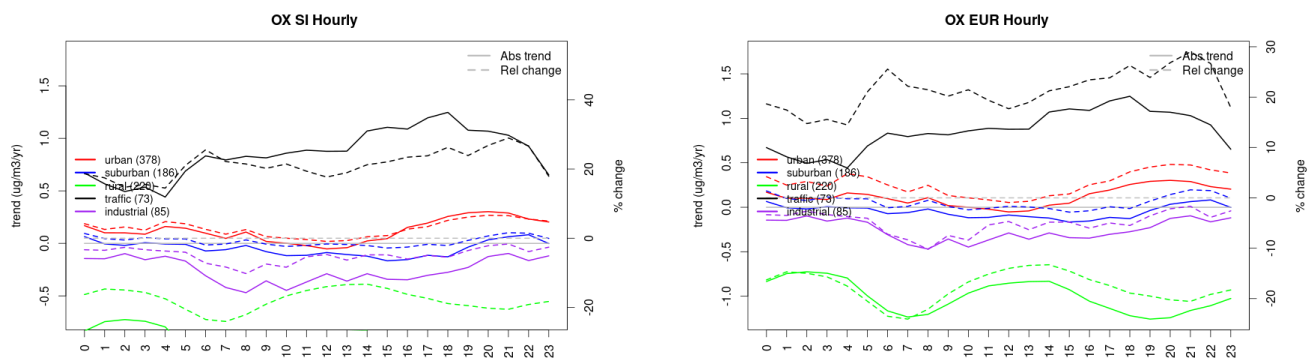


Figure S.592: Absolute (solid lines, left axis) and relative (dashed lines, right axis) trends in the diurnal cycle for Slovenia (left) and Europe (right) of OX (as NO₂+O₃) at various station type.

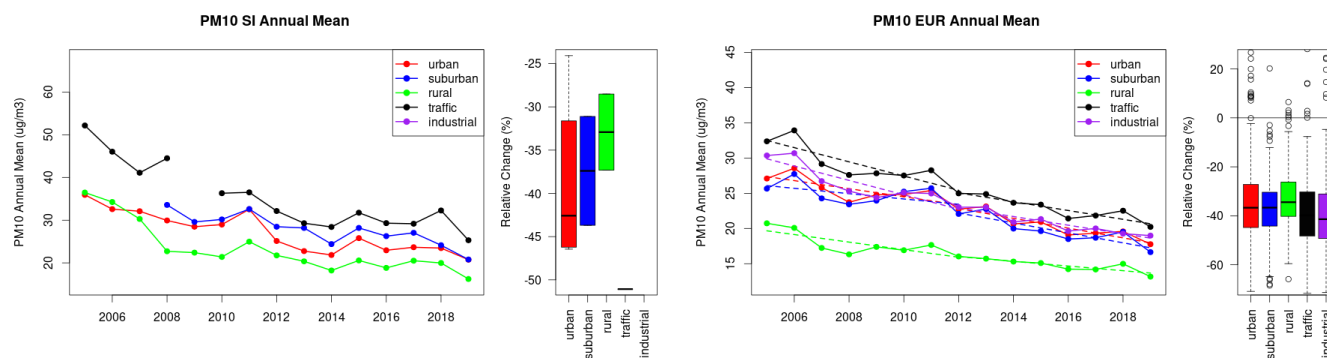


Figure S.593: Time series of the Slovenia (left) and European-wide composite (median) of annual mean PM₁₀ (ug/m³) per station type and area (red: urban background, blue suburban background, green: rural background, black: traffic, violet: industrial) between 2005 and 2019. In the European composite, the dashed lines show the linear fit between 2005 & 2012 and between 2012 & 2019. The boxplots on the right-hand side show the distribution of relative changes (%) between 2005 and 2019 for all stations of each typology in Slovenia and in Europe.

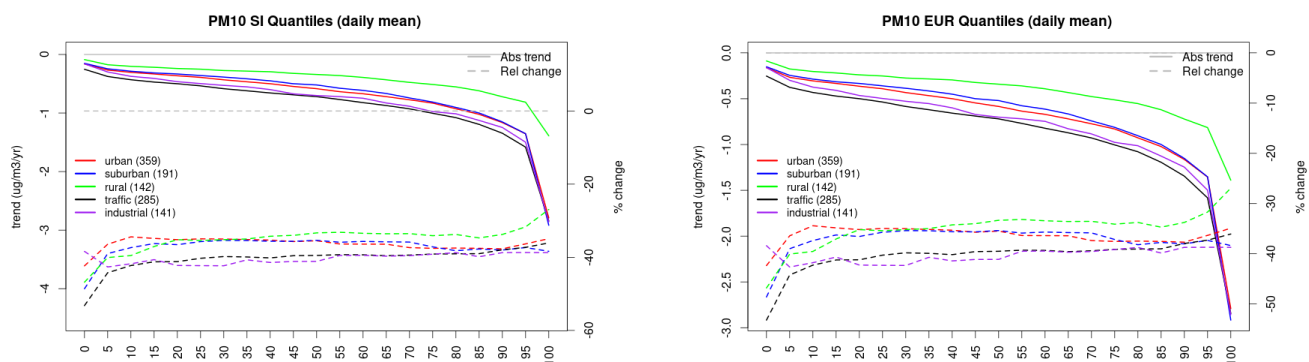


Figure S.594: For PM₁₀ in Slovenia (left) and Europe, and for each typology of station: absolute trend (solid lines, left y-axis) and relative change (dashed lines, right y-axis) of the percentiles of daily means.

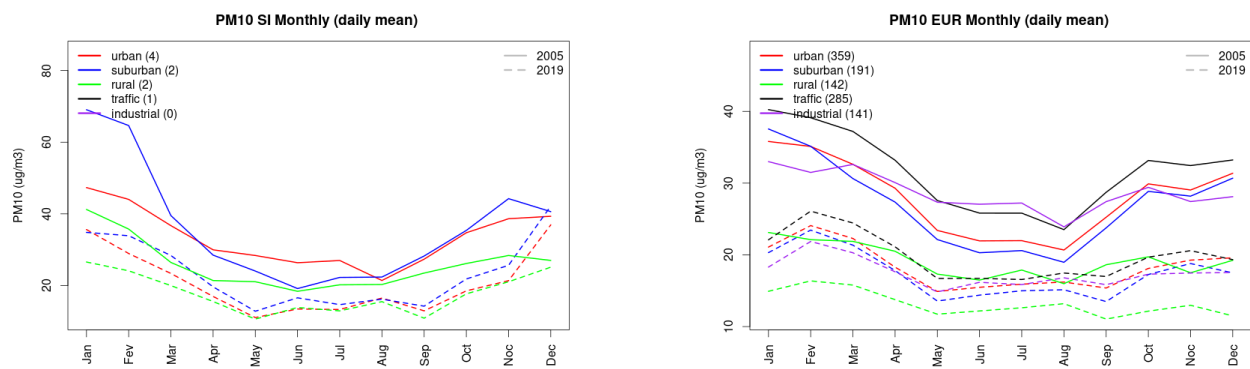


Figure S.595: Monthly cycle of daily mean PM10 for Slovenia (left) and Europe (right) at various station types estimated from the whole time series in 2005 (solid lines) and 2019

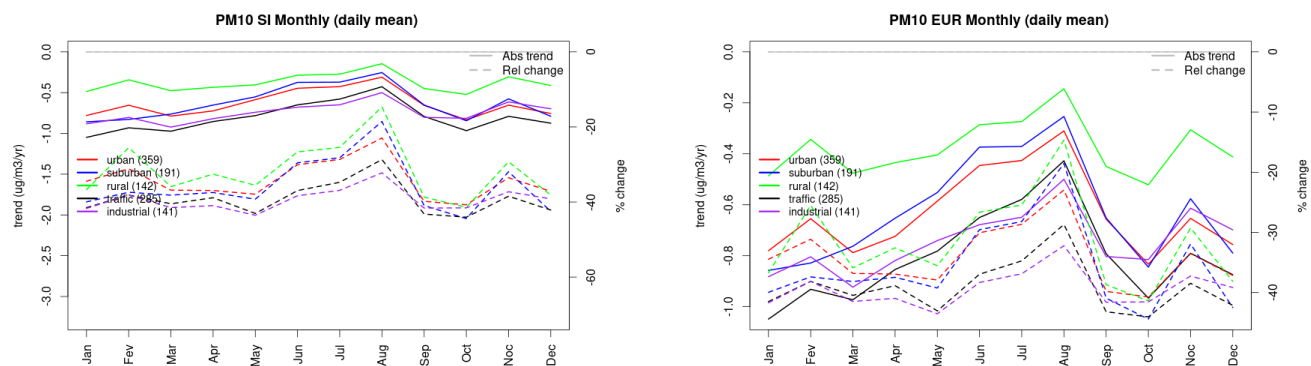


Figure S.596: Absolute (solid lines, left axis) and relative (dashed lines, right axis) trends in the monthly cycle for Slovenia (left) and Europe (right) of PM10 at various station type.

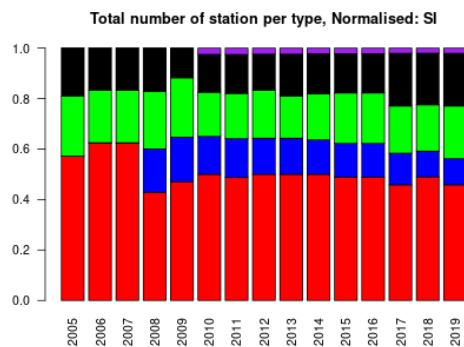
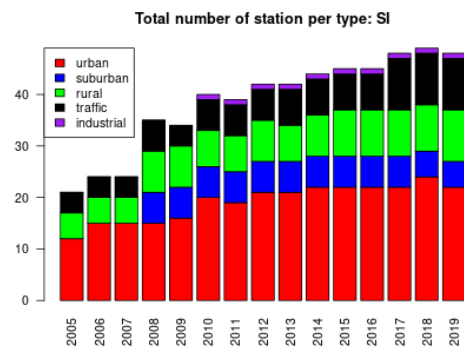
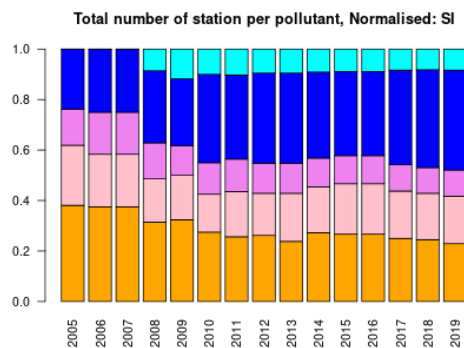
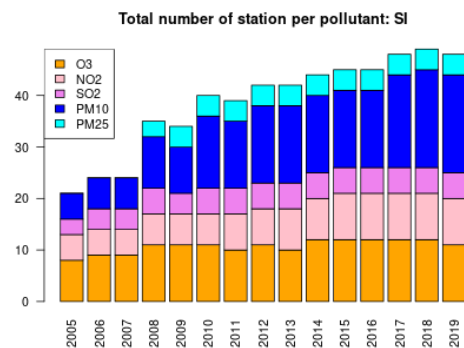
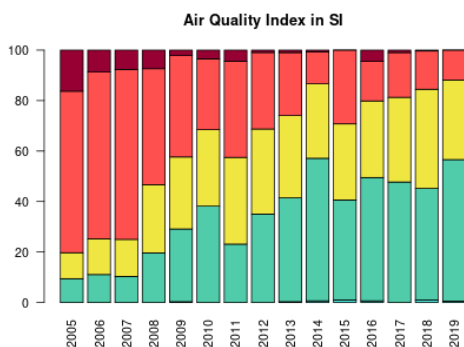


Figure S.597: For Slovenia: overall air quality index (percentage of days in a given year) and distribution of daily categories per pollutant (light blue: good, light green: fair, yellow: moderate, orange: poor, red: very poor, violet: extremely poor).

28 Slovakia

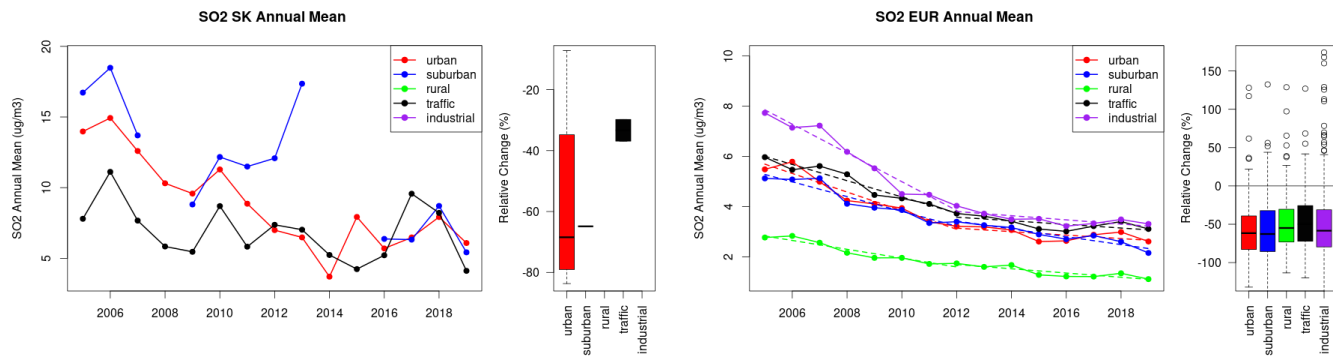


Figure S.598: Time series of the Slovakia (left) and European-wide composite (median) of annual mean SO₂ ($\mu\text{g}/\text{m}^3$) per station type and area (red: urban background, blue suburban background, green: rural background, black: traffic, violet: industrial) between 2005 and 2019. In the European composite, the dashed lines show the linear fit between 2005 & 2012 and between 2012 & 2019. The boxplots on the right-hand side show the distribution of relative changes (%) between 2005 and 2019 for all stations of each typology in Slovakia and in Europe.

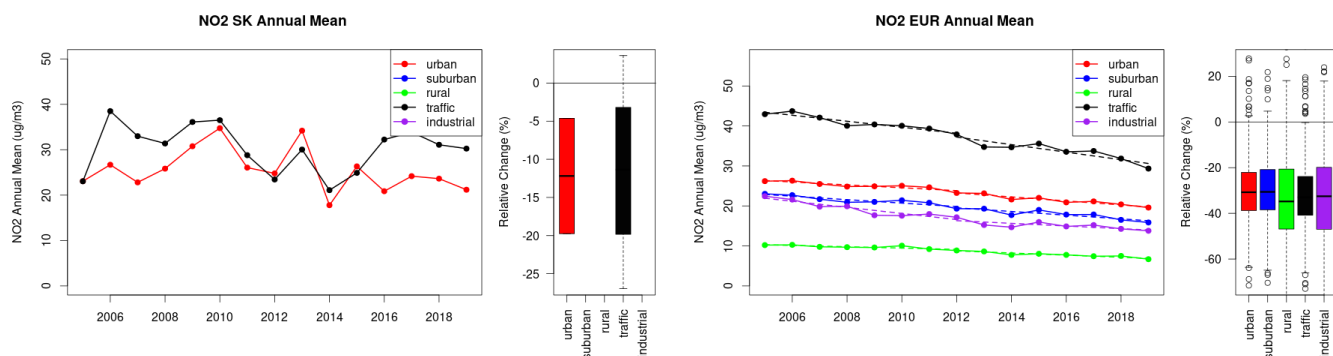


Figure S.599: Time series of the Slovakia (left) and European-wide composite (median) of annual mean NO₂ ($\mu\text{g}/\text{m}^3$) per station type and area (red: urban background, blue suburban background, green: rural background, black: traffic, violet: industrial) between 2005 and 2019. In the European composite, the dashed lines show the linear fit between 2005 & 2012 and between 2012 & 2019. The boxplots on the right-hand side show the distribution of relative changes (%) between 2005 and 2019 for all stations of each typology in Slovakia and in Europe.

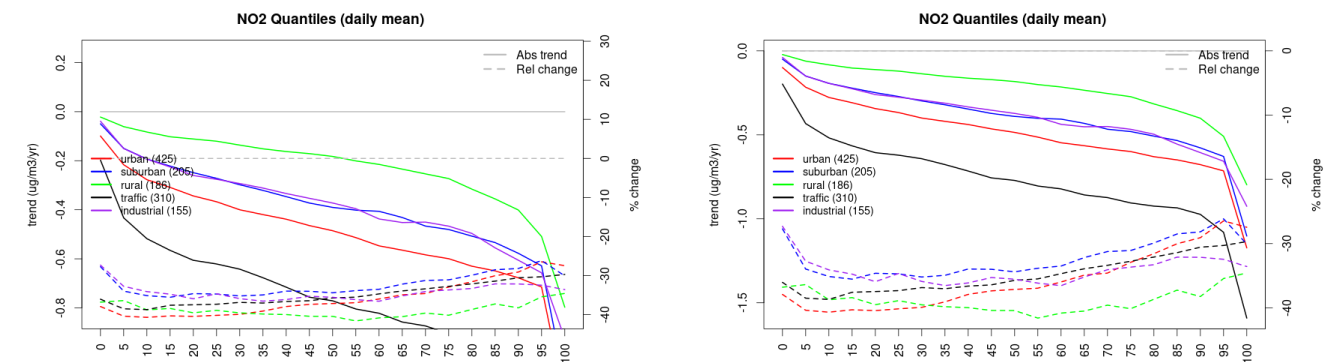


Figure S.600: For NO₂ in Slovakia (left) and Europe, and for each typology of station: absolute trend (solid lines, left y-axis) and relative change (dashed lines, right y-axis) of the percentiles of daily means.

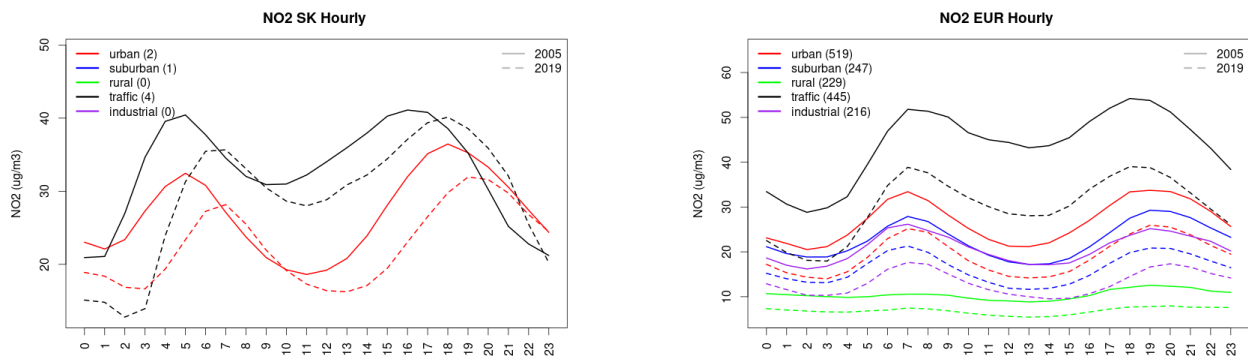


Figure S.601: Diurnal cycle of daily mean NO2 for Slovakia (left) and Europe (right) at various station types estimated from the whole time series in 2005 (solid lines) and 2019

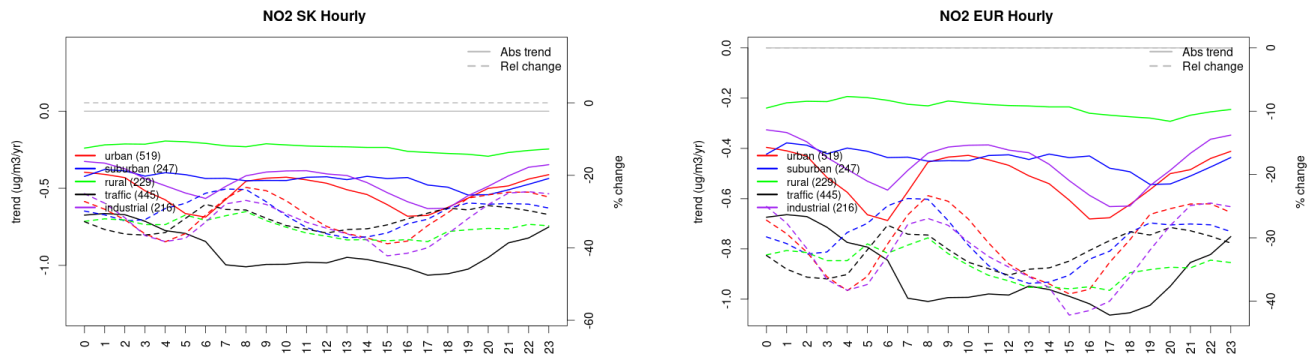


Figure S.602: Absolute (solid lines, left axis) and relative (dashed lines, right axis) trends in the diurnal cycle for Slovakia (left) and Europe (right) of NO2 at various station type.

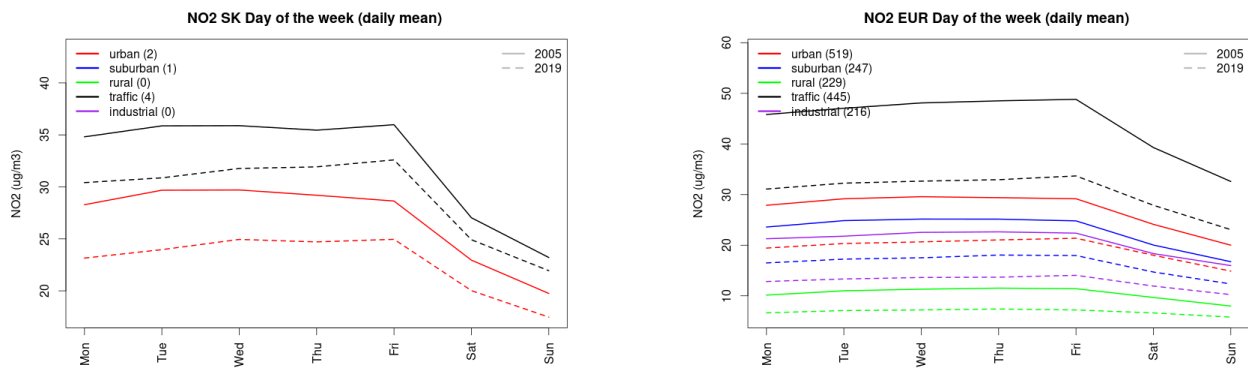


Figure S.603: Weekly cycle of daily mean NO2 for Slovakia (left) and Europe (right) at various station types estimated from the whole time series in 2005 (solid lines) and 2019

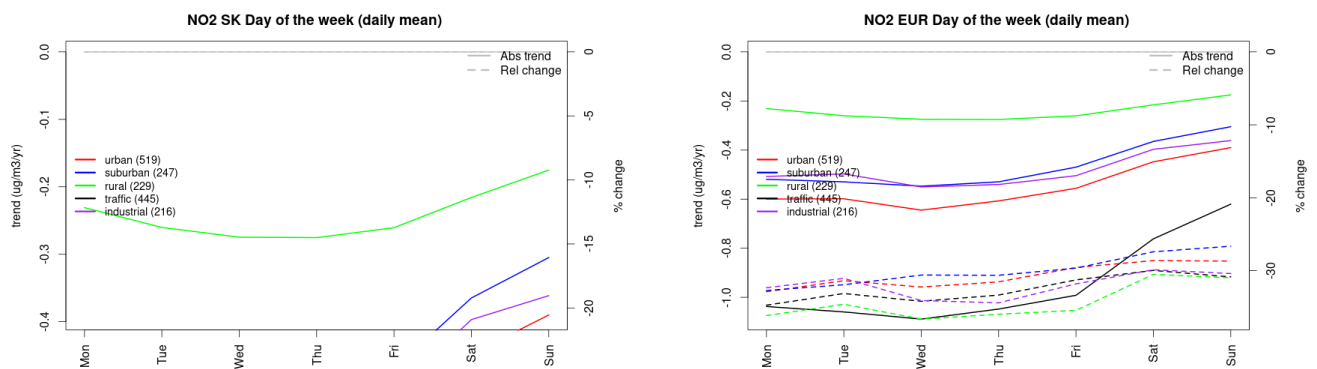


Figure S.604: Absolute (solid lines, left axis) and relative (dashed lines, right axis) trends in the weekly cycle for Slovakia (left) and Europe (right) of NO₂ at various station type.

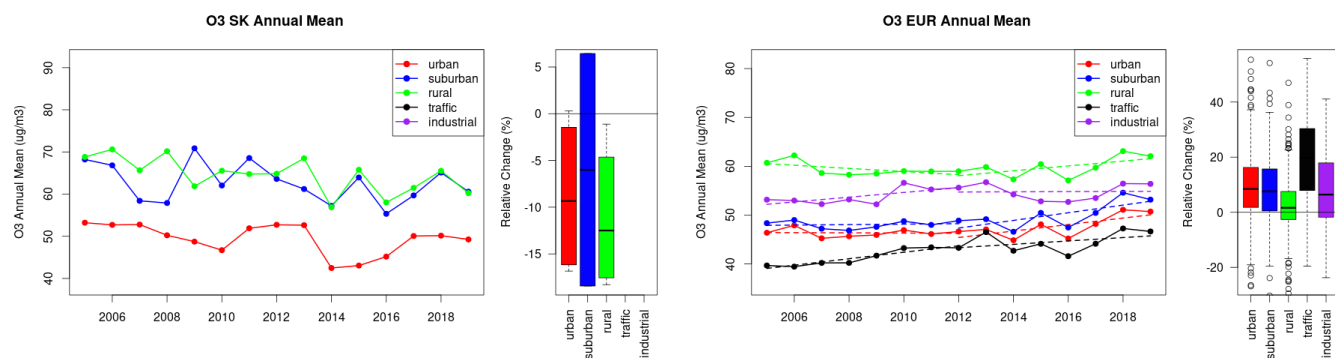


Figure S.605: Time series of the Slovakia (left) and European-wide composite (median) of annual mean ozone (ug/m³) per station type and area (red: urban background, blue suburban background, green: rural background, black: traffic, violet: industrial) between 2005 and 2019. In the European composite, the dashed lines show the linear fit between 2005 & 2012 and between 2012 & 2019. The boxplots on the right-hand side show the distribution of relative changes (%) between 2005 and 2019 for all stations of each typology in Slovakia and in Europe.

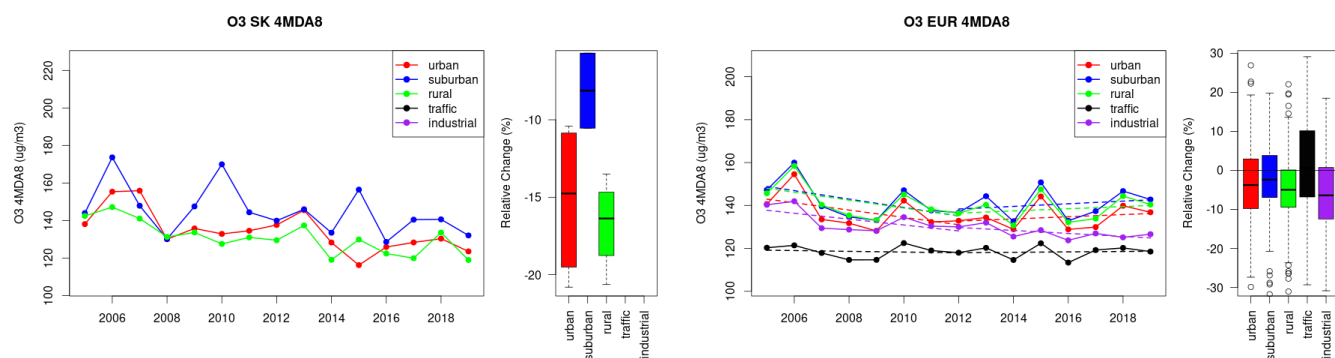


Figure S.606: Time series of the Slovakia (left) and European-wide composite (median) of O₃ fourth highest daily peak (4MDA8, ug/m³) per station type and area (red: urban background, blue suburban background, green: rural background, black: traffic, violet: industrial) between 2005 and 2019. In the European composite, the dashed lines show the linear fit between 2005 & 2012 and between 2012 & 2019. The boxplots on the right-hand side show the distribution of relative changes (%) between 2005 and 2019 for all stations of each typology in Slovakia and in Europe.

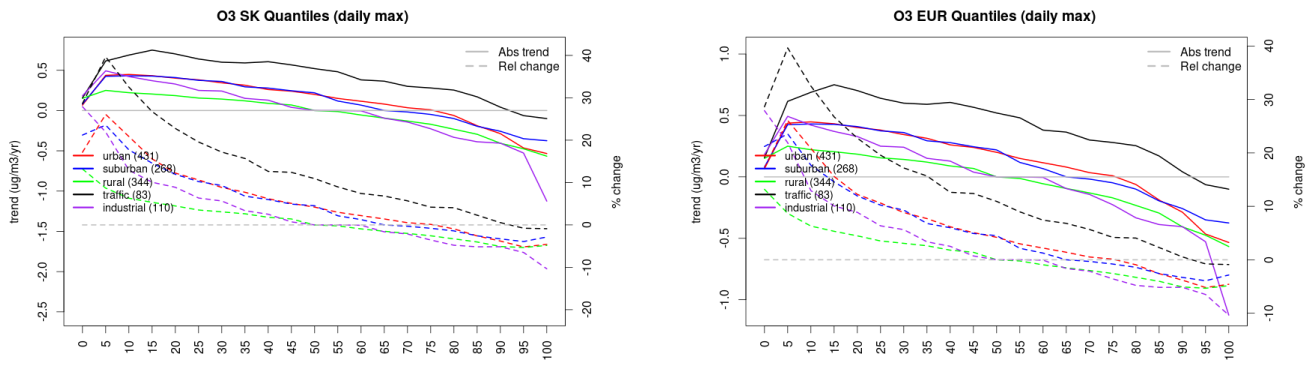


Figure S.607: For ozone in Slovakia (left) and Europe, and for each typology of station: absolute trend (solid lines, left y-axis) and relative change (dashed lines, right y-axis) of the percentiles of daily maxima.

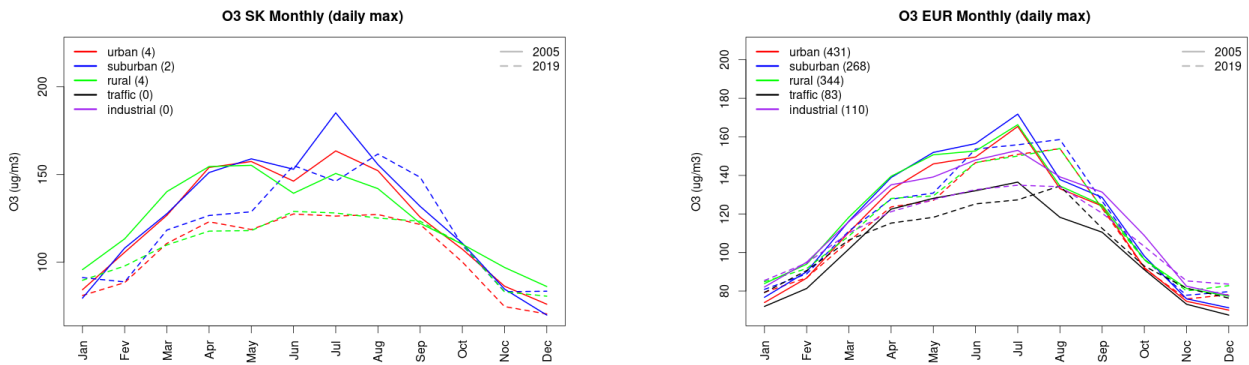


Figure S.608: Monthly cycle of daily max ozone for Slovakia (left) and Europe (right) at various station types estimated from the whole time series in 2005 (solid lines) and 2019

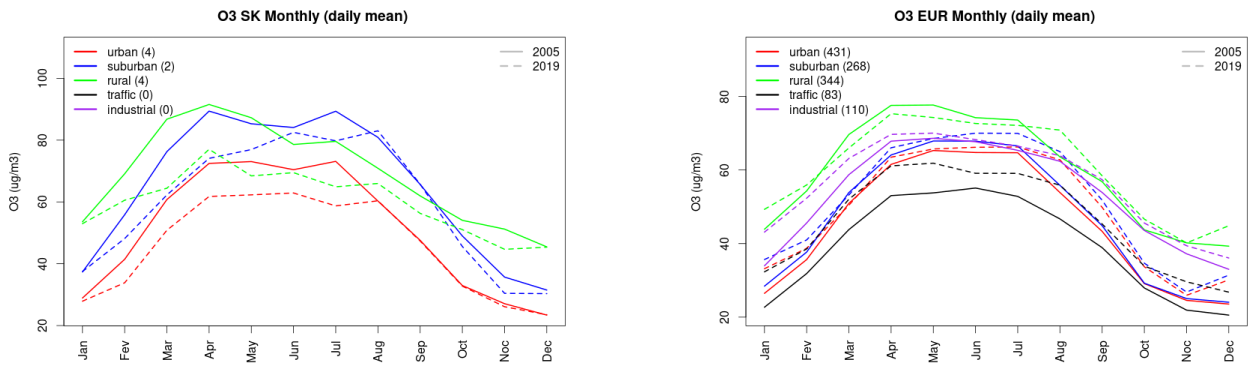


Figure S.609: Monthly cycle of daily mean ozone for Slovakia (left) and Europe (right) at various station types estimated from the whole time series in 2005 (solid lines) and 2019

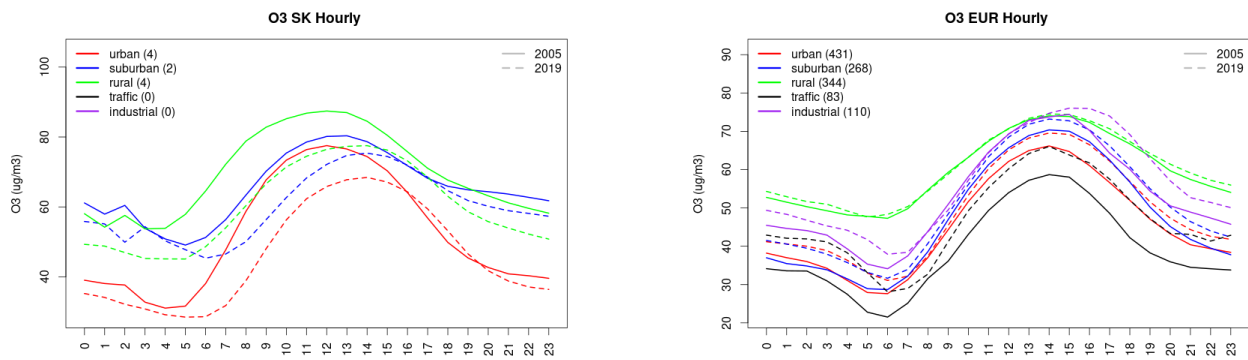


Figure S.610: Diurnal cycle of daily mean ozone for Slovakia (left) and Europe (right) at various station types estimated from the whole time series in 2005 (solid lines) and 2019

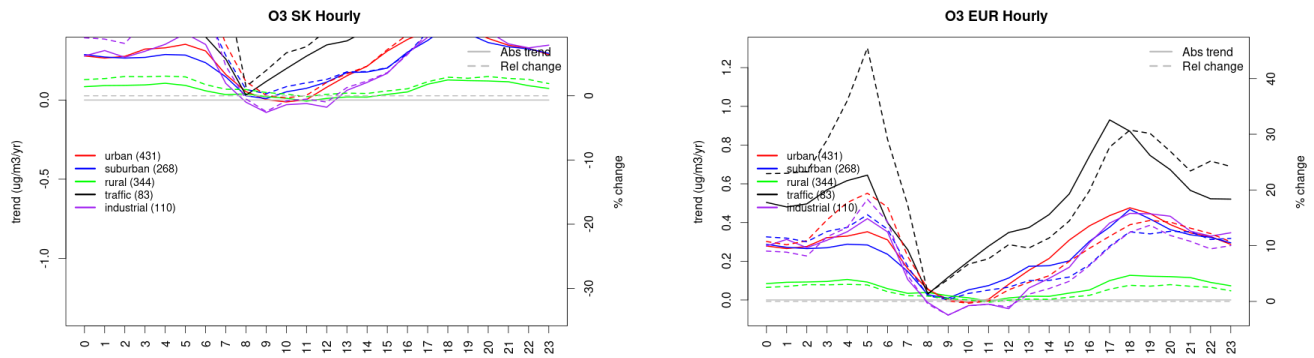


Figure S.611: Absolute (solid lines, left axis) and relative (dashed lines, right axis) trends in the diurnal cycle for Slovakia (left) and Europe (right) of ozone at various station type.

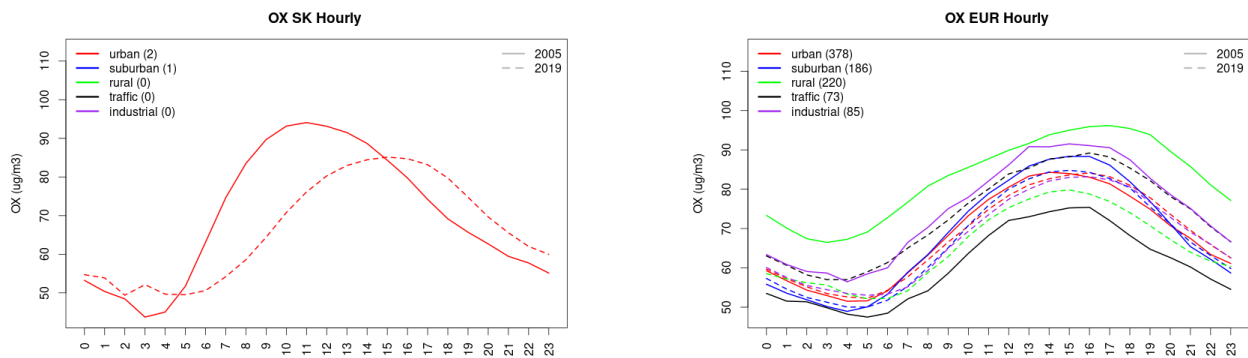


Figure S.612: Diurnal cycle of daily mean OX (as $\text{NO}_2 + \text{O}_3$) for Slovakia (left) and Europe (right) at various station types estimated from the whole time series in 2005 (solid lines) and 2019

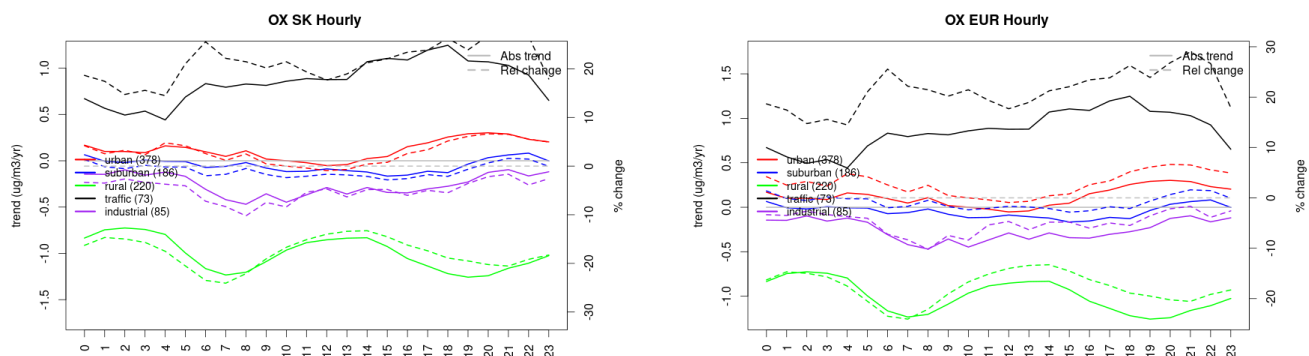


Figure S.613: Absolute (solid lines, left axis) and relative (dashed lines, right axis) trends in the diurnal cycle for Slovakia (left) and Europe (right) of OX (as NO₂+O₃) at various station type.

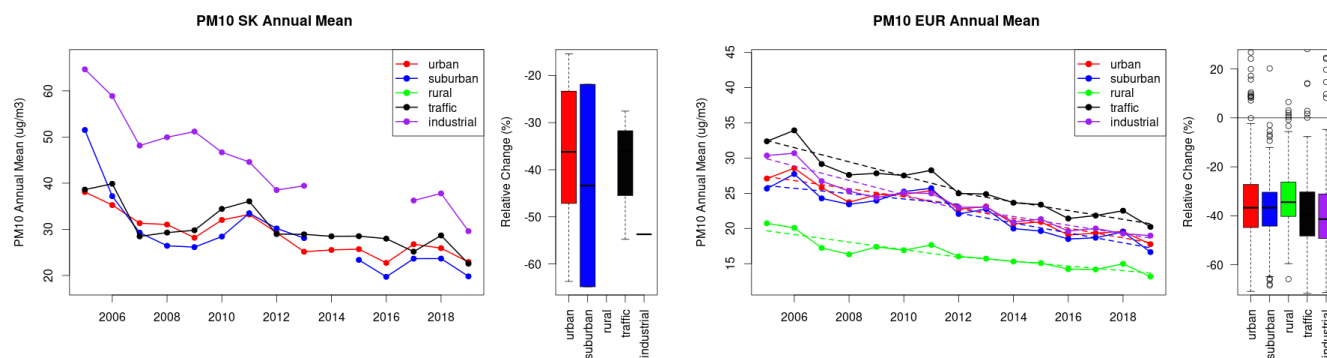


Figure S.614: Time series of the Slovakia (left) and European-wide composite (median) of annual mean PM₁₀ (ug/m³) per station type and area (red: urban background, blue suburban background, green: rural background, black: traffic, violet: industrial) between 2005 and 2019. In the European composite, the dashed lines show the linear fit between 2005 & 2012 and between 2012 & 2019. The boxplots on the right-hand side show the distribution of relative changes (%) between 2005 and 2019 for all stations of each typology in Slovakia and in Europe.

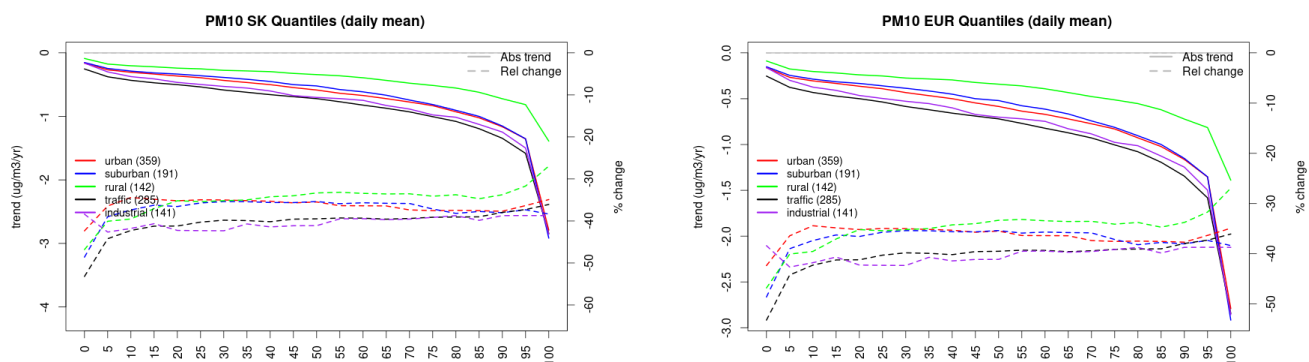


Figure S.615: For PM₁₀ in Slovakia (left) and Europe, and for each typology of station: absolute trend (solid lines, left y-axis) and relative change (dashed lines, right y-axis) of the percentiles of daily means.

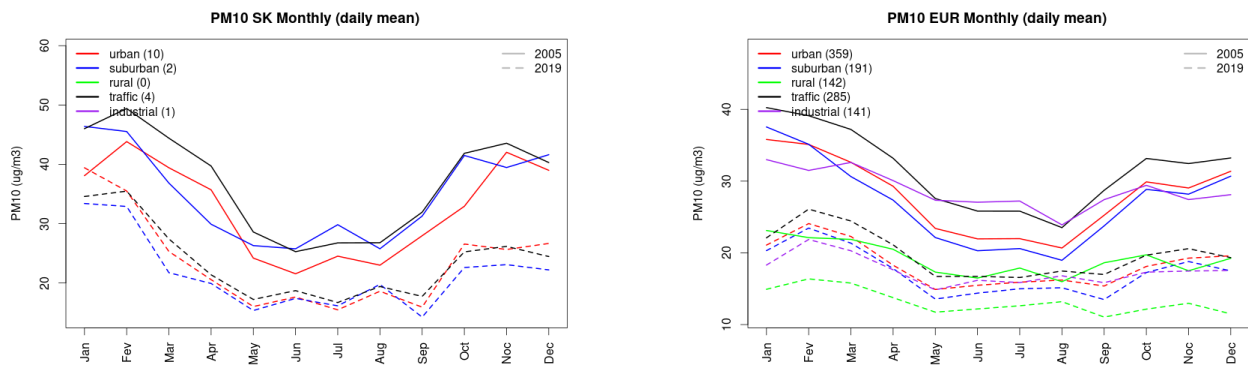


Figure S.616: Monthly cycle of daily mean PM10 for Slovakia (left) and Europe (right) at various station types estimated from the whole time series in 2005 (solid lines) and 2019 (dashed lines)

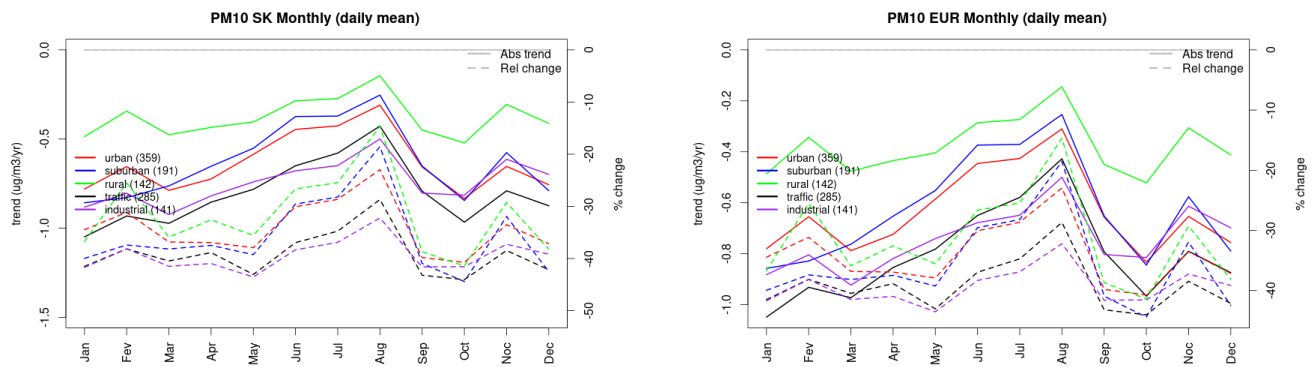


Figure S.617: Absolute (solid lines, left axis) and relative (dashed lines, right axis) trends in the monthly cycle for Slovakia (left) and Europe (right) of PM10 at various station type.

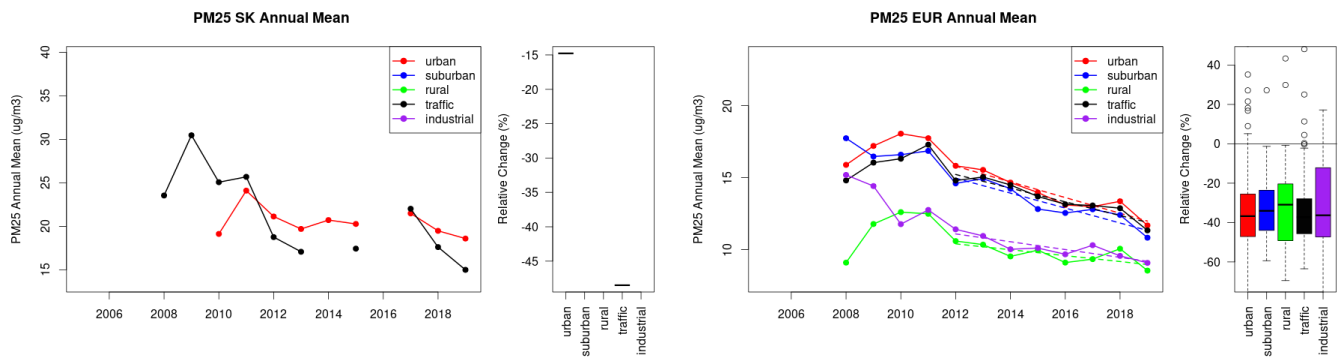


Figure S.618: Time series of the Slovakia (left) and European-wide composite (median) of annual mean PM25 ($\mu\text{g}/\text{m}^3$) per station type and area (red: urban background, blue suburban background, green: rural background, black: traffic, violet: industrial) between 2005 and 2019. In the European composite, the dashed lines show the linear fit between 2005 & 2012 and between 2012 & 2019. The boxplots on the right-hand side show the distribution of relative changes (%) between 2005 and 2019 for all stations of each typology in Slovakia and in Europe.

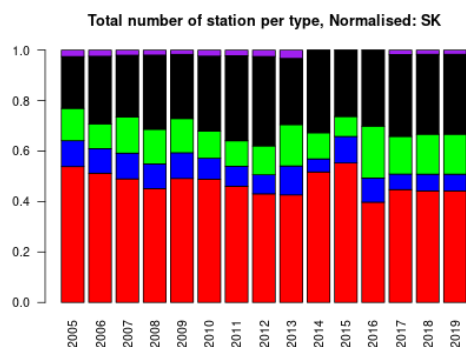
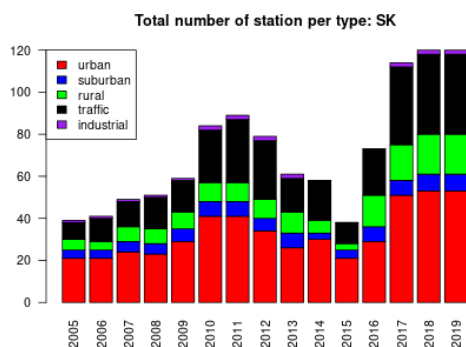
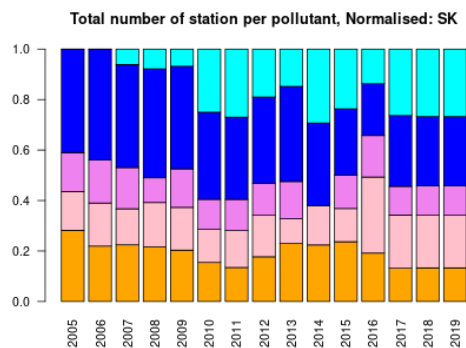
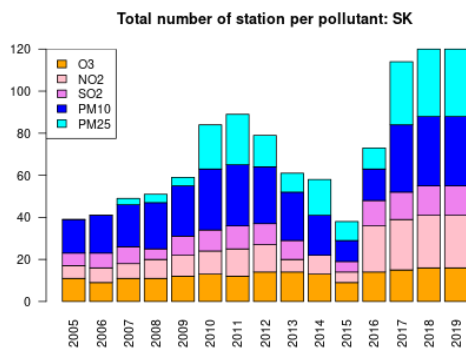
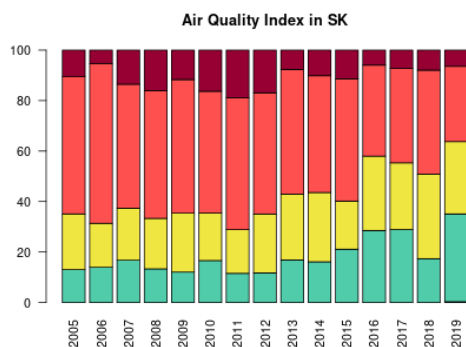


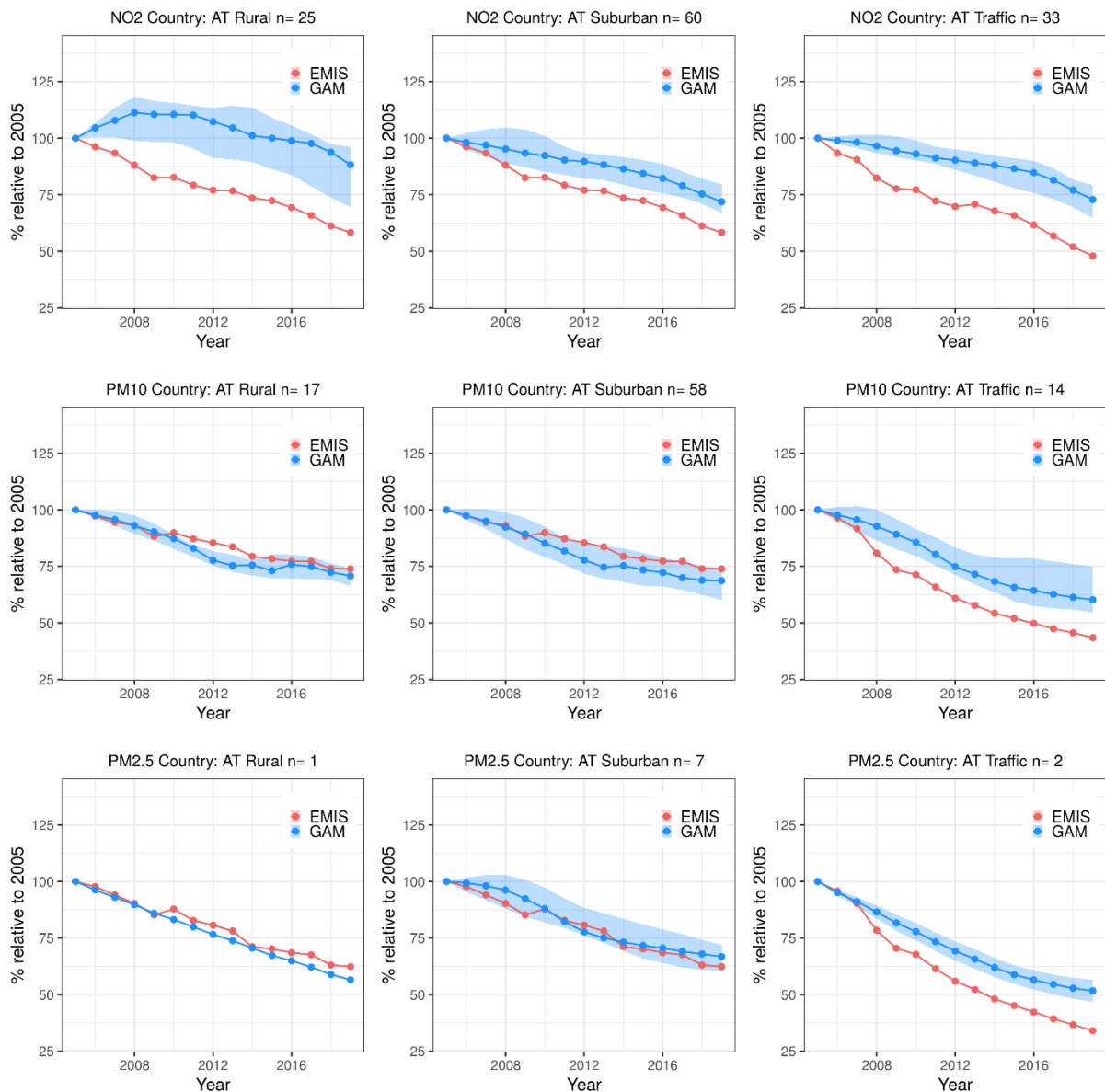
Figure S.619: For Slovakia: overall air quality index (percentage of days in a given year) and distribution of daily categories per pollutant (light blue: good, light green: fair, yellow: moderate, orange: poor, red: very poor, violet: extremely poor).

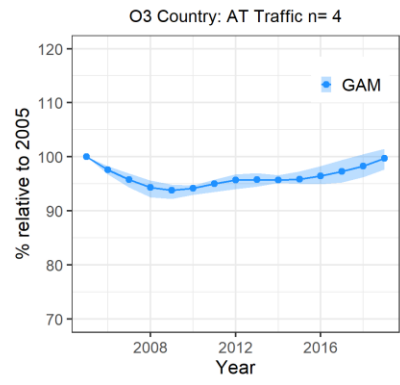
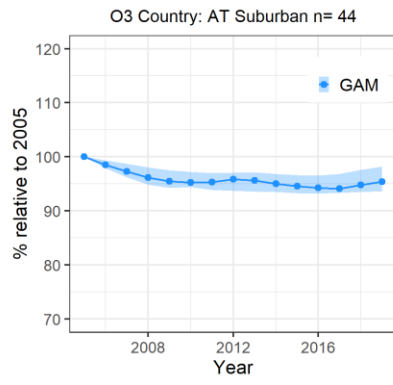
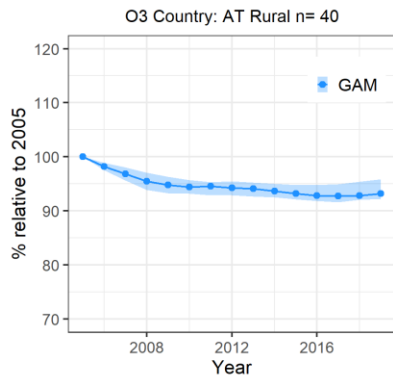
Annex 2

National trends in air concentrations as calculated by AirGAM and reported emissions

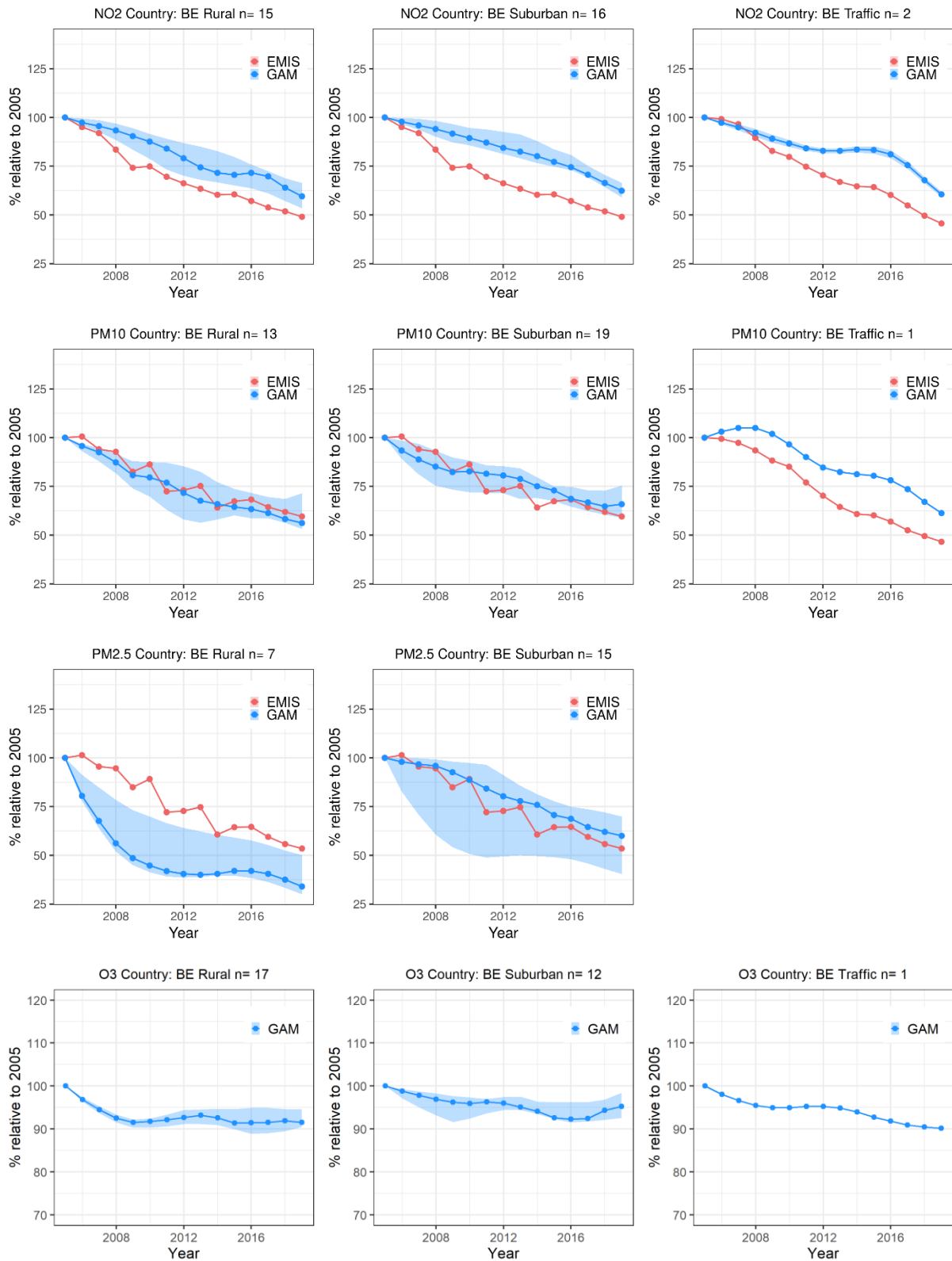
For each country and station category these plots show the median (blue line) and spread (25 and 75 percentile as blue shaded area) of the met.adjusted long-term trend calculated by the AirGAM model for all stations in the respective country/category. The red line gives the national emissions as given by CEIP from road traffic when compared to sites in the traffic category and from all sources when compared to the other two categories.

5.1 Country AT

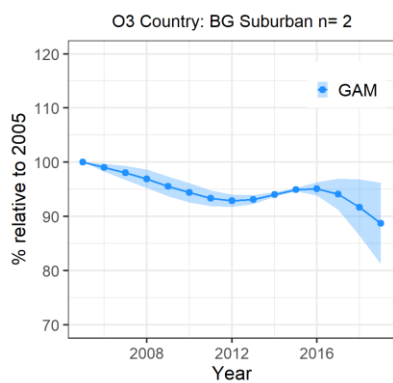
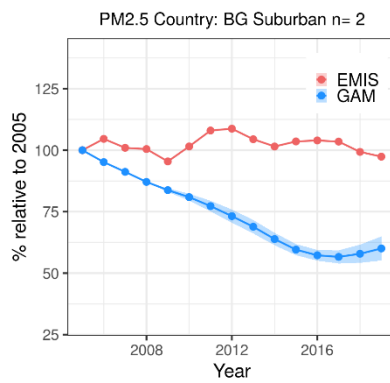
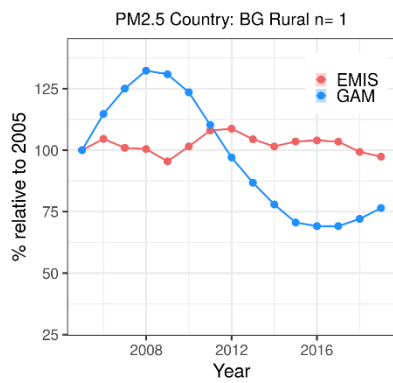
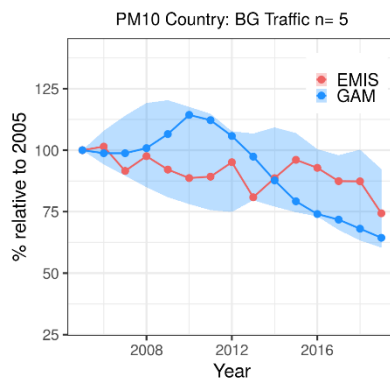
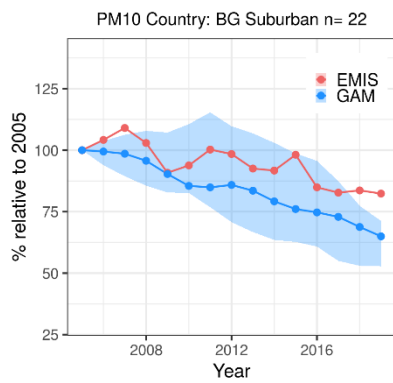
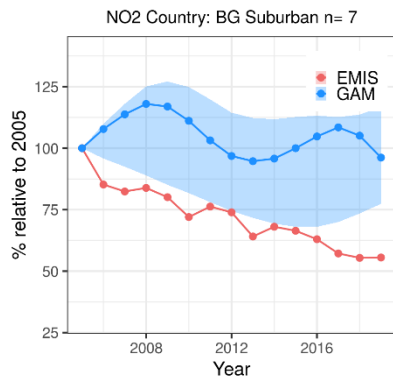




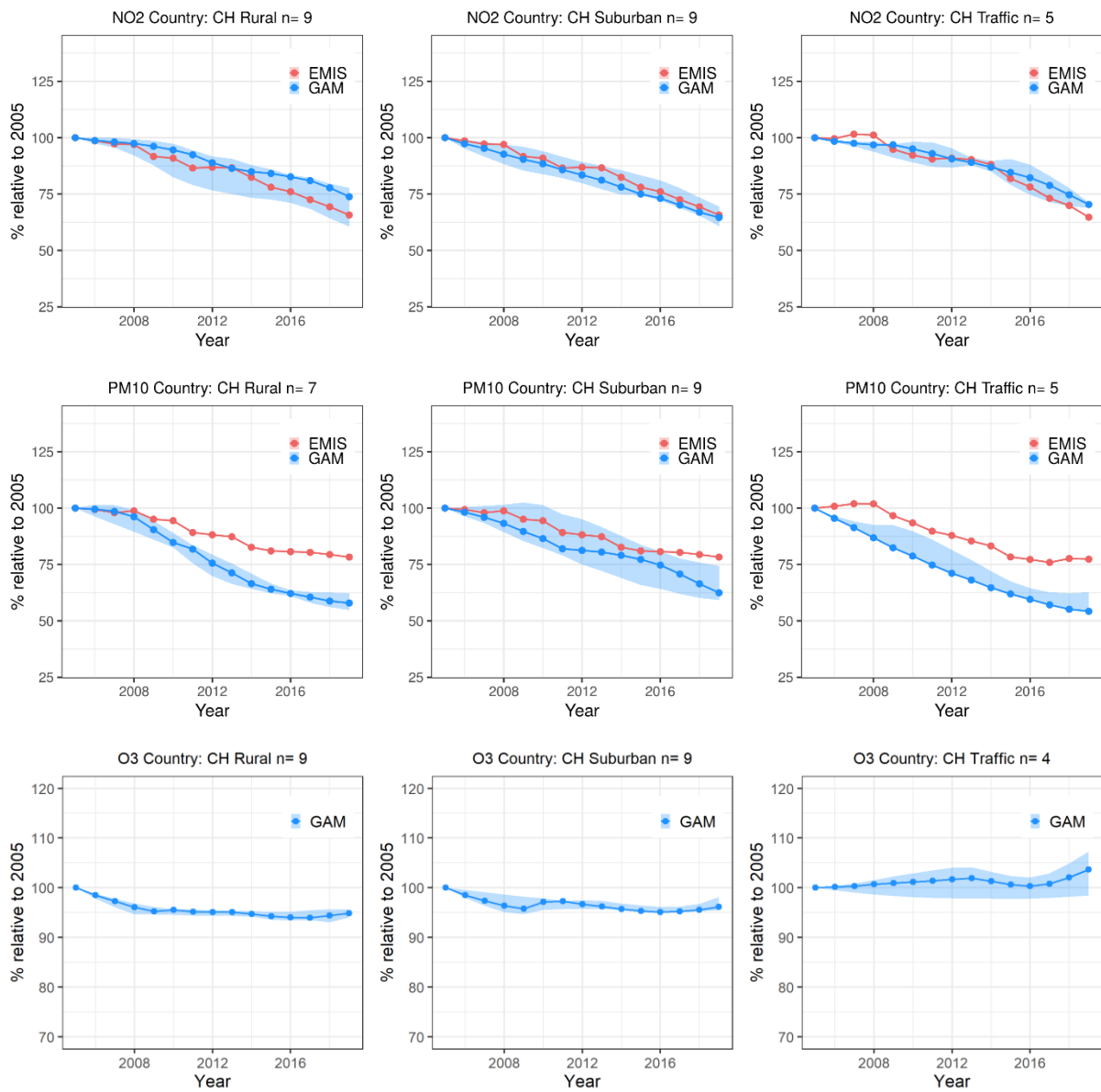
5.2 Country BE



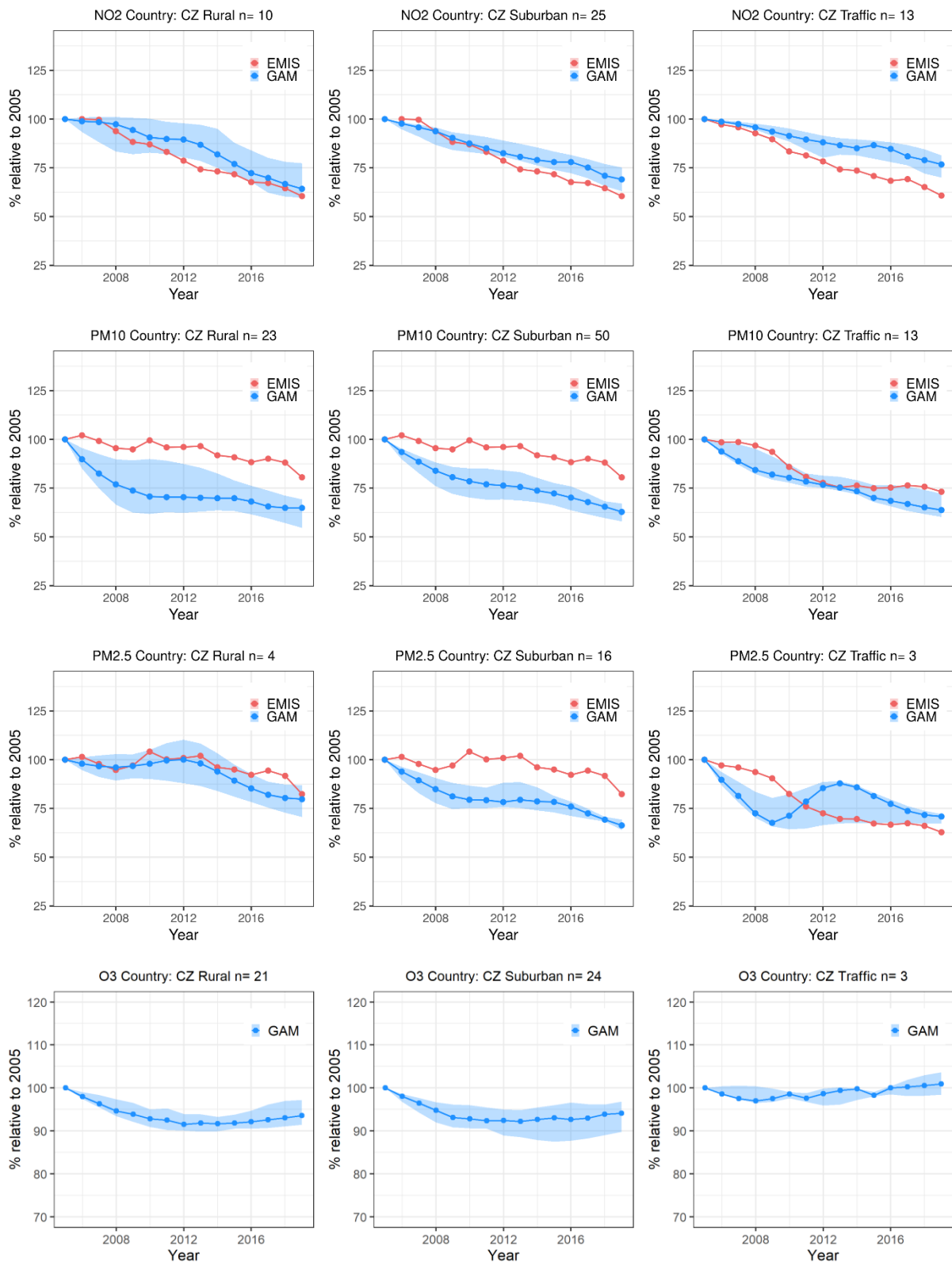
5.3 Country BG



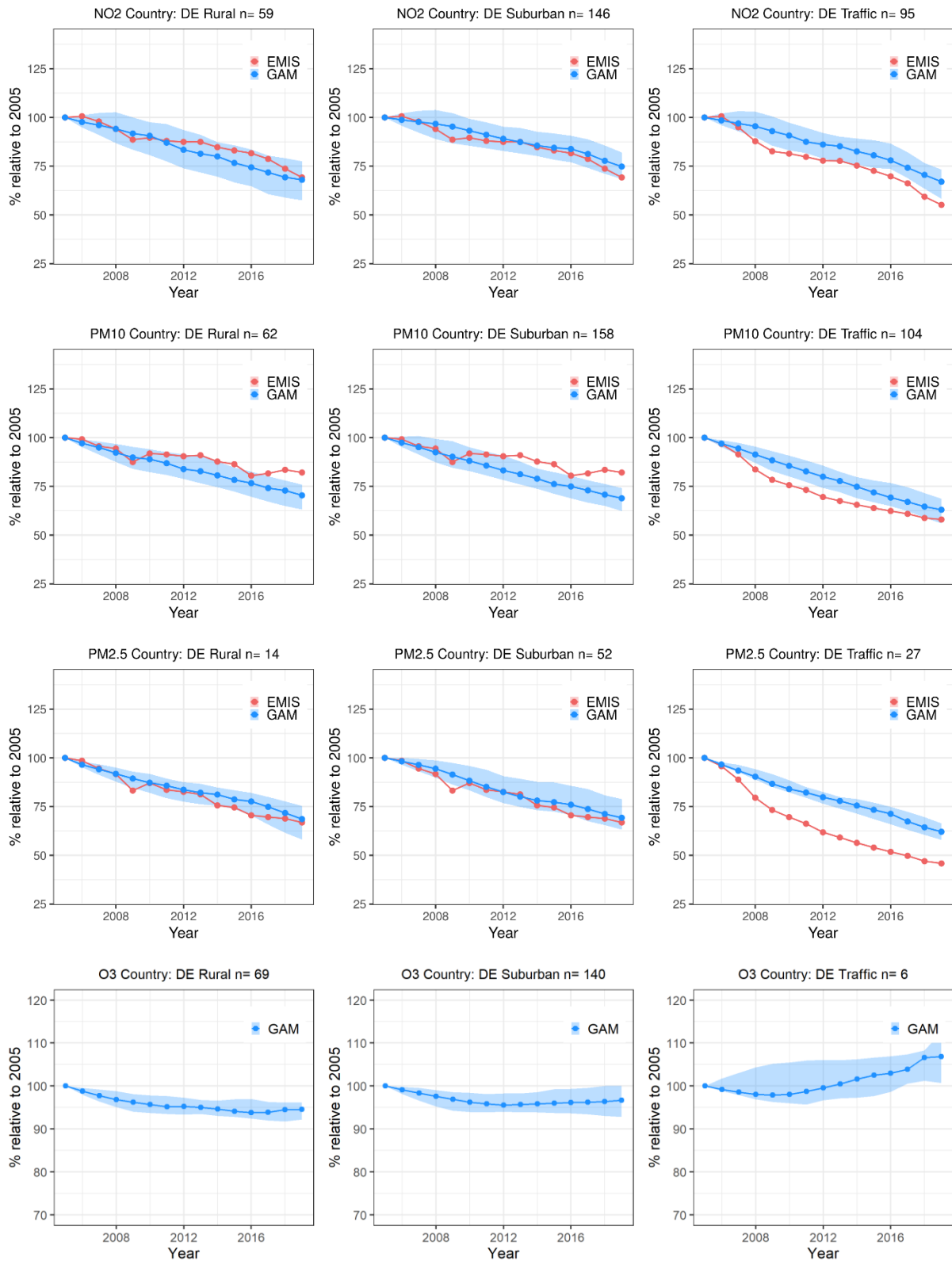
5.4 Country CH



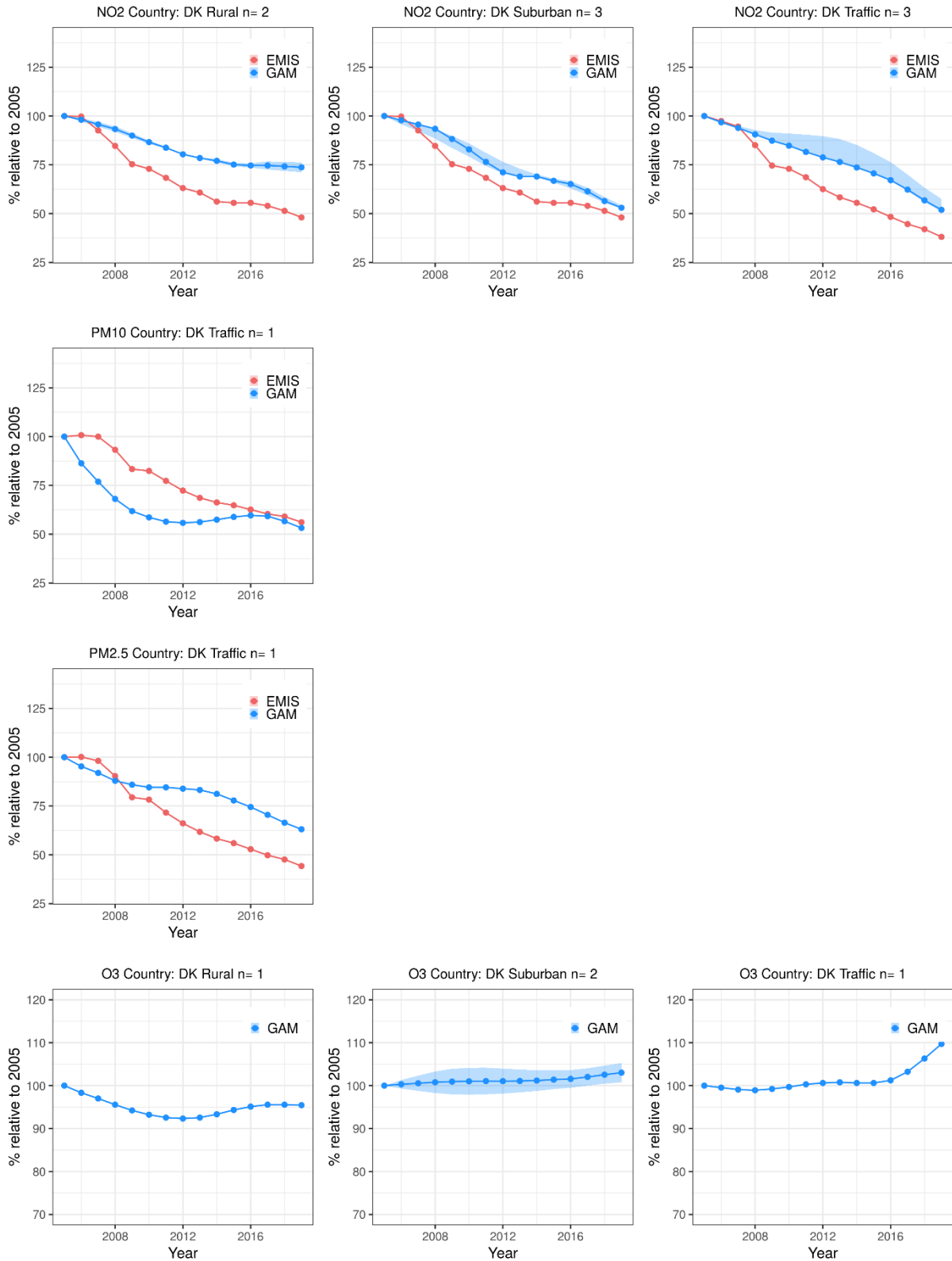
5.5 Country CZ



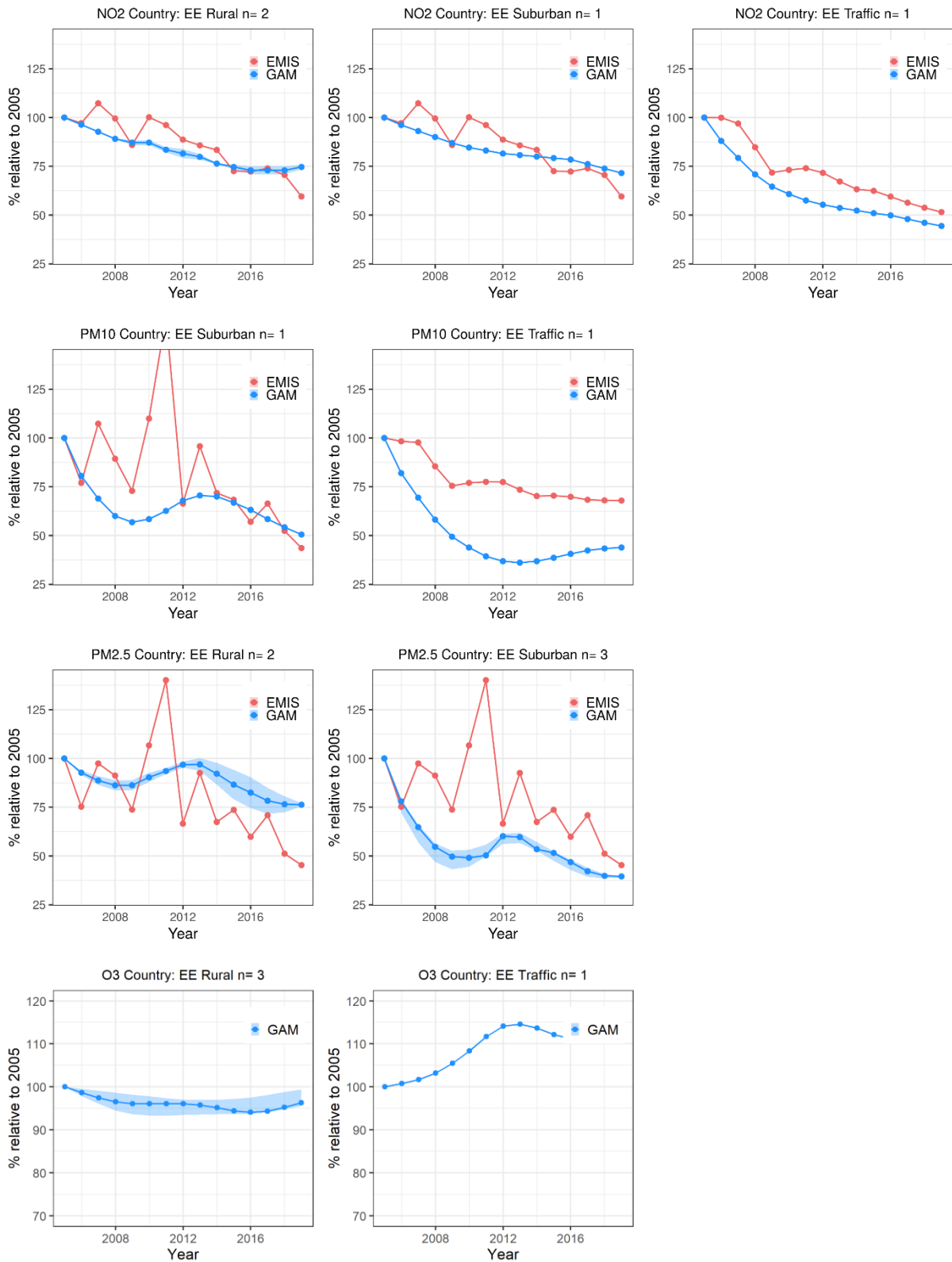
5.6 Country DE



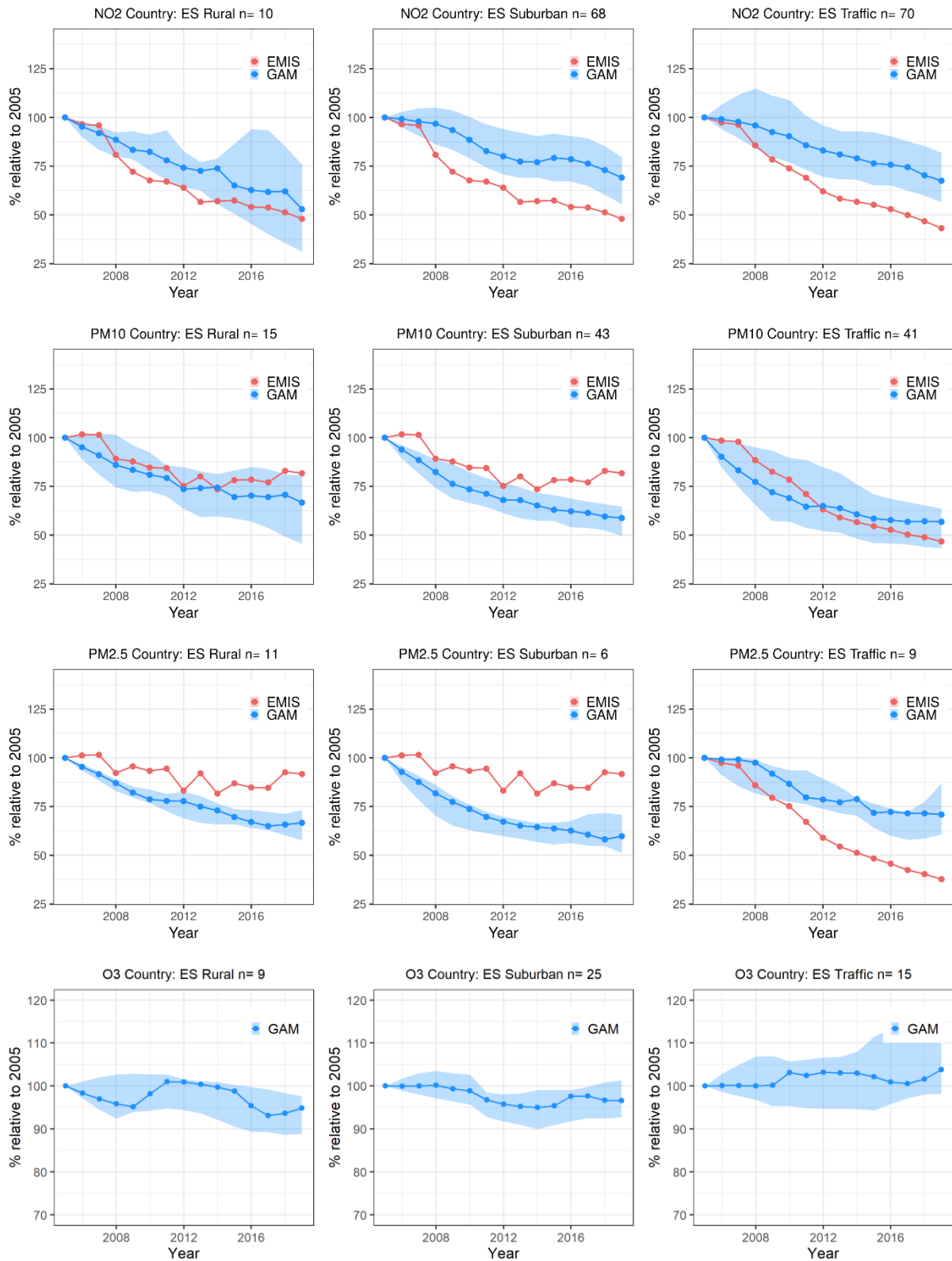
5.7 Country DK



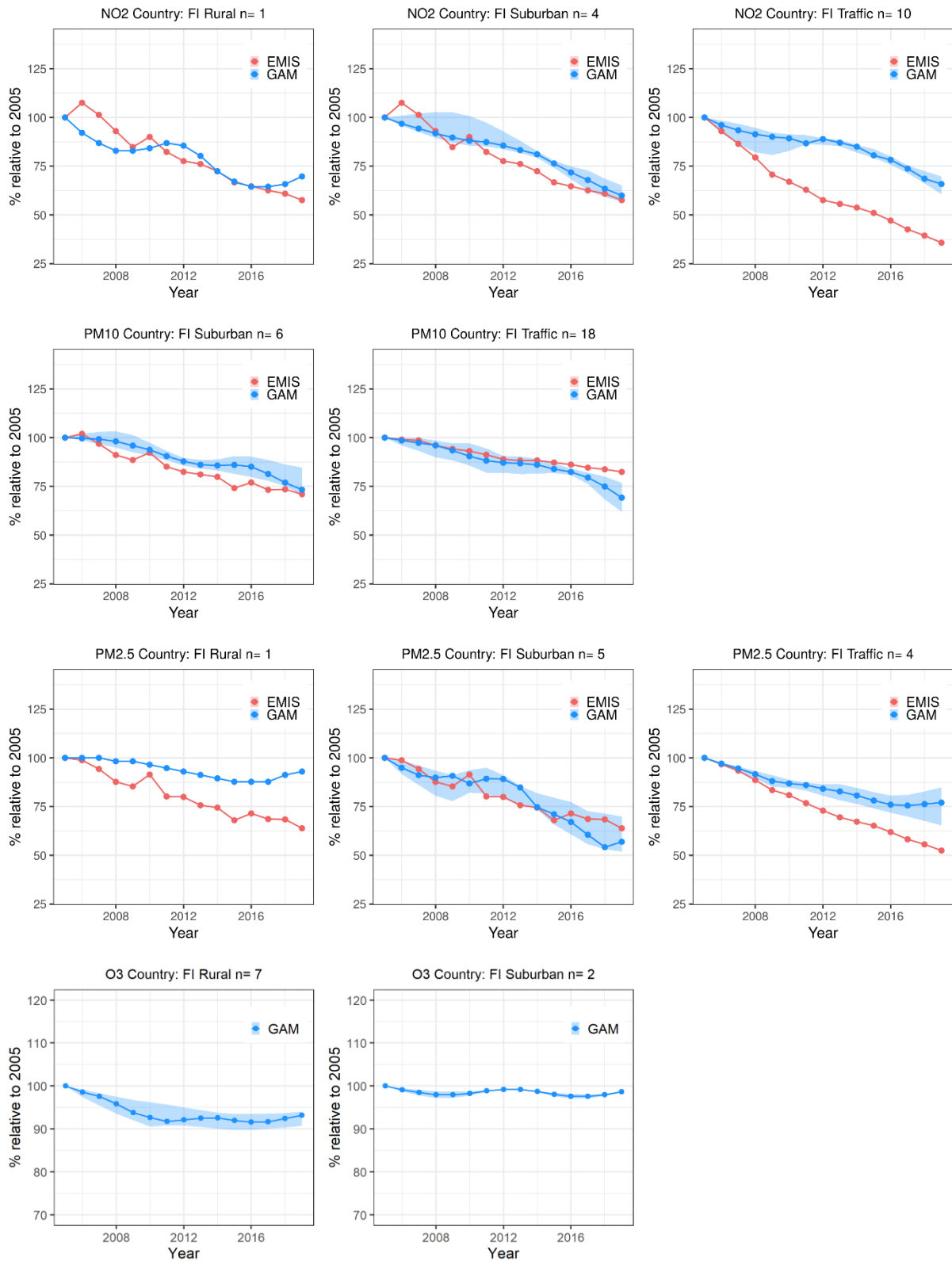
5.8 Country EE



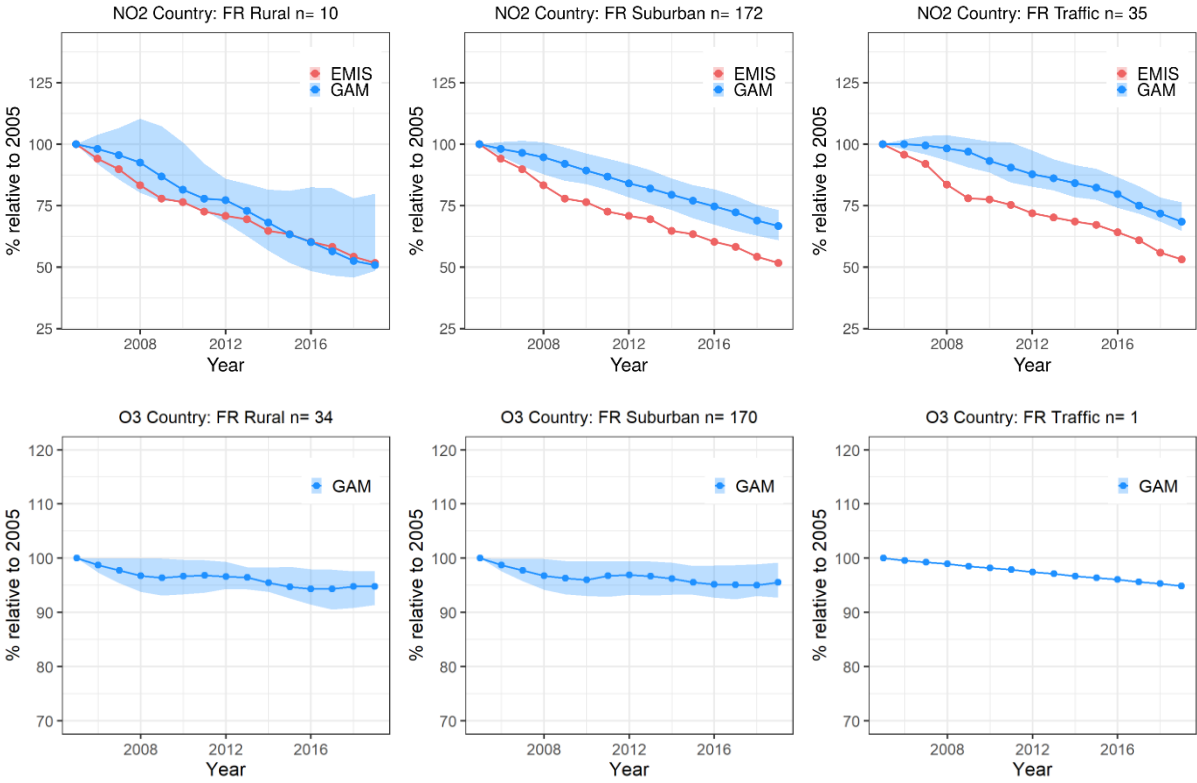
5.9 Country ES



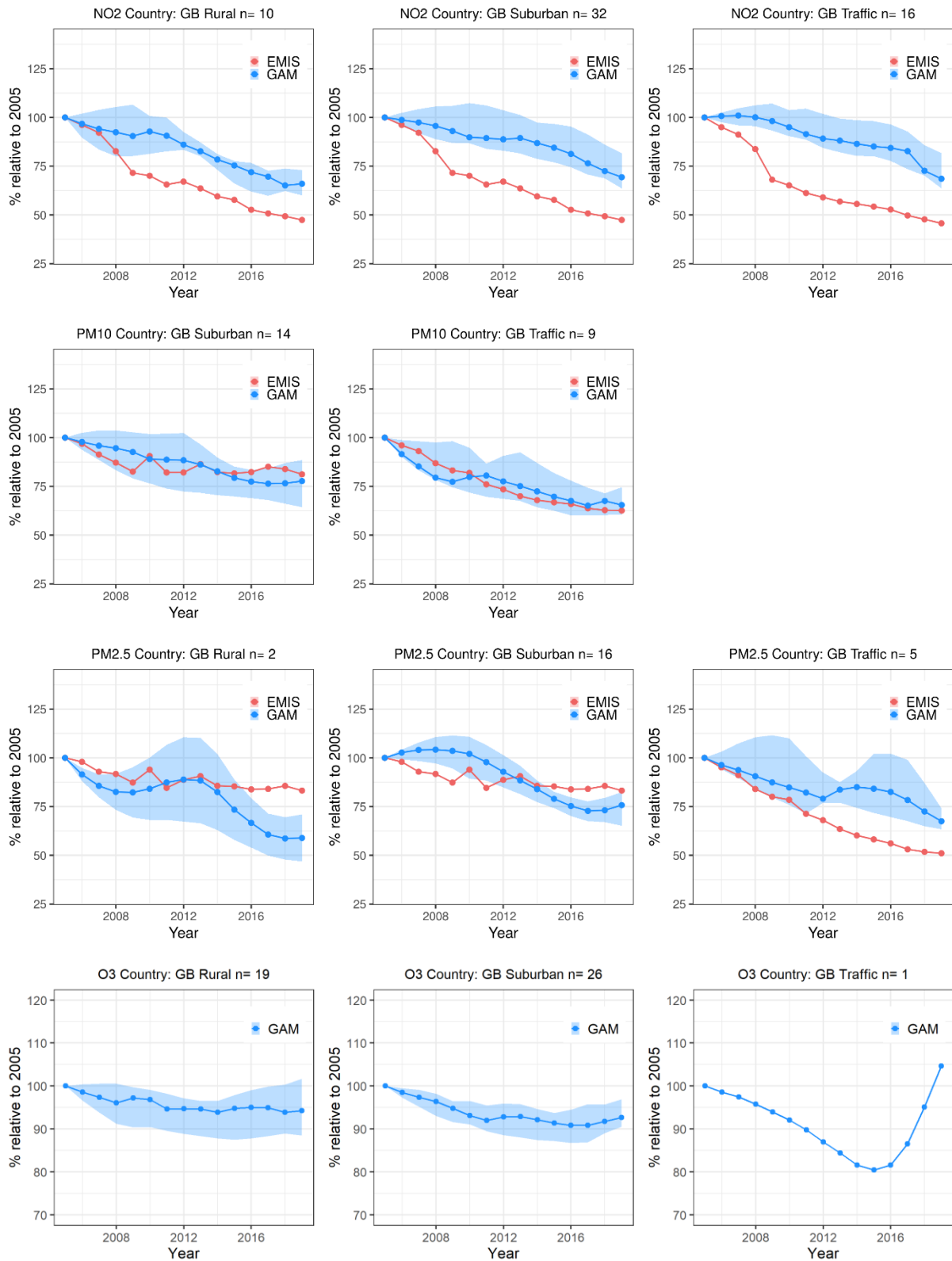
5.10 Country FI



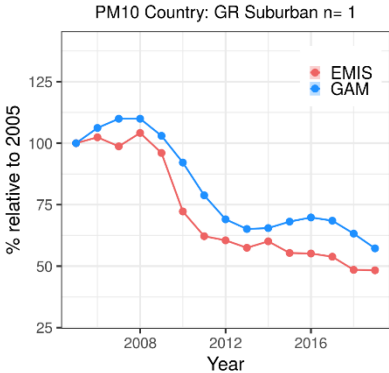
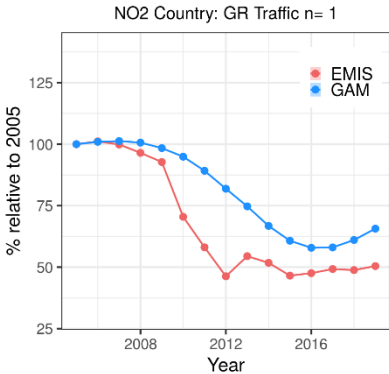
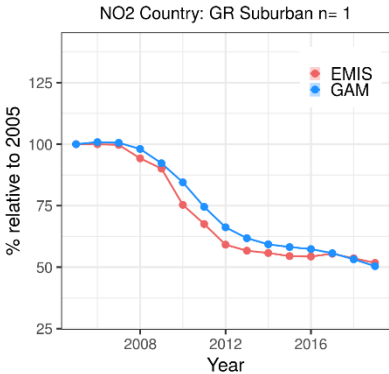
5.11 Country FR



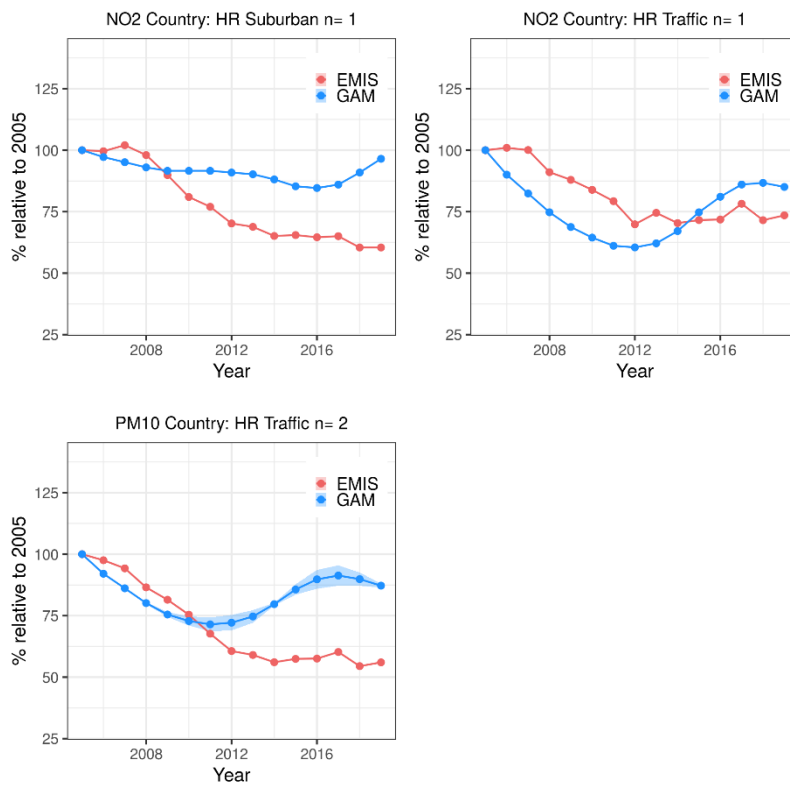
5.12 Country GB



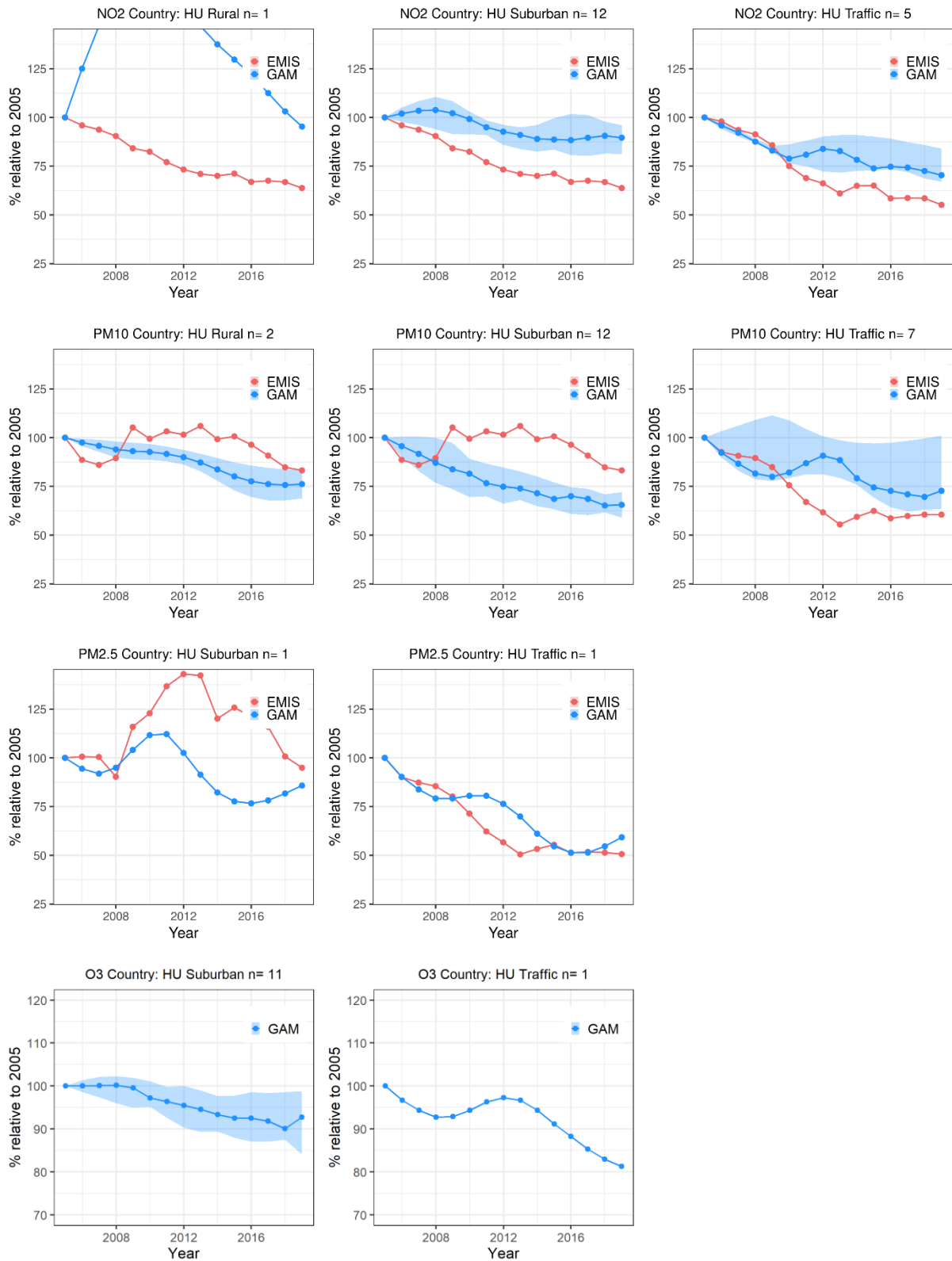
5.13 Country GR



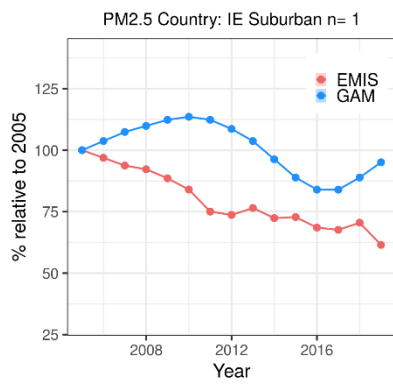
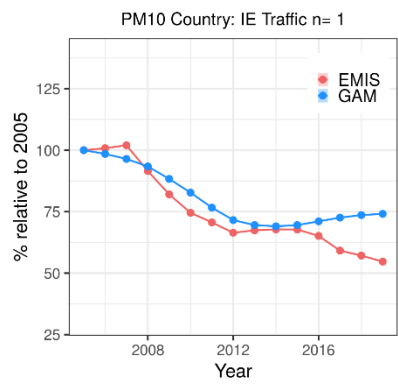
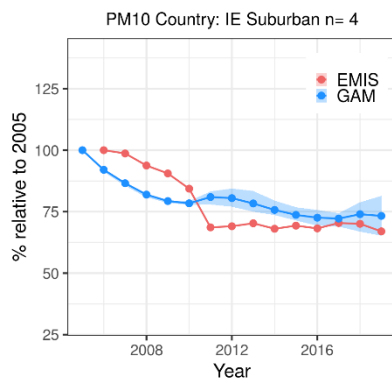
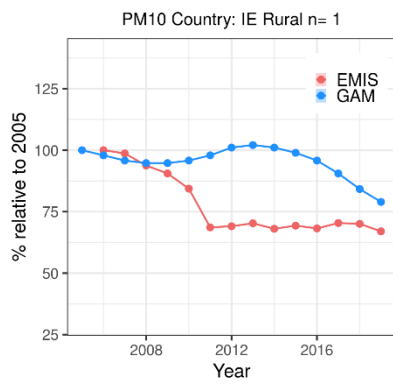
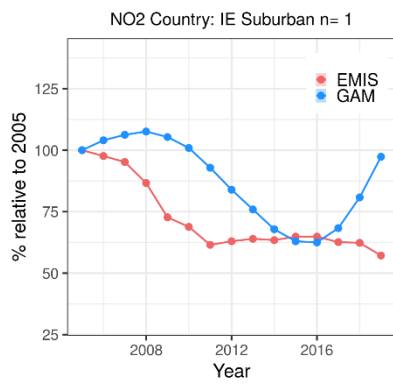
5.14 Country HR



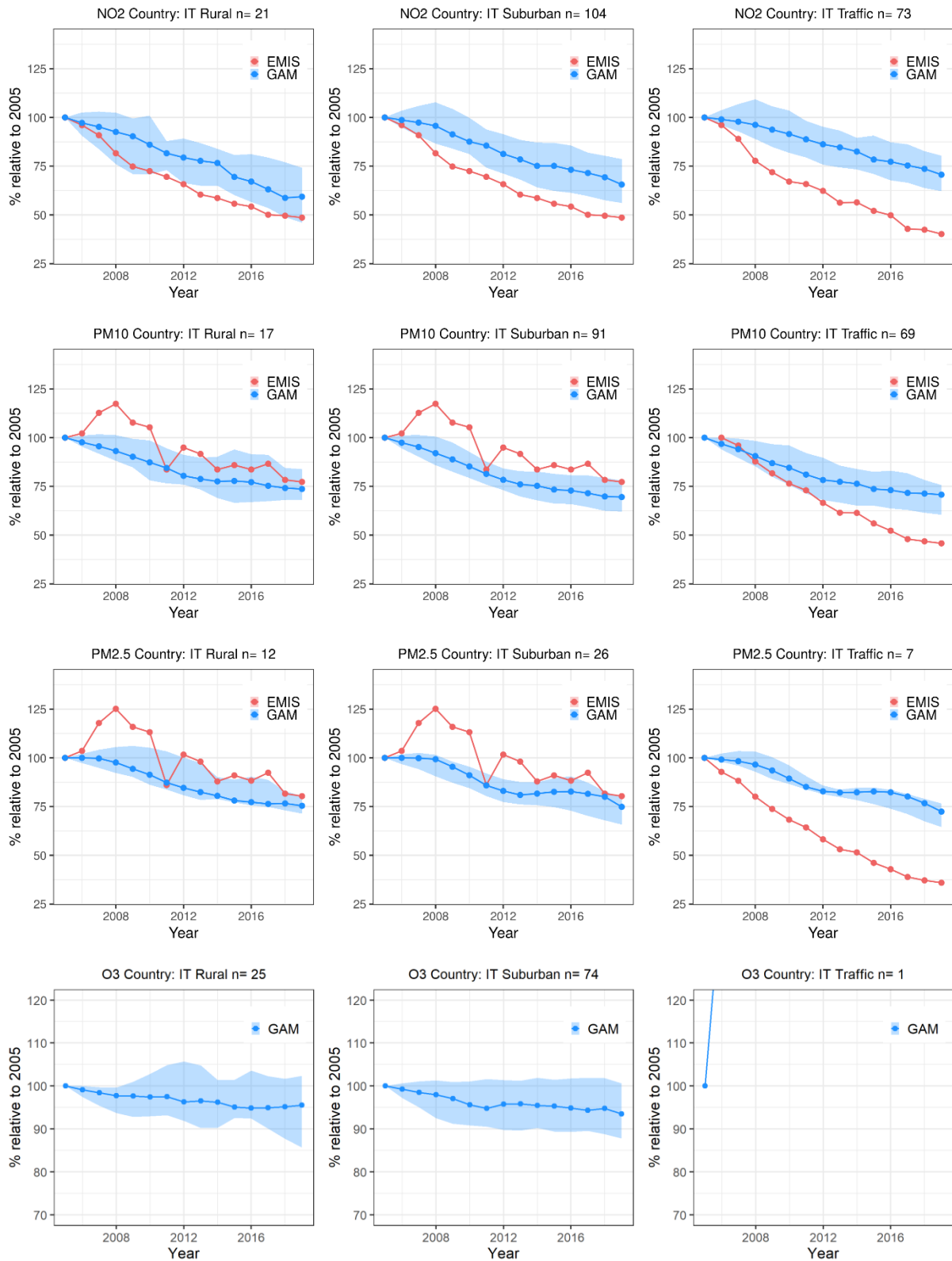
5.15 Country HU



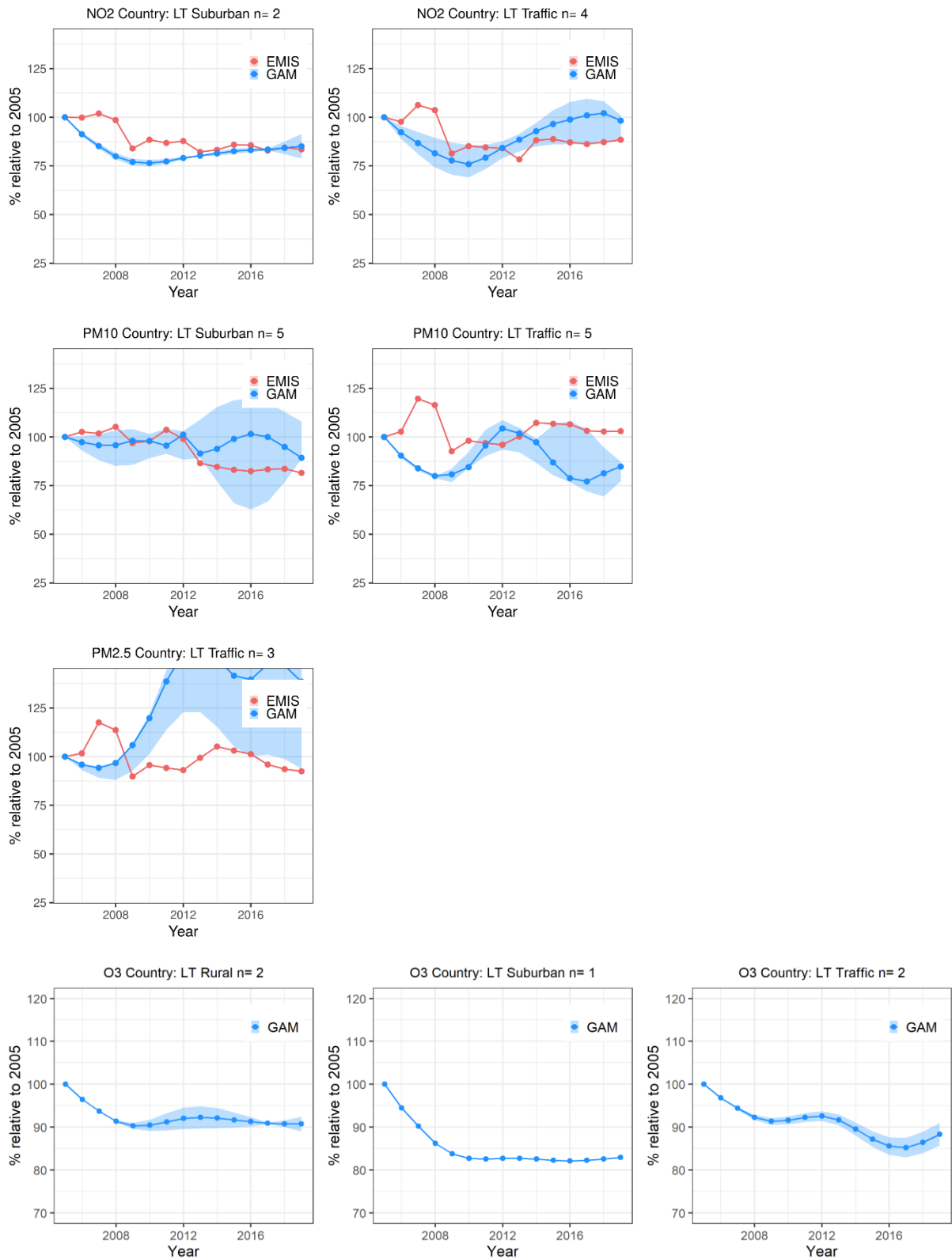
5.16 Country IE



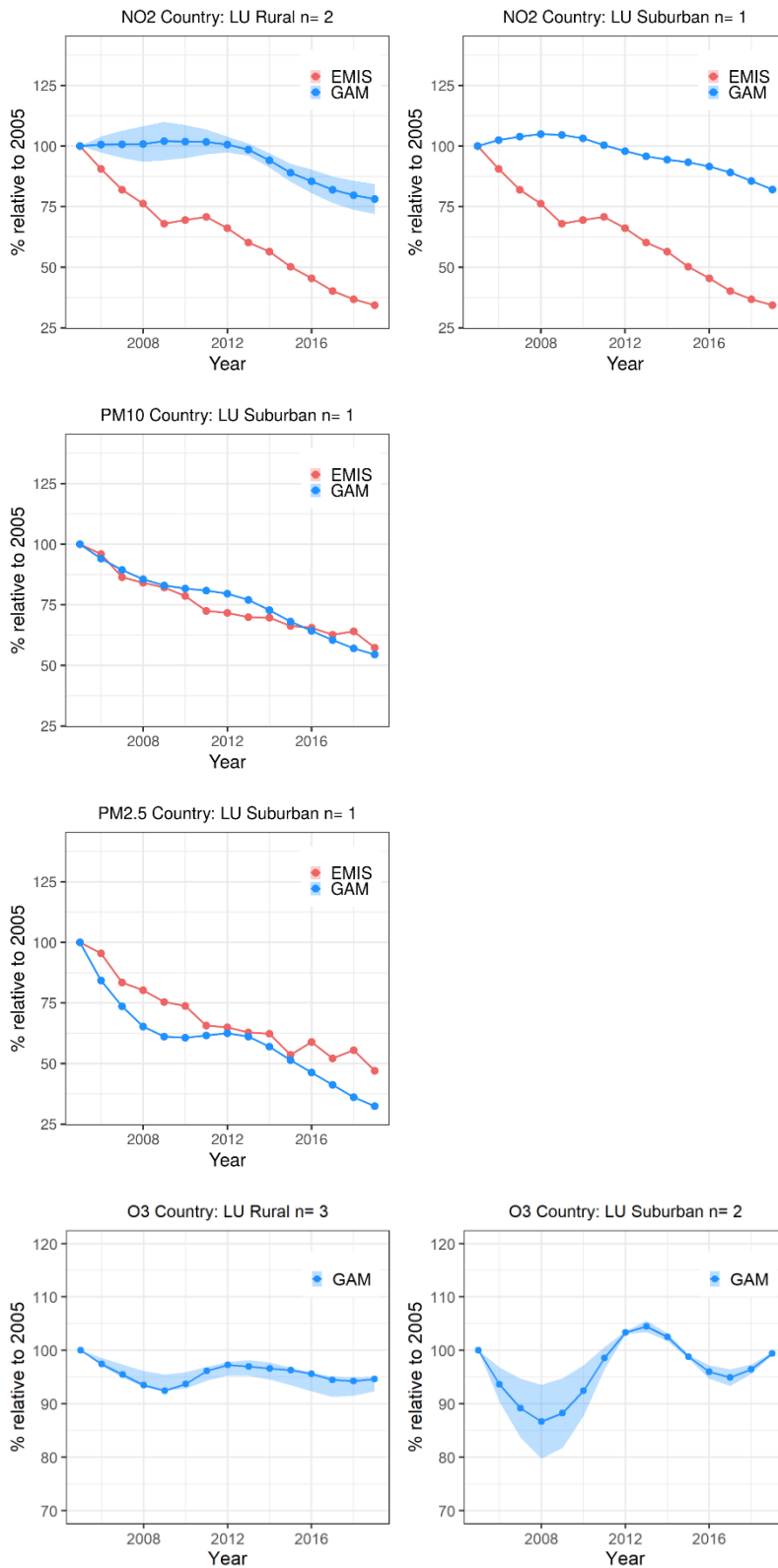
5.17 Country IT



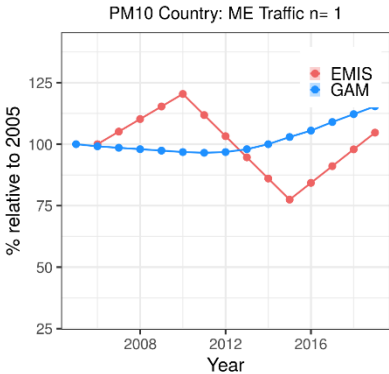
5.18 Country LT



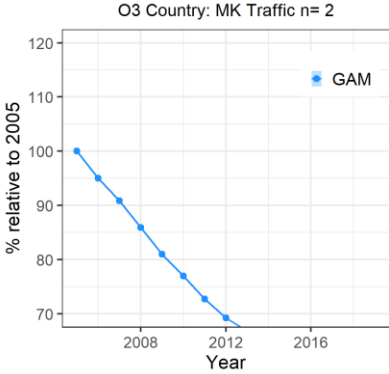
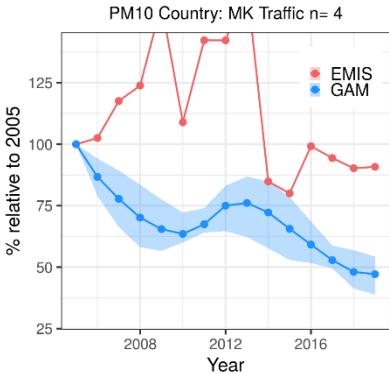
5.19 Country LU



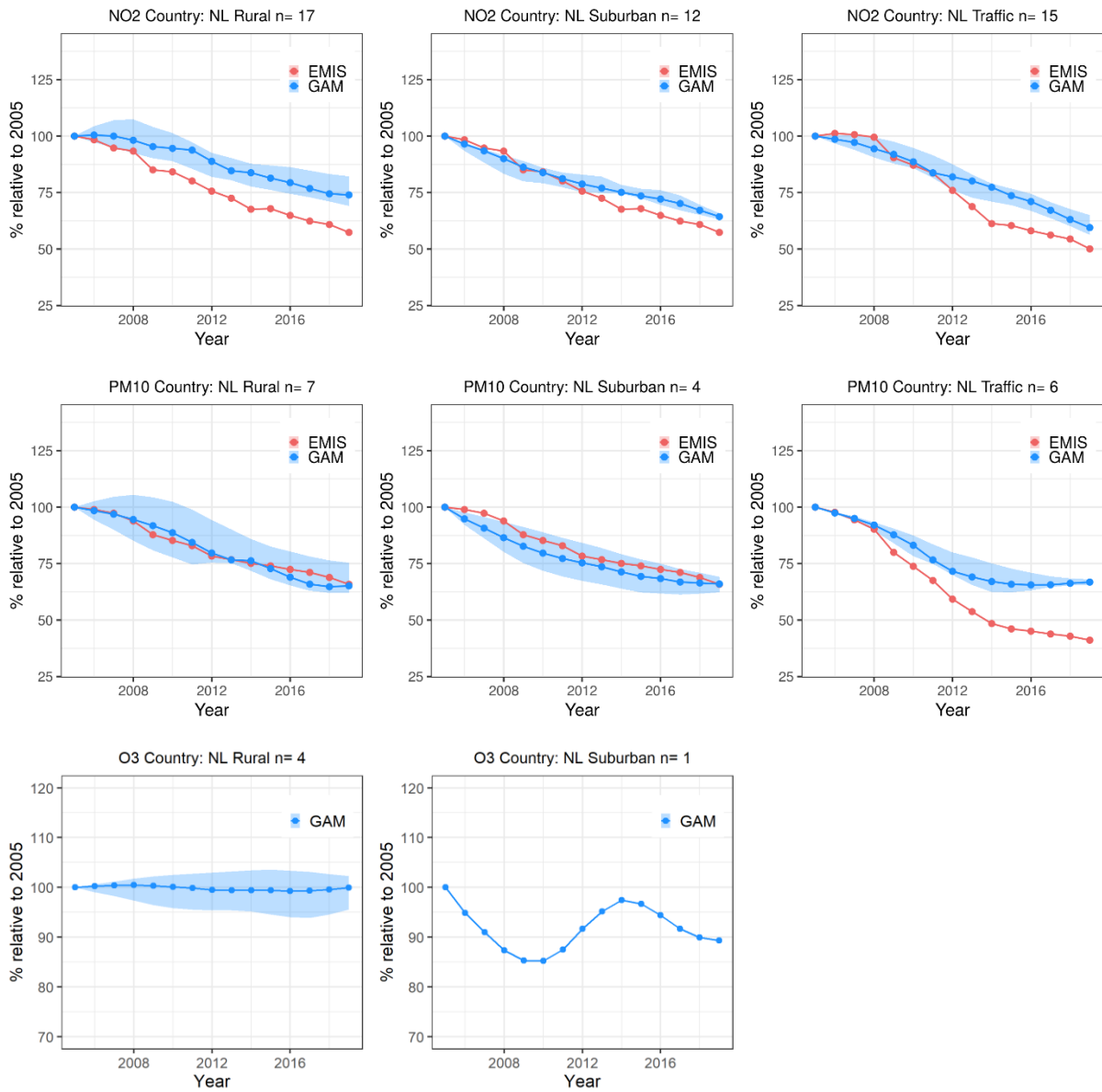
5.20 Country ME



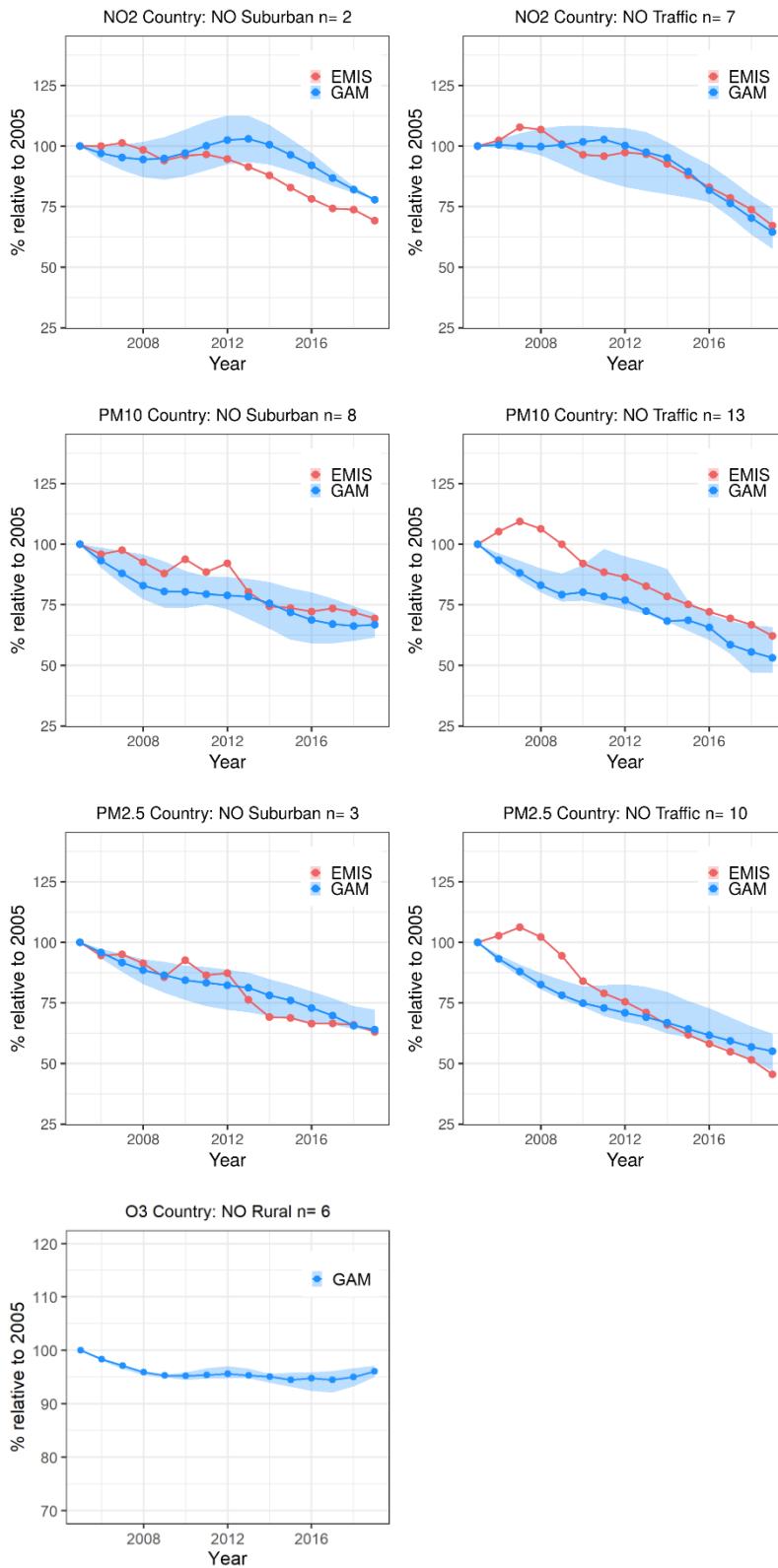
5.21 Country MK



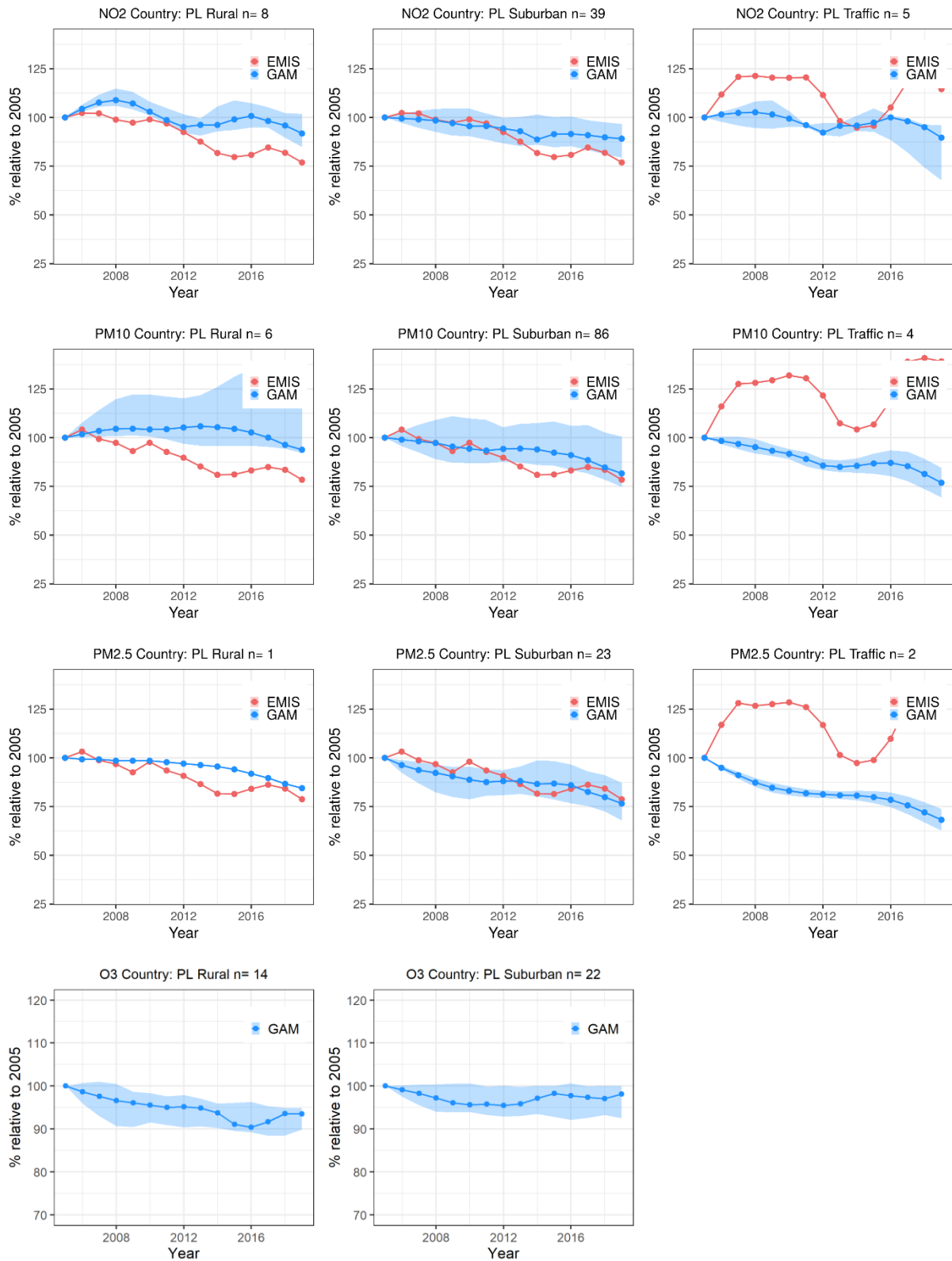
5.22 Country NL



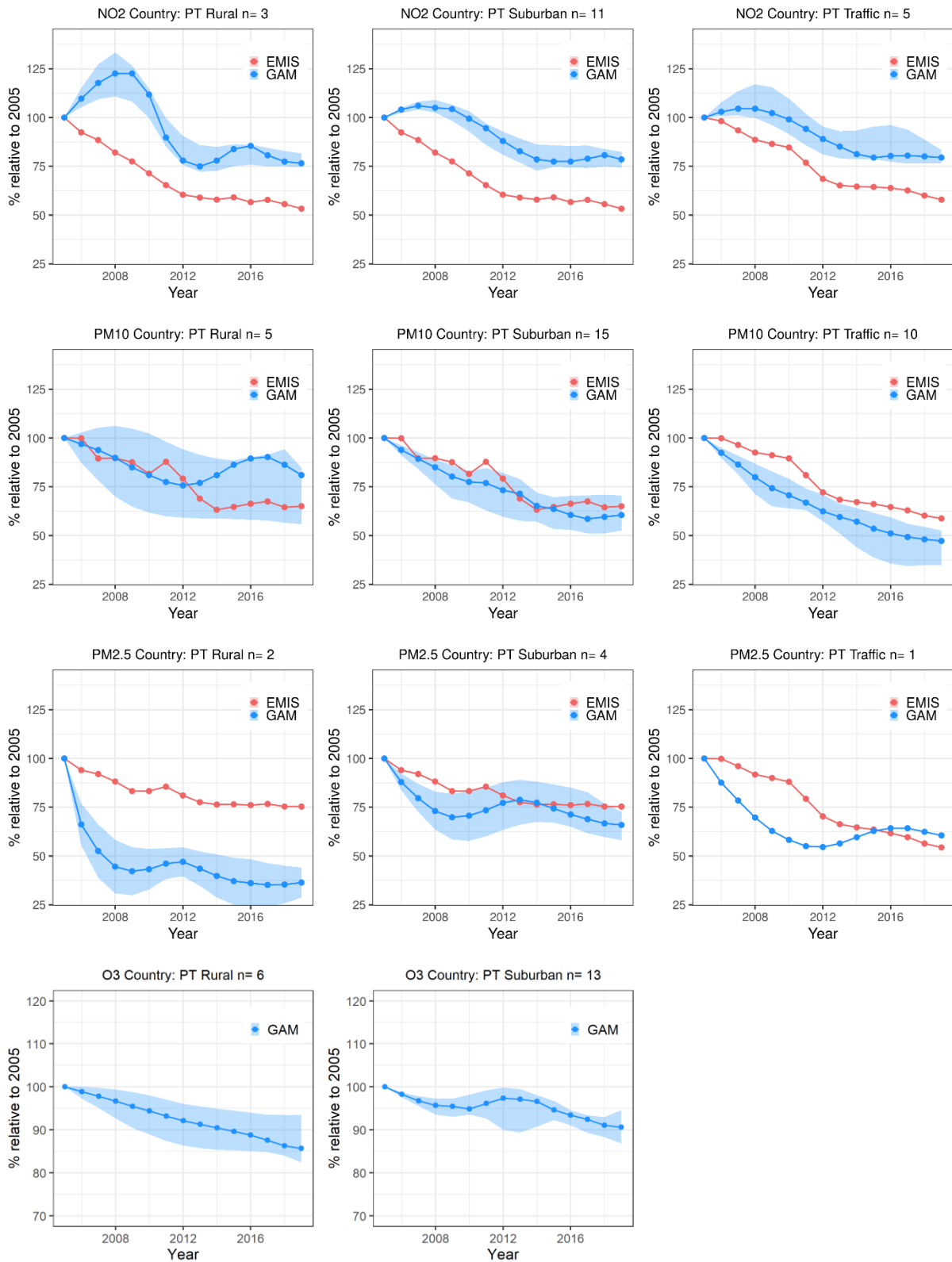
5.23 Country NO



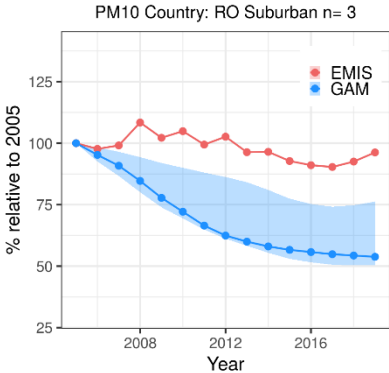
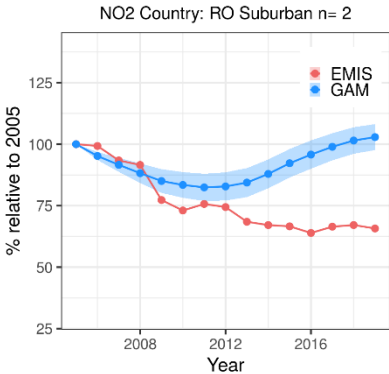
5.24 Country PL



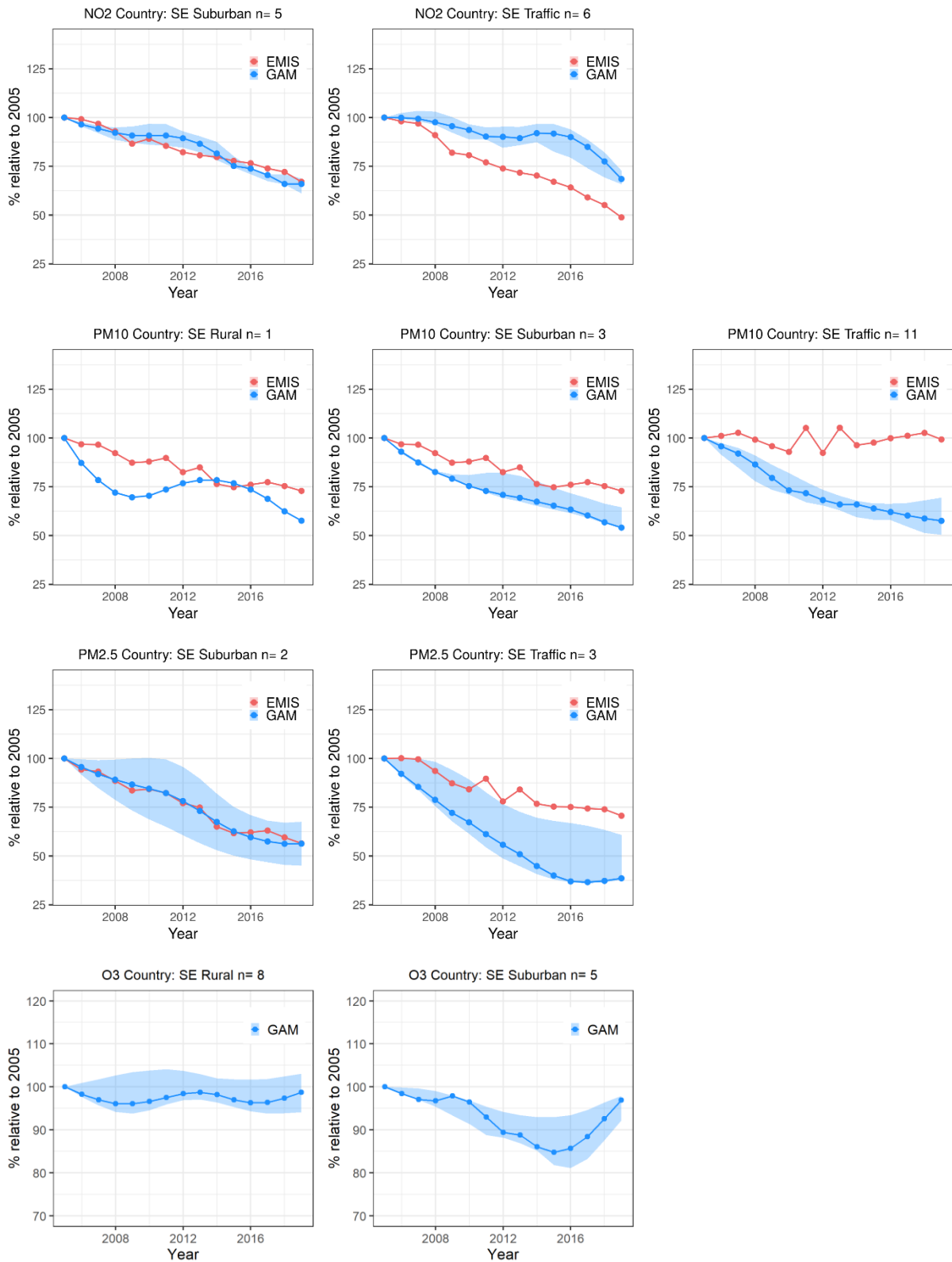
5.25 Country PT



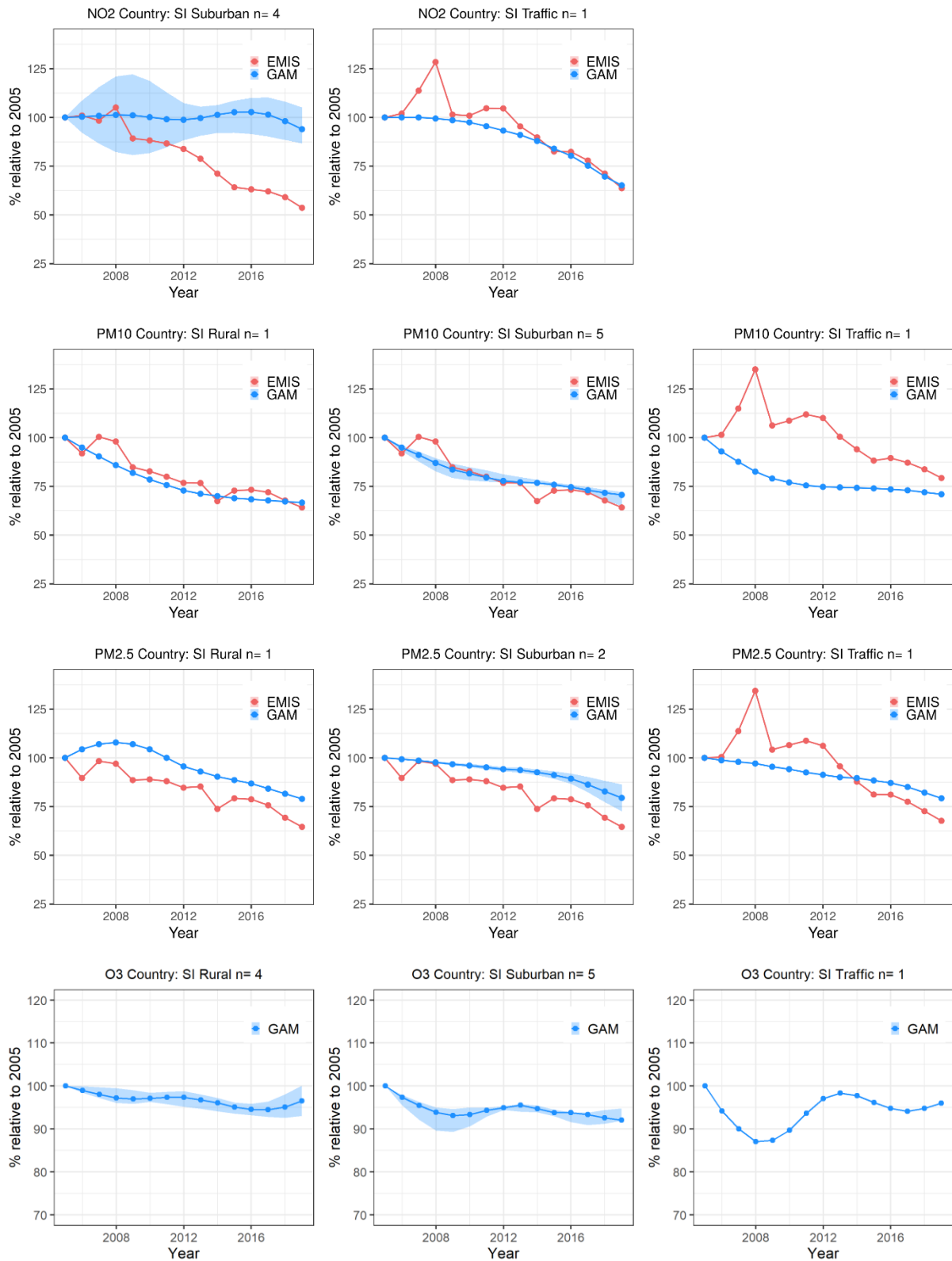
5.26 Country RO



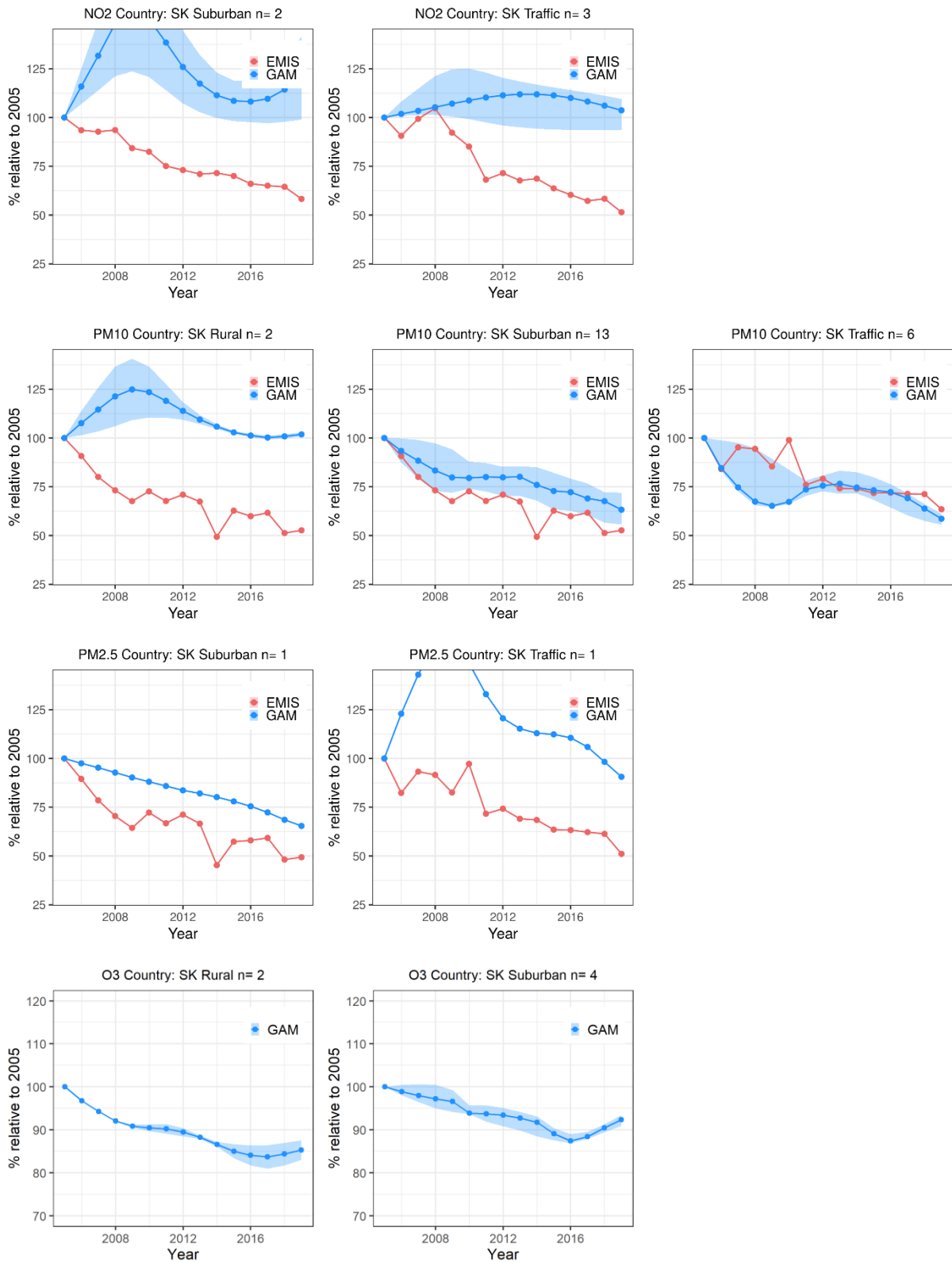
5.27 Country SE



5.28 Country SI



5.29 Country SK



European Topic Centre on Air pollution,
transport, noise and industrial pollution
c/o NILU – Norwegian Institute for Air Research
P.O. Box 100, NO-2027 Kjeller, Norway
Tel.: +47 63 89 80 00
Email: etc.atni@nilu.no
Web :<https://www.eionet.europa.eu/etcs/etc-atni>

The European Topic Centre on Air pollution,
transport, noise and industrial pollution (ETC/ATNI)
is a consortium of European institutes under a
framework partnership contract to the European
Environment Agency.

